

A FLOW REACTOR STUDY OF PYROLYSIS AND OXIDATION
CHARACTERISTICS OF N-DODECANE

A DISSERTATION
SUBMITTED TO THE DEPARTMENT OF MECHANICAL
ENGINEERING
AND THE COMMITTEE ON GRADUATE STUDIES
OF STANFORD UNIVERSITY
IN PARTIAL FULFILLMENT OF THE REQUIREMENTS
FOR THE DEGREE OF
DOCTOR OF PHILOSOPHY

Sayak Banerjee
August 2014

© 2014 by Sayak Banerjee. All Rights Reserved.

Re-distributed by Stanford University under license with the author.



This work is licensed under a Creative Commons Attribution-Noncommercial 3.0 United States License.

<http://creativecommons.org/licenses/by-nc/3.0/us/>

This dissertation is online at: <http://purl.stanford.edu/vh457pj2511>

I certify that I have read this dissertation and that, in my opinion, it is fully adequate in scope and quality as a dissertation for the degree of Doctor of Philosophy.

Craig Bowman, Primary Adviser

I certify that I have read this dissertation and that, in my opinion, it is fully adequate in scope and quality as a dissertation for the degree of Doctor of Philosophy.

Ronald Hanson

I certify that I have read this dissertation and that, in my opinion, it is fully adequate in scope and quality as a dissertation for the degree of Doctor of Philosophy.

Hai Wang

Approved for the Stanford University Committee on Graduate Studies.

Patricia J. Gumport, Vice Provost for Graduate Education

This signature page was generated electronically upon submission of this dissertation in electronic format. An original signed hard copy of the signature page is on file in University Archives.

Abstract

The design of the next generation of energy efficient and fuel flexible air breathing propulsion systems requires the development of increasingly sophisticated turbulent combustion models that incorporate reduced but realistic finite-rate chemical kinetic mechanisms for fuel oxidation and pyrolysis. n-dodecane ($n\text{-C}_{12}\text{H}_{26}$) is a straight chain alkane that is often recommended as an important constituent of the 3-5 component surrogate blends that are used for modeling the combustion characteristics of aviation fuels like JP-8 or Jet-A. Therefore, an experimental investigation of n-dodecane oxidation and pyrolysis kinetics under engine relevant conditions is necessary for the development and validation of chemical mechanisms that seek to predict the combustion characteristics of jet fuels. In the current work, the Stanford Variable Pressure Flow Reactor (VPFR) facility was used to investigate n-dodecane pyrolysis and oxidation at the less studied intermediate temperature regime (950K - 1250 K) in a vitiated environment and at 1 atmosphere pressure. The initial stages of fuel decomposition were investigated in a 1000 K pyrolysis run and a 1050 K rich oxidation run, while the final oxidation and heat generation stages were investigated in 1170 K lean oxidation and 1220 K rich oxidation runs. The species time history data for n-dodecane and oxygen, as well as for 12 intermediate product species including C_2H_4 , CH_4 , H_2 , C_3H_6 , C_2H_2 , CO , CO_2 , CH_2O and several of the higher 1-alkenes, were measured using online Gas Chromatography over a 1-40 ms residence time. The experimental data were used to validate an optimized version of the detailed JetSurf 1.0 mechanism as well as to compare against several other detailed models that are used in the combustion community. The optimized JetSurf model performed relatively well against the flow reactor measurements, though the selected detailed mechanisms were observed to diverge significantly from each other in their species time history predictions. The cause of these

divergences was identified to be uncertainties in several of the C_1 - C_3 reaction rates and thermochemistry values that are responsible for radical build up and for ethylene generation and oxidation kinetics. The experimental results also pointed to a temporal scale separation between the initial stages of fuel breakdown that occur through essentially pyrolytic reactions into a mix of 1-alkenes, and the later stages where the alkenes undergo oxidation to form CO and CO₂. A new methodology of kinetic mechanism reduction was proposed that lumped the pyrolysis stages into a small set of one-step reactions that directly convert the fuel into the final cracked products. An initial proof of concept validation of the new lumping scheme was done by comparing the predictions from a lumped version of the JetSurf mechanism with the flow reactor measurements. The results were found to be promising enough to warrant the further development of the lumping methodology in future investigations.

Acknowledgement

First and foremost, I would like thank my advisor, Professor Tom Bowman for his unfailing guidance and support throughout my years at Stanford. This work would never have seen the light of day without the knowledge and insight I have gained from him in our numerous interactions in the workplace and beyond. It has been a great privilege to have him as my guide. I would also like to thank Professor Hai Wang for the many brainstorming sessions over the intricacies of kinetic mechanism development that have helped give this work its final shape. I would also like to thank Professor Ron Hanson, Dr. Dave Davidson and Professor Reginald Mitchell for always being ready to assist me whenever I came to them with questions about combustion theory or the experimental methodology. I thank all members of my defense committee for providing constructive suggestions that have greatly assisted me in my attempts to present the substance of my research in a meaningful and lucid fashion.

In the laboratory, my heartfelt thanks go first and foremost to my senior and colleague Dr. Adela Bardos in whose understudy I learnt all the tricks involved in mastering the dark arts of conducting a successful experiment. Special thanks to Lakhbir Johal whose unrivaled skills as a machinist and general omniscience about which obscure machine parts need to be procured for which job have helped me avoid the consequences of the Murphy's law on many occasions. Thanks also to all of my friends in the High Temperature Gas Dynamics Laboratory (especially Eli, Rito, Brentan, Matt, Pratap) for being such good company in casual hangouts, lunch-times or in general discussions on the PhD life.

Thanks also to my friends beyond the workplace with whom I had the pleasure to spend many a weekends to re-establish my sanity. Gourab Mukherjee, Rahul Majumdar, the entire crew from ISI, Sukanya Chakraborty and Debarshi Chatterjee especially come

to mind. Thanks also to my old friends in the Stanford Energy Club, the Stanford Indian Association and the cricketers at Stanford for making life fun and interesting. I would also like to express my gratitude to my long time friends, Adhiraj Dasgupta and Baidurja Roy, for showing that friendships never fade with either distance or time.

Three people remain who are forever present in my mind. My parents, Amitava and Sutapa Banerjee, whose unwavering love and support through all these years have nourished my heart. To them I owe everything. And finally my fiancée, Kheya Chakraborty, for always being there with me through the thick and the thin. The love of these three people is the greatest blessing in my life.

Contents

Abstract	iv
Acknowledgement	vi
1 Introduction	1
1.1 Motivation and Objectives	1
1.2 Organization	2
2 Background	5
2.1 The Bigger Picture	5
2.2 Modeling of Engine Fuel Kinetics	7
2.3 Prior Experimental Investigations of N-Dodecane Combustion Kinetics	9
2.4 Current Work	14
3 Experimental Methods	16
3.1 Introduction to Turbulent Plug Flow Reactors	16
3.2 Variable Pressure Flow Reactor Facility	17
3.3 Flow Control and Sample Handling/Diagnostic Systems	21
3.3.1 The Flow Control System	22
3.3.2 The Fuel Evaporation System	22
3.3.3 Measurement Probes	28
3.3.4 Sample Transfer and Conditioning	29
3.3.5 Diagnostics	30
3.4 Flow Reactor Modeling	31

3.4.1	The Plug Flow Assumption	33
3.4.2	Residence Time Calculations	33
3.4.3	One-Dimensional Mixing Reacting Model	35
3.4.4	Zwietering Mixing Reacting Model Description	36
3.5	Summary	42
4	Detailed Mechanisms used for Predictive Modeling	44
4.1	The JetSurf Mechanism	45
4.1.1	The JetSurf Model v 1.0	45
4.1.2	The Optimized JetSurf Model	45
4.2	The Lawrence Livermore Mechanism	51
4.3	The CNRS Mechanism	52
4.4	The CRECK Mechanism	53
5	Experimental and Detailed Modeling Results	63
5.1	Experimental Conditions	63
5.1.1	Axial Temperature Profiles	64
5.1.2	Carbon Dioxide Mixing Experiments	64
5.1.3	Species Profiles	65
5.2	1000 K Pyrolysis Run	65
5.2.1	Initial Flow Composition	65
5.2.2	Temperature and Mixing Data	66
5.2.3	Fuel and Product Species Profiles	66
5.3	1050 K Rich Oxidation Run	74
5.3.1	Initial Flow Composition	74
5.3.2	Temperature and Mixing Data	74
5.3.3	Fuel and Product Species Profiles	76
5.4	1220 K Rich Oxidation Run	81
5.4.1	Initial Flow Composition	81
5.4.2	Temperature Data and Mixing Profile	81
5.4.3	Species Profiles	83
5.5	1170 K Lean Oxidation Run	90

5.5.1	Initial Flow Composition	90
5.5.2	Temperature Data and Mixing Profile	90
5.5.3	Species Profiles	90
5.6	Comparative Analysis with Relevant External Data Sets	98
5.6.1	Overall Fuel Decomposition Rate and Peak Ethylene Yield	98
5.6.2	Species Profiles from Shock Tube Experiments	101
5.6.3	Jet-Stirred Reactor Pyrolysis Experiments	103
5.7	Summary	103
6	A Sensitivity Analysis of the Detailed Mechanisms	109
6.1	Low-Temperature Pyrolysis and Oxidation Runs	110
6.2	High Temperature Oxidation Runs	120
6.3	Summary	125
7	The Lumped JetSurf Mechanism	127
7.1	Motivation	127
7.2	Method	130
7.3	Results	139
7.4	Future Work	143
8	Concluding Remarks	147
8.1	Summary and Discussion	147
8.2	Future Work	149
A	Gas Chromatograph Calibration	152
A.1	Overview	152
A.2	Operating Conditions and Column Calibration	153
B	Uncertainty Analysis	156
B.1	Temperature Uncertainty	157
B.1.1	Radiation Correction Effects	157
B.2	Uncertainties in the Mixing Reacting Model	159
B.3	Species Uncertainty	162

B.3.1	Input Gas Stream Uncertainties	164
B.3.2	Species Concentration Measurements Uncertainty	164
B.4	Residence Time Uncertainty	166
C	Comparing Reaction Rates For Sensitive Reactions	168
D	Reaction Mechanism Files	174
D.1	The Optimized JetSurf Mechanism	174
D.1.1	Mechanism File:-	174
D.1.1.1	Thermodynamic File:-	218
D.1.2	Transport File	266
D.2	The Lumped JetSurf Mechanism	286
	Bibliography	322

List of Tables

2.1	Some Proposed Surrogate Mixtures for Jet Fuels	9
3.1	Gas Streams Entering the Flow Reactor System	23
3.2	List of Columns and the Species Measured by each in the Micro-GC.	32
3.3	PMA and NDIR Analyzer Specifications.	32
3.4	Mixing Model Parameters	40
4.1	Experimental Data Sets Used as Optimization Targets	49
5.1	Experimental Conditions	106
5.2	1000K Pyrolysis Case, Initial Flow Composition	107
5.3	1050 K Rich Oxidation Case, Initial Flow Composition	107
5.4	1220 K Rich Oxidation Case, Initial Flow Composition	107
5.5	1170 K Lean Oxidation Case, Initial Flow Composition	108
6.1	Residence Times to Target Concentrations as Predicted by the Mechanisms	116
6.2	Reaction Rate Comparisons at 1000K between the JetSurf and the LLNL mechanisms for the most Sensitive Reactions pertaining to the 1000 K Py- rolysis and 1050 K Rich Oxidation Experiments.	122
6.3	Reaction Rate Comparisons at 1200K between the JetSurf and the LLNL mechanisms for the most Sensitive Reactions pertaining to the 1220 K Rich Oxidation Experiment.	126
7.1	Comparison of Isomerization and Scission Rates for hexyl and butyl Radicals.	135
A.1	Columns Present in 3000 Micro-GC	154

A.2	GC Column Conditions Used for Species Detection	154
A.3	Response Factors, Elution Times and Standard Errors for the Different Species Detected by the Gas Chromatograph.	155
B.1	Relative Uncertainties in GC Concentration Measurements	165

List of Figures

3.1	Schematic of an Idealized Plug Flow Reactor.	19
3.2	The VPFR facility and the Schematic of the Quartz Flow Reactor.	19
3.3	Stainless Steel Sparger.	25
3.4	Evaporator Bath System.	25
3.5	2nd Injection Bath-FID Flow System.	27
3.6	Calibration Curve for the JUM FID Detector in Propane Equivalents.	27
3.7	Comparison between Gas Chromatograph and PMA, NDIR data for the 1220 K Rich Oxidation Experiment.	32
3.8	Residence Time against Distance Downstream of the Second Injection Stage evaluated for 1220 K Rich Oxidation Condition.	38
3.9	The Mixing Region of the Flow Reactor Shown Schematically.	38
3.10	CO ₂ Mixing Profile Shown for 1000 K Pyrolysis Run at 1 atm.	40
3.11	Comparison of Predicted Profiles from Cantera ODE Solver and Chemkin PFR module under 1000 K Pyrolysis Condition using the optimized JetSurf mechanism.	43
4.1	Simulated Temperature Uncertainty Estimates for Species Time History Measurements. Solid Lines: nominal prediction of the un-optimized Jet- Surf 1.0 model; Long Dashed Lines: computed uncertainty bounds due to ± 10 K uncertainty; short-dashed lines: 20% uncertainty on nominal mole fraction values.	54

4.2	Experimental and Predicted Species Time Histories from the un-optimized JetSurf 1.0 . Dashed Line: Experimental Data; Solid Line: Model Predictions; Dots: Uncertainty Scatter; Filled Circle and Error Bar: Targets and their Uncertainties.	55
4.3	Experimental (symbols) and Predicted (line) Ignition Delay using the un-optimized JetSurf 1.0.	56
4.4	Experimental (symbols) and Predicted (line) Laminar Flames Speeds of n-Dodecane-Air mixture at 1 atm. pressure and an unburned gas temperature of 403K by the un-optimized JetSurf.	56
4.5	Experimental and Predicted Species Time Histories for the optimized JetSurf 1.0. Dashed Line: Experimental Data; Solid Line: Model Predictions; Dots: Uncertainty Scatter; Filled Circle and Error Bar: Targets and their Uncertainties.	57
4.6	Experimental (symbols) and Predicted (line) Ignition Delay using the Optimized JetSurf 1.0.	58
4.7	Experimental (symbols) and Predicted (line) Laminar Flames Speeds of n-Dodecane-Air mixture at 1 atm. pressure and an unburned gas temperature of 403K by the Optimized JetSurf.	58
4.8	Comparison of the Optimized JetSurf against JetSurf 1.0 for n-dodecane ignition delay measurements based on half peak values for OH. 400 ppm dodecane, $\Phi=1$, $P=2.25$ atm., balance argon. Davidson et al. (2011)	59
4.9	Comparison of n-dodecane oxidation reactivity data of Malewicki and Brezinsky (2013) against Optimized JetSurf Predictions; 75 ppm n-dodecane, $\Phi=1.06$, balance argon, $P_{nom}=50$ atm; n-dodecane Profile.	59
4.10	Comparison of n-dodecane oxidation reactivity data of Malewicki and Brezinsky (2013) against Optimized JetSurf Predictions ; 75 ppm n-dodecane, $\Phi=1.06$, balance argon, $P_{nom}=50$ atm; CO_2 , O_2 and CO profiles.	60
4.11	Comparison of n-dodecane oxidation reactivity data of Malewicki and Brezinsky (2013) against Optimized JetSurf Predictions; 75 ppm n-dodecane, $\Phi=1.06$, balance argon, $P_{nom}=50$ atm; C_2H_4 profiles.	60

4.12	Comparison of n-dodecane oxidation reactivity data of Malewicki and Brezinsky (2013) against Optimized JetSurf Predictions; 75 ppm n-dodecane, $\Phi=1.06$, balance argon, $P_{\text{nom}}=50$ atm; other major intermediates.	61
4.13	Comparison of n-dodecane oxidation reactivity data of Malewicki and Brezinsky (2013) against Optimized JetSurf Predictions; 75 ppm n-dodecane, $\Phi=1.06$, balance argon, $P_{\text{nom}}=50$ atm; higher alkenes.	61
4.14	Pyrolysis products of n-dodecane vs residence time by Herbinet et al. (2007) at 973 K for a 2% dodecane-helium mixture. Symbols = data values; Solid Lines = Optimized JetSurf simulations	62
4.15	Conversion of n-dodecane vs residence time by Herbinet et al. (2007) at 973 K for a 2% dodecane-helium pyrolytic mixture; Symbols = data; Line = Optimized JetSurf Simulations	62
5.1	Pyrolysis Temperature Data.	67
5.2	Pyrolysis CO ₂ Mixing Profile.	67
5.3	Pyrolysis Major Species Data compared with the JetSurf and LLNL Mechanisms.	69
5.4	Pyrolysis Major Species Data compared with the JetSurf and CNRS Mechanisms.	70
5.5	Pyrolysis Major Species Data compared with the JetSurf and CRECK mechanisms.	70
5.6	Pyrolysis Minor Species Data compared with the JetSurf and LLNL mechanisms.	71
5.7	Pyrolysis Minor Species Data compared with the JetSurf and CNRS mechanisms.	72
5.8	Pyrolysis Minor Species Data compared with the JetSurf and CRECK mechanisms.	72
5.9	Pyrolysis Run Carbon Balance.	73
5.10	Pyrolysis Run , Carbon Distribution Over Species at 39.5 ms Residence. . .	73
5.11	1050 K Rich Oxidation Temperature Data.	75
5.12	1050 K Oxidation CO ₂ Mixing Profile.	75

5.13	1050 K Rich Oxidation Species Profiles 1.	78
5.14	1050 K Rich Oxidation Species Profiles 2.	78
5.15	1050 K Rich Oxidation Species Profiles 3.	79
5.16	1050 K Rich Oxidation Species Profiles 4.	79
5.17	1050 K Rich Oxidation Carbon Balance.	80
5.18	Carbon Distribution Over Species at 17 ms Residence Time for the 1050 K Oxidation Run.	80
5.19	1220 K Rich Oxidation, Temperature Profile.	82
5.20	1220 K Rich Oxidation, Mixing Profile.	82
5.21	1220 K Rich Oxidation - CO, CO ₂ , O ₂ , H ₂ Profiles Compared to the JetSurf and CNRS Mechanisms.	85
5.22	1220 K Rich Oxidation - CO, CO ₂ , O ₂ , H ₂ Profiles Compared to the JetSurf and LLNL Mechanisms.	85
5.23	1220 K Rich Oxidation - CO, CO ₂ , O ₂ , H ₂ Profiles Compared to the JetSurf and CRECK Mechanisms.	86
5.24	1220 K Rich Oxidation - Major Hydrocarbon Product Profiles Compared to the JetSurf and CNRS Mechanisms.	86
5.25	1220 K Rich Oxidation - Major Hydrocarbon Product Profiles Compared to the JetSurf and LLNL Mechanisms.	87
5.26	1220 K Rich Oxidation - Major Hydrocarbon Product Profiles Compared to the JetSurf and CRECK Mechanisms.	87
5.27	1220 K Rich Oxidation - Minor Product Profiles Compared to the JetSurf and CNRS Mechanisms.	88
5.28	1220 K Rich Oxidation - Minor Product Profiles Compared to the JetSurf and LLNL Mechanisms.	88
5.29	1220 K Rich Oxidation - Minor Product Compared to the JetSurf and CRECK Mechanisms.	89
5.30	1220 K Rich Oxidation - Carbon Balance.	89
5.31	1220 K Rich Oxidation - Carbon Distribution Over Species at 15.8 ms Residence Time.	91
5.32	1170 K Lean Oxidation - Temperature Profile.	91

5.33	1170 K Lean Oxidation - CO ₂ Mixing Profile.	93
5.34	1170 K Lean Oxidation - CO, CO ₂ , O ₂ , H ₂ Profiles Compared to the Jet-Surf and CNRS Mechanisms.	93
5.35	1170 K Lean Oxidation-CO, CO ₂ , O ₂ , H ₂ Profiles Compared to the JetSurf and LLNL Mechanisms.	94
5.36	1170 K Lean Oxidation-CO, CO ₂ , O ₂ , H ₂ Profiles Compared to the JetSurf and CRECK Mechanisms.	94
5.37	1170 K Lean Oxidation - Major Hydrocarbon Product Profiles Compared to the JetSurf and CNRS Mechanisms.	95
5.38	1170 K Lean Oxidation - Major Hydrocarbon Product Profiles Compared to the JetSurf and LLNL Mechanisms.	95
5.39	1170 K Lean Oxidation - Major Hydrocarbon Product Profiles Compared to the JetSurf and CRECK Mechanisms.	96
5.40	1170 K Lean Oxidation - Minor Product Profiles Compared to the JetSurf and CNRS Mechanisms.	96
5.41	1170 K Lean Oxidation - Minor Product Profiles Compared to the JetSurf and CNRS Mechanisms.	97
5.42	1170 K Lean Oxidation - Minor Product Profiles Compared to the JetSurf and CNRS Mechanisms.	97
5.43	1170 K Lean Oxidation - Carbon Balance.	100
5.44	Overall Decomposition Rates of n-dodecane.	100
5.45	Peak Ethylene Yield versus Pyrolysis Temperature.	102
5.46	Normalized n-dodecane Profile, Current 1050 K Rich Run and Fuel Profiles from Davidson et al. (2011)	102
5.47	Ethylene Time History Profile Normalized by the Initial n-dodecane Mole Fraction, 1220 K Rich Profile Compared with Davidson et al. (2011). . . .	104
5.48	Fuel Conversion Time History Profile for 1000 K Pyrolysis Compared With the 973 K JSR profiles of Herbinet et al. (2007) and JetSurf predictions. . .	104
5.49	Species Time History Profiles for the current 1000 K Pyrolysis Experiment Compared with the 973 K JSR data from Herbinet et al. (2007) and JetSurf predictions.	108

6.1	N-Alkane Oxidation Schematic Showing High-Temperature, Low-Temperature and NTC Pathways.	111
6.2	Reaction Flux Analysis for the 1000 K n-dodecane Pyrolysis Conditions as predicted by the JetSurf mechanism at the residence time corresponding to 47% fuel decomposition point.	113
6.3	Largest A factor Sensitivities for reactions that affect n-dodecane concentration at residence times corresponding to the 47% fuel decay point under 1000K Pyrolysis Conditions, JetSurf and LLNL Mechanisms Compared.	115
6.4	Ratio of the Rate of Production of H radicals in the JetSurf vs the LLNL mechanism for the 1000 K Pyrolysis Condition.	116
6.5	Largest A factor Sensitivities for reactions that affect ethylene concentration at 47% fuel decay point under 1000K Pyrolysis Conditions, JetSurf and LLNL Mechanisms Compared	119
6.6	Reaction Flux Analysis for n-dodecane rich oxidation at 1220 K as predicted by the JetSurf mechanism at 0.25% CO concentration point.	122
6.7	Largest A factor Sensitivities for the reactions that affect ethylene mole fractions at residence times corresponding to the 2500 ppm CO concentration point under 1220 K Rich Oxidation Conditions, JetSurf and LLNL Mechanisms Compared.	123
6.8	Largest A factor Sensitivities for the Reactions that affect carbon monoxide mole fraction at residence times corresponding to the 2500 ppm CO concentration point under 1220 K Rich Oxidation Conditions, JetSurf and LLNL Mechanisms Compared.	126
7.1	Simulation of n-dodecane Flame Species Profiles for $\Phi=1.0$, $T_{\text{unburnt}}=298\text{K}$, $P=1$ atm Conditions Showing Fuel Cracking and Fuel Oxidation Zones (Wang, MACCR Meeting 2013).	131
7.2	Simulation of n-dodecane Flame Species Profiles $\Phi=2.0$, $T_{\text{unburnt}}=298\text{K}$, $P=1$ atm (Abid et al. (2009)).	131
7.3	N-decane Flame Species Profile at $\Phi=1.7$ and $P=1$ atm [Doute et al. (1995)].	134

7.4	Schematic of β -scission Pathways for 4-octyl Radical.	134
7.5	Schematic of Radical Isomerization Reaction (1-octyl to 2-octyl, 8ps isomerization).	135
7.6	The Forward Reaction Rates of the Dominant heptyl Isomerization and β -scission Reaction at the High Pressure Limit and at 1 atm. Conditions. . . .	140
7.7	1000 K Pyrolysis Experiment Data Compared with Detailed and Lumped JetSurf Models.	140
7.8	1000 K Pyrolysis Experiment Carbon Balance for Detailed and Lumped JetSurf Models.	141
7.9	1050 K Oxidation, $\Phi=1.56$:- Data Compared with Detailed and Lumped JetSurf Models.	141
7.10	1050 K Oxidation, $\Phi=1.56$:- Data Compared with Detailed and Lumped JetSurf Models.	142
7.11	1050 K oxidation, $\Phi=1.56$:- Carbon Balance.	142
7.12	1170 K Lean ($\Phi=0.79$) Oxidation Data Compared with Detailed and Lumped JetSurf Models.	144
7.13	1170 K Lean ($\Phi=0.79$) Oxidation Data Compared with Detailed and Lumped JetSurf Models.	144
7.14	1170 K Lean ($\Phi=0.79$) Oxidation Data Compared with Detailed and Lumped JetSurf Models.	145
7.15	1220 K Rich ($\Phi=1.32$) Oxidation Data Compared with Detailed and Lumped JetSurf Models.	145
7.16	1220 K Rich ($\Phi=1.32$) Oxidation Data Compared with Detailed and Lumped JetSurf Models.	146
7.17	1220 K Rich ($\Phi=1.32$) Oxidation Data Compared with Detailed and Lumped JetSurf Models.	146
B.1	Differences in the Predicted Species Profiles for the 1000 K Pyrolysis Condition with the Uncorrected Nominal Temperature Profile and a Corrected Profile with a 50 K Wall Temperature Variation. The Optimized JetSurf Mechanism is Used.	160

B.2	Differences in the Predicted Species Profiles for the 1220 K Rich Oxidation Condition with the Uncorrected Nominal Temperature Profile and a Corrected Profile with a 50 K Wall Temperature Variation. The Optimized JetSurf Mechanism is Used.	160
B.3	Differences in the Predicted Species Profiles for the 1220 K Rich Oxidation Condition with the Uncorrected Nominal Temperature Profile and a Corrected Profile with a 50 K Wall Temperature Variation. The Optimized JetSurf Mechanism is Used.	161
B.4	Experimental Ethylene Data Compared with Estimates of the Ethyl-Chloride Decomposition Rate from (Tsang, 1964).	161
B.5	Results of the Mixing Reacting Model for 1000 K Pyrolysis Conditions with Mixing Time Constant 1.3 and 0.7 Times the Original Value (1.4 ms), respectively. The Optimized JetSurf Mechanism is Used.	163
B.6	Results of the Mixing Reacting Model for 1220 K Pyrolysis Conditions with the Mixing Time Constant 1.3 and 0.7 Times the Original Value (1.6 ms), respectively. The Optimized JetSurf Mechanism is Used.	163
B.7	Results of the Mixing Reacting Model for 1220 K Pyrolysis Conditions with the Mixing Time Constant 1.3 and 0.7 Times the Original Value (1.6 ms), respectively. The Optimized JetSurf Mechanism is Used.	165
B.8	Uncertainty in Residence Time (ms) for the 1220 K Rich Oxidation Conditions	167

Chapter 1

Introduction

1.1 Motivation and Objectives

N-dodecane ($n\text{-C}_{12}\text{H}_{26}$) is a 12 carbon straight chain alkane that has attracted increasing interest from the combustion community due to its relevance as a representative hydrocarbon species for the investigation of the combustion chemistry of jet engine fuels. A majority of proposed 3-4 component aviation fuel surrogates incorporate n-dodecane as the representative for the n-paraffin functional group (Chapter 2) and it has also been proposed as a component for RP-1 surrogates, the kerosene fuel frequently used in regeneratively cooled rocket engines (MacDonald, 2012). In this context, an elucidation of the chemical kinetic behavior of n-dodecane in classical experimental systems (ignition delays in shock tubes and rapid compression machines, flame speed and extinction studies, species and reactivity profiles in stirred and flow reactors) under engine relevant conditions is crucial for the development of the next generation of air-breathing propulsion systems that seek to incorporate more realistic fuel chemistry in their combustor simulations. The kinetics of the intermediate temperature regime (950K-1250K) correspond to the preheat zone of a premixed or diffusion flame and play an essential part in determining the characteristics of the pre-induction chemistry occurring in a typical aviation engine. However, previous experimental work has generally focused more on either the high temperature regime ($T > 1300$ K) or the low temperature NTC regimes ($T < 900$ K). The present study uses the Stanford Variable Pressure Flow Reactor (VPFR) facility to investigate the intermediate temperature

regime kinetics for pure n-dodecane and thereby aims to contribute towards a fuller understanding of the pre-induction behavior of jet fuel combustion. The objectives of the study include:-

1. Measuring accurate and repeatable time-history profiles of n-dodecane and important intermediate species (O_2 , CO , CO_2 , H_2 , CH_2O , CH_4 , C_2H_6 , C_2H_4 , C_2H_2 , C_3H_6 , C_4H_8 , C_5H_{10} , C_6H_{12} , C_7H_{14}) under pyrolysis and rich/lean oxidation conditions over the intermediate temperature range and 1 atm. pressure in the flow reactor.
2. Using the current experimental data to validate an optimized version of the Jet Surrogate Fuel Chemistry Model (JetSurf (Sirjean et al. 2009)) that has been under collaborative development at USC and Stanford.
3. Making a comparative study of the predictions of several proposed detailed chemical kinetic schemes from various groups and identifying the degree to which their predictions differ from one another and with the current data sets along with the identification of key reaction rates and pathways that underlie these differences by utilizing sensitivity and rate of production analysis.
4. Conducting a preliminary investigation of the validity of a newly proposed and promising approach towards the reduction of detailed kinetic models that exploit the temporal scale separation between the initial fuel breakdown and the final oxidation stages in a flame to construct a set of lumped single-step pyrolysis reactions attached to a detailed $H_2/CO/C_1 - C_4$ mechanism.

1.2 Organization

The organization of the thesis is outlined below:-

- Chapter 2 surveys the research literature to frame the current work in context of the contemporary combustion kinetics and aviation engine research. The first sections outline the recent trends towards the design of advanced engines by using LES-based turbulent combustion simulations of realistic gas turbine burner configurations with

finite-rate chemistry modules to better capture transient instabilities and pollutant formation processes. The subsequent sections review the literature on jet fuel surrogates highlighting the widespread recommendation of n-dodecane in surrogate models. Finally, previous experimental works on n-dodecane are summarized and their relevance in the context of the current flow reactor experiments are discussed.

- Chapter 3 describes the experimental set-up and diagnostic techniques used for the current investigation and also highlights the relevant theoretical models needed to properly interpret the data. The modifications made to the flow reactor facility to reliably inject low vapor pressure hydrocarbons using a heated bath evaporator system are discussed in detail. The methods used to model the initial mixing zone using a 1D semi-empirical mixing model are also presented.
- Chapter 4 reviews the four detailed chemistry models that are used for comparison and validation purposes in the current study. Primary focus is on an as yet unpublished optimized version of the JetSurf 1.0 mechanism (<http://www.stanford.edu/group/haiwanglab/JetSurF/JetSurF1.0>) that has shown promising results previously. The chapter outlines the optimization scheme and reviews that model prediction against a selected set of n-dodecane experimental data available from previous literature. The other mechanisms considered are the Lawrence Livermore mechanism (https://www-pls.llnl.gov/?url=science_and_technology-chemistry-combustion-2methyl_alkanes), the CNRS mechanism developed by the Orleans research group in France (Mze-Ahmed et al. 2012) and the semi-detailed CRECK mechanism developed by the Milano research group in Italy (<http://creckmodeling.chem.polimi.it/>).
- Chapter 5 presents the experimental data for the four conditions investigated in the flow reactor and compares them with the predictions of the detailed mechanisms. Key features of the time history data trends are highlighted as well as the relative matching between the experiments and the model predictions. The experimental data sets have also been compared with results obtained from external research groups to provide a more complete picture of the n-dodecane chemistry behavior.

- Chapter 6 delves into the chemical kinetic pathways and the rate-limiting steps governing the fuel pyrolysis and oxidation kinetics in the intermediate temperature regime to investigate the reasons for the divergences seen between the various detailed model predictions. Sets of key reactions governing the species mole fraction predictions have been identified and the sources of the differences between the reaction rate parameters among the detailed models discussed.
- Chapter 7 discusses the preliminary validation studies for a new proposal for model reduction using lumping techniques for the initial fuel breakdown stage of the combustion chemistry. The logical validity of this simplification is discussed initially followed by how the reduction is implemented for n-dodecane. Finally, the comparison of the new lumped model with the flow reactor data set is presented.
- Chapter 8 highlights the main results of the current study and recommendations for future studies especially regarding the possible extension of the new lumped approach to real jet engine fuels.

Additional pertinent material including a discussion regarding experimental uncertainty analysis, the development of chromatographic methods for species detection and measurement, a detailed tabulation of the rate parameters of the most sensitive reactions for the mechanisms as well as the full chemistry set for the optimized and lumped JetSurf mechanisms can be found in the Appendices.

Chapter 2

Background

2.1 The Bigger Picture

Aviation represents the fastest growing segment of fuel consumption in the transportation sector and is expected to take an increasing share of transportation energy consumption and Green House Gas emissions over the next decades [IEA (2013)]. In addition most of the emissions stemming from aviation occur at high altitudes as a result of which non-CO₂ emission effects (like high altitude NO_x and cloud generation through contrails) play an important role in enhancing the global warming potential of aviation emissions (Argonne, 2013). In the civil aviation sector, while the overall aircraft energy intensity reduction since the 1960s has been outstanding (50% reduction in energy use per seat-mile), there has been no significant reduction since 2000. Most of the improvements in energy intensity occurred before 1980 due to the introduction of more efficient high bypass ratio turbofan engines, better wing designs that improve lift to drag ratios and better flight patterns that improved passenger load factors from 50% in 1970 to over 80% in 2011. However, most of these advances have tapered off in the recent decade and the increased importance of regional jets with higher fuel intensities due to smaller cruise times have negated fuel efficiency gains considerably. Significant research efforts are currently underway both in civil and military aviation sectors focused on reducing the energy intensity of aviation transportation, decreasing pollutant formation from gas turbine combustion processes and developing engine technologies that can use low carbon intensity alternative fuels. The U.S. government has

committed itself to achieving carbon neutral growth in the commercial aviation sector by 2020 (based on 2005 baseline), and the development of new aviation engine technologies under the Continuous Lower Energy, Emission and Noise (CLEEN) program launched by the FAA in 2010 is expected to play a leading role in this effort (Aviation Greenhouse Gas Reduction Plan 2012). A case in point is the development of the 2nd generation pilot driven Twin Annular Premixed Swirl Combustor (TAPS II, GE) that has achieved significant reductions in NO_x and smoke emissions. Concurrently, the U.S. Air Force has launched the Versatile Affordable Adaptive Turbine Engines (VAATE) program that is aiming to deliver 25-30% range improvements and over 25% fuel efficiencies by developing an efficient core gas turbine engine coupled with an intelligent adaptive feedback system that keeps the system at optimum performance point over the entire operating (take-off/touch-down, cruise, full thrust) range. Decreasing the carbon intensity of aviation fuels by blending current commercial fuels (Jet-A and JP-8) with advanced bio fuels has also been an important target for both sectors. For example, the Air Force Research Laboratory at Wright Patterson Air Force Base has recently performed extensive testing on 50/50 blends of JP-8 and Hydro-Processed Renewable Jet Fuels (HRJ) [James T. Edwards (2012)]. Therefore, the development of improved simulation and diagnostic tools for the design of the next generation of high performance, low emission, fuel flexible air-breathing propulsion systems is a major focus of aviation technology research today.

None of the recent advanced initiatives would have been possible without significant advances in turbulent combustion modeling methods over the last 20 years. The exponential growth of computing power has spurred the development of turbulent combustion modeling approaches from simple non-reacting flow configurations based on RANS methods to increasingly realistic reacting flow configurations using LES methods and more detailed chemistry modeling. Experimental data from swirling flame burners that mimic many of the characteristic of jet engine swirl combustor systems have been successfully reproduced using LES methods [(Kempf, 2008), (Wang et al., 2014)]. A recent review (Gicquel et al., 2012) presents an overview of the ongoing efforts to simulate realistic burner combustor systems including transient phenomena like re-ignition and extinction phases of gas turbine combustion as well as thermo-acoustic instabilities often observed in the next generation of lean premixed swirl burner systems. Increasingly, such high resolution simulations that

seek to capture transient combustion modes or pollutant formation in real gas turbine combustor systems need to incorporate reduced versions of realistic detailed chemistry models for aviation fuels. Such needs have motivated a significant push towards the construction of detailed and reduced kinetic models for kerosene type fuels by the combustion kinetics community over the last decade. A basic overview of the methodology and significant advances towards this endeavor is presented next to provide a context for the current work.

2.2 Modeling of Engine Fuel Kinetics

The early period of the combustion kinetics research on fuel chemistry focused on the elucidation of simpler pure fuels like hydrogen and methane and culminated in the publication of the detailed chemical kinetic model for natural gas, GRI MECH 3.0, consisting of 53 species and 325 reactions that has been widely used in the combustion community. However, the development of kinetic mechanisms for liquid fuels used in IC engines and gas turbines proved to be more complicated. For example, typical jet fuels (JP-8 or Jet-A) contain thousands of hydrocarbon compounds of highly variable compositions (Violi et al., 2002) since the aviation standards based on mean physical and chemical properties (World Jet Fuel Specifications 2012, Exxon Mobil) like freeze point, distillation curve specifications, smoke point and maximum caps on acidity, sulfur content, heat of combustion and aromatic content allow for wide variability in acceptable blends. Military grade JP-8 usually has an antifreeze additive, but otherwise remain similar to Jet-A. Given such variety only averaged out estimates of composition blends in terms of functional groups are possible. Such estimates were made by Shafer et al. (2006) from 55 samples of jet fuels (Jet-A, JP-8, Jet-A1 and JP-5) and the skeletal composition was found to be 20% n-alkanes, 40% iso-alkanes, 20% mono and di-cyclo-alkanes and around 20% aromatics. Even such functional group estimates are expected to have fairly large deviations from one specific batch to another (Shafer et al., 2006). Clearly, a detailed modeling approach based on reconstruction of the entire species set is impossible. As an alternative, the kinetics community has largely focused on developing "surrogate fuel" substitutes made of only a few representative pure species blended together in a certain fraction in order to reproduce a target set of relevant physical and chemical properties of the aviation fuel under consideration. Violi

et al. (2002) identified volatility (boiling range and flash point), sooting tendency (given by a threshold shooting index) and important combustion properties like flammability limits and heat of combustion as the key targets that a surrogate blend must match and generally found that an adequate surrogate must contain a representative from each of the major functional groups present in the real fuel. Further studies have proposed various surrogate mixtures for aviation fuels, (Dooley et al. (2012), Colket et al. (2007), Narayanaswamy (2013), Humer et al. (2007b)) that include properties like threshold sooting index, derived cetane number, H/C ratio, molecular weight matching etc. The surrogate methodology usually proceeds through the following steps:-

1. Construct a 3-5 component surrogate mixture based on chosen targets.
2. Use classical experimental methods (laminar flame speeds, flame extinction and stretch, shock tube and rapid compression machine ignition delay, reactivity and species time history profiles) to compare the quality of the "fit" between the surrogate blend and the real fuel.
3. Construct detailed chemical kinetic models for each species present in the surrogate and validate the model using experimental data on the pure species.
4. Construct a combined chemical mechanism for the surrogate species blend.
5. Validate the surrogate model by comparing its predictions with the data from actual aviation fuel experiments.
6. Develop a reduced mechanism that can be integrated with modern turbulent combustion modeling codes.

Some of the surrogate mechanisms proposed till now are presented in Table (2.1).

A joint multi-university collaborative effort has been underway (Egolfopoulos, 2011) to quantify the combustion relevant properties of practical fuels and promising surrogate species and developing surrogate mixtures that mimic the properties of real fuels. The experimental data are then used to develop and validate a detailed kinetic mechanism for jet surrogate fuels (for example the JetSurf mechanism (B. Sirjean et al. , 2009)). Finally,

Surrogate	n-alkane	iso-alkane	cyclo-alkane	Aromatics
Violi et al. (2002)	30% n Dodecane, 20% n-hexadecane	10% Iso-Octane	20% Me-CycloHexane	15% o-Xylene, 5% teralin
Agosta et al. (2004)	26% n-Dodecane	36% iso-Cetane	14% Me-CycloHexane, 6% Decalin	18% Me-Naphthalene
Humer et al. (2007b) Mixture C	60% n-Dodecane		20% Me-CycloHexane	20% o-Xylene
Montgomery et al. (2002)	32.6 % n-Decane, 34.7 % n-Dodecane		16.7 % Me-CycloHexane	16% Butyl-Benzene
Dooley et al. (2012)	40.4% n-Dodecane	29.5 % iso-Octane		n-propyl Benzene 22.8%, 1,3,5 - trimethyl Benzene 7.3%
Narayanaswamy (2013)	30.3% n-Dodecane		48.5% Me-Cyclohexane	21.2% m-Xylene

Table 2.1: Some Proposed Surrogate Mixtures for Jet Fuels

the mechanism's size and stiffness is reduced so that it can be incorporated into next generation gas turbine combustor simulators. Towards this end, experimental investigations in shock tubes, flow reactors and flames were conducted at Stanford, Princeton, USC and Drexel universities on key fuels (Jet-A, JP-8) and select surrogate species (n-decane, n-dodecane, xylene, n-butyl-cyclohexane and benzene). The JetSurf kinetic scheme, capable of handling n-alkanes up to n-dodecane and cyclic alkanes up to n-butyl cyclohexane at intermediate to high temperatures was developed and validated using experimental data. Current flow-reactor studies of n-dodecane at intermediate temperatures are a part of this effort.

2.3 Prior Experimental Investigations of N-Dodecane Combustion Kinetics

For the n-alkane group, researchers have generally preferred to use n-dodecane ($n\text{-C}_{12}\text{H}_{26}$) as the representative species (2.1). Therefore, there is need to quantify the oxidation, pyrolysis and flame behavior of pure n-dodecane under engine relevant conditions and use

these data to develop and validate kinetic mechanisms for jet engine fuel chemistry. A brief overview of the major experimental results on n-dodecane published in literature is presented next. The survey is thematically arranged and features that will prove relevant to the current work are highlighted.

- Dahm et al. (2004) used a stainless steel isothermal plug flow reactor (61 cm long, 3.04 mm i.d., furnace heated) to investigate the thermal decomposition of 0.336% n-dodecane in N₂ at 950, 1000 and 1050 K and 1 atm pressures. The fuel decomposition and product species profiles were presented as functions of residence time ranging from 0.05 sec to 2 sec. A detailed kinetic model consisting of 1175 reactions generated by the EXGAS software was proposed.
- Herbinet et al. (2007) used a quartz jet stirred reactor (volume of 90 cc and diameter of 50 mm) heated by electric resistance heaters to study the pyrolysis of 2% n-dodecane in helium from 773K-1073K and at residence times between 1 second to 5 seconds at atmospheric pressure. Light species were analyzed online using Gas Chromatography, while the heavier products were accumulated as condensates and analyzed off-line. Both time history profiles (at a given temperature) and reactivity profiles with temperature (at 1 second residence time) were generated and the earlier EXGAS mechanism presented in Dahm et al. (2004) was updated to provide a better fit with the current as well as the previous flow reactor data. The results from this paper has been used to validate JetSurf 1.0 model (Sirjean et al., 2009).
- Kurman et al. (2011) studied lean oxidation ($\Phi=0.23$) of n-dodecane in the low temperature regime (550-830 K) and at high pressure (0.81 MPa) in a pressurized turbulent flow reactor. The flow reactor is 40 cm long with 2.2 cm i.d. quartz reactor enclosed in a pressure vessel through which 530 ppm of n-dodecane diluted in nitrogen is passed along with 42100 ppm of oxygen. Samples were extracted at 120 ms residence time and species profiles were plotted against the temperature range of the study. The LLNL model and the CRECK model (refer to Chapter 4) were used for comparison purposes. The NTC regime was found to start at 675 K and while the mechanisms predicted the overall NTC behavior well, the actual species concentration profiles were not well predicted.

- Mze-Ahmed et al. (2012) studied the high pressure (10 bar) oxidation kinetics of n-dodecane for lean ($\Phi=0.5$), stoichiometric and rich ($\Phi=2.0$) mixtures for temperatures ranging from 550 K-1150 K in a jet stirred reactor. The reactants were diluted in nitrogen so that n-dodecane in the reactor stream was 0.1%. The jet stirred reactor was a 33 cc sphere made of fused silica kept at the desired temperature by insulated heating elements. Samples were collected and analyzed at 1 second residence time and reactivity plots (i.e., concentration vs temperature at fixed residence time) were presented for the fuel and 20 product species. The CNRS mechanism (see chapter 4) was used to compare with the data, and the predictions matched the species profiles well overall.
- Veloo et al. (2012) compared the relative reactivity profiles of n-alkanes from n-heptane to n-tetradecane at stoichiometric conditions for fuel diluted in nitrogen (net 0.3 mol% carbon) between 500-1000 K, 8 atm pressure and 1 second residence time. The Princeton Variable Pressure Turbulent Flow Reactor was used and the time shifting methods described in detail in Jahangirian et al. (2012) was used here as well. The low temperature reactivity region was found to be between 630-700 K. It was found that while high temperature reactivity was similar for all species, n-heptane had significant lower reactivity than n-dodecane and n-tetradecane in the NTC regime.
- Vasu et al. (2009) measured the ignition delay and OH time history behavior of n-dodecane/Air mixtures in the Stanford High Pressure Shock Tube for stoichiometries of 0.5 and 1.0, temperatures from 727-1422 K and pressures from 15-34 atmosphere. The data were compared to predictions of four kinetic mechanisms. NTC behavior was observed between 950 K-750 K region. It was found that overall ignition behavior was well predicted at high temperatures (>1000 K), but the low temperature data match was less good. Wide divergences between the mechanisms were seen for the OH time history predictions. The Ranzi mechanism predicts the NTC region better while at higher temperatures the JetSurf mechanism captured the OH and ignition trends more accurately. The ignition time histories from this experiment were used to optimized the untuned JetSurf 1.0 mechanism (see chapter 4).

- Shen et al. (2009a) measured the ignition delay of n-alkanes from n-heptane to n-hexadecane for stoichiometries of 0.25, 0.5 and 1.0 respectively over temperature and pressure ranges of 786-1396 K and 9-58 atm in a heated high pressure shock tube. The n-dodecane results were found to be consistent with previous data from Vasu et al. (2009). Inter-comparison between the n-alkane ignition delays from the study as well as previous literature values indicated that the differences are slight and fall within joint experimental uncertainties of $\pm 40\%$.
- Laser diagnostics based species and radical concentration profiles in shock tubes are proving to be an increasingly important source of n-dodecane kinetic data especially at high temperatures. MacDonald et al. (2013) investigated n-dodecane decomposition and ethylene generation profiles under pyrolytic conditions in a heated high pressure shock tube for temperatures ranging from 1138 K-1522 K, pressures ranging from 17-23 atm and residence times between 0-1 ms. The data were used to generate overall fuel decomposition rates and peak ethylene yields and compared with LLNL and JetSurf predictions. It was found that both mechanisms over-predicted the fuel decomposition rates and under predicted the peak ethylene yield especially at higher (>1200 K) temperatures. More detailed shock tube studies measuring pre-ignition time history profiles for n-C₁₂H₂₆, CO₂, OH and C₂H₄ for stoichiometric n-dodecane oxidation were performed in the Stanford shock tube facility by Davidson et al. (2011) between 1300K-1600K, 2 atm pressure and 1-2000 μ s residence times. These data sets provide good validation tests for pre-induction chemistry in kinetic mechanisms and are used as optimization targets for the JetSurf model.
- Malewicki and Brezinsky (2013) used a high-pressure single-pulse shock tube with GC diagnostics to measure pyrolysis and oxidative reactions of n-decane and n-dodecane highly diluted in argon (conc. <100 ppm) for temperatures ranging from 850 K-1750 K, pressures between 19-74 atm. and residence times of 1-3.5 ms. Due to highly dilute fuel conditions there is no ignition and near isothermal conditions prevail. The researchers provided species concentration vs temperature plots for the pyrolysis and oxidative conditions and compared the data with predictions from LLNL and their 1st Generation Surrogate models. One of the major conclusions

arrived at by these researchers was that the fuel molecules undergo pyrolytic breakdown into smaller fragments much before oxygen consumption begins while the decay rates are a bit slower for richer stoichiometries. The results also showed that the higher alkenes were consistently over-predicted by both mechanisms. This led them to revise the 1st Generation Model and the new revised model was found to match the data better.

- Gas Turbine combustion typically proceeds with non-premixed or partially premixed burners characterized by high swirl. Understanding premixed and non-premixed flame behavior and characterizing important parameters (laminar flame speed, stretch vs ignition/extinction characteristics, sooting behavior etc.) of jet fuels and their components are essential for developing adequate turbulent combustion models for gas turbine combustors. Kumar and Sung (2007b) used a counterflow twin flame configuration to determine the laminar flame speed and extinction stretch rates of n-dodecane/air flames at stoichiometries ranging from 0.7-1.4 and at different preheat temperatures. The authors used linear extrapolation techniques to the zero stretch axis and found that neither laminar flame speed, nor extinction stretch rates were well predicted by extant mechanisms. Subsequently, Ji et al. (2010) performed laminar flame speed and extinction stretch rates studies on laminar premixed flames for C₅-C₁₂ n-alkanes using twin flame configurations and was able to obtain better match with mechanism predictions by using non-linear extrapolation to zero stretch flame speeds. Only H₂/CO and to some extent C₁-C₃ reactions were found have significant flame speed sensitivity coefficients. It was also found that laminar flame speed profiles for all n-alkanes were almost identical, again underscoring the relative unimportance of the initial fuel breakdown pathways towards flame speed sensitivities. Extinction stretch rates also match numerical predictions well once multi-component diffusive transport was taken into account and the extinction behavior was found to be relatively more sensitive to the binary diffusivity of the fuel in N₂.
- Behavior of non-premixed flames are also an important consideration in gas turbine combustion. Holley et al. (2007) performed an extensive investigation of diffusion flame ignition temperatures and extinction stretch rates for a wide variety of pertinent

species (n-petane to n-tetradecane; iso-C₈H₁₈, 10 different jet fuel types including JP-8 and several Jet-A blends; and two surrogates) in a counterflow configuration. It was found that smaller carbon number species were more resistant to extinction than higher carbon number species, while n-alkanes were more resistant to extinction than branched alkanes. Flame extinction characteristics of n-dodecane was found to be close to those of actual jet fuels, identifying the species as a suitable surrogate candidate. The ignition temperatures of long chain n-alkane diffusion flames were found to be larger than short chain ones, while branched alkanes were found to be harder to ignite when compared to a straight chain alkanes of the same carbon number. Liu et al. (2012) investigated the ignition characteristics of non-premixed n-alkane flames up to n-dodecane under opposed flow configurations and found that the ignition temperature initially drops rapidly with fuel mole fraction before plateauing out. The data matched well with predictions from JetSurf 1.0. Sensitivity analysis shows that the fuel-N₂ diffusion coefficient is the most sensitive factor determining T_{ign} for diffusion flames and progressively increases in importance relative to the main $\text{H} + \text{O}_2 \rightarrow \text{OH} + \text{O}$ chain branching reaction for long chain alkanes. Only $\text{H}_2/\text{CO}/\text{C}_1\text{-C}_3$ reactions were found to have significant sensitivities for ignition temperature of the flame.

2.4 Current Work

In general, prior reactor and shock tube species profile studies have focused on the low temperature ($500 \text{ K} < T < 900 \text{ K}$) or the high temperature ($1300 \text{ K} < T < 1700 \text{ K}$) regions of n-dodecane pyrolysis and oxidation kinetics. Most shock tube experiments have too short a residence time to investigate the species evolution in the intermediate temperature ($1000 \text{ K} < T < 1300 \text{ K}$) regime, while jet stirred and most flow reactors operate at temperatures below 1000 K . However in laminar and diffusion flames, the fuel molecule undergoes rapid thermal dissociation to smaller alkenes between $1000\text{-}1400 \text{ K}$ in the preheat zone, and it is these smaller alkenes that interact with the oxygen molecule within the flame. Therefore, intermediate temperature pyrolysis and oxidation kinetics play an important role in

the overall combustion process in real combustors. The present work aims to provide insight into the pre-ignition kinetics of n-dodecane pyrolysis and oxidation behavior in this intermediate ($1000\text{ K} < T < 1250\text{ K}$) regime using the Stanford Variable Pressure Flow Reactor facility under vitiated conditions and 1 atm. pressure. The data were used to compare the predictive fidelity of several detailed and semi-detailed mechanisms and to examine the primary sensitive reaction pathways in this regime. Furthermore, the data have been used to validate the efficacy of an optimized version of the JetSurf 1.0 model as well as a new promising kinetic scheme reduction technique that leverages the temporal separation between fuel pyrolysis and oxidation stages to considerably simplify the initial fuel decomposition stages.

Chapter 3

Experimental Methods

3.1 Introduction to Turbulent Plug Flow Reactors

The plug flow reactor is an idealized version of the tubular flow reactors that are widely used to study the kinetics of reacting systems, especially for steady-state steady flow systems. The idealized plug flow reactor [schematically shown in Figure(3.1)] assumes perfect mixing in the transverse direction that leads to radially uniform profiles for velocity, temperature and species; and no mixing in the axial direction such that each axially oriented differential fluid element can be tracked in isolation from its neighbors upstream or downstream. Thus, a plug flow reactor can be conceptualized as being made up of infinitesimally thin cylindrical "plugs" of fluid element marching single file through the reactor in the direction of flow. Each such fluid element has uniform temperature, axial velocity and species composition at a given axial location, but these values may change as the element moves downstream. If the mass flow rate and the diameter of the reactor are known, the relationship between residence time of a fluid element and the axial distance can be evaluated resulting in a simple zero-dimensional description of the plug flow system. In general, plug flow assumptions are best approximated by turbulent flow reactors where the high turbulent intensity of the flow causes vigorous mixing along the radial direction considerably flattening the transverse profiles. Thus, plug flow assumptions hold up well for turbulent reactors apart from the very thin near wall region of flow.

Plug Flow Reactors are well suited to kinetic study (Kuo (2005)) as the momentum equations of fluid mechanics can be completely neglected and the system can be modeled by global mass, energy and species balances. For reactors investigating combustion systems, the inlet fuel/oxidizer stream is highly diluted by inert species like N_2 , Ar or He in order to slow down the rate of reaction and decrease the effective temperature and pressure rise during the flame-less oxidation process. Some of the advantages of using Flow Reactor Systems for analyzing heavy hydrocarbon oxidation and pyrolysis conditions include their ability to investigate intermediate and NTC temperature regimes (400 K - 1500K) and to perform detailed measurement of numerous intermediate species as a function of temperature, pressure and/or residence time using Gas Chromatography, Mass Spectrometry or other detection techniques. An isothermal Plug Flow Reactor made of stainless steel was used to investigate n-dodecane pyrolysis by Dahm et al. (2004); Kurman et al. (2011) used a Quartz Pressurized Flow Reactor facility at Drexel University to investigate the low temperature (<900 K) and high pressure (8 atm.) oxidation of n-dodecane by generating reactivity profiles data for fuel decay and intermediate species formation. The Princeton Variable Pressure Quartz Flow Reactor was also recently used to investigate the reactivity profiles for major n-alkanes from n-heptane to n-hexadecane [Jahangirian et al. (2012) and Veloo et al. (2012)] in the 500K-1000K region and at 8 atm. The current study uses the Stanford Variable Pressure Flow Reactor (VPFR) facility to investigate n-dodecane pyrolysis and oxidation kinetics at the intermediate (1000K-1200K) temperature regimes. The details of the facility are outlined next.

3.2 Variable Pressure Flow Reactor Facility

The Stanford Variable Pressure Flow Reactor Facility is a combustion-driven flow reactor that uses the combustion products of an H_2 /Air Flame to generate a hot vitiated flow (roughly 21-24% H_2O and 80-75% N_2) into which metered amounts of gaseous fuel and cooling nitrogen are introduced at a specific point in order to initiate the reactive process. The experimental set up is based upon work done by previous researchers to study thermal de- NO_x reaction [(Schmidt, 2001)], vitiated ethane oxidation [Walters (2008)] and intermediate temperature oxidation studies of binary DME-Methane mixtures [Bardosova (2011)].

Much of the reactor system characterization was performed previously and will be briefly discussed where appropriate. Current modifications include vaporization and detection systems for low vapor pressure and high molecular weight hydrocarbons and will be described in detail in the following sections and the appendices.

The Variable Pressure Flow Reactor, shown schematically in Fig. (3.2) is the central component of the VPFR facility. It is a vertically oriented quartz flow reactor that is shaped as a converging-diverging duct with a constant 3 cm diameter, 30 cm long section at the end comprising of the majority of the reaction zone. The flat flame burner assembly (McKenna burner with high pressure shroud, Prucker et al. (1994)) consists of a 60 mm diameter porous bronze disc on which the H_2 / Air flame is stabilized. The burner has two embedded copper coils through which water at 100 psig pressure and 1.5 SLM flow rate is circulated using a gear pump system for cooling purposes. The water flow extracts enough heat from the hydrogen flame that the flame temperature, characterized previously in Walters (2008), remains well below the adiabatic flame temperature. A Nichrome wire arc discharge with a 10 kV DC power supply is used to ignite the hydrogen flame. For oxidation runs, the hydrogen/air flame is lean, and the excess oxygen in the combustion products is used to oxidize the n-dodecane introduced further downstream. For pyrolysis runs, the Hydrogen/Air Flame is rich so that the bath gas does not contain any free oxygen. The total burner mass flow rate is kept within a narrow range of 0.9-0.97 gm/s so that the flame position is neither too close nor too far from the burner surface that could result in instability or non-optimal heat transfer to the burner surface. The lower temperatures also limit the possibilities for radical presence or NO_x formation in the burnt gas.

Downstream of the flame, the hot vitiated combustion products are guided into a 1.9 cm ID constant area constricted zone through a converging section. Two sets of radially opposed jet injectors are present in this constricted neck region. The first injection stage introduces cold nitrogen gas at high velocities via four radially opposed jets, while 6 cm further downstream, the second injection stage introduces vaporized fuel in N_2 carrier gas through six radially opposed jets. Each injection stage has a quartz toroidal manifold into which the gas to be injected is supplied from external gas lines. The gases then flow from the manifolds into the corresponding sets of four or six radially equi-spaced 0.25 inch O.D. injection tubes (all made of quartz) which constrict and feed their respective gas streams

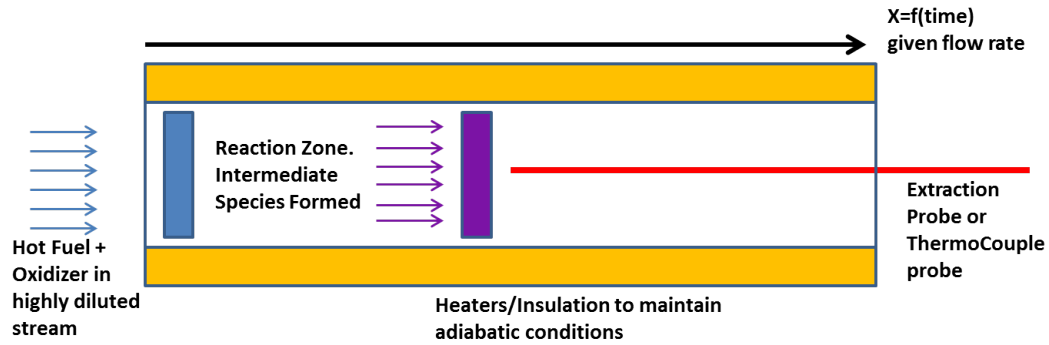


Figure 3.1: Schematic of an Idealized Plug Flow Reactor.

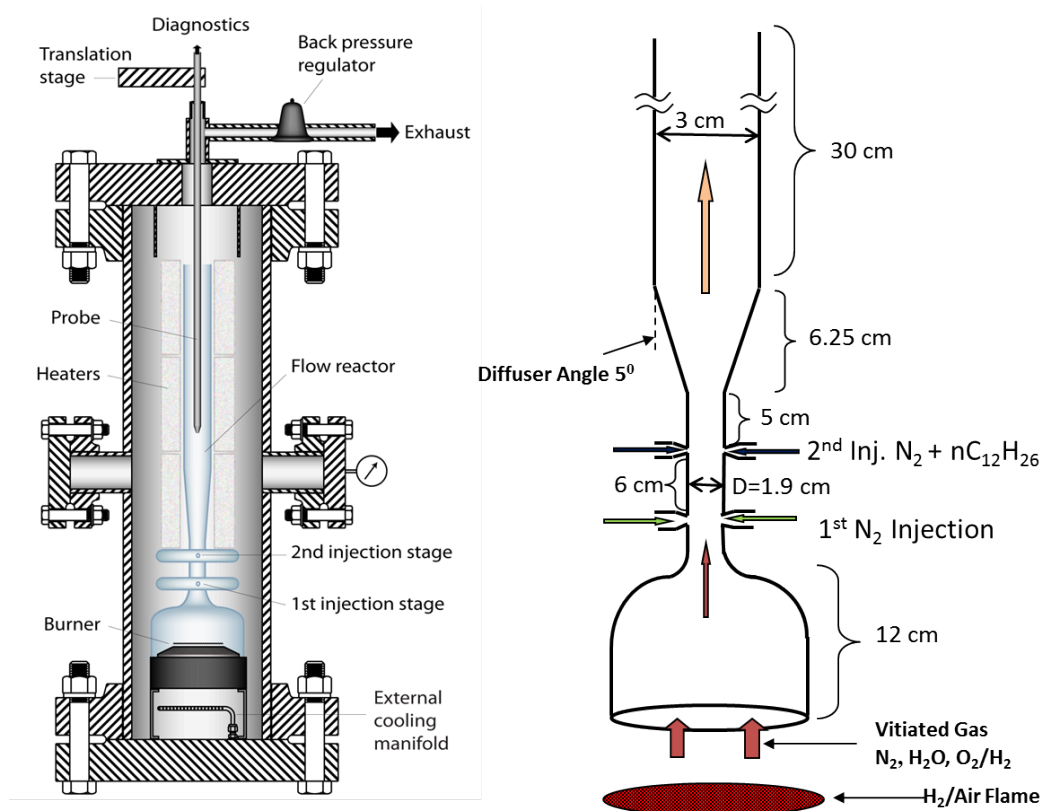


Figure 3.2: The VPFR facility and the Schematic of the Quartz Flow Reactor.

into the main flow through 0.8 mm injection holes laser drilled into the quartz tube wall. To achieve high penetration, rapid mixing and to introduce turbulence into the flow stream, the injectors are designed to provide high jet momentum flux with respect to the main bath flow. The cold nitrogen gas is introduced through the first injector stage in order to decrease the gas temperature and increase the flow turbulence. Therefore this stage has very high momentum flux ratio ($\frac{\rho_{jet}U_{jet}^2}{\rho_{bath}U_{bath}^2} \sim 100$). The first injection Nitrogen flow rate is the primary means by which the reaction region temperature set point is fine-tuned. The second stage introduces the vaporized fuel in nitrogen carrier gas and has a momentum flux ratio of 5-20. The point at which the second injection occurs is called the reactor throat and is defined as the point of origin for the reaction zone. All species and temperature measurements are done between the reactor throat (the second injection point) and the exit of the flow reactor. Past the throat, the reactor diameter remains constant at 1.9 cm for 5 cm. After this the reactor expands into a wider 3 cm diameter and 30 cm long constant area tube by transitioning through a diverging section that is 6.25 cm long and has 5° half angle. Finally, the 30 cm constant area section constricts at a 45° half angle to 2.7 cm at the reactor exit. This brief constriction at the end accelerates the flow as it exists the reactor thus preventing recirculation of the cold surrounding gas back into the reactor. Quartz material is chosen as it provides an inert non-reactive surface thus minimizing surface reactions. The large diameter of the tube (3 cm) also creates a relatively low surface to volume ratio of 1.3 cm⁻¹, further decreasing the possibility of surface activated reaction. A set of three independent electrical resistance heaters enclose the reactor from above the second injection stage. The electrical voltage of the heaters can be adjusted so that the heaters provide adequate thermal flux to compensate for all heat losses from the post-injection region of the flow stream. The Nichrome wire heaters with power rating of 450 W and maximum operating temperature of 1275 K are thus adjusted to maintain near adiabatic conditions in the main reacting region. Thus, when heaters are properly adjusted, the reactor maintains a nearly isothermal profile in the absence of exothermic reactions. This is the case for pyrolysis conditions as well as for inert mixing experiments described in later sections. For oxidative runs at relatively high temperatures, the gas temperature does increase downstream as the fuel oxidizes, but because of the high dilution the temperature rise is kept to a modest 40-60 K. The entire flow tube is enclosed within a stainless steel pressure vessel that is capable of withstanding

a maximum operating pressure of 50 atm. and a temperature of 1400 K. All the gas feed streams going into the injection manifolds are piped through SS flexible tubing that go through the space between the flow reactor and the pressure vessel. Apart from being used for high pressure flow reactor experiments, the steel pressure vessel serves as an effective container of heat and significantly reduce the heat loss from the vitiated flow stream. In fact for the 1200 K oxidation experiments, the electric voltage heaters are unable to maintain the preferred adiabatic conditions unless the heat flux loss is reduced due to the presence of the pressure vessel. Additional nitrogen gas is passed through the purge manifolds present on the periphery of the burner shroud and flows in the space between the quartz reactor and the steel pressure vessel, cooling the latter and also diluting the exhaust stream. The exhaust gas from the flow reactor exits the pressure vessel and flows into water cooled stainless steel piping that are connected to the laboratory exhaust system . A back pressure regulator is installed in this exhaust piping to control the flow reactor pressure for high pressure run conditions.

3.3 Flow Control and Sample Handling/Diagnostic Systems

The primary auxiliary systems attached to the Flow Reactor are:-

1. The flow control system that delivers the inlet gas streams
2. The fuel evaporator assembly that vaporizes n-dodecane and delivers metered amounts of vaporized fuel into the flow reactor
3. The measurement probes
4. Sample Transfer and Conditioning Systems
5. Diagnostics.

Each of these are now described in the sections below.

3.3.1 The Flow Control System

The major gas streams entering the VPFR facility are tabulated in Table (3.1). Critical flow orifices are used to deliver accurate and consistent gas flow rates to each stream during the entire duration of an experiment. From compressible flow theory, the mass flow rate of an ideal gas through a choked orifice is proportional to the stagnation pressure P_0 divided by the square root of the stagnation temperature T_0 upstream of the orifice. The general relationship is given by $\dot{m}_{crit} = C_D \times A_{orifice} \times \frac{P_0}{\sqrt{T_0}} \times \sqrt{\frac{k}{R} \left(\frac{2}{k+1}\right)^{\frac{k+1}{k-1}}}$ where k is the specific heat ratio and C_D is the discharge coefficient accounting for the non-ideality of the flow. The orifice diameter for the flow is chosen based on the maximum upstream pressure (usually 400 psig) and the required flow rate. The stagnation pressure and temperature upstream of a choked orifice are measured using a pressure transducer and a thermocouple, respectively, and the signals are fed into an automated proportional-integral-derivative (PID) controller. The PID controller uses this signal to regulate a pneumatically actuated valve that controls the upstream stagnation pressure P_0 of the given choked flow stream. This automated feedback loop helps in maintaining the flow rate by keeping the process variable $\frac{P_0}{\sqrt{T_0}}$ at its desired value. Due to the non-ideal nature of the flow, each orifice is individually calibrated for the given gas using a dry flow meter (DTM 200-A), thus generating a best fit calibration curve relating the process variable value with the flow rate in mol/s. Further details of the flow control system can be found in the previous work by Schmidt ((Schmidt, 2001)). The orifices used range from diameters of 0.006 inch (2nd injection flow) to 0.030 inch (purge N₂flow).

3.3.2 The Fuel Evaporation System

N-dodecane is a low vapor pressure n-alkane and needs to be vaporized before being injected into the flow reactor. The vaporization system should ensure that a consistent amount of gaseous fuel is being delivered to the flow reactor throughout the steady state operation and that there is no condensation and/or degradation of the fuel before it enters the vitiated flow stream. In the experimental set up, liquid n-dodecane is stored in a 150 cc stainless steel Swagelok cylinder. The cylinder itself is immersed in a thermal bath filled with synthetic polydimethyl siloxane fluid from Dow Corning. The bath is fitted with an

Gas Streams	Source	Destination	Flow Rates (mol/s)
Air	1000 psig Air Compressor, subsequently filtered and dried.	H ₂ /Air Burner	0.031
Hydrogen	Praxair Grade 2.0 Compressed Gas Cylinders	H ₂ /Air Burner	0.012-0.017
1 st injector N ₂	Praxair Grade 2.0 Compressed Gas Cylinders	1 st injection stage	0.009-0.025
2 nd injector N ₂	Praxair Grade 2.0 Compressed Gas Cylinders	The fuel evaporator	0.0025
Purge N ₂	Praxair Grade 2.0 Compressed Gas Cylinders	The purge manifold	0.013
CO ₂ - N ₂	13.5 % CO ₂ in N ₂ , Praxair Primary Standard	The 2 nd injection, for mixing experiment	0.011
N ₂ Diluent	Praxair Grade 2.0 Compressed Gas Cylinder	The diluent gas for Flame Ionization Detector.	0.019

Table 3.1: Gas Streams Entering the Flow Reactor System

SC-150L heated immersion circulator from Thermoscientific with adjustable temperature control. The temperature range of the heater is from 13 °C-150 °C with a temperature stability of ± 0.02 °C. For the flow-reactor runs, the bath temperature is maintained anywhere between 85 °C and 110 °C depending on the evaporated fuel flux requirements. The second injectant nitrogen coming in from the choked orifice is pre-heated to the bath temperature by circulating it through several turns of coiled copper tube also immersed in the heated bath. Subsequently, this preheated nitrogen is introduced into the n-dodecane cylinder in the mode of thousands of tiny gas bubbles using a commercial stainless steel sparger from Mott Corporation with a porous area of 0.009 Ft² (8.36 cm², see Figure (3.3)). The sparging process enhances gas-liquid contact enabling the N₂ carrier gas bubbles to pick up vaporized n-dodecane as they rise through the fuel tank. The fuel cylinder is kept 3/4th full with enough space at the top of the liquid for the N₂-dodecane gas mixture to reach a homogeneous composition for the given bath temperature. This fuel-N₂ gas mixture then leaves the n-dodecane tank at the top through stainless steel lines that are kept heated at 120-130 °C using voltage controlled flexible heating tapes wrapped with fiberglass insulating cloth. Copper-Constantan thermocouples are used to monitor the gas temperature of the exit lines. The length of the entire second injection tubing up to the entry into the flow reactor pressure vessel is kept heated to prevent condensation. Within the pressure vessel proper, the flexible steel tubing absorbs sufficient heat from the hot quartz reactor and the pressure vessel walls to make further external heating unnecessary. A schematic of the fuel evaporation system is shown in Figure (3.4).

Ideally, if the N₂ flow through the n-dodecane tank is slow enough, the exiting gas-vapor stream should be at the 2-phase equilibrium of their respective partial pressures at the set point temperature. However, in practice, the gas flow rate is too rapid and the fuel tank too small for such equilibration to take place. Thus, although the concentration of the fuel vapor in the exiting N₂ stream attains steady-state, the steady-state concentration does not correspond to the 2-phase equilibrium concentration. Therefore, downstream of the thermal bath, the fuel-N₂ stream is passed through a Flame Ionization Detector (THC FID Model 5-100) manufactured by J.U.M. Engineering. The JUM FID is a heated Total Hydrocarbon Analyzer that can measure hydrocarbon concentrations ranging from 0-10 ppm to 0-10⁵ ppm in 5 different ranges. The instrument utilizes a high purity H₂/ Air flame

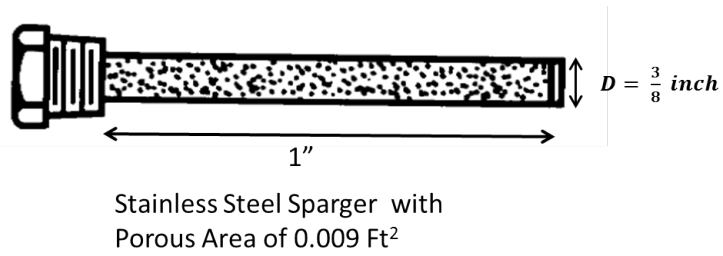


Figure 3.3: Stainless Steel Sparger.

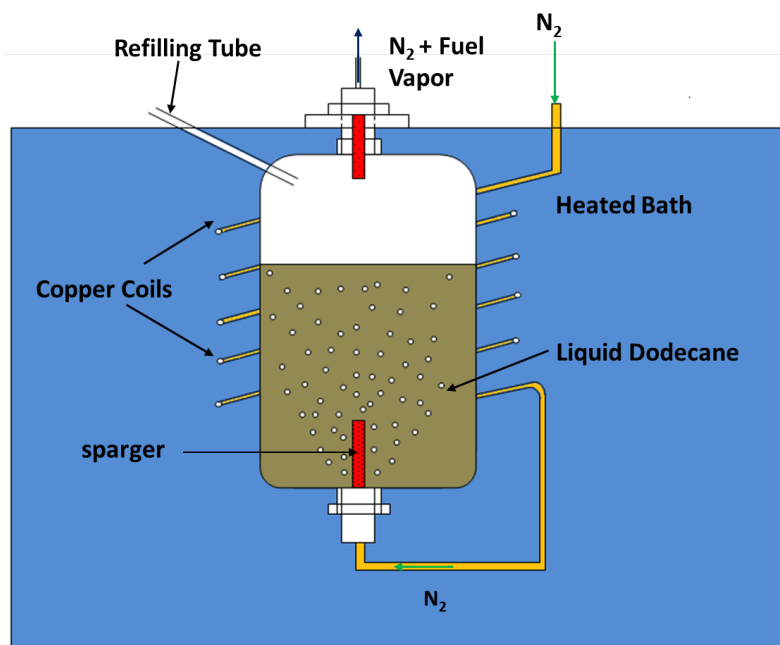


Figure 3.4: Evaporator Bath System.

(supplied by Grade 5.0 Praxair cylinders) into which the gaseous sample containing hydrocarbons is introduced. Once the sample containing hydrocarbon species is introduced into the flame, a complex ionization process generates a large number positive and negative ions. A highly polarizing voltage is applied around the burner nozzle inside the instrument thereby generating an ionization current that is proportional to the hydrocarbon concentration in the sample. A certified standard propane span gas is used to calibrate the instrument and the FID is used to measure the hydrocarbon concentration in terms of propane equivalents. The detected values are then converted into dodecane equivalent ppm concentrations using manufacturer provided Response Factor charts. The FID thus detects the total carbon loading of the flow (in propane equivalents) and is used both to determine the optimum bath temperature set points as well as an online check of the 2nd injection fuel flow rate during the course of the reactor run. Figure (3.5) provides a schematic of the entire evaporator system plumbing diagram. Before an experimental run, the bath flow system is operated for over an hour to ensure that steady state evaporation conditions have been attained before diverting the vaporized fuel stream into the flow reactor.

One of the crucial issues for THC analyzers is ensuring the linearity of the response throughout the operating range of relevance. In general lower operating ranges (i.e. more dilute hydrocarbon streams) generate better linear response from the instrument. Keeping this in mind, the fuel-N₂ flow is diluted with a metered amount of extra N₂ before entering the FID inlet. The diluent stream is also sourced from a choked orifice controlled by the PID system and is preheated before mixing. After dilution, the Range 4 of the Total Hydrocarbon Detector (0-10,000 ppm) can be used to detect n-dodecane concentration in propane equivalents for all flow reactor runs. Range 4 exhibits excellent linear response over its entire span [Fig. (3.6)]. The bath evaporation system is characterized using the FID. The n-dodecane evaporation rates are found to be constant over more than 3 hours of operation with less than $\pm 3\%$ variation in hydrocarbon concentration in the injector flow for a given bath temperature.

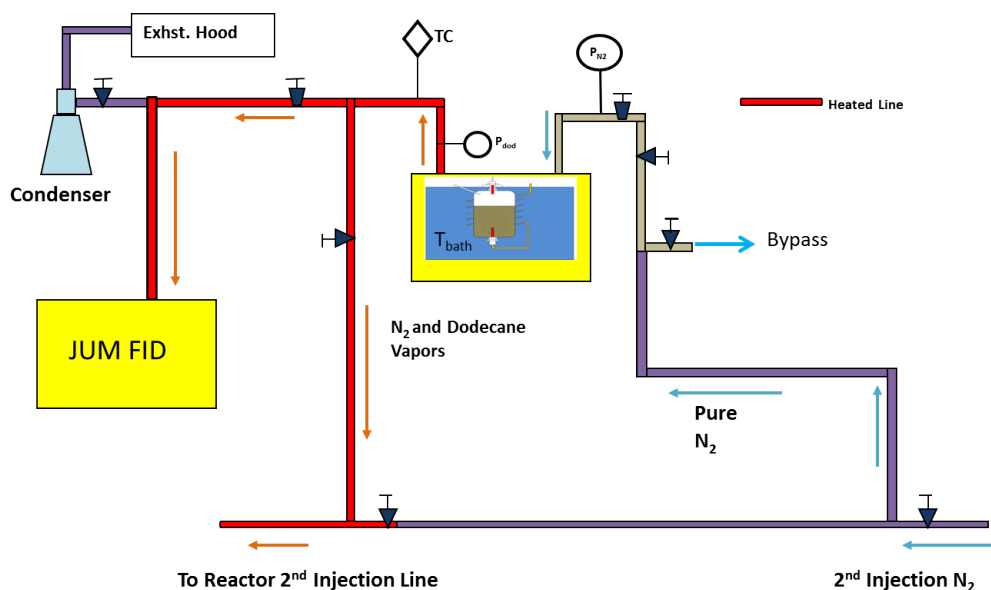


Figure 3.5: 2nd Injection Bath-FID Flow System.

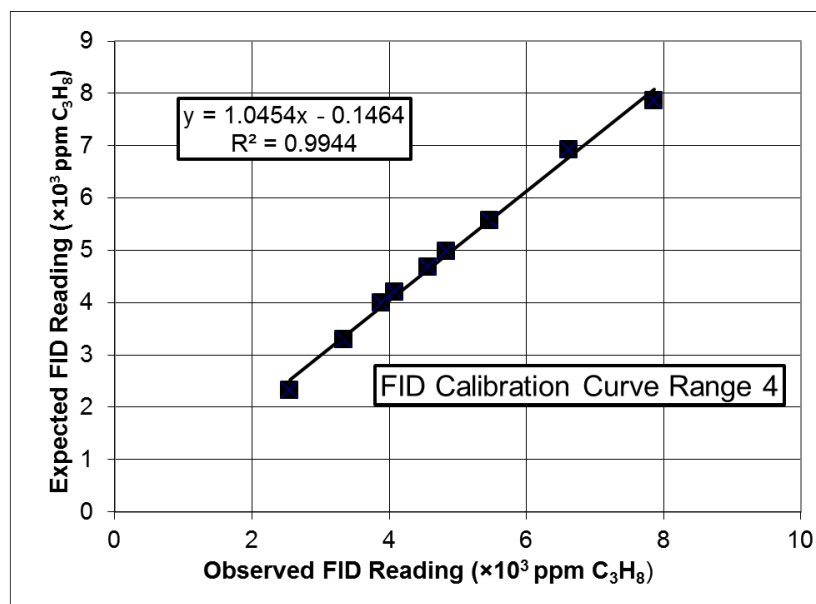


Figure 3.6: Calibration Curve for the JUM FID Detector in Propane Equivalents.

3.3.3 Measurement Probes

Two different probes are used for species extraction and temperature measurement purposes. Temperature is measured axially along the reactor center-line by a Type R (Pt/ 13% Rh-Pt) thermocouple with 0.005" bead diameter (0.002" wire diameter). The thermocouple wire leads are spot welded to 0.02" diameter support wires that go through ceramic insulating tube. The Thermocouple bead is coated with a 0.001" thick passivating SiO_2 film using flame deposition technique discussed previously by Walters [Walters (2008)]. The small thermocouple bead size coupled with high pressure vessel wall temperatures limit radiation losses to values less than 3 K [Bardosova (2011)]. The total uncertainty from measured temperature effects will be treated in detail in Appendix B.

The species extraction probe, discussed in greater detail by Bardosova [Bardosova (2011)] consists of a 1mm diameter choked inlet on a machined stainless steel probe tip that is TIG welded to a 0.25" OD (and 0.17" ID) stainless steel tubing. The probe tip has a convergence half angle of 5° . The species extraction system uses both aerodynamic quench by expansion through a choked nozzle as well as wall cooling in order to "freeze" the species mix at their extraction point concentrations. The steel tube of the extraction probe is housed within two concentric steel tubes through which propylene glycol coolant is pumped. The coolant line pressure and the inlet and exit coolant line temperatures are monitored during the experiment.

Both probes can be mounted along the center-line axis of the flow reactor and can be translated in steps of 1 mm using a stepper motor driven lead screw translation stage that is controlled by a Lab View code. Thus, both probes can access all center-line locations of the 41 cm long reaction zone and are able to measure species and temperature profiles relative to the axial distance from the second injection stage. It is essential that the probes be aligned along the vertical axis of the flow reactor for the plug flow assumptions to hold (Walters, 2008). A torpedo laser level mounted on a custom made vertical frame with a magnetic surface is used to ensure that the burner assembly, the quartz flow reactor, the pressure vessel and the fittings used to mount the probes are all assembled co-axially and are in an upright position with respect to the steel platform attached to the ground. The thermal cycles that the system undergoes tend to degrade the alignment after repeated runs,

thus care is taken to periodically check the alignment using the laser mounting and slightly adjust the top flange of the pressure vessel and probe connector fittings to regain alignment between all the component parts. Well aligned probe connectors result in the measurement of extremely smooth and scatter-free background temperature and CO₂ mixing profiles along the length of the reactor and such diagnostic runs serves as quick checks for the quality of the probe positioning before an experiment.

3.3.4 Sample Transfer and Conditioning

The sample handling systems are identical to those described by Bardosova [Bardosova (2011)] and are briefly outlined in the current work.

Dry Sampling

Many of the species of interest that are measured during the flow reactor experiment are non-polar and non-condensable given their respective partial pressures. Such species include H₂, O₂, CO, CO₂, CH₄, C₂H₆, C₂H₄, C₂H₂, C₃H₆, C₃H₈, 1-C₄H₈, 1-C₅H₁₀, 1-C₆H₁₂ and 1-C₇H₁₄. The higher alkenes exist as vapors because of their low (<50 ppm) concentrations in the flow stream. For such species, it is convenient to desiccate the extracted sample and measure the concentrations on a dry basis in the Gas Chromatograph especially since the large water peak and condensation concerns often make it difficult to measure early eluting species on a wet basis. The extracted gas stream is passed through a refrigerated cold trap where the gases are cooled to 5 °C and the water content is reduced to less than 2 mole % from the initial concentrations of over 20%. Subsequently the sample is passed through a Drierite desiccant bed where the entirety of the remaining water is removed. The sample then passes through the diaphragm pump responsible for driving the extraction process and then splits into three different streams. The first stream goes to the online Gas Chromatograph while the second and third streams go into the paramagnetic analyzer (PMA) and non-dispersive infrared analyzer (NDIR) respectively. These diagnostic tools are described in more detail in the subsequent sections.

Wet Sampling

The wet sampling method is primarily used to measure n-dodecane concentrations for the low temperature pyrolysis and oxidation case and formaldehyde concentration for the high temperature oxidation runs. In this method the extracted gas samples are directly transferred by a separate diaphragm pump to the gas chromatograph through stainless steel tubing that is kept heated and insulated at 130 °C. To improve signal response, the gas chromatograph exit is back-pressured to 3.5 psig when n-dodecane is being measured and 20 psig when formaldehyde is being measured. Care is taken to install proper filters at the GC inlet to prevent the entry of condensates into the columns. Several of the species were measured using both the methods and the concentration values were found to be consistent with each other.

3.3.5 Diagnostics

Gas Chromatograph

The Inficon (formerly Agilent) 3000 Micro Gas Chromatograph is the primary diagnostic instrument used to measure species concentrations in the flow reactor. The Inficon Micro-GC is a bench-top, portable gas chromatograph with four parallel columns each of which is fitted with a thermal conductivity detector that converts the varying thermal conductivities of the eluting species into voltage response peaks that are plotted using the Agilent-Cerity software. The Micro-GC is capable of rapid detection of species peaks. The peak elution times range from 2 minutes for CO, CO₂ to about 7 minutes for n-dodecane. This makes the micro-GC an ideal online diagnostic instrument for a steady state flow reactor system. Both for the dry and wet sampling systems, the extracted gas is fed directly into the micro-GC and the peak responses are noted before translating the extraction probe to a different axial position. There is no need for species storage or offline evaluation systems that are commonly used for more conventional gas chromatographs. The main drawback is relative insensitivity to trace species concentrations. While under ideal conditions the instrument is able to detect peaks at 1-2 ppm levels, in general for actual run conditions where the column set points are tuned to capture a wide band of species with variable concentration levels, getting clean readings for species concentrations below 10 ppm proves difficult.

But overall, the rapid elution of species with concentrations ranging from 10^4 - 10 ppm values remain a decisive advantage. For all dry species that are measured, certified standard calibration mixtures prepared by Praxair at 80% concentration levels of the expected peak values are used to calibrate the GC. For n-dodecane calibration, the bath-FID system is connected with the GC inlet such that the n-dodecane peak area response can be correlated with the Total Hydrocarbon Reading of the JUM FID system. For formaldehyde calibration the method described in [Bardosova (2011)] is followed. The details of GC calibration and species detection methodology as well as associated uncertainties are discussed further in Appendix A. Table (3.2) provides a brief overview of the four GC columns and the species that are detected by each.

Real Time Analyzers

The paramagnetic analyzer (PMA, Rosenmount Analytical, Oxynos 100) and the Non-Dispersive Infrared Analyzer (NDIR, Rosenmount Analytical) are used for rapid real time concentration measurements of oxygen (PMA) and carbon-dioxide and carbon-monoxide (NDIR) respectively. The analyzer response time is less than 5 seconds making them ideal as quick online diagnostics for the flow reactor runs. The species concentration values can also be compared with the GC data to test for compatibility. The analyzer set points are summarized in Table (3.3). While the scales are not as accurate as the GC data, in actuality the measurements correlate well with the measurements from the gas chromatograph. Figure (3.7) shows a sample comparison of GC and NDIR/PMA for one of the oxidative experiments (1220 K Rich Oxidation Experiment).

3.4 Flow Reactor Modeling

Real flow reactors deviate significantly from ideal plug flow assumptions outlined in Section (3.1). Therefore, there is a need to model the non-idealities associated with the presence of transverse gradients, velocity perturbations affecting flow residence times and non-idealities associated with finite mixing times of the reactants. These issues are discussed sequentially in the following subsections.

Channel	Column	Dimension	Carrier Gas	Species Measured
A	Molsieve	12 μm /320 μm /10m	Ar	H ₂ , O ₂ , CH ₄ , CO
B	PLOTU	30 μm / 320 μm / 8m	He	CO ₂ , C ₂ H ₄ , C ₂ H ₆ , C ₂ H ₂
C	Alumina	8 μm / 320 μm / 10m	He	C ₃ H ₆ , 1-C ₄ H ₈
D	OV1 (dry run)	2 μm / 150 μm / 14m	He	1-C ₄ H ₈ , 1-C ₅ H ₁₀ , 1-C ₆ H ₁₂ , 1-C ₇ H ₁₄
D	OV1 (wet run)	2 μm / 150 μm / 14m	He	CH ₂ O, n-C ₁₂ H ₂₆

Table 3.2: List of Columns and the Species Measured by each in the Micro-GC.

Analyzer	Species	Range	Span Gas	Accuracy
PMA	O ₂	0-10%	4.95% and 1.11%	1% of Full Scale ($\pm 0.1\%$)
NDIR	CO ₂	0-0.5%	0.399%	1% of Full Scale ($\pm 50\text{ppm}$)
NDIR	CO ₂	0-5%	0.753%	1% of Full Scale ($\pm 500\text{ppm}$)
NDIR	CO	0-2%	0.8%	1% of Full Scale ($\pm 200\text{ppm}$)

Table 3.3: PMA and NDIR Analyzer Specifications.

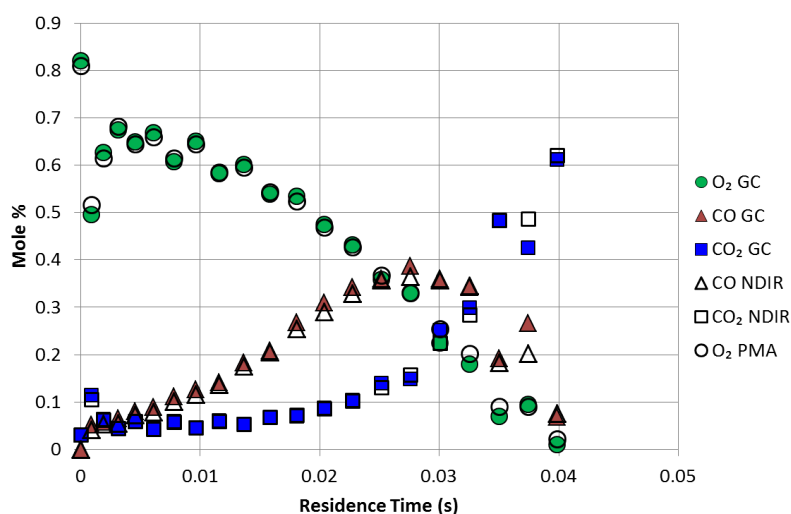


Figure 3.7: Comparison between Gas Chromatograph and PMA, NDIR data for the 1220 K Rich Oxidation Experiment.

3.4.1 The Plug Flow Assumption

A 2-D modeling study was performed in a previous work by Walters [Walters (2008)] to assess the effects of radial gradients in velocity, species and temperature concentrations in the flow reactor. The 2D Navier Stokes equations (for high Reynolds number laminar flows) were solved using Finite Volume discretization using CRESLAF code from the CHEMKIN suite and compared with the solutions of the Plug Flow model along the reactor center line. A detailed ethane oxidation model was implemented and it was found that the species concentration profiles along the reactor center line are virtually identical for the 2D and the plug flow based simulations. This result validates our approach. However substantial deviations from the plug flow model was observed further away from the reactor center-line, underlying the need for careful centering of the temperature and species probes within the flow reactor. The laser level based alignment technique discussed earlier helps in ensuring the positioning of the probe along the reactor axis.

3.4.2 Residence Time Calculations

To report the experimental data in terms of reaction times, the residence time to axial distance correlations need to be developed for the flow reactor. Under the plug flow assumption, the residence time is defined as the age of a small fluid element from its point of origin at the second injector stage and moving downstream along the reactor center-line. In a previous work, Schmidt (Schmidt (2001)) performed hot-wire anemometry characterization of the flow velocity under cold flow conditions and generated the center-line velocity profiles for Reynolds numbers ranging from 1900 to 5200. It was observed that within this Reynolds number range, the center-line velocity profiles collapse into a single dimensionless parameter that is independent of the flow Reynolds number. This simplification helps define a dimensionless mass flow rate parameter that is found to be dependent only on the axial distance z from the 2nd injection point [Bardosova (2011)]. This non-dimensional mass flux is defined by eqn. (3.1).

$$\dot{m}^*(z) = \frac{\dot{m}(z)}{\dot{m}_0} = \left(\frac{M(z)}{M_0} \right) \left(\frac{d(z)}{d_0} \right)^2 \left(\frac{T_0}{T(z)} \right) \left(\frac{U(z)}{U_0} \right) \quad (3.1)$$

where M is the molecular weight, d is the diameter of the reactor, T is the temperature and U the axial velocity. The subscript '0' refers to conditions just after second injection and are given by,

$$U_0 = \frac{\dot{m}_0}{\rho_0 \frac{\pi}{4} d_0^2} \quad (3.2)$$

$$\rho_0 = \frac{P_0 M_0}{R_u T_0} \quad (3.3)$$

The best fit for $\dot{m}^*(z)$ was found to be (Bardosova (2011)),

$$\dot{m}^*(z) = \begin{cases} 1.0, & z \leq 5.0 \\ 13.93 \times \exp\left(\frac{z-5}{113.1}\right) - 12.93, & 5 \leq z \leq 11.25 \\ 0.8048 \times \exp\left(\frac{-(z-11.25)}{8.074}\right) + 0.9869 & 11.25 \leq z \leq 22 \\ 0.06453 \times \exp\left(\frac{-(z-22)}{2.532}\right) + 1.135 & z > 22 \end{cases} \quad (3.4)$$

In the initial 0-5 cm region, the reactor dimension remains constant at 1.9 cm and plug flow conditions hold due to vigorous mixing and turbulence caused by the second injection. Between 5 cm - 11.25 cm, the fluid enters the diffuser section where the diameter expands to 3 cm. However, due to flow separation effects, the velocity along the center-line remains high causing a rapid increase in $\dot{m}^*(z)$ values. Past the diffuser section, the center-line velocity drops as the flow re-attaches itself to the wall. As a result the $\dot{m}^*(z)$ values drops rapidly. However, further downstream, the boundary layer begins to thicken and hence the profile value stops decaying and stays above unity.

Using the fit in eqn. (3.4) and the experimental values for the temperature profile, the axial velocity profile $U(z)$ for a given flow condition can be determined from eqn.(3.1). Finally, the residence time is calculated by numerical integration,

$$t(z) = \int_0^z \frac{dz'}{U(z')} \quad (3.5)$$

A sample residence time vs axial distance correlation for the 1220 K rich oxidation experiment is shown in Fig. (3.8). Similar correlations are obtained for all experimental conditions of interest.

3.4.3 One-Dimensional Mixing Reacting Model

Plug Flow Reactors usually serve as the idealized model for experimental flow reactor facilities. In general, idealized PFR models assume instantaneous mixing of the reactant streams such that well-defined initial conditions at time " $t=0$ " exist. However, in actual flow reactors, the mixing of the fuel and oxidizer flows occurs over a finite time. If the mixing times are negligible compared to subsequent reaction times in the homogeneous fully mixed region, then the mixing effects may be neglected completely. Unfortunately for combustion relevant temperatures, such situations hardly ever arise and reactions do occur between the fuel and the oxidizer streams during the mixing. This violates the plug flow assumptions and different techniques are used to account for this initial non-ideality. A detailed review of some of the commonly used techniques are presented in Zhao et al. (2008) and in Dryer et al. (2014). One popular approach is the "time-shifting" method. In this method, the predicted species time histories are calculated numerically using a time marching zero-dimensional reactor model where the initial conditions are the idealized fully mixed reactant compositions. The resulting calculations are shifted along the time axis until a specified "target" criterion, like the CO peak or 50% fuel decomposition point is matched with the experimental data. The time shifting method gives good results when

a) There is no significant consumption of reactants or generation of product intermediates in the mixing region, and only initial induction chemistry with radical pool build-up is occurring and

b) Perturbations in the early time induction chemistry do not significantly affect the downstream product generation or reactant consumption profiles.

Unfortunately, for the intermediate temperature (900 K-1200 K) regions, there can be significant product generation and reactant removal in the mixing region. In our 1200 K oxidative conditions for example, the complete decomposition of n-dodecane into smaller alkenes occurs before the first millisecond, well within the mixing time scales of 0-5 ms.

Furthermore, for the large hydrocarbon compounds, the reaction mechanisms are not validated well enough so that high confidence can be placed on the profile matching techniques being used to calculate the necessary time shift. As is seen in Chapter (5), identical flow reactor conditions will generate significant differences in the predictions for 50% fuel decomposition time for the pyrolysis condition or the CO peak in oxidation conditions depending on the chosen mechanism. Therefore, the time shifting method is not a good approach for our system. In another method called "initialization conditioning", also described in Dryer et al. (2014), the species composition downstream of the mixing zone are used as the initial conditions for the ideal PFR region. The measurements of the major intermediate species themselves at this point along with estimates of the other minor stables and radicals can be used as the initial "reactant" composition input. This method is likely to be more accurate. However, the estimates for the unmeasured species, especially the important radicals and the high alkenes still require the use of detailed mechanisms, resulting in uncertainties. Once again, different mechanisms will generate different composition estimates at this initial point, undermining our ability to compare between the mechanisms based on the flow-reactor data and mechanism species profile prediction matching.

In the past, a one-dimensional mixing reacting model based on Zwietering ((Zwietering, 1959), (Zwietering, 1984)) was successfully implemented for the Stanford VPFR system by Walters [Walters (2008)] to model vitiated ethane oxidation experiments and by Bardosova [Bardosova (2011)] for modeling the vitiated oxidation of DME-methane binary mixtures. The Zwietering Mixing Reacting Model will be implemented in this work in order to simulate the initial mixing region of the flow reactor. The following sections discuss the mixing theory and its implementation in CHEMKIN-PRO and CANTERA codes.

3.4.4 Zwietering Mixing Reacting Model Description

The Zwietering Mixing Reacting Model utilizes a semi-empirical approach to model the initial inhomogeneities in the species profile distribution during the mixing between the injected vaporized n-dodecane/N₂ stream and the vitiated gas downstream. The flow situation within the mixing region is shown schematically in Figure (3.9). The vitiated gas, hereafter called the "bath gas" is composed of the combustion products of the H₂/Air burner

flame and the nitrogen introduced in the first injection stage. Due to the high momentum flux ratio of the second-injector jets, the fuel/N₂ flow is expected to penetrate rapidly to the reactor center-line and displace the vitiated bath gas to the periphery. Further downstream, the bath-gas remixes back into the center-line stream through entrainment processes. This entrainment alters the species composition as the center-line fuel concentration is diluted and it also heats up the initially cold second injection stream gases back to the bath gas temperatures. Reaction of the fuel species proceeds simultaneously.

A differential control volume, initially consisting only of the pure second injector stream state, is tracked through the reactor center-line as it "marches" downstream while undergoing reaction and entrainment from the peripheral bath gas. Let $m(t)$ denote the changing mass of the control volume, $\dot{m}_e(t)$ the mass-based rate of entrainment of the unreactive bath gas into the control volume, τ_e the characteristic entrainment time, $Y_j(t)$ the time dependent mass-based species composition inside the control volume with $Y_{j,e}$ being the mass fraction of the species j in the bath gas being entrained and $Y_{j,0}$ being the initial mass fraction of the species in the control volume. It is convenient to normalize the mass of the control volume element by the initial mass of the volume element m_0 . Thus, the normalized mass flow rates are given by,

$$\tilde{m}(t) = \frac{m(t)}{m_0} \quad (3.6)$$

and

$$\tilde{m}_e(t) = \frac{\dot{m}_e(t)}{m_0} \quad (3.7)$$

Based on this normalization, the mass and species balance equations for the control volume may be written as (Walters (2008)),

$$\frac{d\tilde{m}}{dt} = \tilde{m}_e(t) \quad (3.8)$$

$$\frac{dY_j}{dt} = \frac{\tilde{m}_e(t)}{\tilde{m}(t)} (Y_{j,e} - Y_j) + \frac{M_{w_j}}{\rho} \dot{\omega}_j \quad (3.9)$$

$$\rho = \frac{P}{R_u T \sum \frac{Y_j}{M_{w_j}}} \quad (3.10)$$

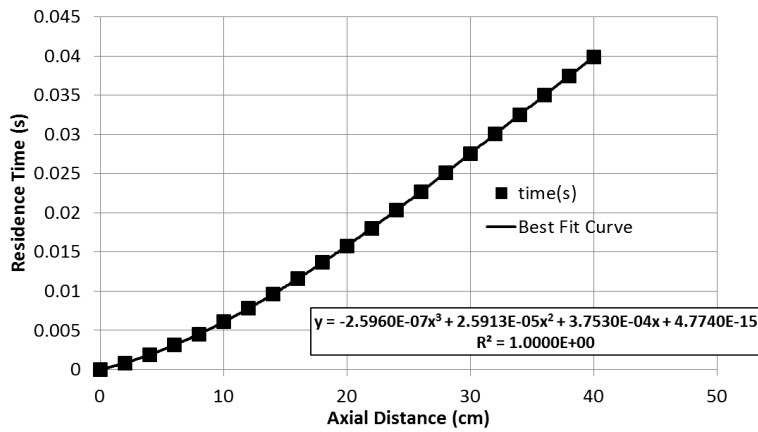


Figure 3.8: Residence Time against Distance Downstream of the Second Injection Stage evaluated for 1220 K Rich Oxidation Condition.

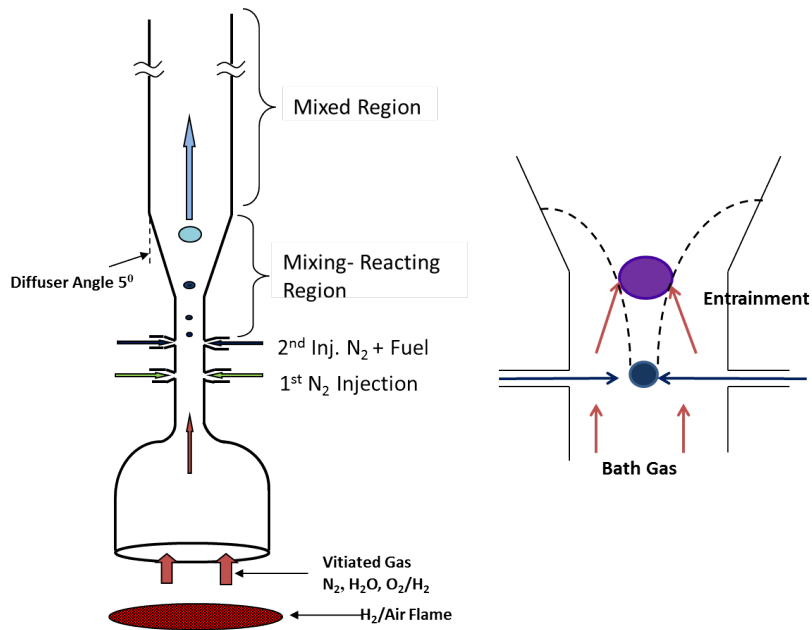


Figure 3.9: The Mixing Region of the Flow Reactor Shown Schematically.

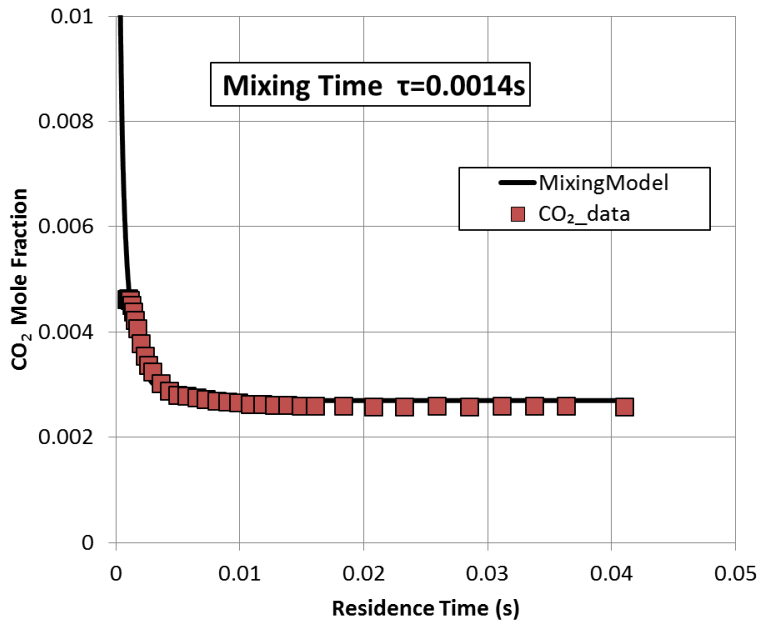
where $\dot{\omega}_j$ is the net volumetric molar production rate of the j^{th} species and is evaluated from reaction kinetics. It is to be noted that the temperature profile is a fit from the measured data over the axial length of the reactor and subsequently converted to residence time basis. Pressure is constant throughout. Thus, the only unknown parameter is the entrainment mass rate $\tilde{m}_e(t)$ itself. This is evaluated semi-empirically. The Zwietering model uses an exponential decay rate for the mixing process given by the equation,

$$\tilde{m}_e(t) = \tilde{M}_e \exp\left(-\frac{t}{\tau_e}\right) \quad (3.11)$$

$$\tilde{M}_e = \left(\frac{\dot{m}_{bath}}{m_{inj}} \right) \frac{1}{\tau_e} \quad (3.12)$$

where the pre-exponential factor is constrained by the bath gas to injected gas mass ratio. The characteristic entrainment time τ_e is determined experimentally by a CO₂ mixing experiment. In the CO₂ mixing experiment, a CO₂-N₂ mixture is injected through the second injector with all other flow conditions (including temperature) being kept identical to the corresponding n-dodecane experimental runs. The mass flow rate of the CO₂-N₂ gas mixture is kept the same as that of the actual second injector mass flow rate so that residence time is the same and the momentum flux ratio through the second injector is also maintained at the same value to ensure sufficient similarity in the mixing behavior. The measured CO₂ concentration profile is then fit using equation (3.11) to determine the optimal value for the characteristic mixing time. An example plot is shown in Fig. (3.10), while the details are discussed in Chapter 5. The relevant values for the mixing parameters are tabulated in the Table (3.4).

The ODE system outlined in this section can be solved directly in any open source code that can handle kinetic and thermodynamic database files. In this instance, the solutions are implemented in open source CANTERA software [Goodwin] in the MATLAB environment using CHEMKIN compatible kinetic and thermodynamic database files and a stiff ODE solver present in MATLAB. However, the CHEMKIN-PRO software is also capable of handling the 1-D mixing scheme and the methodology is described below.

Figure 3.10: CO₂ Mixing Profile Shown for 1000 K Pyrolysis Run at 1 atm.

Parameter	1000 K Pyrolysis Run	1050 K Rich Oxidation Run	1220 K Rich Oxidation Run	1170 K Lean Oxidation Run
$\frac{\dot{m}_{bath}}{\dot{m}_{inj}}$	19.52	21.3	16.44	17.57
$\tau_e(ms)$	1.4	0.69	1.6	2.4

Table 3.4: Mixing Model Parameters

For the standard ODE system outlined in equations (3.8) and (3.9), a differential control volume of a fluid element at constant pressure was tracked as it marched downstream from the injection point entraining bath gas fluid and reacting as it went. An alternate way of looking at the same problem is to think of a series isobaric differential control volumes of variable area into which fluid is flowing in either axially from the previous control volume of the series or laterally from the peripheral bath gas due to entrainment. Of course, the mass flowing in axially from the previous control volume is the total mass entrained thus far along with the mass originally sourced from the second injection stream. Since the residence times corresponding to axial position within the flow reactor has been evaluated before, the mass flux entering a differential control volume at the axial position z can be separated into two sources,

$$\dot{m}(z) = \dot{m}_{inj} + \dot{m}_{bath}(z) \quad (3.13)$$

where,

$$\dot{m}_{bath}(z) = \dot{m}_{inj} \times \int_0^{t(z)} \tilde{m}_e(t) dt \quad (3.14)$$

Since time vs axial distance function is known, the integration can be evaluated numerically to find the profile for $\dot{m}_{bath}(z)$. In Chemkin-Pro, a PFR module with two inlet streams and one outlet stream is constructed. The first stream corresponds to the flow coming from the second injector with the corresponding fuel/N₂ species profile. The second stream is the bath gas stream with a variable mass flow rate profile corresponding to $\dot{m}_{bath}(z)$ of eqn.(3.14) being put in as input. The species composition corresponds to the initial bath gas composition before the fuel injection occurs. The experimental gas temperature profile is set in as input as well. The final data needed are the cross-sectional area. It is noted that we are not modeling the entire flow reactor cross-section but a series of thin differential cylinders straddling the reactor axis whose cross-section grows with time due to isobaric constraint as more gas is entrained. The cross-section is evaluated as a function of axial position as follows,

$$A(z) = \frac{\dot{m}(z)}{\rho(z)U(z)} \quad (3.15)$$

where $U(z)$ is the known axial velocity profile and the density is evaluated from the ideal gas equation using the known temperature profile at constant pressure. This variable cross-section is the final input necessary to run the PFR module in Chemkin. A test profile comparing the matching between the standard mixing o.d.e solution and the Chemkin PFR solution is shown in Fig.(3.11). The match between the two approaches is exact. The ability to directly use Chemkin suite for modeling the Flow Reactor system considerably streamlines the solution diagnostics.

3.5 Summary

This chapter began from a simplified overview of a plug flow reactor system and went on to present a detailed account of the experimental facility and the associated gas handling and diagnostic tools. Further information about measurement uncertainties and GC calibration procedures are presented in the Appendices. In the last section, non-idealities associated with residence times and finite mixing times were accounted for by using a dimensionless mass flow similarity parameter and a 1-D semi-empirical mixing reacting model. The section ended with a brief description of how to implement the reactor model in Chemkin or Cantera software and presented a sample plot demonstrating the efficacy of the theory in capturing the experimental data along the reactor center line. Before presenting the experimental data and associated analysis, an overview of the detailed kinetic schemes that are used for simulation purposes are presented in the next chapter.

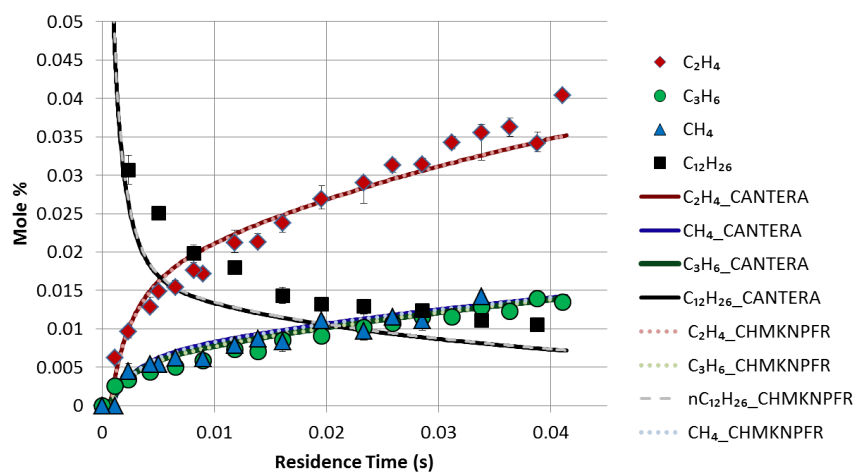


Figure 3.11: Comparison of Predicted Profiles from Cantera ODE Solver and Chemkin PFR module under 1000 K Pyrolysis Condition using the optimized JetSurf mechanism.

Chapter 4

Detailed Mechanisms used for Predictive Modeling

Detailed kinetic mechanisms seek to incorporate all relevant elementary reaction pathways. Consisting of hundreds of reactions for smaller species and thousands of reactions for combustor-relevant heavy fuel compounds, such detailed models, incorporating the best thermodynamic, kinetic and transport data for all species and all reaction pathways aspire to comprehensively predict all aspects of fuel oxidation and pyrolysis chemistry for varied combustion regimes. A well validated detailed mechanism, like the highly cited GRI MECH 3.0 for natural gas combustion (Smith et al., 1999), is often considered the gold standard from which simplified chemistry models are generally constructed for integration with fluid dynamical or flame simulations. A lot of recent efforts have been made by multiple combustion groups to extend the detailed kinetic schemes to heavier hydrocarbons and other more challenging functional groups. Validation against experimental data is crucial for the continuing development of such models. In the present work, four such heavy n-alkane mechanisms were selected and their predictions compared against the flow reactor data. They are 1) an optimized version of JetSurf 1.0 model, 2) the Lawrence Livermore mechanism for n-alkanes up to n-hexadecane, 3) the CNRS n-alkane mechanism developed by Dagaut et al. in Orleans France and 4) an automated semi-detailed model developed by Ranzi et al. of the CRECK group at Milano, Italy. A brief overview of these large kinetic schemes is provided in this chapter.

4.1 The JetSurf Mechanism

4.1.1 The JetSurf Model v 1.0

The Jet Surrogate Fuel Model (Sirjean et al. (2009), <http://www.stanford.edu/group/haiwanglab/JetSurF>) is a detailed kinetic mechanism developed in order to describe high temperature combustion behavior of n-alkanes up to n-dodecane. The mechanism contains 194 species and 1459 reactions and is an extension of the well validated base model USC-Mech II (Wang et al., 2007) that describes the $\text{H}_2/\text{CO}/\text{C}_1\text{-C}_4$ combustion chemistry. USC-Mech II contains 111 species and 784 reactions and in JetSurf, they are appended to 631 additional reactions and 64 species that extend the mechanism to describe high temperature oxidation and pyrolysis chemistry of $\text{C}_5\text{-C}_{12}$ n-alkanes. The main reaction classes that have been considered include C-C fission, H abstraction reactions from alkanes to create alkyl radicals, mutual isomerization of alkyl radicals by H transfer, β -scission of alkyl radicals, H abstraction from alkenes and decomposition of n-alkenyl radicals. Rate parameters for reactions involving higher alkanes, alkenes, alkyl radicals and alkenes are estimated from analogous reactions of n-butane, butyl radicals and 1-butene. JetSurf v 1.0 does not describe low temperature chemistry well, however a 4-species, 12-step lumped low temperature model based on Bikas and Peters (2001) has been added to capture the impact of low temperature chemistry at the intermediate temperature region (900K-1200K) of n-alkane combustion. A detailed discussion of the JetSurf Mechanism and validation tests can be found in You (2008), flame speed and extinction rate comparisons can be found in Ji et al. (2010), while comparisons with ignition delay and species time history profiles in shock tubes can be found in Davidson et al. (2011).

4.1.2 The Optimized JetSurf Model

JetSurf v 1.0 is an untuned model in the sense that it is compiled directly from the best evaluations of rate parameters available for the individual reactions from the literature and no further optimization has been performed. However, each of the elementary reaction rate parameter has its own experimental or theoretical uncertainty limits. A detailed reaction

mechanism is composed of thousands of such reactions creating the possibility that the uncertainties in the individual rate parameters may combine to generate large uncertainties in the predictions made by these detailed mechanisms. Thus, there is a need to quantify the uncertainty ranges of the constructed kinetic mechanism under different operating conditions and, if possible, to increase the accuracy of the model by a judicious selection of the sensitive rate parameter values within their respective uncertainty bands. It is standard practice for most published models to systematically tune the rate parameters within their uncertainty ranges based on data from multiple experiments including species history, ignition delay, reactivity profiles, flame speed, etc. This process is called model optimization or tuning and the final kinetic scheme is called an optimized mechanism. Recently Sheen (Sheen and Wang, 2011a) proposed a systematic methodology for quantifying and minimizing the effects of kinetic rate parameter uncertainties on the accuracy and precision of the overall model predictions by utilizing well-evaluated experimental data sets as tuning targets. The method is known as the Method of Uncertainty Minimization using Polynomial Chaos Expansion (MUM-PCE) and combines the widely used Solution Mapping (SM) optimization methodology with spectral uncertainty propagation techniques. It can be used in conjunction with a set of experimental targets to construct a tuned mechanism that not only has optimized reaction rate parameters but also a substantially reduced uncertainty band for its predictions when compared to the untuned mechanism. MUM-PCE has been used on USC-Mech II to develop an optimized model that generates excellent predictions for ethylene combustion (Sheen et al. (2009)). The method was also used on an earlier version of JetSurf to develop an optimized model for n-heptane combustion (Sheen and Wang, 2011b). The key feature of these optimized models is that not only do the new models predict the experimental data well, but there is also a significant reduction in the uncertainty bands for any predictions made by the newly tuned kinetic scheme. Thus, for ethylene combustion the optimized model achieved a 5-8 times uncertainty reduction in flame speed predictions, a 2 times decrease of the uncertainty band in ignition delay predictions [$\ln(t_{ign})$ predictions] and a decrease in uncertainty in OH concentration predictions with respect to residence time in PSR combustion from a factor of 4 to a factor of 2. Similar trends are seen in the optimized n-heptane model as well. In general, the logic of using such optimization and uncertainty reduction techniques can be summarized as follows:-

1. An unoptimized model compiled from 'as is' literature rate parameter values (and their extensions to higher carbon species using similarity estimates) usually does a poor job of aligning well with experimental data and requires optimization within the uncertainty bands using solution mapping methods.
2. Furthermore, the kinetic parameters for each of the elementary reactions are not well enough sampled to provide a kineticist with anything like a normal distribution about its "mean" value (as is often assumed). Instead most rate parameters are more realistically modeled as being uniformly distributed over the upper and lower uncertainty bounds. This in turn implies that any trajectory within the final uncertainty band of the initial untuned model prediction is equally likely. This, coupled with the much wider uncertainties of the model compared to experiments, makes prior untuned models poor tools both for predictive and validation purposes.
3. In this context, the systematic optimization and uncertainty reduction technique MUM-PCE is able to use high quality experimental data to optimize an untuned model and significantly reduce the uncertainties associated with its predictions. The final model created by such methods has greater accuracy and precision and is a better candidate for comparing with future experimental data. The next section describes the generation of an optimized model from JetSurf 1.0 (H. Wang, private communication) based on good quality species time history, ignition delay and flame speed data for n-dodecane from external experimenters. This optimized JetSurf model will be used to compare with the current PFR data in the next chapter.

The primary data sets for the optimization targets are the multi-species time history data for n-C₁₂H₂₆, OH, C₂H₄, CO₂ and H₂O measurements from the shock heating of a near stoichiometric dilute n-dodecane, oxygen mixture (457 ppm/7500 ppm) with a balance of argon at 2 atm. pressures [Davidson et al. (2011)]. In addition, atmospheric n-dodecane/air laminar flame speed data [You et al. (2009)] and ignition delay data for n-dodecane/air mixtures [Vasu et al. (2009)] have been included as experimental constraints for generating the optimized model. The experimental targets are presented in Table (4.1). For the species time history data, the experimental targets are either the species concentration at a specific time or the time when the species reaches a specific concentration. Which one is

chosen depends on which has the least uncertainty. The absolute uncertainty in the species mole fractions were reported to be $\pm 10\%$. However the temperature uncertainty of the experiment is around ± 10 K as well, and this leads to additional uncertainty. In general, as is seen in Figure (4.1), a 10 K temperature variation leads to around 20% variation in concentration at a given time. Therefore, where necessary, a 20% uncertainty band for experimental data was adopted. The 2σ uncertainty for the laminar flame speed data is ± 2 cm/s while the uncertainty in experimental ignition delay data was estimated to be $\pm 20\%$ based on regression analysis. The Chemkin 2.0 code is used to solve the shock tube problem with constant U and V constraint for both species time histories and ignition delay. Ignition delay is computationally determined from the maximum of $[\text{OH}^*]$ gradient with time. For this purpose a set of $[\text{OH}^*]$ chemiluminescence reactions (Hall and Petersen (2006)) are added to the JetSurf code. The Sandia Premix code is used for the premixed n-dodecane flame simulations.

Before optimization, the simulations from the untuned model are compared with the experimental species time history data. In Figure (4.2) the dashed lines present the experimental data while the solid lines present the mean model prediction. The experimental uncertainty is given by the error bar on blackened symbols while model uncertainty scatter (calculated using Monte Carlo Sampling) is represented by the colored dots. Firstly, it is noted that the model uncertainty far exceeds the experimental uncertainty. Secondly, the mean profile from the untuned JetSurf model predicts a longer induction time as seen by slower OH concentration rise. The mechanism predicts slower oxidation rates in general with a delayed decay of n-dodecane profile and a delayed oxidation of ethylene. Consistent with this trend, the ignition delay times are over-predicted by the model as observed in Figure(4.3) However, much of the deviation lies within the uncertainty scatter of the model; hence, the experimental data sets can be used to optimize the untuned model and constrain the uncertainties associated with the kinetic parameters. The uncertainty bands for laminar flames speeds are particularly large as is seen in Figure (4.4) while the mean prediction diverges from the model on the richer side.

Series 1: Shock Tube Species Profile (457 ppm n-C ₁₂ H ₂₆ /7500 ppm O ₂ /Ar, T ₅ = 1410 K, P ₅ = 2.15 atm. (Davidson et al., 2011))			
Species	Target Data	Exp. Target (Uncertainty factor)	Nominal Value of prediction
n-C ₁₂ H ₂₆	t @ [n-C ₁₂ H ₂₆]=10 ⁻⁵	2.6 × 10 ⁻⁵ (1.25)	2.71 × 10 ⁻⁵ s
C ₂ H ₄	[C ₂ H ₄] @ t = 10 ⁻⁴ sec	1.27 × 10 ⁻³ (1.2)	1.39 × 10 ⁻³ s
C ₂ H ₄	t @ [C ₂ H ₄] = 3.49× 10 ⁻⁴ sec	6.77 × 10 ⁻⁴ (1.2)	1.16 × 10 ⁻³ s
OH	[OH] @ t = 10 ⁻⁴ sec	3.47 × 10 ⁻⁶ (1.2)	2.46 × 10 ⁻⁶ s
	t @ [OH] = 10 ⁻⁵	4.81 × 10 ⁻⁵ (1.25)	8.54 × 10 ⁻⁴ s
	t @ [OH] = 6×10 ⁻⁵	7.18×10 ⁻⁴ (1.2)	1.09×10 ⁻³ s
	[OH] @ t = 10 ⁻³ sec	2.57 × 10 ⁻⁴ (1.2)	2.96×10 ⁻⁵ s
CO ₂	t @ [CO ₂] = 2×10 ⁻⁴	1.21 × 10 ⁻³ (1.2)	1.3 × 10 ⁻³ s
H ₂ O	[H ₂ O] @ t = 10 ⁻⁴ sec	1.58 × 10 ⁻⁴ (1.2)	2.12×10 ⁻⁴ s
	t @ [H ₂ O] =10 ⁻³	5.06 × 10 ⁻⁴ (1.2)	7.71×10 ⁻⁴ s
	[H ₂ O] @ t = 8×10 ⁻⁴ sec	3.74 × 10 ⁻³ (1.2)	1.1×10 ⁻³ s
Series 2: Laminar flame speed (cm/s) (n-C ₁₂ H ₂₆ /air at p=1 atm and T _u = 403 K) (You et al., 2009)			
Φ	Expt. Target	Nominal Prediction	
0.72	40±2	40.5	
0.9	58±2	56.5	
1.04	63±2	60.9	
1.19	59±2	56.6	
1.39	38±2	34.8	
Series 3: Ignition delay (μs) (n-C ₁₂ H ₂₆ /air) (Vasu et al., 2009)			
Φ	T ₅ (K), P ₅ (atm)	Exp. Target (uncertainty factor)	Nominal Prediction
0.56	1117, 30.9	266 (1.2)	594
	910, 22.7	2134 (1.2)	2200
1.12	1109, 23.0	278 (1.2)	360
	907, 23.5	1081 (1.2)	641

Table 4.1: Experimental Data Sets Used as Optimization Targets

The updated model, after optimization using MUM-PCE methodology (H. Wang, private communication), is observed to give significantly better predictions and reduced uncertainties for multi-species time histories (Figure (4.5)), ignition delay time (Figure (4.6)) and laminar flame speed (Figure (4.7)). The species time history profiles (and corresponding ignition delay times) are still somewhat longer than the experimental values, however the discrepancies are fairly minor. The laminar flame speed predictions have improved considerably as well. The results indicate that once systematic optimization and uncertainty minimization is performed, detailed kinetic models like JetSurf are able to perform significantly better in terms of reproducing experimental data.

The Optimized model is subsequently compared with n-dodecane data sets which were not used as targets to gauge its performance. Davidson et al. (2011) measured the ignition delay of stoichiometric mixtures of n-dodecane and oxygen in argon at 2.25 atm. The plots showing the experimental data along with predictions from JetSurf 1.0 and Optimized JetSurf are shown in Figure (4.8). It is seen that the predictions of Optimized JetSurf are an improvement over those of the unoptimized model. Malewicki and Brezinsky (2013) evaluated temperature dependent reactivity profiles for n-dodecane pyrolysis and oxidation at elevated pressures in a heated high-pressure single-pulse shock tube. The reactivity profiles span the range from 900 K to 1700 K, with residence times from 1.5-3.5 ms and provide a good test for the Optimized JetSurf mechanism predictions at the high pressure limit. The n-dodecane shock tube reactivity data for the stoichiometric condition and 50 atm nominal pressure were plotted in Figures S3 and S4 of the supplemental material of Malewicki and Brezinsky (2013) and compared with LLNL and rev1stGen model. Here, in Figures (4.9), (4.10), (4.11), (4.12) and (4.13) , the experimental data from Malewicki and Brezinsky have been compared with Optimized JetSurf predictions using the experimental conditions specified by the researchers in the supplementary data files. Constant U,V conditions have been assumed and are accurate given the very dilute nature of the fuel loading. As can be seen, Optimized JetSurf performs very well in predicting most of the major species profiles and compares favorably with predictions of the mechanisms presented in the original paper. To some extent the ethylene peak is under-predicted and the propylene peak over-predicted by the Optimized JetSurf. The higher alkene peaks are also over-predicted, but this trend is in common with the original LLNL and rev1stGen mechanisms Malewicki and

Brezinsky used for comparison purposes as well. Finally, experimental pyrolysis profiles at 973 K measured by Herbinet et al. (2007) in a jet-stirred reactor have been compared with the Optimized JetSurf model. The fuel conversion rate (Figure (4.15)) is well predicted by optimized JetSurf, however the production of ethylene, propylene and methane is under-predicted in Figure (4.14).

Overall the Optimized JetSurf model performs well against the experimental data. In the next chapter, its predictions will be compared against the flow reactor data set and against other detailed mechanisms.

4.2 The Lawrence Livermore Mechanism

The Combustion Chemistry group at the Lawrence Livermore National Laboratory have been involved in a multi-decade spanning development of detailed chemical kinetic mechanisms for engine relevant fuels. Normal and branched chain alkanes have received particular attention because of their importance as primary reference fuels and more recently due to their importance in developing fuel surrogates. The LLNL n-alkane model is based on a detailed kinetic model of n-heptane oxidation originally proposed by Curran et al. (1998) and was subsequently extended to cover n-alkanes up to n-hexadecane by Westbrook et al. (2009). The model is developed through an essentially hierarchical approach and the reactions are separated out into distinct classes. For high temperature oxidation of n-alkanes, for example, Westbrook et al. (2009) identify 10 reaction classes. These are:-

1. Unimolecular fuel decomposition (C-C fission)
2. H abstraction from fuel
3. Alkyl radical decomposition via β scission
4. Alkyl radical isomerization
5. H abstraction reactions from alkenes
6. Addition of H and OH species to alkenes
7. Reaction of alkenyl radicals with oxygenated radicals like HO_2 , CH_3O_2 and $\text{C}_2\text{H}_5\text{O}_2$

8. Alkenyl radical decompositions
9. Alkene decomposition
10. Retroene decomposition

The LLNL model also include detailed treatment of the low-temperature oxidation regime where as many as 25 different reaction classes have been identified. This enhances the generality of the model, though at the cost of added complexity. The n-dodecane model with detailed low-temperature chemistry thus contains as many as 1282 species and 5030 elementary reactions. The same reaction rate constants are used for analogous reactions of a given reaction class. The rate constants for each reaction class are in turn estimated from experimentally derived kinetic parameters available for lower carbon number species of the same reaction class and extended to the higher molecular number species using similarity rules. Details of the rate estimation methods for each of the reaction classes are presented in Curran et al. (1998) and the values have been continuously updated in lieu of more recent experimental data or theoretical calculations. The Therm software was used to compute thermochemical data using group additivity rules, and reverse rate constants are evaluated using the principle of microscopic reversibility. Westbrook et al. (2009) validated the model using extensive data sets from shock tubes, JSRs, flow reactors and RCMs. The n-alkane LLNL model is used in the current work to model flow reactor experimental conditions using CHEMKIN PRO software code.

The most updated version of the LLNL mechanism can be found in https://www-pls.llnl.gov/?url=science_and_technology-chemistry-combustion-c8c16_n_alkanes

4.3 The CNRS Mechanism

The CNRS group led by Philippe Dagaut at Orleans France has developed detailed chemical kinetic models of important normal, branched and cyclo alkanes using a consistent hierarchical modeling approach [Dagaut (2002)]. Recently, they investigated n-dodecane and n-undecane oxidation kinetics in a Jet Stirred Reactor and concurrently developed a detailed kinetic scheme comprising of 1377 species and 5864 reversible reactions that proved

reasonably accurate against n-dodecane experimental data [Mze-Ahmed et al. (2012)]. This mechanism (henceforth named as the CNRS mechanism) is the third detailed kinetic scheme against which our flow reactor data is compared.

4.4 The CRECK Mechanism

The large size of kinetic schemes for heavy hydrocarbon species have spurred the development of automated kinetic scheme generators. An example is the EXGAS software developed by Battin-Leclerc in Nancy, France [Warth et al. (2000)] or the MAMOX++ program developed by Ranzi et al. at Milano, Italy [Ranzi et al. (1997)]. The CRECK (Chemical Reaction Engineering and Chemical Kinetics) modeling group headed by Ranzi uses an automated code to generate semi-detailed mechanisms for hydrocarbon oxidation and pyrolysis. The semi-detailed kinetic scheme developed by this approach for n-alkanes up to n-hexadecane is described in Ranzi et al. (2005) and is henceforth called the CRECK model. The semi-detailed model uses lumping procedures to reduce the number of species and reaction pathways present in an automatically generated fully detailed model while preserving the descriptive capabilities of the detailed scheme. The main simplifications include the assumption of quasi steady state for the various isomers of a given alkyl radical, classification of the reactions into 10 basic classes with their own rate parameter values and the lumping of primary intermediate radicals and isomers of the primary products into a few groups of pseudo-species (like R_{12}^* or $R_{12}OO^*$ representing the C_{12} alkyl and alkoxy radical isomers). The details of this lumped model for n-dodecane oxidation and pyrolysis case has been outlined in an earlier paper [Ranzi et al. (2001)]. Using such methods, the CRECK modeling group is able to incorporate almost all important functional groups into a single semi-detailed kinetic scheme currently consisting of 460 species and 16039 reactions. This semi-detailed CRECK mechanism is run in CHEMKIN PRO and compared with the flow reactor data.

The CRECK mechanism can be downloaded from <http://creckmodeling.chem.polimi.it>.

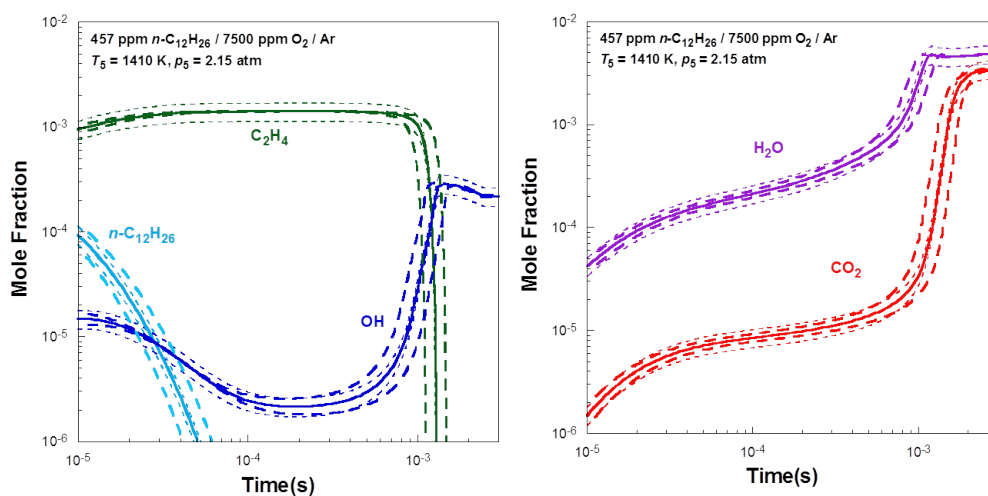


Figure 4.1: Simulated Temperature Uncertainty Estimates for Species Time History Measurements. Solid Lines: nominal prediction of the un-optimized JetSurf 1.0 model; Long Dashed Lines: computed uncertainty bounds due to ± 10 K uncertainty; short-dashed lines: 20% uncertainty on nominal mole fraction values.

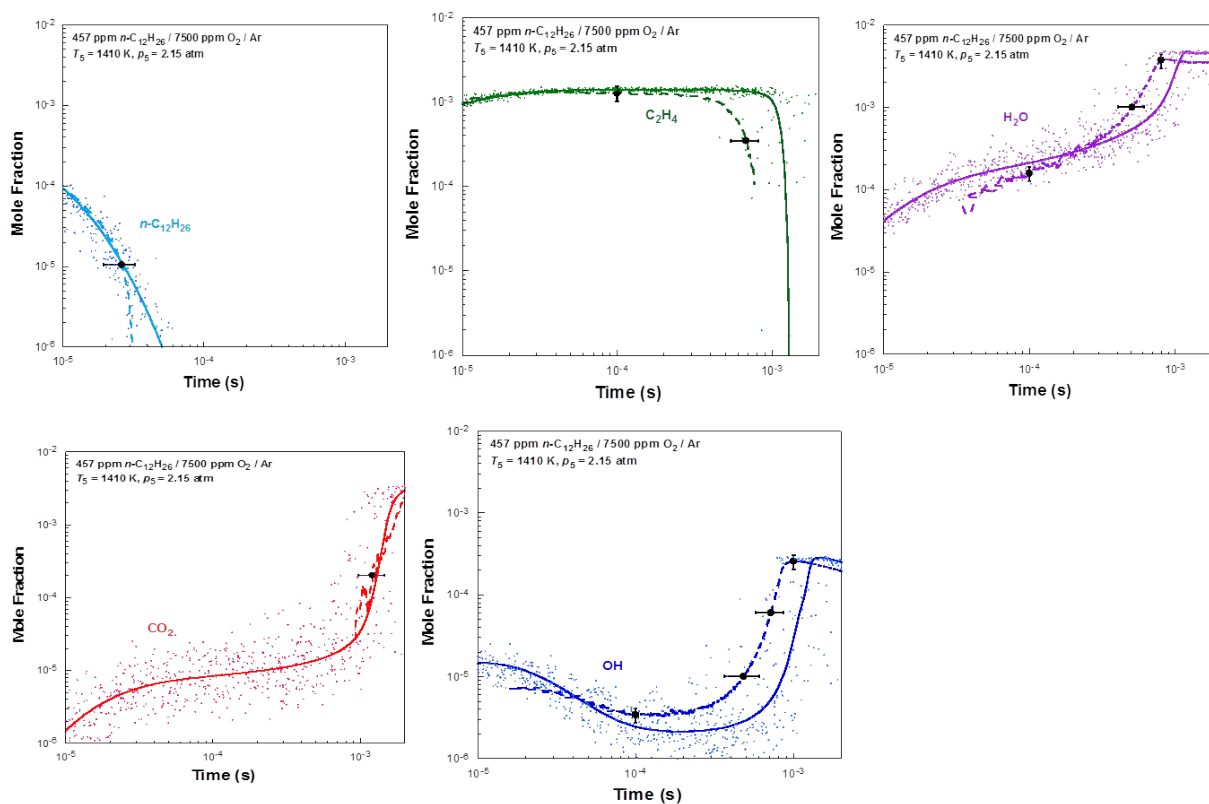


Figure 4.2: Experimental and Predicted Species Time Histories from the un-optimized JetSurf 1.0 . Dashed Line: Experimental Data; Solid Line: Model Predictions; Dots: Uncertainty Scatter; Filled Circle and Error Bar: Targets and their Uncertainties.

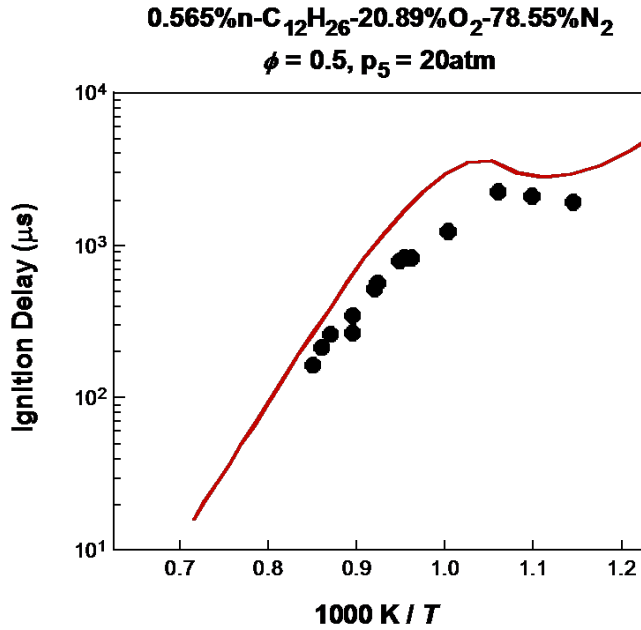


Figure 4.3: Experimental (symbols) and Predicted (line) Ignition Delay using the un-optimized JetSurf 1.0.

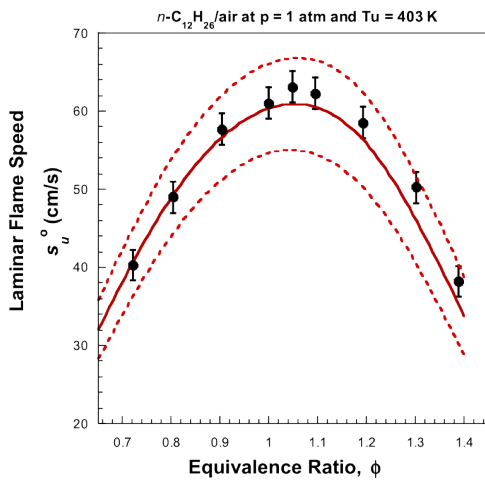


Figure 4.4: Experimental (symbols) and Predicted (line) Laminar Flames Speeds of n -Dodecane-Air mixture at 1 atm. pressure and an unburned gas temperature of 403K by the un-optimized JetSurf.

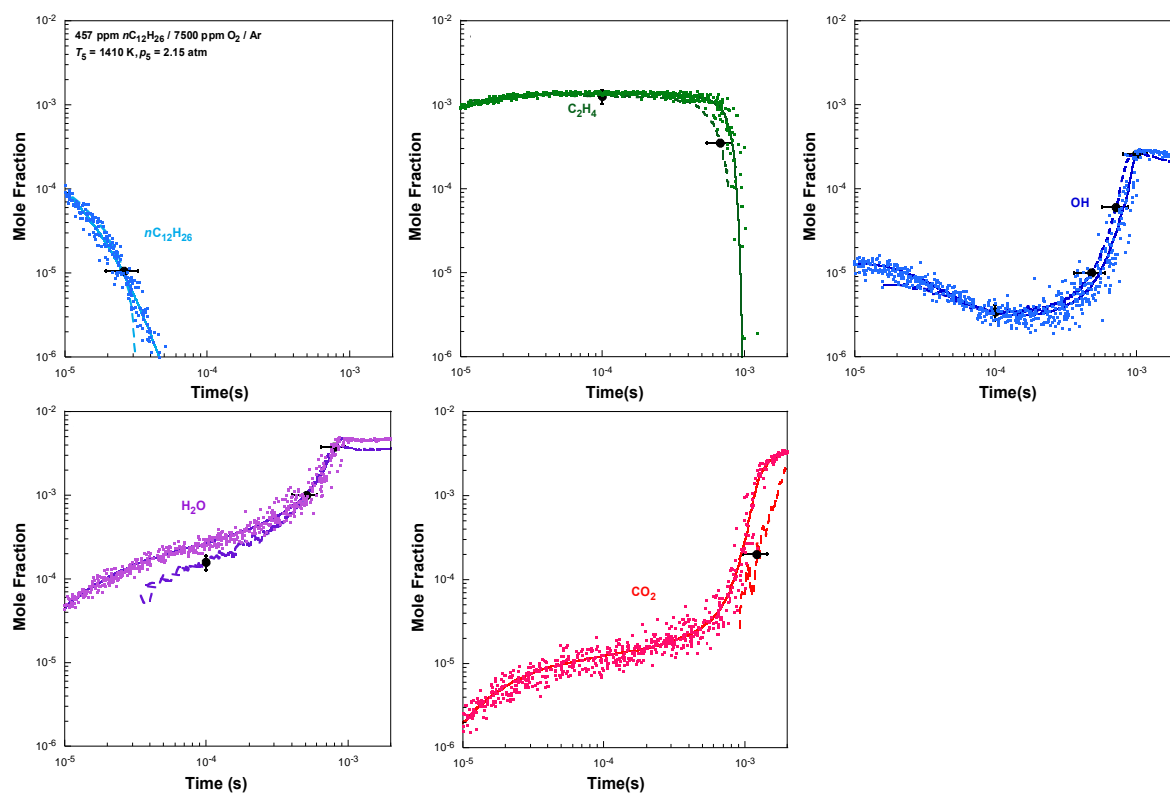


Figure 4.5: Experimental and Predicted Species Time Histories for the optimized JetSurf 1.0. Dashed Line: Experimental Data; Solid Line: Model Predictions; Dots: Uncertainty Scatter; Filled Circle and Error Bar: Targets and their Uncertainties.

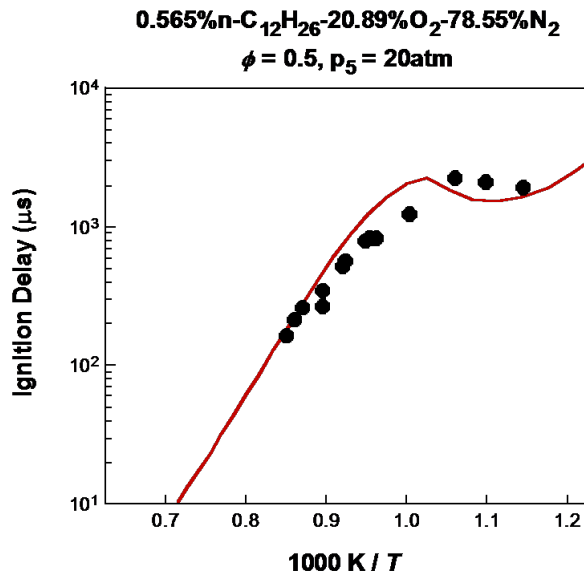


Figure 4.6: Experimental (symbols) and Predicted (line) Ignition Delay using the Optimized JetSurf 1.0.

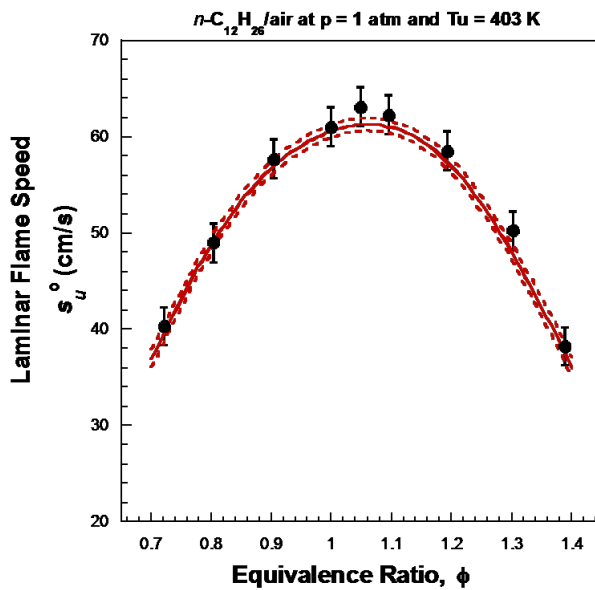


Figure 4.7: Experimental (symbols) and Predicted (line) Laminar Flames Speeds of n -Dodecane-Air mixture at 1 atm. pressure and an unburned gas temperature of 403K by the Optimized JetSurf.

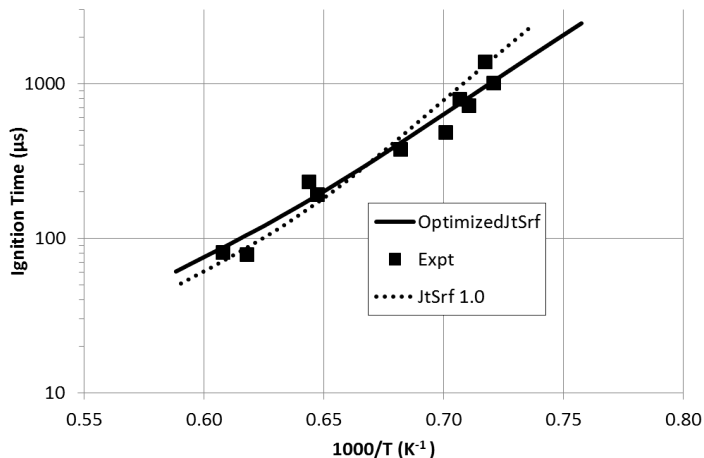


Figure 4.8: Comparison of the Optimized JetSrf against JetSrf 1.0 for n-dodecane ignition delay measurements based on half peak values for OH. 400 ppm dodecane, $\Phi=1$, $P=2.25$ atm., balance argon. Davidson et al. (2011)

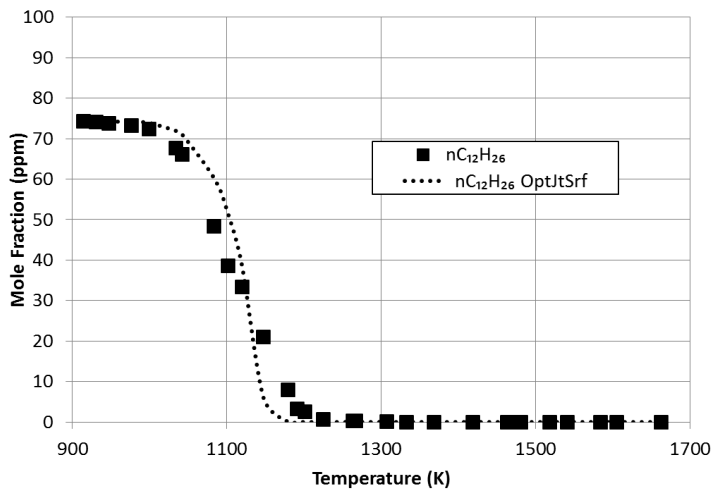


Figure 4.9: Comparison of n-dodecane oxidation reactivity data of Malewicki and Brezinsky (2013) against Optimized JetSrf Predictions; 75 ppm n-dodecane, $\Phi=1.06$, balance argon, $P_{\text{nom}}=50$ atm; n-dodecane Profile.

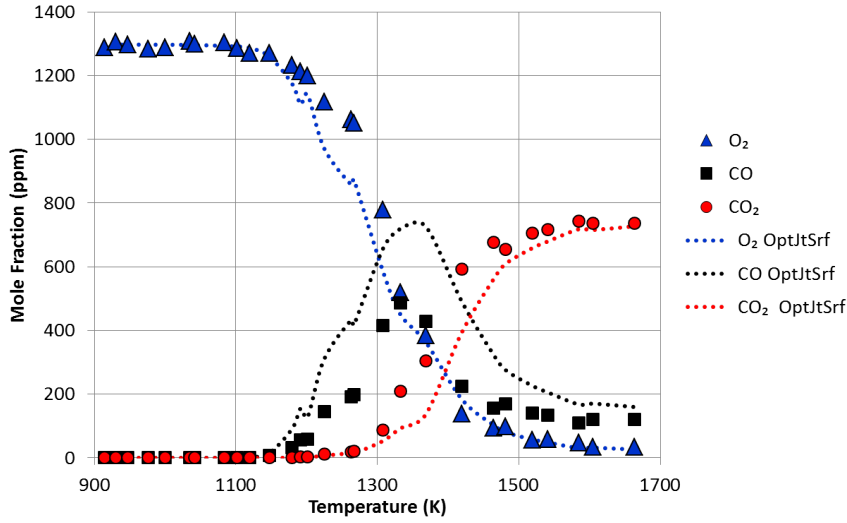


Figure 4.10: Comparison of n-dodecane oxidation reactivity data of Malewicki and Brezinsky (2013) against Optimized JetSrf Predictions ; 75 ppm n-dodecane, $\Phi=1.06$, balance argon, $P_{\text{nom}}=50$ atm; CO₂, O₂ and CO profiles.

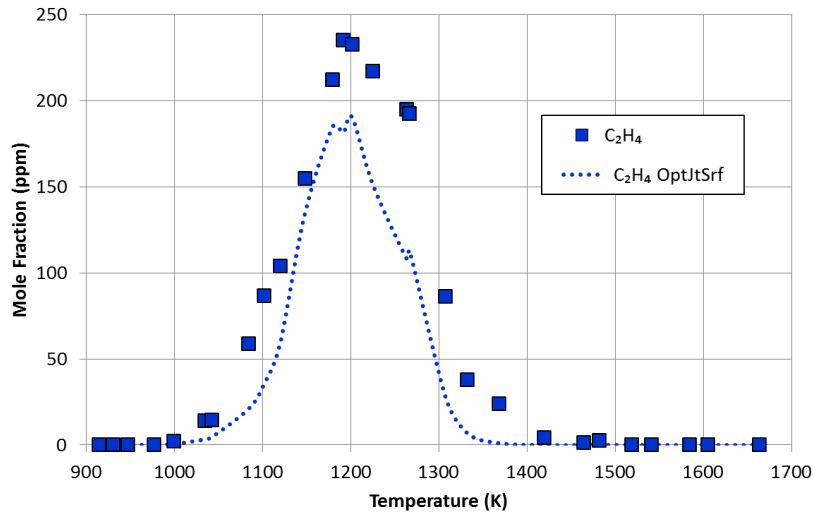


Figure 4.11: Comparison of n-dodecane oxidation reactivity data of Malewicki and Brezinsky (2013) against Optimized JetSrf Predictions; 75 ppm n-dodecane, $\Phi=1.06$, balance argon, $P_{\text{nom}}=50$ atm; C₂H₄ profiles.

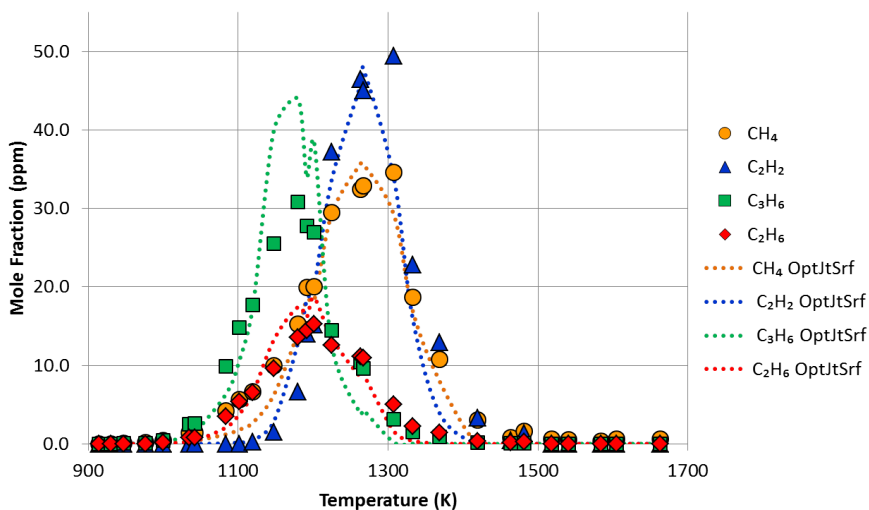


Figure 4.12: Comparison of n-dodecane oxidation reactivity data of Malewicky and Brezinsky (2013) against Optimized JetSurf Predictions; 75 ppm n-dodecane, $\Phi=1.06$, balance argon, $P_{\text{nom}}=50$ atm; other major intermediates.

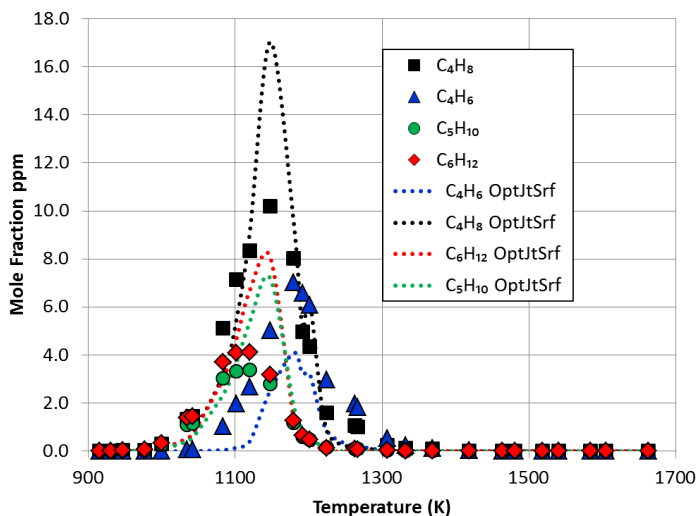


Figure 4.13: Comparison of n-dodecane oxidation reactivity data of Malewicky and Brezinsky (2013) against Optimized JetSurf Predictions; 75 ppm n-dodecane, $\Phi=1.06$, balance argon, $P_{\text{nom}}=50$ atm; higher alkenes.

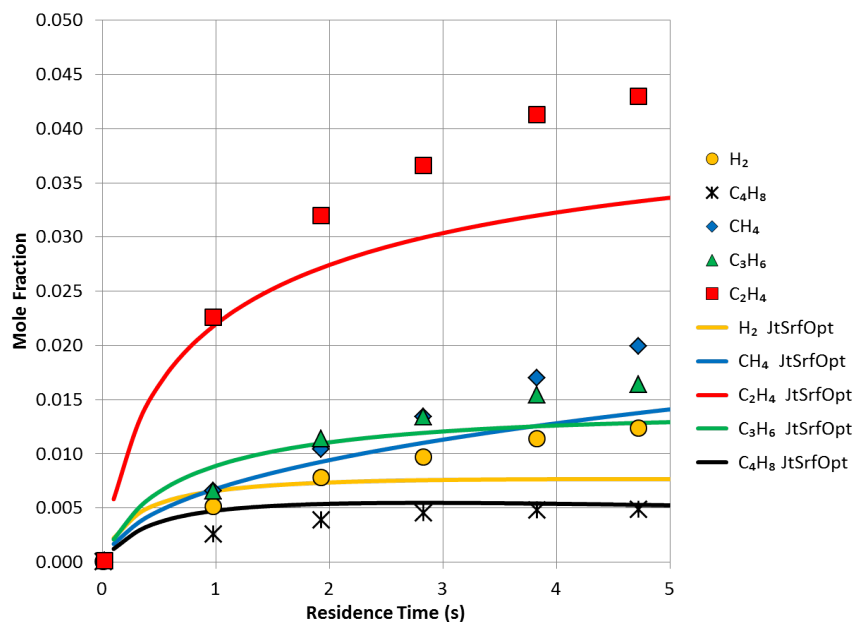


Figure 4.14: Pyrolysis products of n-dodecane vs residence time by Herbinet et al. (2007) at 973 K for a 2% dodecane-helium mixture. Symbols = data values; Solid Lines = Optimized JetSurf simulations

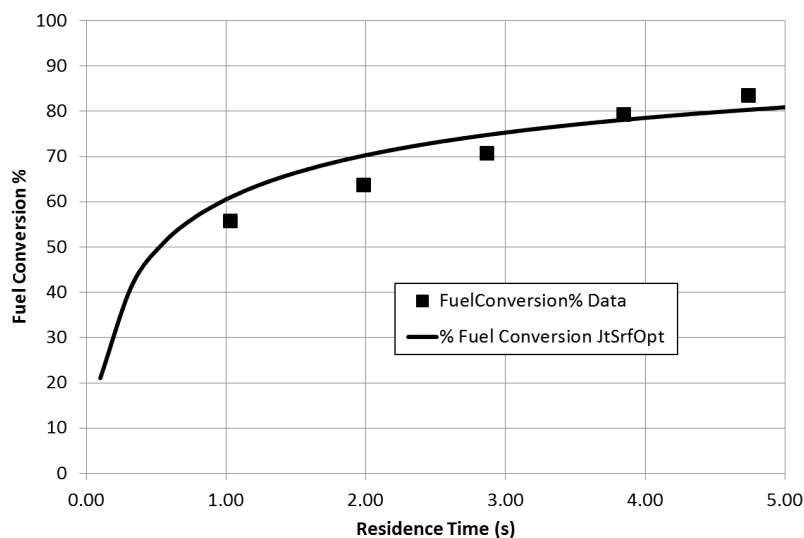


Figure 4.15: Conversion of n-dodecane vs residence time by Herbinet et al. (2007) at 973 K for a 2% dodecane-helium pyrolytic mixture; Symbols = data; Line = Optimized JetSurf Simulations

Chapter 5

Experimental and Detailed Modeling Results

5.1 Experimental Conditions

The Variable Pressure Flow Reactor facility was used to investigate four sets of experimental conditions in the intermediate temperature regime and at atmospheric pressure. The detailed experimental conditions are described in Table (5.1). The results from the experiments are compared with the predictions from the four detailed kinetic mechanisms (Optimized JetSurf, LLNL, CNRS and CRECK) that were described in Chapter 4. The experimental runs may be divided into two classes. The 1000K pyrolysis run and the 1050K rich oxidation run investigate the reaction regime where the decomposition of n-dodecane into C₇-C₂ alkenes predominates. The 1170 K lean oxidation and the 1220 K rich oxidation runs investigate regimes where these intermediate alkenes react to form oxidation products like CO and CO₂. Three types of experimental data were measured in the flow reactor facility and are described below.

5.1.1 Axial Temperature Profiles

For the oxidation runs, both the reacting and the non-reacting (i.e., background) temperature profiles have been measured. The background profile measurements are taken with inert nitrogen added instead of the fuel through the second injection stream in such a manner that the total mass flow rates remain identical to the reacting conditions. The three electric heater voltages are subsequently adjusted such that heat loss effects are negated, creating a nearly uniform axial temperature profile throughout the flow regime. Subsequently, fuel is injected and the temperature along the flow reactor axis is measured keeping the heater settings constant. No heat generation occurs under the pyrolysis run condition, but for the higher temperature oxidation cases the temperature increases as the probe moves towards the reactor exit. The reacting flow temperature data, the background temperature data as well as the best fit temperature profile are plotted together in the following sections. The temperature starts out high at time zero and then decreases as the second injection stream impinges on the reactor axis and cools the bath gas. However, the temperature fits used for the flow reactor simulations start from 400 K at 0 milliseconds, which is the estimated temperature of the second-injection flow stream as it enters the reactor as per estimates made previously (Bardosova, 2011). The best fit temperature profile is a direct input to the Chemkin flow reactor code being used to model the reaction conditions using the selected kinetic mechanisms.

5.1.2 Carbon Dioxide Mixing Experiments

As described in Chapter (3.4.4), the Mixing Reacting Model requires an estimate of the second-injection flow entrainment time constant. This is obtained by injecting a CO_2/N_2 stream through the second-injector such that both the carbon loading and the momentum flux ratio is held the same as the corresponding experimental conditions. The CO_2 concentration data are measured using the NDIR analyzer and used to generate the mixing profile. The mixing profile, the CO_2 concentration data and the mixing time constant have been plotted for the different run conditions.

5.1.3 Species Profiles

A majority of the plots present species profiles data that are compared with the predictions of the various reaction mechanisms. For JetSurf, the optimized JetSurf mechanism described in Chapter (4.1.2) has been used for comparison purposes. The species profile data are plotted as symbols while the mechanism predictions are plotted as lines of the same color. The species data also include experimental scatter over multiple runs as vertical error bars. In all cases the median of the experimental data are plotted. The concentrations are plotted in terms of molar percentages. The uncertainties in the residence time estimates have been plotted as horizontal error bars in some representative data points. The residence time uncertainties range from 0.5 ms at the early times to 3 ms near the reactor exit. The uncertainties in the species measurements range from 2% for the 1220 K rich oxidation and the 1170 K lean oxidation runs, to about 5% for the 1000 K pyrolysis and 1050 K rich oxidation runs. These values are too small to be visible and hence are not included in the data plots. The figures are divided into major species, intermediate species and minor species in terms of the concentration values for easier comparisons. The net carbon balance of all measured species is also plotted along with predictions from the model.

5.2 1000 K Pyrolysis Run

5.2.1 Initial Flow Composition

The first column of Table (5.1) provides the experimental conditions for the pyrolysis experiment. The detailed initial species composition data for the pyrolysis condition are provided in Table (5.2). The composition is tabulated in terms of bath gas (pre-second injection) composition and second-injection composition, respectively. This proves useful in modeling the conditions using the CHEMKIN flow reactor module. For the pyrolysis conditions, the reaction occurs under excess hydrogen (6.6%) and there is also an estimated 13 ppmv. of H radical in the bath gas flow as the products of the H₂- Air flame have not attained full equilibration under these rich flame conditions.

5.2.2 Temperature and Mixing Data

The experimental data for axial temperature along with the best fit profile is shown in Figure (5.1). There is no appreciable scatter in temperature data, hence scatter bars are not shown. The fitting curve starts from 400 K at time zero and corresponds to the temperature of the second-injector gas before mixing. The measured temperature at 0 second residence time corresponds to the bath gas temperature. The temperature fit rises sharply to meet the experimental data points at 1 millisecond where the injected fuel-nitrogen stream impinges on the axis of the flow reactor. This impingement corresponds to the sharp dip in the measured temperature profile between 0 and 1 millisecond after which the temperature reaches its well mixed adiabatic value of 1000 K further downstream.

The CO₂ mixing experiment results are shown next in Figure (5.2). The entrainment time constant is calculated to be 1.4 milliseconds and the mixing curve is plotted using this value. The mixing region is well captured by the modeled profile.

5.2.3 Fuel and Product Species Profiles

The Optimized JetSurf, the Lawrence Livermore mechanism, the CNRS mechanism and the CRECK mechanism predictions are compared with the experimental data for n-dodecane and the major intermediate species C₂H₄, C₃H₆ and CH₄. The JetSurf mechanism (in all cases, the optimized version has been used) is plotted using continuous lines while the other mechanisms are plotted using dotted lines. Experimental data are plotted as symbols with vertical scatter bars depicting the degree of variation across experimental runs. Residence time uncertainties are depicted as horizontal error bars for select data point values. Figure (5.3) compares JetSurf with LLNL; Figure (5.4) compares JetSurf with CNRS, and Figure (5.5) compares JetSurf with CRECK. The next set of figures plots the data for minor products including 1-C₄H₈, 1-C₅H₁₀, 1-C₆H₁₂ and C₂H₆ and compares the data with predictions from the four detailed mechanisms (refer to Figures (5.6), (5.7), (5.8)). The species being measured account for over 90% of the total fuel carbon (Figure 5.9). Note that the carbon balance is relative to the total carbon content in the injected n-dodecane under fully mixed conditions. Thus, the carbon balance profiles are above 100% in the initial mixing region where mixing is still incomplete. The uncertainties associated

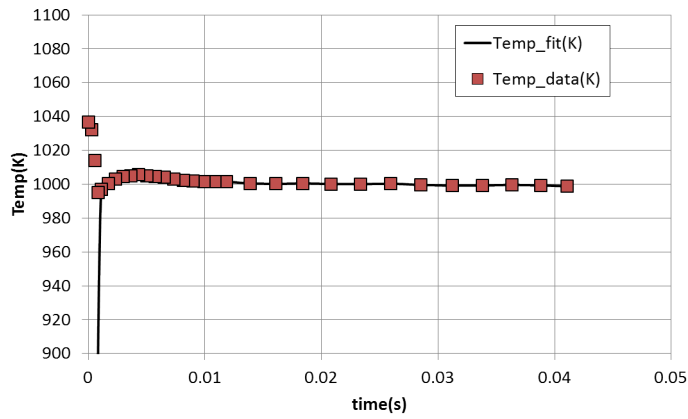
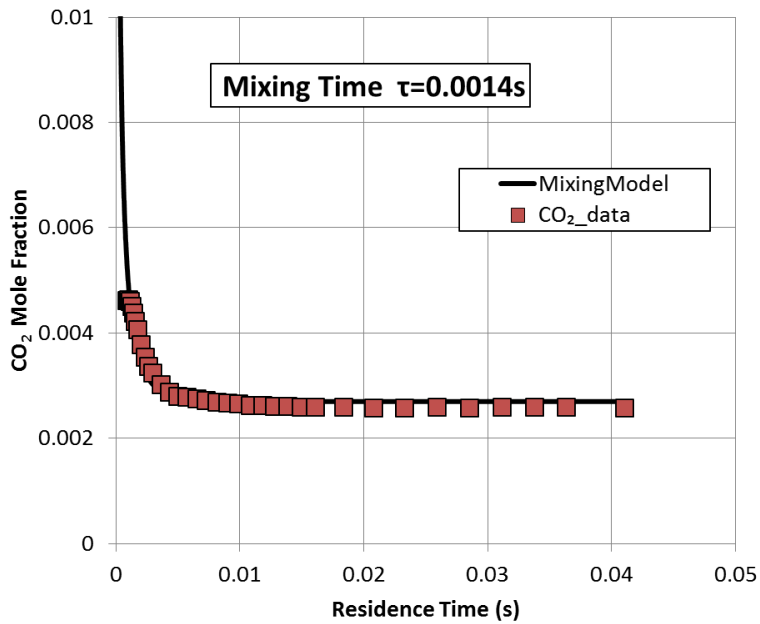


Figure 5.1: Pyrolysis Temperature Data.

Figure 5.2: Pyrolysis CO₂ Mixing Profile.

with the carbon balance measurements is about 5%. All simulations have been performed using the CHEMKIN PFR model using Zweitering Mixing Reacting Model based input profiles. According to the experimental data, 63% of fuel is decomposed by 39.5 milliseconds under these conditions. Figure (5.10) shows a bar graph representing the total carbon content of each of the measured product species at 39.5 millisecond residence time. The most salient points of interest are:-

1. Ethylene, propene, methane and 1-butene are the major products in descending order of importance. As Figure 5.10 demonstrates, in terms of carbon content, ethylene dominates all other product species from fairly early stages of fuel decomposition.
2. In terms of mechanism performance, the CNRS mechanism performs better overall (Figure (5.4) and Figure (5.8)). The optimized JetSurf performs well, though it overpredicts the rate of n-dodecane decomposition. The LLNL and CRECK mechanisms perform relatively poorly as they underpredict the rate of fuel decomposition by a considerable margin (Figure (5.5) and Figure (5.6)). As a result, the LLNL and CRECK mechanisms also underpredict the concentrations of ethylene, propene, 1-butene and most other intermediate species by a large margin (Figure (5.6) and Figure (5.8)). There is 23% variation range among the predictions of the fuel concentration among the 4 mechanisms at 39.5 ms point (see Figure 5.10) and smaller, but correlated variations among the product species. The experimental results fall within the band of predictions.
3. The ethylene species profile does not attain steady state at the end of the reactor exit, therefore calculating an ethylene yield will result in an under-estimate. Bearing this in mind, the exit ethylene yield (defined as maximum moles of ethylene per initial moles of the fuel) for the pyrolysis reaction condition is calculated to be 1.42.

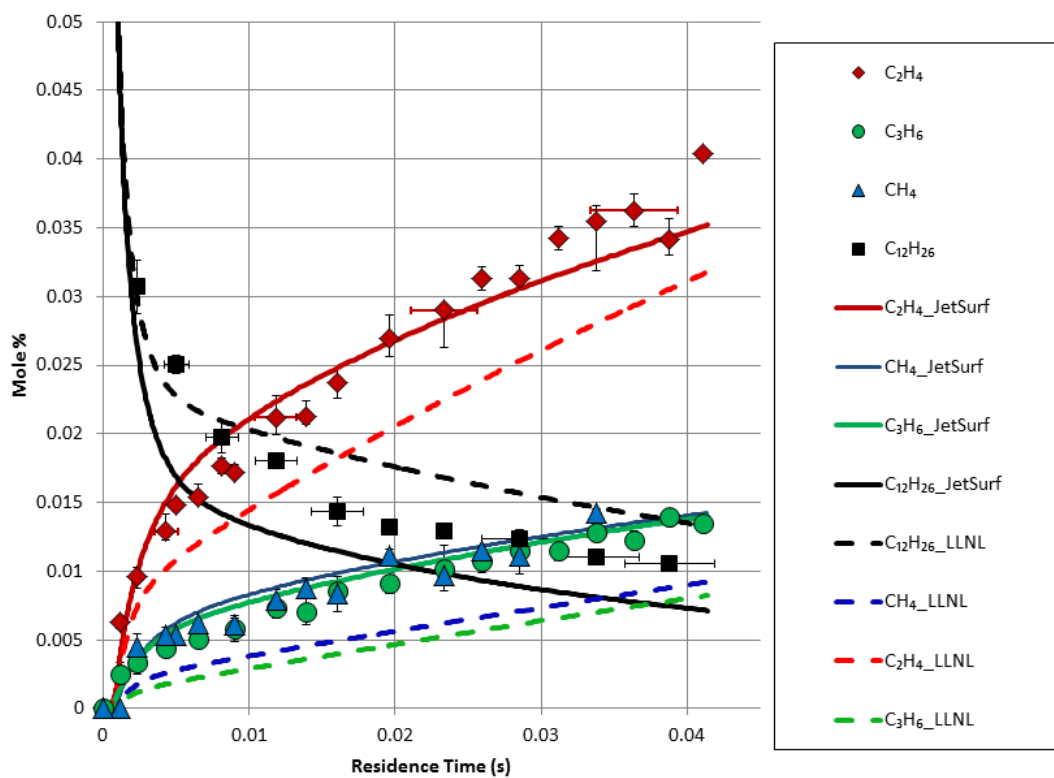


Figure 5.3: Pyrolysis Major Species Data compared with the JetSurf and LLNL Mechanisms.

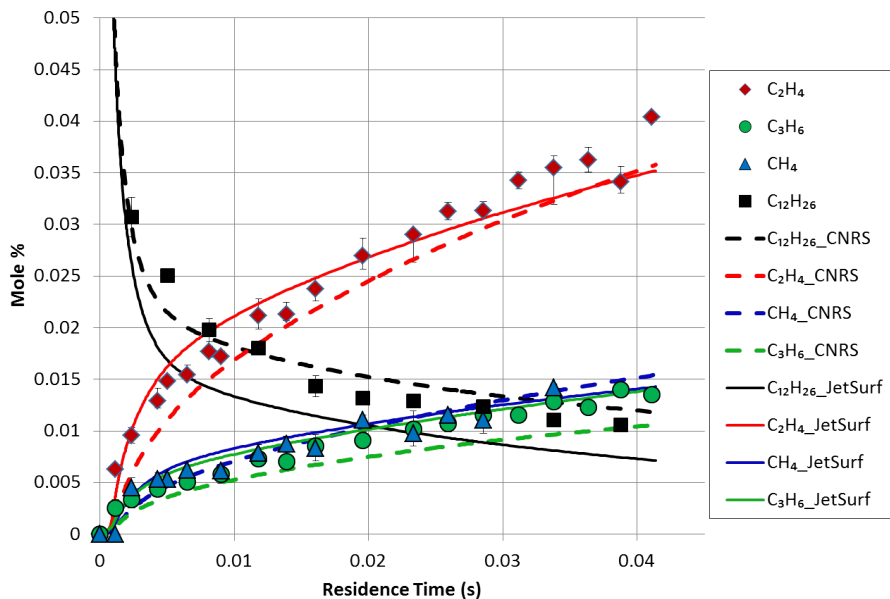


Figure 5.4: Pyrolysis Major Species Data compared with the JetSurf and CNRS Mechanisms.

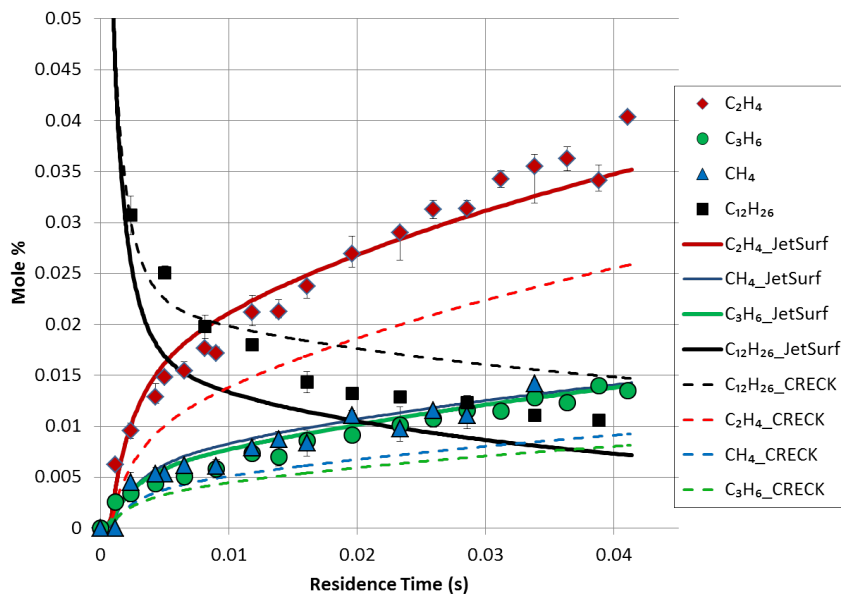


Figure 5.5: Pyrolysis Major Species Data compared with the JetSurf and CRECK mechanisms.

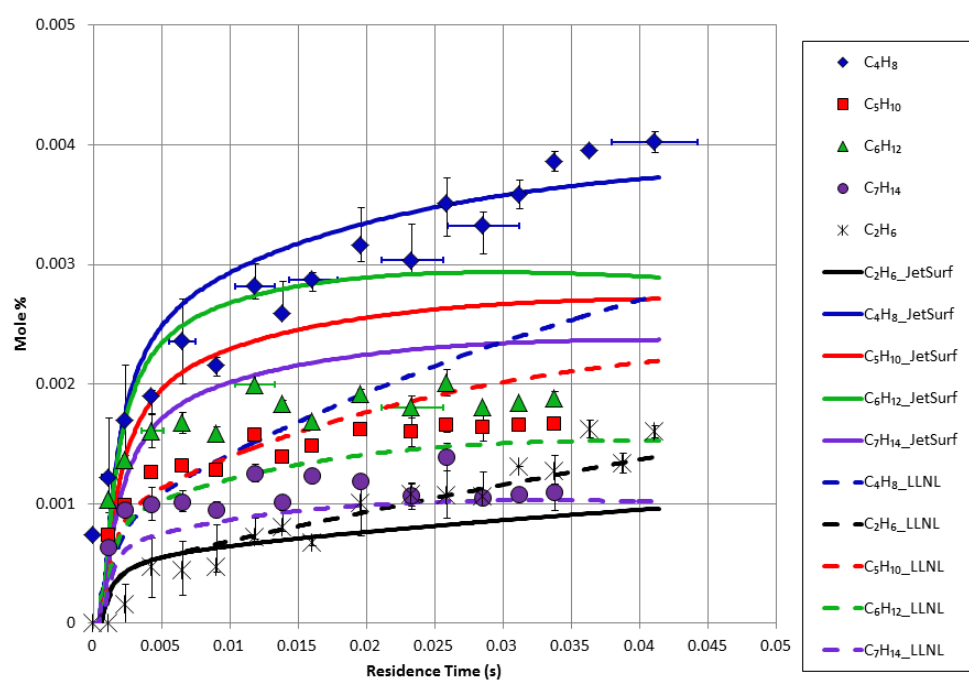


Figure 5.6: Pyrolysis Minor Species Data compared with the JetSurf and LLNL mechanisms.

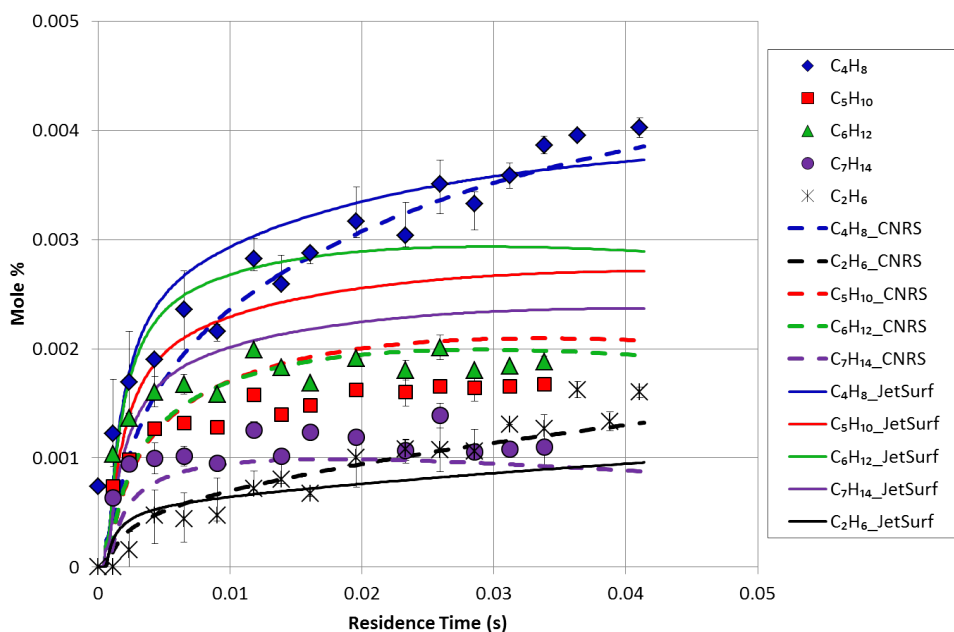


Figure 5.7: Pyrolysis Minor Species Data compared with the JetSurf and CNRS mechanisms.

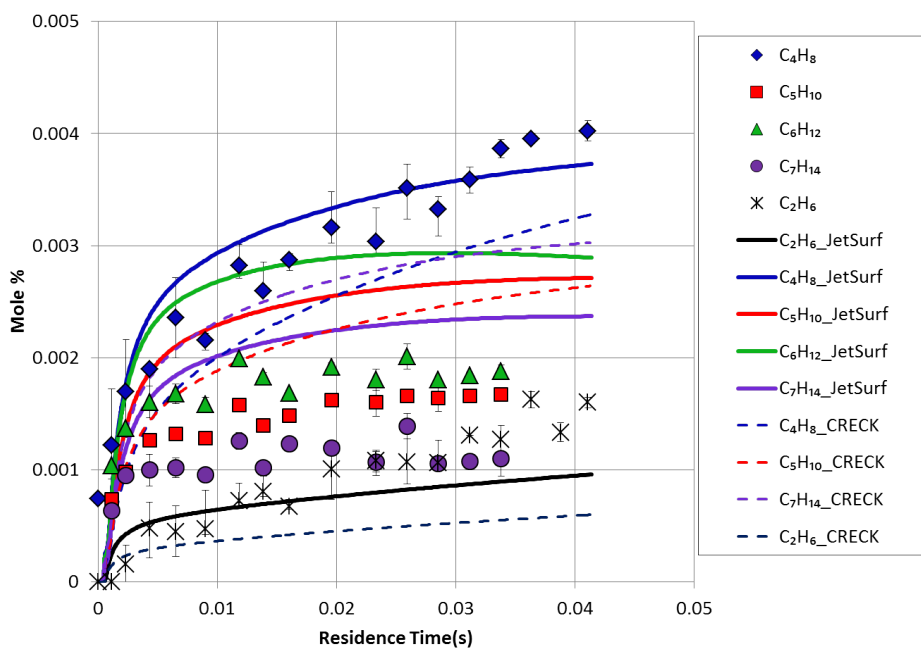


Figure 5.8: Pyrolysis Minor Species Data compared with the JetSurf and CRECK mechanisms.

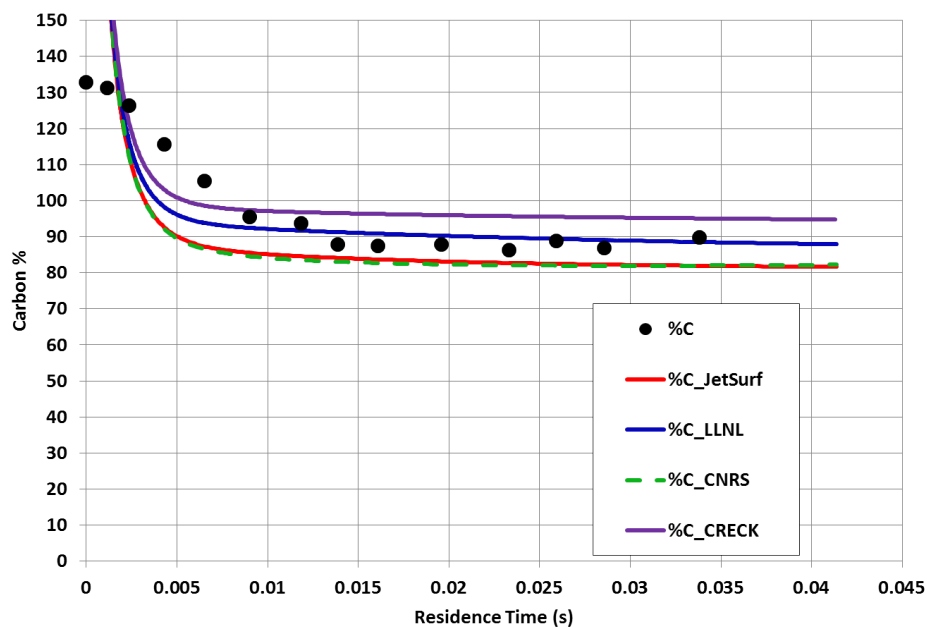


Figure 5.9: Pyrolysis Run Carbon Balance.

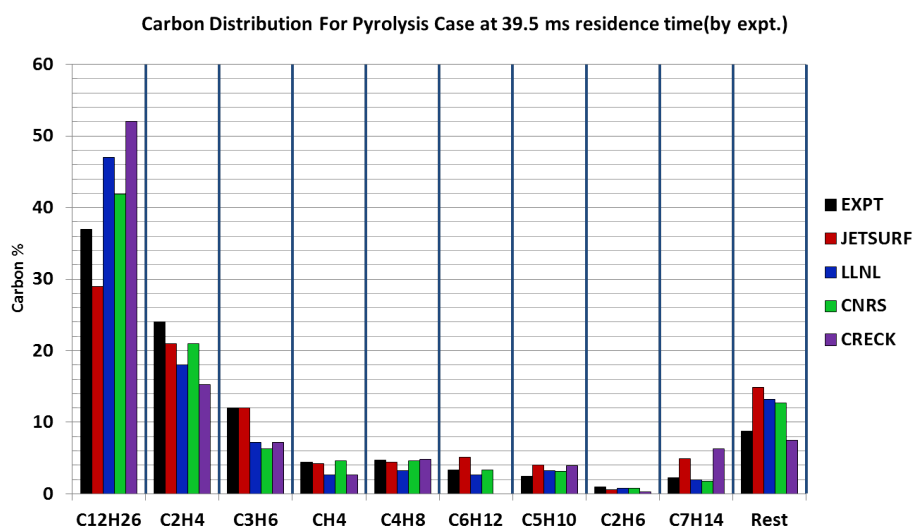


Figure 5.10: Pyrolysis Run, Carbon Distribution Over Species at 39.5 ms Residence.

5.3 1050 K Rich Oxidation Run

5.3.1 Initial Flow Composition

The second column of Table (5.1) provides information about the experimental conditions of the 1050 K run. The experimental stoichiometry is 1.56 and the nominal fuel load is 501 ppmv. The detailed initial species composition data for the 1050 K oxidation condition is provided in Table (5.3). The composition is tabulated in terms of bath gas (pre-second injection) composition and second-injection composition respectively. This proves useful in modeling the conditions using CHEMKIN. For the oxidation conditions, the hydrogen-air flame is lean and therefore there is no excess hydrogen or residual H radicals in the bath gas stream.

5.3.2 Temperature and Mixing Data

The experimental data for axial temperature along with the best fit profile is shown in Figure (5.11). The background temperature data (blue triangles) are plotted in addition to reactive temperature data (red squares). A small initial dip in temperature under fuel injection conditions may be attributed to the endothermic effects of fuel pyrolysis reactions. There is a small temperature rise at the very end of the flow reactor and indicates the onset of exothermic oxidative reactions becoming important. However, for all practical purposes, near isothermal conditions prevail over the majority of the reacting zone and heat generation is insignificant. There is no appreciable scatter in temperature data, hence scatter bars are not shown. The fitting curve starts from 400 K at time zero and corresponds to the temperature of the second-injector gas before mixing. The temperature fit rises sharply to meet the experimental data points at 1 millisecond where the injected fuel-nitrogen stream impinges on the axis of the flow reactor.

The CO₂ mixing experiment results are shown next in Figure (5.12). The entrainment time constant is calculated to be 0.69 milliseconds and the mixing curve is plotted using this value. The mixing region is well captured by the modeled profile.

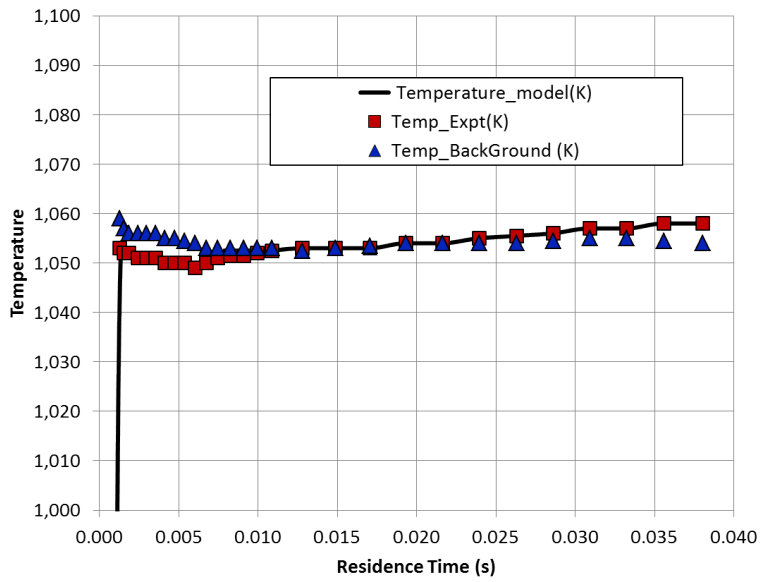
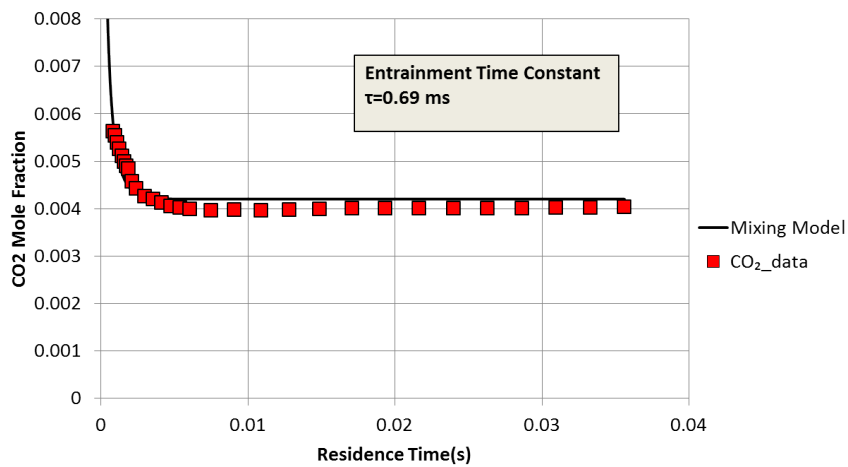


Figure 5.11: 1050 K Rich Oxidation Temperature Data.

Figure 5.12: 1050 K Oxidation CO₂ Mixing Profile.

5.3.3 Fuel and Product Species Profiles

The Optimized JetSurf, the Lawrence Livermore Mechanism, the CNRS mechanism and the CRECK mechanism predictions are compared with the experimental data for n-dodecane and the major intermediate species. Figure 5.13 compares the data for O_2 , $C_{12}H_{26}$ and C_2H_4 with all four mechanisms. Similarly, Figure (5.14) compares H_2 and CH_4 , while Figure (5.15) compares 1- C_3H_6 and 1- C_4H_8 . The minor species data for 1- C_5H_{10} , 1- C_6H_{12} and C_2H_6 are compared with the mechanism predictions in Figure (5.16). Vertical error bars represent the experimental scatter while horizontal error bars represent the residence time uncertainty estimates. All modeling has been performed using the CHEMKIN PFR module and Zweitering Mixing Reacting Model based input profiles (Section (3.4.4)). The experimental carbon balance (Figure (5.17)) for the measured species is around 85% and rising to 90% of the fuel load near the end of the 40 ms residence time. Simulations show that most of the remaining carbon is in the higher C_7 - C_{10} alkenes that exist at concentrations of around 5-15 ppm levels. These have not been measured. The uncertainty in the measured carbon balance is around 4%. According to the experimental data, 63% of original fuel is decomposed by 17 milliseconds under the run conditions. Figure (5.18) shows a bar graph representing the total carbon content of each of the measured product species at 17 millisecond residence time as well as predictions generated by the detailed mechanisms.. The primary observations are:-

1. There is negligible decrease in oxygen concentration pointing to the fact that oxidative reactions are insignificant compared to pyrolytic reactions in the first 40 milliseconds under the low temperature conditions being investigated. The CO concentration rises only to 80 ppmv at the reactor exit. Overall, oxygenated intermediates remain insignificant throughout the reaction zone.
2. The fuel decay rates are fairly well-predicted by all mechanisms apart from LLNL. The Lawrence Livermore mechanism predicts n-dodecane pyrolysis and alkene production to proceed significantly slower than the other mechanisms and the experimental data. In terms of overall performance, CNRS mechanism performs the best, correctly predicting the ethylene, propylene and hydrogen yields. It also performs well in predicting the production and eventual fall-off curves of the higher alkenes

1-hexene and 1-pentene. Optimized JetSurf runs slower than CNRS under these conditions and underpredicts the rate at which the higher alkenes fragment to form ethylene and propylene. Thus, while experimental results show that 1-hexene and 1-pentene peak at 15 ms, Optimized JetSurf predicts the peaks to occur at 30 ms with 50% higher peak values than observed. Curiously CRECK, mechanism predicts no 1-hexene generation at all pointing to a possible defect in the chemical reaction pathways.

3. The species distribution plot at 17 ms clearly demonstrate that ethylene, propylene and to some extent 1-butene contain the majority of the fuel carbon, even though the C₇-C₁₁ alkenes together also comprise a sizable amount. The bar graphs show that CNRS performs better at predicting the overall species distribution compared to other mechanisms. At longer residence times most of the carbon increasingly concentrate in C₂-C₃-C₄ alkenes.

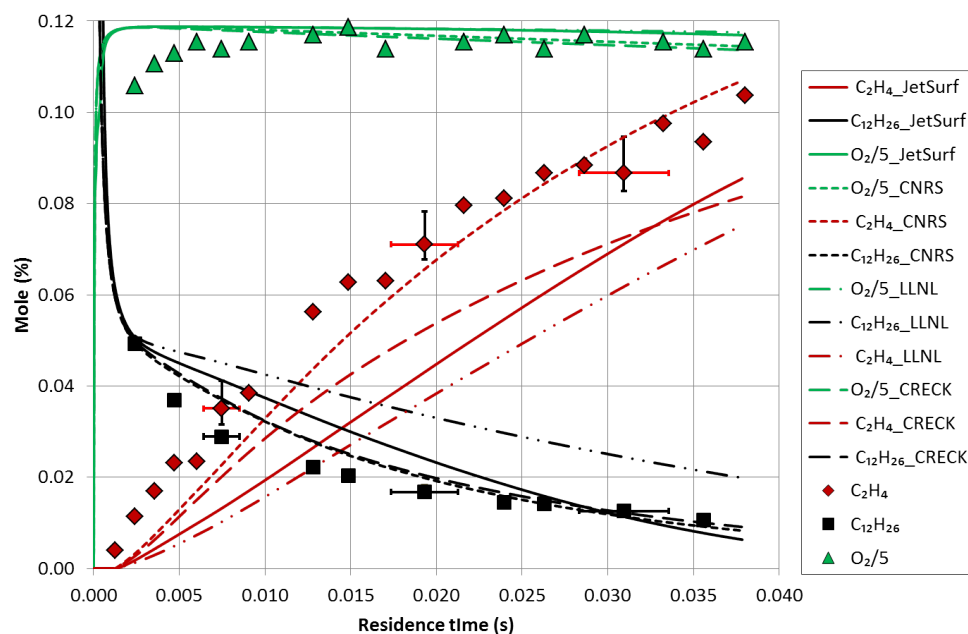


Figure 5.13: 1050 K Rich Oxidation Species Profiles 1.

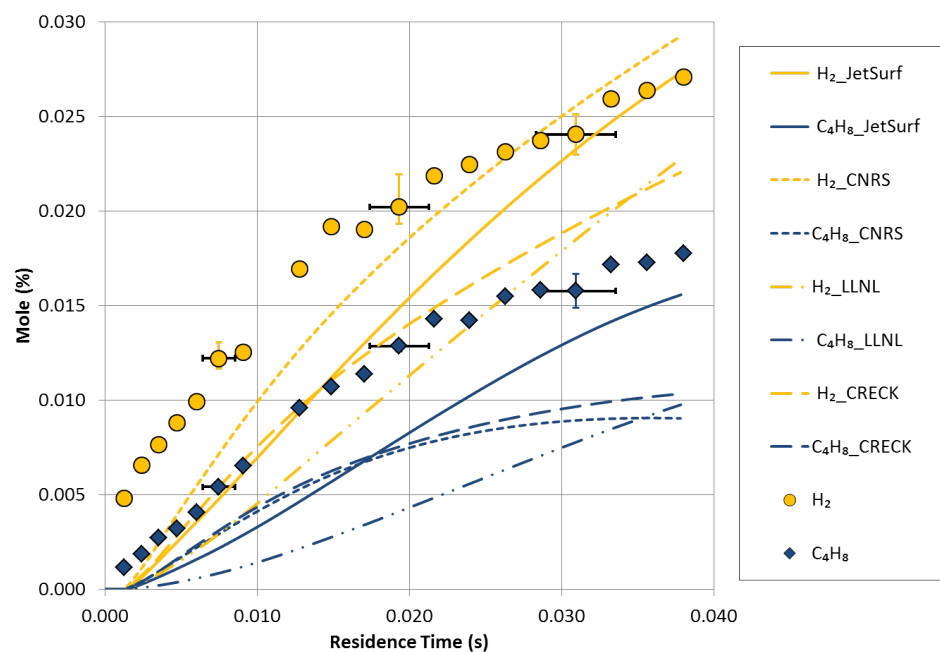


Figure 5.14: 1050 K Rich Oxidation Species Profiles 2.

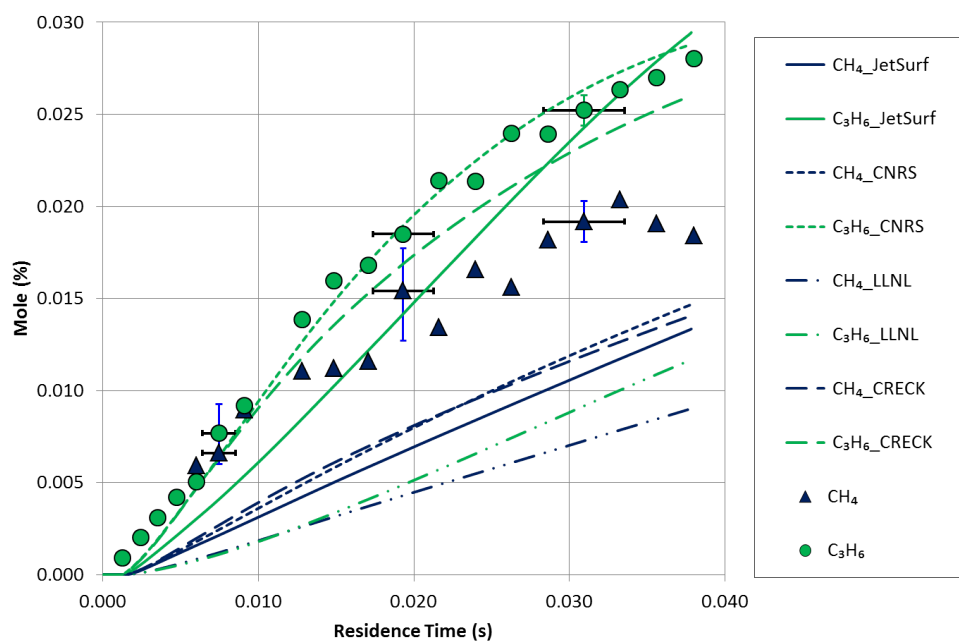


Figure 5.15: 1050 K Rich Oxidation Species Profiles 3.

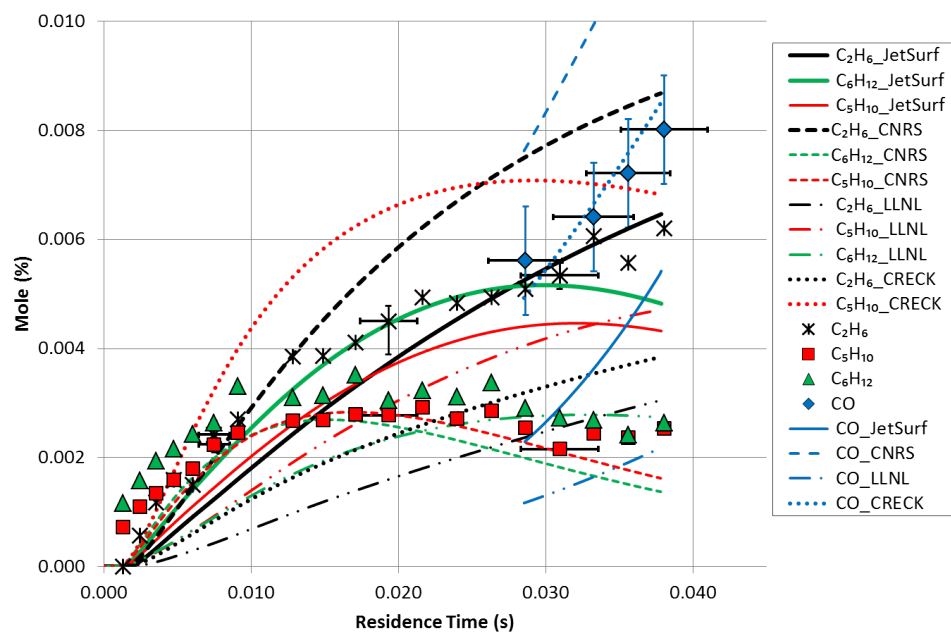


Figure 5.16: 1050 K Rich Oxidation Species Profiles 4.

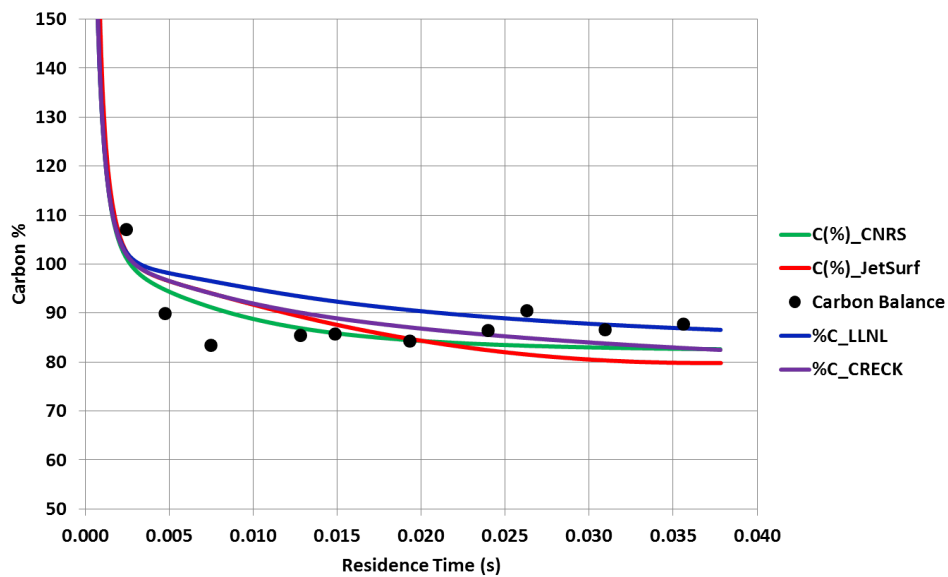


Figure 5.17: 1050 K Rich Oxidation Carbon Balance.

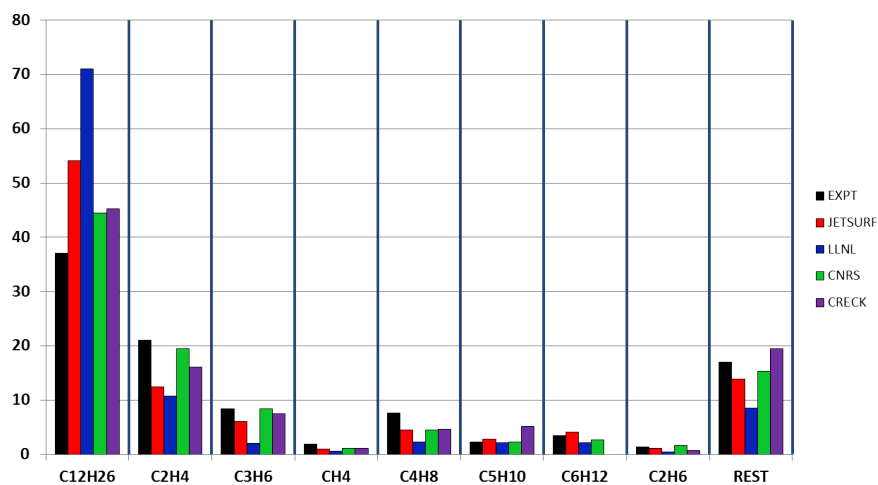


Figure 5.18: Carbon Distribution Over Species at 17 ms Residence Time for the 1050 K Oxidation Run.

5.4 1220 K Rich Oxidation Run

5.4.1 Initial Flow Composition

The third column of Table (5.1) provides the experimental conditions for this relatively higher temperature rich oxidation run. The experimental stoichiometry is 1.325 and the nominal fuel load is 569 ppmv. The detailed initial species composition data for the 1220 K oxidation condition is provided in Table (5.4). The composition is tabulated in terms of bath gas (pre-second injection) composition and second-injection composition respectively. This proves useful in modeling the conditions using CHEMKIN. For the oxidation conditions, the hydrogen-air flame is lean and therefore there is no excess hydrogen or residual H radicals in the bath gas stream.

5.4.2 Temperature Data and Mixing Profile

The experimental data for axial temperature along with the best fit profile is shown in Figure (5.19). The background temperature data (blue triangles) are plotted in addition to the reactive temperature data (red squares). The background temperature is 1220 K. However under fuel injection conditions the axial temperature begins to rise from about 16 ms as oxidative heat release reactions (primarily the conversion of CO to CO₂) assume importance. The final temperature increases to 1280 K near the end of the reaction zone. The fitting curve starts from 400 K at time zero and corresponds to the temperature of the second-injector gas before mixing. The temperature fit rises sharply to meet the experimental data points at 1 millisecond where the injected fuel-nitrogen stream impinges on the axis of the flow reactor.

The CO₂ Mixing Experiment results are shown in Figure (5.20). The entrainment time constant is calculated to be 1.6 milliseconds, and the mixing curve is plotted using this value. The mixing region is well captured by the modeled profile.

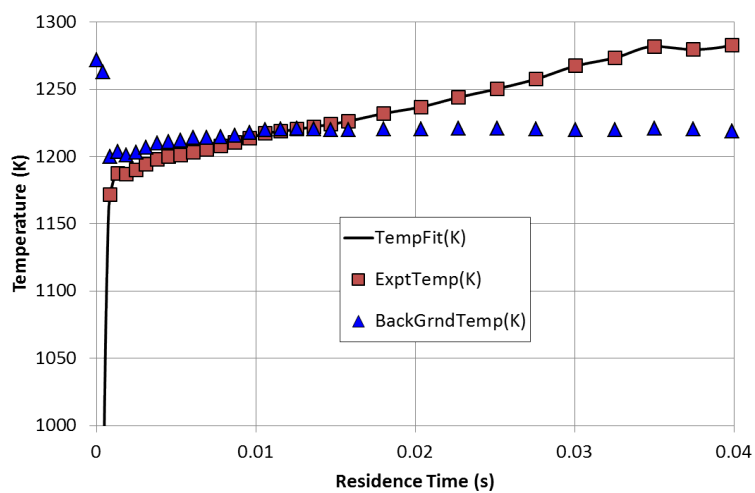


Figure 5.19: 1220 K Rich Oxidation, Temperature Profile.

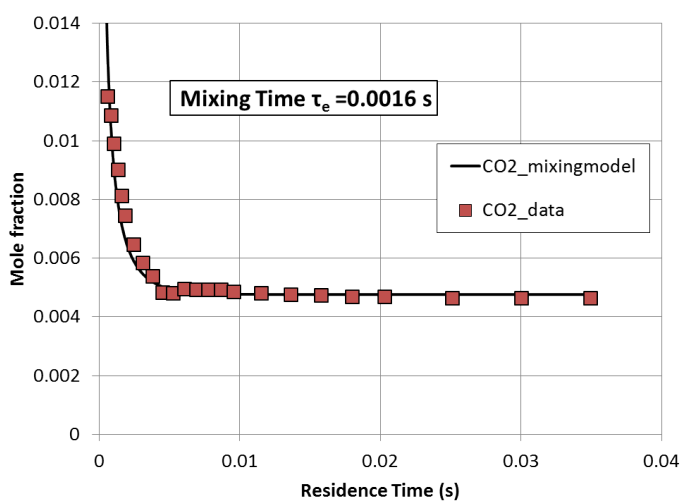


Figure 5.20: 1220 K Rich Oxidation, Mixing Profile.

5.4.3 Species Profiles

The optimized JetSurf, the Lawrence Livermore Mechanism, the CNRS mechanism and the CRECK mechanism predictions are compared with the experimental data for the major intermediate species. At 1220 K condition, the fuel n-dodecane reacts too rapidly to be measured in the flow reactor. Instead, the primary hydrocarbon intermediates, oxygenated species and hydrogen are measured experimentally. The first set of three figures (Figure (5.21), (5.22), (5.23)) compares the data for O_2 , H_2 , CO and CO_2 data with the four detailed mechanism predictions. The next set of three figures (Figure (5.24), (5.25), (5.26)) compares the data for the major hydrocarbon intermediates C_2H_4 , CH_4 and C_2H_2 with all four mechanisms. Similarly, (Figures (5.27), (5.28), (5.29)) compare the relatively minor intermediate products 1- C_3H_6 , 1- C_4H_8 , CH_2O and C_2H_6 with the four mechanisms. Experimental scatter have been plotted as vertical error bars while uncertainties in the residence time estimates have been plotted as horizontal error bars at some representative data points. All modeling has been performed using the CHEMKIN PFR module with Zweitering Mixing Reacting Model based input profiles. The experimental carbon balance, shown in Figure (5.30) for the measured species, is between 95-100% of the fuel load demonstrating that all significant species have been accounted for. The carbon balance uncertainty is estimated to be around 2%. A species distribution profile at a residence time of 15.8 milliseconds is plotted in Figure (5.31). The primary observations are:-

1. N-dodecane is no longer observed as at these temperatures, the rate of decomposition is so rapid that all of the n-dodecane breaks down in smaller fragment before 0.5 ms. The conversion of n-dodecane to smaller alkenes through the pyrolysis chemistry captured at the lower temperature conditions are here essentially complete before the oxidation of the alkene fragments begin. This points to a possible separation between the pyrolysis and the oxidation chemistry for the n-alkanes.
2. The C_2 - C_4 alkenes, the primary products of n-dodecane pyrolysis, peak within the mixing region at 2 ms residence time. The breakdown and oxidation of ethylene, propylene and 1-butene into products like formaldehyde, methane, acetylene and eventually CO and CO_2 are the major reaction processes that are captured in the flow-reactor regime at these higher temperatures. The consumption rate of ethylene

is well captured by the JetSurf mechanism though it predicts slower rates for 1-butene and propylene decay than are observed in the experiment. The CNRS and LLNL mechanisms predict slower rates of ethylene decomposition whereas the match is better for propylene and 1-butene species. CRECK mechanism predicts ethylene destruction profile accurately and does an overall better prediction in the case of 1-butene and propylene as well.

3. Methane and acetylene are the major hydrocarbon intermediates that peak later, at 18 ms and 23 ms, respectively, before decreasing to negligible levels by 38 ms. The behavior of these species and their concentrations are well predicted by the JetSurf and by the CRECK mechanism. However the CNRS and LLNL mechanisms predict a much slower rise and fall-off of CH_4 and C_2H_2 . Thus, for example, the CNRS mechanism predicts the CH_4 peak at 28 ms and the C_2H_2 peak at 38 ms even though the maximum concentration values are well predicted.
4. In concert with the temperature rise, the oxygen consumption rapidly increases from about 15 ms residence time onwards. CO peaks at 28 ms and most of the oxygen is consumed and CO_2 attains near maximum values at the end of the reaction zone. JetSurf predicts the profiles well, though the reaction proceeds somewhat faster than observed in line with ethylene predictions. The CRECK model performs the best, while LLNL and CNRS predict significantly delayed CO peaks at about 38 ms and associated slower rates of O_2 consumption and CO_2 generation. In general, mechanisms that predict C_2H_4 fall off well, also predict the profiles of product species with greater accuracy. The species distribution in terms of total carbon content is plotted at 15.8 ms in Figure (5.31) and show that by the time oxygen consuming reactions and heat release become important, most of the carbon is locked in ethylene and its subsequent oxidation products like carbon monoxide, methane and acetylene. The distribution also shows the very large under-estimations of CO formation by LLNL and CNRS models. An analysis of hydrogen generation profiles also reveal similar traits.

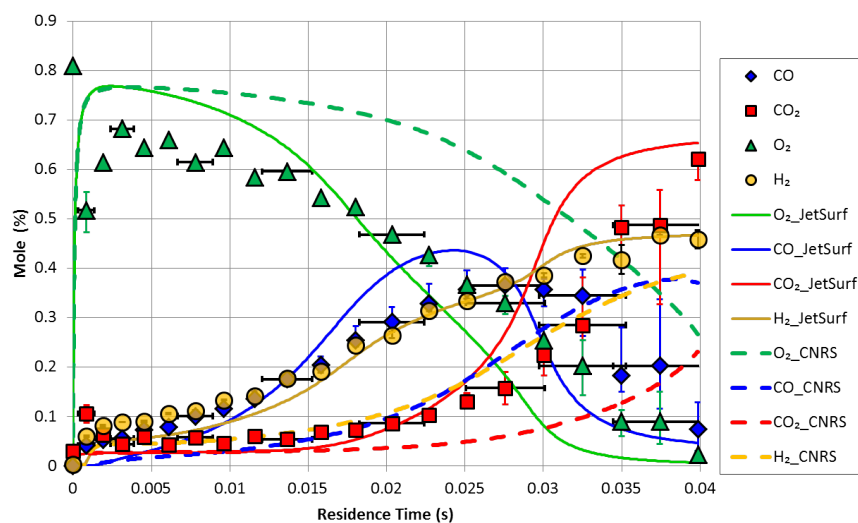


Figure 5.21: 1220 K Rich Oxidation - CO, CO₂, O₂, H₂ Profiles Compared to the JetSurf and CNRS Mechanisms.

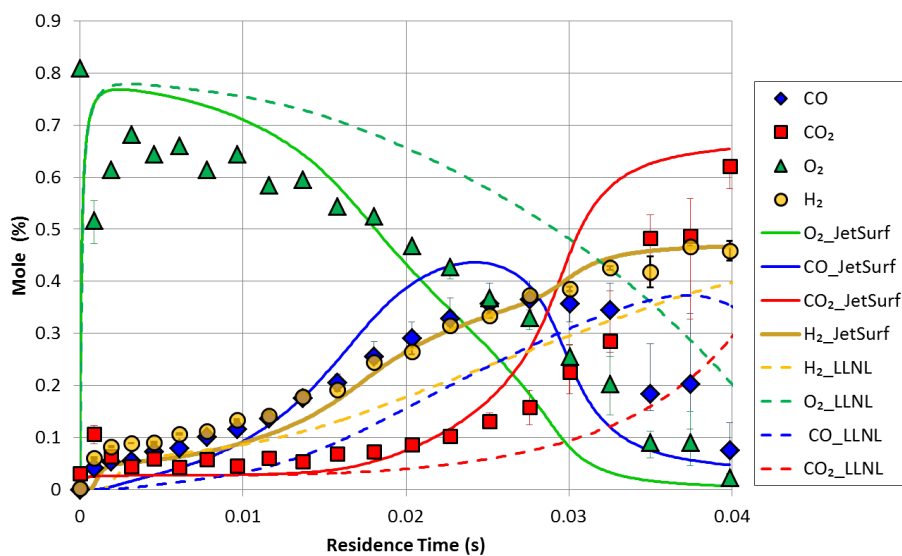


Figure 5.22: 1220 K Rich Oxidation - CO, CO₂, O₂, H₂ Profiles Compared to the JetSurf and LLNL Mechanisms.

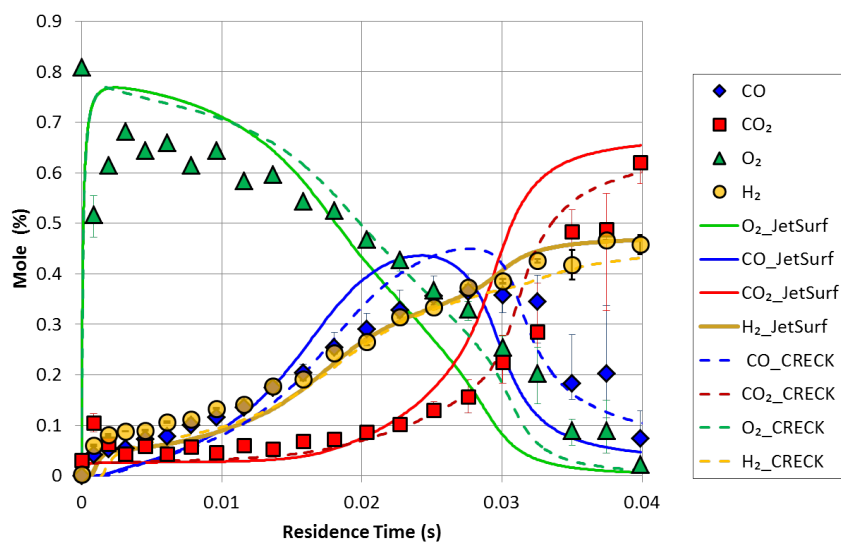


Figure 5.23: 1220 K Rich Oxidation - CO, CO₂, O₂, H₂ Profiles Compared to the JetSurf and CRECK Mechanisms.

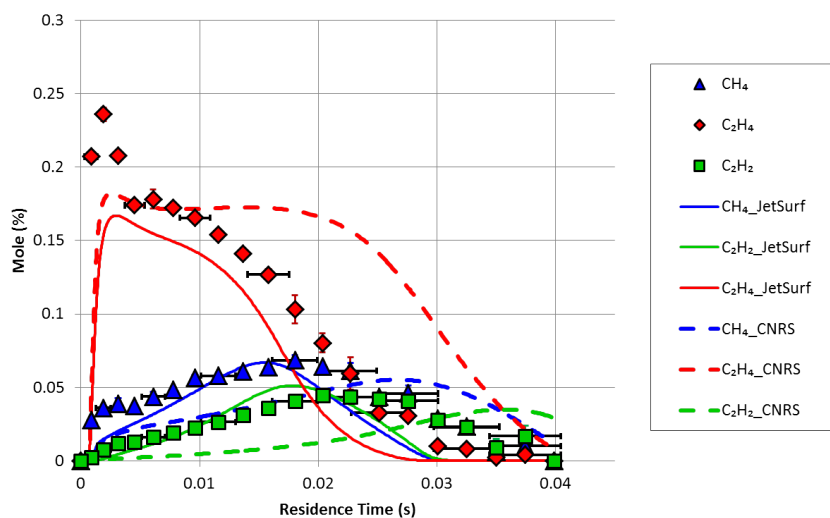


Figure 5.24: 1220 K Rich Oxidation - Major Hydrocarbon Product Profiles Compared to the JetSurf and CNRS Mechanisms.

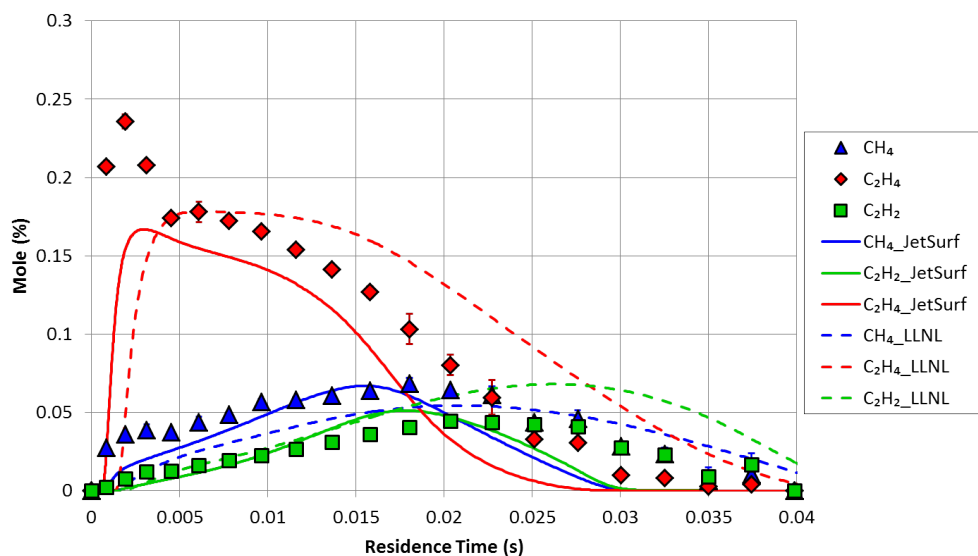


Figure 5.25: 1220 K Rich Oxidation - Major Hydrocarbon Product Profiles Compared to the JetSurf and LLNL Mechanisms.

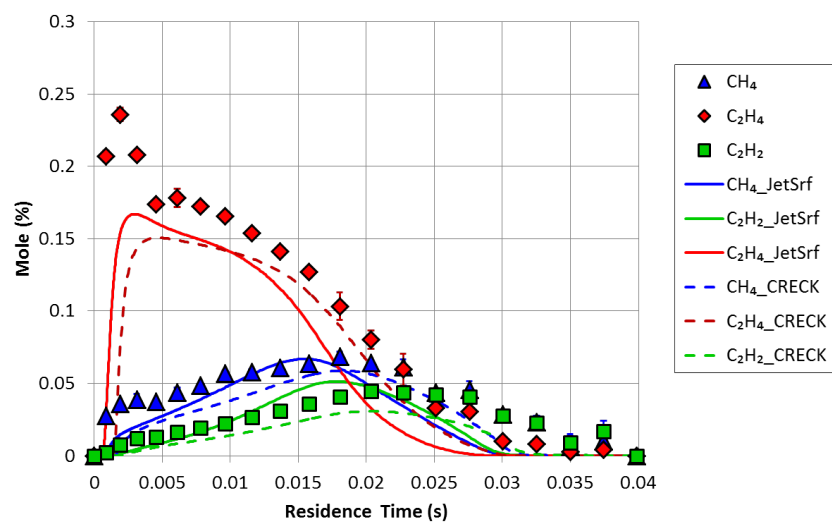


Figure 5.26: 1220 K Rich Oxidation - Major Hydrocarbon Product Profiles Compared to the JetSurf and CRECK Mechanisms.

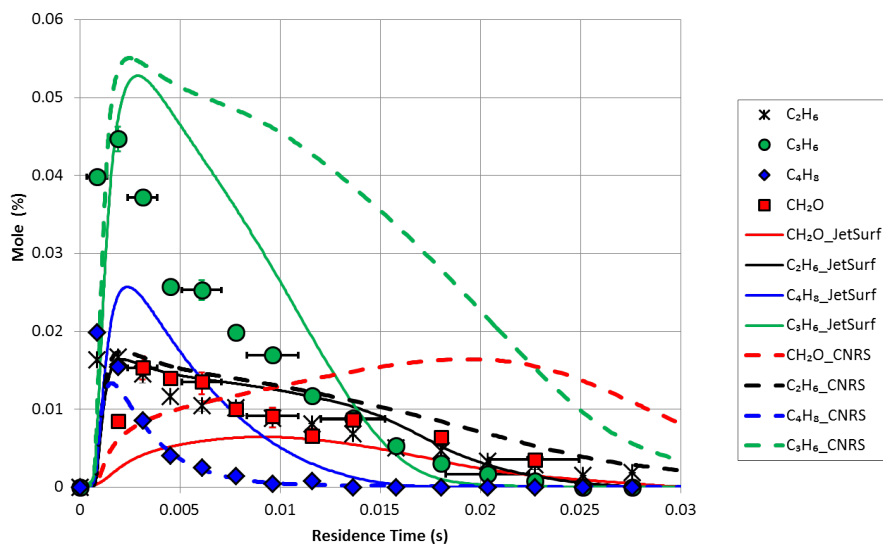


Figure 5.27: 1220 K Rich Oxidation - Minor Product Profiles Compared to the JetSurf and CNRS Mechanisms.

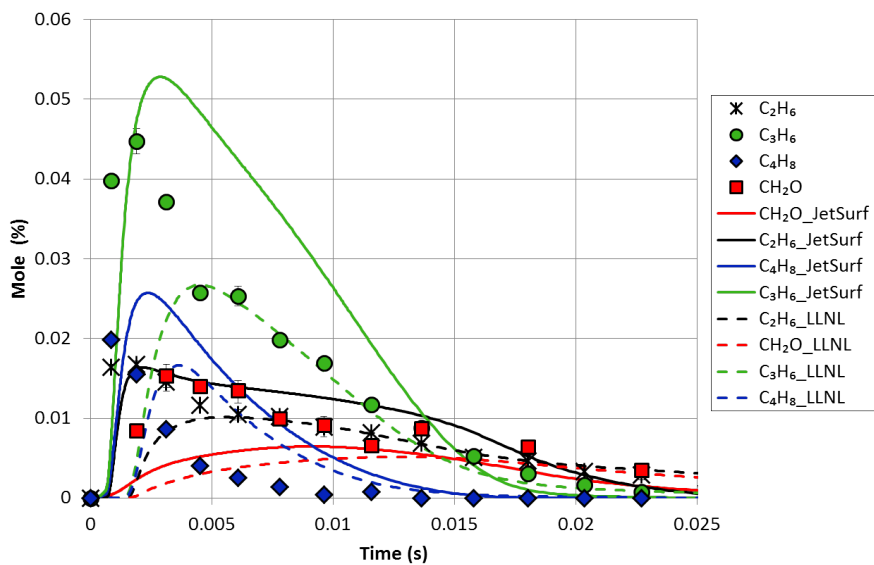


Figure 5.28: 1220 K Rich Oxidation - Minor Product Profiles Compared to the JetSurf and LLNL Mechanisms.

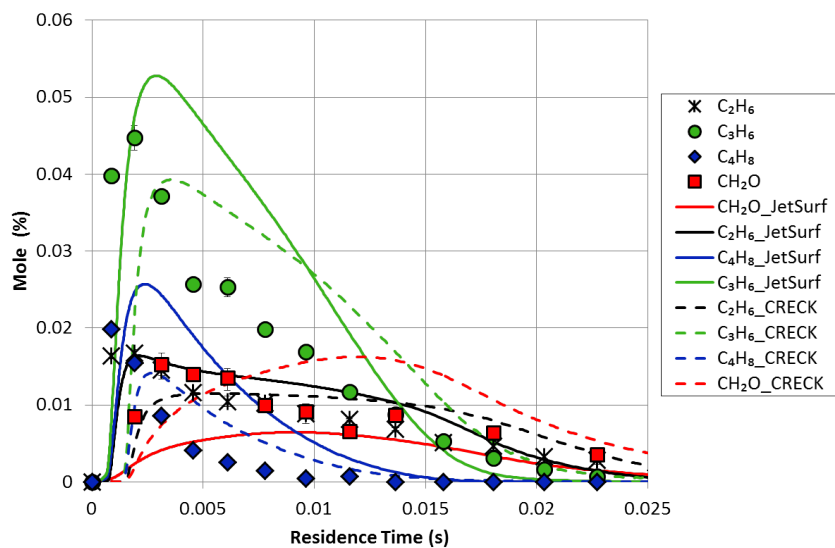


Figure 5.29: 1220 K Rich Oxidation - Minor Product Compared to the JetSurf and CRECK Mechanisms.

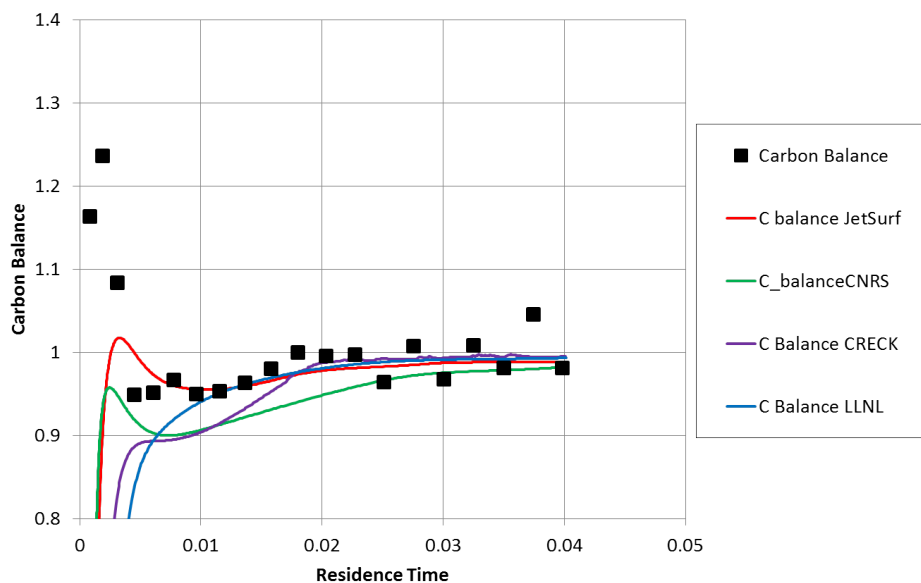


Figure 5.30: 1220 K Rich Oxidation - Carbon Balance.

5.5 1170 K Lean Oxidation Run

5.5.1 Initial Flow Composition

The fourth column of Table (5.1) provides the experimental conditions for the lean oxidation experiment. The experimental stoichiometry is 0.79 and the nominal fuel load is 328 ppmv. The detailed initial species composition data for the 1170 K oxidation condition is provided in Table (5.5). The composition is tabulated in terms of bath gas (pre-second injection) composition and second-injection gas composition respectively. This proves useful in modeling the conditions using CHEMKIN PFR code with two inlet streams.

5.5.2 Temperature Data and Mixing Profile

The experimental data for axial temperature along with the best fit profile is shown in Figure (5.32). The background temperature data (blue triangles) are plotted in addition to reactive temperature data (red squares). The background temperature is 1170 K. However, under fuel injection conditions the axial temperature begins to rise after about 20 ms as oxidative heat release reactions (primarily the conversion of CO to CO₂) assume importance. The final temperature increases to 1210 K by the end of the reaction zone. The fitting curve starts from 400 K at time zero and corresponds to the temperature of the second-injector gas before mixing. The temperature fit rises sharply to meet the experimental data points at 1 millisecond where the injected fuel-nitrogen stream impinges on the axis of the flow reactor thus causing a sharp drop in the measured axial temperature at the mixing region. The CO₂ Mixing Experiment results are presented next in Figure (5.33). The entrainment time constant is calculated to be 2.4 milliseconds and the mixing curve is plotted using this value. The mixing region is well captured by the modeled profile.

5.5.3 Species Profiles

The optimized JetSurf, the Lawrence Livermore Mechanism, the CNRS mechanism and the CRECK mechanism predictions are compared to the experimental data for the major intermediate species. At the 1170 K condition, the fuel n-dodecane reacts too rapidly

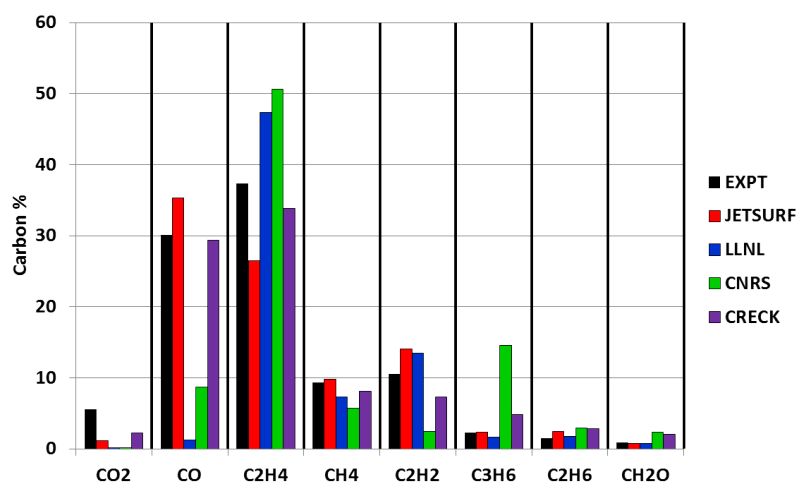


Figure 5.31: 1220 K Rich Oxidation - Carbon Distribution Over Species at 15.8 ms Residence Time.

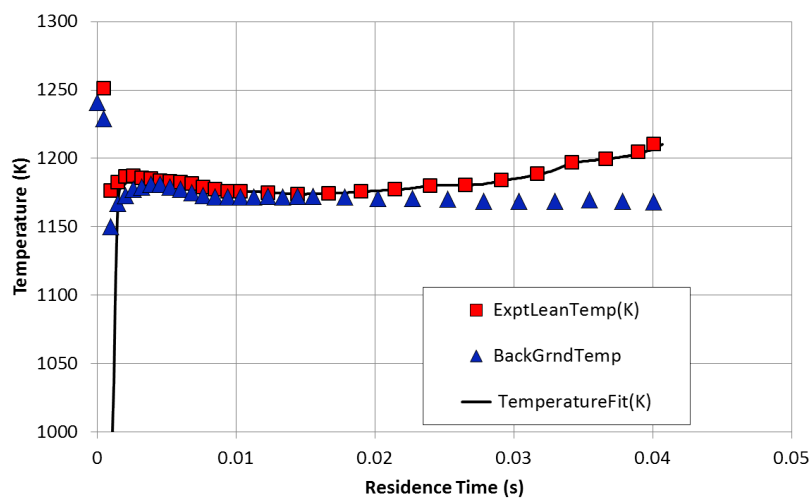
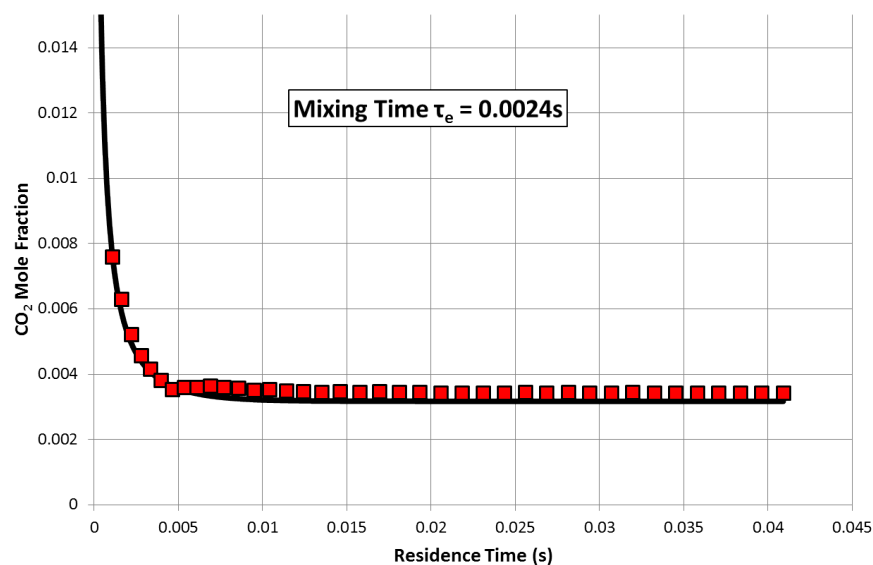
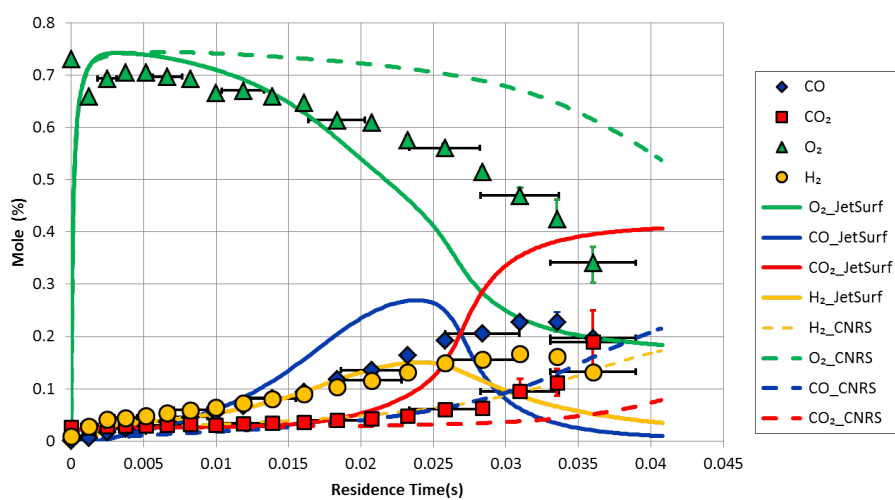


Figure 5.32: 1170 K Lean Oxidation - Temperature Profile.

to be measured in the flow reactor. Instead the primary hydrocarbon intermediates, oxygenated species and hydrogen are measured experimentally. The first set of three figures (Figure (5.34),(5.35),(5.36)) compares the data for O_2 , H_2 , CO and CO_2 with the four detailed mechanism predictions. The next set of three figures (Figure (5.37), (5.38), (5.39)) compares the data of the major hydrocarbon intermediates C_2H_4 , CH_4 and C_2H_2 with all four mechanisms. Similarly the Figures (5.40), (5.41), (5.42) compare the relatively minor intermediate products 1- C_3H_6 , 1- C_4H_8 and C_2H_6 with the predictions of the four mechanisms. All modeling has been performed using CHEMKIN PFR module using Zweitering Mixing Reacting Model based input profiles. The experimental carbon balance (Figure (5.43)) for the measured species is between 95-100% of the fuel load demonstrating that all significant species have been accounted for. The major points of interest are:-

1. Once again, n-dodecane is not observed as it breaks down into small fragments at very early residence time. The pyrolysis and the oxidation stages of the fuel chemistry remain separate for these lean conditions as well.
2. Due to lower temperature than the 1220 K Rich Oxidation run, the reaction proceeds somewhat slowly. The CO profile peaks at 34 ms and H_2 profile peaks at 32 ms. However the C_2 - C_4 alkenes still peak within the mixing region, at 2 ms residence time and the reaction pathways that are primarily observed in the reaction zone of the flow reactor are the decay of the alkenes into products like CO, CO_2 , C_2H_2 and CH_4 .
3. Qualitatively, the mechanism behaviors are very similar to what were noted in the rich 1220 K oxidation case. CNRS proceeds the slowest followed by the LLNL mechanism. The CRECK mechanism provides the most accurate prediction while JetSurf predicts a faster rate of reaction than is observed during the experiment. The predictions of most of the product species are strongly correlated with how well the mechanism under question is able to predict the ethylene consumption profile. Compared to the rich oxidation condition, JetSurf's prediction are somewhat poor, the CO peak is predicted at 25 ms and overall the reaction mechanism proceeds nearly as fast as at 1220 K demonstrating a lesser sensitivity to temperature decrease than what the experimental data suggest.

Figure 5.33: 1170 K Lean Oxidation - CO₂ Mixing Profile.Figure 5.34: 1170 K Lean Oxidation - CO, CO₂, O₂, H₂ Profiles Compared to the JetSurf and CNRS Mechanisms.

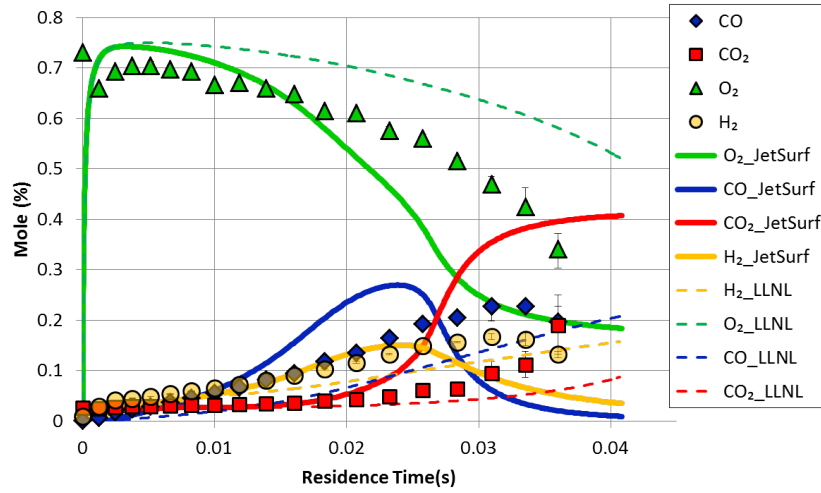


Figure 5.35: 1170 K Lean Oxidation-CO, CO₂, O₂, H₂ Profiles Compared to the JetSurf and LLNL Mechanisms.

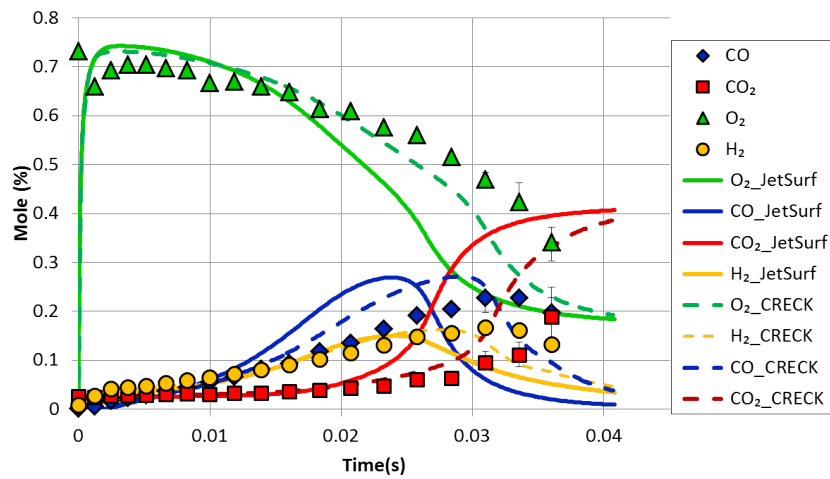


Figure 5.36: 1170 K Lean Oxidation-CO, CO₂, O₂, H₂ Profiles Compared to the JetSurf and CRECK Mechanisms.

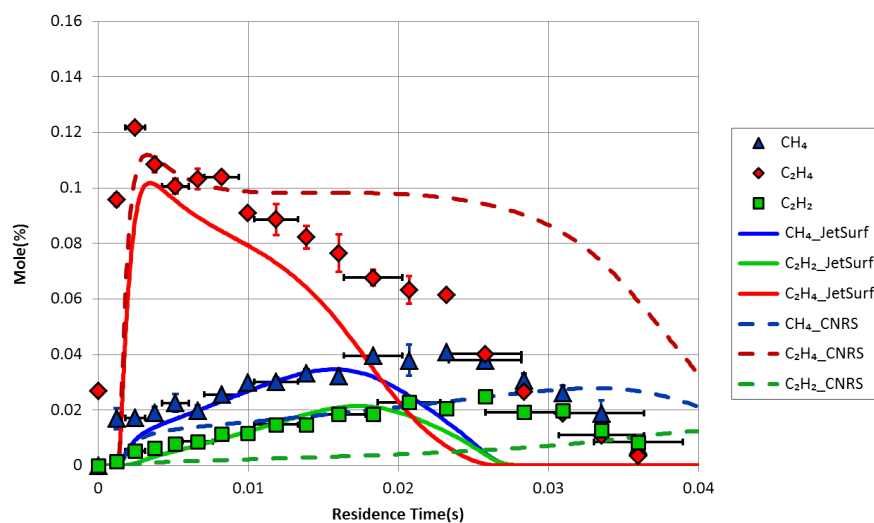


Figure 5.37: 1170 K Lean Oxidation - Major Hydrocarbon Product Profiles Compared to the JetSurf and CNRS Mechanisms.

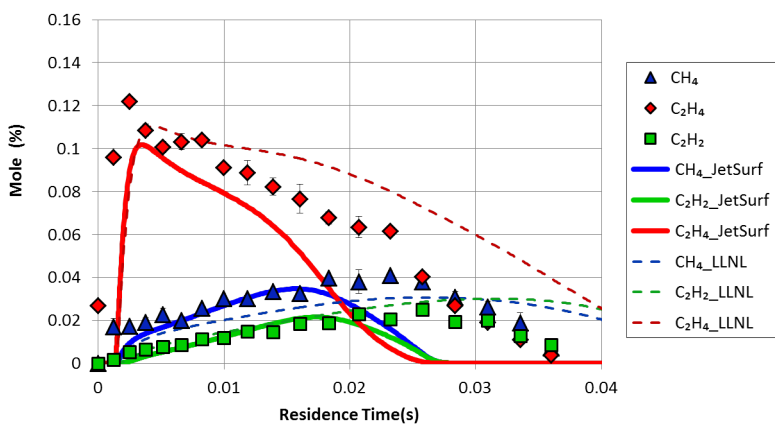


Figure 5.38: 1170 K Lean Oxidation - Major Hydrocarbon Product Profiles Compared to the JetSurf and LLNL Mechanisms.

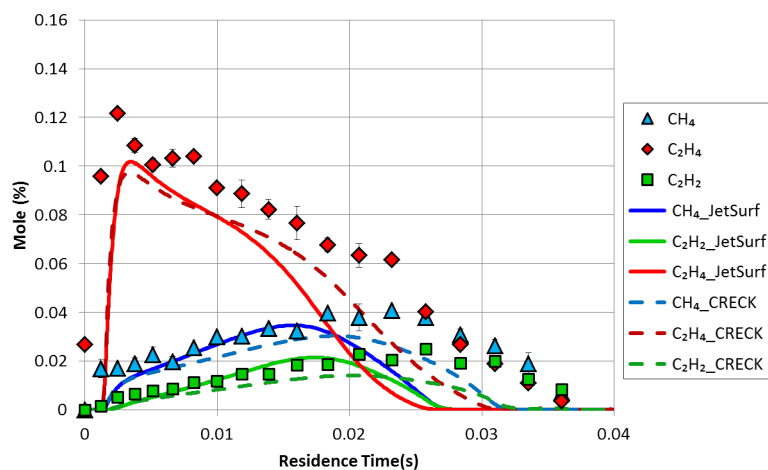


Figure 5.39: 1170 K Lean Oxidation - Major Hydrocarbon Product Profiles Compared to the JetSurf and CRECK Mechanisms.

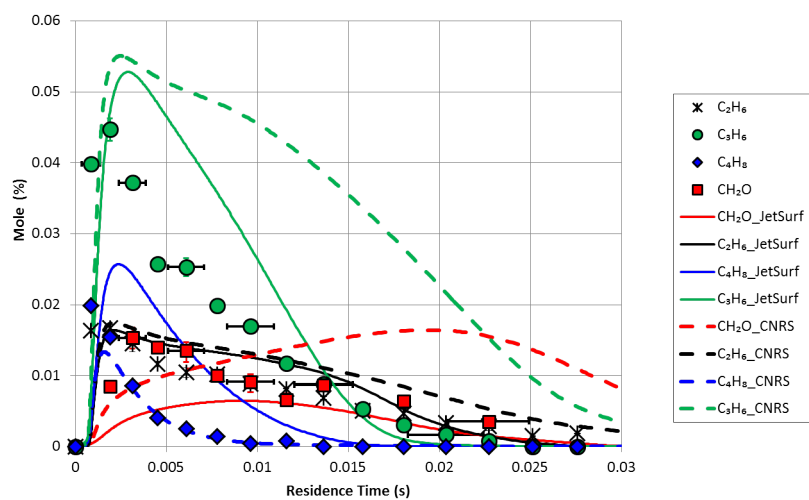


Figure 5.40: 1170 K Lean Oxidation - Minor Product Profiles Compared to the JetSurf and CNRS Mechanisms.

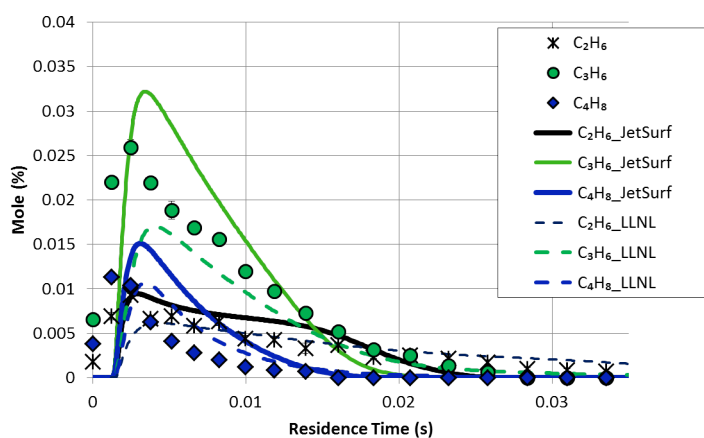


Figure 5.41: 1170 K Lean Oxidation - Minor Product Profiles Compared to the JetSurf and CNRS Mechanisms.

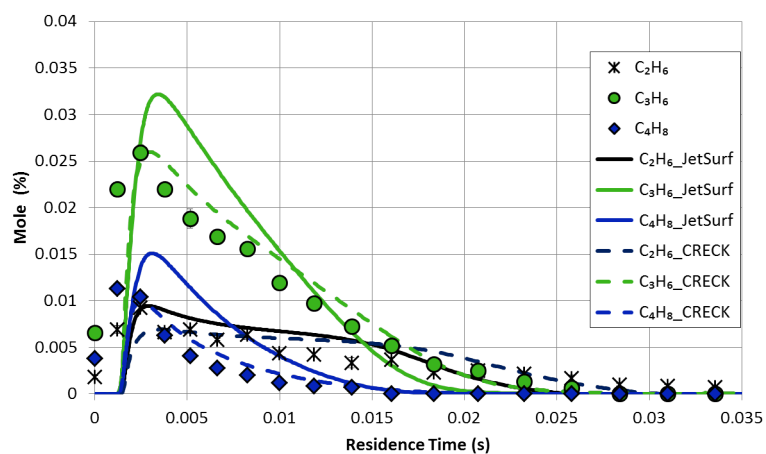


Figure 5.42: 1170 K Lean Oxidation - Minor Product Profiles Compared to the JetSurf and CNRS Mechanisms.

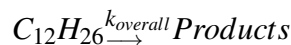
5.6 Comparative Analysis with Relevant External Data Sets

The current work investigates a relatively narrow but crucial temperature range within the n-dodecane combustion chemistry regime. It is therefore necessary to investigate how well the current experimental data set bridges the zone between the low temperature and NTC regime spanning 500 K-800 K and the high temperature regime spanning 1300 K and above. Towards this end the following comparisons have been made in this section,

1. The overall n-dodecane decomposition rate for the 1000 K pyrolysis and 1050 K rich oxidation conditions have been determined and plotted against recent results and an empirical fit developed by MacDonald et al. (2013).
2. An estimate of the peak ethylene yields have been made from the these data sets and compared with data from MacDonald et al. (2013).
3. The 1220 K rich oxidation data set have been compared against the species time history profiles generated from a shock tube study by Davidson et al. (2011) in order to provide a more complete view of the fuel oxidation kinetics over a broad range of temperature and time scales.
4. The molar conversion rates of the fuel and the associated product concentration time histories for the pyrolysis condition have been compared with data sets generated from a Jet Stirred Reactor by Herbinet et al. (2007) at near identical temperatures and the effect of vitiation has been discussed.

5.6.1 Overall Fuel Decomposition Rate and Peak Ethylene Yield

The decomposition of n-dodecane occurs through multiple pathways. Initiation occurs through uni-molecular decomposition, but at the temperatures range of interest, H abstraction reactions facilitated by H and OH radicals soon dominate the process. However it is often convenient to model the decomposition in terms of pseudo first order kinetics of the form :



where a pseudo first order equation for the fuel mole fraction can be written as

$$\frac{[C_{12}H_{26}]}{[C_{12}H_{26}]_0} = \exp(-k_{overall} \times t) \quad (5.1)$$

The fuel time history profile is used to determine the pseudo first order rate coefficient. Since at 1050 K, the fuel breakdown is relatively independent of oxidation effects, $k_{overall}$ has been calculated for the 1050 K run as well. MacDonald (2012) tabulated the overall decomposition rate data for temperatures ranging from 1600 K to 1100 K from several sources. However, there are very few measurements in the intermediate 1100 K-900 K region, and the current calculations prove useful to bridge the gap. The authors provide a best fit for $k_{overall} = A \exp(-E_a/RT)$ for n-dodecane as $A = 7.46 \times 10^{12} \text{ s}^{-1}$ and $E_a = 227 \text{ kJ/mol}$ respectively. The calculated value of k for the 1000 K and 1050 K conditions matches well with the best fit line. The fit is further improved if the effect of water is accounted for. The flow reactor operates under vitiated conditions with 22% water present in the bath gas, the rest being primarily nitrogen. As a third body, water molecules are more efficient than inert molecules like nitrogen or argon. In the pyrolysis reaction water molecules are responsible for increasing the H radical production rate by accelerating the reaction $C_2H_5(+M) \rightleftharpoons C_2H_4 + H(+M)$ which acts as the primary source of H atoms in the system. Based on the water concentration, a correction factor of 2.1 is introduced in the pseudo first order coefficient. As seen from Figure (5.44), this further improves the fit.

The peak or the plateau value for ethylene, the most important product of decomposition, is also an important target for kinetic schemes. MacDonald (2012) obtained data sets plotting the dependence of peak ethylene yield versus temperature under n-dodecane pyrolytic conditions. The current study extends this to intermediate temperatures. As seen in Figure (5.45) the present data fits in nicely. One must be aware that the ethylene yields were measured at 19 atm. pressures while the current data are measured at atmospheric pressure. However, the n-dodecane decomposition rate and the ethylene peak values are relatively insensitive to pressure as the sensitive pressure dependent reactions relevant for

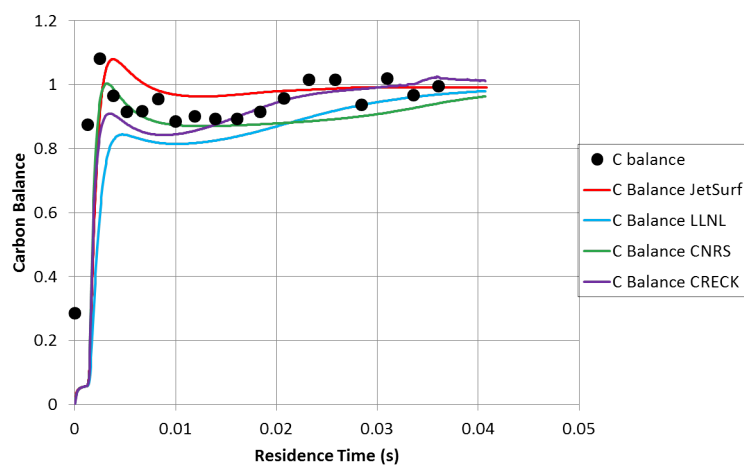


Figure 5.43: 1170 K Lean Oxidation - Carbon Balance.

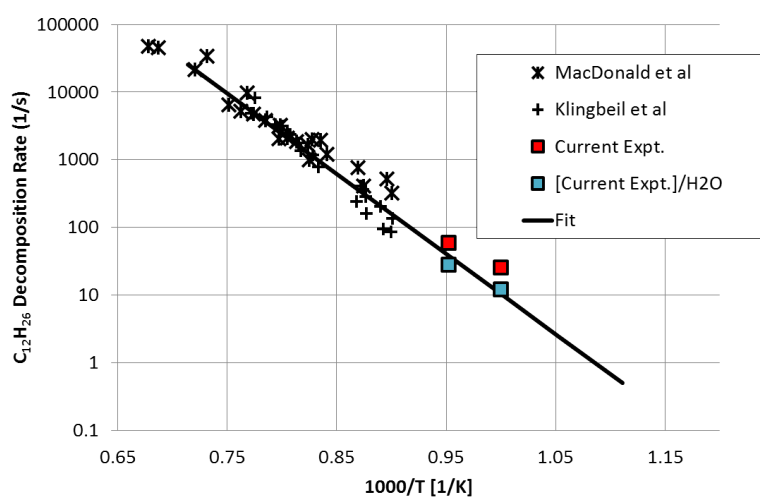


Figure 5.44: Overall Decomposition Rates of n-dodecane.

the pyrolysis pathways are mostly near the high pressure limit. Therefore no significant discrepancies are expected from the pressure mismatch.

5.6.2 Species Profiles from Shock Tube Experiments

Davidson et al. (2011) measured the concentration time histories of n-dodecane, ethylene, OH, carbon dioxide and water between 1170 K-1600 K at 2 atm. pressure and 450 ppm fuel under stoichiometric conditions. The 1 atm. rich 1220 K oxidation data from the current experiment are plotted with the shock tube data in order to gain a better insight as to how the time scales of species profile evolution change with temperature. The n-dodecane conversion profile at 1170 K from the Davidson et al. (2011) data have also been compared with the 1050 K oxidation data.

The comparison is imperfect as the stoichiometry of 1050 K run is 1.56 while the Davidson et al. (2011) data set stoichiometry is 1. The presence of water is also expected to increase the n-dodecane decomposition rates of the current run. However, in Figure (5.46), the temperature dependence of fuel consumption rates are evident. At 1390 K, the fuel consumption begins before 0.01 ms; at 1170 K the n-dodecane profile begins to decrease after 0.7 ms, while at 1050 K the falloff begins at 3 ms. The rapid decay of n-dodecane at 1170 K also shows why the fuel is undetectable at the two high temperature oxidation runs in the flow reactor.

The ethylene data from 1220 K have been plotted against the shock tube species profiles in Figure (5.47). The 1403 K condition and 1330 K condition are from Davidson et al. (2011). It is clear that the peak ethylene value is more or less independent of temperature (at least in a log-log scale). However, the timing of the peak and the ethylene profile itself changes with temperature. All ethylene concentration profiles begin with a gradual rise to a peak and then a very sharp drop off. However, the slope of the rising segment of the ethylene profile becomes steeper with decreasing temperature and the ethylene peak occurs later. Thus, the peak is at 0.5 ms at 1400K, at 0.8 ms at 1330 K and around 5 ms for 1220 K oxidation. For 1050 K case, the C_2H_4 curve continues to rise beyond the observed range of residence time.

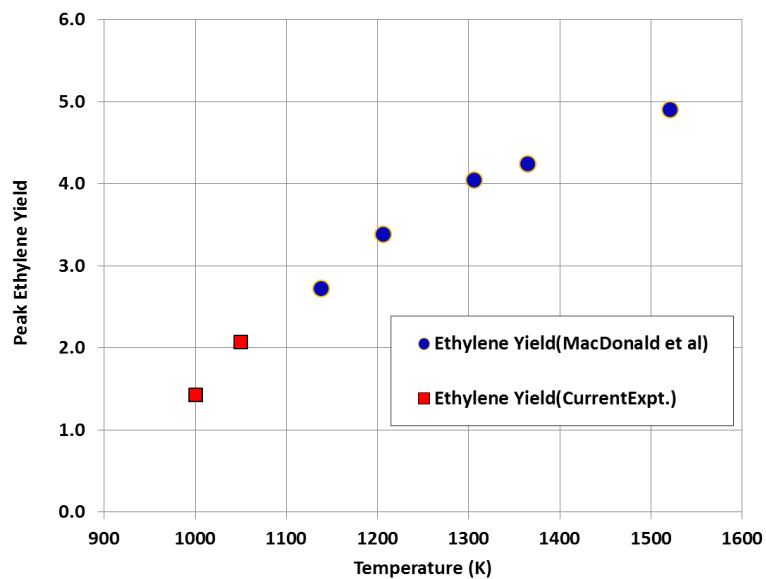


Figure 5.45: Peak Ethylene Yield versus Pyrolysis Temperature.

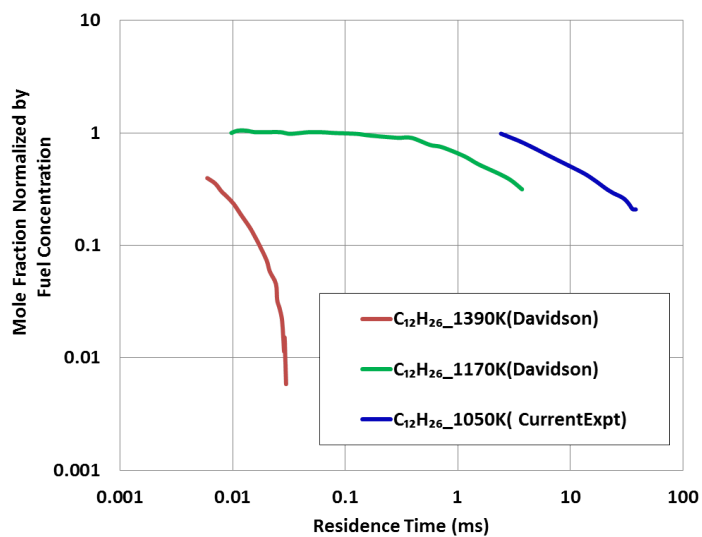


Figure 5.46: Normalized n-dodecane Profile, Current 1050 K Rich Run and Fuel Profiles from Davidson et al. (2011) .

5.6.3 Jet-Stirred Reactor Pyrolysis Experiments

Herbinet et al. (2007) studied the thermal decomposition of n-dodecane (at 2% mole with balance helium) in a Jet Stirred Reactor between 773 and 1073 K and 1 atm pressure. The particular profiles of interest are the fuel and species profiles at 973 K as the temperature conditions are quite close to the current 1000 K pyrolysis. A comparison of the fuel conversion percentages and the product species mole fractions normalized by the fuel load is shown in Figures (5.48) and (5.49). The optimized JetSurf mechanism has been employed to perform CHEMKIN simulations for the conditions in the JSR experiments.

The plots make it clear that the current 1000 K pyrolysis experiment exhibits an accelerated rate of reaction when compared to Herbinet's profile at the same temperature conditions. The optimized JetSurf mechanism replicates this basic divergence between the two experiments though it predicts the flow reactor results far better than the data obtained from the JSR experiments. Since the temperature difference is very small, it is postulated that the presence of excess H_2 and H_2O in the bath gas is responsible for significantly accelerating the process of fuel decomposition by acting as a source of H and OH radicals respectively. Further analysis of the reaction pathways for both the pyrolysis and oxidation cases will be performed in next chapter to validate this conclusion. However, the presence of water molecules and excess H_2 in the reactor at pyrolysis conditions must be taken into account to explain the observed rapidity of fuel breakdown in the flow reactor.

5.7 Summary

This chapter was primarily concerned with a complete tabulation of the experimental data from the four flow reactor runs and comparing the experimental data with predictions from the four detailed mechanisms. Taken as a whole, the optimized JetSurf mechanism performed adequately for all four conditions, thereby showing reliability over the entire range of stoichiometry and temperatures that were studied in the flow reactor. The CNRS mechanism performed exceptionally well at low temperature conditions of 1000 K pyrolysis and 1050 K oxidation, while the CRECK mechanism was most accurate in the 1170 K lean oxidation and 1220 K rich oxidation conditions. The Lawrence Livermore mechanism was

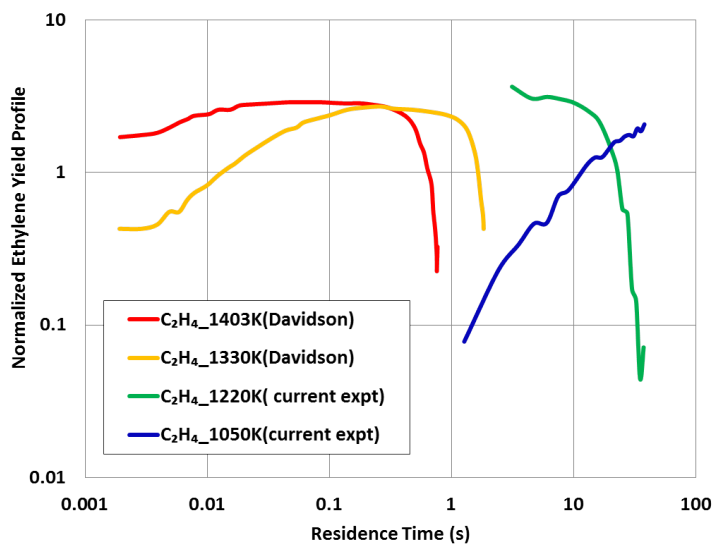


Figure 5.47: Ethylene Time History Profile Normalized by the Initial n-dodecane Mole Fraction, 1220 K Rich Profile Compared with Davidson et al. (2011).

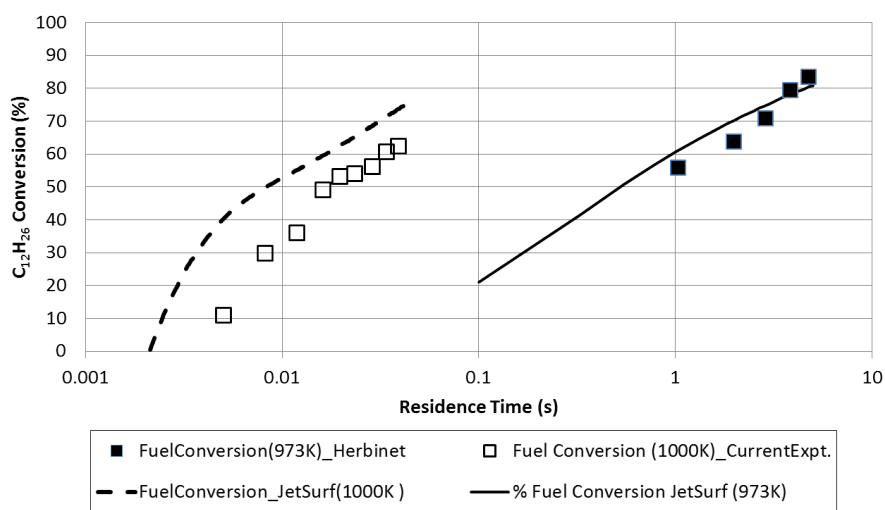


Figure 5.48: Fuel Conversion Time History Profile for 1000 K Pyrolysis Compared With the 973 K JSR profiles of Herbinet et al. (2007) and JetSurf predictions.

found to underpredict the reaction rates in all four instances, while CNRS was slow for the high temperature runs. JetSurf itself tended to proceed faster than what the observed data suggested at higher temperature conditions.

Finally, the experimental data sets were compared with other relevant experimental data from shock tubes and jet stirred reactors. In general, the current data were found to be consistent with previous experimental results performed by other groups. However, it was also observed that the presence of significant amounts of water vapor in the bath gas is responsible for accelerating the reaction rates when compared to experiments done in inert gas or pure nitrogen environments.

The next chapter takes a detailed look at the pathways and the sensitive reactions that control the rate of n-dodecane oxidation and pyrolysis in the detailed mechanism schemes. This in turn aids our understanding of the primary reasons the four mechanisms diverge from each other in their predictions, their relative accuracy as well as possible future improvements.

Parameter	1000 K Pyrolysis	1050 K Rich Oxidation	1220 K Rich Oxidation	1170 K Lean Oxidation
Stoichiometry	∞	1.56	1.32	0.79
Back Ground Temperature(K)	1000	1050	1220	1170
Pressure(atm.)	1	1	1	1
C ₁₂ H ₂₆ (ppmv.)	282	501	569	328
Nominal H ₂ O (%)	22	19.8	25	24.2
Nominal O ₂ (%)	0	0.59	0.79	0.77
Nominal H ₂ (%)	6.6	0	0	0
N ₂ (%)	71	79	73.5	74.4
H ₂ /Air Flame Stoichiometry	1.3	0.94	0.94	0.94
Residence Time (ms)	41.3	37.9	40.3	40.8
Burner Air (mol/s)	0.0309	0.0309	0.0309	0.0309
1 st Injection N ₂ (mol/s)	0.0155	0.0221	0.0092	0.011
2 nd Injection N ₂ (mol/s)	0.00239	0.00239	0.00239	0.00239
Purge N ₂ (mol/s)	0.0133	0.01326	0.0133	0.0133
Hydrogen (mol/s)	0.0168	0.0122	0.0122	0.0122
Dodecane (mol/s)	1.67E-05	3.08E-05	2.77E-05	1.65E-05
Mixing Time (ms)	1.4	0.69	1.6	2.4

Table 5.1: Experimental Conditions

2nd Injection Mass Flow Rate (gm/s)	0.0698
Bath Gas Mass Flow Rate (gm/s)	1.364
X_{N_2} 2nd Injection	0.993
$X_{C_{12}H_{26}}$ 2nd injection	0.00694
X_{N_2} Bath Gas	0.698
X_{H_2O} Bath Gas	0.228
X_{H_2} Bath Gas	0.0687
X_{CO_2} Bath Gas	0.000118
X_{CO} Bath Gas	0.00011
X_{Ar} Bath Gas	0.00508
X_H Bath Gas	0.000013

Table 5.2: 1000K Pyrolysis Case, Initial Flow Composition

2nd Injection Mass Flow Rate (gm/s)	0.0722
Bath Gas Mass Flow Rate (gm/s)	1.5376
X_{N_2} 2nd Injection	0.987
$X_{C_{12}H_{26}}$ 2nd injection	0.0127
X_{N_2} Bath Gas	0.782
X_{H_2O} Bath Gas	0.2066
X_{O_2} Bath Gas	0.00618
X_{CO_2} Bath Gas	0.00022
X_{Ar} Bath Gas	0.00488

Table 5.3: 1050 K Rich Oxidation Case, Initial Flow Composition

2nd Injection Mass Flow Rate (gm/s)	0.0717
Bath Gas Mass Flow Rate (gm/s)	1.178
X_{N_2} 2nd Injection	0.9886
$X_{C_{12}H_{26}}$ 2nd injection	0.0114
X_{N_2} Bath Gas	0.7218
X_{H_2O} Bath Gas	0.2633
X_{O_2} Bath Gas	0.00836
X_{CO_2} Bath Gas	0.000281
X_{Ar} Bath Gas	0.00624

Table 5.4: 1220 K Rich Oxidation Case, Initial Flow Composition

2nd Injection Mass Flow Rate (gm/s)	0.0698
Bath Gas Mass Flow Rate (gm/s)	1.226
X_{N_2} 2nd Injection	0.993
$X_{C_{12}H_{26}}$ 2nd injection	0.00686
X_{N_2} Bath Gas	0.732
X_{H_2O} Bath Gas	0.254
X_{O_2} Bath Gas	0.00806
X_{CO_2} Bath Gas	0.00027
X_{Ar} Bath Gas	0.00602

Table 5.5: 1170 K Lean Oxidation Case, Initial Flow Composition

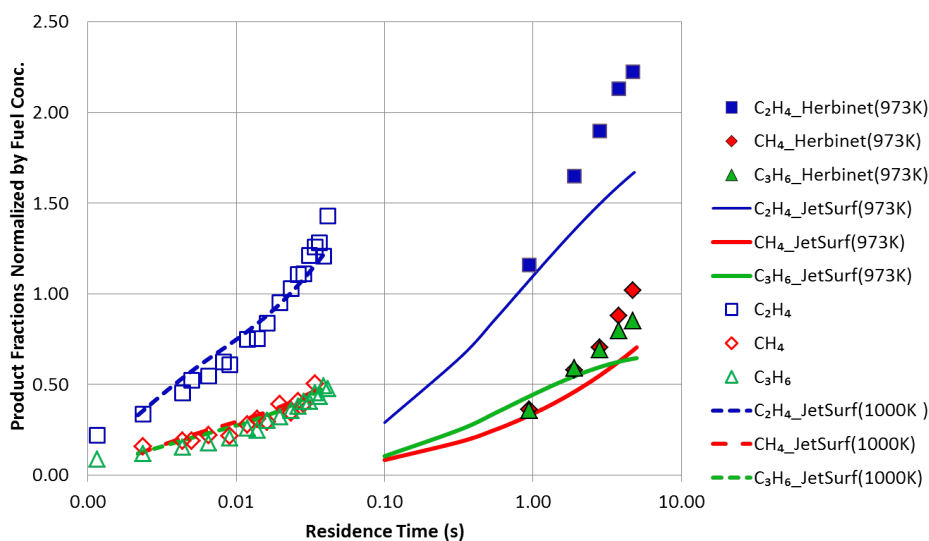


Figure 5.49: Species Time History Profiles for the current 1000 K Pyrolysis Experiment Compared with the 973 K JSR data from Herbina et al. (2007) and JetSurf predictions.

Chapter 6

A Sensitivity Analysis of the Detailed Mechanisms

In Chapter 5, the flow reactor data were compared against four detailed mechanisms developed for n-alkane combustion chemistry. The comparisons revealed significant differences in the predictions of species profiles among the mechanisms. An example of the differences between the predictions of the four mechanisms regarding fuel decay for the low temperature runs and CO concentration for the high temperature runs is shown in Table (6.1). Fuel decay rate is a key indicator of the speed of the reaction under pyrolysis and during the initial stages of oxidation, while CO generation is a good indicator of the rate of progress of the later stages of the oxidation process. JetSurf is seen to be consistently fast and Lawrence Livermore mechanism is found to be consistently slow in all four cases. The CRECK semi-detailed model works well under oxidation conditions, but not under pure pyrolysis. The performance of the CNRS mechanism varies, being superior in pyrolysis and early oxidation zones while predicting slower rates in the late oxidation stages at higher temperatures.

The Lawrence Livermore mechanism has been widely used to model pyrolysis and alkane oxidation by many research groups. In this chapter, the JetSurf mechanism's reaction pathways and key rate-limiting reaction rates are compared with those of the LLNL mechanism in order to better understand the reasons for slower reactions rates of the latter compared to the JetSurf mechanism. It is to be noted that the experimental data exhibit

reaction rates somewhat slower than the JetSurf mechanism but fairly faster than the LLNL predictions. The low-temperature pyrolysis and the high-temperature rich oxidation conditions will be treated in detail with briefer explanations of the features observed for the other two conditions.

6.1 Low-Temperature Pyrolysis and Oxidation Runs

As was seen in Chapter 5, the 1000 K pyrolysis and the 1050 K rich oxidation runs sample the initial fuel breakdown stage of the reaction that produce ethylene and propene as the main decomposition products. There is general agreement regarding the basic kinetic pathways through which large n-alkanes undergo thermal decomposition (Ranzi et al. (2005), Westbrook et al. (2009), You (2008)) and is schematically presented in Figure (6.1).

The formation of alkyl radicals from the n-alkane occur mainly through radical mediated H abstraction reactions though direct C-C fission reactions dominate at temperatures above 1400 K. At temperatures below 900 K (for atmospheric pressure conditions) the O_2 addition pathway that generates alkyl-peroxy radicals is favored. This alkyl-peroxy radical may undergo further O_2 addition to generate ketohydroperoxides that initiate low temperature chain branching, or undergo β scission to produce olefins and unreactive HO_2 in the NTC regime. At temperatures above 900 K (for 1 atm conditions), the decomposition of the alkyl radical is mediated primarily by β scission reactions that generate smaller alkenes and alkyl radicals. At the flow reactor conditions, the low-temperature oxygen addition pathways are insignificant and reaction proceeds through successive β scission of the alkyl radicals. The large alkenes undergo either H abstraction to form alkenyl radicals or addition reactions followed by β scission to form smaller products. The basic pathways are similar for the different mechanisms and a sample flux analysis is shown for the JetSurf mechanism for the 1000K pyrolysis condition at the 47% fuel decay point (Figure 6.2). The alkyl radicals also undergo mutual isomerization (not shown) before undergoing scission reaction. The decomposition fluxes for the relatively stable alkenes are also omitted. As can be seen, the different dodecyl radical isomers decay through multiple scission pathways to create smaller alkyl fragments which in turn undergo one more round of β scission to eventually generate butyl, propyl and ethyl radicals. These radicals are the primary sources

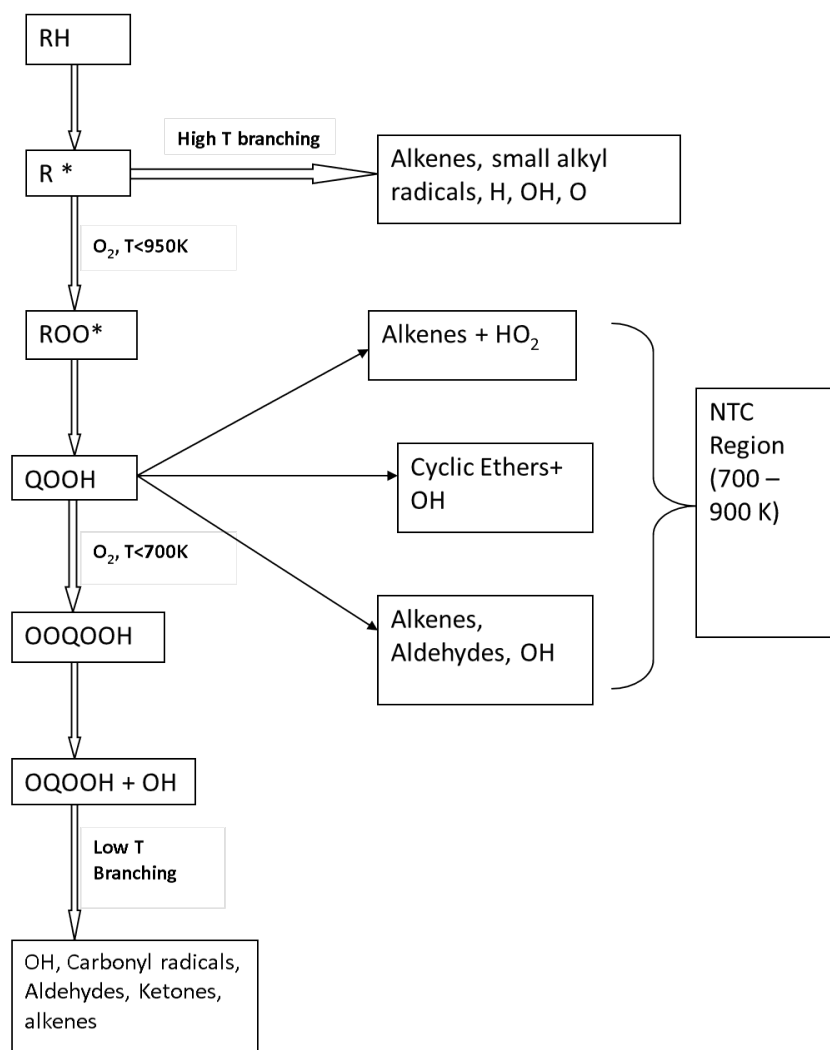


Figure 6.1: N-Alkane Oxidation Schematic Showing High-Temperature, Low-Temperature and NTC Pathways.

of ethylene, the primary pyrolysis product. A Rate of Progress analysis shows that for the 1000 K pyrolysis conditions, the H abstraction reactions are primarily mediated by the H radical. For the 1050 K rich oxidation conditions, the pathways are fairly identical, however OH radical mediated H abstraction reactions also play an important role in the alkyl radical formation.

The CHEMKIN-PRO software is used to calculate the pre-exponential factor sensitivities of important species like n-dodecane, ethylene or the H radical. The sensitivity values are defined as:-

$$\left[S_i^k \right]_t = \left[\frac{A_i}{X_k^{max}} \frac{\partial X_k}{\partial A_i} \right]_t \quad (6.1)$$

where X_k is the mole fraction of the species 'k' whose sensitivity is being evaluated; 'i' denotes the i^{th} reaction involving the species 'k' with a pre-exponential factor A_i ; 't' is the residence time at which the sensitivity coefficient is being evaluated and X_k^{max} is the global maximum mole fraction value the species 'k' has in the system. For the 1000 K pyrolysis condition, the sensitivity analysis was done at the residence time corresponding to the 47% fuel decay point. The largest pre-exponential factor sensitivities pertaining to n-dodecane concentration under pyrolysis conditions are shown in Figure (6.3) for the JetSurf and the LLNL mechanisms. In the figure, reactions with positive A factor sensitivities are those that retard fuel decomposition while reactions with negative A factor sensitivities are those that enhance fuel decomposition. Unsurprisingly, the H abstraction reaction rates show negative sensitivity as they are primarily responsible for the fuel decay. However, the rate at which H abstraction reaction can take place also depends on the concentration of the H atom in the radical pool. Thus, it is the availability of the H radical that determines the rate of dodecane decomposition in the flow reactor. Figure (6.4) compares the rate of production of H radicals in the JetSurf mechanism with the production rate in the LLNL mechanism under the pyrolysis condition. The rate of production values are arrived at by adding the primary sources of the H radicals in both the mechanisms. For both mechanisms, two reactions are responsible for producing almost all of the H radicals present in the radical pool. These source reactions are,

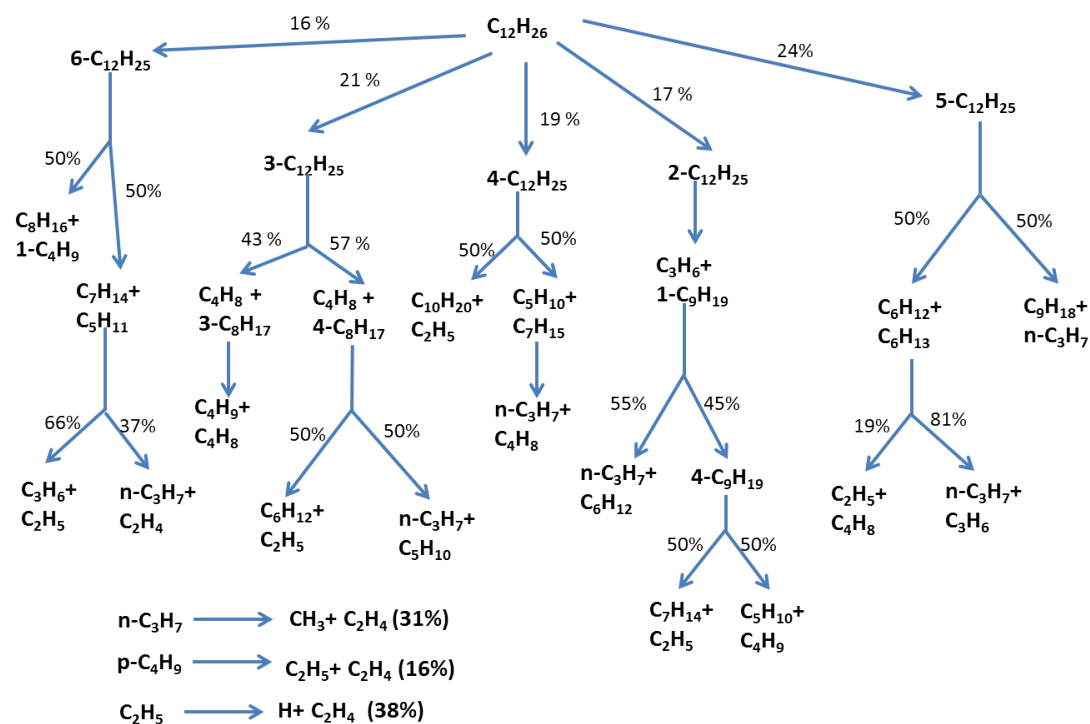
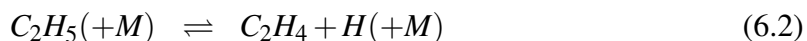


Figure 6.2: Reaction Flux Analysis for the 1000 K n-dodecane Pyrolysis Conditions as predicted by the JetSurf mechanism at the residence time corresponding to 47% fuel decomposition point.



For the JetSurf mechanism, both of these reactions run faster than the LLNL mechanism such that the total positive rate of production values (in mole/cc.s) of H radicals are 2.5-1.5 times that in the LLNL mechanism for the initial 10 ms of the residence time. The increased availability of H radicals at the initial stages of the pyrolysis process speeds up the fuel decay through H abstraction reactions in the JetSurf mechanism.

For the JetSurf mechanism, the most sensitive reaction that enhances $C_{12}H_{26}$ decay is the reaction of the methyl radical with H_2 to generate methane and the H radical. The flux analysis in Figure (6.2) shows that the methyl radical is formed primarily from the n-propyl radical (over 80% of the source flux) and subsequently the methyl radical exclusively generates methane by scavenging a proton from hydrogen. The H_2 mediated methyl to methane formation pathway is one of the primary sources of H radicals under pyrolysis conditions. Though ostensibly a chain propagation reaction, it essentially transforms a relatively unreactive methyl radical into a highly reactive hydrogen radical that can now attack the fuel molecule through the abstraction pathways and thereby enhance the pyrolysis rate. It is to be noted that under pyrolysis conditions, a large excess of H_2 (6.6%) is present in the bath gas which drives the reaction in the direction of methane formation. The dominance of Reaction (6.3) also explains why under the flow reactor conditions of excess hydrogen, pyrolysis proceeds faster than what is generally observed in a pure N_2 or inert gas dilution conditions. In the JetSurf mechanism the forward reaction rate of ethyl to ethylene reaction (Reaction 6.2) and methyl to methane reaction (Reaction 6.3) are 1.5 and 2.5 times that of the LLNL mechanism as shown in Table (6.2). For the ethylene formation reaction (6.2), the JetSurf rate parameters are based on theoretical calculations done by (Miller and Klippenstein, 2004), while for the LLNL, the rate parameters are a factor of 2 increase from those chosen in GRI 3.0 mechanism. GRI 3.0 (http://www.me.berkeley.edu/gri_mech) obtains its rate parameters from the results

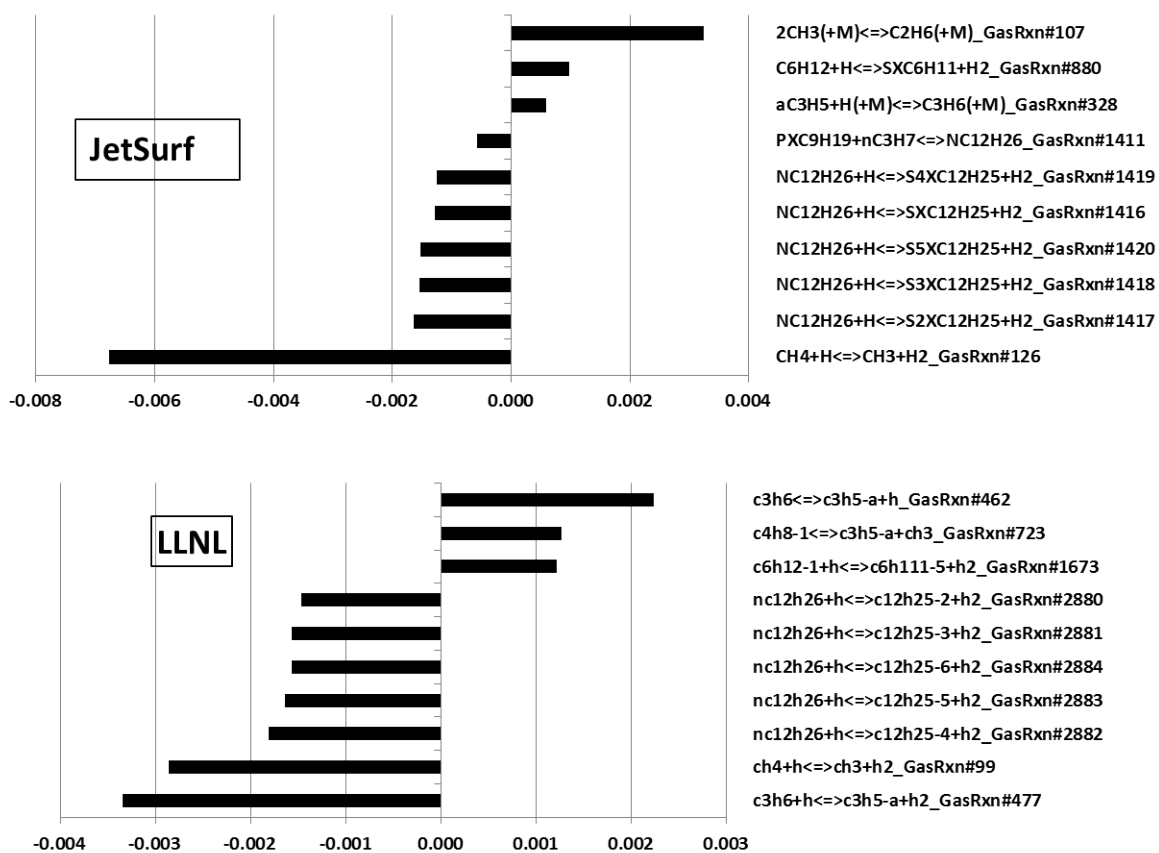


Figure 6.3: Largest A factor Sensitivities for reactions that affect n-dodecane concentration at residence times corresponding to the 47% fuel decay point under 1000K Pyrolysis Conditions, JetSurf and LLNL Mechanisms Compared.

	JetSurf	LLNL	CNRS	CRECK
Time to 47% fuel decay (150 ppm), 1000 K Pyrolysis	6.8 ms	32 ms	21 ms	38.6 ms
Time to 50% fuel decay (250 ppm), 1050 K Oxidation	18.6 ms	30.2 ms	14.7 ms	15.1 ms
Time to 2500 ppm CO concentration, 1220 K Rich Oxidation	16 ms	26 ms	29 ms	17 ms
Time to 1500 ppm CO concentration, 1170 K Lean Oxidation	16 ms	32 ms	35 ms	18 ms

Table 6.1: Residence Times to Target Concentrations as Predicted by the Mechanisms

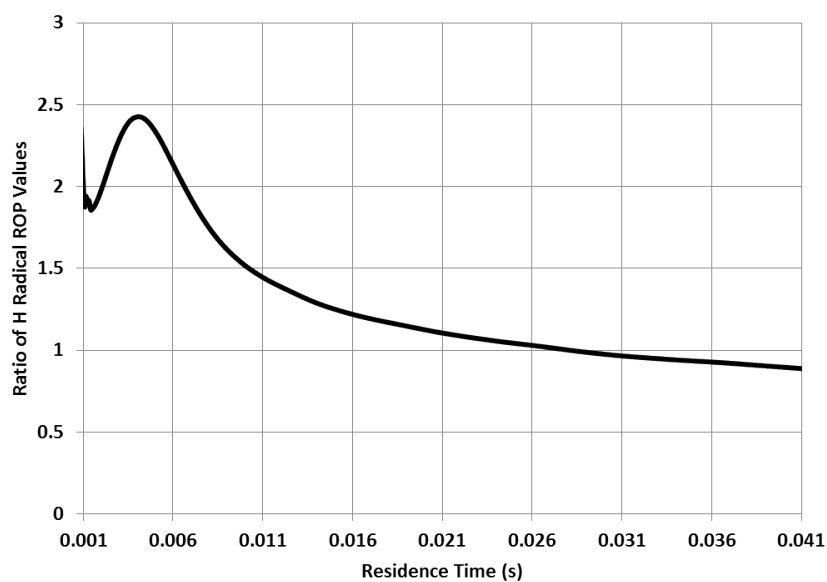


Figure 6.4: Ratio of the Rate of Production of H radicals in the JetSurf vs the LLNL mechanism for the 1000 K Pyrolysis Condition.

obtained by Feng et al. (1993) and Hanning-Lee et al. (1993). For the methane formation reaction (Reaction (6.3)), JetSurf uses the rate parameters adopted by GRI Mech 3.0.

The H_2 mediated methyl to methane reaction remains important for the LLNL mechanism as well. However, the distinctive feature of the LLNL mechanism is the increased importance of the allyl ($a\text{-C}_3\text{H}_5$) pathways in determining the fuel decay sensitivities. In particular, one can see in Figure (6.3) that the Reaction (6.4) has the largest negative sensitivity so that enhancing its rate has a substantial impact towards a general acceleration of the fuel decomposition.



For the LLNL mechanism this reaction proceeds towards the propene formation direction and acts as a source of H radicals in the flow reactor environment. It is, however, balanced by the Reaction (6.5) that also generates propene while consuming a H radical in the process.

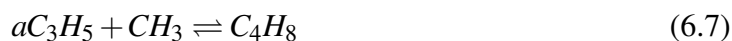


In contrast, the JetSurf mechanism has low sensitivity to the allyl pathways. In a Rate of Production analysis it was found that the Reaction (6.4) proceeds in the reverse direction in JetSurf under identical pyrolysis conditions and acts as a sink for propene and H radicals. Reaction (6.5) goes in the direction of propene formation for both cases. Thus, under pyrolysis conditions, the LLNL mechanism has Reaction (6.4) as the largest sink of allyl radicals and a source of H radicals, while in the JetSurf mechanism the reverse of Reaction (6.4) acts as one of the sources of allyl radical and a minor sink for H radicals. This switching of the direction of reaction progress can be explained from the rate values presented for the reaction in Table (6.2), where it is seen that the reaction rate values for the LLNL mechanism in the propene formation direction is 10 times larger than that of the JetSurf mechanism. This discrepancy is primarily due to the different thermodynamic parameters used for the reaction in the two mechanisms. The JetSurf mechanism follows recommendations from Burcat thermochemical database (Burcat and Ruscic, 2005), while the LLNL mechanism uses the Therm software (Ritter, 1991) that uses group additivity methods to

automatically generate a self-consistent set of thermodynamic parameters. For the reaction under study, the Gibbs energy of formation for propene differs by 2.32 kcal/mol and that for the allyl radical differs by 1.4 kcal/mol at 1000 K between the two mechanisms. As a result the $\Delta_f G^0$ of the Reaction (6.4) for the JetSurf mechanism is -17 kcal/mol while the value for the LLNL mechanism is -21 kcal/mol. Such differences lead to an equilibrium constant (K_c) value that is 6.5 times greater in the JetSurf mechanism for the Reaction (6.4) than the LLNL mechanism. This is sufficient to alter the direction of the Reaction (6.4) when a large excess of H_2 species is present in the bath environment. In the JetSurf mechanism, the higher sensitivity of the reaction (6.3) explains the positive sensitivity associated with the methyl recombination reaction (6.6) that depletes the concentration of methyl radical from the system.



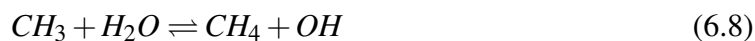
A similar inhibiting role is performed in the LLNL mechanism by the allyl/methyl recombination reaction that removes both these radicals from the system generating a stable 1-butene in the process.



Therefore, it is seen that much of the differences between the LLNL and the JetSurf fuel decay rates can be attributed to distinctively different reaction rate parameters and thermochemistry values associated with the ethyl and allyl formation and destruction reactions.

Sensitivity analysis for C_2H_4 under pyrolysis conditions is shown in Figure (6.5). The H abstraction reactions and methane generation reactions are found to be the most sensitive reactions. Thus, ethylene generation rates are directly tied to the rates of dodecane decay.

In case of the low temperature rich oxidation run (1050 K, 1.56 stoichiometry), H_2O replaces H_2 as the third body mediating the most dominant methyl to methane formation reaction.



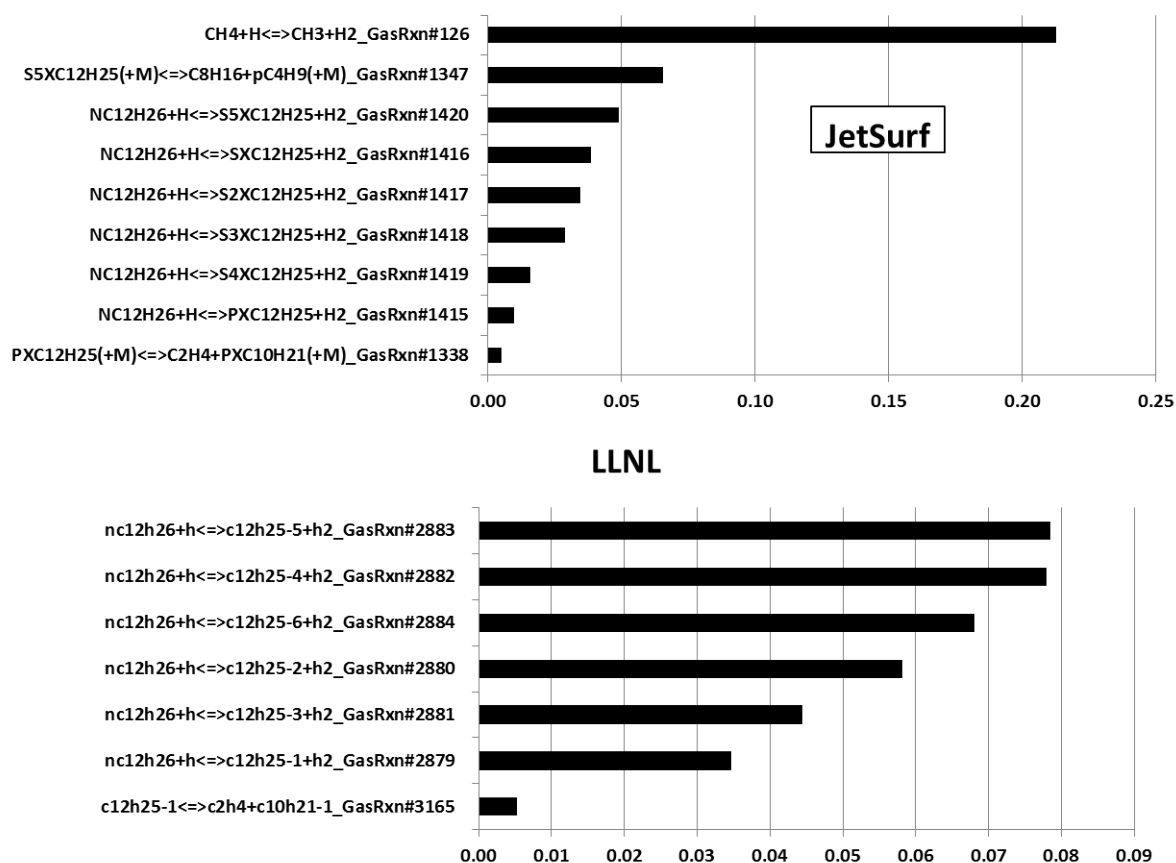


Figure 6.5: Largest A factor Sensitivities for reactions that affect ethylene concentration at 47% fuel decay point under 1000K Pyrolysis Conditions, JetSurf and LLNL Mechanisms Compared

Reaction (6.8) is the most sensitive reaction that enhances n-dodecane decomposition for both JetSurf and LLNL mechanisms by acting as a source of OH radicals. The shift from H_2 to H_2O can be explained by the fact that in the oxidation case, the bath gas does not contain excess hydrogen and the methyl radical instead scavenges a proton from the water molecules present in the vitiated flow reactor environment. The generated hydroxyl radicals begin to play an important part in the H abstraction reactions of n-dodecane. Otherwise the reaction pathways and are more or less identical.

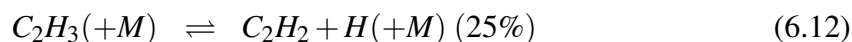
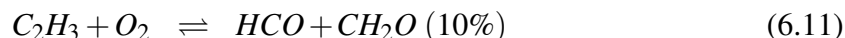
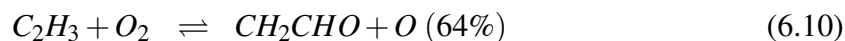
Table (6.2) presents the main reactions associated with fuel decay and ethylene formation for the pyrolysis and low temperature oxidation runs that have significant differences in the reaction rates values between JetSurf and LLNL mechanisms. As is seen, many of the C_2 - C_4 reaction rates associated with ethylene generation also show significant differences between the two mechanisms.

6.2 High Temperature Oxidation Runs

In this section the 1220K rich oxidation run is investigated to identify the important rate limiting reactions and rate parameter differences between the JetSurf and the LLNL mechanisms. The lean 1170 K reaction pathways are essentially similar, though C_2H_2 formation is not prominent in the later stages of oxidation. As previously discussed in Chapter 5 , at higher temperatures n-dodecane decays rapidly into ethylene and propene within the first millisecond and the primary chemistry that occurs in the flow reactor involves the oxidation of ethylene and propene into CO, C_2H_2 and eventually CO_2 . The reaction flux diagram at 2500 ppm CO formation point for the JetSurf mechanism is shown in the Figure (6.6). The primary pathway of ethylene decomposition is through the attack of OH radical to form vinyl ,



The vinyl radical reacts as follows:-



The vinoxy ($\cdot CH_2CHO$) radical rapidly breaks down to methyl and CO. Acetylene persists, but also undergoes oxygen addition to form HCCO that eventually oxidizes to CO. Formaldehyde undergoes OH attack to generate the formyl radical (HCO) and H_2O . HCO acts as the primary source of CO in the system. The methyl radical also plays an important role. Most of it recombines to form ethane that in turn generates ethyl radical and is converted back to ethylene. The rest undergoes oxygen addition to form formaldehyde or hydrogen addition to form methane. The primary source of OH radicals is from the main hydrogen/oxygen chain branching step which is by far the most sensitive reaction at these late stage oxidation conditions.



Figure (6.7) displays the reactions that affect ethylene concentration the most. Positive sensitivities correspond to those reactions where rate increases enhance ethylene concentration, while negative sensitivities correspond to those reactions where rate increases decrease ethylene concentration. JetSurf and LLNL sensitivities are compared at residence times corresponding to the 2500 ppm CO point. The largest negative sensitivity corresponds to the primary hydrogen/oxygen chain branching reaction (Reaction 6.13) that generates OH radicals. The reactions with positive sensitivities (i.e., those which increase ethylene concentration) act as sinks of H or OH radicals with the H mediated methyl to methane formation reaction being the most dominant. The main difference between the JetSurf and LLNL mechanism is that for the LLNL mechanism, the vinyl formation reaction (Reaction 6.9) also has high sensitivity, while in JetSurf, the initial H abstraction from dodecane by the OH radical continues to remain important in determining the ethylene concentration levels.

Reaction	k_f JetSurf	k_f LLNL	Ratio	Effect
$C_{12}H_{26}+H \rightarrow C_{12}H_{25}+H_2$ (avg.)	5.36×10^{12}	4.34×10^{12}	1.235	Fuel Decay
$C_{12}H_{26}+OH \rightarrow C_{12}H_{25}+H_2O$ (avg.)	6.46×10^{12}	6.47×10^{12}	1	Fuel Decay (Oxdn.)
$CH_3+H_2 \rightarrow CH_4+H$	1.18×10^{10}	0.81×10^{10}	1.45	Enhances Pyrolysis
$CH_3+H_2O \rightarrow CH_4+OH$	2.01×10^8	1.8×10^8	1.1	Enhances Oxidation
$aC_3H_5+H_2 \rightarrow C_3H_6+H$	3×10^7	2.63×10^8	0.11	LLNL runs in this direction
$C_3H_6+H \rightarrow aC_3H_5+H_2$	1.17×10^{12}	1.56×10^{12}	0.75	JetSurf runs in this direction
$C_2H_5(+M) \rightarrow C_2H_4+H(+M)$	5.66×10^4	2.14×10^4	2.6	Main source of ethylene
$aC_3H_5+H(+M) \rightarrow C_3H_6(+M)$	1.88×10^{14}	1.15×10^{14}	1.6	Retards Pyrolysis

Table 6.2: Reaction Rate Comparisons at 1000K between the JetSurf and the LLNL mechanisms for the most Sensitive Reactions pertaining to the 1000 K Pyrolysis and 1050 K Rich Oxidation Experiments.

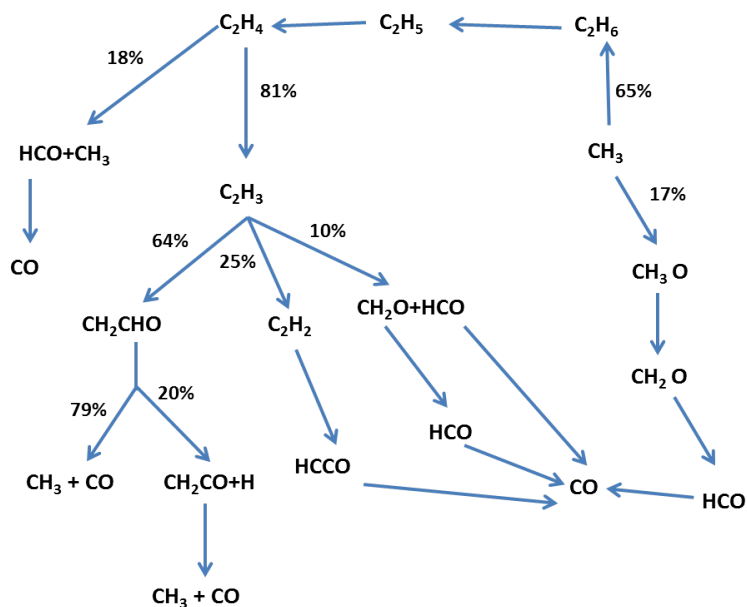


Figure 6.6: Reaction Flux Analysis for n-dodecane rich oxidation at 1220 K as predicted by the JetSurf mechanism at 0.25% CO concentration point.

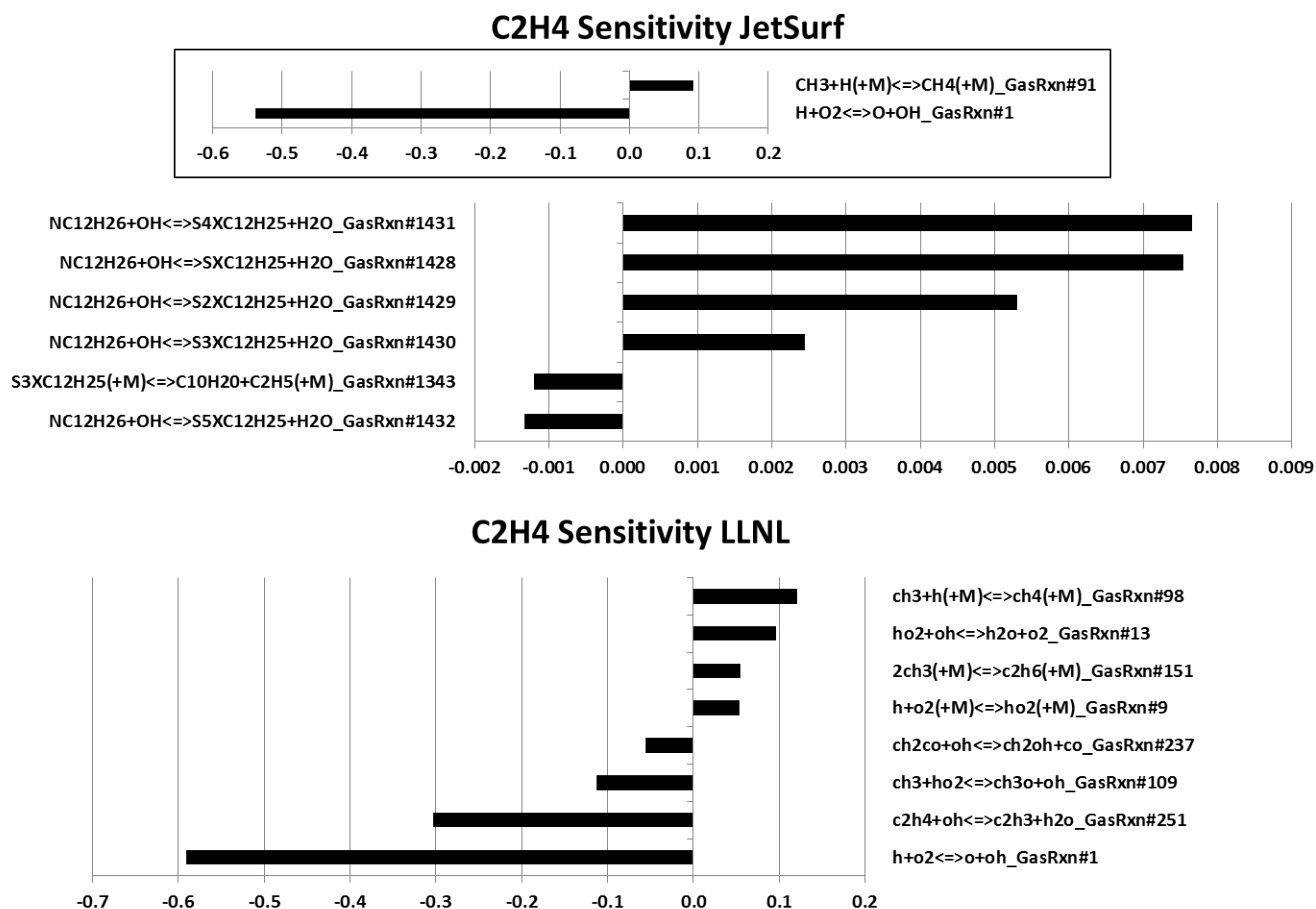


Figure 6.7: Largest A factor Sensitivities for the reactions that affect ethylene mole fractions at residence times corresponding to the 2500 ppm CO concentration point under 1220 K Rich Oxidation Conditions, JetSurf and LLNL Mechanisms Compared.

Next, a sensitivity analysis is done for CO for both the JetSurf and the LLNL mechanisms at residence times corresponding to the 2500 ppmv. CO concentration point. As seen in Figure (6.8), in JetSurf, the Reactions (6.9) and (6.10) have large positive sensitivities and are rate determining for CO generation. However in LLNL, the vinyl pathway reactions are not sensitive, and the hydrogen/oxygen chain branching pathway (Reaction 6.13) assumes the greatest importance. The rate differences between the most sensitive reactions of both mechanisms corresponding to ethylene oxidation and CO formation are presented in Table (6.3) at the 1200K temperature condition. It is clearly seen that the rates associated with the entire ethyl \rightarrow ethylene \rightarrow vinyl \rightarrow vinyloxy pathway are significantly faster for the JetSurf mechanism when compared to the rates in the LLNL mechanism. A factor of 10 difference is observed for the rates corresponding to the vinyl oxygen addition reaction. This difference has a significant effect on the favored vinyl decomposition pathway. In LLNL, the vinyl radical preferentially undergoes unimolecular decomposition to acetylene and the favored reaction chain is ethyl \rightarrow ethylene \rightarrow vinyl \rightarrow acetylene \rightarrow HCCO \rightarrow CO. Thus, while in JetSurf, 64% of the vinyl radical undergoes oxygen addition to form vinyloxy and only 25% follow the unimolecular decomposition route to produce acetylene (refer to Figure (6.6)); for the LLNL mechanism, these flux values are 27% for vinyloxy and 65% for acetylene pathway, respectively. C_2H_2 is a more long lived species than CH_2CHO , thus the LLNL mechanism's branching ratio slows down the overall rate of progress of the reaction. For the JetSurf 1.0 mechanism, the rate parameters of the Reaction (6.10) are taken from GRI 3.0 (based on estimates made by Mebel et al. (1996)) and the pre-exponential factor was increased 3 times the original value in the optimized version. The rate parameters for the Reaction (6.9) were also taken from GRI 3.0 in JetSurf 1.0 and was increased by 20% for the optimized JetSurf. For the LLNL mechanism, the reaction rates were adopted from the work done by Marinov et al. (1998). Historically, the vinyl+O₂ pathway has suffered from large quantification uncertainties. A recent paper by Metcalfe et al. (2013) reviews the various kinetic rate constant values proposed in the literature. It is observed from the discussion in the paper, that Marinov's reaction rate values are the least among all proposed literature rates over the entire temperature range of interest (Figure 23 of Metcalfe et al. (2013)). A majority of the literature rates fall in the range of $2-6 \times 10^{12}$ cc/mol.s while Marinov's estimates fall below 1×10^{12} cc/mol s. Given these ranges, the optimized JetSurf

values of 7.5×10^{12} cc/mol s will lie at the upper limits of literature values. Given the importance of the vinyl decomposition route, further studies may be necessary to accurately quantify the rate parameter values of these reaction pathways.

6.3 Summary

Flux analysis and sensitivity based studies conducted in this chapter uncovered significant differences in the C_3 - C_1 pathway rate values between the JetSurf and the LLNL mechanisms. These differences are likely to be responsible for the divergent predictions between the two mechanisms that were observed in Chapter 5. For the low-temperature oxidation and pyrolysis cases, differences in the rates of H and OH radical generation reactions were found to be responsible for the faster rate of thermal decomposition of n-dodecane into ethylene. The allyl generation and destruction pathways were also found to proceed differently for the two mechanisms due large differences in the thermodynamic parameter estimations. The LLNL mechanism was found to be especially sensitive to the allyl formation and decomposition routes. The presence of H_2 and H_2O species in the bath gas was found to have a significant accelerating impact on fuel decay rates by acting as sources of H and OH radicals to the system. For the high-temperature oxidation pathways, the rate parameters corresponding to the conversion of ethylene to CO through the dominant vinyl formation and oxidation pathways were found to have significantly higher values for the JetSurf mechanism when compared with the LLNL mechanism. This explains the faster rates of progress seen in the JetSurf oxidation predictions when compared to the LLNL model. Most of the differences in the kinetic rate constants and thermochemistry values between the two mechanisms were due to the adoption of different sources of published recommendations from the available literature. An increased effort towards achieving a wider consensus for the C_2 - C_3 reaction rate parameter values based on more up-to-date experimental investigations and theoretical analysis will be needed to improve both the accuracy and the congruency in the predictions of the detailed kinetic schemes.

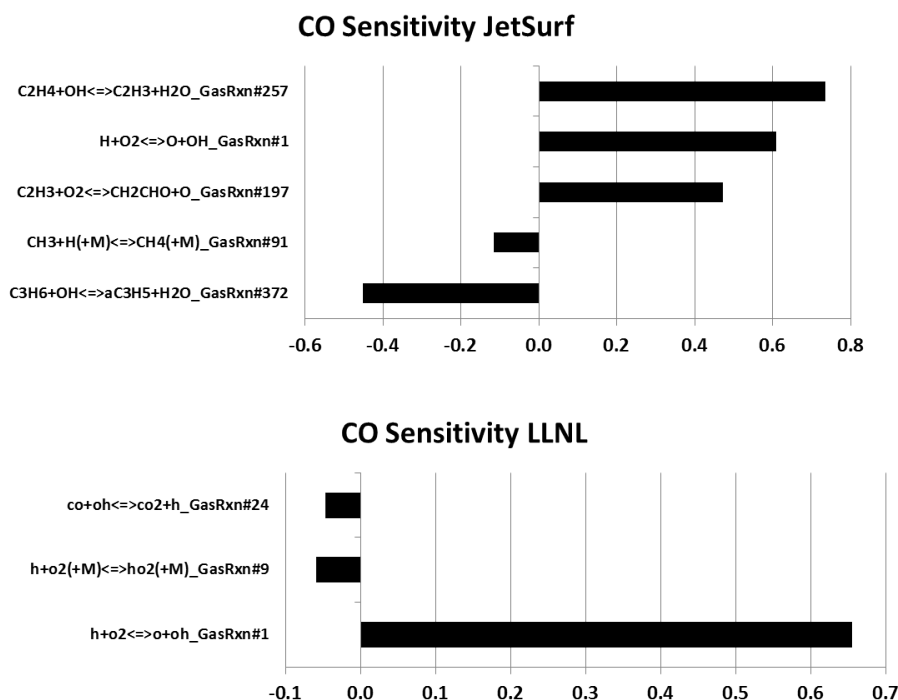


Figure 6.8: Largest A factor Sensitivities for the Reactions that affect carbon monoxide mole fraction at residence times corresponding to the 2500 ppm CO concentration point under 1220 K Rich Oxidation Conditions, JetSurf and LLNL Mechanisms Compared.

Reaction	k_f JetSurf	k_f LLNL	Ratio	Effect
$\text{C}_{12}\text{H}_{26} + \text{OH} \rightarrow \text{C}_{12}\text{H}_{25} + \text{H}_2\text{O}$ (avg.)	7.56×10^{12}	8.08×10^{12}	0.93	Fuel Decay
$\text{CH}_3 + \text{H} (+\text{M}) \rightarrow \text{CH}_4 (+\text{M})$	0.96×10^{13}	1.36×10^{13}	0.7	Retards Ethylene Oxdn.
$\text{C}_2\text{H}_5 (+\text{M}) \rightarrow \text{C}_2\text{H}_4 + \text{H} (+\text{M})$	7.72×10^5	2.3×10^5	3.4	Enhances Ethylene Generation
$\text{C}_2\text{H}_4 + \text{OH} \rightarrow \text{C}_2\text{H}_3 + \text{H}_2\text{O}$	2.16×10^{12}	0.91×10^{12}	2.4	Main Ethylene oxidation pathway
$\text{C}_2\text{H}_3 + \text{O}_2 \rightarrow \text{CH}_2\text{CHO} + \text{O}$	7.48×10^{12}	0.796×10^{12}	9.4	Main Ethylene to CO Formation Pathway in JetSurf
$\text{H} + \text{O}_2 \rightarrow \text{H} + \text{OH}$	1.76×10^{11}	1.89×10^{11}	0.93	Main Chain Branching

Table 6.3: Reaction Rate Comparisons at 1200K between the JetSurf and the LLNL mechanisms for the most Sensitive Reactions pertaining to the 1220 K Rich Oxidation Experiment.

Chapter 7

The Lumped JetSurf Mechanism

7.1 Motivation

The development of detailed kinetic schemes for hydrocarbon pyrolysis and oxidation processes involves multiple challenges. As noted in Chapter 2, a brute force approach towards the development of a comprehensive combustion chemistry mechanisms for commercial fuels remains intractable as they are made up of a complex and variable mixture of thousands of compounds. This motivated the development of the "surrogate fuel" approach. The surrogate approach tries to reproduce the relevant physical and chemical properties of commercial fuels by an intelligent mix of a few (usually three to six) hydrocarbon compounds from the various functional groups. For jet fuels for example, a surrogate mixture usually consists of a suitable n-alkane like n-dodecane, an iso-alkane like iso-octane, a cyclic alkane like methyl-cyclohexane and an aromatic like butyl-benzene (refer to Table (2.1)). However, the surrogate model assumes that it is possible that an accurate and detailed chemistry model for the surrogate components themselves can be developed and that these individual models can be validated over the relevant range of operating conditions. Furthermore, it also assumes that the final kinetic model of the surrogate fuel can successfully deal with the kinetic coupling between the pure components and their reaction intermediaries when they are in a mixture form. Unfortunately, all these assumptions run into separate problems. Firstly, not all surrogate mixtures representing a given fuel perform equally well over all the operating ranges and parameters of interest resulting in multiple

recommendations from various researchers (Table (2.1)) . This increases the number of potential compounds whose detailed chemistry need to be investigated. Furthermore, as noted in Section (4.1.2), even for simple straight chain alkanes of higher carbon numbers (like n-dodecane for jet fuels or n-hexadecane for diesel surrogates), the number of elementary reactions exceed even 10,000, making mechanism development a severely under-defined problem given the relatively few experimental data sets that are available. The problem is even greater for branched or cyclic alkanes and aromatics. Usually functional groups or reaction class assumptions are used to extrapolate kinetic rate parameters for most of the poorly investigated reaction pathways and ab-initio theories are used for the rest. However, as shown in Sheen and Wang (2011a) , such estimations lead to modeling uncertainties whose effects are much larger than most experimental data uncertainties and therefore require significant tuning based on experimental data. Even then, for more complicated surrogate compounds and for many inherently complicated chemistry regimes, the uncertainties remain large. Many reaction pathways have no analogs for the smaller compounds or require experimental conditions that are difficult to realize in a laboratory set up. Finally, the kinetic coupling between the surrogates is as yet not well understood. Such considerations make the surrogate approach both labor intensive and subject to significant uncertainties when quantitative predictions are needed.

Here, an alternative semi-empirical lumping approach is proposed that seeks to improve upon the surrogate approach to modeling the combustion chemistry of commercial fuels. Firstly, it is noted that despite the large variability of species present in a real fuel, the majority of these are large ($C > 6$) hydrocarbon compounds. It is seen that for n-alkanes and most of these larger hydrocarbon species, oxidation at engine relevant conditions occur through a two-stage process (Peters, 2009). The first stage involves the rapid endothermic breakdown of the fuel species into simpler fragments (small alkenes for n-alkane combustion for example) in the pre-heat region of the flame sheet. The second stage involves the exothermic oxidation of these simpler fuel fragments within the flame sheet. Therefore, in many applications, a detailed $H_2/CO/C_1 - C_4$ model supplemented by a lumped semi-empirical pyrolysis model that directly converts the fuel into a mixture of smaller product fragments may prove effective. The relative fractions of these thermal decomposition product fragments are determined through theoretical analysis guided by experimental data. In

this work, a first attempt at constructing such a one-step lumped pyrolysis model is made for n-dodecane and the lumped model predictions are compared against the flow reactor data and the detailed mechanism.

The near-identical laminar flame speed versus stoichiometry profiles for all n-alkanes above n-butane has been noted by multiple researchers (Ji et al. (2010), Ranzi et al. (2012)). In fact, as early as 1981, J. Warnatz in a pioneering kinetic analysis of alkane flames noted:-

"flame velocities of alkane flames can be modeled within a factor of two using the pure H_2 - O_2 -CO mechanism and only the initial attack of H, O and OH on the hydrocarbon...lean and stoichiometric flames, on the whole, can be characterized as H_2 - O_2 -CO flames fed by the hydrocarbon." (Warnatz, 1981) .

Even for rich flames, sensitivity analysis shows that laminar flame speeds are almost entirely insensitive to reactions involving C_4 species and above (Ji et al. (2010)) with H, CO and CH_4 reactions dominating. For binary diffusivities in air flames, the diffusivity of O_2 in N_2 and those of H, OH, O in N_2 are the most sensitive. These results and reaction path analysis confirm that higher n-alkanes break up rapidly through H-abstraction and β -scission pathways to small alkenes and alkyl radicals in the pre-flame region and it is the oxidation of these small carbon fragments that determine heat release and flame speed. A species profile simulation of stoichiometric n-dodecane flame at 1 atm. confirms this picture. As shown in Figure (7.1), the fuel largely decomposes in the 1050 K-1400 K region of the preheat zone over a 100 μs time interval generating smaller scission products like C_2H_4 , C_3H_6 and CH_4 . These smaller fragments then enter the flame sheet (marked by CH^* peak and maximum values of H and OH signaling flame ignition), are oxidized and generate heat. It can be seen that the oxygen fall off begins only after the fuel has decomposed completely. Other fuels, apart from aromatics, also show similar sequential occurrence of cracking-then-oxidation kinetics. It is to be noted that this fuel cracking occurs at a relatively high concentration of H and OH radicals that back diffuse into the preheat region thereby speeding up the cracking process substantially. Figure (7.2) shows the species profile simulations of a rich n-dodecane flame by Abid et al. (2009) showing similar characteristics. Experimental flame species profiles for a premixed rich n-decane burner stabilized flame by Doute et al. (1995), Figure (7.3), show similar characteristics where the fuel decays much faster than the oxygen generating peaks for ethylene, propene

and methane in the preheat zone, followed by their subsequent oxidation. Acetylene is formed at a late stage in this case as the flame is rich. Species profiles for rich n-heptane flames by D'Anna et al. (2007) also exhibit similar behavior in the pre-heat zone before soot formation in the post flame region. Such results confirm that a segregation of cracking kinetics from low-dimensional oxidation kinetics is possible for laminar flames. In the case of turbulent flames, the flamelet model aids in carrying over the key insights of laminar flame structure into much of the turbulent oxidation regime. As discussed by Hamlington et al. (2011), as turbulence intensity increases, the flame becomes broader than laminar flames due to a broadening of the pre-heat region while no appreciable change occurs in the width of the reaction or flame region. Thus, the lumped model approximation is likely to hold even more under such conditions.

7.2 Method

While for complex fuels, the lumping technique requires a semi-empirical approach in order to determine the fractional distribution of the pyrolysis products, a first principle partial equilibrium based lumping approximation can be used for n-dodecane decomposition. In the intermediate temperature regime, n-C₁₂H₂₆ molecules break down primarily through H-abstraction reactions by H and OH radicals to form n-dodecyl radicals. The dodecyl radicals subsequently undergo rapid H shift isomerization among the six dodecyl radicals. The primary and secondary radicals subsequently undergo β -scission reactions to create 1-alkenes and alkyl radicals. The process is repeated for all subsequent smaller alkyl radicals up to C₅. While β -scission is the primary means of n-alkane breakdown into intermediate products, radical isomerization reactions by H shift between the carbon atoms plays an important role in determining the proportion of the different scission products, thus affecting the product composition dramatically. Therefore, knowing the relative composition of the primary and secondary alkyl radical species is important for the successful prediction of the product distribution and species time history data. Also important is the comparative rates of β -scission and H-shift reactions with temperature. A significant number of experimental investigations and theoretical studies have been conducted to elucidate the rates of H-isomerization and β -scission reactions over a wide range of temperatures and

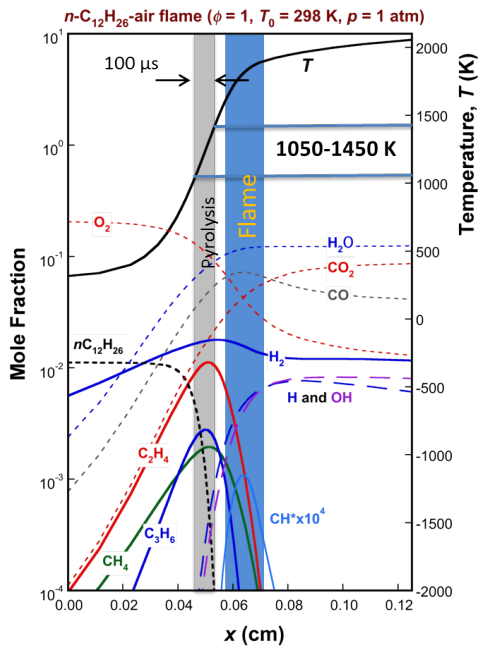


Figure 7.1: Simulation of n-dodecane Flame Species Profiles for $\Phi=1.0$, $T_{\text{unburnt}}=298\text{K}$, $P=1$ atm Conditions Showing Fuel Cracking and Fuel Oxidation Zones (Wang, MACCR Meeting 2013).

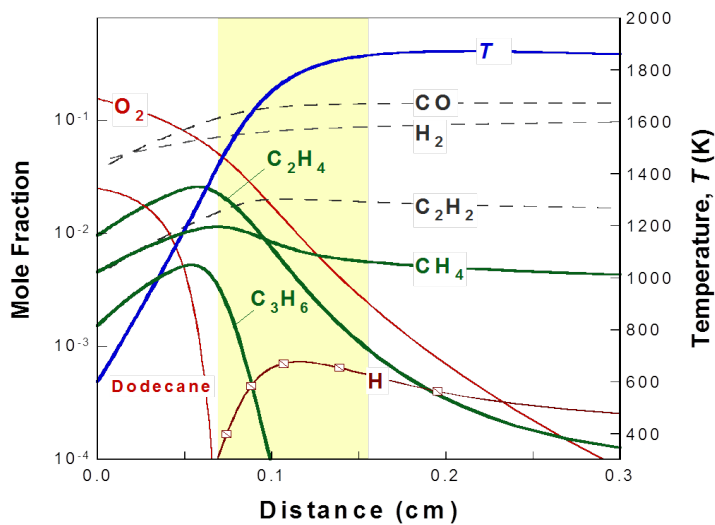


Figure 7.2: Simulation of n-dodecane Flame Species Profiles $\Phi=2.0$, $T_{\text{unburnt}}=298\text{K}$, $P=1$ atm (Abid et al. (2009)).

pressures. Of recent importance are the shock tube studies reported by Tsang and coworkers on n-pentyl (Tsang et al., 1998), n-hexyl (Tsang et al., 2007), n-heptyl (Tsang et al., 2009a), and n-octyl (Tsang et al., 2009b) that looked both into isomerization and scission reactions and recommended high-pressure and fall-off estimates for the major pathways. Sirjean et al. (2011) used Transition State Theory and Electronic Structure Calculations to generate theoretical estimates for H-isomerization rates that were in good agreement with previous experimental data. Ratkiewicz and Truong (2012) used Reaction Class Transition State Theory to obtain estimates for β -scission rate coefficients for various alkyl radicals. Simplified pictures of β -scission and H-isomerization reactions are presented in Figures (7.4) and (7.5). The β -scission reaction proceeds through the radical attack on the β carbon-carbon bond (relative to the initial position of the free electron carbon site) generating a 1-alkene and a primary radical fragment. The H-isomerization reaction proceeds through a cyclic transition state that is often called an N-*ab* state, where N is the ring size, *a* is the nature of the initial radical (primary or secondary) while *b* is the nature of the final radical (primary or secondary). According to the classical theory proposed by Benson (Thermochemical Kinetics, Benson 1974), the activation energy of the H-shift reaction can be evaluated by adding the energy required to abstract the H atom by an alkyl radical and the strain energy associated with the transition state ring structure. The relative magnitude of the reaction barriers between the H-shift and the scission reactions determine which of the competitive unimolecular pathways dominate at which temperature ranges. The estimated barrier heights from *ab-initio* calculations have been performed by several authors. Here, the energy values for H-shift reactions for hexyl radicals calculated by Sirjean et al. (2011), and the β -scission energy barrier for hexyl radicals calculated by Wang et al. (2010) are presented in Table (7.1). It is observed that for H shifts that have ring structures with 5 or more members, the isomerization energy barrier is at least 10 kcal/mol smaller than corresponding barriers for scission reaction. Furthermore, for temperatures less than 900 K, quantum tunneling effects also facilitate the H shift reactions (Sirjean et al., 2011). Thus, at low to intermediate temperatures (below 1400 K), the H-isomerization pathways proceed faster than β -scission pathways for alkyl radicals with 6 or more carbon atoms. The 5ps shift for 1-pentyl to 2-pentyl radical is also favored. However, as is seen in Table (7.1), the activation energy barrier for 4ps ring transition is higher than that of β -scission. Thus, for

smaller alkyl radicals (butyl and below), H isomerization is no longer an important pathway as the high ring strain effectively blocks the possibility of forming the ring transition state. Finally, the reaction rate values comparing the 1-heptyl scission pathway with the 1-heptyl \rightarrow 3-heptyl isomerization pathway are plotted in Figure (7.6). It is seen that at the high-pressure limit, the rates intersect slightly after 1500 K, while in the 1 atmosphere condition (fall off region) the rates intersect above 1700 K. Thus, for all low and intermediate temperature regions of combustion, the isomerization branch proceeds faster than scission paths as indicated by the barrier energy differences.

The Lumping Process pragmatically assumes that there occurs rapid equilibration among the n-alkyl radicals. Thus, the β -scission reaction occurs with the alkyl radicals being held at their equilibrium ratios among themselves. Let us denote the equilibrium concentrations by $[x_p]$ for the primary radical and $[x_{s_i}]$ for the i^{th} secondary radical. Let us also denote the radical in question by C_nH_{2n+1} where n is the carbon number. When n is even, there are $1, 2, \dots, \frac{n}{2}$ radicals ; and all of $2, \dots, \frac{n}{2}$ secondary radical sites are equally likely (to a first approximation). This implies that all $[x_i]$, $i=2, \dots, \frac{n}{2}$ are equal. When n is odd, there are $1, 2, \dots, \frac{n-1}{2}, \frac{n+1}{2}$ radical sites with the central site $\frac{n+1}{2}$ being half as numerous as all the other secondary carbon sites . Therefore, we have,

$$\left[x_{\frac{n+1}{2}} \right] = 0.5 \times [x_i] \quad i = 2, \dots, \frac{n-1}{2} \quad (7.1)$$

when n is odd. In general, the heat of formation of the primary radical is 3 kcal/mol higher than those of the secondary radicals. At equilibrium, the mole preserving reaction denoting the s to p shift can be written as ,



with an equilibrium constant,

$$K_c(T) = \frac{[x_p]}{[x_s]} = \exp\left(\frac{\Delta S_R^o}{R}\right) \times \exp\left(-\frac{\Delta H_R^o}{RT}\right) \quad (7.3)$$

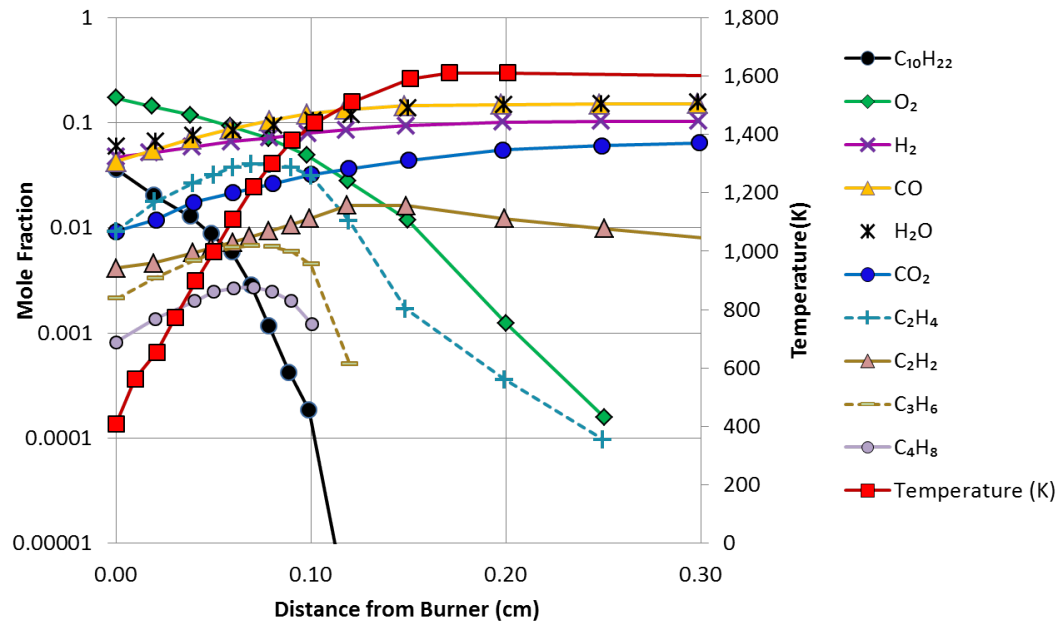


Figure 7.3: N-decane Flame Species Profile at $\Phi=1.7$ and $P=1$ atm [Doute et al. (1995)].

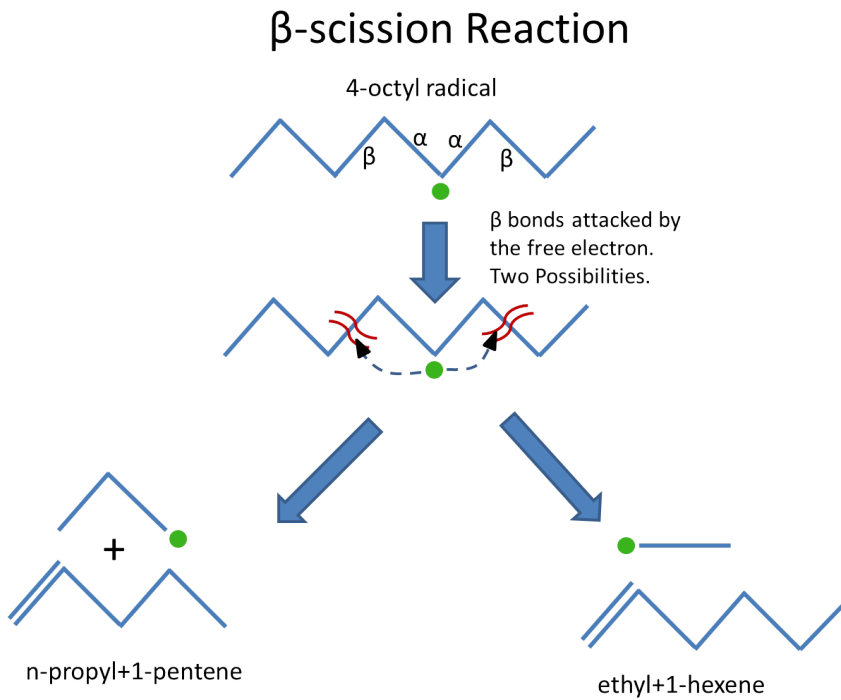


Figure 7.4: Schematic of β -scission Pathways for 4-octyl Radical.

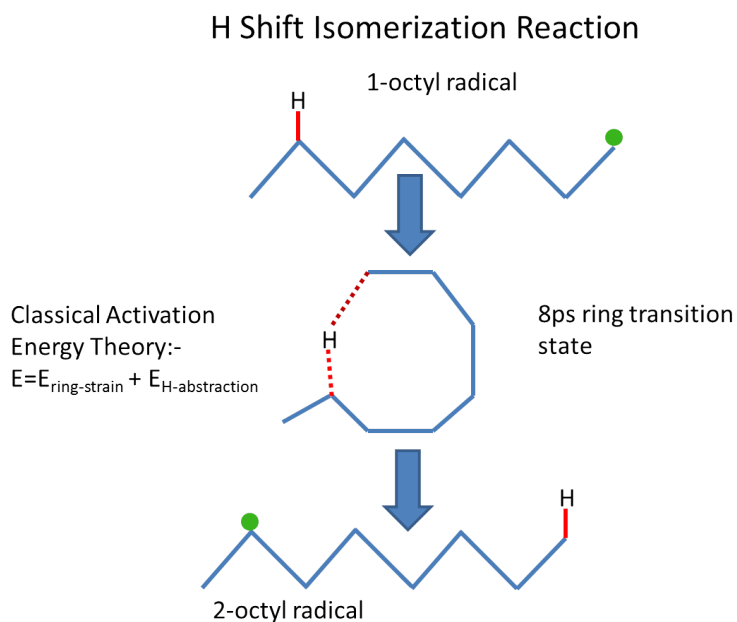


Figure 7.5: Schematic of Radical Isomerization Reaction (1-octyl to 2-octyl, 8ps isomerization).

Reaction	Energy Barrier (kcal/mol)	Ref.
1-hexyl→2-hexyl(6ps)	15.3	Sirjean et al. (2011)
1-hexyl→3-hexyl(5ps)	22.1	Sirjean et al. (2011)
1hexyl→ethene+1-butyl	31.4	Wang et al. (2010)
2hexyl→propene+1-propyl	31.6	Wang et al. (2010)
3hexyl→1-pentene+methyl	32.9	Wang et al. (2010)
3hexyl→1-butene+ethyl	31.4	Wang et al. (2010)
1-butyl→ethene+ethyl	33.9	Ratkiewicz and Truong (2012)
1-butyl→2-butyl (4ps)	39.3	Davis and Francisco (2011)

Table 7.1: Comparison of Isomerization and Scission Rates for hexyl and butyl Radicals.

Neglecting the fairly small entropy change contributions, we obtain $\Delta H_R^o = 3 \text{ kcal/mole}$. Thus,

$$\frac{[x_p]}{[x_s]} \approx \exp\left(-\frac{3000}{RT}\right) \approx e^{-\frac{1500}{T}} \quad (7.4)$$

When n is even,

$$1 = x_p + \sum_{s=2}^{n/2} x_s \quad (7.5)$$

Where x_p and x_s are the mole fractions of the primary and the secondary radicals. Dividing by x_s we get,

$$\frac{1}{x_s} = e^{-\frac{1500}{T}} + \frac{n}{2} - 1 \quad (7.6)$$

using eqn. 7.4 and since all secondary radicals have the same concentration. This gives,

$$f = x_s = \left(\frac{1}{e^{-\frac{1500}{T}} + \frac{n}{2} - 1} \right) = x_p \times e^{\frac{1500}{T}} \quad (7.7)$$

which is the final proportions for the radical fractions.

When n is odd, the central symmetrical secondary radical is present at half the concentration of all the other s -radicals. Therefore,

$$1 = x_p + \sum_{s=2}^{\frac{n-1}{2}} x_s + \frac{x_s}{2} \quad (7.8)$$

Dividing by x_s as before we get once again

$$f = x_s = \left(\frac{1}{e^{-\frac{1500}{T}} + \frac{n}{2} - 1} \right) = 2 \times x_{\frac{n+1}{2}} = x_p \times e^{\frac{1500}{T}}, \quad s = 2 \dots \frac{n-1}{2} \quad (7.9)$$

The lumping process systematically proceeds through the following steps,

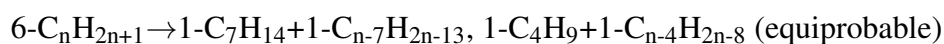
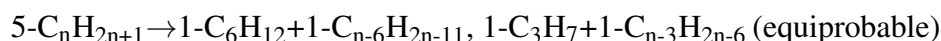
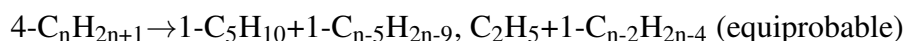
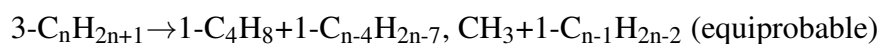
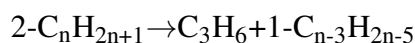
1. In the detailed mechanism, rate coefficients for each of the 6 dodecyl radicals formed by H abstraction by any of the active radicals (H/OH/O/CH₃/HO₂) are separately provided. The first step is to combine all 6 rates into a single dodecane \rightarrow dodecyl pathway for each radical. This is done by summing up all the six rate values as a

function of temperature and then evaluating the best-fit Arrhenius parameters for the effective rate constant. Thus

$$k_{eff}(T) = \sum_{i=1}^{i=6} k_i(T) = A_{eff} T^n \exp\left(-\frac{E_{eff}}{RT}\right) \quad (7.10)$$

for each of the H abstraction reactants (H, OH, O, HO₂, O₂ and CH₃). It is assumed that this H-abstraction is the rate-limiting step and all subsequent β scission and alkene breakdown reactions occur rapidly. Thus, the rates evaluated from eqn. (7.10) are the rate parameters for the lumped dodecane+(H/OH/CH₃/HO₂) pathways in the reduced model.

2. The concentration of the dodecyl radicals are evaluated using eq.(7.7). For the β -scission reactions, all alternate pathways are considered equally probable. The reactions themselves are assumed to occur infinitely fast. The smaller n-alkyl radicals that are formed as a product of β -scission are also assumed to undergo rapid H-isomerization among themselves if their carbon number is greater than 4. In general for the nth alkyl radical, the equilibrium concentration is given by eq. (7.7) or eq.(7.9), whichever is applicable. The radicals break down according to the following scheme when n>4,



Note that due to ring strain constraints, 1-pentyl radical can only isomerize with 2-pentyl radical and not with 3-pentyl radical which requires a 4ps ring structure.

3. The 1-alkenes are assumed to undergo a simple allyl C-C bond fission as follows.

$1\text{-C}_n\text{H}_{2n} \rightarrow \alpha\text{-C}_3\text{H}_5 + 1\text{-C}_{n-3}\text{H}_{2n-5}$; the primary radical will undergo isomerization by usual means if $n \geq 5$. The allyl bond fission pathway is assumed to dominate over all other alkene breakdown pathways in this simple reduced scheme. This is an oversimplification, as alkenyl radicals formed by H abstraction from other sites are possible as well as radical mediated H addition reactions. Future refinements may include explicit considerations of other alkene decomposition pathways.

4. At intermediate temperatures, direct C-C bond fission of n-dodecane is also relatively important and needs to be considered. Here, distinction is made between the two terminal α C-C bonds and the other 9 β C-C bonds. Thus, for n-dodecane fission we have $\text{R-CH}_3 \rightarrow \text{R}^* + \text{CH}_3$ with k_α as the rate constant for the two possible branches and $\text{R-R}' \rightarrow \text{R}^* + \text{R}'^*$ with k_β as the rate constant. Then the probability for each pathways can be determined as follows

$$\text{C}_{12}\text{H}_{26} \rightarrow \text{CH}_3 + \text{C}_{11}\text{H}_{23} \text{ fraction} = 2 \times \frac{k_\alpha}{2k_\alpha + 9k_\beta}$$

$$\text{C}_{12}\text{H}_{26} \rightarrow \text{C}_2\text{H}_5 + \text{C}_{10}\text{H}_{25} \text{ fraction} = 2 \times \frac{k_\beta}{2k_\alpha + 9k_\beta};$$

We proceed similarly for $(\text{C}_3\text{H}_7 + \text{C}_9\text{H}_{19})$, $(\text{C}_4\text{H}_9 + \text{C}_8\text{H}_{17})$, $(\text{C}_5\text{H}_{11} + \text{C}_7\text{H}_{15})$ fissions.

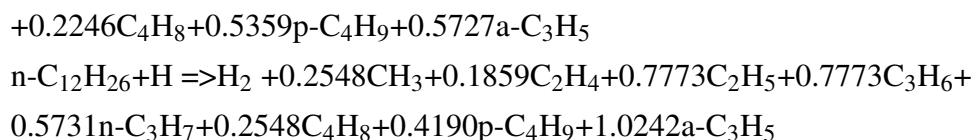
$$\text{Finally } \text{C}_{12}\text{H}_{26} \rightarrow \text{C}_6\text{H}_{13} + \text{C}_6\text{H}_{13} \text{ fraction} = \frac{k_\beta}{2k_\alpha + 9k_\beta};$$

The radicals formed follow the usual isomerization-scission pathways determining the final products. In a process similar to the abstraction reaction, the α and β rate coefficients are summed up to create the effective bond fission rate coefficient whose parameters are adopted in the final lumped fission reaction of n-dodecane.

5. The final lumping is checked for carbon balance and contains only one bond fission reaction and one abstraction reaction per radical species. No products above C_4 are considered.

Thus, the final reduced mechanism contains only six reactions that directly break down n-dodecane into C_1 - C_4 species. Only the abstraction reaction by the H radical has been shown, the other five H abstractions reactions (by O, OH, HO_2 , CH_3 , O_2) have identical stoichiometric coefficients.

$$n\text{-C}_{12}\text{H}_{26} \Rightarrow 0.3117\text{CH}_3 + 0.1884\text{C}_2\text{H}_4 + 0.9924\text{C}_2\text{H}_5 + 0.7895\text{C}_3\text{H}_6 + 0.7327n\text{-C}_3\text{H}_7$$



7.3 Results

Comparisons of the lumped model predictions with the Flow Reactor data are presented in this section. Under-low temperature pyrolysis and oxidation conditions, significant fractions of higher alkenes are formed which the simplified lumped model does not take into account. In order to preserve carbon balance without over-predicting the initial generation rates of ethylene and propene, the n-dodecane H abstraction rates have been reduced by a factor of 2 from the original estimates.

Figure (7.7) presents the comparison between the experimental data and the lumped JetSurf model for the 1000 K pyrolysis run. It is seen that the fuel decay and ethylene generation are relatively well matched. However, it is observed from Figure (7.7) that the predicted propene concentration is two times greater than the experimental data. This discrepancy may be attributed to the exclusive allyl site decomposition pathway assumptions made for all alkenes. The allyl radical is a major producer of propene, and the exclusive allyl pathway fission reaction has the effect of overproducing propene. The carbon balance is 100% as seen in figure (7.8), showing that the lumped mechanism tracks all C-atoms.

The 1050 K Rich Oxidation Data have been compared with the detailed and the lumped JetSurf model in Figures (7.9), (7.10) and (7.11). In this case as well, there are deviations from the detailed species profile, especially propene predictions are too high due to the reasons noted above. The fuel decomposition and ethylene generation are fairly well predicted when compared with the experimental data. The carbon balance predictions continue to remain over 90% throughout. Overall, the simplified lumped mechanism performs fairly well in predicting the species time history profiles in the initial stages of oxidation and pyrolysis reaction if one takes into account the large variations observed previously among the detailed mechanism schemes.

The high-temperature oxidation runs are compared next. For the 1170 K lean oxidation conditions depicted in Figures (7.12), (7.13) and (7.14), it is observed that after the initial

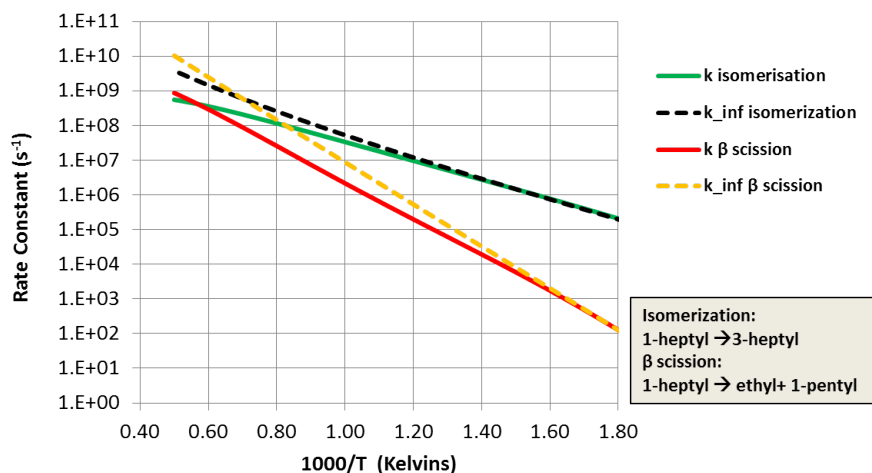


Figure 7.6: The Forward Reaction Rates of the Dominant heptyl Isomerization and β -scission Reaction at the High Pressure Limit and at 1 atm. Conditions.

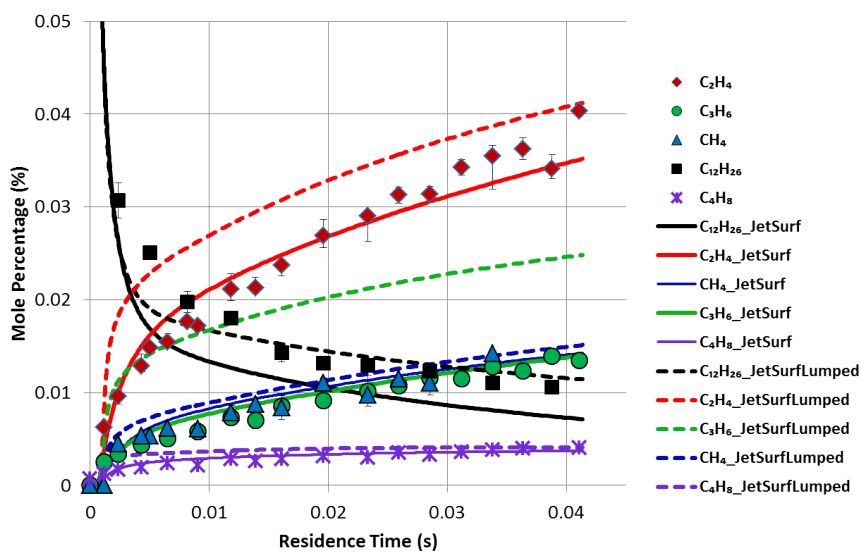


Figure 7.7: 1000 K Pyrolysis Experiment Data Compared with Detailed and Lumped Jet-Surf Models.

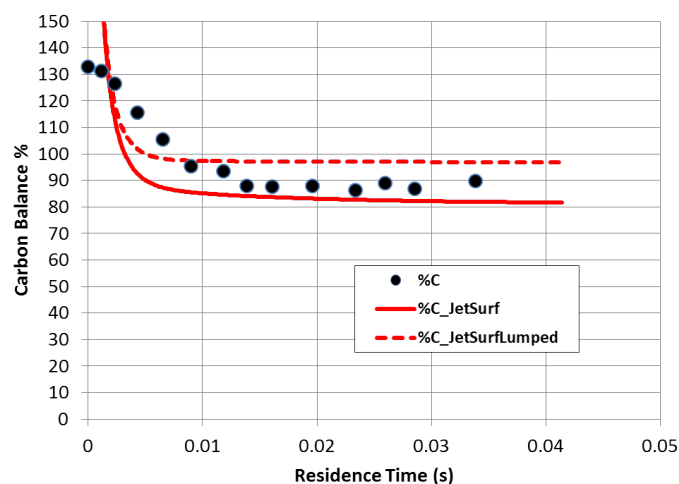


Figure 7.8: 1000 K Pyrolysis Experiment Carbon Balance for Detailed and Lumped JetSurf Models.

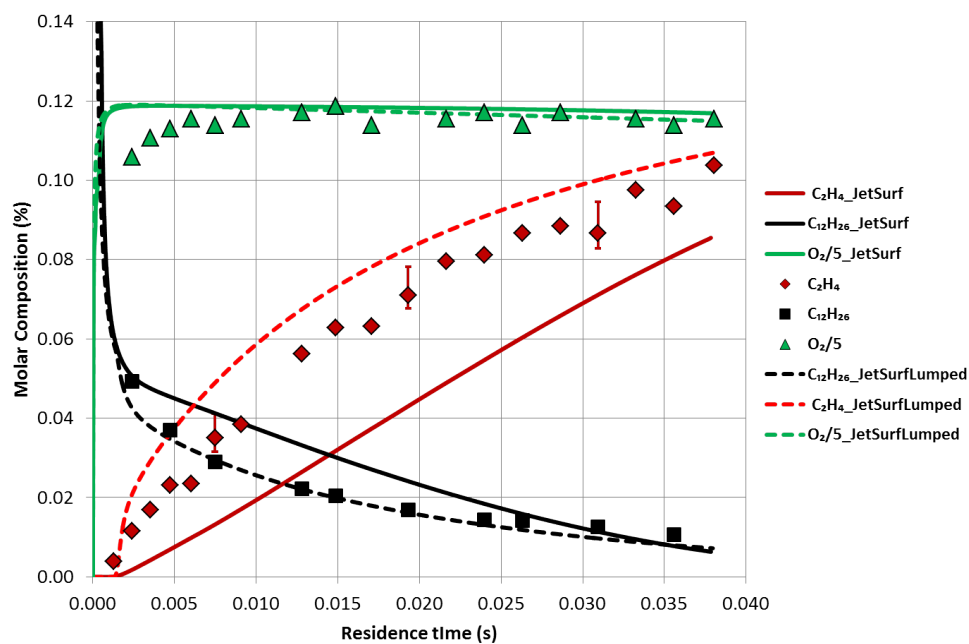


Figure 7.9: 1050 K Oxidation, $\Phi=1.56$:- Data Compared with Detailed and Lumped JetSurf Models.

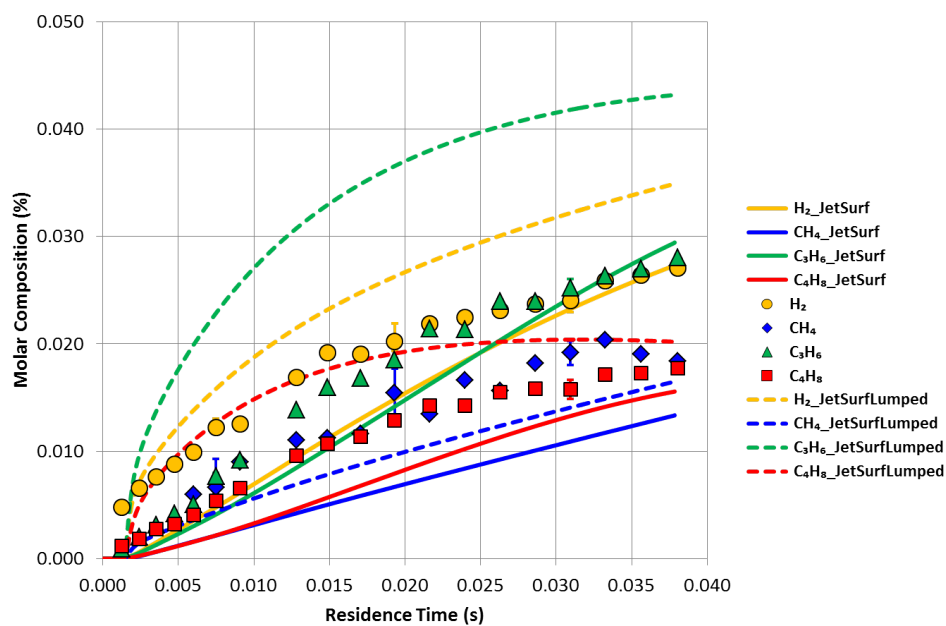


Figure 7.10: 1050 K Oxidation, $\Phi=1.56$:- Data Compared with Detailed and Lumped Jet-Surf Models.

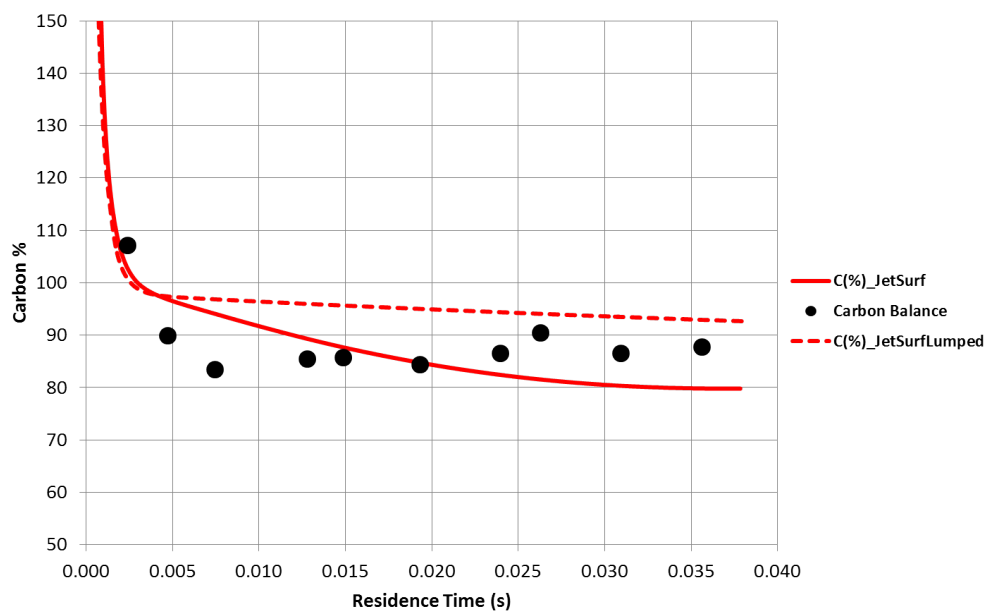


Figure 7.11: 1050 K oxidation, $\Phi=1.56$:- Carbon Balance.

faster rise, the intermediates oxidize at a rate slower than the detailed model. Despite this, the CO, CO₂, CH₄, C₂H₄ species time history profiles match well with the experimental data. 1-butene and particularly propene mole fractions are over predicted. Similar trends are observed for the rich 1220 K oxidation conditions as well [Figures (7.15) , (7.16) , (7.17)]. Overall, the species profile match is of comparable quality to the detailed JetSurf or any of the other detailed mechanisms considered in this study.

7.4 Future Work

The current chapter presents a new lumping methodology that has the potential of considerably simplifying the effort needed to simulate the combustion chemistry of commercial fuels. A preliminary proof of concept analysis for the new methodology has been made against the n-dodecane flow reactor data and the results were found to be satisfactory. Further efforts are underway to refine the model assumptions and test it further against other data and species types. Some of the future work projects are outlined in the concluding chapter. If successful, a direct semi-empirical lumping methodology may replace the current surrogate model-based technique for constructing reduced fuel chemistry models of commercial aviation fuels or for that matter any other fuel types.

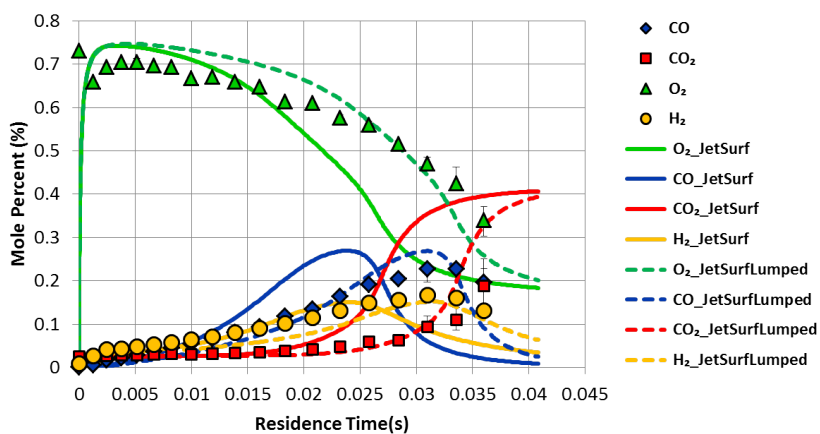


Figure 7.12: 1170 K Lean ($\Phi=0.79$) Oxidation Data Compared with Detailed and Lumped JetSurf Models.

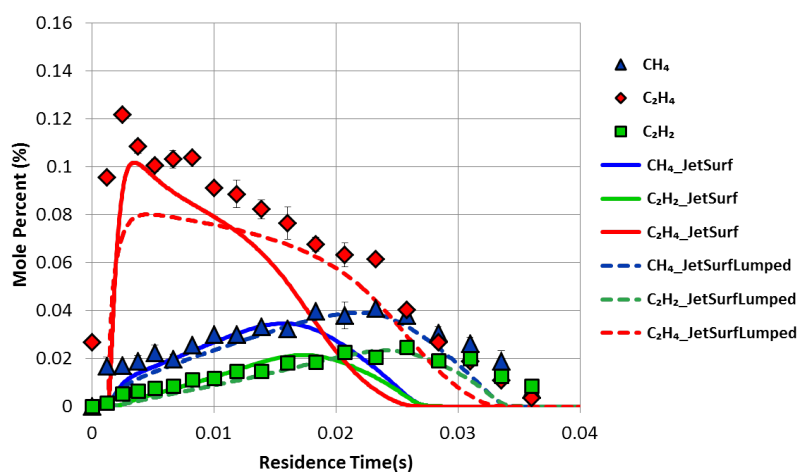


Figure 7.13: 1170 K Lean ($\Phi=0.79$) Oxidation Data Compared with Detailed and Lumped JetSurf Models.

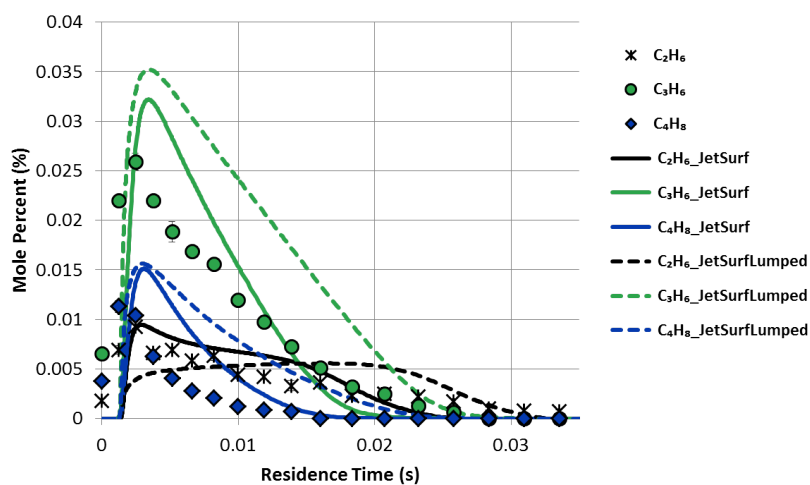


Figure 7.14: 1170 K Lean ($\Phi=0.79$) Oxidation Data Compared with Detailed and Lumped JetSurf Models.

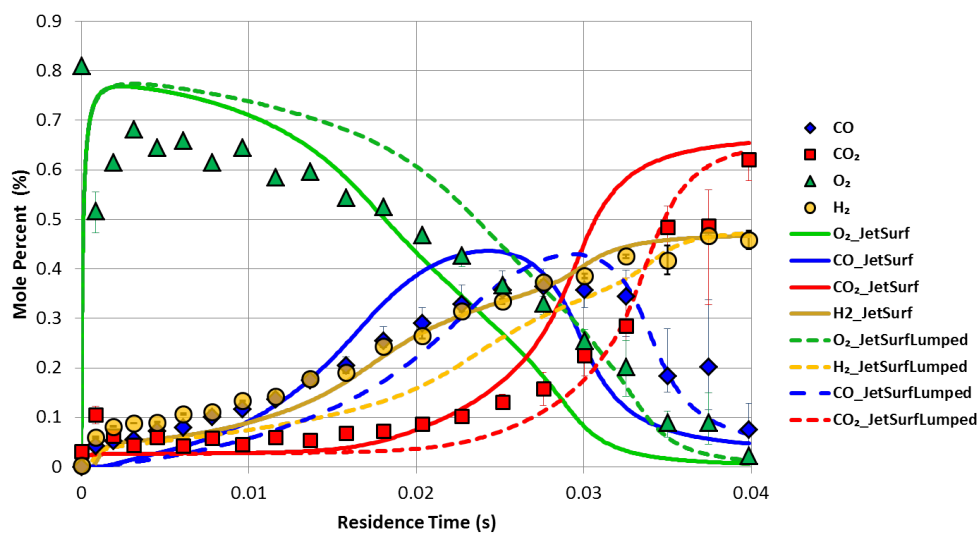


Figure 7.15: 1220 K Rich ($\Phi=1.32$) Oxidation Data Compared with Detailed and Lumped JetSurf Models.

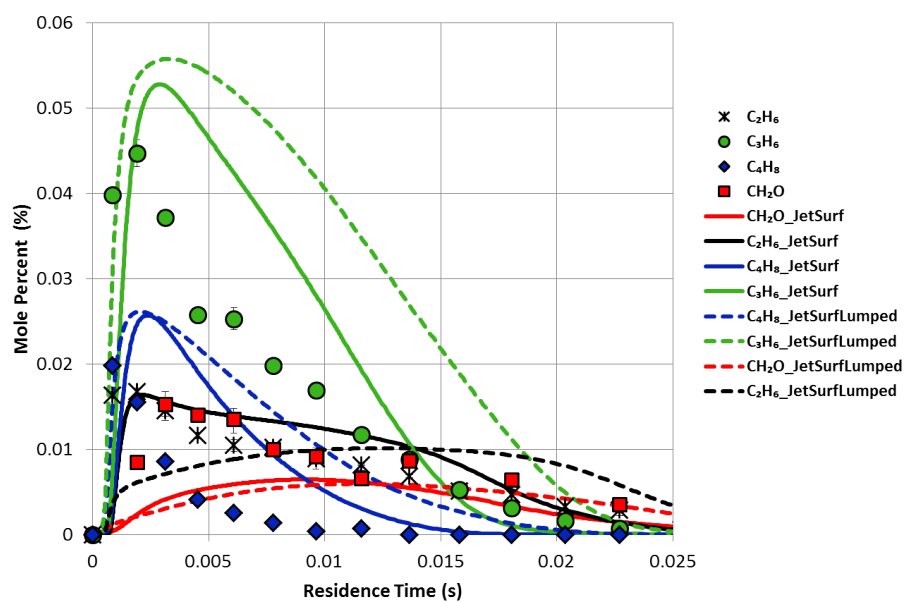


Figure 7.16: 1220 K Rich ($\Phi=1.32$) Oxidation Data Compared with Detailed and Lumped JetSurf Models.

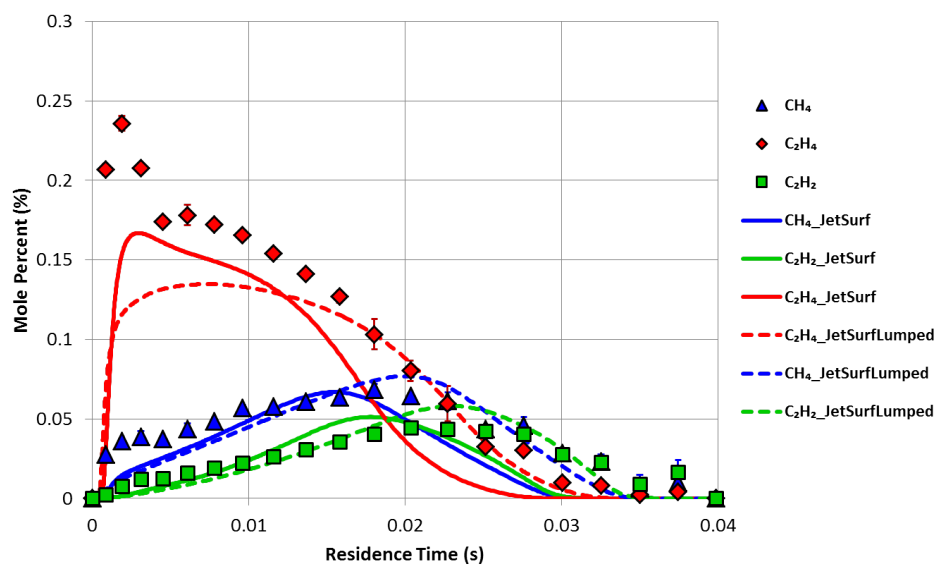


Figure 7.17: 1220 K Rich ($\Phi=1.32$) Oxidation Data Compared with Detailed and Lumped JetSurf Models.

Chapter 8

Concluding Remarks

8.1 Summary and Discussion

The present work investigated n-dodecane oxidation and pyrolysis kinetics in the intermediate temperature regime of 1000K-1250K under atmospheric pressure conditions and extended the experimental database over this critical but somewhat neglected region of n-alkane combustion. The Stanford Variable Pressure Flow Reactor was modified to handle low vapor pressure hydrocarbon fuels and species time-history profiles were obtained for the fuel, oxygen and 12 intermediate products over a 1-40 ms residence time using real-time gas chromatography. The repeatability and carbon balance were excellent under all conditions. The experiments were conducted at four setpoints chosen to investigate fuel pyrolysis as well as early stage and late stage oxidation chemistry pathways under rich and lean conditions. The experimental results were compared against the predictions of several detailed chemical kinetic mechanisms and were also used for an initial proof-of-concept validation study for a new lumping paradigm. Some of the major conclusions that may be drawn from the study are outlined below.

- Under pyrolysis conditions it was observed that the fuel molecule decays by H abstraction and β scission reactions to generate ethylene and propylene as the major products. It was also noted that even under oxidation conditions, n-dodecane decomposition occurs through pyrolytic pathways to generate ethylene, propene and 1-butene without any involvement of oxygen. Only at a later stage do the smaller

alkenes generated from n-dodecane decomposition undergo oxidation to form CO, CH₂O and C₂H₂. The 1000 K pyrolysis run and the rich 1050 K oxidation run investigates the earlier fuel breakdown stages, while the rich 1220K and the lean 1170K oxidation experiments investigate the later oxidation stages of the primary products ethylene and propylene. The initial stages of the fuel breakdown were found to be accelerated by the presence of excess amounts of hydrogen and water molecules in the bath gas since they act as sources of H radicals in the system.

- Four detailed chemical kinetic mechanisms for n-alkane combustion were compared against the experimental results to evaluate their performance in predicting the species profiles at the early thermal decomposition stage and the late oxidation stage of the n-dodecane combustion process. An optimized version of the detailed JetSurf 1.0 mechanism (Sirjean et al., 2009) tuned against shock tube and flame speed data using solution mapping and spectral uncertainty minimization techniques (Section 4.1.2) was used for the comparison along with the Lawrence Livermore mechanism (Westbrook et al., 2009), the CNRS mechanism from the Orleans group (Mze-Ahmed et al., 2012) and the CRECK mechanism from the Milano group (Ranzi et al., 2005). It was found that the CNRS mechanism performs best in predicting the the early stage n-dodecane thermal decomposition processes captured in the 1000K and 1050K experiments, while the CRECK model performs best in predicting the late stage alkene oxidation kinetics captured in the 1170 K and 1220 K experiments. The optimized JetSurf model is the best match overall with fairly accurate predictions for both the lower temperature and the higher temperature run conditions, though in both cases it is found to moderately overpredict the reaction rates. The Lawrence Livermore mechanism predicts reaction rates consistently slower than the experimental results under all conditions.
- The cause of the differences in predictions generated by the different kinetic schemes was investigated through sensitivity and rate-of-production analysis. A comparative analysis between the optimized JetSurf and the LLNL mechanism revealed that significant differences in the rate parameters and equilibrium constants exist in several key H/OH radical formation and ethylene generation pathways and these appear to

be responsible for the differences in the reaction rates observed in the early stage fuel decomposition kinetics between the two mechanisms. Similarly, large differences in reaction rates for the ethylene oxidation through the vinyl radical formation pathways were identified as the source of relatively faster oxidation rates of the JetSurf mechanism when compared against the LLNL mechanism. It was concluded that a better consensus about the kinetic rate parameters of the C₂- C₃ sub-mechanism in the combustion community based on high quality experimental data or improved *ab-initio* studies may be needed to improve the congruence among the predictions made by the detailed mechanism schemes proposed in the literature.

- A new simplified lumping methodology was proposed based on the observation that for heavy hydrocarbons, the combustion process proceeds through an initial thermal decomposition stage to smaller fragments (1-alkenes in the case of paraffins) followed by a final oxidation stage of the cracked products. The lumping method takes into account the fact that the final flame characteristics depend only on the relative fractions of the cracked products of the initial thermal decomposition stage and seeks to replace the entire pyrolysis sub-mechanism with a set of direct one-step reactions that convert the fuel molecule into the cracked products. A proof-of-concept validation of this approach was performed by constructing a lumped n-dodecane mechanism from the optimized JetSurf scheme and its predictions were compared against the flow reactor data. The model matched with the experimental data reasonably well though it over-predicted the propene mole fractions considerably. The source of this over-prediction was identified to an extremely simplified model for higher alkene decomposition pathway. Future efforts will be directed towards fine-tuning the lumping methodology so that it can serve as a superior alternative to the current surrogate modeling approach for aviation fuel kinetics model development.

8.2 Future Work

The continued development of the proposed lumping methodology will be the focus of future experimental and theoretical modeling efforts. The aim of the lumping methodology

is to directly model the chemistry of commercial jet fuels like JP-8 or Jet-A. Experimental work is needed to investigate the thermal decomposition of these complex fuels in order to determine the primary cracking products and their fractional ratios under various temperature and pressure conditions. A semi-empirical lumped model of the fuel decomposition can then be constructed that is able to replicate the ratios of the decomposition products and their generation rates. This lumped mechanism can then be appended to the detailed kinetic schemes that incorporate the oxidation chemistry of the smaller cracked products. A set of experimental projects are proposed to aid this effort.

1. Investigating the thermal decomposition kinetics of JP-8 and Jet-A fuels under low, intermediate and high temperature conditions and at various pressures. The investigation is to be conducted using flow reactors, jet stirred reactors and shock tubes and will be aimed at measuring the concentration of the products of thermal cracking as a function of time, temperature and pressure. The effect of adding H and OH radicals to the fuel/bath-gas mix also needs to be quantified. The pyrolysis products are likely to include all the major functional groups including aromatics. The lumped pyrolysis model will ideally be a set of one-step reactions converting the jet fuel directly to its cracked components and will be based on fitting the composition data obtained from the pyrolysis experiments.
2. The lumped pyrolysis model will then be integrated into a detailed oxidation chemistry sub-mechanism for the products of thermal decomposition. The base model can be selected from any of the well-validated detailed chemical kinetic models that have been developed for the smaller normal and branched alkanes, alkenes, dienes as well as aromatics. The entire model can then be validated against fuel oxidation experiments in the flow reactor or the jet stirred reactor, ignition delay data from the shock tube and RCMs as well as flame speed and extinction studies. If necessary, solution mapping and uncertainty minimization techniques may be applied to optimize the model against target experimental data sets. The effect of the pressure and compositional variations on the yield ratios of the cracked products also needs to be quantified and implemented in the model.

3. For both the stages of model development outlined above, flow reactor experiments that investigate the pyrolysis and oxidation kinetics of commercial jet fuels through species time-history measurements will be necessary. Towards this end, efforts are underway to utilize the Stanford Flow Reactor facility to investigate JP-8 pyrolysis kinetics in the intermediate temperature regime and at various pressures. These experiments will be followed by oxidation experiments for the engine relevant stoichiometric conditions. The experimental set points will be chosen so as to provide the information necessary to construct and validate the lumped mechanism and needs to occur in concert with validation experiments being performed in other experimental facilities. If successful, the new methodology will be able to construct kinetic mechanisms of reasonable size that can replicate most of the combustion behavior of a real jet fuel without the need for adopting the more labor intensive surrogate fuel modeling approach.

Appendix A

Gas Chromatograph Calibration

A.1 Overview

A gas chromatograph consists of one or more analytical columns through which gaseous samples containing the species of interest are injected. The individual species in the gaseous sample are adsorbed by the column and are retained for a specific amount of time before being eluted. The retention time, defined as the time between the start of the sample run and the point when the species exits the column, depends both on the column type and stationary phase material with which its surface is coated as well as the physical and chemical properties of the species. For compounds with similar functional groups, the retention times are, in general, proportional to their relative volatility. The differences in the retention times allow for the separation of the various species in the gas stream based on their chemical composition. The retention times are usually constant for a particular species if the column conditions are kept the same. Thus the retention time values serve to identify a particular species from one experimental run to the next.

The gas chromatograph being used for the present study is a micro gas chromatograph by INFICON (INFICON 3000-MicroGC) that has four capillary columns fitted with thermal conductivity detectors. The different columns are sensitive to different types of chemical compounds. If such a compound is present in the sample gas, the column retains the compound and subsequently elutes it after a characteristic retention time has elapsed. The eluted species is observed as a detector voltage peak whose area is proportion to the

concentration of the species in the sample gas. The proportionality constant is called the response factor R , and for a specific species i , it is given by,

$$X_i = A_i R_i \quad (\text{A.1})$$

where A_i is the peak area and X_i is the species mole fraction (in ppm) in the sample gas. For columns that retain more volatile species, a pre-column with a back-flush module is provided that prevents the slow eluting species from entering the main column and appearing as extraneous peaks in the later runs. The gas chromatograph is also provided with particulate and condensate filters to prevent condensates and impurities from poisoning the columns.

A.2 Operating Conditions and Column Calibration

The four capillary columns present in our GC are described in Table (A.1). The MolSieve column is used to detect H_2 , O_2 , CH_4 and CO . The PLOT U column is used to detect CO_2 , C_2H_4 , C_2H_6 and C_2H_2 . The Alumina PLOT column is used to detect C_3H_6 and C_4H_8 . Depending on the column setpoints, the OV-1 column is used to detect CH_2O , all the higher alkene species as well as n-dodecane. Details of the micro-GC installation, operation and operating instructions are available from the manufacturer's website (INFICON 3000-MicroGC). The species identification and the calibration procedures have been described in detail previously by (Walters, 2008). Standardized calibration gas mixtures were used to evaluate the elution time and response factor of the different chemical species. Formaldehyde calibration was performed through the Multipoint Calibration Technique using manometrically prepared calibration samples of formaldehyde vapor produced by heating solid para-formaldehyde in a quartz glass bulb under vacuum conditions (Bardosova, 2011). The n-dodecane calibration was performed by connecting the heated bath-evaporator system to the GC and using the FID based total hydrocarbon detector to ascertain the concentration of n-dodecane in the sample stream.

Column	Dimensions	Precolumn	Dimensions
MolSieve 5A	10m×0.32 mm	PLOT U	3m×0.32 mm
PLOT U	8m×0.32 mm	PLOT Q	1m×0.32 mm
Alumina PLOT	10m×0.32 mm	PLOT 1	1m×0.32 mm
OV-1	14m×0.15mm, 2 μ m thick	None	

Table A.1: Columns Present in 3000 Micro-GC

Column	Run Conditions	Column Temperature ($^{\circ}$ C)	Column Pressure (psi)	Run Time (s)	Back-flush Time (s)
MolSieve	General	80	32	180	9.1
PLOTU	Dry	50	32	120	6.1
PLOTU	Wet	120	20	120	15.5
Alumina	Dry Only	130	30	75	3.3
OV-1	Formaldehyde Detection	52	15	240	None
OV-1	High Alkenes	90	36	250	None
OV-1	C ₁₂ H ₂₆	180	40	420	None

Table A.2: GC Column Conditions Used for Species Detection

A brief summary of the column conditions used in the experiments is provided in Table (A.2) . Also, Table (A.3) outlines the elution times and response factors for the various species as well as relative errors in the peak area estimates.

Column	Species	Calibration Gas	Response Factor (ppm)	Relative Error (%)	Elution Time (min.)
MolSieve	H ₂	0.303%	1.2	0.13	0.74
	O ₂	1.11%	11.55	0.54	0.89
	CH ₄	0.0802%	5.82	3.02	1.72
	CO	0.401%	14.41	1.06	2.28
PLOT U	CO ₂	0.753%	0.826	0.24	0.79
	C ₂ H ₄	0.159%	0.817	0.605	0.94
	C ₂ H ₆	0.0101%	0.794	4.5	1.1
	C ₂ H ₂	0.0754%	0.987	1.13	1.73
Alumina PLOT	C ₃ H ₆	0.05%	2.58	0.45	0.6
	C ₄ H ₈	0.0199%	2.16	1.73	0.97
OV-1 High Alkenes	C ₄ H ₈	60.7 ppm	0.737	1.14	0.84
	C ₅ H ₁₀	40.5 ppm	0.643	1.58	1.12
	C ₆ H ₁₂	41.1 ppm	0.569	1.42	1.66
	C ₇ H ₁₄	40.8	0.551	5.44	2.77
OV-1, Formaldehyde	CH ₂ O	MCT method	2.47	10	1.61
OV-1, n-C ₁₂ H ₂₆	n-C ₁₂ H ₂₆	366 ppm	0.334	3.72	5.67

Table A.3: Response Factors, Elution Times and Standard Errors for the Different Species Detected by the Gas Chromatograph.

Appendix B

Uncertainty Analysis

The following section presents an analysis of the various uncertainties present in the flow reactor experiments. The uncertainties are classified into those stemming from the temperature measurements, initial flow rate settings, species concentration measurements and those stemming from uncertainties in residence time modeling and the mixing time constant estimates. When multiple uncertainty sources affect a particular variable of interest, the error propagation equations outlined in (Bevington and Robinson, 2002) have been used. The propagation equations are as follows:-

1. One or more independent, random, uncorrelated error sources x_i may be combined to obtain the total error,

$$\sigma_{total} = \sqrt{\sum [\sigma_{x_i}^2]} \quad (B.1)$$

2. If there is a variable y that is a function of several independent variables x_i , each with its own standard error σ_{x_i} , then the standard error in the dependent variable y can be determined by the equation

$$\sigma_y^2 = \sum_i \left[\sigma_{x_i}^2 \left(\frac{\partial y}{\partial x_i} \right)^2 \right] \quad (B.2)$$

3. In linear regression estimates, the parameters 'a' and 'b', in the linear estimate $y = ax + b$, are often derived from multiple measurements of the data pair (x_i, y_i) . In such cases, the standard uncertainty for the regression parameters are calculated from the

equations,

$$\sigma_a^2 = \frac{\sigma_y^2}{\Delta} \sum_{i=1}^N x_i^2 \quad (\text{B.3})$$

$$\sigma_b^2 = N \frac{\sigma_y^2}{\Delta} \quad (\text{B.4})$$

$$\Delta = N \sum_{i=1}^N x_i^2 - \left(\sum_{i=1}^N x_i \right)^2 \quad (\text{B.5})$$

B.1 Temperature Uncertainty

B.1.1 Radiation Correction Effects

A type R (Pt/13% Rh-Pt) thermocouple with 0.005" bead diameter and 0.002" wire diameter is used to measure the temperature within the flow reactor. The thermocouple bead is coated with a 0.001" thick passivating SiO₂ film. A data acquisition system that interfaces with the LabVIEW software is used for monitoring the thermocouple voltages. Cold junction compensation is done aboard the data acquisition board and the non-linearity in the Seebeck coefficient is taken into account by the interfacing software (Bardosova, 2011). The effect of radiation losses from the thermocouple bead to the heated reactor wall needs to be taken into account. Conduction losses through the thin bead wires are considered negligible. Then, the terms of interest include the radiative heat transfer to the walls and the convective heat transfer from the gas to the bead.

$$T = T_b + \frac{\varepsilon_b \sigma d_b}{Nu \lambda_g} (T_b^4 - T_\infty^4) \quad (\text{B.6})$$

where T is the corrected gas temperature, T_b is the measured bead temperature, T_∞ is the reactor wall temperature, d_b is the bead diameter, ε_b is the total emissivity of the bead, σ is the Stefan-Boltzmann constant, λ_g is the thermal conductivity of the gas and Nu is the Nusselt number of the bead. Following (Bardosova, 2011), the Nusselt number is estimated from the hot wire anemometry correlation (Hinze, 1959).

$$Nu = 0.42Pr^{0.2} + 0.57Pr^{0.33}Re^{0.5}, 10^{-2} < Re < 10^4 \quad (B.7)$$

The bead emissivity is taken to be 0.3 based on correlations found in (Sully et al., 1952) and (Bradley and Entwistle, 1961) . The coated bead diameter is estimated to be 0.007" . The axial velocity and the film temperature $T_f = \frac{T+T_b}{2}$ are used to evaluate the Nusselt number values for a specific experimental condition. In a previous work, (Schmidt, 2001) characterized the radial variation of the temperature at different axial points along the reactor for nominal 1200 K, 1 atm flow condition. The temperature differences between the reactor center-line and the reactor walls were found to be about 80 K at 4 cm downstream of the injection point, 50 K at 8 cm , 20 K at 12 cm and less than 10 K for distances further than 20 cm downstream of the second injection point. The corresponding radiation corrections range from 5 K for wall temperature differences of over 50 K and 2K-3K for wall temperature differences of 20 K or lower. For the 1000 K and 1050 K experimental conditions, the radiation corrections are in the 3 K-1 K range.

The overall uncertainty introduced through equation (B.6) is 3.7 K (Bardosova, 2011) , while the uncertainty introduced through signal digitization of the thermocouple measurements is ± 2 K . The net uncertainty in the temperature measurements, obtained through equation (B.1) , is ± 4.2 K. The uncertainty values are relatively insensitive to variations in the reactor temperatures within the 1000 K-1200 K region of interest.

Finally, the effect of temperature variation on the expected molar concentration profiles of the measured species are assessed by comparing the results obtained from using an uncorrected temperature profile to that where a radiation correction effect from a uniform 50 K temperature difference between the walls and the center-line has been considered. Note that the uniform 50 K temperature drop between the axis and the walls represents a worst case scenario and is only being used to assess the impact of the temperature uncertainties on our results. The simulation results for the 1220 K rich experimental condition and the 1000 K pyrolysis condition using the optimized JetSurf mechanism are presented. Figures (B.1), (B.2) and (B.3) show relatively little sensitivity of the species profiles to even the worst possible conditions. Some variations are observed at the longer residence times. However, under actual conditions, the radial temperature gradient smoothens out rapidly to below 20

K at residence times longer than 15 ms. Therefore, the actual effect of radiation correction or temperature uncertainties on the modeling results are fairly insignificant.

B.2 Uncertainties in the Mixing Reacting Model

The one-dimensional mixing reacting model described in Chapter 3 uses the scalar mixing profiles of non-reacting CO₂ to estimate the mixing time constant in the flow reactor experiments. Such a modeling method assumes that the early time reaction chemistry occurring in the mixing region does not significantly perturb the physics of the mixing process when temperature, flow rates, pressure and other relevant conditions are kept identical. One way to test this assumption is to compare the predictions of the mixing model against the results obtained from a species which undergoes a simple one-step reaction with well known kinetic rate parameter values. Ethyl-Chloride (C₂H₅Cl) is known to undergo a simple gas phase elimination reaction that produces ethylene and hydrogen chloride under pyrolysis condition. The reaction is



with a rate constant $k = 10^{13.16} \exp(-\frac{56460}{RT})$ estimated using a shock tube study by (Tsang, 1964) . An ethyl-chloride decomposition experiment was performed in the flow reactor facility (Si et al., 2011, personal communication) at 1055 K and 1 atm. pressure under pyrolysis conditions and the experimental ethylene concentration profiles were compared against the expected profile obtained from the kinetic rate parameters. It is seen in the Figure (B.4) that the best match is found for a rate parameter value 2.4 times the nominal coefficient which is within the uncertainties of the original shock tube study. Furthermore, the data in the mixing region match the expected profiles well for both the nominal and the modified rate coefficient predictions, demonstrating that the mixing physics is relatively insensitive to the effects of chemistry. The results present further grounds to be confident that the mixing reacting model is able to capture the initial stages of the mixing processes occurring in the Stanford Flow Reactor Facility with a fair degree of accuracy.

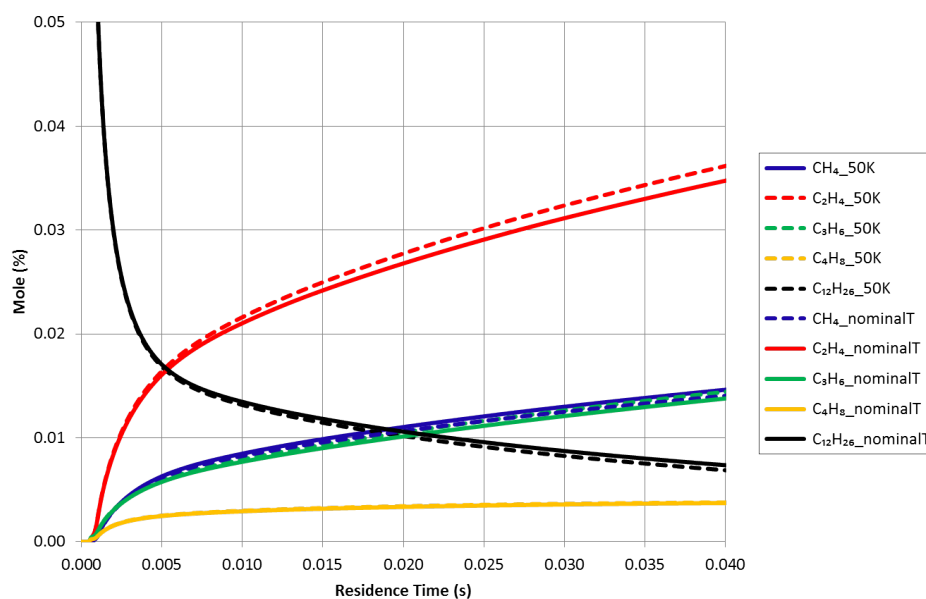


Figure B.1: Differences in the Predicted Species Profiles for the 1000 K Pyrolysis Condition with the Uncorrected Nominal Temperature Profile and a Corrected Profile with a 50 K Wall Temperature Variation. The Optimized JetSurf Mechanism is Used.

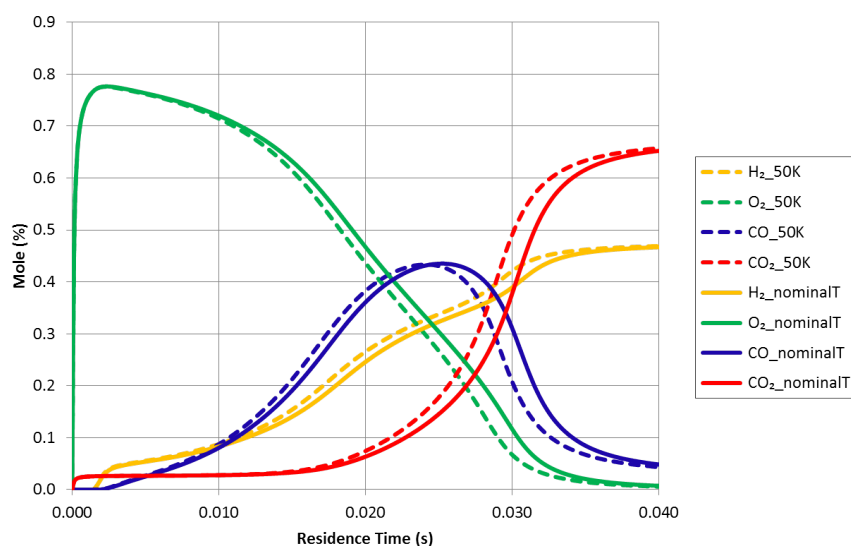


Figure B.2: Differences in the Predicted Species Profiles for the 1220 K Rich Oxidation Condition with the Uncorrected Nominal Temperature Profile and a Corrected Profile with a 50 K Wall Temperature Variation. The Optimized JetSurf Mechanism is Used.

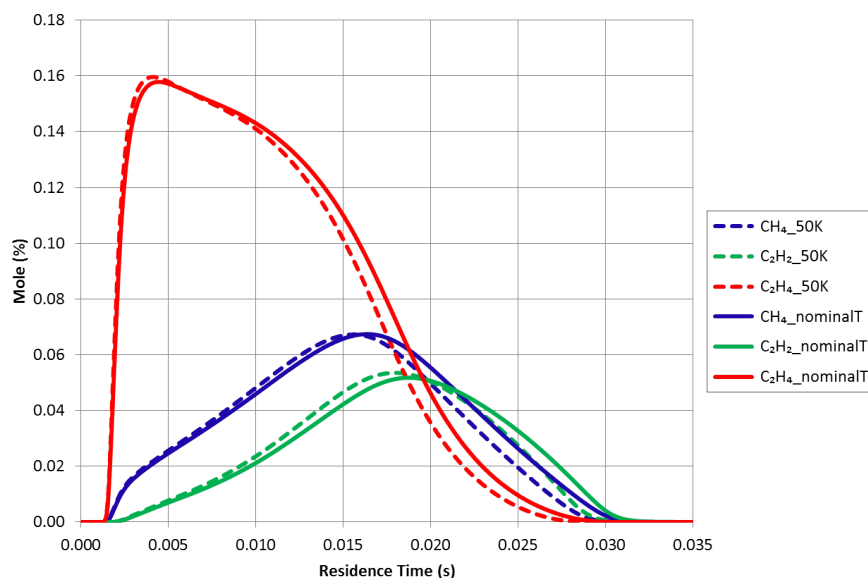


Figure B.3: Differences in the Predicted Species Profiles for the 1220 K Rich Oxidation Condition with the Uncorrected Nominal Temperature Profile and a Corrected Profile with a 50 K Wall Temperature Variation. The Optimized JetSurf Mechanism is Used.

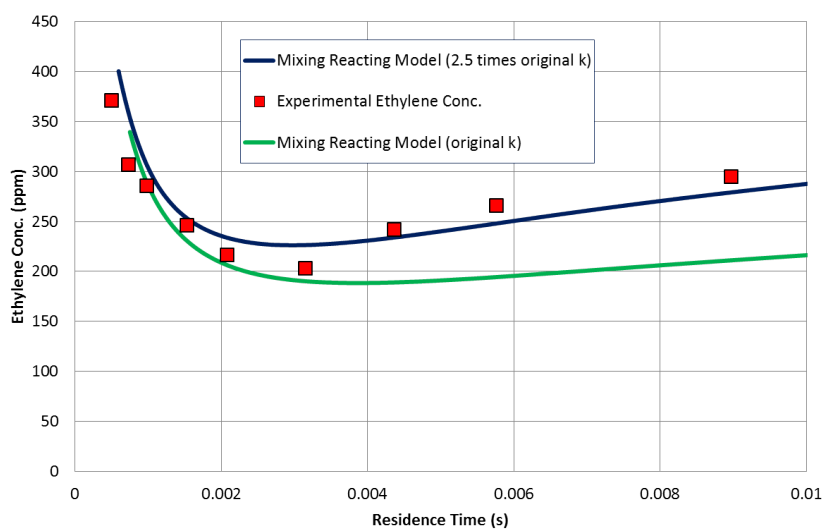


Figure B.4: Experimental Ethylene Data Compared with Estimates of the Ethyl-Chloride Decomposition Rate from (Tsang, 1964).

Next, the sensitivity of the species profiles to variations in the characteristic mixing time constant is assessed. Species profiles for the 1000 K pyrolysis and the 1220 K rich oxidation experiments were modeled using the optimized JetSurf mechanism with mixing time constants at 70% and 130% the original values respectively. The resulting differences are compared in Figure (B.5) for the pyrolysis condition and in Figures (B.6) and (B.7) for the rich oxidation condition respectively. Note that a smaller mixing time constant implies a more efficient mixing while a larger value implies a slower mixing between the bath gas and the second injection gas. In the limit, perfect instantaneous mixing will lead to a mixing constant of 0 seconds. The figures show that variations in mixing times only affect the early time (<5 ms) concentration profiles of those species that have a peak within the mixing region (0-4 ms). In such cases, a slower mixing condition will result in a sharper concentration peak while a faster mixing will result in a more smoothed out maxima. For species like ethylene, propene and 1-butene that do have an early peak for the high temperature oxidation runs, the peak height and shape will be affected by uncertainties in the mixing constant evaluations. Thus such early peaks are not good targets for model validation purposes. It is noted, however, that the effect of such variations become insignificant beyond 8 ms residence times. For species that do not have early peaks, the species profile predictions are insensitive to mixing time variations throughout the reactor regime.

B.3 Species Uncertainty

The uncertainties in the species concentration can be classified into two types. On the one hand, there are uncertainties associated with the flow controllers that meter the flow rates of the various input gas streams. This uncertainty also includes the n-dodecane evaporation and injection system. These are uncertainties in the input gas streams. On the other hand, there are uncertainties in the Gas Chromatographic measurements of the species concentration.

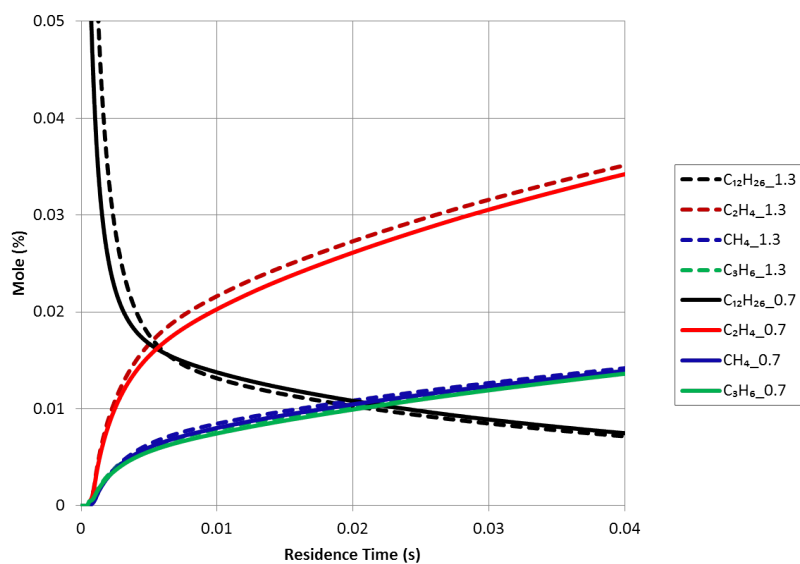


Figure B.5: Results of the Mixing Reacting Model for 1000 K Pyrolysis Conditions with Mixing Time Constant 1.3 and 0.7 Times the Original Value (1.4 ms), respectively. The Optimized JetSurf Mechanism is Used.

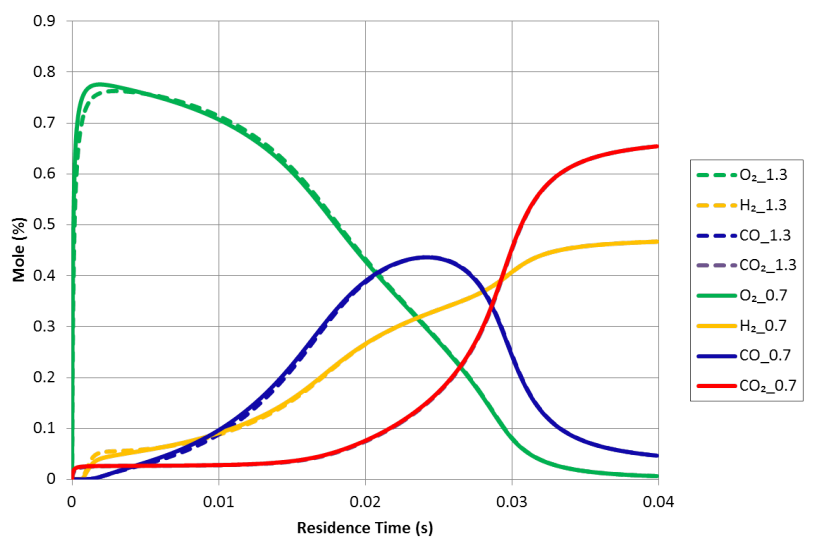


Figure B.6: Results of the Mixing Reacting Model for 1220 K Pyrolysis Conditions with the Mixing Time Constant 1.3 and 0.7 Times the Original Value (1.6 ms), respectively. The Optimized JetSurf Mechanism is Used.

B.3.1 Input Gas Stream Uncertainties

Apart from the fuel, all flow rates are metered using choked flow orifices that are controlled by PID controllers. The PID controllers adjust the stagnation temperature and pressure upstream of the orifices using pneumatically controlled valves. The flow through the choked orifice is proportional to the quantity $\frac{P_0}{\sqrt{T_0}}$. The relationship between the molar flow rate through the orifice and the $\frac{P_0}{\sqrt{T_0}}$ value is determined using a flow meter. The calibration data are fit using a regression analysis and the uncertainty in the relationship is quantified using equations (B.3), (B.4) and (B.5). The uncertainty associated with the metered flows are of the order of 1% and the net uncertainty in the total flow rate (weighed by their relative mass contribution) is around 2%. The uncertainty associated with the n-dodecane injection rates stem from variations in the fuel concentrations in the bath evaporator flow stream (3%) and uncertainties in the FID based total hydrocarbon analyzer used to calibrate the evaporator. The combined uncertainty from these two sources is estimated to be 4%.

B.3.2 Species Concentration Measurements Uncertainty

Species concentrations are primarily measured using the Inficon Micro-GC described in Appendix A. The uncertainty in the concentration estimates from the GC stem from uncertainties in the calibration gas concentrations used to evaluate the response factors for each species and the uncertainties in measured area values of the chromatographic peaks. The uncertainties in the calibration standard mixtures are reported by the supplier (Praxair) and the standard deviations associated with peak area values are evaluated through repeated measurements. The combined uncertainties are listed in Table (B.1). The uncertainty in the n-dodecane measurement is the combined effect of uncertainties of the bath-FID flow system and the standard error in the GC chromatographic peak. The two evaluations for the case of n-butene correspond to the two separate calibration standards that have been used for different experimental conditions. The formaldehyde calibration uncertainty has been discussed in Appendix A and in (Bardosova, 2011).

The combined uncertainty in the carbon balance is evaluated using equation (B.2) with different weighing factors for the different species in proportion to their relative carbon

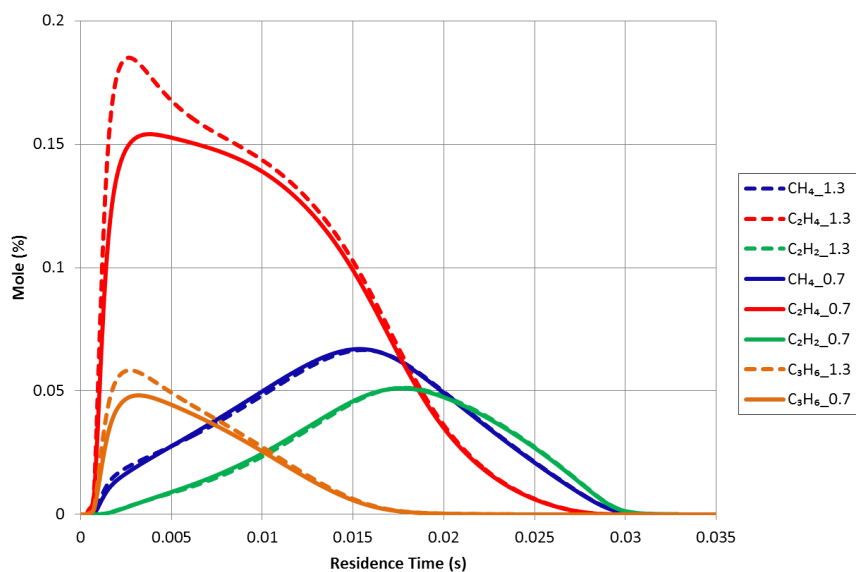


Figure B.7: Results of the Mixing Reacting Model for 1220 K Pyrolysis Conditions with the Mixing Time Constant 1.3 and 0.7 Times the Original Value (1.6 ms), respectively. The Optimized JetSurf Mechanism is Used.

Species	Relative Uncertainty
H ₂	2%
O ₂	2%
CH ₄	3.6%
CO	2.3%
CO ₂	2%
C ₂ H ₄	2.1%
C ₂ H ₆	6.7%
C ₂ H ₂	2.3%
C ₃ H ₆	2%
C ₄ H ₈	2.6%, 5.1%
C ₅ H ₁₀	5.2%
C ₆ H ₁₂	5.2%
C ₇ H ₁₄	7.4%
C ₁₂ H ₂₆	6.2%
CH ₂ O	10%

Table B.1: Relative Uncertainties in GC Concentration Measurements

content. The uncertainty in the carbon balance varies from 3% for the high temperature oxidation conditions to 5% for the pyrolysis and the low temperature oxidation condition.

B.4 Residence Time Uncertainty

The residence time is evaluated by integrating equation (3.5) using the trapezoidal method. The uncertainties associated with the estimation of the residence time are propagated from the uncertainties associated with estimating the axial velocity profile $U(z)$. The uncertainties in the velocity profile include contributions from the uncertainties in the non-dimensional mass flow rate correlation in equation (3.1), the total mass flow rate, reactor temperature measurements and the estimated molecular weight of the gas. The total uncertainty in the center line velocity is estimated to be 9.5% (Bardosova, 2011). The trapezoidal method equation

$$\Delta t_i = \frac{\Delta z_i}{2} \left[\frac{1}{U(i)} + \frac{1}{U(i+1)} \right] \quad (\text{B.9})$$

is used to combine the standard errors in the velocity profiles and evaluate the residence time uncertainty along the reactor axis. The residence time uncertainty values are plotted for the 1220 K rich oxidation conditions in Figure (B.8). The residence time uncertainties vary from 0.5 ms to 3 ms between the 0-40 ms residence time interval of the experiment. Other experimental conditions also give similar results. The residence time uncertainty estimates have been incorporated as horizontal error bars in the flow reactor data presented in the Chapter 5 of the present thesis.

The impact of flow disturbance due to the extraction probe were investigated previously by (Bardosova, 2011) and were found to be not significant.

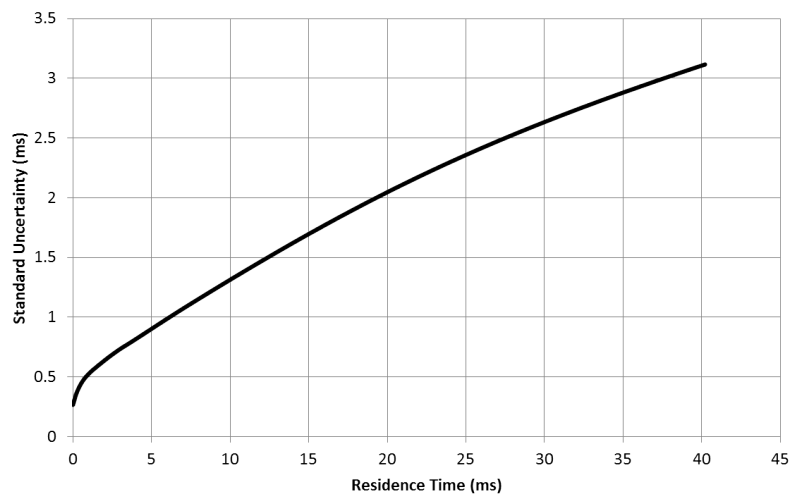


Figure B.8: Uncertainty in Residence Time (ms) for the 1220 K Rich Oxidation Conditions

Appendix C

Comparing Reaction Rates For Sensitive Reactions

The following section tabulates the rate coefficient values for the reactions that were found to have the greatest A factor sensitivities for the major species and H/OH radical concentrations under the flow reactor experiment conditions. The values from the three detailed mechanisms have been compared at 1000 K and 1200 K under 1 atm pressure. Significant variations in the rate coefficients exist for several sensitive reactions primarily due to the adoption of differing values from the published literature. A detailed discussion of the most important differences between the optimized JetSurf and LLNL mechanism reaction rates and pathways thought to be responsible for the differences between their pr have been discussed in Chapter 6.

1. $\text{H} + \text{O}_2 \rightleftharpoons \text{O} + \text{OH}$

	1000 K		1200 K	
Mechanisms	k_f	k_r	k_f	k_r
JetSurf	4.76E+10	9.64E+12	17.6E+10	9.33E+12
CNRS	4.02E+10	7.94E+12	16.5E+10	8.55E+12
LLNL	5.05E+10	9.9E+12	18.9E+10	9.76E+12

2. $\text{OH} + \text{H}_2 \rightleftharpoons \text{H} + \text{H}_2\text{O}$

	1000 K		1200 K	
Mechanisms	k_f	k_r	k_f	k_r
JetSurf	1.29E+12	3.54E+09	2.26E+12	2.16E+10
CNRS	1.22E+12	3.46E+09	2.13E+12	2.1E+10
LLNL	1.3E+12	3.7E+9	2.29E+12	2.22E+10

3. $\text{H} + \text{O}_2 (+\text{M}) \rightleftharpoons \text{HO}_2 + \text{M}$

	1000 K		1200 K	
Mechanisms	k_f	k_r	k_f	k_r
JetSurf	3.22E+15	8.74E+04	2.52E+15	4.14E+06
CNRS	3.18E+15	6.69E+04	2.75E+15	3.66E+06
LLNL	3.75E+10	0.997	2.72E+10	43.9

4. $\text{OH} + \text{HO}_2 \rightleftharpoons \text{H}_2\text{O} + \text{O}_2$

	1000 K		1200 K	
Mechanisms	k_f	k_r	k_f	k_r
JetSurf	3.4E+13	0.216	3.26E+13	74.8
CNRS	1.86E+13	0.157	1.79E+13	52
LLNL	1.79E+13	0.119	2.08E+13	49.5

5. $\text{CH}_3 + \text{HO}_2 \rightleftharpoons \text{CH}_3\text{O} + \text{OH}$

	1000 K		1200 K	
Mechanisms	k_f	k_r	k_f	k_r
JetSurf	3.02E+13	2.62E+08	3.02E+13	1.85E+09
CNRS	9.06E+12	1.83E+08	8.99E+12	1.44E+09
LLNL	9.06E+12	7.36E+07	8.99E+12	5.93E+08

6. $2\text{CH}_3 + (+\text{M}) \rightleftharpoons \text{C}_2\text{H}_6 (+\text{M})$

	1000 K		1200 K	
Mechanisms	k_f	k_r	k_f	k_r
JetSurf	1.2E+13	1.27E-03	6.53E+12	1.22
CNRS	1.2E+13	1.81E-03	7.41E+12	1.88
LLNL	1.26E+13	1.68E-03	7.89E+12	1.76

7. $\text{CH}_4 + \text{H} \rightleftharpoons \text{CH}_3 + \text{H}_2$

	1000 K		1200 K	
Mechanisms	k_f	k_r	k_f	k_r
JetSurf	2.04E+11	1.18E+10	6.81E+11	3.57E+10
CNRS	2.74E+11	1.34E+10	9.88E+11	4.37E+10
LLNL	1.56E+11	8.08E+09	5.49E+11	2.71E+10

8. $\text{CH}_4 + \text{OH} \rightleftharpoons \text{CH}_3 + \text{H}_2\text{O}$

	1000 K		1200 K	
Mechanisms	k_f	k_r	k_f	k_r
JetSurf	1.27E+12	2.01E+08	2.2E+12	1.1E+09
CNRS	9.25E+11	1.28E+08	1.67E+12	7.28E+08
LLNL	1.22E+12	1.8E+08	2.36E+12	1.13E+09

9. $\text{C}_2\text{H}_6 + \text{OH} \rightleftharpoons \text{C}_2\text{H}_5 + \text{H}_2\text{O}$

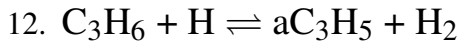
	1000 K		1200 K	
Mechanisms	k_f	k_r	k_f	k_r
JetSurf	5.11E+12	3.16E+07	8.09E+12	2.42E+08
CNRS	5.03E+12	1.96E+07	7.87E+12	1.59E+08
LLNL	4.6E+12	4.36E+07	7.04E+12	3.12E+08

10. $\text{aC}_3\text{H}_5 + \text{H} (+\text{M}) \rightleftharpoons \text{C}_3\text{H}_6 (+\text{M})$

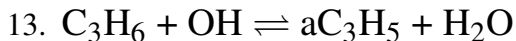
	1000 K		1200 K	
Mechanisms	k_f	k_r	k_f	k_r
JetSurf	1.88E+14	4.59E-04	1.73E+14	7.3E-01
CNRS	3.53E+14	4.21E-03	3.21E+14	5.6
LLNL	1.15E+14	4.2E-05	1.27E+14	7.76E-02

11. $\text{aC}_3\text{H}_5 + \text{CH}_3 \rightleftharpoons \text{C}_4\text{H}_8 (+\text{M})$

	1000 K		1200 K	
Mechanisms	k_f	k_r	k_f	k_r
JetSurf	1.2E+13	0.235	1.01E+13	105
CNRS	3.81E+12	1.36	3.33E+12	534
LLNL	1.35E+13	0.164	1.35E+13	854



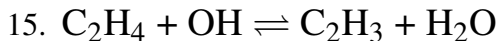
	1000 K		1200 K	
Mechanisms	k _f	k _r	k _f	k _r
JetSurf	1.17E+12	3E+07	2.27E+12	2.13E+08
CNRS	6.89E+11	3.59E+06	1.00E+12	2.25E+07
LLNL	1.56E+12	2.63E+08	3.03E+12	1.91E+09



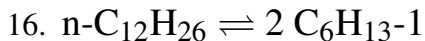
	1000 K		1200 K	
Mechanisms	k _f	k _r	k _f	k _r
JetSurf	2.91E+12	2.05E+05	4.08E+12	3.66E+06
CNRS	2.47E+12	3.66E+04	3.89E+12	8.63E+05
LLNL	3.62E+12	1.73E+06	5.09E+12	3.11E+07



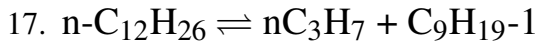
	1000 K		1200 K	
Mechanisms	k _f	k _r	k _f	k _r
JetSurf	5.6E+12	5.66E+04	3.74E+12	7.72E+05
CNRS	2.62E+12	1.62E+04	2.43E+12	3.3E+05
LLNL	1.55E+12	2.14E+04	8.53E+11	2.3E+05



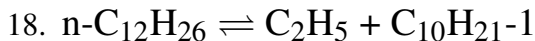
	1000 K		1200 K	
Mechanisms	k _f	k _r	k _f	k _r
JetSurf	1.22E+12	2.23E+09	2.16E+12	7.67E+09
CNRS	1.02E+12	2.08E+09	1.68E+12	6.78E+09
LLNL	5.12E+11	7.5E+08	9.08E+11	2.61E+09



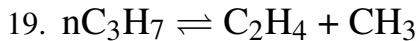
	1000 K		1200 K	
Mechanisms	k _f	k _r	k _f	k _r
JetSurf	0.197	2.81E+13	2.02E+02	2.57E+13
CNRS	3.51E-02	7.77E+12	4.37E+01	8.28E+12
LLNL	5.59E-02	8.0E+12	6.28E+01	8.0E+12



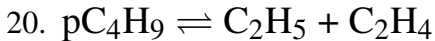
	1000 K		1200 K	
Mechanisms	k _f	k _r	k _f	k _r
JetSurf	2.85E-01	5.95E+12	2.87E+02	5.43E+12
CNRS	3.46E-01	7.58E+12	3.12E+02	7.1E+12
LLNL	3.42E-02	8.0E+12	3.98E+01	8.0E+12



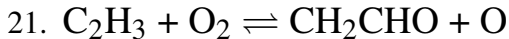
	1000 K		1200 K	
Mechanisms	k _f	k _r	k _f	k _r
JetSurf	2.91E-02	5.23E+12	2.94E+01	4.78E+12
CNRS	5.71E-01	7.72E+12	4.58E+02	7.27E+12
LLNL	3.42E-02	8.0E+12	3.98E+01	8.0E+12



	1000 K		1200 K	
Mechanisms	k _f	k _r	k _f	k _r
JetSurf	1.43E+06	6.85E+09	1.68E+07	1.31E+10
CNRS	3.39E+06	1.00E+10	4.35E+07	2.24E+10
LLNL	8.12E+06	2.13E+10	1.23E+08	5.5E+10



	1000 K		1200 K	
Mechanisms	k _f	k _r	k _f	k _r
JetSurf	3.42E+06	3.81E+09	2.98E+07	7.02E+09
CNRS	1.25E+07	2.82E+09	1.41E+08	7.2E+09
LLNL	3.11E+07	1.66E+10	4.0E+08	4.37E+10



	1000 K		1200 K	
Mechanisms	k _f	k _r	k _f	k _r
JetSurf	7.09E+12	2.01E+11	7.48E+12	4.24E+11
CNRS	1.37E+12	3.9E+10	1.54E+12	8.11E+10
LLNL	5.72E+11	5.71E+10	7.96E+11	1.74E+11

22. $\text{CH}_4 (+\text{M}) \rightleftharpoons \text{CH}_3 + \text{H} (+\text{M})$

	1000 K		1200 K	
Mechanisms	k_f	k_r	k_f	k_r
JetSurf	2.0E-08	1.84E+13	7.23E-05	9.59E+12
CNRS	3.46E-08	2.71E+13	8.01E-05	9.04E+12
LLNL	3.25E-08	2.64E+13	1.13E-04	1.36E+13

23. $\text{C}_3\text{H}_6 \rightleftharpoons \text{C}_2\text{H}_3 + \text{CH}_3$

	1000 K		1200 K	
Mechanisms	k_f	k_r	k_f	k_r
JetSurf	2.11E-05	2.34E+13	8.19E-02	2.05E+13
CNRS	1.21E-04	3.79E+14	3.53E-01	2.71E+14
LLNL	1.2E+11	1.22E+03	7.13E+10	1.66E+04

24. $\text{H} + \text{CH}_2\text{CO} (+\text{M}) \rightleftharpoons \text{CH}_2\text{HCO} (+\text{M})$

	1000 K		1200 K	
Mechanisms	k_f	k_r	k_f	k_r
JetSurf	1.02E+11	3.34E+03	2.88E+11	2.19E+05
CNRS	2.91E+12	4.03E+04	1.35E+12	3.86E+05
LLNL	1.2E+11	1.22E+3	7.13E+10	1.66E+04

25. $\text{C}_2\text{H}_4 + \text{OH} \rightleftharpoons \text{C}_2\text{H}_3 + \text{H}_2\text{O}$

	1000 K		1200 K	
Mechanisms	k_f	k_r	k_f	k_r
JetSurf	1.22E+12	2.23E+09	2.16E+12	7.67E+09
CNRS	1.02E+12	2.08E+09	1.68E+12	6.78E+09
LLNL	5.12E+11	7.5E+08	9.08E+11	2.61E+09

Appendix D

Reaction Mechanism Files

D.1 The Optimized JetSurf Mechanism

D.1.1 Mechanism File:-

```

ELEMENTS
O  H  C  N  AR HE
END
SPECIES
AR          N2          HE          H          O          OH
OH*         HO2         H2         H2O         H2O2         O2
C           CH          CH*        CH2         CH2*        CH3
CH4         HCO         CH2O       CH3O       CH2OH       CH3OH
CO          CO2         C2O        C2H         C2H2        H2CC
C2H3        C2H4         C2H5       C2H6        HCCO        HCCOH
CH2CO       CH3CO        CH2CHO     CH2OCH     CH3CHO      CH2OCH2
C3H3        pC3H4        aC3H4      cC3H4      aC3H5      CH3CCH2
CH3CHCH     C3H6        nC3H7      iC3H7      C3H8       CH2CHCO
C2H3CHO     CH3CHOCH2   CH3CH2CHO  CH3COCH3   C4H2       nC4H3
iC4H3       C4H4        nC4H5      iC4H5      C4H5-2     c-C4H5
C4H6        C4H612     C4H6-2     C4H7       iC4H7      C4H81
C4H82       iC4H8       pC4H9      sC4H9      iC4H9      tC4H9
C4H10       iC4H10     H2C4O      C4H4O      CH2CHCHCHO CH3CHCHCO
C2H3CHOCH2  C4H6O23    CH3CHCHCHO C4H6O25    C5H4O      C5H5O (1,3)
C5H5O (2,4) C5H4OH     C5H5OH     C5H5       C5H6       1C5H7
cC5H9       cC5H8       C6H2       C6H3       1-C6H4     o-C6H4
C6H5        C6H6       C6H5CH2    C6H5CH3    C6H5C2H    C6H5O
C6H5OH      C6H4O2     C6H5CO     C6H5CHO    C6H5CH2OH  OC6H4CH3
HOC6H4CH3  C6H4CH3    NC12H26    PXC12H25   SXC12H25   C12H24

PXC12H23    NC11H24    PXC11H23    SXC11H23    C11H22     PXC11H21
NC10H22     PXC10H21   SXC10H21    C10H20     PXC10H19   NC9H20
PXC9H19     SXC9H19    C9H18       PXC9H17     NC8H18     PXC8H17
SXC8H17     C8H16      PXC8H15     NC7H16      PXC7H15    SXC7H15
C7H14       PXC7H13    NC6H14      PXC6H13     SXC6H13    C6H12
PXC6H11     SXC6H11    S2XC6H11    SAXC6H11    cC6H11     cC6H10
SAXC6H11-3  cC5H9CH2   CH2C5H8     m1C5H81     CH3cC5H83  C6H10-13
NC5H12      PXC5H11    SXC5H11     C5H10       PXC5H9     SXC5H9
SAXC5H9     CH2C4H7    C5H8-13     C5H8-14     S2XC12H25  S3XC12H25
S4XC12H25   S5XC12H25  S2XC11H23   S3XC11H23   S4XC11H23  S5XC11H23
S2XC10H21   S3XC10H21  S4XC10H21   S2XC9H19    S3XC9H19   S4XC9H19
S2XC8H17    S3XC8H17   S2XC7H15    S3XC7H15    S2XC6H13   S2XC5H11
PC12H25O2   P12O0HX2   SOO12O0H    OC12O0H

END
REACTIONS
H+O2<=>O+OH          2.6023E+16   -0.671   17041.00
O+H2<=>H+OH          3.8390E+04    2.700    6260.00
OH+H2<=>H+H2O        2.1384E+08    1.510    3430.00
2OH<=>O+H2O          3.5700E+04    2.400   -2110.00
2H+M<=>H2+M          1.0000E+18   -1.000     0.00
AR/0.63/ HE/0.63/ H2/0.00/ H2O/0.00/ CO2/0.00/
2H+H2<=>2H2          9.0000E+16   -0.600     0.00
2H+H2O<=>H2+H2O      6.0000E+19   -1.250     0.00
2H+CO2<=>H2+CO2      5.5000E+20   -2.000     0.00
H+OH+M<=>H2O+M       2.5102E+22   -2.000     0.00
AR/0.38/ HE/0.38/ H2/2.00/ H2O/6.30/ CO/1.75/ CO2/3.60/
O+H+M<=>OH+M         4.7140E+18   -1.000     0.00
AR/ 0.70/ HE/ 0.70/ H2/ 2.00/ H2O/12.00/ CO/ 1.75/ CO2/ 3.60/
2O+M<=>O2+M          1.2000E+17   -1.000     0.00

```

```

AR/ 0.83/ HE/ 0.83/ H2/ 2.40/ H2O/15.40/ CO/ 1.75/ CO2/ 3.60/
H+O2+M<=>HO2+M          5.2413E+19  -1.397      94.56
AR/0.00/ HE/0.00/ H2/0.00/ H2O/0.00/ O2/0.00/ CO/0.00/
CO2/0.00/
H+O2+H2<=>HO2+H2          5.2204E+19  -1.397      94.56
H+2O2<=>HO2+O2           3.8564E+19  -1.395      82.11
H+O2+CO<=>HO2+CO          6.3427E+19  -1.398     103.74
H+O2+CO2<=>HO2+CO2        1.3670E+20  -1.408     150.94
H+O2+H2O<=>HO2+H2O        7.9988E+20  -1.438     217.44
H+O2+AR<=>HO2+AR           6.4519E+18  -1.190      57.52
H+O2+HE<=>HO2+HE           6.4519E+18  -1.190      57.52
H2+O2<=>HO2+H             7.3580E+05   2.433    53502.00
2OH (+M) <=>H2O2 (+M)      7.4000E+13  -0.370       0.00
      LOW / 1.3400E+17  -0.584  -2293.00/
      TROE/ 0.7346      94.00    1756.00    5182.00 /
AR/0.70/ HE/0.70/ H2/2.00/ H2O/6.00/ CO/1.75/ CO2/3.60/
HO2+H<=>O+H2O             3.9700E+12   0.000      671.00
HO2+H<=>2OH                6.4286E+13   0.000      295.00
HO2+O<=>OH+O2              2.0000E+13   0.000       0.00
2HO2<=>O2+H2O2            1.3000E+11   0.000    -1630.00
  DUPLICATE
2HO2<=>O2+H2O2            3.5070E+14   0.000    12000.00
  DUPLICATE
OH+HO2<=>H2O+O2            2.6415E+13   0.000     -500.00
H2O2+H<=>HO2+H2            1.2100E+07   2.000     5200.00
H2O2+H<=>OH+H2O            2.4100E+13   0.000     3970.00
H2O2+O<=>OH+HO2            9.6300E+06   2.000     3970.00
H2O2+OH<=>HO2+H2O          2.0000E+12   0.000      427.00
  DUPLICATE
H2O2+OH<=>HO2+H2O          2.6700E+41  -7.000     37600.00
  DUPLICATE
CO+O (+M) <=>CO2 (+M)      1.8000E+10   0.000     2384.00
      LOW / 1.5500E+24  -2.790   4191.00/
AR/ 0.70/ HE/ 0.70/ H2/ 2.00/ H2O/12.00/ CO/ 1.75/ CO2/ 3.60/
CO+OH<=>CO2+H              6.8417E+04   2.053     -355.67
  DUPLICATE
CO+OH<=>CO2+H              5.7340E+12  -0.664      331.83
  DUPLICATE
CO+O2<=>CO2+O              2.5300E+12   0.000     47700.00
CO+HO2<=>CO2+OH            3.0100E+13   0.000     23000.00
HCO+H<=>CO+H2              1.3692E+14   0.000       0.00
HCO+O<=>CO+OH              3.0000E+13   0.000       0.00
HCO+O<=>CO2+H              3.0000E+13   0.000       0.00
HCO+OH<=>CO+H2O            3.4066E+13   0.000       0.00
HCO+M<=>CO+H+M             1.0023E+17  -1.000     17000.00
H2/2.00/ H2O/0.00/ CO/1.75/ CO2/3.60/
HCO+H2O<=>CO+H+H2O         9.5033E+17  -1.000     17000.00
HCO+O2<=>CO+HO2            1.2209E+10   0.807     -727.00
CO+H2 (+M) <=>CH2O (+M)    4.3000E+07   1.500     79600.00
      LOW / 5.0700E+27  -3.420   84350.00/
      TROE/ 0.9320      197.00    1540.00    10300.00 /
AR/0.70/ H2/2.00/ H2O/6.00/ CH4/2.00/ CO/1.50/ CO2/2.00/
C2H6/3.00/
C+OH<=>CO+H                5.0000E+13   0.000       0.00

```

```

C+O2<=>CO+O          5.8000E+13    0.000    576.00
CH+H<=>C+H2          1.1077E+14    0.000     0.00
CH+O<=>CO+H          5.7000E+13    0.000     0.00
CH+OH<=>HCO+H        3.0000E+13    0.000     0.00
CH+H2<=>CH2+H        1.1070E+08    1.790    1670.00
CH+H2O<=>CH2O+H      5.7100E+12    0.000   -755.00
CH+O2<=>HCO+O        2.4453E+13    0.000     0.00
CH+CO (+M) <=>HCCO (+M) 5.0000E+13    0.000     0.00
      LOW / 2.6900E+28   -3.740   1936.00/
      TROE/ 0.5757      237.00   1652.00   5069.00 /
AR/0.70/ H2/2.00/ H2O/6.00/ CH4/2.00/ CO/1.50/ CO2/2.00/
C2H6/3.00/
CH+CO2<=>HCO+CO          3.4000E+12    0.000    690.00
HCO+H (+M) <=>CH2O (+M) 1.0900E+12    0.480   -260.00
      LOW / 1.3500E+24   -2.570   1425.00/
      TROE/ 0.7824      271.00   2755.00   6570.00 /
AR/0.70/ H2/2.00/ H2O/6.00/ CH4/2.00/ CO/1.50/ CO2/2.00/
C2H6/3.00/
CH2+H (+M) <=>CH3 (+M)    2.5000E+16   -0.800     0.00
      LOW / 3.2000E+27   -3.140   1230.00/
      TROE/ 0.6800      78.00   1995.00   5590.00 /
AR/0.70/ H2/2.00/ H2O/6.00/ CH4/2.00/ CO/1.50/ CO2/2.00/
C2H6/3.00/
CH2+O<=>HCO+H          8.0000E+13    0.000     0.00
CH2+OH<=>CH2O+H        2.0000E+13    0.000     0.00
CH2+OH<=>CH+H2O        1.1300E+07    2.000    3000.00
CH2+H2<=>H+CH3         5.0000E+05    2.000    7230.00
CH2+O2<=>HCO+OH        1.0452E+13    0.000    1500.00
CH2+O2<=>CO2+2H        2.6030E+12    0.000    1500.00
CH2+HO2<=>CH2O+OH      2.0000E+13    0.000     0.00
CH2+C<=>C2H+H          5.0000E+13    0.000     0.00
CH2+CO (+M) <=>CH2CO (+M) 8.1000E+11    0.500   4510.00
      LOW / 2.6900E+33   -5.110   7095.00/
      TROE/ 0.5907      275.00   1226.00   5185.00 /
AR/0.70/ H2/2.00/ H2O/6.00/ CH4/2.00/ CO/1.50/ CO2/2.00/
C2H6/3.00/
CH2+CH<=>C2H2+H        4.0000E+13    0.000     0.00
2CH2<=>C2H2+H2         3.2000E+13    0.000     0.00
CH2*+N2<=>CH2+N2       1.5000E+13    0.000    600.00
CH2*+AR<=>CH2+AR       9.0000E+12    0.000    600.00
CH2*+H<=>CH+H2         3.0000E+13    0.000     0.00
CH2*+O<=>CO+H2         1.5000E+13    0.000     0.00
CH2*+O<=>HCO+H         1.5000E+13    0.000     0.00
CH2*+OH<=>CH2O+H       3.0000E+13    0.000     0.00
CH2*+H2<=>CH3+H        7.0000E+13    0.000     0.00
CH2*+O2<=>H+OH+CO      2.6684E+13    0.000     0.00
CH2*+O2<=>CO+H2O       1.2000E+13    0.000     0.00
CH2*+H2O (+M) <=>CH3OH (+M) 2.0000E+13    0.000     0.00
      LOW / 2.7000E+38   -6.300   3100.00/
      TROE/ 0.1507      134.00   2383.00   7265.00 /
H2/2.00/ H2O/6.00/ CH4/2.00/ CO/1.50/ CO2/2.00/ C2H6/3.00/
CH2*+H2O<=>CH2+H2O     3.0000E+13    0.000     0.00
CH2*+CO<=>CH2+CO       9.0000E+12    0.000     0.00
CH2*+CO2<=>CH2+CO2     7.0000E+12    0.000     0.00

```

```

CH2*+CO2<=>CH2O+CO          1.4000E+13    0.000    0.00
CH2O+H (+M) <=>CH2OH (+M)      5.4000E+11    0.454    3600.00
    LOW / 1.2700E+32    -4.820    6530.00/
    TROE/ 0.7187      103.00    1291.00    4160.00 /
H2/2.00/ H2O/6.00/ CH4/2.00/ CO/1.50/ CO2/2.00/ C2H6/3.00/
CH2O+H (+M) <=>CH3O (+M)      5.4000E+11    0.454    2600.00
    LOW / 2.2000E+30    -4.800    5560.00/
    TROE/ 0.7580      94.00    1555.00    4200.00 /
H2/2.00/ H2O/6.00/ CH4/2.00/ CO/1.50/ CO2/2.00/ C2H6/3.00/
CH2O+H<=>HCO+H2              2.3000E+10    1.050    3275.00
CH2O+O<=>HCO+OH              3.9000E+13    0.000    3540.00
CH2O+OH<=>HCO+H2O            3.4300E+09    1.180    -447.00
CH2O+O2<=>HCO+HO2            1.0000E+14    0.000    40000.00
CH2O+HO2<=>HCO+H2O2          1.0000E+12    0.000    8000.00
CH2O+CH<=>CH2CO+H            9.4600E+13    0.000    -515.00
CH3+H (+M) <=>CH4 (+M)        1.0109E+16    -0.630    383.00
    LOW / 1.9717E+33    -4.760    2440.00/
    TROE/ 0.7830      74.00    2941.00    6964.00 /
AR/0.70/ H2/2.00/ H2O/6.00/ CH4/2.00/ CO/1.50/ CO2/2.00/
C2H6/3.00/
CH3+O<=>CH2O+H              8.2024E+13    0.000    0.00
CH3+OH (+M) <=>CH3OH (+M)     9.4185E+13    0.000    0.00
    LOW / 4.0365E+38    -6.300    3100.00/
    TROE/ 0.2105      83.50    5398.00    8370.00 /
H2/2.00/ H2O/6.00/ CH4/2.00/ CO/1.50/ CO2/2.00/ C2H6/3.00/
CH3+OH<=>CH2+H2O              5.6000E+07    1.600    5420.00
CH3+OH<=>CH2*+H2O             7.7281E+12    0.000    0.00
CH3+O2<=>O+CH3O              3.4776E+13    0.000    28800.00
CH3+O2<=>OH+CH2O              3.6000E+10    0.000    8940.00
CH3+HO2<=>CH4+O2              1.0000E+12    0.000    0.00
CH3+HO2<=>CH3O+OH             3.0217E+13    0.000    0.00
CH3+H2O2<=>CH4+HO2            2.4500E+04    2.470    5180.00
CH3+C<=>C2H2+H                5.0000E+13    0.000    0.00
CH3+CH<=>C2H3+H               3.0000E+13    0.000    0.00
CH3+HCO<=>CH4+CO              8.4800E+12    0.000    0.00
CH3+CH2O<=>CH4+HCO            3.3200E+03    2.810    5860.00
CH3+CH2<=>C2H4+H              4.0000E+13    0.000    0.00
CH3+CH2* <=>C2H4+H            1.2000E+13    0.000    -570.00
2CH3 (+M) <=>C2H6 (+M)        2.4359E+16    -0.970    620.00
    LOW / 2.0337E+50    -9.670    6220.00/
    TROE/ 0.5325      151.00    1038.00    4970.00 /
AR/0.70/ H2/2.00/ H2O/6.00/ CH4/2.00/ CO/1.50/ CO2/2.00/
C2H6/3.00/
2CH3<=>H+C2H5                5.5838E+12    0.100    10600.00
CH3+HCCO<=>C2H4+CO            5.0000E+13    0.000    0.00
CH3+C2H<=>C3H3+H              2.4100E+13    0.000    0.00
CH3O+H (+M) <=>CH3OH (+M)     5.0000E+13    0.000    0.00
    LOW / 8.6000E+28    -4.000    3025.00/
    TROE/ 0.8902      144.00    2838.00    45569.00 /
H2/2.00/ H2O/6.00/ CH4/2.00/ CO/1.50/ CO2/2.00/ C2H6/3.00/
CH3O+H<=>CH2OH+H              3.4000E+06    1.600    0.00
CH3O+H<=>CH2O+H2              2.0000E+13    0.000    0.00
CH3O+H<=>CH3+OH               3.2000E+13    0.000    0.00
CH3O+H<=>CH2*+H2O             1.6000E+13    0.000    0.00

```

```

CH3O+O<=>CH2O+OH          1.0000E+13    0.000    0.00
CH3O+OH<=>CH2O+H2O          5.0000E+12    0.000    0.00
CH3O+O2<=>CH2O+HO2          4.2800E-13    7.600   -3530.00
CH2OH+H (+M) <=>CH3OH (+M)    1.8000E+13    0.000    0.00
      LOW / 3.0000E+31   -4.800   3300.00/
      TROE/ 0.7679      338.00   1812.00   5081.00 /
H2/2.00/ H2O/6.00/ CH4/2.00/ CO/1.50/ CO2/2.00/ C2H6/3.00/
CH2OH+H<=>CH2O+H2          2.0000E+13    0.000    0.00
CH2OH+H<=>CH3+OH            1.2000E+13    0.000    0.00
CH2OH+H<=>CH2*+H2O          6.0000E+12    0.000    0.00
CH2OH+O<=>CH2O+OH          1.0000E+13    0.000    0.00
CH2OH+OH<=>CH2O+H2O         5.0000E+12    0.000    0.00
CH2OH+O2<=>CH2O+HO2         1.8000E+13    0.000    900.00
CH4+H<=>CH3+H2              6.6000E+08    1.620   10840.00
CH4+O<=>CH3+OH              1.0200E+09    1.500   8600.00
CH4+OH<=>CH3+H2O            9.6400E+07    1.600   3120.00
CH4+CH<=>C2H4+H             6.0000E+13    0.000    0.00
CH4+CH2<=>2CH3              2.4600E+06    2.000   8270.00
CH4+CH2* <=>2CH3            1.6000E+13    0.000   -570.00
CH4+C2H<=>C2H2+CH3          1.8100E+12    0.000   500.00
CH3OH+H<=>CH2OH+H2          1.7000E+07    2.100   4870.00
CH3OH+H<=>CH3O+H2           4.2000E+06    2.100   4870.00
CH3OH+O<=>CH2OH+OH          3.8800E+05    2.500   3100.00
CH3OH+O<=>CH3O+OH           1.3000E+05    2.500   5000.00
CH3OH+OH<=>CH2OH+H2O        1.4400E+06    2.000   -840.00
CH3OH+OH<=>CH3O+H2O         6.3000E+06    2.000   1500.00
CH3OH+CH3<=>CH2OH+CH4       3.0000E+07    1.500   9940.00
CH3OH+CH3<=>CH3O+CH4        1.0000E+07    1.500   9940.00
C2H+H (+M) <=>C2H2 (+M)      1.0000E+17   -1.000    0.00
      LOW / 3.7500E+33   -4.800   1900.00/
      TROE/ 0.6464      132.00   1315.00   5566.00 /
AR/0.70/ H2/2.00/ H2O/6.00/ CH4/2.00/ CO/1.50/ CO2/2.00/
C2H6/3.00/
C2H+O<=>CH+CO               5.0000E+13    0.000    0.00
C2H+OH<=>H+HCCO             2.0000E+13    0.000    0.00
C2H+O2<=>HCO+CO             5.0000E+13    0.000   1500.00
C2H+H2<=>H+C2H2             4.9000E+05    2.500   560.00
C2O+H<=>CH+CO               5.0000E+13    0.000    0.00
C2O+O<=>2CO                 5.0000E+13    0.000    0.00
C2O+OH<=>2CO+H              2.0000E+13    0.000    0.00
C2O+O2<=>2CO+O              2.0000E+13    0.000    0.00
HCCO+H<=>CH2*+CO            1.0350E+14    0.000    0.00
HCCO+O<=>H+2CO              1.0000E+14    0.000    0.00
HCCO+O2<=>OH+2CO            1.9104E+12    0.000   854.00
HCCO+CH<=>C2H2+CO           5.0000E+13    0.000    0.00
HCCO+CH2<=>C2H3+CO          3.0000E+13    0.000    0.00
2HCCO<=>C2H2+2CO            1.0000E+13    0.000    0.00
HCCO+OH<=>C2O+H2O           3.0000E+13    0.000    0.00
C2H2 (+M) <=>H2CC (+M)       8.0000E+14   -0.520   50750.00
      LOW / 2.4500E+15   -0.640  49700.00/
H2/2.00/ H2O/6.00/ CH4/2.00/ CO/1.50/ CO2/2.00/ C2H4/2.50/
C2H6/3.00/
C2H3 (+M) <=>C2H2+H (+M)     3.6323E+08    1.620   37048.20
      LOW / 2.4137E+27   -3.400  35798.72/

```



```

TROE/ 1.9816      5383.70      4.29      -0.08 /
AR/0.70/ H2/2.00/ H2O/6.00/ CH4/2.00/ CO/1.50/ CO2/2.00/
C2H2/3.00/ C2H4/3.00/ C2H6/3.00/
C2H2+O<=>C2H+OH      4.6000E+19      -1.410      28950.00
C2H2+O<=>CH2+CO      4.0800E+06      2.000      1900.00
C2H2+O<=>HCCO+H      1.6124E+07      2.000      1900.00
C2H2+OH<=>CH2CO+H      2.1800E-04      4.500      -1000.00
C2H2+OH<=>HCCOH+H      5.0400E+05      2.300      13500.00
C2H2+OH<=>C2H+H2O      3.3700E+07      2.000      14000.00
C2H2+OH<=>CH3+CO      4.8300E-04      4.000      -2000.00
C2H2+HCO<=>C2H3+CO      1.0000E+07      2.000      6000.00
C2H2+CH2<=>C3H3+H      1.2000E+13      0.000      6620.00
C2H2+CH2*<=>C3H3+H      2.0000E+13      0.000      0.00
C2H2+C2H<=>C4H2+H      9.6000E+13      0.000      0.00
C2H2+C2H (+M) <=>nC4H3 (+M)      8.3000E+10      0.899      -363.00
LOW / 1.2400E+31      -4.718      1871.00/
TROE/ 1.0000      100.00      5613.00      13387.00 /
H2/2.00/ H2O/6.00/ CH4/2.00/ CO/1.50/ CO2/2.00/ C2H2/2.50/
C2H4/2.50/ C2H6/3.00/
C2H2+C2H (+M) <=>iC4H3 (+M)      8.3000E+10      0.899      -363.00
LOW / 1.2400E+31      -4.718      1871.00/
TROE/ 1.0000      100.00      5613.00      13387.00 /
H2/2.00/ H2O/6.00/ CH4/2.00/ CO/1.50/ CO2/2.00/ C2H2/2.50/
C2H4/2.50/ C2H6/3.00/
C2H2+HCCO<=>C3H3+CO      1.0000E+11      0.000      3000.00
C2H2+CH3<=>pC3H4+H      2.4218E+09      1.100      13644.00
C2H2+CH3<=>aC3H4+H      5.1400E+09      0.860      22153.00
C2H2+CH3<=>CH3CCH2      4.9900E+22      -4.390      18850.00
C2H2+CH3<=>CH3CHCH      3.2000E+35      -7.760      13300.00
C2H2+CH3<=>aC3H5      2.6800E+53      -12.820      35730.00
H2CC+H<=>C2H2+H      1.0000E+14      0.000      0.00
H2CC+OH<=>CH2CO+H      2.0000E+13      0.000      0.00
H2CC+O2<=>2HCO      1.0000E+13      0.000      0.00
H2CC+C2H2 (+M) <=>C4H4 (+M)      3.5000E+05      2.055      -2400.00
LOW / 1.4000E+60      -12.599      7417.00/
TROE/ 0.9800      56.00      580.00      4164.00 /
H2/2.00/ H2O/6.00/ CH4/2.00/ CO/1.50/ CO2/2.00/ C2H2/3.00/
C2H4/3.00/ C2H6/3.00/
H2CC+C2H4<=>C4H6      1.0000E+12      0.000      0.00
CH2CO+H (+M) <=>CH2CHO (+M)      3.3000E+14      -0.060      8500.00
LOW / 3.8000E+41      -7.640      11900.00/
TROE/ 0.3370      1707.00      3200.00      4131.00 /
AR/0.70/ H2/2.00/ H2O/6.00/ CH4/2.00/ CO/1.50/ CO2/2.00/
C2H2/3.00/ C2H4/3.00/ C2H6/3.00/
CH2CO+H<=>HCCO+H2      5.0000E+13      0.000      8000.00
CH2CO+H<=>CH3+CO      1.5000E+09      1.430      2690.00
CH2CO+O<=>HCCO+OH      1.0000E+13      0.000      8000.00
CH2CO+O<=>CH2+CO2      1.7500E+12      0.000      1350.00
CH2CO+OH<=>HCCO+H2O      7.5000E+12      0.000      2000.00
HCCOH+H<=>CH2CO+H      1.0000E+13      0.000      0.00
C2H3+H (+M) <=>C2H4 (+M)      6.0800E+12      0.270      280.00
LOW / 1.4000E+30      -3.860      3320.00/
TROE/ 0.7820      207.50      2663.00      6095.00 /
AR/0.70/ H2/2.00/ H2O/6.00/ CH4/2.00/ CO/1.50/ CO2/2.00/

```

```

C2H2/3.00/ C2H4/3.00/ C2H6/3.00/
C2H3+H<=>C2H2+H2      8.8020E+13      0.000      0.00
C2H3+H<=>H2CC+H2      6.3960E+13      0.000      0.00
C2H3+O<=>CH2CO+H      4.8000E+13      0.000      0.00
C2H3+O<=>CH3+CO      4.8000E+13      0.000      0.00
C2H3+OH<=>C2H2+H2O      3.0110E+13      0.000      0.00
C2H3+O2<=>C2H2+HO2      1.3400E+06      1.610     -383.40
C2H3+O2<=>CH2CHO+O      9.6120E+11      0.290      11.00
C2H3+O2<=>HCO+CH2O      3.8410E+16     -1.390     1010.00
C2H3+HO2<=>CH2CHO+OH      1.0000E+13      0.000      0.00
C2H3+H2O2<=>C2H4+HO2      1.2100E+10      0.000     -596.00
C2H3+HCO<=>C2H4+CO      9.0330E+13      0.000      0.00
C2H3+HCO<=>C2H3CHO      1.8000E+13      0.000      0.00
C2H3+CH3<=>C2H2+CH4      3.9200E+11      0.000      0.00
C2H3+CH3 (+M) <=>C3H6 (+M)      2.5000E+13      0.000      0.00
    LOW / 4.2700E+58   -11.940   9769.80/
    TROE/  0.1750     1340.60   60000.00   10139.80 /
AR/0.70/ H2/2.00/ H2O/6.00/ CH4/2.00/ CO/1.50/ CO2/2.00/
C2H4/3.00/ C2H6/3.00/
C2H3+CH3<=>aC3H5+H      1.5000E+24     -2.830     18618.00
C2H3+C2H2<=>C4H4+H      2.0000E+18     -1.680     10600.00
C2H3+C2H2<=>nC4H5      9.3000E+38     -8.760     12000.00
C2H3+C2H2<=>iC4H5      1.6000E+46    -10.980     18600.00
2C2H3<=>C4H6      1.5000E+42     -8.840     12483.00
2C2H3<=>iC4H5+H      1.2000E+22     -2.440     13654.00
2C2H3<=>nC4H5+H      2.4000E+20     -2.040     15361.00
2C2H3<=>C2H2+C2H4      9.6000E+11      0.000      0.00
CH2CHO<=>CH3+CO      7.8000E+41     -9.147     46900.00
CH2CHO+H (+M) <=>CH3CHO (+M)      1.0000E+14      0.000      0.00
    LOW / 5.2000E+39   -7.297   4700.00/
    TROE/  0.5500     8900.00   4350.00   7244.00 /
H2/2.00/ H2O/6.00/ CH4/2.00/ CO/1.50/ CO2/2.00/ C2H2/3.00/
C2H4/3.00/ C2H6/3.00/
CH2CHO+H<=>CH3CO+H      5.0000E+12      0.000      0.00
CH2CHO+H<=>CH3+HCO      9.0000E+13      0.000      0.00
CH2CHO+H<=>CH2CO+H2      2.0000E+13      0.000     4000.00
CH2CHO+O<=>CH2CO+OH      2.0000E+13      0.000     4000.00
CH2CHO+OH<=>CH2CO+H2O      1.0000E+13      0.000     2000.00
CH2CHO+O2<=>CH2CO+HO2      1.4000E+11      0.000      0.00
CH2CHO+O2<=>CH2O+CO+OH      1.8000E+10      0.000      0.00
CH3+CO (+M) <=>CH3CO (+M)      4.8500E+07      1.650     6150.00
    LOW / 7.8000E+30   -5.395   8600.00/
    TROE/  0.2580     598.00   21002.00   1773.00 /
AR/0.70/ H2/2.00/ H2O/6.00/ CH4/2.00/ CO/1.50/ CO2/2.00/
C2H2/3.00/ C2H4/3.00/ C2H6/3.00/
CH3CO+H (+M) <=>CH3CHO (+M)      9.6000E+13      0.000      0.00
    LOW / 3.8500E+44   -8.569   5500.00/
    TROE/  1.0000     2900.00   2900.00   5132.00 /
H2/2.00/ H2O/6.00/ CH4/2.00/ CO/1.50/ CO2/2.00/ C2H2/3.00/
C2H4/3.00/ C2H6/3.00/
CH3CO+H<=>CH3+HCO      9.6000E+13      0.000      0.00
CH3CO+O<=>CH2CO+OH      3.9000E+13      0.000      0.00
CH3CO+O<=>CH3+CO2      1.5000E+14      0.000      0.00
CH3CO+OH<=>CH2CO+H2O      1.2000E+13      0.000      0.00

```

```

CH3CO+OH<=>CH3+CO+OH          3.0000E+13    0.000    0.00
CH3CO+HO2<=>CH3+CO2+OH          3.0000E+13    0.000    0.00
CH3CO+H2O2<=>CH3CHO+HO2         1.8000E+11    0.000    8226.00
CH3+HCO (+M) <=>CH3CHO (+M)      1.8000E+13    0.000    0.00
      LOW / 2.2000E+48   -9.588   5100.00/
      TROE/ 0.6173      13.08    2078.00    5093.00 /
H2/2.00/ H2O/6.00/ CH4/2.00/ CO/1.50/ CO2/2.00/ C2H2/3.00/
C2H4/3.00/ C2H6/3.00/
CH3CHO+H<=>CH3CO+H2             4.1000E+09    1.160    2400.00
CH3CHO+H<=>CH4+HCO              5.0000E+10    0.000    0.00
CH3CHO+O<=>CH3CO+OH             5.8000E+12    0.000    1800.00
CH3CHO+OH<=>CH3CO+H2O           2.3500E+10    0.730   -1110.00
CH3CHO+CH3<=>CH3CO+CH4          2.0000E-06    5.600    2460.00
CH3CHO+HCO<=>CO+HCO+CH4         8.0000E+12    0.000    10400.00
CH3CHO+O2<=>CH3CO+HO2           3.0000E+13    0.000    39100.00
CH2OCH2<=>CH3+HCO              3.6300E+13    0.000    57200.00
CH2OCH2<=>CH3CHO               7.2600E+13    0.000    57200.00
CH2OCH2<=>CH4+CO               1.2100E+13    0.000    57200.00
CH2OCH2+H<=>CH2OCH+H2           2.0000E+13    0.000    8300.00
CH2OCH2+H<=>C2H3+H2O            5.0000E+09    0.000    5000.00
CH2OCH2+H<=>C2H4+OH             9.5100E+10    0.000    5000.00
CH2OCH2+O<=>CH2OCH+OH           1.9100E+12    0.000    5250.00
CH2OCH2+OH<=>CH2OCH+H2O         1.7800E+13    0.000    3610.00
CH2OCH2+CH3<=>CH2OCH+CH4        1.0700E+12    0.000    11830.00
CH2OCH+M<=>CH3+CO+M             3.1600E+14    0.000    12000.00
CH2OCH+M<=>CH2CHO+M             5.0000E+09    0.000    0.00
CH2OCH+M<=>CH2CO+H+M            3.0000E+13    0.000    8000.00
C2H4+M<=>H2+H2CC+M             9.6835E+14    0.000    54250.00
AR/0.70/ H2/2.00/ H2O/6.00/ CH4/2.00/ CO/1.50/ CO2/2.00/
C2H6/3.00/
C2H4+H (+M) <=>C2H5 (+M)         1.2385E+09    1.463    1355.00
      LOW / 1.8365E+39   -6.642   5769.00/
      TROE/ -0.5690     299.00    9147.00    -152.40 /
AR/0.70/ H2/2.00/ H2O/6.00/ CH4/2.00/ CO/1.50/ CO2/2.00/
C2H6/3.00/
C2H4+H<=>C2H3+H2               4.9990E+07    1.900    12950.00
C2H4+O<=>C2H3+OH               1.7425E+07    1.900    3740.00
C2H4+O<=>CH3+HCO                1.6032E+07    1.830    220.00
C2H4+O<=>CH2+CH2O               3.8400E+05    1.830    220.00
C2H4+OH<=>C2H3+H2O             4.2804E+06    2.000    2500.00
C2H4+HCO<=>C2H5+CO              1.0000E+07    2.000    8000.00
C2H4+CH<=>aC3H4+H               3.0000E+13    0.000    0.00
C2H4+CH<=>pC3H4+H               3.0000E+13    0.000    0.00
C2H4+CH2<=>aC3H5+H              2.0000E+13    0.000    6000.00
C2H4+CH2*<=>H2CC+CH4            5.0000E+13    0.000    0.00
C2H4+CH2*<=>aC3H5+H              5.0000E+13    0.000    0.00
C2H4+CH3<=>C2H3+CH4            4.4628E+05    2.000    9200.00
C2H4+CH3<=>nC3H7                3.3000E+11    0.000    7700.00
C2H4+C2H<=>C4H4+H              1.2000E+13    0.000    0.00
C2H4+O2<=>C2H3+HO2             4.2200E+13    0.000    60800.00
C2H4+C2H3<=>C4H7               7.9300E+38   -8.470    14220.00
C2H4+HO2<=>CH2OCH2+OH           2.8200E+12    0.000    17100.00
C2H5+H (+M) <=>C2H6 (+M)         5.2100E+17   -0.990    1580.00
      LOW / 1.9900E+41   -7.080   6685.00/

```

```

TROE/ 0.8422      125.00      2219.00      6882.00 /
AR/0.70/ H2/2.00/ H2O/6.00/ CH4/2.00/ CO/1.50/ CO2/2.00/
C2H6/3.00/
C2H5+H<=>C2H4+H2          2.0000E+12      0.000      0.00
C2H5+O<=>CH3+CH2O          1.6040E+13      0.000      0.00
C2H5+O<=>CH3CHO+H          8.0200E+13      0.000      0.00
C2H5+O2<=>C2H4+HO2        2.0000E+10      0.000      0.00
C2H5+HO2<=>C2H6+O2        3.0000E+11      0.000      0.00
C2H5+HO2<=>C2H4+H2O2       3.0000E+11      0.000      0.00
C2H5+HO2<=>CH3+CH2O+OH     2.4000E+13      0.000      0.00
C2H5+H2O2<=>C2H6+HO2      8.7000E+09      0.000      974.00
C2H5+CH3 (+M) <=>C3H8 (+M) 4.9000E+14     -0.500      0.00
LOW / 6.8000E+61 -13.420 6000.00/
TROE/ 1.0000      1000.00      1433.90      5328.80 /
AR/0.70/ H2/2.00/ H2O/6.00/ CH4/2.00/ CO/1.50/ CO2/2.00/
C2H6/3.00/
C2H5+C2H3 (+M) <=>C4H81 (+M) 1.5000E+13      0.000      0.00
LOW / 1.5500E+56 -11.790 8984.50/
TROE/ 0.1980      2277.90      60000.00      5723.20 /
AR/0.70/ H2/2.00/ H2O/6.00/ CH4/2.00/ CO/1.50/ CO2/2.00/
C2H6/3.00/
C2H5+C2H3<=>aC3H5+CH3      3.9000E+32     -5.220     19747.00
C2H6+H<=>C2H5+H2          1.1500E+08      1.900      7530.00
C2H6+O<=>C2H5+OH          8.9800E+07      1.920      5690.00
C2H6+OH<=>C2H5+H2O        3.4550E+06      2.120      870.00
C2H6+CH2*<=>C2H5+CH3      4.0000E+13      0.000     -550.00
C2H6+CH3<=>C2H5+CH4       6.1400E+06      1.740     10450.00
C3H3+H<=>pC3H4            1.5000E+13      0.000      0.00
C3H3+H<=>aC3H4            2.5000E+12      0.000      0.00
C3H3+O<=>CH2O+C2H         2.0000E+13      0.000      0.00
C3H3+O2<=>CH2CO+HCO       3.0000E+10      0.000     2868.00
C3H3+HO2<=>OH+CO+C2H3     8.0000E+11      0.000      0.00
C3H3+HO2<=>aC3H4+O2       3.0000E+11      0.000      0.00
C3H3+HO2<=>pC3H4+O2       2.5000E+12      0.000      0.00
C3H3+HCO<=>aC3H4+CO       2.5000E+13      0.000      0.00
C3H3+HCO<=>pC3H4+CO       2.5000E+13      0.000      0.00
C3H3+HCCO<=>C4H4+CO       2.5000E+13      0.000      0.00
C3H3+CH<=>iC4H3+H         5.0000E+13      0.000      0.00
C3H3+CH2<=>C4H4+H         5.0000E+13      0.000      0.00
C3H3+CH3 (+M) <=>C4H612 (+M) 1.5000E+12      0.000      0.00
LOW / 2.6000E+57 -11.940 9770.00/
TROE/ 0.1750      1340.60      60000.00      9769.80 /
AR/0.70/ H2/2.00/ H2O/6.00/ CH4/2.00/ CO/1.50/ CO2/2.00/
C2H6/3.00/
C3H3+C2H2<=>C5H5          6.8700E+55     -12.500     42025.00
2C3H3=>C6H5+H            5.0000E+12      0.000      0.00
2C3H3=>C6H6            2.0000E+12      0.000      0.00
C3H3+C4H4<=>C6H5CH2       6.5300E+05      1.280     -4611.00
C3H3+C4H6<=>C6H5CH3+H     6.5300E+05      1.280     -4611.00
aC3H4+H<=>C3H3+H2        1.3000E+06      2.000      5500.00
aC3H4+H<=>CH3CHCH         5.4000E+29     -6.090     16300.00
aC3H4+H<=>CH3CCH2         9.4600E+42     -9.430     11190.00
aC3H4+H<=>aC3H5           1.6173E+59    -13.540     26949.00
aC3H4+O<=>C2H4+CO        2.0000E+07      1.800      1000.00

```

aC3H4+OH<=>C3H3+H2O	5.3000E+06	2.000	2000.00
aC3H4+CH3<=>C3H3+CH4	1.3000E+12	0.000	7700.00
aC3H4+CH3<=>iC4H7	2.0000E+11	0.000	7500.00
aC3H4+C2H<=>C2H2+C3H3	1.0000E+13	0.000	0.00
pC3H4<=>cC3H4	1.2000E+44	-9.920	69250.00
pC3H4<=>aC3H4	5.1500E+60	-13.930	91117.00
pC3H4+H<=>aC3H4+H	6.2700E+17	-0.910	10079.00
pC3H4+H<=>CH3CCH2	1.6600E+47	-10.580	13690.00
pC3H4+H<=>CH3CHCH	5.5000E+28	-5.740	4300.00
pC3H4+H<=>aC3H5	4.9100E+60	-14.370	31644.00
pC3H4+H<=>C3H3+H2	1.3000E+06	2.000	5500.00
pC3H4+C3H3<=>aC3H4+C3H3	6.1400E+06	1.740	10450.00
pC3H4+O<=>HCCO+CH3	7.3000E+12	0.000	2250.00
pC3H4+O<=>C2H4+CO	1.0000E+13	0.000	2250.00
pC3H4+OH<=>C3H3+H2O	1.0000E+06	2.000	100.00
pC3H4+C2H<=>C2H2+C3H3	1.0000E+13	0.000	0.00
pC3H4+CH3<=>C3H3+CH4	1.8000E+12	0.000	7700.00
cC3H4<=>aC3H4	4.8900E+41	-9.170	49594.00
aC3H5+H (+M) <=>C3H6 (+M)	1.9560E+14	0.000	0.00
LOW / 1.3007E+60 -12.000 5967.80/			
TROE/ 0.0200 1096.60 1096.60 6859.50 /			
AR/0.70/ H2/2.00/ H2O/6.00/ CH4/2.00/ CO/1.50/ CO2/2.00/			
C2H6/3.00/			
aC3H5+H<=>aC3H4+H2	1.8000E+13	0.000	0.00
aC3H5+O<=>C2H3CHO+H	5.6820E+13	0.000	0.00
aC3H5+OH<=>C2H3CHO+2H	4.2000E+32	-5.160	30126.00
aC3H5+OH<=>aC3H4+H2O	6.0000E+12	0.000	0.00
aC3H5+O2<=>aC3H4+HO2	4.9900E+15	-1.400	22428.00
aC3H5+O2<=>CH3CO+CH2O	1.1900E+15	-1.010	20128.00
aC3H5+O2<=>C2H3CHO+OH	1.8200E+13	-0.410	22859.00
aC3H5+HO2<=>C3H6+O2	2.6600E+12	0.000	0.00
aC3H5+HO2<=>OH+C2H3+CH2O	9.1740E+12	0.000	0.00
aC3H5+HCO<=>C3H6+CO	6.0000E+13	0.000	0.00
aC3H5+CH3 (+M) <=>C4H81 (+M)	9.9200E+13	-0.320	-262.30
LOW / 3.8787E+60 -12.810 6250.00/			
TROE/ 0.1040 1606.00 60000.00 6118.40 /			
AR/0.70/ H2/2.00/ H2O/6.00/ CH4/2.00/ CO/1.50/ CO2/2.00/			
C2H6/3.00/			
aC3H5+CH3<=>aC3H4+CH4	3.0000E+12	-0.320	-131.00
aC3H5<=>CH3CCH2	7.0600E+56	-14.080	75868.00
aC3H5<=>CH3CHCH	5.0000E+51	-13.020	73300.00
aC3H5+C2H2<=>1C5H7	8.3800E+30	-6.242	12824.00
CH3CCH2<=>CH3CHCH	1.5000E+48	-12.710	53900.00
CH3CCH2+H<=>pC3H4+H2	3.3400E+12	0.000	0.00
CH3CCH2+O<=>CH3+CH2CO	6.0000E+13	0.000	0.00
CH3CCH2+OH<=>CH3+CH2CO+H	5.0000E+12	0.000	0.00
CH3CCH2+O2<=>CH3CO+CH2O	1.0000E+11	0.000	0.00
CH3CCH2+HO2<=>CH3+CH2CO+OH	2.0000E+13	0.000	0.00
CH3CCH2+HCO<=>C3H6+CO	9.0000E+13	0.000	0.00
CH3CCH2+CH3<=>pC3H4+CH4	1.0000E+11	0.000	0.00
CH3CCH2+CH3<=>iC4H8	2.0000E+13	0.000	0.00
CH3CHCH+H<=>pC3H4+H2	3.3400E+12	0.000	0.00
CH3CHCH+O<=>C2H4+HCO	6.0000E+13	0.000	0.00
CH3CHCH+OH<=>C2H4+HCO+H	5.0000E+12	0.000	0.00

```

CH3CHCH+O2<=>CH3CHO+HCO          1.0000E+11    0.000    0.00
CH3CHCH+HO2<=>C2H4+HCO+OH          2.0000E+13    0.000    0.00
CH3CHCH+HCO<=>C3H6+CO              9.0000E+13    0.000    0.00
CH3CHCH+CH3<=>pC3H4+CH4            1.0000E+11    0.000    0.00
C3H6+H(+M)<=>nC3H7(+M)              1.3300E+13    0.000    3260.70
    LOW / 6.2600E+38    -6.660    7000.00/
    TROE/ 1.0000    1000.00    1310.00    48097.00 /
AR/0.70/ H2/2.00/ H2O/6.00/ CH4/2.00/ CO/1.50/ CO2/2.00/
C2H6/3.00/
C3H6+H(+M)<=>iC3H7(+M)              1.3300E+13    0.000    1559.80
    LOW / 8.7000E+42    -7.500    4721.80/
    TROE/ 1.0000    1000.00    645.40    6844.30 /
AR/0.70/ H2/2.00/ H2O/6.00/ CH4/2.00/ CO/1.50/ CO2/2.00/
C2H6/3.00/
C3H6+H<=>C2H4+CH3                  7.7840E+21    -2.390    11180.00
C3H6+H<=>aC3H5+H2                  1.2923E+05    2.500    2490.00
C3H6+H<=>CH3CCH2+H2                4.0000E+05    2.500    9790.00
C3H6+H<=>CH3CHCH+H2                8.0400E+05    2.500    12283.00
C3H6+O<=>CH2CO+CH3+H               8.0000E+07    1.650    327.00
C3H6+O<=>C2H3CHO+2H                4.0640E+07    1.650    327.00
C3H6+O<=>C2H5+HCO                  3.5735E+07    1.650    -972.00
C3H6+O<=>aC3H5+OH                   1.8000E+11    0.700    5880.00
C3H6+O<=>CH3CCH2+OH                6.0000E+10    0.700    7630.00
C3H6+O<=>CH3CHCH+OH                1.2100E+11    0.700    8960.00
C3H6+OH<=>aC3H5+H2O                2.5017E+06    2.000    -298.00
C3H6+OH<=>CH3CCH2+H2O              1.1000E+06    2.000    1450.00
C3H6+OH<=>CH3CHCH+H2O              2.1400E+06    2.000    2778.00
C3H6+HO2<=>aC3H5+H2O2              9.6000E+03    2.600    13910.00
C3H6+CH3<=>aC3H5+CH4               2.2000E+00    3.500    5675.00
C3H6+CH3<=>CH3CCH2+CH4             8.4000E-01    3.500    11660.00
C3H6+CH3<=>CH3CHCH+CH4             1.3500E+00    3.500    12848.00
C3H6+C2H3<=>C4H6+CH3               7.2300E+11    0.000    5000.00
C3H6+HO2<=>CH3CHOCH2+OH            1.0900E+12    0.000    14200.00
C2H3CHO+H<=>C2H4+HCO               1.0800E+11    0.454    5820.00
C2H3CHO+O<=>C2H3+OH+CO              3.0000E+13    0.000    3540.00
C2H3CHO+O<=>CH2O+CH2CO              1.9000E+07    1.800    220.00
C2H3CHO+OH<=>C2H3+H2O+CO           3.4300E+09    1.180    -447.00
C2H3CHO+CH3<=>CH2CHCO+CH4           2.0000E+13    0.000    11000.00
C2H3CHO+C2H3<=>C4H6+HCO            2.8000E+21    -2.440    14720.00
CH2CHCO<=>C2H3+CO                  1.0000E+14    0.000    27000.00
CH2CHCO+H<=>C2H3CHO                1.0000E+14    0.000    0.00
CH3CHOCH2<=>CH3CH2CHO               1.8400E+14    0.000    58500.00
CH3CHOCH2<=>C2H5+HCO                2.4500E+13    0.000    58500.00
CH3CHOCH2<=>CH3+CH2CHO              2.4500E+13    0.000    58800.00
CH3CHOCH2<=>CH3COCH3                1.0100E+14    0.000    59900.00
CH3CHOCH2<=>CH3+CH3CO               4.5400E+13    0.000    59900.00
iC3H7+H(+M)<=>C3H8(+M)              2.4000E+13    0.000    0.00
    LOW / 1.7000E+58    -12.080    11263.70/
    TROE/ 0.6490    1213.10    1213.10    13369.70 /
AR/0.70/ H2/2.00/ H2O/6.00/ CH4/2.00/ CO/1.50/ CO2/2.00/
C2H6/3.00/
iC3H7+H<=>CH3+C2H5                 1.4000E+28    -3.940    15916.00
iC3H7+H<=>C3H6+H2                  3.2000E+12    0.000    0.00
iC3H7+O<=>CH3CHO+CH3               9.6000E+13    0.000    0.00

```

iC3H7+OH<=>C3H6+H2O	2.4000E+13	0.000	0.00
iC3H7+O2<=>C3H6+HO2	1.3000E+11	0.000	0.00
iC3H7+HO2<=>CH3CHO+CH3+OH	2.4000E+13	0.000	0.00
iC3H7+HCO<=>C3H8+CO	1.2000E+14	0.000	0.00
iC3H7+CH3<=>CH4+C3H6	2.2000E+14	-0.680	0.00
nC3H7+H(+M)<=>C3H8(+M)	3.6000E+13	0.000	0.00
LOW / 3.0100E+48 -9.320 5833.60/			
TROE/ 0.4980 1314.00 1314.00 50000.00 /			
AR/0.70/ H2/2.00/ H2O/6.00/ CH4/2.00/ CO/1.50/ CO2/2.00/			
C2H6/3.00/			
nC3H7+H<=>C2H5+CH3	3.7000E+24	-2.920	12505.00
nC3H7+H<=>C3H6+H2	1.8000E+12	0.000	0.00
nC3H7+O<=>C2H5+CH2O	9.6000E+13	0.000	0.00
nC3H7+OH<=>C3H6+H2O	2.4000E+13	0.000	0.00
nC3H7+O2<=>C3H6+HO2	9.0000E+10	0.000	0.00
nC3H7+HO2<=>C2H5+OH+CH2O	2.4000E+13	0.000	0.00
nC3H7+HCO<=>C3H8+CO	6.0000E+13	0.000	0.00
nC3H7+CH3<=>CH4+C3H6	1.1000E+13	0.000	0.00
C3H8+H<=>H2+nC3H7	1.3000E+06	2.540	6756.00
C3H8+H<=>H2+iC3H7	1.3000E+06	2.400	4471.00
C3H8+O<=>nC3H7+OH	1.9000E+05	2.680	3716.00
C3H8+O<=>iC3H7+OH	4.7600E+04	2.710	2106.00
C3H8+OH<=>nC3H7+H2O	1.4000E+03	2.660	527.00
C3H8+OH<=>iC3H7+H2O	2.7000E+04	2.390	393.00
C3H8+O2<=>nC3H7+HO2	4.0000E+13	0.000	50930.00
C3H8+O2<=>iC3H7+HO2	4.0000E+13	0.000	47590.00
C3H8+HO2<=>nC3H7+H2O2	4.7600E+04	2.550	16490.00
C3H8+HO2<=>iC3H7+H2O2	9.6400E+03	2.600	13910.00
C3H8+CH3<=>CH4+nC3H7	9.0300E-01	3.650	7153.00
C3H8+CH3<=>CH4+iC3H7	1.5100E+00	3.460	5480.00
C4H2+H<=>nC4H3	1.1000E+42	-8.720	15300.00
C4H2+H<=>iC4H3	1.1000E+30	-4.920	10800.00
C4H2+OH<=>H2C4O+H	6.6000E+12	0.000	-410.00
C4H2+C2H<=>C6H2+H	9.6000E+13	0.000	0.00
C4H2+C2H<=>C6H3	4.5000E+37	-7.680	7100.00
H2C4O+H<=>C2H2+HCCO	5.0000E+13	0.000	3000.00
H2C4O+OH<=>CH2CO+HCCO	1.0000E+07	2.000	2000.00
nC4H3<=>iC4H3	4.1000E+43	-9.490	53000.00
nC4H3+H<=>iC4H3+H	2.5000E+20	-1.670	10800.00
nC4H3+H<=>C2H2+H2CC	6.3000E+25	-3.340	10014.00
nC4H3+H<=>C4H4	2.0000E+47	-10.260	13070.00
nC4H3+H<=>C4H2+H2	3.0000E+13	0.000	0.00
nC4H3+OH<=>C4H2+H2O	2.0000E+12	0.000	0.00
nC4H3+C2H2<=>1-C6H4+H	2.5000E+14	-0.560	10600.00
nC4H3+C2H2<=>C6H5	9.6000E+70	-17.770	31300.00
nC4H3+C2H2<=>o-C6H4+H	6.9000E+46	-10.010	30100.00
iC4H3+H<=>C2H2+H2CC	2.8000E+23	-2.550	10780.00
iC4H3+H<=>C4H4	3.4000E+43	-9.010	12120.00
iC4H3+H<=>C4H2+H2	6.0000E+13	0.000	0.00
iC4H3+OH<=>C4H2+H2O	4.0000E+12	0.000	0.00
iC4H3+O2<=>HCCO+CH2CO	7.8600E+16	-1.800	0.00
C4H4+H<=>nC4H5	1.3000E+51	-11.920	16500.00
C4H4+H<=>iC4H5	4.9000E+51	-11.920	17700.00
C4H4+H<=>nC4H3+H2	6.6500E+05	2.530	12240.00

C4H4+H<=>iC4H3+H2	3.3300E+05	2.530	9240.00
C4H4+OH<=>nC4H3+H2O	3.1000E+07	2.000	3430.00
C4H4+OH<=>iC4H3+H2O	1.5500E+07	2.000	430.00
C4H4+O<=>C3H3+HCO	6.0000E+08	1.450	-860.00
C4H4+C2H<=>1-C6H4+H	1.2000E+13	0.000	0.00
nC4H5<=>iC4H5	1.5000E+67	-16.890	59100.00
nC4H5+H<=>iC4H5+H	3.1000E+26	-3.350	17423.00
nC4H5+H<=>C4H4+H2	1.5000E+13	0.000	0.00
nC4H5+OH<=>C4H4+H2O	2.0000E+12	0.000	0.00
nC4H5+HCO<=>C4H6+CO	5.0000E+12	0.000	0.00
nC4H5+HO2<=>C2H3+CH2CO+OH	6.6000E+12	0.000	0.00
nC4H5+H2O2<=>C4H6+HO2	1.2100E+10	0.000	-596.00
nC4H5+HO2<=>C4H6+O2	6.0000E+11	0.000	0.00
nC4H5+O2<=>CH2CHCHCHO+O	3.0000E+11	0.290	11.00
nC4H5+O2<=>HCO+C2H3CHO	9.2000E+16	-1.390	1010.00
nC4H5+C2H2<=>C6H6+H	1.6000E+16	-1.330	5400.00
nC4H5+C2H3<=>C6H6+H2	1.8400E-13	7.070	-3611.00
iC4H5+H<=>C4H4+H2	3.0000E+13	0.000	0.00
iC4H5+H<=>C3H3+CH3	2.0000E+13	0.000	2000.00
iC4H5+OH<=>C4H4+H2O	4.0000E+12	0.000	0.00
iC4H5+HCO<=>C4H6+CO	5.0000E+12	0.000	0.00
iC4H5+HO2<=>C4H6+O2	6.0000E+11	0.000	0.00
iC4H5+HO2<=>C2H3+CH2CO+OH	6.6000E+12	0.000	0.00
iC4H5+H2O2<=>C4H6+HO2	1.2100E+10	0.000	-596.00
iC4H5+O2<=>CH2CO+CH2CHO	2.1600E+10	0.000	2500.00
C4H5-2<=>iC4H5	1.5000E+67	-16.890	59100.00
iC4H5+H<=>C4H5-2+H	3.1000E+26	-3.350	17423.00
C4H5-2+HO2<=>OH+C2H2+CH3CO	8.0000E+11	0.000	0.00
C4H5-2+O2<=>CH3CO+CH2CO	2.1600E+10	0.000	2500.00
C4H5-2+C2H2<=>C6H6+H	5.0000E+14	0.000	25000.00
C4H5-2+C2H4<=>C5H6+CH3	5.0000E+14	0.000	25000.00
C4H6<=>iC4H5+H	5.7000E+36	-6.270	112353.00
C4H6<=>nC4H5+H	5.3000E+44	-8.620	123608.00
C4H6<=>C4H4+H2	2.5000E+15	0.000	94700.00
C4H6+H<=>nC4H5+H2	1.3300E+06	2.530	12240.00
C4H6+H<=>iC4H5+H2	6.6500E+05	2.530	9240.00
C4H6+H<=>C2H4+C2H3	1.4600E+30	-4.340	21647.00
C4H6+H<=>pC3H4+CH3	2.0000E+12	0.000	7000.00
C4H6+H<=>aC3H4+CH3	2.0000E+12	0.000	7000.00
C4H6+O<=>nC4H5+OH	7.5000E+06	1.900	3740.00
C4H6+O<=>iC4H5+OH	7.5000E+06	1.900	3740.00
C4H6+O<=>CH3CHCHCO+H	1.5000E+08	1.450	-860.00
C4H6+O<=>CH2CHCHCHO+H	4.5000E+08	1.450	-860.00
C4H6+OH<=>nC4H5+H2O	6.2000E+06	2.000	3430.00
C4H6+OH<=>iC4H5+H2O	3.1000E+06	2.000	430.00
C4H6+HO2<=>C4H6O25+OH	1.2000E+12	0.000	14000.00
C4H6+HO2<=>C2H3CHOCH2+OH	4.8000E+12	0.000	14000.00
C4H6+CH3<=>nC4H5+CH4	2.0000E+14	0.000	22800.00
C4H6+CH3<=>iC4H5+CH4	1.0000E+14	0.000	19800.00
C4H6+C2H3<=>nC4H5+C2H4	5.0000E+13	0.000	22800.00
C4H6+C2H3<=>iC4H5+C2H4	2.5000E+13	0.000	19800.00
C4H6+C3H3<=>nC4H5+aC3H4	1.0000E+13	0.000	22500.00
C4H6+C3H3<=>iC4H5+aC3H4	5.0000E+12	0.000	19500.00
C4H6+aC3H5<=>nC4H5+C3H6	1.0000E+13	0.000	22500.00

C4H6+aC3H5<=>iC4H5+C3H6	5.0000E+12	0.000	19500.00
C4H6+C2H3<=>C6H6+H2+H	5.6200E+11	0.000	3240.00
C4H612<=>iC4H5+H	4.2000E+15	0.000	92600.00
C4H612+H<=>C4H6+H	2.0000E+13	0.000	4000.00
C4H612+H<=>iC4H5+H2	1.7000E+05	2.500	2490.00
C4H612+H<=>aC3H4+CH3	2.0000E+13	0.000	2000.00
C4H612+H<=>pC3H4+CH3	2.0000E+13	0.000	2000.00
C4H612+CH3<=>iC4H5+CH4	7.0000E+13	0.000	18500.00
C4H612+O<=>CH2CO+C2H4	1.2000E+08	1.650	327.00
C4H612+O<=>iC4H5+OH	1.8000E+11	0.700	5880.00
C4H612+OH<=>iC4H5+H2O	3.1000E+06	2.000	-298.00
C4H612<=>C4H6	3.0000E+13	0.000	65000.00
C4H6-2<=>C4H6	3.0000E+13	0.000	65000.00
C4H6-2<=>C4H612	3.0000E+13	0.000	67000.00
C4H6-2+H<=>C4H612+H	2.0000E+13	0.000	4000.00
C4H6-2+H<=>C4H5-2+H2	3.4000E+05	2.500	2490.00
C4H6-2+H<=>CH3+pC3H4	2.6000E+05	2.500	1000.00
C4H6-2<=>H+C4H5-2	5.0000E+15	0.000	87300.00
C4H6-2+CH3<=>C4H5-2+CH4	1.4000E+14	0.000	18500.00
C2H3CHOCH2<=>C4H6O23	2.0000E+14	0.000	50600.00
C4H6O23<=>CH3CHCHCHO	1.9500E+13	0.000	49400.00
C4H6O23<=>C2H4+CH2CO	5.7500E+15	0.000	69300.00
C4H6O23<=>C2H2+CH2OCH2	1.0000E+16	0.000	75800.00
C4H6O25<=>C4H4O+H2	5.3000E+12	0.000	48500.00
C4H4O<=>CO+pC3H4	1.7800E+15	0.000	77500.00
C4H4O<=>C2H2+CH2CO	5.0100E+14	0.000	77500.00
CH3CHCHCHO<=>C3H6+CO	3.9000E+14	0.000	69000.00
CH3CHCHCHO+H<=>CH2CHCHCHO+H2	1.7000E+05	2.500	2490.00
CH3CHCHCHO+H<=>CH3CHCHCO+H2	1.0000E+05	2.500	2490.00
CH3CHCHCHO+H<=>CH3+C2H3CHO	4.0000E+21	-2.390	11180.00
CH3CHCHCHO+H<=>C3H6+HCO	4.0000E+21	-2.390	11180.00
CH3CHCHCHO+CH3<=>CH2CHCHCHO+CH4	2.1000E+00	3.500	5675.00
CH3CHCHCHO+CH3<=>CH3CHCHCO+CH4	1.1000E+00	3.500	5675.00
CH3CHCHCHO+C2H3<=>CH2CHCHCHO+C2H4	2.2100E+00	3.500	4682.00
CH3CHCHCHO+C2H3<=>CH3CHCHCO+C2H4	1.1100E+00	3.500	4682.00
CH3CHCHCO<=>CH3CHCH+CO	1.0000E+14	0.000	30000.00
CH3CHCHCO+H<=>CH3CHCHCHO	1.0000E+14	0.000	0.00
CH2CHCHCHO<=>aC3H5+CO	1.0000E+14	0.000	25000.00
CH2CHCHCHO+H<=>CH3CHCHCHO	1.0000E+14	0.000	0.00
C4H7<=>C4H6+H	2.4800E+53	-12.300	52000.00
C4H7+H (+M) <=>C4H81 (+M)	3.6000E+13	0.000	0.00
LOW / 3.0100E+48 -9.320 5833.60/			
TROE/ 0.4980 1314.00 1314.00 50000.00 /			
AR/0.70/ H2/2.00/ H2O/6.00/ CH4/2.00/ CO/1.50/ CO2/2.00/			
C2H6/3.00/			
C4H7+H<=>CH3+aC3H5	2.0000E+21	-2.000	11000.00
C4H7+H<=>C4H6+H2	1.8000E+12	0.000	0.00
C4H7+O2<=>C4H6+HO2	1.0000E+11	0.000	0.00
C4H7+HO2<=>CH2O+OH+aC3H5	2.4000E+13	0.000	0.00
C4H7+HCO<=>C4H81+CO	6.0000E+13	0.000	0.00
C4H7+CH3<=>C4H6+CH4	1.1000E+13	0.000	0.00
iC4H7+H (+M) <=>iC4H8 (+M)	2.0000E+14	0.000	0.00
LOW / 1.3300E+60 -12.000 5967.80/			
TROE/ 0.0200 1096.60 1096.60 6859.50 /			

```

AR/0.70/ H2/2.00/ H2O/6.00/ CH4/2.00/ CO/1.50/ CO2/2.00/
C2H6/3.00/
iC4H7+H<=>CH3CCH2+CH3          2.6000E+45   -8.190   37890.00
iC4H7+O<=>CH2O+CH3CCH2          9.0000E+13    0.000    0.00
iC4H7+HO2<=>CH3CCH2+CH2O+OH     4.0000E+12    0.000    0.00
C4H81+H(+M)<=>pC4H9(+M)          1.3300E+13    0.000   3260.70
    LOW / 6.2600E+38   -6.660   7000.00/
    TROE/ 1.0000    1000.00   1310.00   48097.00 /
AR/0.70/ H2/2.00/ H2O/6.00/ CH4/2.00/ CO/1.50/ CO2/2.00/
C2H6/3.00/
C4H81+H(+M)<=>sC4H9(+M)          1.3300E+13    0.000   1559.80
    LOW / 8.7000E+42   -7.500   4721.80/
    TROE/ 1.0000    1000.00   645.40    6844.30 /
AR/0.70/ H2/2.00/ H2O/6.00/ CH4/2.00/ CO/1.50/ CO2/2.00/
C2H6/3.00/
C4H81+H<=>C2H4+C2H5              1.3872E+22   -2.390   11180.00
C4H81+H<=>C3H6+CH3              3.5232E+22   -2.390   11180.00
C4H81+H<=>C4H7+H2              6.5000E+05    2.540    6756.00
C4H81+O<=>nC3H7+HCO            3.3000E+08    1.450   -402.00
C4H81+O<=>C4H7+OH              1.5000E+13    0.000   5760.00
    DUPLICATE
C4H81+O<=>C4H7+OH              2.6000E+13    0.000   4470.00
    DUPLICATE
C4H81+OH<=>C4H7+H2O             7.0000E+02    2.660    527.00
C4H81+O2<=>C4H7+HO2            2.0000E+13    0.000  50930.00
C4H81+HO2<=>C4H7+H2O2          1.0000E+12    0.000  14340.00
C4H81+CH3<=>C4H7+CH4           4.5000E-01    3.650   7153.00
C4H82+H(+M)<=>sC4H9(+M)          1.3300E+13    0.000   1559.80
    LOW / 8.7000E+42   -7.500   4721.80/
    TROE/ 1.0000    1000.00   645.40    6844.30 /
AR/0.70/ H2/2.00/ H2O/6.00/ CH4/2.00/ CO/1.50/ CO2/2.00/
C2H6/3.00/
C4H82+H<=>C4H7+H2              3.4000E+05    2.500   2490.00
C4H82+O<=>C2H4+CH3CHO          2.4000E+08    1.650    327.00
C4H82+OH<=>C4H7+H2O            6.2000E+06    2.000   -298.00
C4H82+O2<=>C4H7+HO2            5.0000E+13    0.000  53300.00
C4H82+HO2<=>C4H7+H2O2          1.9000E+04    2.600  13910.00
C4H82+CH3<=>C4H7+CH4           4.4000E+00    3.500   5675.00
iC4H8+H(+M)<=>iC4H9(+M)          1.3300E+13    0.000   3260.70
    LOW / 6.2600E+38   -6.660   7000.00/
    TROE/ 1.0000    1000.00   1310.00   48097.00 /
AR/0.70/ H2/2.00/ H2O/6.00/ CH4/2.00/ CO/1.50/ CO2/2.00/
C2H6/3.00/
iC4H8+H<=>iC4H7+H2              1.2000E+06    2.540   6760.00
iC4H8+H<=>C3H6+CH3              8.0000E+21   -2.390   11180.00
iC4H8+O<=>2CH3+CH2CO            1.2000E+08    1.650    327.00
iC4H8+O<=>iC3H7+HCO            3.5000E+07    1.650   -972.00
iC4H8+O<=>iC4H7+OH              2.9000E+05    2.500   3640.00
iC4H8+OH<=>iC4H7+H2O            1.5000E+08    1.530    775.00
iC4H8+HO2<=>iC4H7+H2O2          2.0000E+04    2.550  15500.00
iC4H8+O2<=>iC4H7+HO2            2.7000E+13    0.000  50900.00
iC4H8+CH3<=>iC4H7+CH4           9.1000E-01    3.650   7150.00
C2H4+C2H5<=>pC4H9              1.5000E+11    0.000   7300.00
pC4H9+H(+M)<=>C4H10(+M)         3.6000E+13    0.000    0.00

```

```

LOW / 3.0100E+48 -9.320 5833.60/
TROE/ 0.4980 1314.00 1314.00 50000.00 /
AR/0.70/ H2/2.00/ H2O/6.00/ CH4/2.00/ CO/1.50/ CO2/2.00/
C2H6/3.00/
pC4H9+H<=>2C2H5 3.7000E+24 -2.920 12505.00
pC4H9+H<=>C4H81+H2 1.8000E+12 0.000 0.00
pC4H9+O<=>nC3H7+CH2O 9.6000E+13 0.000 0.00
pC4H9+OH<=>C4H81+H2O 2.4000E+13 0.000 0.00
pC4H9+O2<=>C4H81+HO2 2.7000E+11 0.000 0.00
pC4H9+HO2<=>nC3H7+OH+CH2O 2.4000E+13 0.000 0.00
pC4H9+HCO<=>C4H10+CO 9.0000E+13 0.000 0.00
pC4H9+CH3<=>C4H81+CH4 1.1000E+13 0.000 0.00
C3H6+CH3 (+M) <=>sC4H9 (+M) 1.7000E+11 0.000 7403.60
LOW / 2.3100E+28 -4.270 1831.00/
TROE/ 0.5650 60000.00 534.20 3007.20 /
AR/0.70/ H2/2.00/ H2O/6.00/ CH4/2.00/ CO/1.50/ CO2/2.00/
C2H6/3.00/
sC4H9+H (+M) <=>C4H10 (+M) 2.4000E+13 0.000 0.00
LOW / 1.7000E+58 -12.080 11263.70/
TROE/ 0.6490 1213.10 1213.10 13369.70 /
AR/0.70/ H2/2.00/ H2O/6.00/ CH4/2.00/ CO/1.50/ CO2/2.00/
C2H6/3.00/
sC4H9+H<=>2C2H5 1.4000E+28 -3.940 15916.00
sC4H9+H<=>C4H81+H2 3.2000E+12 0.000 0.00
sC4H9+H<=>C4H82+H2 2.1000E+12 0.000 0.00
sC4H9+O<=>CH3CHO+C2H5 9.6000E+13 0.000 0.00
sC4H9+OH<=>C4H81+H2O 2.4000E+13 0.000 0.00
sC4H9+OH<=>C4H82+H2O 1.6000E+13 0.000 0.00
sC4H9+O2<=>C4H81+HO2 5.1000E+10 0.000 0.00
sC4H9+O2<=>C4H82+HO2 1.2000E+11 0.000 0.00
sC4H9+HO2<=>CH3CHO+C2H5+OH 2.4000E+13 0.000 0.00
sC4H9+HCO<=>C4H10+CO 1.2000E+14 0.000 0.00
sC4H9+CH3<=>CH4+C4H81 2.2000E+14 -0.680 0.00
sC4H9+CH3<=>CH4+C4H82 1.5000E+14 -0.680 0.00
C3H6+CH3 (+M) <=>iC4H9 (+M) 9.6000E+10 0.000 8003.60
LOW / 1.3000E+28 -4.270 2431.10/
TROE/ 0.5650 60000.00 534.20 3007.20 /
AR/0.70/ H2/2.00/ H2O/6.00/ CH4/2.00/ CO/1.50/ CO2/2.00/
C2H6/3.00/
iC4H9+H (+M) <=>iC4H10 (+M) 3.6000E+13 0.000 0.00
LOW / 3.2700E+56 -11.740 6430.80/
TROE/ 0.5060 1266.60 1266.60 50000.00 /
AR/0.70/ H2/2.00/ H2O/6.00/ CH4/2.00/ CO/1.50/ CO2/2.00/
C2H6/3.00/
iC4H9+H<=>iC3H7+CH3 1.9000E+35 -5.830 22470.00
iC4H9+H<=>iC4H8+H2 9.0000E+11 0.000 0.00
iC4H9+O<=>iC3H7+CH2O 9.6000E+13 0.000 0.00
iC4H9+OH<=>iC4H8+H2O 1.2000E+13 0.000 0.00
iC4H9+O2<=>iC4H8+HO2 2.4000E+10 0.000 0.00
iC4H9+HO2<=>iC3H7+CH2O+OH 2.4100E+13 0.000 0.00
iC4H9+HCO<=>iC4H10+CO 3.6000E+13 0.000 0.00
iC4H9+CH3<=>iC4H8+CH4 6.0000E+12 -0.320 0.00
tC4H9 (+M) <=>iC4H8+H (+M) 8.3000E+13 0.000 38150.40
LOW / 1.9000E+41 -7.360 36631.70/

```

```

TROE/ 0.2930      649.00      60000.00      3425.90 /
AR/0.70/ H2/2.00/ H2O/6.00/ CH4/2.00/ CO/1.50/ CO2/2.00/
C2H6/3.00/
tC4H9+H(+M)<=>iC4H10(+M)      2.4000E+13      0.000      0.00
LOW / 1.4700E+61 -12.940      8000.00/
TROE/ 0.0000      1456.40      1000.00      10000.50 /
AR/0.70/ H2/2.00/ H2O/6.00/ CH4/2.00/ CO/1.50/ CO2/2.00/
C2H6/3.00/
tC4H9+H<=>iC3H7+CH3      2.6000E+36      -6.120      25640.00
tC4H9+H<=>iC4H8+H2      5.4200E+12      0.000      0.00
tC4H9+O<=>iC4H8+OH      1.8000E+14      0.000      0.00
tC4H9+O<=>CH3COCH3+CH3      1.8000E+14      0.000      0.00
tC4H9+OH<=>iC4H8+H2O      1.8000E+13      0.000      0.00
tC4H9+O2<=>iC4H8+HO2      4.8000E+11      0.000      0.00
tC4H9+HO2<=>CH3+CH3COCH3+OH      1.8000E+13      0.000      0.00
tC4H9+HCO<=>iC4H10+CO      6.0000E+13      0.000      0.00
tC4H9+CH3<=>iC4H8+CH4      3.8000E+15      -1.000      0.00
CH3COCH3+H<=>H2+CH2CO+CH3      1.3000E+06      2.540      6756.00
CH3COCH3+O<=>OH+CH2CO+CH3      1.9000E+05      2.680      3716.00
CH3COCH3+OH<=>H2O+CH2CO+CH3      3.2000E+07      1.800      934.00
CH3+CH3CO<=>CH3COCH3      4.0000E+15      -0.800      0.00
nC3H7+CH3(+M)<=>C4H10(+M)      1.9300E+14      -0.320      0.00
LOW / 2.6800E+61 -13.240      6000.00/
TROE/ 1.0000      1000.00      1433.90      5328.80 /
AR/0.70/ H2/2.00/ H2O/6.00/ CH4/2.00/ CO/1.50/ CO2/2.00/
C2H6/3.00/
2C2H5(+M)<=>C4H10(+M)      1.8800E+14      -0.500      0.00
LOW / 2.6100E+61 -13.420      6000.00/
TROE/ 1.0000      1000.00      1433.90      5328.80 /
AR/0.70/ H2/2.00/ H2O/6.00/ CH4/2.00/ CO/1.50/ CO2/2.00/
C2H6/3.00/
C4H10+H<=>pC4H9+H2      9.2000E+05      2.540      6756.00
C4H10+H<=>sC4H9+H2      2.4000E+06      2.400      4471.00
C4H10+O<=>pC4H9+OH      4.9000E+06      2.400      5500.00
C4H10+O<=>sC4H9+OH      4.3000E+05      2.600      2580.00
C4H10+OH<=>pC4H9+H2O      3.3000E+07      1.800      954.00
C4H10+OH<=>sC4H9+H2O      5.4000E+06      2.000      -596.00
C4H10+O2<=>pC4H9+HO2      4.0000E+13      0.000      50930.00
C4H10+O2<=>sC4H9+HO2      8.0000E+13      0.000      47590.00
C4H10+HO2<=>pC4H9+H2O2      4.7600E+04      2.550      16490.00
C4H10+HO2<=>sC4H9+H2O2      1.9000E+04      2.600      13910.00
C4H10+CH3<=>pC4H9+CH4      9.0300E-01      3.650      7153.00
C4H10+CH3<=>sC4H9+CH4      3.0000E+00      3.460      5480.00
iC3H7+CH3(+M)<=>iC4H10(+M)      1.4000E+15      -0.680      0.00
LOW / 4.1600E+61 -13.330      3903.40/
TROE/ 0.9310      60000.00      1265.30      5469.80 /
AR/0.70/ H2/2.00/ H2O/6.00/ CH4/2.00/ CO/1.50/ CO2/2.00/
C2H6/3.00/
iC4H10+H<=>iC4H9+H2      1.8000E+06      2.540      6760.00
iC4H10+H<=>tC4H9+H2      6.0000E+05      2.400      2580.00
iC4H10+O<=>iC4H9+OH      4.3000E+05      2.500      3640.00
iC4H10+O<=>tC4H9+OH      1.5700E+05      2.500      1110.00
iC4H10+OH<=>iC4H9+H2O      2.3000E+08      1.530      775.00
iC4H10+OH<=>tC4H9+H2O      5.7300E+10      0.510      64.00

```

iC4H10+HO2<=>iC4H9+H2O2	3.0000E+04	2.550	15500.00
iC4H10+HO2<=>tC4H9+H2O2	3.6000E+03	2.550	10500.00
iC4H10+O2<=>iC4H9+HO2	4.0000E+13	0.000	50900.00
iC4H10+O2<=>tC4H9+HO2	4.0000E+13	0.000	44000.00
iC4H10+CH3<=>iC4H9+CH4	1.3600E+00	3.650	7150.00
iC4H10+CH3<=>tC4H9+CH4	9.0000E-01	3.460	4600.00
C6H2+H<=>C6H3	1.1000E+30	-4.920	10800.00
C6H3+H<=>C4H2+C2H2	2.8000E+23	-2.550	10780.00
C6H3+H<=>l-C6H4	3.4000E+43	-9.010	12120.00
C6H3+H<=>C6H2+H2	3.0000E+13	0.000	0.00
C6H3+OH<=>C6H2+H2O	4.0000E+12	0.000	0.00
l-C6H4+H<=>C6H5	1.7000E+78	-19.720	31400.00
l-C6H4+H<=>o-C6H4+H	1.4000E+54	-11.700	34500.00
l-C6H4+H<=>C6H3+H2	1.3300E+06	2.530	9240.00
l-C6H4+OH<=>C6H3+H2O	3.1000E+06	2.000	430.00
C4H2+C2H2<=>o-C6H4	5.0000E+78	-19.310	67920.00
o-C6H4+OH<=>CO+C5H5	1.0000E+13	0.000	0.00
C6H5+CH3<=>C6H5CH3	1.3800E+13	0.000	46.00
C6H5CH3+O2<=>C6H5CH2+HO2	3.0000E+14	0.000	42992.00
C6H5CH3+OH<=>C6H5CH2+H2O	1.6200E+13	0.000	2770.00
C6H5CH3+OH<=>C6H4CH3+H2O	1.3330E+08	1.420	1450.00
C6H5CH3+H<=>C6H5CH2+H2	1.2590E+14	0.000	8359.00
C6H5CH3+H<=>C6H6+CH3	1.9300E+06	2.170	4163.00
C6H5CH3+O<=>OC6H4CH3+H	2.6000E+13	0.000	3795.00
C6H5CH3+CH3<=>C6H5CH2+CH4	3.1600E+11	0.000	9500.00
C6H5CH3+C6H5<=>C6H5CH2+C6H6	2.1030E+12	0.000	4400.00
C6H5CH3+HO2<=>C6H5CH2+H2O2	3.9750E+11	0.000	14069.00
C6H5CH3+HO2<=>C6H4CH3+H2O2	5.4200E+12	0.000	28810.00
C6H5CH2+H (+M) <=>C6H5CH3 (+M)	1.0000E+14	0.000	0.00
LOW / 1.1000+103 -24.630 14590.00/			
TROE/ 0.4310 383.00 152.00 4730.00 /			
H2/2.00/ H2O/6.00/ CH4/2.00/ CO/1.50/ CO2/2.00/ C2H6/3.00/			
C6H5CH2+H<=>C6H5+CH3	1.5000E+66	-13.940	64580.00
C6H5CH2+O<=>C6H5CHO+H	4.0000E+14	0.000	0.00
C6H5CH2+OH<=>C6H5CH2OH	2.0000E+13	0.000	0.00
C6H5CH2+HO2<=>C6H5CHO+H+OH	5.0000E+12	0.000	0.00
C6H5CH2+C6H5OH<=>C6H5CH3+C6H5O	1.0500E+11	0.000	9500.00
C6H5CH2+HOC6H4CH3<=>C6H5CH3+OC6H4CH3	1.0500E+11	0.000	9500.00
C6H5CH2OH+OH<=>C6H5CHO+H2O+H	5.0000E+12	0.000	0.00
C6H5CH2OH+H<=>C6H5CHO+H2+H	8.0000E+13	0.000	8235.00
C6H5CH2OH+H<=>C6H6+CH2OH	1.2000E+13	0.000	5148.00
C6H5CH2OH+C6H5<=>C6H5CHO+C6H6+H	1.4000E+12	0.000	4400.00
C6H5+HCO<=>C6H5CHO	1.0000E+13	0.000	0.00
C6H5CHO<=>C6H5CO+H	3.9800E+15	0.000	86900.00
C6H5CHO+O2<=>C6H5CO+HO2	1.0200E+13	0.000	38950.00
C6H5CHO+OH<=>C6H5CO+H2O	2.3500E+10	0.730	-1110.00
C6H5CHO+H<=>C6H5CO+H2	4.1000E+09	1.160	2400.00
C6H5CHO+H<=>C6H6+HCO	1.9300E+06	2.170	4163.00
C6H5CHO+O<=>C6H5CO+OH	5.8000E+12	0.000	1800.00
C6H5CHO+C6H5CH2<=>C6H5CO+C6H5CH3	2.0000E-06	5.600	2460.00
C6H5CHO+CH3<=>C6H5CO+CH4	2.0000E-06	5.600	2460.00
C6H5CHO+C6H5<=>C6H5CO+C6H6	2.1030E+12	0.000	4400.00
C6H5CO+H2O2<=>C6H5CHO+HO2	1.8000E+11	0.000	8226.00
OC6H4CH3+H (+M) <=>HOC6H4CH3 (+M)	1.0000E+14	0.000	0.00

```

LOW / 4.0000E+93 -21.840 13880.00/
TROE/ 0.0430 304.20 60000.00 5896.40 /
H2/2.00/ H2O/6.00/ CH4/2.00/ CO/1.50/ CO2/2.00/
OC6H4CH3+H<=>C6H5O+CH3 1.9300E+06 2.170 4163.00
OC6H4CH3+O<=>C6H4O2+CH3 8.0000E+13 0.000 0.00
HOC6H4CH3+OH<=>OC6H4CH3+H2O 6.0000E+12 0.000 0.00
HOC6H4CH3+H<=>OC6H4CH3+H2 1.1500E+14 0.000 12400.00
HOC6H4CH3+H<=>C6H5CH3+OH 2.2100E+13 0.000 7910.00
HOC6H4CH3+H<=>C6H5OH+CH3 1.2000E+13 0.000 5148.00
C6H5CO<=>C6H5+CO 5.2700E+14 0.000 29013.00
C6H5+H (+M) <=>C6H6 (+M) 1.0000E+14 0.000 0.00
LOW / 6.6000E+75 -16.300 7000.00/
TROE/ 1.0000 0.10 584.90 6113.00 /
H2/2.00/ H2O/6.00/ CH4/2.00/ CO/1.50/ CO2/2.00/
C6H6+OH<=>C6H5+H2O 3.9850E+05 2.286 1058.00
C6H6+OH<=>C6H5OH+H 1.3000E+13 0.000 10600.00
C6H6+O<=>C6H5O+H 1.3900E+13 0.000 4910.00
C6H6+O<=>C5H5+HCO 1.3900E+13 0.000 4530.00
C6H5+H2<=>C6H6+H 5.7070E+04 2.430 6273.00
C6H5 (+M) <=>o-C6H4+H (+M) 4.3000E+12 0.616 77313.00
LOW / 1.0000E+84 -18.866 90064.00/
TROE/ 0.9020 696.00 358.00 3856.00 /
H2/2.00/ H2O/6.00/ CH4/2.00/ CO/1.50/ CO2/2.00/
C6H5+H<=>o-C6H4+H2 2.0000E+11 1.100 24500.00
C6H5+O2<=>C6H5O+O 2.6000E+13 0.000 6120.00
C6H5+O2<=>C6H4O2+H 3.0000E+13 0.000 8980.00
C6H5+O<=>C5H5+CO 1.0000E+14 0.000 0.00
C6H5+OH<=>C6H5O+H 3.0000E+13 0.000 0.00
C6H5+HO2<=>C6H5O+OH 3.0000E+13 0.000 0.00
C6H5+HO2<=>C6H6+O2 1.0000E+12 0.000 0.00
C6H5+CH4<=>C6H6+CH3 3.8900E-03 4.570 5256.00
C6H5+C2H6<=>C6H6+C2H5 2.1000E+11 0.000 4443.00
C6H5+CH2O<=>C6H6+HCO 8.5500E+04 2.190 38.00
C6H4O2<=>C5H4O+CO 7.4000E+11 0.000 59000.00
C6H4O2+H<=>CO+C5H5O (1,3) 4.3000E+09 1.450 3900.00
C6H4O2+O<=>2CO+C2H2+CH2CO 3.0000E+13 0.000 5000.00
C6H5O+H<=>C5H5+HCO 1.0000E+13 0.000 12000.00
C6H5O+H<=>C5H6+CO 5.0000E+13 0.000 0.00
C6H5O<=>CO+C5H5 3.7600E+54 -12.060 72800.00
C6H5O+O<=>C6H4O2+H 2.6000E+10 0.470 795.00
C6H5OH<=>C5H6+CO 1.0000E+12 0.000 60808.00
C6H5OH+OH<=>C6H5O+H2O 2.9500E+06 2.000 -1312.00
C6H5OH+H<=>C6H5O+H2 1.1500E+14 0.000 12398.00
C6H5OH+O<=>C6H5O+OH 2.8100E+13 0.000 7352.00
C6H5OH+C2H3<=>C6H5O+C2H4 6.0000E+12 0.000 0.00
C6H5OH+nC4H5<=>C6H5O+C4H6 6.0000E+12 0.000 0.00
C6H5OH+C6H5<=>C6H5O+C6H6 4.9100E+12 0.000 4400.00
C5H6+H<=>C2H2+aC3H5 7.7400E+36 -6.180 32890.00
C5H6+H<=>1C5H7 8.2700+126 -32.300 82348.00
C5H6+H<=>C5H5+H2 3.0300E+08 1.710 5590.00
C5H6+O<=>C5H5+OH 4.7700E+04 2.710 1106.00
C5H6+O<=>C5H5O (1,3) +H 8.9100E+12 -0.150 590.00
DUPLICATE
C5H6+O<=>C5H5O (1,3) +H 5.6000E+12 -0.060 200.00

```

```

DUPLICATE
C5H6+O<=>nC4H5+CO+H      8.7000E+51  -11.090  33240.00
C5H6+OH<=>C5H5+H2O        3.0800E+06   2.000    0.00
C5H6+HO2<=>C5H5+H2O2      1.1000E+04   2.600  12900.00
C5H6+O2<=>C5H5+HO2        4.0000E+13   0.000  37150.00
C5H6+HCO<=>C5H5+CH2O      1.0800E+08   1.900  16000.00
C5H6+CH3<=>C5H5+CH4       1.8000E-01   4.000    0.00
C5H5+H (+M) <=>C5H6 (+M)   1.0000E+14   0.000    0.00
      LOW / 4.4000E+80  -18.280  12994.00/
      TROE/ 0.0680    400.70    4135.80    5501.90 /
H2/2.00/ H2O/6.00/ CH4/2.00/ CO/1.50/ CO2/2.00/
C5H5+O2<=>C5H5O (2,4) +O   7.7800E+15   -0.730  48740.00
C5H5+O<=>C5H5O (2,4)      1.1200E-12   5.870 -17310.00
C5H5+O<=>C5H4O+H          5.8100E+13   -0.020   20.00
C5H5+O<=>nC4H5+CO         3.2000E+13   -0.170   440.00
C5H5+OH<=>C5H4OH+H        3.5100E+57  -12.180  48350.00
C5H5+OH<=>C5H5O (2,4) +H   1.3600E+51  -10.460  57100.00
C5H5+HO2<=>C5H5O (2,4) +OH 6.2700E+29   -4.690  11650.00
C5H5+OH<=>C5H5OH          6.4900E+14   -0.850  -2730.00
DUPLICATE
C5H5+OH<=>C5H5OH          1.1500E+43   -8.760  18730.00
DUPLICATE
DUPLICATE
C5H5+OH<=>C5H5OH          1.0600E+59  -13.080  33450.00
DUPLICATE
C5H5+O2<=>C5H4O+OH        1.8000E+12   0.080  18000.00
C5H5OH+H<=>C5H5O (2,4) +H2 1.1500E+14   0.000  15400.00
C5H5OH+H<=>C5H4OH+H2       1.2000E+05   2.500  1492.00
C5H5OH+OH<=>C5H5O (2,4) +H2O 6.0000E+12   0.000    0.00
C5H5OH+OH<=>C5H4OH+H2O     3.0800E+06   2.000    0.00
C5H5O (2,4) +H<=>C5H5OH    1.0000E+14   0.000    0.00
C5H5O (2,4) <=>C5H4O+H     2.0000E+13   0.000  30000.00
C5H5O (2,4) +O2<=>C5H4O+HO2 1.0000E+11   0.000    0.00
C5H4O+H<=>C5H5O (1,3)     2.0000E+13   0.000  2000.00
C5H5O (1,3) <=>c-C4H5+CO   1.0000E+12   0.000  36000.00
C5H5O (1,3) +O2<=>C5H4O+HO2 1.0000E+11   0.000    0.00
C5H4OH<=>C5H4O+H         2.1000E+13   0.000  48000.00
C5H4O<=>2C2H2+CO          6.2000E+41  -7.870  98700.00
C5H4O+H<=>CO+c-C4H5       4.3000E+09   1.450  3900.00
C5H4O+O<=>CO+HCO+C3H3     6.2000E+08   1.450  -858.00
c-C4H5+H<=>C4H6           1.0000E+13   0.000    0.00
c-C4H5+H<=>C2H4+C2H2       1.0000E+13   0.000    0.00
c-C4H5+O<=>CH2CHO+C2H2     1.0000E+14   0.000    0.00
c-C4H5+O2<=>CH2CHO+CH2CO   4.8000E+11   0.000  19000.00
c-C4H5<=>C4H4+H           3.0000E+12   0.000  52000.00
c-C4H5<=>C2H3+C2H2         2.0000E+12   0.000  58000.00
aC3H5+C2H3<=>1C5H7+H      1.0000E+13   0.000    0.00
1C5H7+O<=>C2H3CHO+C2H3     5.0000E+13   0.000    0.00
1C5H7+OH<=>C2H3CHO+C2H4    2.0000E+13   0.000    0.00
PXC5H9+H (+M) <=>C5H10 (+M) 3.6000E+13   0.000    0.00
      LOW / 3.0100E+48  -9.320   5833.60/
      TROE/ 0.4980    1314.00    1314.00    50000.00 /
AR/0.70/ H2/2.00/ H2O/6.00/ CH4/2.00/ CO/1.50/ CO2/2.00/
C2H6/3.00/

```

PXC5H9+H<=>CH3+C4H7	2.0000E+21	-2.000	11000.00
PXC5H9+HO2<=>CH2O+OH+C4H7	2.4000E+13	0.000	0.00
PXC5H9+HCO<=>C5H10+CO	6.0000E+13	0.000	0.00
PXC5H9<=>C2H4+aC3H5	1.0400E+12	-0.370	25124.00
cC5H9<=>PXC5H9	2.1500E+12	-0.300	33721.00
cC5H9<=>cC5H8+H	6.5300E+11	-0.550	33140.00
SXC5H9<=>C5H8-13+H	3.5000E+08	-1.350	32487.00
SXC5H9<=>C3H6+C2H3	1.3900E+12	-0.580	37797.00
SXC5H9<=>C5H8-14+H	5.6900E-09	-1.170	37097.00
SXC5H9<=>CH2C4H7	5.5200E+08	-1.420	14609.00
CH2C4H7<=>C4H6+CH3	4.6000E+11	-0.410	31254.00
SAXC5H9<=>CH3+C4H6	5.7000E+12	-0.100	35891.00
C5H10<=>C2H5+aC3H5	7.3052E+22	-1.940	75470.00
C5H10<=>C3H6+C2H4	1.6200E+06	1.810	53454.00
C5H10+H<=>C2H4+nC3H7	8.0000E+21	-2.390	11180.00
C5H10+H<=>C3H6+C2H5	1.6000E+22	-2.390	11180.00
C5H10+H<=>PXC5H9+H2	6.5000E+05	2.540	6756.00
C5H10+H<=>SXC5H9+H2	1.3000E+06	2.400	4471.00
C5H10+H<=>SAXC5H9+H2	5.4000E+04	2.500	-1900.00
C5H10+O<=>pC4H9+HCO	3.3000E+08	1.450	-402.00
C5H10+O<=>PXC5H9+OH	1.5000E+13	0.000	5760.00
DUPLICATE			
C5H10+O<=>PXC5H9+OH	2.6000E+13	0.000	4470.00
DUPLICATE			
C5H10+OH<=>PXC5H9+H2O	7.0000E+02	2.660	527.00
C5H10+O2<=>PXC5H9+HO2	2.0000E+13	0.000	50930.00
C5H10+HO2<=>PXC5H9+H2O2	1.0000E+12	0.000	14340.00
C5H10+CH3<=>PXC5H9+CH4	4.5000E-01	3.650	7153.00
PXC5H11 (+M) <=>C2H4+nC3H7 (+M)	1.0660E+13	0.000	28366.40
LOW / 7.5686E-35 15.411 -600.00/			
TROE/ -5.9100 333.00 28.00 50000.00 /			
AR/0.70/ H2/2.00/ H2O/6.00/ CH4/2.00/ CO/1.50/ CO2/2.00/			
C2H6/3.00/			
SXC5H11 (+M) <=>C3H6+C2H5 (+M)	8.0000E+12	0.000	27392.80
LOW / 3.7000E-33 14.910 -600.00/			
TROE/ -6.5300 333.00 28.00 50000.00 /			
AR/0.70/ H2/2.00/ H2O/6.00/ CH4/2.00/ CO/1.50/ CO2/2.00/			
C2H6/3.00/			
S2XC5H11 (+M) <=>C4H81+CH3 (+M)	1.8000E+13	0.000	29348.00
LOW / 4.0000E-39 16.782 -600.40/			
TROE/ -7.0300 314.00 28.00 50000.00 /			
AR/0.70/ H2/2.00/ H2O/6.00/ CH4/2.00/ CO/1.50/ CO2/2.00/			
C2H6/3.00/			
SXC5H11+H (+M) <=>NC5H12 (+M)	2.4000E+13	0.000	0.00
LOW / 1.7000E+58 -12.080 11263.70/			
TROE/ 0.6490 1213.10 1213.10 13369.70 /			
AR/0.70/ H2/2.00/ H2O/6.00/ CH4/2.00/ CO/1.50/ CO2/2.00/			
C2H6/3.00/			
SXC5H11+H<=>nC3H7+C2H5	1.4000E+28	-3.940	15916.00
SXC5H11+H<=>C5H10+H2	3.2000E+12	0.000	0.00
SXC5H11+O<=>CH3CHO+nC3H7	9.6000E+13	0.000	0.00
SXC5H11+OH<=>C5H10+H2O	2.4000E+13	0.000	0.00
SXC5H11+O2<=>C5H10+HO2	1.3000E+11	0.000	0.00
SXC5H11+HO2<=>CH3CHO+nC3H7+OH	2.4000E+13	0.000	0.00


```

SXC5H11+HCO<=>NC5H12+CO          1.2000E+14    0.000    0.00
SXC5H11+CH3<=>CH4+C5H10            2.2000E+14   -0.680    0.00
PXC5H11+H(+M)<=>NC5H12(+M)          3.6000E+13    0.000    0.00
    LOW / 3.0100E+48   -9.320   5833.60/
    TROE/ 0.4980    1314.00    1314.00    50000.00 /
AR/0.70/ H2/2.00/ H2O/6.00/ CH4/2.00/ CO/1.50/ CO2/2.00/
C2H6/3.00/
PXC5H11+H<=>nC3H7+C2H5              3.7000E+24   -2.920   12505.00
PXC5H11+H<=>C5H10+H2                1.8000E+12    0.000    0.00
PXC5H11+O<=>pC4H9+CH2O              9.6000E+13    0.000    0.00
PXC5H11+OH<=>C5H10+H2O              2.4000E+13    0.000    0.00
PXC5H11+O2<=>C5H10+HO2              9.0000E+10    0.000    0.00
PXC5H11+HO2<=>pC4H9+OH+CH2O         2.4000E+13    0.000    0.00
PXC5H11+HCO<=>NC5H12+CO            9.0000E+13    0.000    0.00
PXC5H11+CH3<=>C5H10+CH4            1.1000E+13    0.000    0.00
pC4H9+CH3<=>NC5H12                  1.9300E+14   -0.320    0.00
nC3H7+C2H5<=>NC5H12                 1.8800E+14   -0.500    0.00
NC5H12+H<=>PXC5H11+H2               1.3000E+06    2.540   6756.00
NC5H12+H<=>SXC5H11+H2               2.6000E+06    2.400   4471.00
NC5H12+H<=>S2XC5H11+H2              1.3000E+06    2.400   4471.00
NC5H12+O<=>PXC5H11+OH               4.4000E+06    2.400   5504.00
NC5H12+O<=>SXC5H11+OH               6.2000E+05    2.500   2225.00
NC5H12+O<=>S2XC5H11+OH              3.1000E+05    2.500   2225.00
NC5H12+OH<=>PXC5H11+H2O             2.7300E+07    1.810    868.30
NC5H12+OH<=>SXC5H11+H2O             1.4100E+10    0.940    504.70
NC5H12+OH<=>S2XC5H11+H2O            5.7200E+06    1.810  -1015.40
NC5H12+O2<=>PXC5H11+HO2             4.0000E+13    0.000   50930.00
NC5H12+O2<=>SXC5H11+HO2            8.0000E+13    0.000   47590.00
NC5H12+O2<=>S2XC5H11+HO2           4.0000E+13    0.000   47590.00
NC5H12+HO2<=>PXC5H11+H2O2           4.7600E+04    2.550   16490.00
NC5H12+HO2<=>SXC5H11+H2O2           1.9000E+04    2.600   13910.00
NC5H12+HO2<=>S2XC5H11+H2O2          9.5000E+03    2.600   13910.00
NC5H12+CH3<=>PXC5H11+CH4            9.0300E-01    3.650    7153.00
NC5H12+CH3<=>SXC5H11+CH4            3.0000E+00    3.460    5480.00
NC5H12+CH3<=>S2XC5H11+CH4           1.5000E+00    3.460    5480.00
PXC6H11+H(+M)<=>C6H12(+M)           3.6000E+13    0.000    0.00
    LOW / 3.0100E+48   -9.320   5833.60/
    TROE/ 0.4980    1314.00    1314.00    50000.00 /
AR/0.70/ H2/2.00/ H2O/6.00/ CH4/2.00/ CO/1.50/ CO2/2.00/
C2H6/3.00/
PXC6H11+H<=>CH3+PXC5H9              2.0000E+21   -2.000   11000.00
PXC6H11+HO2<=>CH2O+OH+PXC5H9        2.4000E+13    0.000    0.00
PXC6H11+HCO<=>C6H12+CO              6.0000E+13    0.000    0.00
cC6H11<=>cC6H10+H                    3.3400E+11    0.690   33948.00
cC5H9CH2<=>CH2C5H8+H                7.7600E+08    1.110   34616.00
SAXC6H11<=>C4H6+C2H5                 3.3900E+11    0.660   32263.00
PXC6H11<=>C4H7+C2H4                  3.9800E+12    0.120   27572.00
SAXC6H11-3<=>C5H8-13+CH3            4.9000E+13   -0.210   33346.00
SXC6H11<=>C3H6+aC3H5                 4.5700E+12    0.130   24386.00
m1C5H81<=>aC3H5+C3H6                 5.3700E+12    0.120   23947.00
cC6H11<=>PXC6H11                     6.0300E+12    0.070   27983.00
PXC6H11<=>cC5H9CH2                   9.5500E+08    0.360   10704.00
CH3cC5H83<=>SXC6H11                 7.5900E+12    0.150   32940.00
CH3cC5H83<=>m1C5H81                  3.5500E+12    0.150   32404.00

```

```

PXC6H11<=>SAXC6H11          1.5500E+02    2.830    15566.00
cC5H9CH2<=>CH3cC5H83        6.6100E+01    2.850    21082.00
PXC6H11<=>SAXC6H11-3        9.3300E+03    2.380    22141.00
S2XC6H11<=>C6H10-13+H       3.0000E+13    0.000    38000.00
C6H12<=>aC3H5+nC3H7         1.0315E+23   -2.030    74958.00
C6H12<=>2C3H6                7.0800E+06    1.650    53752.00
C6H12+H<=>C2H4+pC4H9        8.0000E+21   -2.390    11180.00
C6H12+H<=>C3H6+nC3H7        1.6000E+22   -2.390    11180.00
C6H12+H<=>PXC6H11+H2        6.5000E+05    2.540     6756.00
C6H12+H<=>SXC6H11+H2        1.3000E+06    2.400     4471.00
C6H12+H<=>S2XC6H11+H2       1.4781E+06    2.400     4471.00
C6H12+H<=>SAXC6H11+H2       5.4000E+04    2.500    -1900.00
C6H12+O<=>PXC5H11+HCO       3.3000E+08    1.450     -402.00
C6H12+O<=>PXC6H11+OH        1.5000E+13    0.000     5760.00
    DUPLICATE
C6H12+O<=>PXC6H11+OH        2.6000E+13    0.000     4470.00
    DUPLICATE
C6H12+OH<=>PXC6H11+H2O       7.0000E+02    2.660      527.00
C6H12+O2<=>PXC6H11+HO2       2.0000E+13    0.000    50930.00
C6H12+HO2<=>PXC6H11+H2O2     1.0000E+12    0.000    14340.00
C6H12+CH3<=>PXC6H11+CH4      4.5000E-01    3.650     7153.00
PXC6H13 (+M) <=>C2H4+pC4H9 (+M) 6.0486E+11    0.300    27273.60
    LOW / 4.2103E-35    15.411   -600.00/
    TROE/ -5.9100      333.00    28.00    50000.00 /
AR/0.70/ H2/2.00/ H2O/6.00/ CH4/2.00/ CO/1.50/ CO2/2.00/
C2H6/3.00/
SXC6H13 (+M) <=>C3H6+nC3H7 (+M) 4.4700E+11    0.570    28044.50
    LOW / 3.7000E-33    14.910   -600.00/
    TROE/ -6.5300      333.00    28.00    50000.00 /
AR/0.70/ H2/2.00/ H2O/6.00/ CH4/2.00/ CO/1.50/ CO2/2.00/
C2H6/3.00/
S2XC6H13 (+M) <=>C2H5+C4H81 (+M) 3.5500E+12    0.290    28296.90
    LOW / 4.5000E-26    13.090   -600.50/
    TROE/ -0.7400      308.00    28.00    50000.00 /
AR/0.70/ H2/2.00/ H2O/6.00/ CH4/2.00/ CO/1.50/ CO2/2.00/
C2H6/3.00/
S2XC6H13 (+M) <=>C5H10+CH3 (+M) 8.1300E+10    0.780    29648.00
    LOW / 4.0000E-39    16.782   -600.40/
    TROE/ -7.0300      314.00    28.00    50000.00 /
AR/0.70/ H2/2.00/ H2O/6.00/ CH4/2.00/ CO/1.50/ CO2/2.00/
C2H6/3.00/
PXC6H13+H<=>pC4H9+C2H5       3.7000E+24   -2.920    12505.00
PXC6H13+H<=>C6H12+H2        1.8000E+12    0.000      0.00
PXC6H13+O<=>PXC5H11+CH2O     9.6000E+13    0.000      0.00
PXC6H13+OH<=>C6H12+H2O       2.4000E+13    0.000      0.00
PXC6H13+O2<=>C6H12+HO2       9.0000E+10    0.000      0.00
PXC6H13+HO2<=>PXC5H11+OH+CH2O 2.4000E+13    0.000      0.00
PXC6H13+HCO<=>NC6H14+CO      9.0000E+13    0.000      0.00
PXC6H13+CH3<=>C6H12+CH4      1.1000E+13    0.000      0.00
SXC6H13+H (+M) <=>NC6H14 (+M) 2.4000E+13    0.000      0.00
    LOW / 1.7000E+58   -12.080  11263.70/
    TROE/ 0.6490      1213.10    1213.10    13369.70 /
AR/0.70/ H2/2.00/ H2O/6.00/ CH4/2.00/ CO/1.50/ CO2/2.00/
C2H6/3.00/

```

SXC6H13+H<=>pC4H9+C2H5	1.4000E+28	-3.940	15916.00
SXC6H13+H<=>C6H12+H2	3.2000E+12	0.000	0.00
SXC6H13+O<=>CH3CHO+pC4H9	9.6000E+13	0.000	0.00
SXC6H13+OH<=>C6H12+H2O	2.4000E+13	0.000	0.00
SXC6H13+O2<=>C6H12+HO2	1.3000E+11	0.000	0.00
SXC6H13+HO2<=>CH3CHO+pC4H9+OH	2.4000E+13	0.000	0.00
SXC6H13+HCO<=>NC6H14+CO	1.2000E+14	0.000	0.00
SXC6H13+CH3<=>CH4+C6H12	2.2000E+14	-0.680	0.00
S2XC6H13+O2<=>C6H12+HO2	1.3000E+11	0.000	0.00
PXC5H11+CH3<=>NC6H14	1.9300E+14	-0.320	0.00
pC4H9+C2H5<=>NC6H14	1.8800E+14	-0.500	0.00
2nC3H7<=>NC6H14	1.8800E+14	-0.500	0.00
NC6H14+H<=>PXC6H13+H2	1.3000E+06	2.540	6756.00
NC6H14+H<=>SXC6H13+H2	2.6000E+06	2.400	4471.00
NC6H14+H<=>S2XC6H13+H2	2.6000E+06	2.400	4471.00
NC6H14+O<=>PXC6H13+OH	3.7000E+06	2.400	5504.00
NC6H14+O<=>SXC6H13+OH	3.5000E+05	2.600	2106.00
NC6H14+O<=>S2XC6H13+OH	3.5000E+05	2.600	2106.00
NC6H14+OH<=>PXC6H13+H2O	2.7300E+07	1.810	868.30
NC6H14+OH<=>SXC6H13+H2O	1.4100E+10	0.940	504.70
NC6H14+OH<=>S2XC6H13+H2O	1.1400E+07	1.810	-1015.40
NC6H14+O2<=>PXC6H13+HO2	4.0000E+13	0.000	50930.00
NC6H14+O2<=>SXC6H13+HO2	8.0000E+13	0.000	47590.00
NC6H14+O2<=>S2XC6H13+HO2	8.0000E+13	0.000	47590.00
NC6H14+HO2<=>PXC6H13+H2O2	4.7600E+04	2.550	16490.00
NC6H14+HO2<=>SXC6H13+H2O2	1.9000E+04	2.600	13910.00
NC6H14+HO2<=>S2XC6H13+H2O2	1.9000E+04	2.600	13910.00
NC6H14+CH3<=>PXC6H13+CH4	9.0300E-01	3.650	7153.00
NC6H14+CH3<=>SXC6H13+CH4	3.0000E+00	3.460	5480.00
NC6H14+CH3<=>S2XC6H13+CH4	3.0000E+00	3.460	5480.00
PXC7H13+H (+M) <=>C7H14 (+M)	3.6000E+13	0.000	0.00
LOW / 3.0100E+48 -9.320 5833.60/			
TROE/ 0.4980 1314.00 1314.00 50000.00 /			
AR/0.70/ H2/2.00/ H2O/6.00/ CH4/2.00/ CO/1.50/ CO2/2.00/			
C2H6/3.00/			
PXC7H13+H<=>CH3+PXC6H11	2.0000E+21	-2.000	11000.00
PXC7H13+HO2<=>CH2O+OH+PXC6H11	2.4000E+13	0.000	0.00
PXC7H13+HCO<=>C7H14+CO	6.0000E+13	0.000	0.00
C2H4+PXC5H9<=>PXC7H13	3.0000E+11	0.000	7300.00
C7H14<=>pC4H9+aC3H5	1.0700E+23	-2.030	74958.00
C7H14<=>C4H81+C3H6	7.0800E+06	1.650	53752.00
C7H14+H<=>C2H4+PXC5H11	8.0000E+21	-2.390	11180.00
C7H14+H<=>C3H6+pC4H9	1.6000E+22	-2.390	11180.00
C7H14+H<=>PXC7H13+H2	6.5000E+05	2.540	6756.00
C7H14+O<=>PXC6H13+HCO	3.3000E+08	1.450	-402.00
C7H14+O<=>PXC7H13+OH	1.5000E+13	0.000	5760.00
DUPLICATE			
C7H14+O<=>PXC7H13+OH	2.6000E+13	0.000	4470.00
DUPLICATE			
C7H14+OH<=>PXC7H13+H2O	7.0000E+02	2.660	527.00
C7H14+O2<=>PXC7H13+HO2	2.0000E+13	0.000	50930.00
C7H14+HO2<=>PXC7H13+H2O2	1.0000E+12	0.000	14340.00
C7H14+CH3<=>PXC7H13+CH4	4.5000E-01	3.650	7153.00
PXC7H15 (+M) <=>C2H4+PXC5H11 (+M)	7.9400E+11	0.330	27210.00

```

LOW / 2.8000E-44 18.729 -602.50/
TROE/-14.6600 219.00 28.00 50000.00 /
AR/0.70/ H2/2.00/ H2O/6.00/ CH4/2.00/ CO/1.50/ CO2/2.00/
C2H6/3.00/
SXC7H15 (+M) <=> pC4H9+C3H6 (+M) 5.0100E+11 0.560 28092.20
LOW / 8.9000E-39 16.934 -602.50/
TROE/-25.2700 223.00 28.00 50000.00 /
AR/0.70/ H2/2.00/ H2O/6.00/ CH4/2.00/ CO/1.50/ CO2/2.00/
C2H6/3.00/
S2XC7H15 (+M) <=> nC3H7+C4H81 (+M) 2.9235E+12 0.310 28257.10
LOW / 1.9820E-38 16.814 -602.40/
TROE/-20.9600 221.00 28.00 50000.00 /
AR/0.70/ H2/2.00/ H2O/6.00/ CH4/2.00/ CO/1.50/ CO2/2.00/
C2H6/3.00/
S2XC7H15 (+M) <=> C6H12+CH3 (+M) 1.1198E+11 0.750 29401.60
LOW / 1.0791E-42 18.004 -602.40/
TROE/-20.9400 217.00 28.00 50000.00 /
AR/0.70/ H2/2.00/ H2O/6.00/ CH4/2.00/ CO/1.50/ CO2/2.00/
C2H6/3.00/
S3XC7H15 (+M) <=> C2H5+C5H10 (+M) 5.8900E+12 0.310 28257.10
LOW / 2.1000E-38 16.897 -602.50/
TROE/-27.5400 224.00 28.00 50000.00 /
AR/0.70/ H2/2.00/ H2O/6.00/ CH4/2.00/ CO/1.50/ CO2/2.00/
C2H6/3.00/
PXC7H15+H (+M) <=> NC7H16 (+M) 3.6000E+13 0.000 0.00
LOW / 3.0100E+48 -9.320 5833.60/
TROE/ 0.4980 1314.00 1314.00 50000.00 /
AR/0.70/ H2/2.00/ H2O/6.00/ CH4/2.00/ CO/1.50/ CO2/2.00/
C2H6/3.00/
PXC7H15+H<=>PXC5H11+C2H5 3.7000E+24 -2.920 12505.00
PXC7H15+H<=>C7H14+H2 1.8000E+12 0.000 0.00
PXC7H15+O<=>PXC6H13+CH2O 9.6000E+13 0.000 0.00
PXC7H15+OH<=>C7H14+H2O 2.4000E+13 0.000 0.00
PXC7H15+O2<=>C7H14+HO2 9.0000E+10 0.000 0.00
PXC7H15+HO2<=>PXC6H13+OH+CH2O 2.4000E+13 0.000 0.00
PXC7H15+HCO<=>NC7H16+CO 9.0000E+13 0.000 0.00
PXC7H15+CH3<=>C7H14+CH4 1.1000E+13 0.000 0.00
SXC7H15+H<=>PXC5H11+C2H5 1.4000E+28 -3.940 15916.00
SXC7H15+H<=>C7H14+H2 3.2000E+12 0.000 0.00
SXC7H15+O<=>CH3CHO+PXC5H11 9.6000E+13 0.000 0.00
SXC7H15+OH<=>C7H14+H2O 2.4000E+13 0.000 0.00
SXC7H15+O2<=>C7H14+HO2 1.3000E+11 0.000 0.00
SXC7H15+HO2<=>CH3CHO+PXC5H11+OH 2.4000E+13 0.000 0.00
SXC7H15+HCO<=>NC7H16+CO 1.2000E+14 0.000 0.00
SXC7H15+CH3<=>CH4+C7H14 2.2000E+14 -0.680 0.00
S2XC7H15+O2<=>C7H14+HO2 1.3000E+11 0.000 0.00
S3XC7H15+O2<=>C7H14+HO2 1.3000E+11 0.000 0.00
PXC6H13+CH3<=>NC7H16 1.9300E+14 -0.320 0.00
PXC5H11+C2H5<=>NC7H16 1.8800E+14 -0.500 0.00
pC4H9+nC3H7<=>NC7H16 1.8800E+14 -0.500 0.00
NC7H16+H<=>PXC7H15+H2 1.3000E+06 2.540 6756.00
NC7H16+H<=>SXC7H15+H2 2.6000E+06 2.400 4471.00
NC7H16+H<=>S2XC7H15+H2 2.6000E+06 2.400 4471.00
NC7H16+H<=>S3XC7H15+H2 1.3000E+06 2.400 4471.00

```

NC7H16+O<=>PXC7H15+OH	2.9000E+06	2.400	5504.00
NC7H16+O<=>SXC7H15+OH	2.8000E+05	2.600	1908.00
NC7H16+O<=>S2XC7H15+OH	2.8000E+05	2.600	1908.00
NC7H16+O<=>S3XC7H15+OH	1.4000E+05	2.600	1908.00
NC7H16+OH<=>PXC7H15+H2O	2.7300E+07	1.810	868.30
NC7H16+OH<=>SXC7H15+H2O	1.4100E+10	0.940	504.70
NC7H16+OH<=>S2XC7H15+H2O	1.1400E+07	1.810	-1015.40
NC7H16+OH<=>S3XC7H15+H2O	5.6200E+11	0.320	846.50
NC7H16+O2<=>PXC7H15+HO2	4.0000E+13	0.000	50930.00
NC7H16+O2<=>SXC7H15+HO2	8.0000E+13	0.000	47590.00
NC7H16+O2<=>S2XC7H15+HO2	8.0000E+13	0.000	47590.00
NC7H16+O2<=>S3XC7H15+HO2	4.0000E+13	0.000	47590.00
NC7H16+HO2<=>PXC7H15+H2O2	4.7600E+04	2.550	16490.00
NC7H16+HO2<=>SXC7H15+H2O2	1.9000E+04	2.600	13910.00
NC7H16+HO2<=>S2XC7H15+H2O2	1.9000E+04	2.600	13910.00
NC7H16+HO2<=>S3XC7H15+H2O2	9.5000E+03	2.600	13910.00
NC7H16+CH3<=>PXC7H15+CH4	9.0300E-01	3.650	7153.00
NC7H16+CH3<=>SXC7H15+CH4	3.0000E+00	3.460	5480.00
NC7H16+CH3<=>S2XC7H15+CH4	3.0000E+00	3.460	5480.00
NC7H16+CH3<=>S3XC7H15+CH4	1.5000E+00	3.460	5480.00
PXC8H15+H (+M) <=>C8H16 (+M)	3.6000E+13	0.000	0.00
LOW / 3.0100E+48 -9.320 5833.60/			
TROE/ 0.4980 1314.00 1314.00 50000.00 /			
AR/0.70/ H2/2.00/ H2O/6.00/ CH4/2.00/ CO/1.50/ CO2/2.00/			
C2H6/3.00/			
PXC8H15+H<=>CH3+PXC7H13	2.0000E+21	-2.000	11000.00
PXC8H15+HO2<=>CH2O+OH+PXC7H13	2.4000E+13	0.000	0.00
PXC8H15+HCO<=>C8H16+CO	6.0000E+13	0.000	0.00
C2H4+PXC6H11<=>PXC8H15	3.0000E+11	0.000	7300.00
C8H16<=>PXC5H11+aC3H5	1.0700E+23	-2.030	74958.00
C8H16<=>C5H10+C3H6	7.0800E+06	1.650	53752.00
C8H16+H<=>C2H4+PXC6H13	8.0000E+21	-2.390	11180.00
C8H16+H<=>C3H6+PXC5H11	1.6000E+22	-2.390	11180.00
C8H16+H<=>PXC8H15+H2	6.5000E+05	2.540	6756.00
C8H16+O<=>PXC7H15+HCO	3.3000E+08	1.450	-402.00
C8H16+O<=>PXC8H15+OH	1.5000E+13	0.000	5760.00
DUPLICATE			
C8H16+O<=>PXC8H15+OH	2.6000E+13	0.000	4470.00
DUPLICATE			
C8H16+OH<=>PXC8H15+H2O	7.0000E+02	2.660	527.00
C8H16+O2<=>PXC8H15+HO2	2.0000E+13	0.000	50930.00
C8H16+HO2<=>PXC8H15+H2O2	1.0000E+12	0.000	14340.00
C8H16+CH3<=>PXC8H15+CH4	4.5000E-01	3.650	7153.00
PXC8H17 (+M) <=>C2H4+PXC6H13 (+M)	9.1200E+11	0.310	27237.80
LOW / 1.8000E-57 23.463 -602.40/			
TROE/ -2.4600 206.00 28.00 50000.00 /			
AR/0.70/ H2/2.00/ H2O/6.00/ CH4/2.00/ CO/1.50/ CO2/2.00/			
C2H6/3.00/			
SXC8H17 (+M) <=>PXC5H11+C3H6 (+M)	6.0300E+10	0.840	27820.00
LOW / 1.0000E-43 18.591 -602.50/			
TROE/-43.3200 200.00 28.00 50000.00 /			
AR/0.70/ H2/2.00/ H2O/6.00/ CH4/2.00/ CO/1.50/ CO2/2.00/			
C2H6/3.00/			
S2XC8H17 (+M) <=>pC4H9+C4H81 (+M)	2.0400E+13	0.040	28493.60

```

LOW / 3.0000E-43 18.430 -602.80/
TROE/-34.4700 208.00 28.00 50000.00 /
AR/0.70/ H2/2.00/ H2O/6.00/ CH4/2.00/ CO/1.50/ CO2/2.00/
C2H6/3.00/
S2XC8H17 (+M) <=> C7H14+CH3 (+M) 9.5500E+09 1.080 29387.70
LOW / 5.3000E-46 19.133 -602.70/
TROE/-34.3600 210.00 28.00 50000.00 /
AR/0.70/ H2/2.00/ H2O/6.00/ CH4/2.00/ CO/1.50/ CO2/2.00/
C2H6/3.00/
S3XC8H17 (+M) <=> nC3H7+C5H10 (+M) 5.4505E+11 0.550 28084.30
LOW / 3.0721E-43 18.418 -602.90/
TROE/-32.1300 207.00 28.00 50000.00 /
AR/0.70/ H2/2.00/ H2O/6.00/ CH4/2.00/ CO/1.50/ CO2/2.00/
C2H6/3.00/
S3XC8H17 (+M) <=> C6H12+C2H5 (+M) 6.8208E+09 1.110 27023.20
LOW / 8.2738E-43 18.276 -602.90/
TROE/-30.0400 210.00 28.00 50000.00 /
AR/0.70/ H2/2.00/ H2O/6.00/ CH4/2.00/ CO/1.50/ CO2/2.00/
C2H6/3.00/
PXC8H17+H (+M) <=> NC8H18 (+M) 3.6000E+13 0.000 0.00
LOW / 3.0100E+48 -9.320 5833.60/
TROE/ 0.4980 1314.00 1314.00 50000.00 /
AR/0.70/ H2/2.00/ H2O/6.00/ CH4/2.00/ CO/1.50/ CO2/2.00/
C2H6/3.00/
PXC8H17+H<=>PXC6H13+C2H5 3.7000E+24 -2.920 12505.00
PXC8H17+H<=>C8H16+H2 1.8000E+12 0.000 0.00
PXC8H17+O<=>PXC7H15+CH2O 9.6000E+13 0.000 0.00
PXC8H17+OH<=>C8H16+H2O 2.4000E+13 0.000 0.00
PXC8H17+O2<=>C8H16+HO2 9.0000E+10 0.000 0.00
PXC8H17+HO2<=>PXC7H15+OH+CH2O 2.4000E+13 0.000 0.00
PXC8H17+HCO<=>NC8H18+CO 9.0000E+13 0.000 0.00
PXC8H17+CH3<=>C8H16+CH4 1.1000E+13 0.000 0.00
SXC8H17+H (+M) <=> NC8H18 (+M) 2.4000E+13 0.000 0.00
LOW / 1.7000E+58 -12.080 11263.70/
TROE/ 0.6490 1213.10 1213.10 13369.70 /
AR/0.70/ H2/2.00/ H2O/6.00/ CH4/2.00/ CO/1.50/ CO2/2.00/
C2H6/3.00/
SXC8H17+H<=>PXC6H13+C2H5 1.4000E+28 -3.940 15916.00
SXC8H17+H<=>C8H16+H2 3.2000E+12 0.000 0.00
SXC8H17+O<=>CH3CHO+PXC6H13 9.6000E+13 0.000 0.00
SXC8H17+OH<=>C8H16+H2O 2.4000E+13 0.000 0.00
SXC8H17+O2<=>C8H16+HO2 1.3000E+11 0.000 0.00
SXC8H17+HO2<=>CH3CHO+PXC6H13+OH 2.4000E+13 0.000 0.00
SXC8H17+HCO<=>NC8H18+CO 1.2000E+14 0.000 0.00
SXC8H17+CH3<=>CH4+C8H16 2.2000E+14 -0.680 0.00
S2XC8H17+O2<=>C8H16+HO2 1.3000E+11 0.000 0.00
S3XC8H17+O2<=>C8H16+HO2 1.3000E+11 0.000 0.00
PXC7H15+CH3<=>NC8H18 1.9300E+14 -0.320 0.00
PXC6H13+C2H5<=>NC8H18 1.8800E+14 -0.500 0.00
PXC5H11+nC3H7<=>NC8H18 1.8800E+14 -0.500 0.00
2pC4H9<=>NC8H18 1.8800E+14 -0.500 0.00
NC8H18+H<=>PXC8H17+H2 1.3000E+06 2.540 6756.00
NC8H18+H<=>SXC8H17+H2 2.6000E+06 2.400 4471.00
NC8H18+H<=>S2XC8H17+H2 2.6000E+06 2.400 4471.00

```

```

NC8H18+H<=>S3XC8H17+H2      2.6000E+06      2.400      4471.00
NC8H18+O<=>PXC8H17+OH        2.5000E+06      2.400      5504.00
NC8H18+O<=>SXC8H17+OH        2.3000E+05      2.600      1768.00
NC8H18+O<=>S2XC8H17+OH        2.3000E+05      2.600      1768.00
NC8H18+O<=>S3XC8H17+OH        2.3000E+05      2.600      1768.00
NC8H18+OH<=>PXC8H17+H2O      2.7300E+07      1.810      868.30
NC8H18+OH<=>SXC8H17+H2O      1.4100E+10      0.940      504.70
NC8H18+OH<=>S2XC8H17+H2O      1.1400E+07      1.810     -1015.40
NC8H18+OH<=>S3XC8H17+H2O      1.1200E+12      0.320      846.50
NC8H18+O2<=>PXC8H17+HO2      4.0000E+13      0.000     50930.00
NC8H18+O2<=>SXC8H17+HO2      8.0000E+13      0.000     47590.00
NC8H18+O2<=>S2XC8H17+HO2      8.0000E+13      0.000     47590.00
NC8H18+O2<=>S3XC8H17+HO2      8.0000E+13      0.000     47590.00
NC8H18+HO2<=>PXC8H17+H2O2     4.7600E+04      2.550     16490.00
NC8H18+HO2<=>SXC8H17+H2O2     1.9000E+04      2.600     13910.00
NC8H18+HO2<=>S2XC8H17+H2O2     1.9000E+04      2.600     13910.00
NC8H18+HO2<=>S3XC8H17+H2O2     1.9000E+04      2.600     13910.00
NC8H18+CH3<=>PXC8H17+CH4      9.0300E-01      3.650      7153.00
NC8H18+CH3<=>SXC8H17+CH4      3.0000E+00      3.460      5480.00
NC8H18+CH3<=>S2XC8H17+CH4      3.0000E+00      3.460      5480.00
NC8H18+CH3<=>S3XC8H17+CH4      3.0000E+00      3.460      5480.00
PXC9H17+H (+M) <=>C9H18 (+M)  3.6000E+13      0.000        0.00
  LOW / 3.0100E+48   -9.320   5833.60/
  TROE/ 0.4980      1314.00   1314.00   50000.00 /
AR/0.70/ H2/2.00/ H2O/6.00/ CH4/2.00/ CO/1.50/ CO2/2.00/
C2H6/3.00/
PXC9H17+H<=>CH3+PXC8H15      2.0000E+21     -2.000     11000.00
PXC9H17+HO2<=>CH2O+OH+PXC8H15 2.4000E+13      0.000        0.00
PXC9H17+HCO<=>C9H18+CO       6.0000E+13      0.000        0.00
C2H4+PXC7H13<=>PXC9H17      3.0000E+11      0.000     7300.00
C9H18<=>PXC6H13+aC3H5        1.0700E+23     -2.030     74958.00
C9H18<=>C6H12+C3H6           7.0800E+06      1.650     53752.00
C9H18+H<=>C2H4+PXC7H15       8.0000E+21     -2.390     11180.00
C9H18+H<=>C3H6+PXC6H13       1.6000E+22     -2.390     11180.00
C9H18+H<=>PXC9H17+H2        6.5000E+05      2.540     6756.00
C9H18+O<=>PXC8H17+HCO       3.3000E+08      1.450     -402.00
C9H18+O<=>PXC9H17+OH        1.5000E+13      0.000     5760.00
  DUPLICATE
C9H18+O<=>PXC9H17+OH        2.6000E+13      0.000     4470.00
  DUPLICATE
C9H18+OH<=>PXC9H17+H2O       7.0000E+02      2.660      527.00
C9H18+O2<=>PXC9H17+HO2      2.0000E+13      0.000     50930.00
C9H18+HO2<=>PXC9H17+H2O2     1.0000E+12      0.000     14340.00
C9H18+CH3<=>PXC9H17+CH4      4.5000E-01      3.650      7153.00
PXC9H19 (+M) <=>C2H4+PXC7H15 (+M) 9.1200E+11      0.310     27237.80
  LOW / 1.8000E-57   23.463   -602.40/
  TROE/ -2.4600      206.00    28.00   50000.00 /
AR/0.70/ H2/2.00/ H2O/6.00/ CH4/2.00/ CO/1.50/ CO2/2.00/
C2H6/3.00/
SXC9H19 (+M) <=>C3H6+PXC6H13 (+M) 6.0300E+10      0.840     27820.00
  LOW / 1.0000E-43   18.591   -602.50/
  TROE/-43.3200      200.00    28.00   50000.00 /
AR/0.70/ H2/2.00/ H2O/6.00/ CH4/2.00/ CO/1.50/ CO2/2.00/
C2H6/3.00/

```

S2XC9H19 (+M) <=> PXC5H11+C4H81 (+M)	2.0400E+13	0.040	28493.60
LOW / 3.0000E-43 18.430 -602.80/			
TROE/-34.4700 208.00 28.00 50000.00 /			
AR/0.70/ H2/2.00/ H2O/6.00/ CH4/2.00/ CO/1.50/ CO2/2.00/			
C2H6/3.00/			
S2XC9H19 (+M) <=> C8H16+CH3 (+M)	9.5500E+09	1.080	29387.70
LOW / 5.3000E-46 19.133 -602.70/			
TROE/-34.3600 210.00 28.00 50000.00 /			
AR/0.70/ H2/2.00/ H2O/6.00/ CH4/2.00/ CO/1.50/ CO2/2.00/			
C2H6/3.00/			
S3XC9H19 (+M) <=> pC4H9+C5H10 (+M)	5.5000E+11	0.550	28084.30
LOW / 3.1000E-43 18.418 -602.90/			
TROE/-32.1300 207.00 28.00 50000.00 /			
AR/0.70/ H2/2.00/ H2O/6.00/ CH4/2.00/ CO/1.50/ CO2/2.00/			
C2H6/3.00/			
S3XC9H19 (+M) <=> C7H14+C2H5 (+M)	6.7600E+09	1.110	27023.20
LOW / 8.2000E-43 18.276 -602.90/			
TROE/-30.0400 210.00 28.00 50000.00 /			
AR/0.70/ H2/2.00/ H2O/6.00/ CH4/2.00/ CO/1.50/ CO2/2.00/			
C2H6/3.00/			
S4XC9H19 (+M) <=> nC3H7+C6H12 (+M)	1.1000E+12	0.550	28084.30
LOW / 6.2000E-43 18.418 -602.90/			
TROE/-32.1300 207.00 28.00 50000.00 /			
AR/0.70/ H2/2.00/ H2O/6.00/ CH4/2.00/ CO/1.50/ CO2/2.00/			
C2H6/3.00/			
PXC9H19+H (+M) <=> NC9H20 (+M)	3.6000E+13	0.000	0.00
LOW / 3.0100E+48 -9.320 5833.60/			
TROE/ 0.4980 1314.00 1314.00 50000.00 /			
AR/0.70/ H2/2.00/ H2O/6.00/ CH4/2.00/ CO/1.50/ CO2/2.00/			
C2H6/3.00/			
PXC9H19+H <=> PXC7H15+C2H5	3.7000E+24	-2.920	12505.00
PXC9H19+H <=> C9H18+H2	1.8000E+12	0.000	0.00
PXC9H19+O <=> PXC8H17+CH2O	9.6000E+13	0.000	0.00
PXC9H19+OH <=> C9H18+H2O	2.4000E+13	0.000	0.00
PXC9H19+O2 <=> C9H18+HO2	9.0000E+10	0.000	0.00
PXC9H19+HO2 <=> PXC8H17+OH+CH2O	2.4000E+13	0.000	0.00
PXC9H19+HCO <=> NC9H20+CO	9.0000E+13	0.000	0.00
PXC9H19+CH3 <=> C9H18+CH4	1.1000E+13	0.000	0.00
SXC9H19+H (+M) <=> NC9H20 (+M)	2.4000E+13	0.000	0.00
LOW / 1.7000E+58 -12.080 11263.70/			
TROE/ 0.6490 1213.10 1213.10 13369.70 /			
AR/0.70/ H2/2.00/ H2O/6.00/ CH4/2.00/ CO/1.50/ CO2/2.00/			
C2H6/3.00/			
SXC9H19+H <=> PXC7H15+C2H5	1.4000E+28	-3.940	15916.00
SXC9H19+H <=> C9H18+H2	3.2000E+12	0.000	0.00
SXC9H19+O <=> CH3CHO+PXC7H15	9.6000E+13	0.000	0.00
SXC9H19+OH <=> C9H18+H2O	2.4000E+13	0.000	0.00
SXC9H19+O2 <=> C9H18+HO2	1.3000E+11	0.000	0.00
SXC9H19+HO2 <=> CH3CHO+PXC7H15+OH	2.4000E+13	0.000	0.00
SXC9H19+HCO <=> NC9H20+CO	1.2000E+14	0.000	0.00
SXC9H19+CH3 <=> CH4+C9H18	2.2000E+14	-0.680	0.00
S2XC9H19+O2 <=> C9H18+HO2	1.3000E+11	0.000	0.00
S3XC9H19+O2 <=> C9H18+HO2	1.3000E+11	0.000	0.00
S4XC9H19+O2 <=> C9H18+HO2	1.3000E+11	0.000	0.00

PXC8H17+CH3<=>NC9H20	1.9300E+14	-0.320	0.00
PXC7H15+C2H5<=>NC9H20	1.8800E+14	-0.500	0.00
PXC6H13+nC3H7<=>NC9H20	1.8800E+14	-0.500	0.00
PXC5H11+pC4H9<=>NC9H20	1.8800E+14	-0.500	0.00
NC9H20+H<=>PXC9H19+H2	1.3000E+06	2.540	6756.00
NC9H20+H<=>SXC9H19+H2	2.6000E+06	2.400	4471.00
NC9H20+H<=>S2XC9H19+H2	2.6000E+06	2.400	4471.00
NC9H20+H<=>S3XC9H19+H2	2.6000E+06	2.400	4471.00
NC9H20+H<=>S4XC9H19+H2	1.3000E+06	2.400	4471.00
NC9H20+O<=>PXC9H19+OH	2.5000E+06	2.400	5504.00
NC9H20+O<=>SXC9H19+OH	2.3000E+05	2.600	1768.00
NC9H20+O<=>S2XC9H19+OH	2.3000E+05	2.600	1768.00
NC9H20+O<=>S3XC9H19+OH	2.3000E+05	2.600	1768.00
NC9H20+O<=>S4XC9H19+OH	1.1500E+05	2.600	1768.00
NC9H20+OH<=>PXC9H19+H2O	2.7300E+07	1.810	868.30
NC9H20+OH<=>SXC9H19+H2O	1.4100E+10	0.940	504.70
NC9H20+OH<=>S2XC9H19+H2O	1.1400E+07	1.810	-1015.40
NC9H20+OH<=>S3XC9H19+H2O	1.1200E+12	0.320	846.50
NC9H20+OH<=>S4XC9H19+H2O	5.6200E+11	0.320	846.50
NC9H20+O2<=>PXC9H19+HO2	4.0000E+13	0.000	50930.00
NC9H20+O2<=>SXC9H19+HO2	8.0000E+13	0.000	47590.00
NC9H20+O2<=>S2XC9H19+HO2	8.0000E+13	0.000	47590.00
NC9H20+O2<=>S3XC9H19+HO2	8.0000E+13	0.000	47590.00
NC9H20+O2<=>S4XC9H19+HO2	4.0000E+13	0.000	47590.00
NC9H20+HO2<=>PXC9H19+H2O2	4.7600E+04	2.550	16490.00
NC9H20+HO2<=>SXC9H19+H2O2	1.9000E+04	2.600	13910.00
NC9H20+HO2<=>S2XC9H19+H2O2	1.9000E+04	2.600	13910.00
NC9H20+HO2<=>S3XC9H19+H2O2	1.9000E+04	2.600	13910.00
NC9H20+HO2<=>S4XC9H19+H2O2	9.5000E+03	2.600	13910.00
NC9H20+CH3<=>PXC9H19+CH4	9.0300E-01	3.650	7153.00
NC9H20+CH3<=>SXC9H19+CH4	3.0000E+00	3.460	5480.00
NC9H20+CH3<=>S2XC9H19+CH4	3.0000E+00	3.460	5480.00
NC9H20+CH3<=>S3XC9H19+CH4	3.0000E+00	3.460	5480.00
NC9H20+CH3<=>S4XC9H19+CH4	1.5000E+00	3.460	5480.00
PXC10H19+H (+M) <=>C10H20 (+M)	3.6000E+13	0.000	0.00
LOW / 3.0100E+48 -9.320 5833.60/			
TROE/ 0.4980 1314.00 1314.00 50000.00 /			
AR/0.70/ H2/2.00/ H2O/6.00/ CH4/2.00/ CO/1.50/ CO2/2.00/			
C2H6/3.00/			
PXC10H19+H<=>CH3+PXC9H17	2.0000E+21	-2.000	11000.00
PXC10H19+HO2<=>CH2O+OH+PXC9H17	2.4000E+13	0.000	0.00
PXC10H19+HCO<=>C10H20+CO	6.0000E+13	0.000	0.00
C2H4+PXC8H15<=>PXC10H19	3.0000E+11	0.000	7300.00
C10H20<=>PXC7H15+aC3H5	1.0700E+23	-2.030	74958.00
C10H20<=>C7H14+C3H6	7.0800E+06	1.650	53752.00
C10H20+H<=>C2H4+PXC8H17	8.0000E+21	-2.390	11180.00
C10H20+H<=>C3H6+PXC7H15	1.6000E+22	-2.390	11180.00
C10H20+H<=>PXC10H19+H2	6.5000E+05	2.540	6756.00
C10H20+O<=>PXC9H19+HCO	3.3000E+08	1.450	-402.00
C10H20+O<=>PXC10H19+OH	1.5000E+13	0.000	5760.00
DUPLICATE			
C10H20+O<=>PXC10H19+OH	2.6000E+13	0.000	4470.00
DUPLICATE			
C10H20+OH<=>PXC10H19+H2O	7.0000E+02	2.660	527.00

```

C10H20+O2<=>PXC10H19+HO2          2.0000E+13    0.000    50930.00
C10H20+HO2<=>PXC10H19+H2O2         1.0000E+12    0.000    14340.00
C10H20+CH3<=>PXC10H19+CH4          4.5000E-01    3.650    7153.00
PXC10H21 (+M) <=>C2H4+PXC8H17 (+M)    9.1200E+11    0.310    27237.80
    LOW / 1.8000E-57    23.463    -602.40/
    TROE/ -2.4600    206.00    28.00    50000.00 /
AR/0.70/ H2/2.00/ H2O/6.00/ CH4/2.00/ CO/1.50/ CO2/2.00/
C2H6/3.00/
SXC10H21 (+M) <=>C3H6+PXC7H15 (+M)    6.0300E+10    0.840    27820.00
    LOW / 1.0000E-43    18.591    -602.50/
    TROE/-43.3200    200.00    28.00    50000.00 /
AR/0.70/ H2/2.00/ H2O/6.00/ CH4/2.00/ CO/1.50/ CO2/2.00/
C2H6/3.00/
S2XC10H21 (+M) <=>PXC6H13+C4H81 (+M)    2.0400E+13    0.040    28493.60
    LOW / 3.0000E-43    18.430    -602.80/
    TROE/-34.4700    208.00    28.00    50000.00 /
AR/0.70/ H2/2.00/ H2O/6.00/ CH4/2.00/ CO/1.50/ CO2/2.00/
C2H6/3.00/
S2XC10H21 (+M) <=>C9H18+CH3 (+M)    9.5500E+09    1.080    29387.70
    LOW / 5.3000E-46    19.133    -602.70/
    TROE/-34.3600    210.00    28.00    50000.00 /
AR/0.70/ H2/2.00/ H2O/6.00/ CH4/2.00/ CO/1.50/ CO2/2.00/
C2H6/3.00/
S3XC10H21 (+M) <=>PXC5H11+C5H10 (+M)    5.5000E+11    0.550    28084.30
    LOW / 3.1000E-43    18.418    -602.90/
    TROE/-32.1300    207.00    28.00    50000.00 /
AR/0.70/ H2/2.00/ H2O/6.00/ CH4/2.00/ CO/1.50/ CO2/2.00/
C2H6/3.00/
S3XC10H21 (+M) <=>C8H16+C2H5 (+M)    6.7600E+09    1.110    27023.20
    LOW / 8.2000E-43    18.276    -602.90/
    TROE/-30.0400    210.00    28.00    50000.00 /
AR/0.70/ H2/2.00/ H2O/6.00/ CH4/2.00/ CO/1.50/ CO2/2.00/
C2H6/3.00/
S4XC10H21 (+M) <=>PXC4H9+C6H12 (+M)    5.5000E+11    0.550    28084.30
    LOW / 3.1000E-43    18.418    -602.90/
    TROE/-32.1300    207.00    28.00    50000.00 /
AR/0.70/ H2/2.00/ H2O/6.00/ CH4/2.00/ CO/1.50/ CO2/2.00/
C2H6/3.00/
S4XC10H21 (+M) <=>C7H14+nC3H7 (+M)    5.5000E+11    0.550    28084.30
    LOW / 3.1000E-43    18.418    -602.90/
    TROE/-32.1300    207.00    28.00    50000.00 /
AR/0.70/ H2/2.00/ H2O/6.00/ CH4/2.00/ CO/1.50/ CO2/2.00/
C2H6/3.00/
PXC10H21+H (+M) <=>NC10H22 (+M)    3.6000E+13    0.000    0.00
    LOW / 3.0100E+48    -9.320    5833.60/
    TROE/ 0.4980    1314.00    1314.00    50000.00 /
AR/0.70/ H2/2.00/ H2O/6.00/ CH4/2.00/ CO/1.50/ CO2/2.00/
C2H6/3.00/
PXC10H21+H<=>PXC8H17+C2H5          3.7000E+24    -2.920    12505.00
PXC10H21+H<=>C10H20+H2            1.8000E+12    0.000    0.00
PXC10H21+O<=>PXC9H19+CH2O          9.6000E+13    0.000    0.00
PXC10H21+OH<=>C10H20+H2O          2.4000E+13    0.000    0.00
PXC10H21+O2<=>C10H20+HO2          9.0000E+10    0.000    0.00
PXC10H21+HO2<=>PXC9H19+OH+CH2O    2.4000E+13    0.000    0.00

```

PXC10H21+HCO<=>NC10H22+CO	9.0000E+13	0.000	0.00
PXC10H21+CH3<=>C10H20+CH4	1.1000E+13	0.000	0.00
SXC10H21+H(+M)<=>NC10H22(+M)	2.4000E+13	0.000	0.00
LOW / 1.7000E+58 -12.080 11263.70/			
TROE/ 0.6490 1213.10 1213.10 13369.70 /			
AR/0.70/ H2/2.00/ H2O/6.00/ CH4/2.00/ CO/1.50/ CO2/2.00/			
C2H6/3.00/			
SXC10H21+H<=>PXC8H17+C2H5	1.4000E+28	-3.940	15916.00
SXC10H21+H<=>C10H20+H2	3.2000E+12	0.000	0.00
SXC10H21+O<=>CH3CHO+PXC8H17	9.6000E+13	0.000	0.00
SXC10H21+OH<=>C10H20+H2O	2.4000E+13	0.000	0.00
SXC10H21+O2<=>C10H20+HO2	1.3000E+11	0.000	0.00
SXC10H21+HO2<=>CH3CHO+PXC8H17+OH	2.4000E+13	0.000	0.00
SXC10H21+HCO<=>NC10H22+CO	1.2000E+14	0.000	0.00
SXC10H21+CH3<=>CH4+C10H20	2.2000E+14	-0.680	0.00
S2XC10H21+O2<=>C10H20+HO2	1.3000E+11	0.000	0.00
S3XC10H21+O2<=>C10H20+HO2	1.3000E+11	0.000	0.00
S4XC10H21+O2<=>C10H20+HO2	1.3000E+11	0.000	0.00
PXC9H19+CH3<=>NC10H22	1.9300E+14	-0.320	0.00
PXC8H17+C2H5<=>NC10H22	1.8800E+14	-0.500	0.00
PXC7H15+nC3H7<=>NC10H22	1.8800E+14	-0.500	0.00
PXC6H13+pC4H9<=>NC10H22	1.8800E+14	-0.500	0.00
2PXC5H11<=>NC10H22	1.8800E+14	-0.500	0.00
NC10H22+H<=>PXC10H21+H2	1.3000E+06	2.540	6756.00
NC10H22+H<=>SXC10H21+H2	2.6000E+06	2.400	4471.00
NC10H22+H<=>S2XC10H21+H2	2.6000E+06	2.400	4471.00
NC10H22+H<=>S3XC10H21+H2	2.6000E+06	2.400	4471.00
NC10H22+H<=>S4XC10H21+H2	2.6000E+06	2.400	4471.00
NC10H22+O<=>PXC10H21+OH	2.5000E+06	2.400	5504.00
NC10H22+O<=>SXC10H21+OH	2.3000E+05	2.600	1768.00
NC10H22+O<=>S2XC10H21+OH	2.3000E+05	2.600	1768.00
NC10H22+O<=>S3XC10H21+OH	2.3000E+05	2.600	1768.00
NC10H22+O<=>S4XC10H21+OH	2.3000E+05	2.600	1768.00
NC10H22+OH<=>PXC10H21+H2O	2.7300E+07	1.810	868.30
NC10H22+OH<=>SXC10H21+H2O	1.4100E+10	0.940	504.70
NC10H22+OH<=>S2XC10H21+H2O	1.1400E+07	1.810	-1015.40
NC10H22+OH<=>S3XC10H21+H2O	1.1200E+12	0.320	846.50
NC10H22+OH<=>S4XC10H21+H2O	1.1200E+12	0.320	846.50
NC10H22+O2<=>PXC10H21+HO2	4.0000E+13	0.000	50930.00
NC10H22+O2<=>SXC10H21+HO2	8.0000E+13	0.000	47590.00
NC10H22+O2<=>S2XC10H21+HO2	8.0000E+13	0.000	47590.00
NC10H22+O2<=>S3XC10H21+HO2	8.0000E+13	0.000	47590.00
NC10H22+O2<=>S4XC10H21+HO2	8.0000E+13	0.000	47590.00
NC10H22+HO2<=>PXC10H21+H2O2	4.7600E+04	2.550	16490.00
NC10H22+HO2<=>SXC10H21+H2O2	1.9000E+04	2.600	13910.00
NC10H22+HO2<=>S2XC10H21+H2O2	1.9000E+04	2.600	13910.00
NC10H22+HO2<=>S3XC10H21+H2O2	1.9000E+04	2.600	13910.00
NC10H22+HO2<=>S4XC10H21+H2O2	1.9000E+04	2.600	13910.00
NC10H22+CH3<=>PXC10H21+CH4	9.0300E-01	3.650	7153.00
NC10H22+CH3<=>SXC10H21+CH4	3.0000E+00	3.460	5480.00
NC10H22+CH3<=>S2XC10H21+CH4	3.0000E+00	3.460	5480.00
NC10H22+CH3<=>S3XC10H21+CH4	3.0000E+00	3.460	5480.00
NC10H22+CH3<=>S4XC10H21+CH4	3.0000E+00	3.460	5480.00
PXC11H21+H(+M)<=>C11H22(+M)	3.6000E+13	0.000	0.00

```

LOW / 3.0100E+48 -9.320 5833.60/
TROE/ 0.4980 1314.00 1314.00 50000.00 /
AR/0.70/ H2/2.00/ H2O/6.00/ CH4/2.00/ CO/1.50/ CO2/2.00/
C2H6/3.00/
PXC11H21+H<=>CH3+PXC10H19 2.0000E+21 -2.000 11000.00
PXC11H21+HO2<=>CH2O+OH+PXC10H19 2.4000E+13 0.000 0.00
PXC11H21+HCO<=>C11H22+CO 6.0000E+13 0.000 0.00
C2H4+PXC9H17<=>PXC11H21 3.0000E+11 0.000 7300.00
C11H22<=>PXC8H17+aC3H5 1.0700E+23 -2.030 74958.00
C11H22<=>C8H16+C3H6 7.0800E+06 1.650 53752.00
C11H22+H<=>C2H4+PXC9H19 8.0000E+21 -2.390 11180.00
C11H22+H<=>C3H6+PXC8H17 1.6000E+22 -2.390 11180.00
C11H22+H<=>PXC11H21+H2 6.5000E+05 2.540 6756.00
C11H22+O<=>PXC10H21+HCO 3.3000E+08 1.450 -402.00
C11H22+O<=>PXC11H21+OH 1.5000E+13 0.000 5760.00
DUPLICATE
C11H22+O<=>PXC11H21+OH 2.6000E+13 0.000 4470.00
DUPLICATE
C11H22+OH<=>PXC11H21+H2O 7.0000E+02 2.660 527.00
C11H22+O2<=>PXC11H21+HO2 2.0000E+13 0.000 50930.00
C11H22+HO2<=>PXC11H21+H2O2 1.0000E+12 0.000 14340.00
C11H22+CH3<=>PXC11H21+CH4 4.5000E-01 3.650 7153.00
PXC11H23 (+M) <=>C2H4+PXC9H19 (+M) 9.1200E+11 0.310 27237.80
LOW / 1.8000E-57 23.463 -602.40/
TROE/ -2.4600 206.00 28.00 50000.00 /
AR/0.70/ H2/2.00/ H2O/6.00/ CH4/2.00/ CO/1.50/ CO2/2.00/
C2H6/3.00/
SXC11H23 (+M) <=>PXC8H17+C3H6 (+M) 6.0300E+10 0.840 27820.00
LOW / 1.0000E-43 18.591 -602.50/
TROE/-43.3200 200.00 28.00 50000.00 /
AR/0.70/ H2/2.00/ H2O/6.00/ CH4/2.00/ CO/1.50/ CO2/2.00/
C2H6/3.00/
S2XC11H23 (+M) <=>PXC7H15+C4H81 (+M) 2.0400E+13 0.040 28493.60
LOW / 3.0000E-43 18.430 -602.80/
TROE/-34.4700 208.00 28.00 50000.00 /
AR/0.70/ H2/2.00/ H2O/6.00/ CH4/2.00/ CO/1.50/ CO2/2.00/
C2H6/3.00/
S2XC11H23 (+M) <=>C10H20+CH3 (+M) 9.5500E+09 1.080 29387.70
LOW / 5.3000E-46 19.133 -602.70/
TROE/-34.3600 210.00 28.00 50000.00 /
AR/0.70/ H2/2.00/ H2O/6.00/ CH4/2.00/ CO/1.50/ CO2/2.00/
C2H6/3.00/
S3XC11H23 (+M) <=>PXC6H13+C5H10 (+M) 5.5000E+11 0.550 28084.30
LOW / 3.1000E-43 18.418 -602.90/
TROE/-32.1300 207.00 28.00 50000.00 /
AR/0.70/ H2/2.00/ H2O/6.00/ CH4/2.00/ CO/1.50/ CO2/2.00/
C2H6/3.00/
S3XC11H23 (+M) <=>C9H18+C2H5 (+M) 6.7600E+09 1.110 27023.20
LOW / 8.2000E-43 18.276 -602.90/
TROE/-30.0400 210.00 28.00 50000.00 /
AR/0.70/ H2/2.00/ H2O/6.00/ CH4/2.00/ CO/1.50/ CO2/2.00/
C2H6/3.00/
S4XC11H23 (+M) <=>PXC5H11+C6H12 (+M) 5.5000E+11 0.550 28084.30
LOW / 3.1000E-43 18.418 -602.90/

```

```

TROE/-32.1300      207.00      28.00      50000.00 /
AR/0.70/ H2/2.00/ H2O/6.00/ CH4/2.00/ CO/1.50/ CO2/2.00/
C2H6/3.00/
S4XC11H23 (+M) <=> C8H16+nC3H7 (+M)      5.5000E+11      0.550      28084.30
LOW / 3.1000E-43      18.418      -602.90/
TROE/-32.1300      207.00      28.00      50000.00 /
AR/0.70/ H2/2.00/ H2O/6.00/ CH4/2.00/ CO/1.50/ CO2/2.00/
C2H6/3.00/
S5XC11H23 (+M) <=> pC4H9+C7H14 (+M)      1.1000E+12      0.550      28084.30
LOW / 6.2000E-43      18.418      -602.90/
TROE/-32.1300      207.00      28.00      50000.00 /
AR/0.70/ H2/2.00/ H2O/6.00/ CH4/2.00/ CO/1.50/ CO2/2.00/
C2H6/3.00/
PXC11H23+H (+M) <=> NC11H24 (+M)      3.6000E+13      0.000      0.00
LOW / 3.0100E+48      -9.320      5833.60/
TROE/ 0.4980      1314.00      1314.00      50000.00 /
AR/0.70/ H2/2.00/ H2O/6.00/ CH4/2.00/ CO/1.50/ CO2/2.00/
C2H6/3.00/
PXC11H23+H <=> PXC9H19+C2H5      3.7000E+24      -2.920      12505.00
PXC11H23+H <=> C11H22+H2      1.8000E+12      0.000      0.00
PXC11H23+O <=> PXC10H21+CH2O      9.6000E+13      0.000      0.00
PXC11H23+OH <=> C11H22+H2O      2.4000E+13      0.000      0.00
PXC11H23+O2 <=> C11H22+HO2      9.0000E+10      0.000      0.00
PXC11H23+HO2 <=> PXC10H21+OH+CH2O      2.4000E+13      0.000      0.00
PXC11H23+HCO <=> NC11H24+CO      9.0000E+13      0.000      0.00
PXC11H23+CH3 <=> C11H22+CH4      1.1000E+13      0.000      0.00
SXC11H23+H (+M) <=> NC11H24 (+M)      2.4000E+13      0.000      0.00
LOW / 1.7000E+58      -12.080      11263.70/
TROE/ 0.6490      1213.10      1213.10      13369.70 /
AR/0.70/ H2/2.00/ H2O/6.00/ CH4/2.00/ CO/1.50/ CO2/2.00/
C2H6/3.00/
SXC11H23+H <=> PXC9H19+C2H5      1.4000E+28      -3.940      15916.00
SXC11H23+H <=> C11H22+H2      3.2000E+12      0.000      0.00
SXC11H23+O <=> CH3CHO+PXC9H19      9.6000E+13      0.000      0.00
SXC11H23+OH <=> C11H22+H2O      2.4000E+13      0.000      0.00
SXC11H23+O2 <=> C11H22+HO2      1.3000E+11      0.000      0.00
SXC11H23+HO2 <=> CH3CHO+PXC9H19+OH      2.4000E+13      0.000      0.00
SXC11H23+HCO <=> NC11H24+CO      1.2000E+14      0.000      0.00
SXC11H23+CH3 <=> CH4+C11H22      2.2000E+14      -0.680      0.00
S2XC11H23+O2 <=> C11H22+HO2      1.3000E+11      0.000      0.00
S3XC11H23+O2 <=> C11H22+HO2      1.3000E+11      0.000      0.00
S4XC11H23+O2 <=> C11H22+HO2      1.3000E+11      0.000      0.00
S5XC11H23+O2 <=> C11H22+HO2      1.3000E+11      0.000      0.00
PXC10H21+CH3 <=> NC11H24      1.9300E+14      -0.320      0.00
PXC9H19+C2H5 <=> NC11H24      1.8800E+14      -0.500      0.00
PXC8H17+nC3H7 <=> NC11H24      1.8800E+14      -0.500      0.00
PXC7H15+pC4H9 <=> NC11H24      1.8800E+14      -0.500      0.00
PXC6H13+PXC5H11 <=> NC11H24      1.8800E+14      -0.500      0.00
NC11H24+H <=> PXC11H23+H2      1.3000E+06      2.540      6756.00
NC11H24+H <=> SXC11H23+H2      2.6000E+06      2.400      4471.00
NC11H24+H <=> S2XC11H23+H2      2.6000E+06      2.400      4471.00
NC11H24+H <=> S3XC11H23+H2      2.6000E+06      2.400      4471.00
NC11H24+H <=> S4XC11H23+H2      2.6000E+06      2.400      4471.00
NC11H24+H <=> S5XC11H23+H2      1.3000E+06      2.400      4471.00

```

NC11H24+O<=>PXC11H23+OH	2.5000E+06	2.400	5504.00
NC11H24+O<=>SXC11H23+OH	2.3000E+05	2.600	1768.00
NC11H24+O<=>S2XC11H23+OH	2.3000E+05	2.600	1768.00
NC11H24+O<=>S3XC11H23+OH	2.3000E+05	2.600	1768.00
NC11H24+O<=>S4XC11H23+OH	2.3000E+05	2.600	1768.00
NC11H24+O<=>S5XC11H23+OH	1.2500E+05	2.600	1768.00
NC11H24+OH<=>PXC11H23+H2O	2.7300E+07	1.810	868.30
NC11H24+OH<=>SXC11H23+H2O	1.4100E+10	0.940	504.70
NC11H24+OH<=>S2XC11H23+H2O	1.1400E+07	1.810	-1015.40
NC11H24+OH<=>S3XC11H23+H2O	1.1200E+12	0.320	846.50
NC11H24+OH<=>S4XC11H23+H2O	1.1200E+12	0.320	846.50
NC11H24+OH<=>S5XC11H23+H2O	5.6200E+11	0.320	846.50
NC11H24+O2<=>PXC11H23+HO2	4.0000E+13	0.000	50930.00
NC11H24+O2<=>SXC11H23+HO2	8.0000E+13	0.000	47590.00
NC11H24+O2<=>S2XC11H23+HO2	8.0000E+13	0.000	47590.00
NC11H24+O2<=>S3XC11H23+HO2	8.0000E+13	0.000	47590.00
NC11H24+O2<=>S4XC11H23+HO2	8.0000E+13	0.000	47590.00
NC11H24+O2<=>S5XC11H23+HO2	4.0000E+13	0.000	47590.00
NC11H24+HO2<=>PXC11H23+H2O2	4.7600E+04	2.550	16490.00
NC11H24+HO2<=>SXC11H23+H2O2	1.9000E+04	2.600	13910.00
NC11H24+HO2<=>S2XC11H23+H2O2	1.9000E+04	2.600	13910.00
NC11H24+HO2<=>S3XC11H23+H2O2	1.9000E+04	2.600	13910.00
NC11H24+HO2<=>S4XC11H23+H2O2	1.9000E+04	2.600	13910.00
NC11H24+HO2<=>S5XC11H23+H2O2	9.5000E+03	2.600	13910.00
NC11H24+CH3<=>PXC11H23+CH4	9.0300E-01	3.650	7153.00
NC11H24+CH3<=>SXC11H23+CH4	3.0000E+00	3.460	5480.00
NC11H24+CH3<=>S2XC11H23+CH4	3.0000E+00	3.460	5480.00
NC11H24+CH3<=>S3XC11H23+CH4	3.0000E+00	3.460	5480.00
NC11H24+CH3<=>S4XC11H23+CH4	3.0000E+00	3.460	5480.00
NC11H24+CH3<=>S5XC11H23+CH4	1.5000E+00	3.460	5480.00
PXC12H23+H (+M) <=>C12H24 (+M)	3.6000E+13	0.000	0.00
LOW / 3.0100E+48 -9.320 5833.60/			
TROE/ 0.4980 1314.00 1314.00 50000.00 /			
AR/0.70/ H2/2.00/ H2O/6.00/ CH4/2.00/ CO/1.50/ CO2/2.00/			
C2H6/3.00/			
PXC12H23+H<=>CH3+PXC11H21	2.0000E+21	-2.000	11000.00
PXC12H23+HO2<=>CH2O+OH+PXC11H21	2.4000E+13	0.000	0.00
PXC12H23+HCO<=>C12H24+CO	6.0000E+13	0.000	0.00
C2H4+PXC10H19<=>PXC12H23	3.0000E+11	0.000	7300.00
C12H24<=>PXC9H19+ac3H5	1.0700E+23	-2.030	74958.00
C12H24<=>C9H18+C3H6	7.0800E+06	1.650	53752.00
C12H24+H<=>C2H4+PXC10H21	8.0000E+21	-2.390	11180.00
C12H24+H<=>C3H6+PXC9H19	1.6000E+22	-2.390	11180.00
C12H24+H<=>PXC12H23+H2	6.5000E+05	2.540	6756.00
C12H24+O<=>PXC11H23+HCO	3.3000E+08	1.450	-402.00
C12H24+O<=>PXC12H23+OH	1.5000E+13	0.000	5760.00
DUPLICATE			
C12H24+O<=>PXC12H23+OH	2.6000E+13	0.000	4470.00
DUPLICATE			
C12H24+OH<=>PXC12H23+H2O	7.0000E+02	2.660	527.00
C12H24+O2<=>PXC12H23+HO2	2.0000E+13	0.000	50930.00
C12H24+HO2<=>PXC12H23+H2O2	1.0000E+12	0.000	14340.00
C12H24+CH3<=>PXC12H23+CH4	4.5000E-01	3.650	7153.00
PXC12H25 (+M) <=>C2H4+PXC10H21 (+M)	9.1200E+11	0.310	27237.80

```

        LOW / 1.8000E-57    23.463    -602.40/
        TROE/ -2.4600      206.00      28.00      50000.00 /
AR/0.70/ H2/2.00/ H2O/6.00/ CH4/2.00/ CO/1.50/ CO2/2.00/
C2H6/3.00/
SXC12H25 (+M) <=> C3H6+PXC9H19 (+M)          6.0300E+10    0.840    27820.00
        LOW / 1.0000E-43    18.591    -602.50/
        TROE/-43.3200      200.00      28.00      50000.00 /
AR/0.70/ H2/2.00/ H2O/6.00/ CH4/2.00/ CO/1.50/ CO2/2.00/
C2H6/3.00/
S2XC12H25 (+M) <=> C4H81+PXC8H17 (+M)         2.0400E+13    0.040    28493.60
        LOW / 3.0000E-43    18.430    -602.80/
        TROE/-34.4700      208.00      28.00      50000.00 /
AR/0.70/ H2/2.00/ H2O/6.00/ CH4/2.00/ CO/1.50/ CO2/2.00/
C2H6/3.00/
S2XC12H25 (+M) <=> C11H22+CH3 (+M)           9.5500E+09    1.080    29387.70
        LOW / 5.3000E-46    19.133    -602.70/
        TROE/-34.3600      210.00      28.00      50000.00 /
AR/0.70/ H2/2.00/ H2O/6.00/ CH4/2.00/ CO/1.50/ CO2/2.00/
C2H6/3.00/
S3XC12H25 (+M) <=> C5H10+PXC7H15 (+M)         5.5000E+11    0.550    28084.30
        LOW / 3.1000E-43    18.418    -602.90/
        TROE/-32.1300      207.00      28.00      50000.00 /
AR/0.70/ H2/2.00/ H2O/6.00/ CH4/2.00/ CO/1.50/ CO2/2.00/
C2H6/3.00/
S3XC12H25 (+M) <=> C10H20+C2H5 (+M)           6.7600E+09    1.110    27023.20
        LOW / 8.2000E-43    18.276    -602.90/
        TROE/-30.0400      210.00      28.00      50000.00 /
AR/0.70/ H2/2.00/ H2O/6.00/ CH4/2.00/ CO/1.50/ CO2/2.00/
C2H6/3.00/
S4XC12H25 (+M) <=> C6H12+PXC6H13 (+M)         5.5000E+11    0.550    28084.30
        LOW / 3.1000E-43    18.418    -602.90/
        TROE/-32.1300      207.00      28.00      50000.00 /
AR/0.70/ H2/2.00/ H2O/6.00/ CH4/2.00/ CO/1.50/ CO2/2.00/
C2H6/3.00/
S4XC12H25 (+M) <=> C9H18+nC3H7 (+M)         5.5000E+11    0.550    28084.30
        LOW / 3.1000E-43    18.418    -602.90/
        TROE/-32.1300      207.00      28.00      50000.00 /
AR/0.70/ H2/2.00/ H2O/6.00/ CH4/2.00/ CO/1.50/ CO2/2.00/
C2H6/3.00/
S5XC12H25 (+M) <=> C7H14+PXC5H11 (+M)         5.5000E+11    0.550    28084.30
        LOW / 3.1000E-43    18.418    -602.90/
        TROE/-32.1300      207.00      28.00      50000.00 /
AR/0.70/ H2/2.00/ H2O/6.00/ CH4/2.00/ CO/1.50/ CO2/2.00/
C2H6/3.00/
S5XC12H25 (+M) <=> C8H16+pC4H9 (+M)         5.5000E+11    0.550    28084.30
        LOW / 3.1000E-43    18.418    -602.90/
        TROE/-32.1300      207.00      28.00      50000.00 /
AR/0.70/ H2/2.00/ H2O/6.00/ CH4/2.00/ CO/1.50/ CO2/2.00/
C2H6/3.00/
PXC12H25+H (+M) <=> NC12H26 (+M)           3.6000E+13    0.000          0.00
        LOW / 3.0100E+48    -9.320    5833.60/
        TROE/  0.4980      1314.00      1314.00      50000.00 /
AR/0.70/ H2/2.00/ H2O/6.00/ CH4/2.00/ CO/1.50/ CO2/2.00/
C2H6/3.00/

```

```

SXC12H25+H<=>PXC10H21+C2H5          1.4000E+28   -3.940   15916.00
SXC12H25+H<=>C12H24+H2                3.2000E+12    0.000    0.00
SXC12H25+O<=>CH3CHO+PXC10H21          9.6000E+13    0.000    0.00
SXC12H25+OH<=>C12H24+H2O              2.4000E+13    0.000    0.00
SXC12H25+O2<=>C12H24+HO2              1.3000E+11    0.000    0.00
SXC12H25+HO2<=>CH3CHO+PXC10H21+OH     2.4000E+13    0.000    0.00
SXC12H25+HCO<=>NC12H26+CO             1.2000E+14    0.000    0.00
SXC12H25+CH3<=>CH4+C12H24             2.2000E+14   -0.680    0.00
S2XC12H25+O2<=>C12H24+HO2             1.3000E+11    0.000    0.00
S3XC12H25+O2<=>C12H24+HO2             1.3000E+11    0.000    0.00
S4XC12H25+O2<=>C12H24+HO2             1.3000E+11    0.000    0.00
S5XC12H25+O2<=>C12H24+HO2             1.3000E+11    0.000    0.00
PXC12H25 (+M) <=>S3XC12H25 (+M)        5.1300E+00    3.230   16847.80
    LOW / 5.1000E-44   18.749   -602.90/
    TROE/-20.1500     205.00    28.00   5000000.00 /
AR/0.70/ H2/2.00/ H2O/6.00/ CH4/2.00/ CO/1.50/ CO2/2.00/
C2H6/3.00/
PXC11H23 (+M) <=>S3XC11H23 (+M)        5.1300E+00    3.230   16847.80
    LOW / 5.1000E-44   18.749   -602.90/
    TROE/-20.1500     205.00    28.00   5000000.00 /
AR/0.70/ H2/2.00/ H2O/6.00/ CH4/2.00/ CO/1.50/ CO2/2.00/
C2H6/3.00/
PXC10H21 (+M) <=>S3XC10H21 (+M)        5.1300E+00    3.230   16847.80
    LOW / 5.1000E-44   18.749   -602.90/
    TROE/-20.1500     205.00    28.00   5000000.00 /
AR/0.70/ H2/2.00/ H2O/6.00/ CH4/2.00/ CO/1.50/ CO2/2.00/
C2H6/3.00/
PXC9H19 (+M) <=>S3XC9H19 (+M)          5.1300E+00    3.230   16847.80
    DUPLICATE
    LOW / 5.1000E-44   18.749   -602.90/
    TROE/-20.1500     205.00    28.00   5000000.00 /
AR/0.70/ H2/2.00/ H2O/6.00/ CH4/2.00/ CO/1.50/ CO2/2.00/
C2H6/3.00/
PXC8H17 (+M) <=>S3XC8H17 (+M)          5.1300E+00    3.230   16847.80
    DUPLICATE
    LOW / 5.1000E-44   18.749   -602.90/
    TROE/-20.1500     205.00    28.00   5000000.00 /
AR/0.70/ H2/2.00/ H2O/6.00/ CH4/2.00/ CO/1.50/ CO2/2.00/
C2H6/3.00/
PXC7H15 (+M) <=>S3XC7H15 (+M)          1.1700E+02    2.850   17247.20
    LOW / 1.9000E-31   14.521   -599.00/
    TROE/ -8.1000     259.00    28.00   5000000.00 /
AR/0.70/ H2/2.00/ H2O/6.00/ CH4/2.00/ CO/1.50/ CO2/2.00/
C2H6/3.00/
PXC6H13 (+M) <=>S2XC6H13 (+M)          6.7287E+00    3.200   16557.70
    LOW / 1.9280E-26   12.833   -600.70/
    TROE/-10.1400     307.00    28.00   5000000.00 /
AR/0.70/ H2/2.00/ H2O/6.00/ CH4/2.00/ CO/1.50/ CO2/2.00/
C2H6/3.00/
PXC5H11 (+M) <=>SXC5H11 (+M)           9.2900E+11    0.000   22453.10
    LOW / 1.8580E-26   12.833   -600.70/
    TROE/-10.1400     307.00    28.00   5000000.00 /
AR/0.70/ H2/2.00/ H2O/6.00/ CH4/2.00/ CO/1.50/ CO2/2.00/
C2H6/3.00/

```



```

PXC12H25 (+M) <=> S4XC12H25 (+M)                2.2900E+01    2.820    10755.60
  LOW / 9.9000E-38    17.215    -603.00/
  TROE/-16.3300      200.00      28.00    5000000.00 /
AR/0.70/ H2/2.00/ H2O/6.00/ CH4/2.00/ CO/1.50/ CO2/2.00/
C2H6/3.00/
PXC11H23 (+M) <=> S4XC11H23 (+M)                2.2900E+01    2.820    10755.60
  LOW / 9.9000E-38    17.215    -603.00/
  TROE/-16.3300      200.00      28.00    5000000.00 /
AR/0.70/ H2/2.00/ H2O/6.00/ CH4/2.00/ CO/1.50/ CO2/2.00/
C2H6/3.00/
PXC10H21 (+M) <=> S4XC10H21 (+M)                2.2900E+01    2.820    10755.60
  DUPLICATE
  LOW / 9.9000E-38    17.215    -603.00/
  TROE/-16.3300      200.00      28.00    5000000.00 /
AR/0.70/ H2/2.00/ H2O/6.00/ CH4/2.00/ CO/1.50/ CO2/2.00/
C2H6/3.00/
PXC9H19 (+M) <=> S4XC9H19 (+M)                  2.2900E+01    2.820    10755.60
  LOW / 9.9000E-38    17.215    -603.00/
  TROE/-16.3300      200.00      28.00    5000000.00 /
AR/0.70/ H2/2.00/ H2O/6.00/ CH4/2.00/ CO/1.50/ CO2/2.00/
C2H6/3.00/
PXC8H17 (+M) <=> S3XC8H17 (+M)                  2.2900E+01    2.820    10755.60
  DUPLICATE
  LOW / 9.9000E-38    17.215    -603.00/
  TROE/-16.3300      200.00      28.00    5000000.00 /
AR/0.70/ H2/2.00/ H2O/6.00/ CH4/2.00/ CO/1.50/ CO2/2.00/
C2H6/3.00/
PXC7H15 (+M) <=> S2XC7H15 (+M)                   6.7600E+02    2.390    10405.90
  LOW / 5.4000E-26    13.202    -602.60/
  TROE/-25.3900      215.00      28.00    5000000.00 /
AR/0.70/ H2/2.00/ H2O/6.00/ CH4/2.00/ CO/1.50/ CO2/2.00/
C2H6/3.00/
PXC6H13 (+M) <=> SXC6H13 (+M)                    2.5693E+02    2.550    10960.30
  LOW / 7.5816E-26    13.087    -602.60/
  TROE/-25.3800      215.00      28.00    5000000.00 /
AR/0.70/ H2/2.00/ H2O/6.00/ CH4/2.00/ CO/1.50/ CO2/2.00/
C2H6/3.00/
PXC12H25 (+M) <=> S5XC12H25 (+M)                2.9500E+00    3.080    11015.90
  LOW / 3.9000E-34    15.855    -606.20/
  TROE/-15.2400      216.00      28.00    5000000.00 /
AR/0.70/ H2/2.00/ H2O/6.00/ CH4/2.00/ CO/1.50/ CO2/2.00/
C2H6/3.00/
PXC11H23 (+M) <=> S5XC11H23 (+M)                2.9500E+00    3.080    11015.90
  LOW / 3.9000E-34    15.855    -606.20/
  TROE/-15.2400      216.00      28.00    5000000.00 /
AR/0.70/ H2/2.00/ H2O/6.00/ CH4/2.00/ CO/1.50/ CO2/2.00/
C2H6/3.00/
PXC10H21 (+M) <=> S4XC10H21 (+M)                2.9500E+00    3.080    11015.90
  DUPLICATE
  LOW / 3.9000E-34    15.855    -606.20/
  TROE/-15.2400      216.00      28.00    5000000.00 /
AR/0.70/ H2/2.00/ H2O/6.00/ CH4/2.00/ CO/1.50/ CO2/2.00/
C2H6/3.00/
PXC9H19 (+M) <=> S3XC9H19 (+M)                  2.9500E+00    3.080    11015.90

```

```

DUPLICATE
    LOW / 3.9000E-34 15.855 -606.20/
    TROE/-15.2400 216.00 28.00 5000000.00 /
AR/0.70/ H2/2.00/ H2O/6.00/ CH4/2.00/ CO/1.50/ CO2/2.00/
C2H6/3.00/
PXC8H17 (+M) <=> S2XC8H17 (+M) 2.9500E+00 3.080 11015.90
    LOW / 3.9000E-34 15.855 -606.20/
    TROE/-15.2400 216.00 28.00 5000000.00 /
AR/0.70/ H2/2.00/ H2O/6.00/ CH4/2.00/ CO/1.50/ CO2/2.00/
C2H6/3.00/
PXC7H15 (+M) <=> SXC7H15 (+M) 2.4500E+02 2.510 12502.20
    LOW / 3.3000E-30 14.309 -602.50/
    TROE/-27.1900 220.00 28.00 5000000.00 /
AR/0.70/ H2/2.00/ H2O/6.00/ CH4/2.00/ CO/1.50/ CO2/2.00/
C2H6/3.00/
S3XC12H25 (+M) <=> S5XC12H25 (+M) 1.4100E+00 3.320 16144.40
    LOW / 5.2000E-30 14.079 -606.40/
    TROE/-21.9300 219.00 28.00 5000000.00 /
AR/0.70/ H2/2.00/ H2O/6.00/ CH4/2.00/ CO/1.50/ CO2/2.00/
C2H6/3.00/
S2XC12H25 (+M) <=> S5XC12H25 (+M) 1.4100E+00 3.320 16144.40
DUPLICATE
    LOW / 5.2000E-30 14.079 -606.40/
    TROE/-21.9300 219.00 28.00 5000000.00 /
AR/0.70/ H2/2.00/ H2O/6.00/ CH4/2.00/ CO/1.50/ CO2/2.00/
C2H6/3.00/
SXC12H25 (+M) <=> S4XC12H25 (+M) 1.4100E+00 3.320 16144.40
    LOW / 5.2000E-30 14.079 -606.40/
    TROE/-21.9300 219.00 28.00 5000000.00 /
AR/0.70/ H2/2.00/ H2O/6.00/ CH4/2.00/ CO/1.50/ CO2/2.00/
C2H6/3.00/
S3XC11H23 (+M) <=> S4XC11H23 (+M) 1.4100E+00 3.320 16144.40
    LOW / 5.2000E-30 14.079 -606.40/
    TROE/-21.9300 219.00 28.00 5000000.00 /
AR/0.70/ H2/2.00/ H2O/6.00/ CH4/2.00/ CO/1.50/ CO2/2.00/
C2H6/3.00/
S2XC11H23 (+M) <=> S5XC11H23 (+M) 1.4100E+00 3.320 16144.40
    LOW / 5.2000E-30 14.079 -606.40/
    TROE/-21.9300 219.00 28.00 5000000.00 /
AR/0.70/ H2/2.00/ H2O/6.00/ CH4/2.00/ CO/1.50/ CO2/2.00/
C2H6/3.00/
SXC11H23 (+M) <=> S4XC11H23 (+M) 1.4100E+00 3.320 16144.40
DUPLICATE
    LOW / 5.2000E-30 14.079 -606.40/
    TROE/-21.9300 219.00 28.00 5000000.00 /
AR/0.70/ H2/2.00/ H2O/6.00/ CH4/2.00/ CO/1.50/ CO2/2.00/
C2H6/3.00/
S4XC10H21 (+M) <=> S2XC10H21 (+M) 1.4100E+00 3.320 16144.40
    LOW / 5.2000E-30 14.079 -606.40/
    TROE/-21.9300 219.00 28.00 5000000.00 /
AR/0.70/ H2/2.00/ H2O/6.00/ CH4/2.00/ CO/1.50/ CO2/2.00/
C2H6/3.00/
S4XC10H21 (+M) <=> SXC10H21 (+M) 1.4100E+00 3.320 16144.40
DUPLICATE

```

```

LOW / 5.2000E-30 14.079 -606.40/
TROE/-21.9300 219.00 28.00 5000000.00 /
AR/0.70/ H2/2.00/ H2O/6.00/ CH4/2.00/ CO/1.50/ CO2/2.00/
C2H6/3.00/
SXC9H19 (+M) <=> S4XC9H19 (+M) 1.4100E+00 3.320 16144.40
LOW / 5.2000E-30 14.079 -606.40/
TROE/-21.9300 219.00 28.00 5000000.00 /
AR/0.70/ H2/2.00/ H2O/6.00/ CH4/2.00/ CO/1.50/ CO2/2.00/
C2H6/3.00/
S3XC9H19 (+M) <=> S2XC9H19 (+M) 1.4100E+00 3.320 16144.40
LOW / 5.2000E-30 14.079 -606.40/
TROE/-21.9300 219.00 28.00 5000000.00 /
AR/0.70/ H2/2.00/ H2O/6.00/ CH4/2.00/ CO/1.50/ CO2/2.00/
C2H6/3.00/
SXC8H17 (+M) <=> S3XC8H17 (+M) 1.4100E+00 3.320 16144.40
LOW / 5.2000E-30 14.079 -606.40/
TROE/-21.9300 219.00 28.00 5000000.00 /
AR/0.70/ H2/2.00/ H2O/6.00/ CH4/2.00/ CO/1.50/ CO2/2.00/
C2H6/3.00/
SXC7H15 (+M) <=> S2XC7H15 (+M) 2.4500E+01 3.090 18107.50
LOW / 1.3000E-32 14.834 -602.60/
TROE/-28.4100 219.00 28.00 5000000.00 /
AR/0.70/ H2/2.00/ H2O/6.00/ CH4/2.00/ CO/1.50/ CO2/2.00/
C2H6/3.00/
SXC12H25 (+M) <=> S5XC12H25 (+M) 1.8600E+00 3.270 13197.70
DUPLICATE
LOW / 3.0000E-27 13.481 -606.50/
TROE/-19.7000 215.00 28.00 5000000.00 /
AR/0.70/ H2/2.00/ H2O/6.00/ CH4/2.00/ CO/1.50/ CO2/2.00/
C2H6/3.00/
S2XC12H25 (+M) <=> S5XC12H25 (+M) 1.8600E+00 3.270 13197.70
DUPLICATE
LOW / 3.0000E-27 13.481 -606.50/
TROE/-19.7000 215.00 28.00 5000000.00 /
AR/0.70/ H2/2.00/ H2O/6.00/ CH4/2.00/ CO/1.50/ CO2/2.00/
C2H6/3.00/
S3XC12H25 (+M) <=> S4XC12H25 (+M) 1.8600E+00 3.270 13197.70
LOW / 3.0000E-27 13.481 -606.50/
TROE/-19.7000 215.00 28.00 5000000.00 /
AR/0.70/ H2/2.00/ H2O/6.00/ CH4/2.00/ CO/1.50/ CO2/2.00/
C2H6/3.00/
SXC11H23 (+M) <=> S5XC11H23 (+M) 1.8600E+00 3.270 13197.70
LOW / 3.0000E-27 13.481 -606.50/
TROE/-19.7000 215.00 28.00 5000000.00 /
AR/0.70/ H2/2.00/ H2O/6.00/ CH4/2.00/ CO/1.50/ CO2/2.00/
C2H6/3.00/
S2XC11H23 (+M) <=> S4XC11H23 (+M) 1.8600E+00 3.270 13197.70
LOW / 3.0000E-27 13.481 -606.50/
TROE/-19.7000 215.00 28.00 5000000.00 /
AR/0.70/ H2/2.00/ H2O/6.00/ CH4/2.00/ CO/1.50/ CO2/2.00/
C2H6/3.00/
S2XC10H21 (+M) <=> S3XC10H21 (+M) 1.8600E+00 3.270 13197.70
LOW / 3.0000E-27 13.481 -606.50/
TROE/-19.7000 215.00 28.00 5000000.00 /

```

```

AR/0.70/ H2/2.00/ H2O/6.00/ CH4/2.00/ CO/1.50/ CO2/2.00/
C2H6/3.00/
SXC10H21 (+M) <=> S4XC10H21 (+M)          1.8600E+00    3.270    13197.70
  DUPLICATE
    LOW / 3.0000E-27    13.481    -606.50/
    TROE/-19.7000      215.00      28.00    5000000.00 /
AR/0.70/ H2/2.00/ H2O/6.00/ CH4/2.00/ CO/1.50/ CO2/2.00/
C2H6/3.00/
SXC9H19 (+M) <=> S2XC9H19 (+M)          1.8600E+00    3.270    13197.70
  DUPLICATE
    LOW / 3.0000E-27    13.481    -606.50/
    TROE/-19.7000      215.00      28.00    5000000.00 /
AR/0.70/ H2/2.00/ H2O/6.00/ CH4/2.00/ CO/1.50/ CO2/2.00/
C2H6/3.00/
SXC8H17 (+M) <=> S2XC8H17 (+M)          1.8600E+00    3.270    13197.70
  DUPLICATE
    LOW / 3.0000E-27    13.481    -606.50/
    TROE/-19.7000      215.00      28.00    5000000.00 /
AR/0.70/ H2/2.00/ H2O/6.00/ CH4/2.00/ CO/1.50/ CO2/2.00/
C2H6/3.00/
S2XC12H25 (+M) <=> S4XC12H25 (+M)        2.9500E+00    3.080    12865.90
  DUPLICATE
    LOW / 3.9000E-34    15.855    1243.80/
    TROE/-15.2400      216.00      28.00    5000000.00 /
AR/0.70/ H2/2.00/ H2O/6.00/ CH4/2.00/ CO/1.50/ CO2/2.00/
C2H6/3.00/
SXC12H25 (+M) <=> S5XC12H25 (+M)        2.9500E+00    3.080    12865.90
  DUPLICATE
    LOW / 3.9000E-34    15.855    1243.80/
    TROE/-15.2400      216.00      28.00    5000000.00 /
AR/0.70/ H2/2.00/ H2O/6.00/ CH4/2.00/ CO/1.50/ CO2/2.00/
C2H6/3.00/
S2XC11H23 (+M) <=> S3XC11H23 (+M)        2.9500E+00    3.080    12865.90
  DUPLICATE
    LOW / 3.9000E-34    15.855    1243.80/
    TROE/-15.2400      216.00      28.00    5000000.00 /
AR/0.70/ H2/2.00/ H2O/6.00/ CH4/2.00/ CO/1.50/ CO2/2.00/
C2H6/3.00/
SXC11H23 (+M) <=> S4XC11H23 (+M)        2.9500E+00    3.080    12865.90
  DUPLICATE
    LOW / 3.9000E-34    15.855    1243.80/
    TROE/-15.2400      216.00      28.00    5000000.00 /
AR/0.70/ H2/2.00/ H2O/6.00/ CH4/2.00/ CO/1.50/ CO2/2.00/
C2H6/3.00/
SXC10H21 (+M) <=> S3XC10H21 (+M)        2.9500E+00    3.080    12865.90
  DUPLICATE
    LOW / 3.9000E-34    15.855    1243.80/
    TROE/-15.2400      216.00      28.00    5000000.00 /
AR/0.70/ H2/2.00/ H2O/6.00/ CH4/2.00/ CO/1.50/ CO2/2.00/
C2H6/3.00/
SXC9H19 (+M) <=> S2XC9H19 (+M)          2.9500E+00    3.080    12865.90
  DUPLICATE
    LOW / 3.9000E-34    15.855    1243.80/
    TROE/-15.2400      216.00      28.00    5000000.00 /
AR/0.70/ H2/2.00/ H2O/6.00/ CH4/2.00/ CO/1.50/ CO2/2.00/
C2H6/3.00/
PXC11H23+CH3 <=> NC12H26                1.9300E+14    -0.320    0.00
PXC10H21+C2H5 <=> NC12H26                1.6544E+14    -0.500    0.00

```

PXC9H19+nC3H7<=>NC12H26	1.8800E+14	-0.500	0.00
PXC8H17+pC4H9<=>NC12H26	1.4025E+14	-0.500	0.00
PXC7H15+PXC5H11<=>NC12H26	1.7315E+14	-0.500	0.00
2PXC6H13<=>NC12H26	8.9018E+14	-0.500	0.00
NC12H26+H<=>PXC12H25+H2	1.3000E+06	2.540	6756.00
NC12H26+H<=>SXC12H25+H2	3.0654E+06	2.400	4471.00
NC12H26+H<=>S2XC12H25+H2	3.4866E+06	2.400	4471.00
NC12H26+H<=>S3XC12H25+H2	2.9562E+06	2.400	4471.00
NC12H26+H<=>S4XC12H25+H2	3.8558E+06	2.400	4471.00
NC12H26+H<=>S5XC12H25+H2	2.6962E+06	2.400	4471.00
NC12H26+O<=>PXC12H25+OH	2.5000E+06	2.400	5504.00
NC12H26+O<=>SXC12H25+OH	2.3000E+05	2.600	1768.00
NC12H26+O<=>S2XC12H25+OH	2.3000E+05	2.600	1768.00
NC12H26+O<=>S3XC12H25+OH	2.3000E+05	2.600	1768.00
NC12H26+O<=>S4XC12H25+OH	2.3000E+05	2.600	1768.00
NC12H26+O<=>S5XC12H25+OH	2.3000E+05	2.600	1768.00
NC12H26+OH<=>PXC12H25+H2O	2.7300E+07	1.810	868.30
NC12H26+OH<=>SXC12H25+H2O	1.4100E+10	0.940	504.70
NC12H26+OH<=>S2XC12H25+H2O	1.1400E+07	1.810	-1015.40
NC12H26+OH<=>S3XC12H25+H2O	1.1200E+12	0.320	846.50
NC12H26+OH<=>S4XC12H25+H2O	1.1200E+12	0.320	846.50
NC12H26+OH<=>S5XC12H25+H2O	1.1200E+12	0.320	846.50
NC12H26+O2<=>PXC12H25+HO2	4.0000E+13	0.000	50930.00
NC12H26+O2<=>SXC12H25+HO2	8.0000E+13	0.000	47590.00
NC12H26+O2<=>S2XC12H25+HO2	8.0000E+13	0.000	47590.00
NC12H26+O2<=>S3XC12H25+HO2	8.0000E+13	0.000	47590.00
NC12H26+O2<=>S4XC12H25+HO2	8.0000E+13	0.000	47590.00
NC12H26+O2<=>S5XC12H25+HO2	8.0000E+13	0.000	47590.00
NC12H26+HO2<=>PXC12H25+H2O2	4.7600E+04	2.550	16490.00
NC12H26+HO2<=>SXC12H25+H2O2	1.9000E+04	2.600	13910.00
NC12H26+HO2<=>S2XC12H25+H2O2	1.9000E+04	2.600	13910.00
NC12H26+HO2<=>S3XC12H25+H2O2	1.9000E+04	2.600	13910.00
NC12H26+HO2<=>S4XC12H25+H2O2	1.9000E+04	2.600	13910.00
NC12H26+HO2<=>S5XC12H25+H2O2	1.9000E+04	2.600	13910.00
NC12H26+CH3<=>PXC12H25+CH4	9.0300E-01	3.650	7153.00
NC12H26+CH3<=>SXC12H25+CH4	3.0000E+00	3.460	5480.00
NC12H26+CH3<=>S2XC12H25+CH4	3.0000E+00	3.460	5480.00
NC12H26+CH3<=>S3XC12H25+CH4	3.0000E+00	3.460	5480.00
NC12H26+CH3<=>S4XC12H25+CH4	3.0000E+00	3.460	5480.00
NC12H26+CH3<=>S5XC12H25+CH4	3.0000E+00	3.460	5480.00
PXC12H25+O2<=>PC12H25O2	4.0000E+11	0.000	0.00
SXC12H25+O2<=>PC12H25O2	4.0000E+11	0.000	0.00
S2XC12H25+O2<=>PC12H25O2	4.0000E+11	0.000	0.00
S3XC12H25+O2<=>PC12H25O2	4.0000E+11	0.000	0.00
S4XC12H25+O2<=>PC12H25O2	4.0000E+11	0.000	0.00
S5XC12H25+O2<=>PC12H25O2	4.0000E+11	0.000	0.00
PC12H25O2=>P12OOHX2	2.0000E+12	0.000	17017.20
P12OOHX2=>PC12H25O2	1.0000E+11	0.000	12500.00
P12OOHX2<=>C12H24+HO2	8.5000E+12	0.000	25573.60
P12OOHX2+O2<=>SOO12OOH	5.4640E+11	0.000	0.00
SOO12OOH<=>OC12OOH+OH	1.5000E+12	0.000	0.00
OC12OOH=>CH2O+4C2H4+C2H5+OH+CO	7.0000E+14	0.000	42065.00
CH*=>CH	1.9000E+06	0.000	0.00
CH*+M=>CH+M	4.0000E+10	0.500	0.00

CH*+O2=>CH+O2	2.4000E+12	0.500	0.00
C2H+O2=>CH*+CO2	4.5000E+15	0.000	25000.00
H+O+M<=>OH*+M	3.1000E+14	0.000	10000.00
OH*+AR<=>OH+AR	2.1700E+10	0.500	2060.00
OH*+H2O<=>OH+H2O	5.9200E+12	0.500	-861.00
OH*+CO2<=>OH+CO2	2.7500E+12	0.500	-968.00
OH*+CO<=>OH+CO	3.2300E+12	0.500	-787.00
OH*+H2<=>OH+H2	2.9500E+12	0.500	-444.00
OH*+O2<=>OH+O2	2.1000E+12	0.500	-482.00
OH*+OH<=>2OH	1.5000E+12	0.500	0.00
OH*+H<=>OH+H	1.5000E+12	0.500	0.00
OH*+O<=>OH+O	1.5000E+12	0.500	0.00
OH*+CH4<=>OH+CH4	3.3600E+12	0.500	-635.00
OH*<=>OH	1.4000E+06	0.000	0.00
END			

D.1.1.1 Thermodynamic File:-

```

THERMO
  298.000  1000.000  5000.000
N2          121286N  2          G  0300.00  5000.00
1000.00      1
  0.02926640E+02  0.14879768E-02-0.05684760E-05
  0.10097038E-09-0.06753351E-13      2
-0.09227977E+04  0.05980528E+02  0.03298677E+02
  0.14082404E-02-0.03963222E-04      3
  0.05641515E-07-0.02444854E-10-0.10208999E+04  0.03950372E+02
4
AR          120186AR  1          G  0300.00  5000.00
1000.00      1
  0.025000000E+02  0.000000000E+00  0.000000000E+00  0.000000000E+00
  0.000000000E+00      2
-0.07453750E+04  0.04366000E+02  0.025000000E+02  0.000000000E+00
  0.000000000E+00      3
  0.000000000E+00  0.000000000E+00-0.07453750E+04  0.04366000E+02
4
HE          L10/90HE  1      0      0      OG  200.000  6000.000 1000.
1
  2.500000000E+00  0.000000000E+00  0.000000000E+00  0.000000000E+00
  0.000000000E+00      2
-7.45375000E+02  9.28723974E-01  2.500000000E+00  0.000000000E+00
  0.000000000E+00      3
  0.000000000E+00  0.000000000E+00-7.45375000E+02  9.28723974E-01
  0.000000000E+00      4
NE          L10/92NE  1      0      0      OG  200.000  6000.000
1000.00      1
  0.250000000E+01  0.          0.          0.          0.
2
-0.74537500E+03  0.33553227E+01  0.250000000E+01  0.          0.
3
  0.          0.          -0.74537498E+03  0.33553227E+01
  0.000000000E+00      4
C(S)        P 4/83C  1      0      0      OC  200.000  5000.000
12.01100  1
  0.14556924e+01  0.17170638e-02-0.69758410e-06
  0.13528316e-09-0.96764905e-14      2
-0.69512804e+03-0.85256842e+01-0.31087207e+00  0.44035369e-02
  0.19039412e-05      3
-0.63854697e-08  0.29896425e-11-0.10865079e+03  0.11138295e+01
4
O          L 1/90O  1      00      00      00G  200.000  3500.000
1000.000      1
  2.56942078E+00-8.59741137E-05  4.19484589E-08-1.00177799E-11
  1.22833691E-15      2
  2.92175791E+04  4.78433864E+00  3.16826710E+00-3.27931884E-03
  6.64306396E-06      3
-6.12806624E-09  2.11265971E-12  2.91222592E+04  2.05193346E+00
  6.72540300E+03      4
O2          TPIS89O  2      00      00      00G  200.000  3500.000
1000.000      1

```



```
3.28253784E+00 1.48308754E-03-7.57966669E-07
2.09470555E-10-2.16717794E-14      2
-1.08845772E+03 5.45323129E+00 3.78245636E+00-2.99673416E-03
9.84730201E-06      3
-9.68129509E-09 3.24372837E-12-1.06394356E+03 3.65767573E+00
8.68010400E+03      4
H      L 7/88H      1      00      00      00G      200.000      3500.000
1000.00      1
2.50000001E+00-2.30842973E-11 1.61561948E-14-4.73515235E-18
4.98197357E-22      2
2.54736599E+04-4.46682914E-01 2.50000000E+00
7.05332819E-13-1.99591964E-15      3
2.30081632E-18-9.27732332E-22 2.54736599E+04-4.46682853E-01
6.19742800E+03      4
H2      TPIS78H      2      00      00      00G      200.000      3500.000
1000.00      1
3.33727920E+00-4.94024731E-05 4.99456778E-07-1.79566394E-10
2.00255376E-14      2
-9.50158922E+02-3.20502331E+00 2.34433112E+00
7.98052075E-03-1.94781510E-05      3
2.01572094E-08-7.37611761E-12-9.17935173E+02 6.83010238E-01
8.46810200E+03      4
OH      S 9/01O      1H      1      0      0G      200.000      6000.000
1000.00      1
2.86472886E+00 1.05650448E-03-2.59082758E-07
3.05218674E-11-1.33195876E-15      2
3.71885774E+03 5.70164073E+00 4.12530561E+00-3.22544939E-03
6.52764691E-06      3
-5.79853643E-09 2.06237379E-12 3.38153812E+03-6.90432960E-01
4.51532273E+03      4
H2O      L 8/89H      20      1      00      00G      200.000      3500.000
1000.000      1
3.03399249E+00 2.17691804E-03-1.64072518E-07-9.70419870E-11
1.68200992E-14      2
-3.00042971E+04 4.96677010E+00 4.19864056E+00-2.03643410E-03
6.52040211E-06      3
-5.48797062E-09 1.77197817E-12-3.02937267E+04-8.49032208E-01
9.90409200E+03      4
HO2      L 5/89H      10      2      00      00G      200.000      3500.000
1000.000      1
4.01721090E+00 2.23982013E-03-6.33658150E-07
1.14246370E-10-1.07908535E-14      2
1.11856713E+02 3.78510215E+00 4.30179801E+00-4.74912051E-03
2.11582891E-05      3
-2.42763894E-08 9.29225124E-12 2.94808040E+02 3.71666245E+00
1.00021620E+04      4
H2O2      L 7/88H      20      2      00      00G      200.000      3500.000
1000.000      1
4.16500285E+00 4.90831694E-03-1.90139225E-06
3.71185986E-10-2.87908305E-14      2
-1.78617877E+04 2.91615662E+00 4.27611269E+00-5.42822417E-04
1.67335701E-05      3
```

```

-2.15770813E-08 8.62454363E-12-1.77025821E+04 3.43505074E+00
1.11588350E+04 4
C L11/88C 1 00 00 00G 200.000 3500.000
1000.000 1
2.49266888E+00 4.79889284E-05-7.24335020E-08
3.74291029E-11-4.87277893E-15 2
8.54512953E+04 4.80150373E+00 2.55423955E+00-3.21537724E-04
7.33792245E-07 3
-7.32234889E-10 2.66521446E-13 8.54438832E+04 4.53130848E+00
6.53589500E+03 4
CH TPIS79C 1H 1 00 00G 200.000 3500.000
1000.000 1
2.87846473E+00 9.70913681E-04 1.44445655E-07-1.30687849E-10
1.76079383E-14 2
7.10124364E+04 5.48497999E+00 3.48981665E+00
3.23835541E-04-1.68899065E-06 3
3.16217327E-09-1.40609067E-12 7.07972934E+04 2.08401108E+00
8.62500000E+03 4
CH2 L S/93C 1H 2 00 00G 200.000 3500.000
1000.000 1
2.87410113E+00 3.65639292E-03-1.40894597E-06
2.60179549E-10-1.87727567E-14 2
4.62636040E+04 6.17119324E+00 3.76267867E+00 9.68872143E-04
2.79489841E-06 3
-3.85091153E-09 1.68741719E-12 4.60040401E+04 1.56253185E+00
1.00274170E+04 4
CH2* L S/93C 1H 2 00 00G 200.000 3500.000
1000.000 1
2.29203842E+00 4.65588637E-03-2.01191947E-06
4.17906000E-10-3.39716365E-14 2
5.09259997E+04 8.62650169E+00 4.19860411E+00-2.36661419E-03
8.23296220E-06 3
-6.68815981E-09 1.94314737E-12 5.04968163E+04-7.69118967E-01
9.93967200E+03 4
CH3 L11/89C 1H 3 00 00G 200.000 3500.000
1000.000 1
2.28571772E+00 7.23990037E-03-2.98714348E-06
5.95684644E-10-4.67154394E-14 2
1.67755843E+04 8.48007179E+00 3.67359040E+00 2.01095175E-03
5.73021856E-06 3
-6.87117425E-09 2.54385734E-12 1.64449988E+04 1.60456433E+00
1.03663400E+04 4
CH4 L 8/88C 1H 4 00 00G 200.000 3500.000
1000.000 1
7.48514950E-02 1.33909467E-02-5.73285809E-06
1.22292535E-09-1.01815230E-13 2
-9.46834459E+03 1.84373180E+01 5.14987613E+00-1.36709788E-02
4.91800599E-05 3
-4.84743026E-08 1.66693956E-11-1.02466476E+04-4.64130376E+00
1.00161980E+04 4
CO TPIS79C 1O 1 00 00G 200.000 3500.000
1000.000 1

```

```
2.71518561E+00 2.06252743E-03-9.98825771E-07
2.30053008E-10-2.03647716E-14      2
-1.41518724E+04 7.81868772E+00 3.57953347E+00-6.10353680E-04
1.01681433E-06      3
9.07005884E-10-9.04424499E-13-1.43440860E+04 3.50840928E+00
8.67100000E+03      4
CO2      L 7/88C      1O      2      00      00G      200.000      3500.000
1000.000      1
3.85746029E+00 4.41437026E-03-2.21481404E-06
5.23490188E-10-4.72084164E-14      2
-4.87591660E+04 2.27163806E+00 2.35677352E+00
8.98459677E-03-7.12356269E-06      3
2.45919022E-09-1.43699548E-13-4.83719697E+04 9.90105222E+00
9.36546900E+03      4
HCO      L12/89H      1C      1O      1      00G      200.000      3500.000
1000.000      1
2.77217438E+00 4.95695526E-03-2.48445613E-06
5.89161778E-10-5.33508711E-14      2
4.01191815E+03 9.79834492E+00 4.22118584E+00-3.24392532E-03
1.37799446E-05      3
-1.33144093E-08 4.33768865E-12 3.83956496E+03 3.39437243E+00
9.98945000E+03      4
CH2O      L 8/88H      2C      1O      1      00G      200.000      3500.000
1000.000      1
1.76069008E+00 9.20000082E-03-4.42258813E-06
1.00641212E-09-8.83855640E-14      2
-1.39958323E+04 1.36563230E+01 4.79372315E+00-9.90833369E-03
3.73220008E-05      3
-3.79285261E-08 1.31772652E-11-1.43089567E+04 6.02812900E-01
1.00197170E+04      4
CH2OH      IU2/03C      1H      3O      1      00G      200.000      6000.00
1
5.09314370E+00 5.94761260E-03-2.06497460E-06
3.23008173E-10-1.88125902E-14      2
-4.03409640E+03-1.84691493E+00 4.47834367E+00-1.35070310E-03
2.78484980E-05      3
-3.64869060E-08 1.47907450E-11-3.50072890E+03
3.30913500E+00-2.04462770E+03      4
CH3O      IU1/03C      1H      3O      1      G      200.000      6000.00
1
4.75779238E+00 7.44142474E-03-2.69705176E-06
4.38090504E-10-2.63537098E-14      2
3.78111940E+02-1.96680028E+00 3.71180502E+00-2.80463306E-03
3.76550971E-05      3
-4.73072089E-08 1.86588420E-11 1.29569760E+03 6.57240864E+00
2.52571660E+03      4
CH3OH      L 8/88C      1H      4O      1      00G      200.000      3500.000
1000.000      1
1.78970791E+00 1.40938292E-02-6.36500835E-06
1.38171085E-09-1.17060220E-13      2
-2.53748747E+04 1.45023623E+01 5.71539582E+00-1.52309129E-02
6.52441155E-05      3
```

-7.10806889E-08 2.61352698E-11-2.56427656E+04-1.50409823E+00
1.14352770E+04 4
C2H L 1/91C 2H 1 00 00G 200.000 3500.000
1000.000 1
3.16780652E+00 4.75221902E-03-1.83787077E-06
3.04190252E-10-1.77232770E-14 2
6.71210650E+04 6.63589475E+00 2.88965733E+00
1.34099611E-02-2.84769501E-05 3
2.94791045E-08-1.09331511E-11 6.68393932E+04 6.22296438E+00
1.04544720E+04 4
C2H2 L 1/91C 2H 2 00 00G 200.000 3500.000
1000.000 1
4.14756964E+00 5.96166664E-03-2.37294852E-06
4.67412171E-10-3.61235213E-14 2
2.59359992E+04-1.23028121E+00 8.08681094E-01
2.33615629E-02-3.55171815E-05 3
2.80152437E-08-8.50072974E-12 2.64289807E+04 1.39397051E+01
1.00058390E+04 4
H2CC L12/89H 2C 2 0 0G 200.000 6000.000
1000.000 1
0.42780340E+01 0.47562804E-02-0.16301009E-05
0.25462806E-09-0.14886379E-13 2
0.48316688E+05 0.64023701E+00 0.32815483E+01
0.69764791E-02-0.23855244E-05 3
-0.12104432E-08 0.98189545E-12 0.48621794E+05 0.59203910E+01
0.49887266E+05 4
C2H3 L 2/92C 2H 3 00 00G 200.000 3500.000
1000.000 1
3.01672400E+00 1.03302292E-02-4.68082349E-06
1.01763288E-09-8.62607041E-14 2
3.46128739E+04 7.78732378E+00 3.21246645E+00 1.51479162E-03
2.59209412E-05 3
-3.57657847E-08 1.47150873E-11 3.48598468E+04 8.51054025E+00
1.05750490E+04 4
C2H4 L 1/91C 2H 4 00 00G 200.000 3500.000
1000.000 1
2.03611116E+00 1.46454151E-02-6.71077915E-06
1.47222923E-09-1.25706061E-13 2
4.93988614E+03 1.03053693E+01 3.95920148E+00-7.57052247E-03
5.70990292E-05 3
-6.91588753E-08 2.69884373E-11 5.08977593E+03 4.09733096E+00
1.05186890E+04 4
C2H5 L12/92C 2H 5 00 00G 200.000 3500.000
1000.000 1
1.95465642E+00 1.73972722E-02-7.98206668E-06
1.75217689E-09-1.49641576E-13 2
1.28575200E+04 1.34624343E+01 4.30646568E+00-4.18658892E-03
4.97142807E-05 3
-5.99126606E-08 2.30509004E-11 1.28416265E+04 4.70720924E+00
1.21852440E+04 4
C2H6 L 8/88C 2H 6 00 00G 200.000 3500.000
1000.000 1

```
1.07188150E+00 2.16852677E-02-1.00256067E-05
2.21412001E-09-1.90002890E-13      2
-1.14263932E+04 1.51156107E+01 4.29142492E+00-5.50154270E-03
5.99438288E-05      3
-7.08466285E-08 2.68685771E-11-1.15222055E+04 2.66682316E+00
1.18915940E+04      4
CH2CO"OLD"      L 5/90C      2H      2O      1      00G      200.000      3500.000
1000.000      1
4.51129732E+00 9.00359745E-03-4.16939635E-06
9.23345882E-10-7.94838201E-14      2
-7.55105311E+03 6.32247205E-01 2.13583630E+00
1.81188721E-02-1.73947474E-05      3
9.34397568E-09-2.01457615E-12-7.04291804E+03 1.22156480E+01
1.17977430E+04      4
CH2CO      D05/90C      2H      2O      1      00G      200.000      3500.000
1000.000      1
4.51129732E+00 9.00359745E-03-4.16939635E-06
9.23345882E-10-7.94838201E-14      2
-7.77850000E+03 6.32247205E-01 2.13583630E+00
1.81188721E-02-1.73947474E-05      3
9.34397568E-09-2.01457615E-12-7.27000000E+03 1.22156480E+01
1.17977430E+04      4
CH2CHO"OLD"      T04/83O      1H      3C      2      0G      300.000      5000.000
1
0.59756699E+01 0.81305914E-02-0.27436245E-05
0.40703041E-09-0.21760171E-13      2
0.49032178E+03-0.50320879E+01 0.34090624E+01 0.10738574E-01
0.18914925E-05      3
-0.71585831E-08 0.28673851E-11 0.15214766E+04 0.95714535E+01
0.30474436E+04      4
CH2CHO      D05/83O      1H      3C      2      0G      300.000      5000.000
1
0.59756699E+01 0.81305914E-02-0.27436245E-05
0.40703041E-09-0.21760171E-13      2
-0.96950000E+03-0.50320879E+01 0.34090624E+01 0.10738574E-01
0.18914925E-05      3
-0.71585831E-08 0.28673851E-11 0.62000000E+02 0.95714535E+01
0.30474436E+04      4
CH2OCH      A12/04C      2H      3O      1      0G      298.150      3000.000
500.0      1
0.44994054E+01 0.11552625E-01-0.48144129E-05
0.89234919E-09-0.56870585E-13      2
0.17473963E+05 0.33925515E+00-0.38396084E+00
0.23879038E-01-0.12467587E-04      3
-0.17686411E-08 0.28142438E-11 0.18836203E+05 0.25741745E+02
4
CH2OCH2      T 6/92C      2H      4O      1      0G      298.150      3000.0
1000.0      1
0.54887641E+01 0.12046190E-01-0.43336931E-05
0.70028311E-09-0.41949088E-13      2
-0.91804251E+04-0.70799605E+01 0.37590532E+01-0.94412180E-02
0.80309721E-04      3
```

-0.10080788E-06 0.40039921E-10-0.75608143E+04
0.78497475E+01-0.63304657E+04 4
CH3CO T 9/92C 2H 3O 1 OG 200.000 6000.0
1000.0 1
0.59447731E+01 0.78667205E-02-0.28865882E-05
0.47270875E-09-0.28599861E-13 2
-0.37873075E+04-0.50136751E+01 0.41634257E+01-0.23261610E-03
0.34267820E-04 3
-0.44105227E-07 0.17275612E-10-0.26574529E+04
0.73468280E+01-0.12027167E+04 4
CH3CHO L 8/88C 2H 4O 1 OG 200.000 6000.0
1000.0 1
0.54041108E+01 0.11723059E-01-0.42263137E-05
0.68372451E-09-0.40984863E-13 2
-0.22593122E+05-0.34807917E+01 0.47294595E+01-0.31932858E-02
0.47534921E-04 3
-0.57458611E-07 0.21931112E-10-0.21572878E+05
0.41030159E+01-0.19987949E+05 4
HCCO SRIC91H 1C 2O 1 G 0300.00 4000.00
1000.00 1
0.56282058E+01 0.40853401E-02-0.15934547E-05
0.28626052E-09-0.19407832E-13 2
0.19327215E+05-0.39302595E+01 0.22517214E+01
0.17655021E-01-0.23729101E-04 3
0.17275759E-07-0.50664811E-11 0.20059449E+05 0.12490417E+02
4
HCCOH SRI91C 2O 1H 20 OG 300.000 5000.000
1000.G 1
0.59238291E+01 0.67923600E-02-0.25658564E-05
0.44987841E-09-0.29940101E-13 2
0.72646260E+04-0.76017742E+01 0.12423733E+01
0.31072201E-01-0.50866864E-04 3
0.43137131E-07-0.14014594E-10 0.80316143E+04 0.13874319E+02
4
C2O RUS 79C 2O 1 0 OG 200.000 6000.000
1
0.51512722E+01 0.23726722E-02-0.76135971E-06
0.11706415E-09-0.70257804E-14 2
0.33241888E+05-0.22183135E+01 0.28648610E+01
0.11990216E-01-0.18362448E-04 3
0.15769739E-07-0.53897452E-11 0.33749932E+05 0.88867772E+01
0.35003406E+05 4
C3H2 T12/00C 3H 2 0 OG 200.000 6000.000
1
0.73481207E+01 0.44476404E-02-0.12610332E-05 0.78131814E-10
0.13216298E-13 2
0.62551656E+05-0.91040211E+01 0.45094776E+01
0.17438605E-01-0.24516321E-04 3
0.18993967E-07-0.57996520E-11 0.63080191E+05 0.42892461E+01
4
C3H2-2 S 4/01C 3H 2 0 OG 200.000 3000.000
1

```
7.47247827E+00 4.57765160E-03-1.56482125E-06
2.43991965E-10-1.42462924E-14      2
8.83321441E+04-1.27113314E+01 3.74356467E+00
2.51955211E-02-4.62608277E-05      3
4.34360520E-08-1.53992558E-11 8.89297787E+04 4.22612394E+00
9.08356403E+04      4
cC3H2      121686C      3H      2      G      0300.00      5000.00
1000.00      1
0.06530853E+02 0.05870316E-01-0.01720777E-04
0.02127498E-08-0.08291910E-13      2
0.05115214E+06-0.01122728E+03 0.02691077E+02
0.01480366E+00-0.03250551E-04      3
-0.08644363E-07 0.05284878E-10 0.05219072E+06 0.08757391E+02
4
C3H3      T 5/97C      3H      3      0      OG      200.000      6000.000
1
7.14221880E+00 7.61902005E-03-2.67459950E-06
4.24914801E-10-2.51475415E-14      2
3.89087427E+04-1.25848436E+01 1.35110927E+00
3.27411223E-02-4.73827135E-05      3
3.76309808E-08-1.18540923E-11 4.01057783E+04 1.52058924E+01
4.16139977E+04      4
aC3H4      L 8/89C      3H      4      0      OG      200.000      6000.000
1
0.63168722E+01 0.11133728E-01-0.39629378E-05
0.63564238E-09-0.37875540E-13      2
0.20117495E+05-0.10995766E+02 0.26130445E+01 0.12122575E-01
0.18539880E-04      3
-0.34525149E-07 0.15335079E-10 0.21541567E+05 0.10226139E+02
0.22962267E+05      4
pC3H4      T 2/90H      4C      3      0      OG      200.000      6000.000
1
0.60252400E+01 0.11336542E-01-0.40223391E-05
0.64376063E-09-0.38299635E-13      2
0.19620942E+05-0.86043785E+01 0.26803869E+01 0.15799651E-01
0.25070596E-05      3
-0.13657623E-07 0.66154285E-11 0.20802374E+05 0.98769351E+01
0.22302059E+05      4
cC3H4      T12/81C      3H      4      0      OG      300.000      5000.000
1
0.66999931E+01 0.10357372E-01-0.34551167E-05
0.50652949E-09-0.26682276E-13      2
0.30199051E+05-0.13378770E+02-0.24621047E-01
0.23197215E-01-0.18474357E-05      3
-0.15927593E-07 0.86846155E-11 0.32334137E+05 0.22729762E+02 0.3332728
E+05      4
C3H8      F11/94C      3H      8      0      OG      300.000      3000.000
1
0.75244152E+01 0.18898282E-01-0.62921041E-05
0.92161457E-09-0.48684478E-13      2
-0.16564394E+05-0.17838375E+02 0.92851093E+00 0.26460566E-01
0.60332446E-05      3
```

```
-0.21914953E-07 0.94961544E-11-0.14057907E+05 0.19225538E+02
4
nC3H7          P11/94C   3H   7   0   OG   300.000  3000.000
1
  0.77097479E+01 0.16031485E-01-0.52720238E-05
0.75888352E-09-0.38862719E-13   2
  0.79762236E+04-0.15515297E+02 0.10491173E+01 0.26008973E-01
0.23542516E-05   3
-0.19595132E-07 0.93720207E-11 0.10312346E+05 0.21136034E+02
4
iC3H7          P11/94C   3H   7   0   OG   300.000  3000.000
1
  0.65192741E+01 0.17220104E-01-0.57364217E-05
0.84130732E-09-0.44565913E-13   2
  0.73227193E+04-0.90830215E+01 0.14449199E+01 0.20999112E-01
0.77036222E-05   3
-0.18476253E-07 0.71282962E-11 0.94223724E+04 0.20116317E+02
4
C3H6           120186C   3H   6           G   0300.00  5000.00
1000.00   1
  0.06732257E+02 0.01490834E+00-0.04949899E-04
0.07212022E-08-0.03766204E-12   2
-0.09235703E+04-0.01331335E+03 0.01493307E+02 0.02092518E+00
0.04486794E-04   3
-0.01668912E-06 0.07158146E-10 0.01074826E+05 0.01614534E+03
4
CH2CHCO        T05/99C   3H   3O   1   OG   200.000  6000.0
1000.0   1
  6.95842227E+00 1.07193211E-02-3.85218494E-06
6.22009064E-10-3.72401640E-14   2
  5.64826498E+03-1.14745786E+01 3.21169467E+00 1.18422105E-02
1.67462582E-05   3
-3.06947176E-08 1.33048816E-11 7.12815750E+03 1.00881663E+01
8.70564832E+03   4
CH2CHCO        USC/07C   3H   3O   1   OG   300.000  5000.000
1
  0.73338666E+01 0.11401899E-01-0.45696443E-05
0.79430967E-09-0.44163078E-13   2
  0.83094941E+04-0.11019943E+02 0.23135836E+01
0.28253129E-01-0.25737754E-04   3
  0.12222654E-07-0.21353429E-11 0.95213496E+04 0.14105129E+02
4
CH3CHOCH2      T 6/92C   3H   6O   1   OG   298.150  3000.0
1000.0   1
  0.86900558E 01 0.16020987E-01-0.53971753E-05
0.79941542E-09-0.42656366E-13   2
-0.15420691E 05-0.22485016E 02 0.48733836E 00 0.28519690E-01
0.30096162E-05   3
-0.22652642E-07 0.10706728E-10-0.12556434E 05 0.22605270E 02-0.11156446E
05   4
CH3CH2CHO      USC/07C   3H   6O   1   OG   300.000  5000.000
1
```


0.62637410E+01 0.19976260E-01-0.76195147E-05
0.11687118E-08-0.41959993E-13 2
-0.25885953E+05-0.57786498E+01 0.27255676E+01 0.23236005E-01
0.29740656E-05 3
-0.16613415E-07 0.74250103E-11-0.24556711E+05 0.14166277E+02
4
CH3COCH3 T 5/92C 3H 6O 1 OG 200.000 6000.000
1000.0 1
0.72975991E+01 0.17566207E-01-0.63170456E-05
0.10203086E-08-0.61094016E-13 2
-0.29817680E+05-0.12756981E+02 0.55557943E+01-0.28365428E-02
0.70568945E-04 3
-0.87810488E-07 0.34028266E-10-0.28113337E+05
0.23226600E+01-0.26116945E+05 4
C2H3CHO USC/07C 3H 4O 1 OG 300.000 5000.000
1
0.58111868E+01 0.17114256E-01-0.74834161E-05
0.14252249E-08-0.91746841E-13 2
-0.10784054E+05-0.48588004E+01 0.12713498E+01
0.26231054E-01-0.92912305E-05 3
-0.47837272E-08 0.33480543E-11-0.93357344E+04 0.19498077E+02
4
aC3H5 PD5/98C 3H 5 0 OG 300.000 3000.000
1
0.65007877E+01 0.14324731E-01-0.56781632E-05
0.11080801E-08-0.90363887E-13 2
0.17482449E+05-0.11243050E+02 0.13631835E+01 0.19813821E-01
0.12497060E-04 3
-0.33355555E-07 0.15846571E-10 0.19245629E+05 0.17173214E+02
4
CH3CCH2 PD5/98C 3H 5 0 OG 300.000 3000.000
1
0.54255528E+01 0.15511072E-01-0.56678350E-05
0.79224388E-09-0.16878034E-13 2
0.27843027E+05-0.33527184E+01 0.17329209E+01
0.22394620E-01-0.51490611E-05 3
-0.67596466E-08 0.38253211E-11 0.29040498E+05 0.16568878E+02
4
CH3CHCH PD5/98C 3H 5 0 OG 300.000 3000.000
1
0.53725281E+01 0.15780509E-01-0.59922850E-05
0.93089664E-09-0.36550966E-13 2
0.29614760E+05-0.34186478E+01 0.91372931E+00
0.26432343E-01-0.11758950E-04 3
-0.23035678E-08 0.27715488E-11 0.30916867E+05 0.19989269E+02
4
C4H P 1/93C 4H 1 0 OG 300.000 3000.000
1
0.77697593E+01 0.49829976E-02-0.17628546E-05
0.28144284E-09-0.16689869E-13 2
0.94345900E+05-0.14165274E+02 0.13186295E+01
0.38582956E-01-0.71385623E-04 3

0.65356359E-07-0.22617666E-10 0.95456106E+05 0.15567583E+02
4
C4H2 D11/99C 4H 2 0 OG 300.000 3000.000
1
0.91576328E+01 0.55430518E-02-0.13591604E-05 0.18780075E-10
0.23189536E-13 2
0.52588039E+05-0.23711460E+02 0.10543978E+01
0.41626960E-01-0.65871784E-04 3
0.53257075E-07-0.16683162E-10 0.54185211E+05 0.14866591E+02
4
nC4H3 USC/07C 4H 3O 0 OG 300.000 5000.000
1
0.78045716E+01 0.10712364E-01-0.41939124E-05
0.70446277E-09-0.36271326E-13 2
0.62987805E+05-0.14129741E+02 0.81667686E+00
0.38716201E-01-0.48045651E-04 3
0.32066808E-07-0.85628215E-11 0.64455754E+05 0.19740503E+02
4
iC4H3 USC/07C 4H 3O 0 OG 300.000 5000.000
1
0.76538548E+01 0.11204055E-01-0.46401342E-05
0.86786639E-09-0.57430562E-13 2
0.57954363E+05-0.11756476E+02 0.37221482E+01
0.25957543E-01-0.26356343E-04 3
0.15508920E-07-0.38040565E-11 0.58837121E+05 0.75637245E+01
4
H2C4O USC/07C 4H 2O 1 OG 300.000 5000.000
1
0.84292183E+01 0.10502701E-01-0.42066836E-05
0.71184902E-09-0.35796602E-13 2
0.22907807E+05-0.16511997E+02 0.31811900E+01
0.29840752E-01-0.32832409E-04 3
0.20631813E-07-0.54200598E-11 0.24125576E+05 0.94210100E+01
4
C4H4 USC/07C 4H 4O 0 OG 300.000 5000.000
1
0.72539601E+01 0.13914094E-01-0.52932214E-05
0.83480450E-09-0.35197882E-13 2
0.31766016E+05-0.12629521E+02 0.58857048E+00
0.36546685E-01-0.34106968E-04 3
0.16652619E-07-0.30064623E-11 0.33359492E+05 0.20657881E+02
4
nC4H5 USC/07C 4H 5O 0 OG 300.000 5000.000
1
0.74087291E+01 0.17752748E-01-0.75601506E-05
0.14203795E-08-0.91100182E-13 2
0.40438762E+05-0.13150027E+02 0.22611290E+00
0.36742371E-01-0.22120474E-04 3
0.14390138E-08 0.26435809E-11 0.42428410E+05 0.24066401E+02
4
iC4H5 USC/07C 4H 5O 0 OG 300.000 5000.000
1

```

0.69646029E+01 0.18274333E-01-0.78133735E-05
0.15292154E-08-0.10920493E-12 2
0.34725098E+05-0.10649321E+02 0.11308105E+00
0.40950615E-01-0.35413581E-04 3
0.15530969E-07-0.23355122E-11 0.36383371E+05 0.23692457E+02
4
C4H5-2 H6W/94C 4H 5 0 0G 300.000 3000.000
1
1.45381710E+01-8.56770560E-03 2.35595240E-05-1.36763790E-08
2.44369270E-12 2
3.32590950E+04-4.53694970E+01 2.96962800E+00
2.44422450E-02-9.12514240E-06 3
-4.24668710E-18 1.63047280E-21 3.55033160E+04 1.20360510E+01
3.73930550E+04 4
c-C4H5 PUPM3 C 4H 5 0 0G 300.000 3000.000
1
0.67467155E+01 0.17283000E-01-0.65168579E-05
0.98917574E-09-0.34604908E-13 2
0.32808359E+05-0.12912880E+02-0.26397593E+01
0.41549157E-01-0.21920954E-04 3
-0.46559014E-08 0.61348890E-11 0.35373828E+05 0.35701797E+02
4
C4H7 USC/07C 4H 7O 0 0G 300.000 5000.000
1
0.70134835E+01 0.22634558E-01-0.92545470E-05
0.16807927E-08-0.10408617E-12 2
0.20955008E+05-0.88893080E+01 0.74449432E+00
0.39678857E-01-0.22898086E-04 3
0.21352973E-08 0.23096375E-11 0.22653328E+05 0.23437878E+02
4
C4H6 H6W/94C 4H 6 0 0G 300.000 3000.000
1
0.88673134E+01 0.14918670E-01-0.31548716E-05-0.41841330E-09
0.15761258E-12 2
0.91338516E+04-0.23328171E+02 0.11284465E+00
0.34369022E-01-0.11107392E-04 3
-0.92106660E-08 0.62065179E-11 0.11802270E+05 0.23089996E+02
4
C4H612 A 8/83C 4H 6 0 0G 300. 3000.
1000.0 1
0.1781557E 02 -0.4257502E-02 0.1051185E-04 -0.4473844E-08
0.5848138E-12 2
0.1267342E 05 -0.6982662E 02 0.1023467E 01 0.3495919E-01
-0.2200905E-04 3
0.6942272E-08 -0.7879187E-12 0.1811799E 05 0.1975066E 02
0.1950807E+05 4
C4H6-2 A 8/83C 4H 6 0 0G 300. 3000.
1000.0 1
9.0338133E+00 8.2124510E-03 7.1753952E-06 -5.8834334E-09
1.0343915E-12 2
1.4335068E+04 -2.0985762E+01 2.1373338E+00 2.6486229E-02
-9.0568711E-06 3

```

-5.5386397E-19 2.1281884E-22 1.5710902E+04 1.3529426E+01
1.7488676E+04 4
C4H10 P11/94C 4H 10 0 OG 300.000 3000.000
1
0.10526774E+02 0.23590738E-01-0.78522480E-05
0.11448408E-08-0.59827703E-13 2
-0.20479223E+05-0.32198579E+02 0.15685419E+01 0.34652278E-01
0.68168129E-05 3
-0.27995097E-07 0.12307742E-10-0.17129977E+05 0.17908045E+02
4
iC4H10 P11/94C 4H 10 0 OG 300.000 3000.000
1
0.10846169E+02 0.23338389E-01-0.77833962E-05
0.11393807E-08-0.59918289E-13 2
-0.21669854E+05-0.35870573E+02 0.54109489E+00 0.37860301E-01
0.55459804E-05 3
-0.30500110E-07 0.14033357E-10-0.17977644E+05 0.21150935E+02
4
pC4H9 USC/07C 4H 90 0 OG 300.000 5000.000
1
0.86822395E+01 0.23691071E-01-0.75948865E-05 0.66427136E-09
0.54845136E-13 2
0.49644058E+04-0.17891747E+02 0.12087042E+01
0.38297497E-01-0.72660509E-05 3
-0.15428547E-07 0.86859435E-11 0.73221040E+04 0.22169268E+02
4
sC4H9 P11/94C 4H 9 0 OG 300.000 3000.000
1
0.94263839E+01 0.21918998E-01-0.72868375E-05
0.10630334E-08-0.55649464E-13 2
0.31965874E+04-0.22406051E+02 0.69428423E+00 0.33113346E-01
0.62942577E-05 3
-0.27025274E-07 0.11989315E-10 0.64175654E+04 0.26279789E+02
4
tC4H9 P11/94C 4H 9 0 OG 300.000 3000.000
1
0.76607261E+01 0.23879414E-01-0.80890353E-05
0.12057521E-08-0.65009814E-13 2
0.16207623E+04-0.14800281E+02 0.96167553E+00 0.25735856E-01
0.15609033E-04 3
-0.26656519E-07 0.89418010E-11 0.46564412E+04 0.24805366E+02
4
iC4H9 USC/07C 4H 90 0 OG 300.000 5000.000
1
0.84981728E+01 0.24689538E-01-0.86487589E-05
0.10779325E-08-0.64340570E-15 2
0.44288174E+04-0.18441397E+02 0.97527862E+00
0.41613799E-01-0.14467331E-04 3
-0.93852393E-08 0.68797377E-11 0.66688267E+04 0.21277582E+02
4
C4H81 T 6/83C 4H 8 0 OG 300.000 5000.000
1

0.20535841E+01 0.34350507E-01-0.15883197E-04
0.33089662E-08-0.25361045E-12 2
-0.21397231E+04 0.15543201E+02 0.11811380E+01 0.30853380E-01
0.50865247E-05 3
-0.24654888E-07 0.11110193E-10-0.17904004E+04 0.21062469E+02
4
C4H82 T 6/83C 4H 8 0 0G 300.000 5000.00
1
0.82797676E+00 0.35864539E-01-0.16634498E-04
0.34732759E-08-0.26657398E-12 2
-0.30521033E+04 0.21342545E+02 0.12594252E+01 0.27808424E-01
0.87013932E-05 3
-0.24402205E-07 0.98977710E-11-0.29647742E+04 0.20501129E+02
4
iC4H8 T 6/83H 8C 4 0 0G 300.000 5000.0
1
0.44609470E+01 0.29611487E-01-0.13077129E-04
0.26571934E-08-0.20134713E-12 2
-0.50066758E+04 0.10671549E+01 0.26471405E+01 0.25902957E-01
0.81985354E-05 3
-0.22193259E-07 0.88958580E-11-0.40373069E+04 0.12676388E+02
4
iC4H7 USC/07C 4H 7O 0 0G 300.000 5000.000
1
0.71485939E+01 0.22189671E-01-0.84400172E-05
0.13133353E-08-0.51617927E-13 2
0.12712294E+05-0.12131183E+02-0.10375890E+01
0.45566667E-01-0.30476231E-04 3
0.71102568E-08 0.99685722E-12 0.14896458E+05 0.29863663E+02
4
C2H3CHOCH2 A 8/83C 4H 6O 1 0G 300. 3000.
1000.0 1
-4.72093360E+00 3.91413780E-02-6.52872650E-06-7.68209500E-09
2.51473310E-12 2
1.75352252E+03 5.17190420E+01 7.97985440E-01
3.44034320E-02-1.24598510E-05 3
-5.18062790E-18 1.99359540E-21-6.48927540E+02 2.18896980E+01
1.00654250E+03 4
CH3CHCHCHO T 5/92C 4H 6O 1 0G 298.150 3000.0
1000.0 1
1.98794540E+01-2.09130550E-02 4.45360508E-05-2.60374870E-08
4.86836120E-12 2
-1.95278768E+04-6.87200320E+01-1.55577660E+00
4.09640630E-02-1.69868810E-05 3
-6.00928140E-18 2.31368530E-21-1.41394920E+04
3.74707580E+01-1.29340710E+04 4
CH2CHCOCH3 T 3/97C 4H 6O 1 0G 200.000 3000.0
1000.0 1
1.98794540E+01-2.09130550E-02 4.45360580E-05-2.60374870E-08
4.86836120E-12 2
-1.90786168E+04-6.97265750E+01-1.55577660E+00
4.09640630E-02-1.69868810E-05 3

-6.00928140E-18 2.31368530E-21-1.49447258E+04
3.64642160E+01-1.66079520E+04 4
C4H4O T03/97C 4H 4O 1 OG 200.000 6000.0
1000.0 1
9.38935003E+00 1.40291241E-02-5.07755110E-06
8.24137332E-10-4.95319963E-14 2
-8.68241814E+03-2.79162920E+01 8.47469463E-01 1.31773796E-02
5.99735901E-05 3
-9.71562904E-08 4.22733796E-11-5.36785445E+03
2.14945172E+01-4.17166616E+03 4
CH3CHCHCO USC/07C 4H 5O 1 OG 300.000 5000.000
1
0.77608204E+01 0.20031804E-01-0.80631016E-05
0.13361392E-08-0.62308408E-13 2
0.45708291E+04-0.11095638E+02 0.53053460E+01 0.15749373E-01
0.21623913E-04 3
-0.36607769E-07 0.14932489E-10 0.57588633E+04 0.42043533E+01
4
CH2CHCHCHO USC/07C 4H 5O 1 OG 300.000 5000.000
1
0.83010607E+01 0.19945331E-01-0.82903771E-05
0.15100753E-08-0.91581155E-13 2
0.15788387E+03-0.16910566E+02 0.12108673E+01
0.35205878E-01-0.10939090E-04 3
-0.11720642E-07 0.76174908E-11 0.22665703E+04 0.20613544E+02
4
CH2CHCH2CHO T 5/92C 4H 6O 1 OG 298.150 3000.0
1000.0 1
1.98794540E+01-2.09130550E-02 4.45360508E-05-2.60374870E-08
4.86836120E-12 2
-1.58539966E+04-6.71095639E+01-1.55577660E+00
4.09640630E-02-1.69868810E-05 3
-6.00928140E-18 2.31368530E-21-1.04656118E+04
3.90812260E+01-1.29340710E+04 4
C4H6O25 T 3/97C 4H 6O 1 OG 200.000 5000.000
1000.0 1
8.60658242E+00 2.08310051E-02-8.42229481E-06
1.56717640E-09-1.09391202E-13 2
-1.76177415E+04-2.32464750E+01 2.67053463E+00 4.92586420E-03
8.86967406E-05 3
-1.26219194E-07 5.23991321E-11-1.46572472E+04
1.45722395E+01-1.30831522E+04 4
C4H6O23 T 3/97C 4H 6O 1 OG 200.000 5000.000
1000.0 1
8.60658242E+00 2.08310051E-02-8.42229481E-06
1.56717640E-09-1.09391202E-13 2
-1.32392815E+04-2.32464750E+01 2.67053463E+00 4.92586420E-03
8.86967406E-05 3
-1.26219194E-07 5.23991321E-11-1.02787872E+04
1.45722395E+01-1.30831522E+04 4
sC4H9 T07/95C 4H 9 0 OG 200.000 6000.000
1000.0 1

```
0.88057265E+01 0.23630381E-01-0.84564737E-05
0.13612584E-08-0.81313232E-13      2
0.37941169E+04-0.19996770E+02 0.46457042E+01 0.79313214E-02
0.70027013E-04      3
-0.95973349E-07 0.38628890E-10 0.62341181E+04 0.79642808E+01
0.84190169E+04      4
C5H2      20587C      5H      2      G      0300.00      5000.00
1000.00      1
0.01132917E+03 0.07424057E-01-0.02628189E-04
0.04082541E-08-0.02301333E-12      2
0.07878706E+06-0.03617117E+03 0.03062322E+02
0.02709998E+00-0.01009170E-03      3
-0.01272745E-06 0.09167219E-10 0.08114969E+06 0.07071078E+02
4
C5H3      20387C      5H      3      G      0300.00      5000.00
1000.00      1
0.01078762E+03 0.09539619E-01-0.03206745E-04
0.04733323E-08-0.02512135E-12      2
0.06392904E+06-0.03005444E+03 0.04328720E+02
0.02352480E+00-0.05856723E-04      3
-0.01215449E-06 0.07726478E-10 0.06588531E+06 0.04173259E+02
4
C5H6      T 1/90C      5H      6      0      OG      200.000      6000.000
1
0.99757848E+01 0.18905543E-01-0.68411461E-05
0.11099340E-08-0.66680236E-13      2
0.11081693E+05-0.32209454E+02 0.86108957E+00 0.14804031E-01
0.72108895E-04      3
-0.11338055E-06 0.48689972E-10 0.14801755E+05 0.21353453E+02
0.16152485E+05      4
C5H5      T12/89C      5H      5      0      OG      300.00      2000.000
1000.00      1
0.74743938E+01 0.16012733E-01-0.64823148E-08-0.35819703E-08
0.92365071E-12      2
2.80860000E+04-0.16133000E+02 0.98349822E+00
0.33651476E-01-0.11054181E-06      3
-0.36743394E-07 0.23141184E-10 2.96260000E+04 0.16585519E+02
4
cC5H8      T03/97C      5H      8O      0      OG      200.000      6000.000
1000.0      1
0.77244792E+01 0.28322316E-01-0.11545236E-04
0.21540815E-08-0.15054178E-12      2
-0.78261573E+03-0.19769698E+02 0.26898140E+01 0.20954550E-02
0.11303687E-03      3
-0.15408070E-06 0.62763658E-10 0.23139663E+04 0.15294056E+02
0.39328836E+04      4
1C5H9      T03/97C      5H      9O      0      OG      200.000      6000.000
1000.0      1
0.20313000E+02 0.10869880E-01-0.19063805E-05 0.00000000E+00
0.00000000E+00      2
0.94061603E+04-0.82533815E+02 0.11430827E+01
0.44350789E-01-0.17825470E-04      3
```

```
0.00000000E+00 0.00000000E+00 0.16967656E+05 0.24181940E+02
0.19122233E+05      4
cC5H9      T03/97C      5H      9O      0      OG      200.000      6000.000
1000.0      1
0.11406802E+02 0.22563988E-01-0.70235595E-05
0.11321968E-08-0.73438204E-13      2
0.75268769E+04-0.39636280E+02 0.29427128E+00 0.13823374E-01
0.90847653E-04      3
-0.13008694E-06 0.53051811E-10 0.12565712E+05 0.27389773E+02
0.13838458E+05      4
C5H4O      T 8/99C      5H      4O      1      OG      200.000      6000.000
1
1.00806824E+01 1.61143465E-02-5.83314509E-06
9.46759320E-10-5.68972206E-14      2
1.94364771E+03-2.94521623E+01 2.64576497E-01 3.34873827E-02
1.67738470E-06      3
-2.96207455E-08 1.54431476E-11 5.11159287E+03 2.35409513E+01
6.64245999E+03      4
C5H4OH      T 8/99C      5H      5O      1      OG      200.000      6000.000
1
1.33741248E+01 1.51996469E-02-5.45685046E-06
8.80944866E-10-5.27493258E-14      2
2.20358027E+03-4.59569069E+01-1.28398054E+00
4.90298511E-02-1.35844414E-05      3
-2.92983743E-08 1.90820619E-11 6.37364803E+03 3.08073591E+01
8.00114499E+03      4
C5H5O(2,4)      D 9/97C      5H      5O      1      00G      300.000      3000.000
1
0.85405312E+01 0.22989510E-01-0.95437563E-05
0.17061612E-08-0.97459360E-13      2
0.22263699E+05-0.20818825E+02-0.30777600E+01
0.52581679E-01-0.28856513E-04      3
-0.33885479E-08 0.63361399E-11 0.25510455E+05 0.39591522E+02
0.26570048E+05      4
C5H5O(1,3)      DU0997C      5H      5O      1      00G      300.000      3000.000
1000.00      1
0.92431440E+01 0.22201257E-01-0.93105946E-05
0.17155222E-08-0.10613969E-12      2
0.15908394E+04-0.24087738E+02-0.29566984E+01
0.55851892E-01-0.37241636E-04      3
0.41624357E-08 0.39272010E-11 0.48573193E+04 0.38676682E+02
4
C5H5OH      HWZD99C      5H      6O      1      OG      300.000      3000.000
1
0.34893970E+01 0.38052600E-01-0.21654527E-04
0.59238574E-08-0.62763461E-12      2
-0.82131025E+04 0.71248055E+01-0.50430169E+01
0.71253479E-01-0.70918177E-04      3
0.38680220E-07-0.87888264E-11-0.64167788E+04 0.48617100E+02
4
bi-C5H4O      DU0997C      5H      4O      1      00G      300.000      3000.000
1000.00      1
```



```
0.10514051E+02 0.16667502E-01-0.61001861E-05
0.81804008E-09-0.88743752E-14      2
0.27501334E+05-0.30678673E+02-0.35879545E+01
0.59943721E-01-0.52969943E-04      3
0.19971461E-07-0.14667430E-11 0.31091709E+05 0.40873169E+02
4
1C5H6          HWZD99C   5H   6   0   0G   300.    3000.
1000.          1
0.86914568E+01 0.21268958E-01-0.79818547E-05
0.11795985E-08-0.35253359E-13      2
0.25763865E+05-0.19189083E+02 0.58391756E+00
0.42602919E-01-0.24962495E-04      3
0.25815752E-08 0.23169964E-11 0.28043699E+05 0.22916780E+02
4
1C5H7          HWZD99C   5H   7   0   0G   300.000  3000.000
1
0.22246480E+01 0.39601296E-01-0.22345617E-04
0.60649676E-08-0.63840047E-12      2
0.22303428E+05 0.14009951E+02-0.40974307E+01
0.61832044E-01-0.48770780E-04      3
0.16696418E-07-0.75334899E-12 0.23683646E+05 0.45148109E+02
4
C6H2          D11/99C   6H   2   0   0G   300.000  3000.000
1
0.12893918E+02 0.79145068E-02-0.24027240E-05 0.24340149E-09
0.31383246E-14      2
0.79832406E+05-0.40771996E+02 0.45099974E+00
0.67475192E-01-0.11809925E-03      3
0.10367632E-06-0.34851039E-10 0.82173062E+05 0.17704124E+02
4
C6H          P 1/93C   6H   1   0   0G   300.000  3000.000
1
0.12370055E+02 0.52177699E-02-0.16885009E-05
0.25807149E-09-0.15472851E-13      2
0.12158739E+06-0.34952797E+02-0.25630299E+00
0.63793827E-01-0.11440118E-03      3
0.10136744E-06-0.34361855E-10 0.12408855E+06 0.24930750E+02
4
1-C6H4          H6W/94C   6H   4   0   0G   300.000  3000.000
1
0.12715182E+02 0.13839662E-01-0.43765440E-05 0.31541636E-09
0.46619026E-13      2
0.57031148E+05-0.39464600E+02 0.29590225E+00
0.58053318E-01-0.67766756E-04      3
0.43376762E-07-0.11418864E-10 0.60001371E+05 0.22318970E+02
4
1-C6H6          H6W/94C   6H   6   0   0G   300.000  3000.000
1
0.17584442E+02 0.64486600E-02 0.48933980E-05-0.34696221E-08
0.56150749E-12      2
0.34111988E+05-0.66017838E+02-0.10170622E+01
0.61794821E-01-0.59461061E-04      3
```

```

0.31873491E-07-0.71717693E-11 0.39202707E+05 0.29460373E+02
4
c-C6H7          H6W/94C   6H   7   0   0G   300.000   3000.000
1
0.19996841E+02 0.11189543E-02 0.11649756E-04-0.62779471E-08
0.94939508E-12 2
0.16730059E+05-0.83746933E+02-0.30328493E+01
0.50804518E-01-0.69150292E-05 3
-0.29715974E-07 0.16296353E-10 0.23895383E+05 0.38909180E+02
4
n-C6H7          H6W/94C   6H   7   0   0G   300.000   3000.000
1
0.22577469E+02-0.30737517E-02 0.14225234E-04-0.69880848E-08
0.10232874E-11 2
0.41228980E+05-0.91568619E+02 0.13248032E+00
0.57103366E-01-0.43712644E-04 3
0.15538603E-07-0.12976356E-11 0.47730512E+05 0.25339081E+02
4
C6H8            H6W/94C   6H   8   0   0G   300.000   3000.000
1
0.28481979E+02-0.15702948E-01 0.26771697E-04-0.11780109E-07
0.16573427E-11 2
0.93346445E+04-0.12500226E+03 0.15850439E+01 0.40215142E-01
0.78439543E-05 3
-0.38761325E-07 0.18545207E-10 0.17949613E+05 0.19112625E+02
4
cC6H8            T03/97C   6H   8O   0   0G   200.000   6000.000
1000.0 1
0.11779870E+02 0.25519980E-01-0.92666947E-05
0.15068122E-08-0.90658701E-13 2
0.65486686E+04-0.41618805E+02 0.17265319E+01 0.14887612E-01
0.94809230E-04 3
-0.14083394E-06 0.58859873E-10 0.11021297E+05 0.19130886E+02
0.12784878E+05 4
1cC6H9           T 2/92C   6H   9O   0   0G   200.000   3000.000
1000.0 1
0.23165919E+02 0.10813608E-01-0.17638168E-05 0.00000000E+00
0.00000000E+00 2
0.11162402E+05-0.98600332E+02 0.31671271E+00
0.52069818E-01-0.21965057E-04 3
0.00000000E+00 0.00000000E+00 0.19926824E+05 0.27879902E+02
0.22141533E+05 4
cC6H9            T 2/92C   6H   9O   0   0G   200.000   3000.000
1000.0 1
0.26295828E+02 0.86828857E-02-0.15770376E-05 0.00000000E+00
0.00000000E+00 2
0.20863563E+04-0.12573825E+03-0.35714300E+01
0.61696043E-01-0.26928803E-04 3
0.00000000E+00 0.00000000E+00 0.13657039E+05 0.39986250E+02
0.15096500E+05 4
cC6H10           T03/97C   6H  10O   0   0G   200.000   6000.000
1000.0 1

```

```
0.11773904E+02 0.30947360E-01-0.11234330E-04
0.18262494E-08-0.10985119E-12      2
-0.72028376E+04-0.42658688E+02 0.23662378E+01 0.10681712E-01
0.11822112E-03      3
-0.16567854E-06 0.67612802E-10-0.24824973E+04
0.16769357E+02-0.55324968E+03      4
C6H3          H6W/94C  6H  3    0    OG  300.000  3000.000
1
0.58188343E+01 0.27933408E-01-0.17825427E-04
0.53702536E-08-0.61707627E-12      2
0.85188250E+05-0.92147827E+00 0.11790619E+01
0.55547360E-01-0.73076168E-04      3
0.52076736E-07-0.15046964E-10 0.85647312E+05 0.19179199E+02
4
i-C6H5          H6W/94C  6H  5    0    OG  300.000  3000.000
1
0.22501663E+02-0.81009977E-02 0.15955695E-04-0.72310371E-08
0.10310424E-11      2
0.58473410E+05-0.91224777E+02-0.78585434E+00
0.60221825E-01-0.62890264E-04      3
0.36310730E-07-0.87000259E-11 0.64942270E+05 0.28658905E+02
4
i-C6H7          H6W/94C  6H  7    0    OG  300.000  3000.000
1
0.20481506E+02 0.79439697E-03 0.11450761E-04-0.60991177E-08
0.91756724E-12      2
0.37728426E+05-0.81812073E+02-0.17099094E+01
0.62486034E-01-0.54290707E-04      3
0.26959682E-07-0.58999090E-11 0.44086621E+05 0.33344772E+02
4
o-C6H4          D11/99C  6H  4    0    OG  300.000  3000.000
1
0.88432961E+01 0.20301474E-01-0.88674269E-05
0.17264292E-08-0.11786047E-12      2
0.49317113E+05-0.24014301E+02-0.38454189E+01
0.58391564E-01-0.48644750E-04      3
0.16770320E-07-0.78580680E-12 0.52592500E+05 0.40587132E+02
4
m-C6H4          D11/99C  6H  4    0    OG  300.000  3000.000
1
0.95307283E+01 0.19178549E-01-0.80941481E-05
0.14811132E-08-0.88632260E-13      2
0.56865535E+05-0.27623203E+02-0.39450364E+01
0.59887171E-01-0.50811577E-04      3
0.17603140E-07-0.72608743E-12 0.60323117E+05 0.40899506E+02
4
p-C6H4          D11/99C  6H  4    0    OG  300.000  3000.000
1
0.98300371E+01 0.18499156E-01-0.75165058E-05
0.12727610E-08-0.61767120E-13      2
0.64446117E+05-0.29418266E+02-0.39744728E+01
0.58399867E-01-0.44950713E-04      3
```

```
0.10307744E-07 0.22412619E-11 0.68058992E+05 0.41168865E+02
4
1-C6H4Z          D11/99C   6H   4   0   0G   300.000  3000.000
1
0.11186811E+02 0.17122138E-01-0.73898623E-05
0.14678845E-08-0.10733922E-12 2
0.60743207E+05-0.29537384E+02 0.20895090E+01
0.53276263E-01-0.63299172E-04 3
0.40811642E-07-0.10598600E-10 0.62662203E+05 0.14613283E+02
4
nC6H5            D11/99C   6H   5   0   0G   300.000  3000.000
1
0.11263281E+02 0.19379666E-01-0.76874276E-05
0.12866819E-08-0.63244650E-13 2
0.68052773E+05-0.30487534E+02-0.27013230E+00
0.59389681E-01-0.60963321E-04 3
0.33169378E-07-0.71466453E-11 0.70785828E+05 0.26953651E+02
4
C6H5             D11/99C   6H   5   0   0G   300.000  3000.000
1
0.85973110E+01 0.22241630E-01-0.87199978E-05
0.13788785E-08-0.53146056E-13 2
0.36261047E+05-0.22954643E+02-0.36931453E+01
0.52178968E-01-0.25558427E-04 3
-0.70661121E-08 0.75833975E-11 0.39779590E+05 0.41332535E+02
4
C6H6             D11/99C   6H   6   0   0G   300.000  3000.000
1
0.91381245E+01 0.23854433E-01-0.88127726E-05
0.12099021E-08-0.18221503E-13 2
0.52043462E+04-0.29115665E+02-0.48437734E+01
0.58427613E-01-0.29485855E-04 3
-0.69390440E-08 0.82125253E-11 0.91817773E+04 0.43889832E+02
4
C5H5CH3          P 1/93C   6H   8   0   0G   300.000  2500.000
1
0.14628364E+02 0.19849248E-01-0.50529134E-05 0.10556275E-10
0.11381723E-12 2
0.55674092E+04-0.56114021E+02-0.45763016E-01 0.29978730E-01
0.61898092E-04 3
-0.11171783E-06 0.49435803E-10 0.10927480E+05 0.26558569E+02
4
C5H4CH2          P 1/93C   6H   6   0   0G   300.000  2500.000
1
0.75731055E+04-0.18843678E+02 0.17058320E-01-0.65980571E-05
0.93053393E-09 2
-0.22894220E+07-0.40003195E+05 0.78428810E+02-0.43919629E+00
0.13370259E-02 3
-0.14196110E-05 0.56357985E-09 0.22226365E+05-0.41005380E+03
4
C6H5C6H5         HW /94C   12H  10   0   0G   300.000  3000.000
1
```

0.50761871E+02-0.34501564E-01 0.50293413E-04-0.21559579E-07
0.30097192E-11 2
0.21538867E+04-0.24670712E+03-0.10283234E+02
0.12428707E+00-0.95990268E-04 3
0.32294793E-07-0.23045229E-11 0.20165258E+05 0.72707947E+02
4
C6H5C2H H6W/94C 8H 6 0 OG 300.000 3000.000
1
0.24090759E+02 0.78232400E-03 0.11453964E-04-0.61620504E-08
0.93346685E-12 2
0.27429445E+05-0.10499631E+03-0.52645016E+01
0.84511042E-01-0.76597848E-04 3
0.33216978E-07-0.47673063E-11 0.35566242E+05 0.46378815E+02
4
C6H5CH3 L 6/87C 7H 8 0 OG 200.000 6000.000
1
0.12940034E+02 0.26691287E-01-0.96838505E-05
0.15738629E-08-0.94663601E-13 2
-0.69764908E+03-0.46728785E+02 0.16152663E+01 0.21099438E-01
0.85366018E-04 3
-0.13261066E-06 0.55956604E-10 0.40756300E+04 0.20282210E+02
0.60135835E+04 4
C6H5CH2 T08/90C 7H 7 0 OG 200.000 6000.000
1
0.14043980E+02 0.23493873E-01-0.85375367E-05
0.13890841E-08-0.83614420E-13 2
0.18564203E+05-0.51665589E+02 0.48111540E+00 0.38512832E-01
0.32861492E-04 3
-0.76972721E-07 0.35423068E-10 0.23307027E+05 0.23548820E+02
0.25317186E+05 4
C6H5C2H3 T12/94C 8H 8 0 OG 298.150 5000.000
1
0.16139277E+02 0.24210847E-01-0.72678359E-05
0.11392276E-08-0.72984881E-13 2
0.10249251E+05-0.61169437E+02-0.10717708E+02
0.12666725E+00-0.17762493E-03 3
0.14344049E-06-0.47616577E-10 0.16597133E+05 0.71526331E+02
0.17723291E+05 4
C6H5CH2OH L 7/87C 7H 8O 1 OG 200.000 6000.000
1000.00 1
0.15281154E+02 0.27208501E-01-0.98584660E-05
0.16012183E-08-0.96278057E-13 2
-0.19700471E+05-0.59418673E+02 0.20642021E+01 0.22775140E-01
0.95972053E-04 3
-0.15085110E-06 0.64175832E-10-0.14285021E+05
0.18148312E+02-0.12077200E+05 4
C6H5CHO L 3/86C 7H 6O 1 OG 298.150 5000.000
1000.00 1
0.13650737E+02 0.25680419E-01-0.10466729E-04
0.19413430E-08-0.13483792E-12 2
-0.11019744E+05-0.47965796E+02-0.31627334E+01
0.66369245E-01-0.34816353E-04 3

```

-0.62999377E-08 0.85807101E-11-0.61169349E+04
0.40231735E+02-0.44259974E+04      4
C6H5CO      EST/BUR P 1/93C      7H      5O      1      OG      300.000      2500.000
1
  0.13374409E+02 0.23999289E-01-0.10465724E-04
0.21669131E-08-0.18007045E-12      2
  0.69147837E+04-0.44659218E+02-0.20251155E+01
0.61512541E-01-0.31603653E-04      3
-0.69724599E-08 0.79835149E-11 0.11255803E+05 0.35778175E+02
4
C6H4O2      PUML96C      6H      4O      2      OG      300.000      5000.000
1000.000      1
  0.11730840E+02 0.23614995E-01-0.10234576E-04
0.19532174E-08-0.12746022E-12      2
-0.21085770E+05-0.36300453E+02-0.95193005E+00
0.57842445E-01-0.38214439E-04      3
  0.46312656E-08 0.36296651E-11-0.17611047E+05 0.29239513E+02
4
C6H5O      T05/02C      6H      5O      1      OG      200.000      6000.000
1000.000      1
  1.37221720E+01 1.74688771E-02-6.35504520E-06
1.03492308E-09-6.23410504E-14      2
  2.87274751E+02-4.88181680E+01-4.66204455E-01 4.13443975E-02
1.32412991E-05      3
-5.72872769E-08 2.89763707E-11 4.77858391E+03 2.76990274E+01
6.49467016E+03      4
C6H5OH      L 4/84C      6H      6O      1      OG      300.000      5000.000
1
  0.14912073E 02 0.18378135E-01-0.61983128E-05
0.91983221E-09-0.49209565E-13      2
-0.18375199E 05-0.55924103E 02-0.16956539E 01
0.52271299E-01-0.72024050E-05      3
-0.35859603E-07 0.20449073E-10-0.13284121E 05 0.32542160E 02-0.11594207E
05      4
C6H5C2H5      A 6/83C      8H      10      0      OG      300.      3000.
1000.00      1
  0.3878978E 01 0.5810059E-01 -0.3196380E-04 0.8448993E-08
-0.8694825E-12      2
  -0.5024922E 03 0.3837099E 01 -0.7266845E 01 0.1003089E 00
-0.9651715E-04      3
  0.5565908E-07 -0.1453370E-10 0.1987290E 04 0.5857746E 02
0.3529492E+04      4
HOC6H4CH3 AVG CRESOL6/87C      7H      8O      1      OG      200.000      6000.000
1000.00      1
  0.15932987E+02 0.27011160E-01-0.99448722E-05
0.16296689E-08-0.98513298E-13      2
-0.23592065E+05-0.59732841E+02 0.42258267E+00 0.45551636E-01
0.32012513E-04      3
-0.81121959E-07 0.37665658E-10-0.18202621E+05
0.26032903E+02-0.15911701E+05      4
OC6H4CH3 EST/BUR P 1/93C      7H      7O      1      OG      300.000      2500.000
1

```

```
0.22609371E+02 0.75646150E-02 0.65960894E-05-0.47150865E-08
0.80409063E-12      2
-0.82025244E+04-0.97292511E+02-0.28855777E+00 0.48003536E-01
0.18032993E-04      3
-0.61741488E-07 0.28852587E-10-0.68945581E+03 0.26720068E+02
4
bi-C6H5CH2          A 6/83C 14H 14      0      0G      300.      3000.
1000.00      1
0.7292035E 01 0.9250200E-01 -0.5168641E-04 0.1362709E-07
-0.1381148E-11      2
0.1031673E 05 -0.1132738E 02 -0.1388958E 02 0.1720984E 00
-0.1700660E-03      3
0.9601888E-07 -0.2373253E-10 0.1503234E 05 0.9270736E 02
0.1721641E+05      4
C10H8              H6W/94C 10H 8      0      0G      300.000 3000.000
1
0.36468643E+02-0.15419513E-01 0.30160038E-04-0.13700120E-07
0.19582730E-11      2
0.35091445E+04-0.17329489E+03-0.94505043E+01
0.11137849E+00-0.10345667E-03      3
0.52800392E-07-0.11804439E-10 0.16695594E+05 0.65187668E+02
4
C6H4CH3            P 1/93C 7H 7      0      0G      300.000 2500.000
1
0.11615498E+02 0.27431838E-01-0.10899345E-04
0.18641830E-08-0.10191607E-12      2
0.31209334E+05-0.38994637E+02-0.31415942E+01
0.56723077E-01-0.86885111E-05      3
-0.34249616E-07 0.19266902E-10 0.35738547E+05 0.39742840E+02
4
NC5H12      1/ 2/ 7 THERMC 5H 12      0      0G      300.000 5000.000
1390.000      41
1.57257603E+01 2.61086045E-02-8.90970996E-06
1.38102248E-09-8.00296536E-14      2
-2.60519543E+04-6.03365457E+01-7.36766122E-01
6.07200973E-02-3.57592761E-05      3
1.04907042E-08-1.21487315E-12-1.98934934E+04 2.95358287E+01
4
PXC5H11      1/ 2/ 7 THERMC 5H 11      0      0G      300.000 5000.000
1390.000      41
1.52977446E+01 2.39735310E-02-8.18392948E-06
1.26883076E-09-7.35409055E-14      2
-9.80712307E+02-5.44829293E+01 5.24384081E-02
5.60796958E-02-3.31545803E-05      3
9.77533781E-09-1.14009660E-12 4.71611460E+03 2.87238666E+01
4
SXC5H11      1/ 2/ 7 THERMC 5H 11      0      0G      300.000 5000.000
1377.000      41
1.50998007E+01 2.37225333E-02-8.01388900E-06
1.23431039E-09-7.12300125E-14      2
-2.33420039E+03-5.29613979E+01 4.98943592E-01
5.09850184E-02-2.40687488E-05      3
```

```
3.59465211E-09 3.01383099E-13 3.40702366E+03 2.78600953E+01
4
S2XC5H11 1/ 2/ 7 THERMC 5H 11 0 OG 300.000 5000.000
1377.000 41
1.50998007E+01 2.37225333E-02-8.01388900E-06
1.23431039E-09-7.12300125E-14 2
-2.33420039E+03-5.29613979E+01 4.98943592E-01
5.09850184E-02-2.40687488E-05 3
3.59465211E-09 3.01383099E-13 3.40702366E+03 2.78600953E+01
4
C5H10 1/ 2/ 7 THERMC 5H 10 0 OG 300.000 5000.000
1392.000 31
1.45851539E+01 2.24072471E-02-7.63348025E-06
1.18188966E-09-6.84385139E-14 2
-1.00898205E+04-5.23683936E+01-1.06223481E+00
5.74218294E-02-3.74486890E-05 3
1.27364989E-08-1.79609789E-12-4.46546666E+03 3.22739790E+01
4
PXC5H9 1/ 2/ 7 THERMC 5H 9 0 OG 300.000 5000.000
1386.000 31
1.45546753E+01 2.04331611E-02-7.07391431E-06
1.10720105E-09-6.46021493E-14 2
6.76813422E+03-5.37243740E+01-1.22720644E+00
5.49419289E-02-3.56284020E-05 3
1.18245127E-08-1.61716004E-12 1.25391664E+04 3.19626373E+01
4
NC6H14 1/ 2/ 7 THERMC 6H 14 0 OG 300.000 5000.000
1390.000 51
1.89634117E+01 3.04480204E-02-1.03794829E-05
1.60775457E-09-9.31269728E-14 2
-3.01628739E+04-7.62839355E+01-9.69606184E-01
7.29085608E-02-4.38853919E-05 3
1.32312807E-08-1.58437423E-12-2.27803862E+04 3.23069798E+01
4
PXC6H13 1/ 2/ 7 THERMC 6H 13 0 OG 300.000 5000.000
1390.000 51
1.85385470E+01 2.83107962E-02-9.65307246E-06
1.49547585E-09-8.66336064E-14 2
-5.09299041E+03-7.04490943E+01-2.04871465E-01
6.83801272E-02-4.14447912E-05 3
1.26155802E-08-1.53120058E-12 1.83280393E+03 3.16075093E+01
4
SXC6H13 1/ 2/ 7 THERMC 6H 13 0 OG 300.000 5000.000
1380.000 51
1.83687363E+01 2.80268110E-02-9.47032396E-06
1.45888527E-09-8.42002461E-14 2
-6.46093974E+03-6.90934018E+01 2.29560149E-01
6.33327323E-02-3.24135431E-05 3
6.46387687E-09-9.61420427E-14 5.25639156E+02 3.08006138E+01
4
S2XC6H13 1/ 2/ 7 THERMC 6H 13 0 OG 300.000 5000.000
1380.000 51
```



```
1.83687363E+01 2.80268110E-02-9.47032396E-06
1.45888527E-09-8.42002461E-14      2
-6.46093974E+03-6.90934018E+01 2.29560149E-01
6.33327323E-02-3.24135431E-05      3
6.46387687E-09-9.61420427E-14 5.25639156E+02 3.08006138E+01
4
C6H12      1/22/ 7 THERMC      6H 12      0      OG      300.000 5000.000
1392.000    41
1.78337529E+01 2.67377658E-02-9.10036773E-06
1.40819768E-09-8.15124244E-14      2
-1.42062860E+04-6.83818851E+01-1.35275205E+00
6.98655426E-02-4.59408022E-05      3
1.56967343E-08-2.21296175E-12-7.34368617E+03 3.53120691E+01
4
PXC6H11    1/22/ 7 THERMC      6H 11      0      OG      300.000 5000.000
1389.000    41
1.77336550E+01 2.48934775E-02-8.59991450E-06
1.34412828E-09-7.83475666E-14      2
2.68017174E+03-6.93471508E+01-1.55544944E+00
6.76865602E-02-4.47048635E-05      3
1.52236630E-08-2.14346377E-12 9.66316695E+03 3.51482658E+01
4
NC7H16     1/ 2/ 7 THERMC      7H 16      0      OG      300.000 5000.000
1391.000    61
2.22148969E+01 3.47675750E-02-1.18407129E-05
1.83298478E-09-1.06130266E-13      2
-3.42760081E+04-9.23040196E+01-1.26836187E+00
8.54355820E-02-5.25346786E-05      3
1.62945721E-08-2.02394925E-12-2.56586565E+04 3.53732912E+01
4
PXC7H15     1/ 2/ 7 THERMC      7H 15      0      OG      300.000 5000.000
1390.000    61
2.17940709E+01 3.26280243E-02-1.11138244E-05
1.72067148E-09-9.96366999E-14      2
-9.20938221E+03-8.64954311E+01-4.99570406E-01
8.08826467E-02-5.00532754E-05      3
1.56549308E-08-1.96616227E-12-1.04590223E+03 3.46564011E+01
4
SXC7H15     1/ 2/ 7 THERMC      7H 15      0      OG      300.000 5000.000
1382.000    61
2.16368842E+01 3.23324804E-02-1.09273807E-05
1.68357060E-09-9.71774091E-14      2
-1.05873616E+04-8.52209653E+01-3.79155767E-02
7.56726570E-02-4.07473634E-05      3
9.32678943E-09-4.92360745E-13-2.35605303E+03 3.37321506E+01
4
S2XC7H15    1/ 2/ 7 THERMC      7H 15      0      OG      300.000 5000.000
1382.000    61
2.16368842E+01 3.23324804E-02-1.09273807E-05
1.68357060E-09-9.71774091E-14      2
-1.05873616E+04-8.52209653E+01-3.79155767E-02
7.56726570E-02-4.07473634E-05      3
```

9.32678943E-09-4.92360745E-13-2.35605303E+03 3.37321506E+01
4
S3XC7H15 1/ 2/ 7 THERMC 7H 15 0 OG 300.000 5000.000
1382.000 61
2.16368842E+01 3.23324804E-02-1.09273807E-05
1.68357060E-09-9.71774091E-14 2
-1.05873616E+04-8.52209653E+01-3.79155767E-02
7.56726570E-02-4.07473634E-05 3
9.32678943E-09-4.92360745E-13-2.35605303E+03 3.37321506E+01
4
C7H14 1/ 2/ 7 THERMC 7H 14 0 OG 300.000 5000.000
1392.000 51
2.10898039E+01 3.10607878E-02-1.05644793E-05
1.63405780E-09-9.45598219E-14 2
-1.83260065E+04-8.44391108E+01-1.67720549E+00
8.24611601E-02-5.46504108E-05 3
1.87862303E-08-2.65737983E-12-1.02168601E+04 3.85068032E+01
4
PXC7H13 1/ 2/ 7 THERMC 7H 13 0 OG 300.000 5000.000
1389.000 51
2.09278134E+01 2.92841022E-02-1.00899640E-05
1.57425554E-09-9.16505991E-14 2
-1.41296217E+03-8.50447021E+01-1.66945935E+00
7.93202117E-02-5.20231516E-05 3
1.74804211E-08-2.40912996E-12 6.75927466E+03 3.73759517E+01
4
NC8H18 1/ 2/ 7 THERMC 8H 18 0 OG 300.000 5000.000
1391.000 71
2.54710194E+01 3.90887037E-02-1.33038777E-05
2.05867527E-09-1.19167174E-13 2
-3.83962755E+04-1.08361094E+02-1.54218406E+00
9.78112063E-02-6.09318358E-05 3
1.92005591E-08-2.42996250E-12-2.85395641E+04 3.83327978E+01
4
PXC8H17 1/ 2/ 7 THERMC 8H 17 0 OG 300.000 5000.000
1390.000 71
2.50510356E+01 3.69480162E-02-1.25765264E-05
1.94628409E-09-1.12668898E-13 2
-1.33300535E+04-1.02557384E+02-7.72759438E-01
9.32549705E-02-5.84447245E-05 3
1.85570214E-08-2.37127483E-12-3.92689511E+03 3.76130631E+01
4
SXC8H17 1/ 2/ 7 THERMC 8H 17 0 OG 300.000 5000.000
1383.000 71
2.49043504E+01 3.66393792E-02-1.23849888E-05
1.90835394E-09-1.10160725E-13 2
-1.47135299E+04-1.01344740E+02-3.04233324E-01
8.80077253E-02-4.90742611E-05 3
1.21857563E-08-8.87773198E-13-5.23792835E+03 3.66582632E+01
4
S2XC8H17 1/ 2/ 7 THERMC 8H 17 0 OG 300.000 5000.000
1383.000 71

```
2.49043504E+01 3.66393792E-02-1.23849888E-05
1.90835394E-09-1.10160725E-13 2
-1.47135299E+04-1.01344740E+02-3.04233324E-01
8.80077253E-02-4.90742611E-05 3
1.21857563E-08-8.87773198E-13-5.23792835E+03 3.66582632E+01
4
S3XC8H17 1/ 2/ 7 THERMC 8H 17 0 0G 300.000 5000.000
1383.000 71
2.49043504E+01 3.66393792E-02-1.23849888E-05
1.90835394E-09-1.10160725E-13 2
-1.47135299E+04-1.01344740E+02-3.04233324E-01
8.80077253E-02-4.90742611E-05 3
1.21857563E-08-8.87773198E-13-5.23792835E+03 3.66582632E+01
4
C8H16 1/ 2/ 7 THERMC 8H 16 0 0G 300.000 5000.000
1392.000 61
2.43540125E+01 3.53666462E-02-1.20208388E-05
1.85855053E-09-1.07522262E-13 2
-2.24485674E+04-1.00537716E+02-1.89226915E+00
9.46066357E-02-6.27385521E-05 3
2.15158309E-08-3.02718683E-12-1.31074559E+04 4.11878981E+01
4
PXC8H15 1/ 2/ 7 THERMC 8H 15 0 0G 300.000 5000.000
1390.000 61
2.41485380E+01 3.36466429E-02-1.15692934E-05
1.80261649E-09-1.04847473E-13 2
-5.51631151E+03-1.00894875E+02-1.90098561E+00
9.15067740E-02-6.01588113E-05 3
2.02337556E-08-2.78235289E-12 3.87213558E+03 4.01405031E+01
4
NC9H20 1/ 2/ 7 THERMC 9H 20 0 0G 300.000 5000.000
1391.000 81
2.87289600E+01 4.34074576E-02-1.47660985E-05
2.28420987E-09-1.32194796E-13 2
-4.25174479E+04-1.24428751E+02-1.81390458E+00
1.10176644E-01-6.93124463E-05 3
2.20957601E-08-2.83355715E-12-3.14207716E+04 4.12827220E+01
4
PXC9H19 1/ 2/ 7 THERMC 9H 19 0 0G 300.000 5000.000
1390.000 81
2.83097514E+01 4.12657344E-02-1.40383289E-05
2.17174871E-09-1.25692307E-13 2
-1.74516030E+04-1.16837897E+02-1.04387292E+00
1.05617283E-01-6.68199971E-05 3
2.14486166E-08-2.77404275E-12-6.80818512E+03 4.23518992E+01
4
SXC9H19 1/ 2/ 7 THERMC 9H 19 0 0G 300.000 5000.000
1386.000 81
2.80393256E+01 4.11440297E-02-1.39260043E-05
2.14745952E-09-1.24022172E-13 2
-1.87727855E+04-1.16696832E+02-5.76046059E-01
1.00511821E-01-5.77755119E-05 3
```

```
1.53276702E-08-1.35056750E-12-8.12289806E+03 3.95795606E+01
4
S2XC9H19 1/ 2/ 7 THERMC 9H 19 0 OG 300.000 5000.000
1386.000 81
2.80393256E+01 4.11440297E-02-1.39260043E-05
2.14745952E-09-1.24022172E-13 2
-1.87727855E+04-1.16696832E+02-5.76046059E-01
1.00511821E-01-5.77755119E-05 3
1.53276702E-08-1.35056750E-12-8.12289806E+03 3.95795606E+01
4
S3XC9H19 1/ 2/ 7 THERMC 9H 19 0 OG 300.000 5000.000
1386.000 81
2.80393256E+01 4.11440297E-02-1.39260043E-05
2.14745952E-09-1.24022172E-13 2
-1.87727855E+04-1.16696832E+02-5.76046059E-01
1.00511821E-01-5.77755119E-05 3
1.53276702E-08-1.35056750E-12-8.12289806E+03 3.95795606E+01
4
S4XC9H19 1/ 2/ 7 THERMC 9H 19 0 OG 300.000 5000.000
1386.000 81
2.80393256E+01 4.11440297E-02-1.39260043E-05
2.14745952E-09-1.24022172E-13 2
-1.87727855E+04-1.16696832E+02-5.76046059E-01
1.00511821E-01-5.77755119E-05 3
1.53276702E-08-1.35056750E-12-8.12289806E+03 3.95795606E+01
4
C9H18 1/ 2/ 7 THERMC 9H 18 0 OG 300.000 5000.000
1392.000 71
2.76142176E+01 3.96825287E-02-1.34819446E-05
2.08390452E-09-1.20539294E-13 2
-2.65709061E+04-1.16618623E+02-2.16108263E+00
1.06958297E-01-7.10973244E-05 3
2.43971077E-08-3.42771547E-12-1.59890847E+04 4.41245128E+01
4
PXC9H17 1/ 3/ 7 THERMC 9H 17 0 OG 300.000 5000.000
1390.000 71
2.73846125E+01 3.79931250E-02-1.30425564E-05
2.02998652E-09-1.17985203E-13 2
-9.62653063E+03-1.17685762E+02-2.20061475E+00
1.03997426E-01-6.87316813E-05 3
2.32482420E-08-3.21153346E-12 9.95158605E+02 4.23691203E+01
4
NC10H22 1/ 2/ 7 THERMC 10H 22 0 OG 300.000 5000.000
1391.000 91
3.19882239E+01 4.77244922E-02-1.62276391E-05
2.50963259E-09-1.45215772E-13 2
-4.66392840E+04-1.40504121E+02-2.08416969E+00
1.22535012E-01-7.76815739E-05 3
2.49834877E-08-3.23548038E-12-3.43021863E+04 4.42260140E+01
4
PXC10H21 1/ 2/ 7 THERMC 10H 21 0 OG 300.000 5000.000
1390.000 91
```

```
3.15697160E+01 4.55818403E-02-1.54994965E-05
2.39710933E-09-1.38709559E-13      2
-2.15737832E+04-1.34708986E+02-1.31358348E+00
1.17972813E-01-7.51843079E-05      3
2.43331106E-08-3.17522852E-12-9.68967550E+03 4.35010452E+01
4
SXC10H21 1/ 2/ 7 THERMC 10H 21 0 0G 300.000 5000.000
1385.000 91
3.14447580E+01 4.52778532E-02-1.53145696E-05
2.36072411E-09-1.36311835E-13      2
-2.29702700E+04-1.33634423E+02-9.30536886E-01
1.13137924E-01-6.64034118E-05      3
1.83220872E-08-1.77128003E-12-1.09890165E+04 4.29335080E+01
4
S2XC10H21 1/ 2/ 7 THERMC 10H 21 0 0G 300.000 5000.000
1385.000 91
3.14447580E+01 4.52778532E-02-1.53145696E-05
2.36072411E-09-1.36311835E-13      2
-2.29702700E+04-1.33634423E+02-9.30536886E-01
1.13137924E-01-6.64034118E-05      3
1.83220872E-08-1.77128003E-12-1.09890165E+04 4.29335080E+01
4
S3XC10H21 1/ 2/ 7 THERMC 10H 21 0 0G 300.000 5000.000
1385.000 91
3.14447580E+01 4.52778532E-02-1.53145696E-05
2.36072411E-09-1.36311835E-13      2
-2.29702700E+04-1.33634423E+02-9.30536886E-01
1.13137924E-01-6.64034118E-05      3
1.83220872E-08-1.77128003E-12-1.09890165E+04 4.29335080E+01
4
S4XC10H21 1/ 2/ 7 THERMC 10H 21 0 0G 300.000 5000.000
1385.000 91
3.14447580E+01 4.52778532E-02-1.53145696E-05
2.36072411E-09-1.36311835E-13      2
-2.29702700E+04-1.33634423E+02-9.30536886E-01
1.13137924E-01-6.64034118E-05      3
1.83220872E-08-1.77128003E-12-1.09890165E+04 4.29335080E+01
4
C10H20 1/22/ 7 THERMC 10H 20 0 0G 300.000 5000.000
1392.000 81
3.08753903E+01 4.39971526E-02-1.49425530E-05
2.30917678E-09-1.33551477E-13      2
-3.06937307E+04-1.32705172E+02-2.42901688E+00
1.19305598E-01-7.94489025E-05      3
2.72736596E-08-3.82718373E-12-1.88708365E+04 4.70571383E+01
4
PXC10H19 1/22/ 7 THERMC 10H 19 0 0G 300.000 5000.000
1390.000 81
3.06442992E+01 4.23089356E-02-1.45032261E-05
2.25520722E-09-1.30991162E-13      2
-1.37453412E+04-1.32907157E+02-2.49340025E+00
1.16496175E-01-7.73332421E-05      3
```

```
2.62845301E-08-3.64630937E-12-1.88400568E+03 4.62584816E+01
4
NC11H24 1/22/ 7 THERMC 11H 24 0 OG 300.000 5000.000
1391.000 11
3.52484813E+01 5.20402416E-02-1.76886732E-05
2.73497226E-09-1.58231832E-13 2
-5.07616214E+04-1.56585288E+02-2.35338447E+00
1.34888270E-01-8.60424000E-05 3
2.78658195E-08-3.63619953E-12-3.71837502E+04 4.71645217E+01
4
PXC11H23 1/22/ 7 THERMC 11H 23 0 OG 300.000 5000.000
1391.000 11
3.48306023E+01 4.98967610E-02-1.69601993E-05
2.62239406E-09-1.51722334E-13 2
-2.56964317E+04-1.50793815E+02-1.58230042E+00
1.30323530E-01-8.35408417E-05 3
2.72125730E-08-3.57529580E-12-1.25713075E+04 4.64373071E+01
4
SXC11H23 1/22/ 7 THERMC 11H 23 0 OG 300.000 5000.000
1385.000 11
3.47027943E+01 4.95633551E-02-1.67588574E-05
2.58285265E-09-1.49118584E-13 2
-2.70891758E+04-1.49690851E+02-1.10250355E+00
1.25021794E-01-7.40802024E-05 3
2.07818900E-08-2.07855904E-12-1.38839647E+04 4.54310281E+01
4
S2XC11H23 1/22/ 7 THERMC 11H 23 0 OG 300.000 5000.000
1385.000 11
3.47027943E+01 4.95633551E-02-1.67588574E-05
2.58285265E-09-1.49118584E-13 2
-2.70891758E+04-1.49690851E+02-1.10250355E+00
1.25021794E-01-7.40802024E-05 3
2.07818900E-08-2.07855904E-12-1.38839647E+04 4.54310281E+01
4
S3XC11H23 1/22/ 7 THERMC 11H 23 0 OG 300.000 5000.000
1385.000 11
3.47027943E+01 4.95633551E-02-1.67588574E-05
2.58285265E-09-1.49118584E-13 2
-2.70891758E+04-1.49690851E+02-1.10250355E+00
1.25021794E-01-7.40802024E-05 3
2.07818900E-08-2.07855904E-12-1.38839647E+04 4.54310281E+01
4
S4XC11H23 1/22/ 7 THERMC 11H 23 0 OG 300.000 5000.000
1385.000 11
3.47027943E+01 4.95633551E-02-1.67588574E-05
2.58285265E-09-1.49118584E-13 2
-2.70891758E+04-1.49690851E+02-1.10250355E+00
1.25021794E-01-7.40802024E-05 3
2.07818900E-08-2.07855904E-12-1.38839647E+04 4.54310281E+01
4
S5XC11H23 1/22/ 7 THERMC 11H 23 0 OG 300.000 5000.000
1385.000 11
```

```
3.47027943E+01 4.95633551E-02-1.67588574E-05
2.58285265E-09-1.49118584E-13      2
-2.70891758E+04-1.49690851E+02-1.10250355E+00
1.25021794E-01-7.40802024E-05      3
2.07818900E-08-2.07855904E-12-1.38839647E+04 4.54310281E+01
4
C11H22      1/ 2/ 7 THERMC 11H 22      0      0G      300.000 5000.000
1392.000      91
3.41376800E+01 4.83102359E-02-1.64025319E-05
2.53434308E-09-1.46557255E-13      2
-3.48170932E+04-1.48798197E+02-2.69653994E+00
1.31650370E-01-8.77957172E-05      3
3.01467965E-08-4.22584486E-12-2.17526343E+04 4.99879917E+01
4
PXC11H21    1/ 2/ 7 THERMC 11H 21      0      0G      300.000 5000.000
1390.000      91
3.38968067E+01 4.66347047E-02-1.59682128E-05
2.48119562E-09-1.44045675E-13      2
-1.78637749E+04-1.48943146E+02-2.77277326E+00
1.28897937E-01-8.57717335E-05      3
2.92169310E-08-4.05817299E-12-4.76410432E+03 4.92434369E+01
4
NC12H26     1/ 2/ 7 THERMC 12H 26      0      0G      300.000 5000.000
1391.000      11
3.85095037E+01 5.63550048E-02-1.91493200E-05
2.96024862E-09-1.71244150E-13      2
-5.48843465E+04-1.72670922E+02-2.62181594E+00
1.47237711E-01-9.43970271E-05      3
3.07441268E-08-4.03602230E-12-4.00654253E+04 5.00994626E+01
4
PXC12H25    1/ 2/ 7 THERMC 12H 25      0      0G      300.000 5000.000
1390.000      11
3.80921885E+01 5.42107848E-02-1.84205517E-05
2.84762173E-09-1.64731748E-13      2
-2.98194375E+04-1.66882734E+02-1.85028741E+00
1.42670708E-01-9.18916555E-05      3
3.00883392E-08-3.97454300E-12-1.54530435E+04 4.93702421E+01
4
SXC12H25    1/ 2/ 7 THERMC 12H 25      0      0G      300.000 5000.000
1385.000      11
3.79688268E+01 5.38719464E-02-1.82171263E-05
2.80774503E-09-1.62108420E-13      2
-3.12144988E+04-1.65805933E+02-1.36787089E+00
1.37355348E-01-8.24076158E-05      3
2.36421562E-08-2.47435932E-12-1.67660539E+04 4.83521895E+01
4
S2XC12H25   1/ 2/ 7 THERMC 12H 25      0      0G      300.000 5000.000
1385.000      11
3.79688268E+01 5.38719464E-02-1.82171263E-05
2.80774503E-09-1.62108420E-13      2
-3.12144988E+04-1.65805933E+02-1.36787089E+00
1.37355348E-01-8.24076158E-05      3
```

2.36421562E-08-2.47435932E-12-1.67660539E+04 4.83521895E+01
4
S3XC12H25 1/ 2/ 7 THERMC 12H 25 0 OG 300.000 5000.000
1385.000 11
3.79688268E+01 5.38719464E-02-1.82171263E-05
2.80774503E-09-1.62108420E-13 2
-3.12144988E+04-1.65805933E+02-1.36787089E+00
1.37355348E-01-8.24076158E-05 3
2.36421562E-08-2.47435932E-12-1.67660539E+04 4.83521895E+01
4
S4XC12H25 1/ 2/ 7 THERMC 12H 25 0 OG 300.000 5000.000
1385.000 11
3.79688268E+01 5.38719464E-02-1.82171263E-05
2.80774503E-09-1.62108420E-13 2
-3.12144988E+04-1.65805933E+02-1.36787089E+00
1.37355348E-01-8.24076158E-05 3
2.36421562E-08-2.47435932E-12-1.67660539E+04 4.83521895E+01
4
S5XC12H25 1/ 2/ 7 THERMC 12H 25 0 OG 300.000 5000.000
1385.000 11
3.79688268E+01 5.38719464E-02-1.82171263E-05
2.80774503E-09-1.62108420E-13 2
-3.12144988E+04-1.65805933E+02-1.36787089E+00
1.37355348E-01-8.24076158E-05 3
2.36421562E-08-2.47435932E-12-1.67660539E+04 4.83521895E+01
4
C12H24 1/22/ 7 THERMC 12H 24 0 OG 300.000 5000.000
1391.000 11
3.74002111E+01 5.26230753E-02-1.78624319E-05
2.75949863E-09-1.59562499E-13 2
-3.89405962E+04-1.64892663E+02-2.96342681E+00
1.43992360E-01-9.61384015E-05 3
3.30174473E-08-4.62398190E-12-2.46345299E+04 5.29158870E+01
4
PXC12H23 1/22/ 7 THERMC 12H 23 0 OG 300.000 5000.000
1391.000 11
3.71516071E+01 5.09574750E-02-1.74320046E-05
2.70698624E-09-1.57088382E-13 2
-2.19833461E+04-1.64992468E+02-3.04897817E+00
1.41284540E-01-9.41858477E-05 3
3.21335288E-08-4.46649750E-12-7.64465960E+03 5.22139103E+01
4
PC2H5O2 1/24/ 7 THERMC 2H 50 2 OG 300.000 5000.000
1382.000 21
9.48931216E+00 1.24402783E-02-4.31809356E-06
6.76915985E-10-3.95348408E-14 2
-7.52261739E+03-2.17786688E+01 2.30095124E+00
2.75312844E-02-1.68081734E-05 3
5.69376219E-09-8.76790905E-13-4.74134679E+03 1.76237375E+01
4
CH2CH2OOH 1/24/ 7 THERMC 2H 50 2 OG 300.000 5000.000
1382.000 31

1.15505529E+01 1.04299962E-02-3.66358169E-06
5.78998600E-10-3.40113553E-14 2
-7.80691513E+02-3.17628437E+01 2.04987307E+00
3.20347201E-02-2.27815550E-05 3
8.49241660E-09-1.33090473E-12 2.62922119E+03 1.95586851E+01
4
OOC2H4OOH 1/24/ 7 THERMC 2H 5O 4 OG 300.000 5000.000
1380.000 41
1.54580704E+01 1.19277842E-02-4.21396998E-06
6.68549393E-10-3.93768340E-14 2
-1.96569195E+04-4.69248307E+01 3.40736063E+00
4.09221341E-02-3.20927884E-05 3
1.34150840E-08-2.34667668E-12-1.54603745E+04 1.76595898E+01
4
PX22OOH 1/24/ 7 THERMC 2H 5O 4 OG 300.000 5000.000
1378.000 51
1.67992281E+01 1.04805951E-02-3.74283905E-06
5.98116130E-10-3.54072328E-14 2
-1.40531787E+04-5.24230006E+01 3.20263505E+00
4.28067975E-02-3.37303553E-05 3
1.35610096E-08-2.23338556E-12-9.35423134E+03 2.04591974E+01
4
C2H4O3 1/24/ 7 THERMC 2H 4O 3 OG 300.000 5000.000
1392.000 31
1.32937132E+01 9.01153234E-03-3.18927469E-06
5.06625091E-10-2.98677537E-14 2
-3.40338147E+04-3.99732856E+01-2.06900994E+00
5.25847638E-02-5.18552940E-05 3
2.54086373E-08-4.86654489E-12-2.94278951E+04 3.98760686E+01
4
C2H3O2 1/24/ 7 THERMC 2H 3O 2 OG 300.000 5000.000
1388.000 11
8.19923244E+00 8.90299466E-03-3.10715408E-06
4.88920007E-10-2.86317312E-14 2
-1.39601291E+04-1.48830229E+01-1.94624296E-01
3.03512584E-02-2.51547825E-05 3
1.11865557E-08-2.05106603E-12-1.11603465E+04 2.96606902E+01
4
PC3H7O2 1/24/ 7 THERMC 3H 7O 2 OG 300.000 5000.000
1384.000 31
1.26357393E+01 1.69827075E-02-5.88449466E-06
9.21409117E-10-5.37718183E-14 2
-1.16176813E+04-3.72565529E+01 2.13045105E+00
3.94902478E-02-2.47276910E-05 3
8.43817447E-09-1.27443437E-12-7.63844515E+03 2.00989657E+01
4
C3H6OOH 1/24/ 7 THERMC 3H 7O 2 OG 300.000 5000.000
1369.000 41
1.45698875E+01 1.45471186E-02-4.97634313E-06
7.73606581E-10-4.49528816E-14 2
-6.23146757E+03-4.60581941E+01 2.24247295E+00
3.92932185E-02-2.21205540E-05 3

5.25219959E-09-3.03945067E-13-1.56553748E+03 2.15536099E+01
4
SOO3OOH 1/24/ 7 THERMC 3H 7O 4 OG 300.000 5000.000
1386.000 51
1.91746808E+01 1.59836134E-02-5.61163915E-06
8.86584005E-10-5.20674192E-14 2
-2.60898463E+04-6.65194463E+01 2.65369491E+00
5.73946173E-02-4.70605755E-05 3
2.04360185E-08-3.65661909E-12-2.05292590E+04 2.13875379E+01
4
PX23OOH 1/24/ 7 THERMC 3H 7O 4 OG 300.000 5000.000
1383.000 61
2.05603679E+01 1.45470162E-02-5.15526020E-06
8.19639773E-10-4.83499291E-14 2
-2.05279108E+04-7.23203440E+01 3.16202783E+00
5.58668519E-02-4.32748674E-05 3
1.71231784E-08-2.77162256E-12-1.45254858E+04 2.09298268E+01
4
OC3OOH 1/24/ 7 THERMC 3H 6O 3 OG 300.000 5000.000
1388.000 41
1.70756225E+01 1.31013491E-02-4.61949408E-06
7.31991329E-10-4.30788679E-14 2
-4.14341300E+04-6.00660684E+01 1.10507238E+00
5.27396706E-02-4.31805774E-05 3
1.81618292E-08-3.10535568E-12-3.60960199E+04 2.49229905E+01
4
C3H5O2 1/24/ 7 THERMC 3H 5O 2 OG 300.000 5000.000
1395.000 21
1.27827539E+01 1.21529347E-02-4.21228103E-06
6.59844007E-10-3.85228684E-14 2
-2.15946846E+04-3.94512036E+01 5.06096897E-01
4.26121702E-02-3.37628379E-05 3
1.39422914E-08-2.35317319E-12-1.74952136E+04 2.58742916E+01
4
PC4H9O2 7/21/ 7 THERMC 4H 9O 2 OG 300.000 5000.000
1385.000 41
1.57885198E+01 2.15113203E-02-7.44430353E-06
1.16468602E-09-6.79304977E-14 2
-1.57130491E+04-5.27655101E+01 1.96571170E+00
5.14318324E-02-3.26177841E-05 3
1.11567625E-08-1.66463146E-12-1.05367011E+04 2.25454581E+01
4
P4OOHX2 7/21/ 7 THERMC 4H 9O 2 OG 300.000 5000.000
1378.000 51
1.75660043E+01 1.92995354E-02-6.62807784E-06
1.03236762E-09-6.00471622E-14 2
-1.02570294E+04-6.06710767E+01 1.99364612E+00
5.16680683E-02-3.07831330E-05 3
8.52209906E-09-8.26023222E-13-4.45218241E+03 2.43797452E+01
4
SOO4OOH 7/21/ 7 THERMC 4H 9O 4 OG 300.000 5000.000
1386.000 61

```
2.23375875E+01 2.05289862E-02-7.18257603E-06
1.13213314E-09-6.63793653E-14      2
-3.01526876E+04-8.20048369E+01 2.89457505E+00
6.84091648E-02-5.42459976E-05      3
2.29905385E-08-4.05214453E-12-2.35131454E+04 2.17695099E+01
4
PX24OOH      7/21/ 7 THERMC      4H      9O      4      OG      300.000 5000.000
1384.000      71
2.36907774E+01 1.91226272E-02-6.73730913E-06
1.06700255E-09-6.27709453E-14      2
-2.46195340E+04-8.77139674E+01 3.02159850E+00
6.76990412E-02-5.10265711E-05      3
1.97840777E-08-3.15505435E-12-1.74272393E+04 2.32647720E+01
4
OC4OOH      7/21/ 7 THERMC      4H      8O      3      OG      300.000 5000.000
1388.000      51
2.02458485E+01 1.76440360E-02-6.19054598E-06
9.77688024E-10-5.74053258E-14      2
-4.55474174E+04-7.57027174E+01 8.05387149E-01
6.52375119E-02-5.18373651E-05      3
2.13454896E-08-3.59860255E-12-3.89728623E+04 2.80026741E+01
4
C4H7O2      7/21/ 7 THERMC      4H      7O      2      OG      300.000 5000.000
1394.000      31
1.59446603E+01 1.66618871E-02-5.76277391E-06
9.01410802E-10-5.25718677E-14      2
-2.56924242E+04-5.50091509E+01 3.17744215E-01
5.46400822E-02-4.17564571E-05      3
1.67073275E-08-2.75020492E-12-2.03894402E+04 2.84337893E+01
4
PC5H11O2     7/22/ 7 THERMC      5H     11O      2      OG      300.000 5000.000
1387.000      51
1.89824681E+01 2.60214213E-02-9.00135472E-06
1.40790906E-09-8.21012334E-14      2
-1.98249259E+04-6.85173928E+01 1.41983707E+00
6.52267797E-02-4.33517452E-05      3
1.56669657E-08-2.45437421E-12-1.33819243E+04 2.67222874E+01
4
P5OOHX2      7/22/ 7 THERMC      5H     11O      2      OG      300.000 5000.000
1380.000      61
2.08416568E+01 2.36351604E-02-8.10335374E-06
1.26070679E-09-7.32695103E-14      2
-1.43977675E+04-7.68684713E+01 1.72033478E+00
6.40156524E-02-3.91021679E-05      3
1.13900588E-08-1.22859688E-12-7.33261274E+03 2.73415581E+01
4
SOO5OOH      7/22/ 7 THERMC      5H     11O      4      OG      300.000 5000.000
1387.000      71
2.55592601E+01 2.50247849E-02-8.73680730E-06
1.37514179E-09-8.05469362E-14      2
-3.42869979E+04-9.79406604E+01 2.52410060E+00
8.12115701E-02-6.32391949E-05      3
```

2.63186824E-08-4.56646696E-12-2.63797224E+04 2.51754337E+01
4
PX25OOH 7/22/ 7 THERMC 5H 110 4 OG 300.000 5000.000
1386.000 81
2.68348828E+01 2.36685990E-02-8.30519400E-06
1.31174779E-09-7.70232202E-14 2
-2.87121458E+04-1.03175816E+02 2.85622158E+00
7.96549256E-02-5.89528565E-05 3
2.25355531E-08-3.55442817E-12-2.03256817E+04 2.57119698E+01
4
OC5OOH 7/22/ 7 THERMC 5H 100 3 OG 300.000 5000.000
1389.000 61
2.34427049E+01 2.21540692E-02-7.74817880E-06
1.22107095E-09-7.15883644E-14 2
-4.96683256E+04-9.14852543E+01 5.64845658E-01
7.74889690E-02-6.00818427E-05 3
2.42432817E-08-4.02329880E-12-4.18594976E+04 3.08029042E+01
4
C5H9O2 7/22/ 7 THERMC 5H 90 2 OG 300.000 5000.000
1394.000 41
1.91083079E+01 2.11672546E-02-7.31157960E-06
1.14266852E-09-6.66010584E-14 2
-2.97898371E+04-7.05745277E+01 1.46352927E-01
6.66042570E-02-4.96612966E-05 3
1.94183992E-08-3.13536799E-12-2.32865742E+04 3.09121584E+01
4
PC6H13O2 7/23/ 7 THERMC 6H 130 2 OG 300.000 5000.000
1387.000 61
2.21334608E+01 3.05481753E-02-1.05598344E-05
1.65091157E-09-9.62413767E-14 2
-2.39223175E+04-8.40214284E+01 1.25016716E+00
7.71245157E-02-5.11312712E-05 3
1.83000166E-08-2.82326599E-12-1.62775792E+04 2.92057449E+01
4
P6OOHX2 7/23/ 7 THERMC 6H 130 2 OG 300.000 5000.000
1383.000 71
2.39171282E+01 2.82747269E-02-9.70956200E-06
1.51192849E-09-8.79148147E-14 2
-1.84595636E+04-9.19362687E+01 1.51238631E+00
7.61892915E-02-4.74214582E-05 3
1.44213983E-08-1.69480959E-12-1.02250902E+04 2.99815152E+01
4
SOO6OOH 7/23/ 7 THERMC 6H 130 4 OG 300.000 5000.000
1388.000 81
2.87911006E+01 2.95103558E-02-1.02872369E-05
1.61753482E-09-9.46779632E-14 2
-3.84279173E+04-1.13939723E+02 2.18820873E+00
9.38148007E-02-7.18812053E-05 3
2.94075675E-08-5.02502378E-12-2.92504137E+04 2.84300982E+01
4
PX26OOH 7/23/ 7 THERMC 6H 130 4 OG 300.000 5000.000
1386.000 91

2.99831673E+01 2.82004173E-02-9.86590110E-06
1.55513766E-09-9.11872003E-14 2
-3.28044110E+04-1.18656463E+02 2.68555415E+00
9.16313678E-02-6.69052410E-05 3
2.52952900E-08-3.95379637E-12-2.32232462E+04 2.81842684E+01
4
OC6OOH 7/23/ 7 THERMC 6H 120 3 OG 300.000 5000.000
1389.000 71
2.66361304E+01 2.66581586E-02-9.30182328E-06
1.46363129E-09-8.57154695E-14 2
-5.37857426E+04-1.07242249E+02 3.70119591E-01
8.95274436E-02-6.80060352E-05 3
2.69373082E-08-4.40174703E-12-4.47527753E+04 3.33930705E+01
4
C6H11O2 7/23/ 7 THERMC 6H 110 2 OG 300.000 5000.000
1394.000 51
2.22727578E+01 2.56709901E-02-8.85962065E-06
1.38378656E-09-8.06213153E-14 2
-3.38871575E+04-8.61434536E+01-1.78738656E-02
7.85411929E-02-5.75279491E-05 3
2.21061716E-08-3.51539687E-12-2.61849273E+04 3.33563267E+01
4
PC7H15O2 7/23/ 7 THERMC 7H 150 2 OG 300.000 5000.000
1388.000 71
2.52805212E+01 3.50686994E-02-1.21140690E-05
1.89303487E-09-1.10321620E-13 2
-2.80153904E+04-9.94952300E+01 1.16872823E+00
8.86227339E-02-5.83104983E-05 3
2.05545044E-08-3.10713200E-12-1.91863784E+04 3.12821091E+01
4
P7OOHX2 7/23/ 7 THERMC 7H 150 2 OG 300.000 5000.000
1383.000 81
2.72132171E+01 3.25191534E-02-1.11379006E-05
1.73139496E-09-1.00559996E-13 2
-2.25930020E+04-1.08210835E+02 1.16890785E+00
8.88852920E-02-5.63088643E-05 3
1.76221371E-08-2.16358175E-12-1.30956911E+04 3.32616848E+01
4
SOO7OOH 7/23/ 7 THERMC 7H 150 4 OG 300.000 5000.000
1388.000 91
3.21342162E+01 3.39120040E-02-1.18112913E-05
1.85609745E-09-1.08598138E-13 2
-4.26106800E+04-1.30572580E+02 2.11485737E+00
1.05420561E-01-7.89368006E-05 3
3.14573966E-08-5.24630757E-12-3.21671216E+04 3.04245085E+01
4
PX27OOH 7/23/ 7 THERMC 7H 150 4 OG 300.000 5000.000
1387.000 01
3.31332803E+01 3.27239308E-02-1.14222936E-05
1.79770658E-09-1.05297523E-13 2
-3.68963515E+04-1.34144680E+02 2.51302821E+00
1.03610884E-01-7.48591563E-05 3

2.80514337E-08-4.35133762E-12-2.61203734E+04 3.06663357E+01
4
OC7OOH 7/23/ 7 THERMC 7H 14O 3 OG 300.000 5000.000
1390.000 81
2.98309487E+01 3.11575033E-02-1.08530721E-05
1.70574095E-09-9.98133019E-14 2
-5.79044572E+04-1.23008918E+02 1.40412408E-01
1.01694435E-01-7.61014621E-05 3
2.97275336E-08-4.79971555E-12-4.76400035E+04 3.61510273E+01
4
C7H13O2 7/23/ 7 THERMC 7H 13O 2 OG 300.000 5000.000
1393.000 61
2.54484609E+01 3.01518721E-02-1.03969304E-05
1.62294039E-09-9.45157396E-14 2
-3.79867982E+04-1.01771399E+02-2.04456941E-01
9.05778473E-02-6.55330934E-05 3
2.48675838E-08-3.90908323E-12-2.90799627E+04 3.59036730E+01
4
PC8H17O2 7/23/ 7 THERMC 8H 17O 2 OG 300.000 5000.000
1388.000 81
2.84302449E+01 3.95840608E-02-1.36658948E-05
2.13471787E-09-1.24373659E-13 2
-3.21095752E+04-1.14984838E+02 1.04091476E+00
1.00316326E-01-6.57704913E-05 3
2.29761685E-08-3.42654205E-12-2.20878679E+04 3.35755185E+01
4
P8OOHX2 7/23/ 7 THERMC 8H 17O 2 OG 300.000 5000.000
1385.000 91
3.03669825E+01 3.70383586E-02-1.26921785E-05
1.97354168E-09-1.14641217E-13 2
-2.66867096E+04-1.23722044E+02 9.59955361E-01
1.00992720E-01-6.44085076E-05 3
2.04462840E-08-2.57230312E-12-1.59864847E+04 3.59190575E+01
4
SOO8OOH 7/23/ 7 THERMC 8H 17O 4 OG 300.000 5000.000
1388.000 01
3.54136730E+01 3.83615941E-02-1.33505074E-05
2.09688181E-09-1.22641764E-13 2
-4.67797084E+04-1.46864750E+02 1.85311068E+00
1.17574065E-01-8.67169257E-05 3
3.39346549E-08-5.55919430E-12-3.50464051E+04 3.33576174E+01
4
PX28OOH 7/23/ 7 THERMC 8H 17O 4 OG 300.000 5000.000
1388.000 11
3.62844119E+01 3.72420506E-02-1.29758593E-05
2.03973644E-09-1.19372589E-13 2
-4.09880728E+04-1.49636918E+02 2.33966984E+00
1.15589699E-01-8.28100543E-05 3
3.08028911E-08-4.74720708E-12-2.90172395E+04 3.31532589E+01
4
OC8OOH 7/23/ 7 THERMC 8H 16O 3 OG 300.000 5000.000
1390.000 91

3.30306734E+01 3.56490492E-02-1.24008543E-05
1.94723076E-09-1.13871925E-13 2
-6.20229707E+04-1.38798244E+02-3.43441330E-02
1.13643959E-01-8.38830081E-05 3
3.23245110E-08-5.15504930E-12-5.05363609E+04 3.86484073E+01
4
C8H15O2 7/23/ 7 THERMC 8H 15O 2 0G 300.000 5000.000
1389.000 91
2.96179863E+01 3.34336914E-02-1.16323669E-05
1.82679865E-09-1.06839333E-13 2
-4.25836942E+04-1.23225296E+02-5.09122236E-01
1.02678797E-01-7.28395985E-05 3
2.67137726E-08-4.04491435E-12-3.19471351E+04 3.90811586E+01
4
PC9H19O2 7/23/ 7 THERMC 9H 19O 2 0G 300.000 5000.000
1388.000 91
3.15899231E+01 4.40952875E-02-1.52172499E-05
2.37642684E-09-1.38431228E-13 2
-3.62061771E+04-1.30528998E+02 8.84542185E-01
1.12206665E-01-7.35657702E-05 3
2.56222121E-08-3.79805529E-12-2.49870439E+04 3.59860090E+01
4
P9OOHX2 7/23/ 7 THERMC 9H 19O 2 0G 300.000 5000.000
1386.000 01
3.35220087E+01 4.15545664E-02-1.42451353E-05
2.21546266E-09-1.28708813E-13 2
-3.07805559E+04-1.39239129E+02 7.56421032E-01
1.13085975E-01-7.24983977E-05 3
2.32689264E-08-2.98140317E-12-1.88783467E+04 3.85493660E+01
4
SOO9OOH 7/23/ 7 THERMC 9H 19O 4 0G 300.000 5000.000
1388.000 11
3.86978865E+01 4.28068092E-02-1.48881806E-05
2.33742506E-09-1.36671441E-13 2
-5.09514745E+04-1.63185611E+02 1.61474515E+00
1.29613653E-01-9.43117826E-05 3
3.62914339E-08-5.84483896E-12-3.79290082E+04 3.61842500E+01
4
PX29OOH 7/23/ 7 THERMC 9H 19O 4 0G 300.000 5000.000
1388.000 21
3.94361752E+01 4.17564767E-02-1.45274806E-05
2.28139522E-09-1.33423385E-13 2
-4.50796411E+04-1.65131553E+02 2.16600426E+00
1.27566594E-01-9.07569127E-05 3
3.35500540E-08-5.14172057E-12-3.19139564E+04 3.56423608E+01
4
OC9OOH 7/23/ 7 THERMC 9H 18O 3 0G 300.000 5000.000
1390.000 01
3.62313913E+01 4.01378645E-02-1.39472937E-05
2.18847057E-09-1.27914399E-13 2
-6.61416812E+04-1.54592687E+02-2.10756952E-01
1.25597792E-01-9.16678732E-05 3

3.49212756E-08-5.50989215E-12-5.34323864E+04 4.11540880E+01
4
C9H17O2 7/23/ 7 THERMC 9H 17O 2 OG 300.000 5000.000
1393.000 81
3.17676033E+01 3.91799062E-02-1.35027571E-05
2.10696848E-09-1.22671395E-13 2
-4.61817700E+04-1.32863726E+02-5.66522945E-01
1.14562919E-01-8.14143456E-05 3
3.03357499E-08-4.69044767E-12-3.48704558E+04 4.09561651E+01
4
PC10H21O2 7/23/ 7 THERMC 10H 21O 2 OG 300.000 5000.000
1389.000 01
3.47500473E+01 4.86054563E-02-1.67680957E-05
2.61804172E-09-1.52482744E-13 2
-4.03027403E+04-1.46075198E+02 7.28991608E-01
1.24094712E-01-8.13580187E-05 3
2.82660217E-08-4.16896982E-12-2.78863857E+04 3.83923835E+01
4
P10OOHX2 7/23/ 7 THERMC 10H 21O 2 OG 300.000 5000.000
1386.000 11
3.66792326E+01 4.60670805E-02-1.57965124E-05
2.45711260E-09-1.42759860E-13 2
-3.48750025E+04-1.54767837E+02 5.55912405E-01
1.25171778E-01-8.05819527E-05 3
2.60890204E-08-3.39012894E-12-2.17708307E+04 4.11643973E+01
4
SOO10OOH 7/23/ 7 THERMC 10H 21O 4 OG 300.000 5000.000
1388.000 21
4.19829527E+01 4.72518019E-02-1.64259128E-05
2.57799359E-09-1.50703301E-13 2
-5.51243761E+04-1.79512774E+02 1.39255905E+00
1.41572125E-01-1.01777822E-04 3
3.85665506E-08-6.11239303E-12-4.08138150E+04 3.89378438E+01
4
PX210OOH 7/23/ 7 THERMC 10H 21O 4 OG 300.000 5000.000
1388.000 31
4.25883473E+01 4.62682846E-02-1.60777186E-05
2.52278985E-09-1.47456903E-13 2
-4.91710934E+04-1.80627663E+02 1.99234205E+00
1.39541096E-01-9.86995634E-05 3
3.62934567E-08-5.53513690E-12-3.48105983E+04 3.81320008E+01
4
OC10OOH 7/23/ 7 THERMC 10H 20O 3 OG 300.000 5000.000
1390.000 11
3.94333213E+01 4.46237652E-02-1.54923252E-05
2.42944983E-09-1.41940086E-13 2
-7.02604396E+04-1.70392954E+02-3.84573919E-01
1.37541633E-01-9.94377658E-05 3
3.75076006E-08-5.86215012E-12-5.63288547E+04 4.36473794E+01
4
C10H19O2 7/23/ 7 THERMC 10H 19O 2 OG 300.000 5000.000
1393.000 91


```
3.49330730E+01 4.36817320E-02-1.50499222E-05
2.34792823E-09-1.36681596E-13      2
-5.02794848E+04-1.48438412E+02-7.34414425E-01
1.26513810E-01-8.92992155E-05      3
3.30332261E-08-5.07233088E-12-3.77681939E+04 4.34177804E+01
4
PC11H23O2 7/23/ 7 THERMC 11H 23O 2 OG 300.000 5000.000
1389.000 11
3.79134101E+01 5.31263309E-02-1.83256016E-05
2.86100432E-09-1.66625168E-13      2
-4.44045245E+04-1.61650234E+02 4.81830796E-01
1.36401407E-01-8.97875259E-05      3
3.13184008E-08-4.63303120E-12-3.07721548E+04 4.12207947E+01
4
P11OOHX2 7/23/ 7 THERMC 11H 23O 2 OG 300.000 5000.000
1387.000 21
3.98385109E+01 5.05764523E-02-1.73465657E-05
2.69853616E-09-1.56797085E-13      2
-3.89701118E+04-1.70307720E+02 3.57493344E-01
1.37251628E-01-8.86583357E-05      3
2.89048423E-08-3.79791851E-12-2.46637286E+04 4.37690148E+01
4
SOO11OOH 7/23/ 7 THERMC 11H 23O 4 OG 300.000 5000.000
1388.000 31
4.52700291E+01 5.16946662E-02-1.79628400E-05
2.81843083E-09-1.64727346E-13      2
-5.92983397E+04-1.95851738E+02 1.18498703E+00
1.53462918E-01-1.09138096E-04      3
4.07744578E-08-6.36496407E-12-4.37007796E+04 4.16242140E+01
4
PX211OOH 7/23/ 7 THERMC 11H 23O 4 OG 300.000 5000.000
1389.000 41
4.57407884E+01 5.07781866E-02-1.76269459E-05
2.76399132E-09-1.61477785E-13      2
-5.32624527E+04-1.96124677E+02 1.81886105E+00
1.51513075E-01-1.06638152E-04      3
3.90335941E-08-5.92765458E-12-3.77072119E+04 4.06212074E+01
4
OC11OOH 7/23/ 7 THERMC 11H 22O 3 OG 300.000 5000.000
1390.000 21
4.26345464E+01 4.91093398E-02-1.70370471E-05
2.67036084E-09-1.55961013E-13      2
-7.43791003E+04-1.86189582E+02-5.70148343E-01
1.49530761E-01-1.07272397E-04      3
4.01327129E-08-6.22271556E-12-5.92233311E+04 4.61967088E+01
4
C11H21O2 7/23/ 7 THERMC 11H 21O 2 OG 300.000 5000.000
1393.000 01
3.80995197E+01 4.81809978E-02-1.65958315E-05
2.58865395E-09-1.50676658E-13      2
-5.43768336E+04-1.64016785E+02-8.90208649E-01
1.38418692E-01-9.71202083E-05      3
```

3.56919512E-08-5.44569741E-12-4.06679857E+04 4.58216743E+01
4
PC12H25O2 7/23/ 7 THERMC 12H 250 2 0G 300.000 5000.000
1389.000 21
4.10720559E+01 5.76223879E-02-1.98682057E-05
3.10098353E-09-1.80567383E-13 2
-4.84961160E+04-1.77176648E+02 4.13301762E-01
1.47893311E-01-9.69755376E-05 3
3.35724323E-08-4.91454646E-12-3.36844450E+04 4.32258761E+01
4
P12OOHX2 7/23/ 7 THERMC 12H 250 2 0G 300.000 5000.000
1387.000 31
4.29994696E+01 5.50833554E-02-1.88955870E-05
2.93978363E-09-1.70823564E-13 2
-4.30658136E+04-1.85856878E+02 1.60721186E-01
1.49325879E-01-9.67266789E-05 3
3.17154092E-08-4.20449417E-12-2.75569298E+04 4.63656051E+01
4
SOO12OOH 7/23/ 7 THERMC 12H 250 4 0G 300.000 5000.000
1389.000 41
4.78237378E+01 5.66012764E-02-1.96226767E-05
3.07404604E-09-1.79468346E-13 2
-6.30929400E+04-2.07768890E+02 6.91692611E-01
1.67000994E-01-1.20729787E-04 3
4.63412670E-08-7.45842745E-12-4.65446291E+04 4.56074372E+01
4
PX212OOH 7/23/ 7 THERMC 12H 250 4 0G 300.000 5000.000
1389.000 51
4.89358966E+01 5.52991412E-02-1.91904385E-05
3.00850701E-09-1.75735606E-13 2
-5.73849295E+04-2.11902966E+02 1.58567624E+00
1.63721110E-01-1.14803987E-04 3
4.18812947E-08-6.34154032E-12-4.05947115E+04 4.33893943E+01
4
OC12OOH 7/23/ 7 THERMC 12H 240 3 0G 300.000 5000.000
1390.000 31
4.58270142E+01 5.36021643E-02-1.85842108E-05
2.91164544E-09-1.70003340E-13 2
-7.84952427E+04-2.01938484E+02-8.15246773E-01
1.61762409E-01-1.15472154E-04 3
4.29870811E-08-6.63426907E-12-6.21080428E+04 4.90271786E+01
4
PX212POO 7/23/ 7 THERMC 12H 230 2 0G 300.000 5000.000
1393.000 11
4.12649751E+01 5.26828938E-02-1.81430355E-05
2.82962147E-09-1.64687384E-13 2
-5.84747908E+04-1.79591985E+02-1.06370326E+00
1.50390366E-01-1.05033191E-04 3
3.84058041E-08-5.83104375E-12-4.35647594E+04 4.83101291E+01
4
PXC6H11 8/29/ 8 G C 6H 11 0 0G 300.000 5000.000
1387.000 01

```
1.88127079E+01 2.24707969E-02-7.39640607E-06
1.12968081E-09-6.50216800E-14      2
1.04951457E+04-7.13311281E+01-1.34535943E+00
6.92921569E-02-4.88150205E-05      3
1.77673074E-08-2.63116535E-12 1.74972691E+04 3.69855102E+01
4
SXC6H11      8/29/ 8 G      C      6H 11      0      OG      300.000 5000.000
1388.000      01
1.75342278E+01 2.37700257E-02-7.73998759E-06
1.17076496E-09-6.69110170E-14      2
9.29122079E+03-6.35766942E+01-1.11464755E+00
6.69717331E-02-4.59611004E-05      3
1.65804004E-08-2.46116141E-12 1.57975469E+04 3.66990880E+01
4
S2XC6H11      8/29/ 8 G      C      6H 11      0      OG      300.000 5000.000
1388.000      01
1.75342278E+01 2.37700257E-02-7.73998759E-06
1.17076496E-09-6.69110170E-14      2
9.29122079E+03-6.35766942E+01-1.11464755E+00
6.69717331E-02-4.59611004E-05      3
1.65804004E-08-2.46116141E-12 1.57975469E+04 3.66990880E+01
4
SAXC6H11      8/29/ 8 G      C      6H 11      0      OG      300.000 5000.000
1389.000      01
1.82778003E+01 2.36537811E-02-7.75072414E-06
1.17603845E-09-6.73353698E-14      2
1.13087491E+03-7.13034099E+01-1.37770930E+00
6.97369420E-02-4.91344265E-05      3
1.81492072E-08-2.75290394E-12 7.92711562E+03 3.41796309E+01
4
cC6H11      8/29/ 8 G      C      6H 11      0      OG      300.000 5000.000
1387.000      01
1.67134967E+01 2.64723419E-02-8.73186729E-06
1.32580368E-09-7.59023046E-14      2
-6.80682328E+02-7.01816482E+01-6.12523837E+00
7.84159467E-02-5.30466359E-05      3
1.81779786E-08-2.48668647E-12 7.33042324E+03 5.28759955E+01
4
cC6H10      8/29/ 8 G      C      6H 10      0      OG      300.000 5000.000
1385.000      01
1.62562432E+01 2.35093706E-02-7.33289134E-06
1.07949279E-09-6.07965496E-14      2
-9.31410436E+03-6.91215468E+01-6.42092564E+00
7.54181347E-02-5.13700157E-05      3
1.74397214E-08-2.29155931E-12-1.47017604E+03 5.28194329E+01
4
cC5H9CH2      8/29/ 8 G      C      6H 11      0      OG      300.000 5000.000
1394.000      01
1.81101178E+01 2.23566781E-02-6.16163818E-06
8.36809653E-10-4.48982805E-14      2
2.57344918E+03-7.38881366E+01-8.00155548E+00
8.69261896E-02-6.61725074E-05      3
```

```
2.56782868E-08-3.90470114E-12 1.10356516E+04 6.46693881E+01
4
CH2C5H8      8/29/ 8 G      C      6H  10      0      OG      300.000  5000.000
1390.000      01
1.87430625E+01 2.17683653E-02-7.21394229E-06
1.10067312E-09-6.32280178E-14      2
-7.90122236E+03-8.00632170E+01-1.83749129E+00
7.13516757E-02-5.32002188E-05      3
2.06335809E-08-3.26391062E-12-9.34546298E+02 2.98847691E+01
4
C6H10-13     8/29/ 8 G      C      6H  10      0      OG      300.000  5000.000
1395.000      01
1.75263752E+01 2.18447910E-02-7.07364536E-06
1.06374721E-09-6.05245347E-14      2
-1.71855602E+03-6.76539587E+01-2.74170140E+00
7.44458966E-02-6.04686268E-05      3
2.60487709E-08-4.55730700E-12 4.78762455E+03 3.93238815E+01
4
SAXC6H11-3   8/29/ 8 G      C      6H  11      0      OG      300.000  5000.000
1386.000      01
1.79088347E+01 2.40206083E-02-7.92205050E-06
1.20719104E-09-6.93087184E-14      2
-2.58715836E+02-6.97326294E+01-9.20881834E-01
6.63768552E-02-4.38897352E-05      3
1.49618341E-08-2.07564376E-12 6.44041386E+03 3.19697168E+01
4
m1C5H81      8/29/ 8 G      C      6H  11      0      OG      300.000  5000.000
1389.000      01
1.87248033E+01 2.26408474E-02-7.40593401E-06
1.12566451E-09-6.45783709E-14      2
9.41104884E+03-7.15447685E+01-2.12565812E+00
7.23499603E-02-5.28655648E-05      3
2.01123555E-08-3.11929929E-12 1.65181910E+04 4.00256810E+01
4
CH3cC5H83    8/29/ 8 G      C      6H  11      0      OG      300.000  5000.000
1397.000      01
1.58686016E+01 2.59804698E-02-7.97036739E-06
1.15372372E-09-6.40749985E-14      2
1.61686671E+03-6.04011739E+01-7.44055145E+00
8.34654024E-02-6.19825570E-05      3
2.40905431E-08-3.77166969E-12 9.27714420E+03 6.34899056E+01
4
PXC5H9       8/29/ 8 G      C      5H   9      0      OG      300.000  5000.000
1388.000      01
1.53696377E+01 1.83676679E-02-6.01677545E-06
9.15695271E-10-5.25804651E-14      2
1.47343004E+04-5.42387364E+01-1.09492416E+00
5.68655697E-02-4.03292203E-05      3
1.48071178E-08-2.21133463E-12 2.04219611E+04 3.41306974E+01
4
SXC5H9       8/29/ 8 G      C      5H   9      0      OG      300.000  5000.000
1388.000      01
```

1.45766840E+01 1.86937690E-02-5.75318620E-06
8.42596121E-10-4.73125100E-14 2
1.34103542E+04-4.89933658E+01-9.72736306E-01
5.53607813E-02-3.86033065E-05 3
1.41485618E-08-2.10517703E-12 1.87272947E+04 3.43153414E+01
4
C5H8-13 8/29/ 8 G C 5H 8 0 OG 300.000 5000.000
1391.000 01
1.43257851E+01 1.76169669E-02-5.80042088E-06
8.82118331E-10-5.05625946E-14 2
2.21575220E+03-5.21896211E+01-1.48584236E+00
5.79258726E-02-4.62461588E-05 3
1.97299445E-08-3.45027610E-12 7.39913837E+03 3.15833848E+01
4
C5H8-14 8/29/ 8 G C 5H 8 0 OG 300.000 5000.000
1390.000 01
1.38824133E+01 1.77427021E-02-5.79515709E-06
8.77549990E-10-5.01822180E-14 2
5.88792983E+03-4.81519427E+01-1.45429789E+00
5.42940716E-02-3.92475616E-05 3
1.48763980E-08-2.30893184E-12 1.11219293E+04 3.39271603E+01
4
CH2C4H7 8/29/ 8 G C 5H 9 0 OG 300.000 5000.000
1394.000 01
1.49484359E+01 1.79111376E-02-5.33022509E-06
7.62624635E-10-4.21709731E-14 2
1.48422892E+04-5.16317137E+01-1.32159546E+00
5.87180938E-02-4.46130375E-05 3
1.79676724E-08-2.92481115E-12 2.01371798E+04 3.46311211E+01
4
SAXC5H9 8/29/ 8 G C 5H 9 0 OG 300.000 5000.000
1389.000 01
1.51441327E+01 1.93268901E-02-6.34197189E-06
9.62600971E-10-5.51208154E-14 2
5.16943043E+03-5.59956467E+01-1.08167008E+00
5.72222617E-02-4.01416553E-05 3
1.46881058E-08-2.19955709E-12 1.07882469E+04 3.11232057E+01
4
cC5H9 8/29/ 8 G C 5H 9 0 OG 300.000 5000.000
1396.000 01
1.29317351E+01 2.11424763E-02-6.36999876E-06
9.11625180E-10-5.02979354E-14 2
6.70980336E+03-4.61414406E+01-6.45191478E+00
6.80782118E-02-4.92096917E-05 3
1.83894771E-08-2.73634944E-12 1.31374506E+04 5.71442754E+01
4
cC5H8 8/29/ 8 G C 5H 8 0 OG 300.000 5000.000
1390.000 01
1.32959097E+01 1.89098135E-02-6.03053478E-06
8.98443521E-10-5.09028504E-14 2
-3.02608717E+03-5.12794740E+01-5.47936621E+00
6.28323837E-02-4.45346566E-05 3

```
1.58975948E-08-2.23821209E-12 3.38122309E+03 4.93568170E+01
4
OH*          ATcT AO   1H   1   0   0G   200.000  6000.000
1000.00      1
2.75582920E+00 1.39848756E-03-4.19428493E-07
6.33453282E-11-3.56042218E-15      2
5.09751756E+04 5.62581429E+00 3.46084428E+00
5.01872172E-04-2.00254474E-06      3
3.18901984E-09-1.35451838E-12 5.07349466E+04 1.73976415E+00
5.17770741E+04      4
CH*          TPIS79C   1H   1   00   00G   200.000  3500.000
1000.000     1
2.78220752E+00 1.47246754E-03-4.63436227E-07
7.32736021E-11-4.19705404E-15      2
1.04547060E+05 5.17421018E+00 3.47250101E+00
4.26443626E-04-1.95181794E-06      3
3.51755043E-09-1.60436174E-12 1.04334869E+05 1.44799533E+00
1.05378099E+05      4
ENDOFDATA
```

D.1.2 Transport File

AR	0	136.500	3.330	0.000	0.000
0.000					
C	0	71.400	3.298	0.000	0.000
0.000 ! *					
CH	1	80.000	2.750	0.000	0.000
0.000					
CH*	1	80.000	2.750	0.000	0.000
0.000					
CH2	1	144.000	3.800	0.000	0.000
0.000					
CH2*	1	144.000	3.800	0.000	0.000
0.000					
CH3	1	144.000	3.800	0.000	0.000
0.000					
CH4	2	141.400	3.746	0.000	2.600
13.000					
CO	1	98.100	3.650	0.000	1.950
1.800					
CO2	1	244.000	3.763	0.000	2.650
2.100					
HCO	2	498.000	3.590	0.000	0.000
0.000					
CH2O	2	498.000	3.590	0.000	0.000
2.000					
CH2OH	2	417.000	3.690	1.700	0.000
2.000					
CH3O	2	417.000	3.690	1.700	0.000
2.000					
CH3OH	2	481.800	3.626	0.000	0.000
1.000 ! SVE					
C2	1	97.530	3.621	0.000	1.760
4.000					
C2O	1	232.400	3.828	0.000	0.000
1.000 ! *					
C2H	1	209.000	4.100	0.000	0.000
2.500					
C2H2	1	209.000	4.100	0.000	0.000
2.500					
H2CC	2	209.000	4.100	0.000	0.000
2.500					
C2H3	2	209.000	4.100	0.000	0.000
1.000 ! *					
C2H4	2	280.800	3.971	0.000	0.000
1.500					
C2H5	2	252.300	4.302	0.000	0.000
1.500					
C2H6	2	252.300	4.302	0.000	0.000
1.500					
HCCO	2	150.000	2.500	0.000	0.000
1.000 ! *					

HCCOH 2.000	2	436.000	3.970	0.000	0.000
CH2CO 2.000	2	436.000	3.970	0.000	0.000
CH2CHO 2.000	2	436.000	3.970	0.000	0.000
C2H2OH 1.000 ! *	2	224.700	4.162	0.000	0.000
C3H2 1.000 ! *	2	209.000	4.100	0.000	0.000
C3H3 1.000 ! JAM	2	252.000	4.760	0.000	0.000
aC3H4 1.000	1	252.000	4.760	0.000	0.000
pC3H4 1.000	1	252.000	4.760	0.000	0.000
cC3H4 1.000	1	252.000	4.760	0.000	0.000
CH2OCH2 1.000	1	252.000	4.760	0.000	0.000
CH2OCH 1.000	1	252.000	4.760	0.000	0.000
CH3CH2CHO 1.000	1	252.000	4.760	0.000	0.000
C4H 1.000	1	357.000	5.180	0.000	0.000
C4H2 1.000	1	357.000	5.180	0.000	0.000
H2C4O 1.000 ! JAM	2	357.000	5.180	0.000	0.000
C4H2OH 1.000 ! *	2	224.700	4.162	0.000	0.000
iC4H3 1.000 ! JAM	2	357.000	5.180	0.000	0.000
nC4H3 1.000 ! JAM	2	357.000	5.180	0.000	0.000
C4H4 1.000 ! JAM	2	357.000	5.180	0.000	0.000
iC4H5 1.000 ! JAM	2	357.000	5.180	0.000	0.000
nC4H5 1.000 ! JAM	2	357.000	5.180	0.000	0.000
C4H5-2 1.000 !	2	357.000	5.180	0.000	0.000
C4H6 1.000	2	357.000	5.180	0.000	0.000
C4H6-2 1.000	2	357.000	5.180	0.000	0.000
C4H612 1.000	2	357.000	5.180	0.000	0.000

CH3CHOCH2 1.000	2	357.000	5.180	0.000	0.000
C5H2 1.000	1	357.000	5.180	0.000	0.000
C5H3 1.000	1	357.000	5.180	0.000	0.000
C5H5 1.000	1	357.000	5.180	0.000	0.000
C5H6 1.000	1	357.000	5.180	0.000	0.000
1C5H7 1.000	1	357.000	5.180	0.000	0.000
C4H6O25 1.000	1	357.000	5.180	0.000	0.000
C4H6O23 1.000	1	357.000	5.180	0.000	0.000
C4H4O 1.000	1	357.000	5.180	0.000	0.000
CH2CHCO 1.000	1	357.000	5.180	0.000	0.000
CH3CHOCH2 1.000	1	357.000	5.180	0.000	0.000
CH2CHCHCHO 1.000	1	357.000	5.180	0.000	0.000
CH3CHCHCO 1.000	1	357.000	5.180	0.000	0.000
C2H3CHOCH2 1.000	1	357.000	5.180	0.000	0.000
CH3CHCHCHO 1.000	1	357.000	5.180	0.000	0.000
C6H 1.000	1	357.000	5.180	0.000	0.000
C6H2 1.000	1	357.000	5.180	0.000	0.000
C6H3 1.000 !	2	357.000	5.180	0.000	0.000
1-C6H4 1.000 !(JAM)	2	412.300	5.349	0.000	0.000
nC6H5 1.000 !(JAM)	2	412.300	5.349	0.000	0.000
i-C6H5 1.000 !(JAM)	2	412.300	5.349	0.000	0.000
1-C6H6 1.000 !(SVE)	2	412.300	5.349	0.000	0.000
n-C6H7 1.000 !(JAM)	2	412.300	5.349	0.000	0.000
i-C6H7 1.000 !(JAM)	2	412.300	5.349	0.000	0.000
C6H8 1.000 !(JAM)	2	412.300	5.349	0.000	0.000

HE	0	10.200	2.576	0.000	0.000
0.000 ! *					
H	0	145.000	2.050	0.000	0.000
0.000					
H2	1	38.000	2.920	0.000	0.790
280.000					
H2O	2	572.400	2.605	1.844	0.000
4.000					
H2O2	2	107.400	3.458	0.000	0.000
3.800					
HO2	2	107.400	3.458	0.000	0.000
1.000 ! *					
N2	1	97.530	3.621	0.000	1.760
4.000					
O	0	80.000	2.750	0.000	0.000
0.000					
O2	1	107.400	3.458	0.000	1.600
3.800					
OH	1	80.000	2.750	0.000	0.000
0.000					
OH*	1	80.000	2.750	0.000	0.000
0.000					

The Lennard-Jones parameters of polycyclic aromatic hydrocarbons were estimated based on the critical temperature and pressure. See H. Wang and M. Frenklach, "Transport Properties of Polycyclic Aromatic Hydrocarbons for Flame Modeling." Combustion and Flame, 96:163-170 (1994)

c-C6H4	2	464.8	5.29	0.00	10.32
0.000 ! benze					
C6H6	2	464.8	5.29	0.00	10.32
0.000 ! benze					
C6H5	2	464.8	5.29	0.00	10.32
0.000 ! benze					
C6H5CH3	2	495.3	5.68	0.43	12.30
1.000 !					
C6H5C2H3	2	546.2	6.00	0.13	15.00
1.000 !					
C6H5CH2	2	495.3	5.68	0.43	12.30
1.000 !					
C6H5C2H	2	535.6	5.72	0.77	12.00
1.000 !					
A2	2	630.4	6.18	0.00	16.50
1.000 !					
c-C6H7	2	464.8	5.29	0.00	10.32
0.000 ! benze					
C5H4O	2	464.8	5.29	0.00	10.32

0.000	!	benze				
C5H5O			2	464.8	5.29	0.00 10.32
0.000	!	benze				
C5H4OH			2	464.8	5.29	0.00 10.32
0.000	!	benze				
C6H5O			2	464.8	5.29	0.00 10.32
0.000	!	benze				
C6H5OH			2	464.8	5.29	0.00 10.32
0.000	!	benze				
aC3H5			2	266.800	4.982	0.000 0.000
1.000						
CH3CCH2			2	266.800	4.982	0.000 0.000
1.000						
CH3CHCH			2	266.800	4.982	0.000 0.000
1.000						
C3H6			2	266.800	4.982	0.000 0.000
1.000						
C3H7			2	266.800	4.982	0.000 0.000
1.000						
C4H6			2	357.000	5.180	0.000 0.000
1.000						
iC3H7			2	266.800	4.982	0.000 0.000
1.000						
nC3H7			2	266.800	4.982	0.000 0.000
1.000						
C3H8			2	266.800	4.982	0.000 0.000
1.000						
C4H			1	357.000	5.180	0.000 0.000
1.000						
C4H2			1	357.000	5.180	0.000 0.000
1.000						
C4H2OH			2	224.700	4.162	0.000 0.000
1.000	!	*				
iC4H5			2	357.000	5.176	0.000 0.000
1.000						
C4H6			2	357.000	5.176	0.000 0.000
1.000						
C4H7			2	357.000	5.176	0.000 0.000
1.000						
iC4H7			2	357.000	5.176	0.000 0.000
1.000						
C4H81			2	357.000	5.176	0.000 0.000
1.000						
C4H82			2	357.000	5.176	0.000 0.000
1.000						
iC4H8			2	357.000	5.176	0.000 0.000
1.000						
tC4H9			2	357.000	5.176	0.000 0.000
1.000						
iC4H9			2	357.000	5.176	0.000 0.000
1.000						

pC4H9	2	357.000	5.176	0.000	0.000
1.000					
sC4H9	2	357.000	5.176	0.000	0.000
1.000					
C4H10	2	357.000	5.176	0.000	0.000
1.000					
iC4H10	2	357.000	5.176	0.000	0.000
1.000					
CH3COCH3	2	357.000	5.176	0.000	0.000
1.000					
C2H3CHO	2	357.000	5.176	0.000	0.000
1.000					
iC4H7O	2	450.000	5.500	0.000	0.000
1.000 ! JAM					
CH3CHO	2	436.000	3.970	0.000	0.000
2.000					
CH3CO	2	436.000	3.970	0.000	0.000
2.000					
C5H7	1	357.000	5.180	0.000	0.000
1.000					
C6H5CH2O	2	572	5.82	1.7	0.0
1.0					
C5H5O(2,4)	2	494	5.2	1.6	0.0
1.0					
C5H5O(1,2)	2	494	5.2	1.6	0.0
1.0					
C5H5O(1,3)	2	494	5.2	1.6	0.0
1.0					
C4H5	2	329	5.1	0.0	0.0
1.0					
c-C4H5	2	329	5.1	0.0	0.0
1.0					
C6H5CO	2	593	5.5	2.8	0.0
1.0					
C6H5CHO	2	593	5.47	2.8	0.0
1.0					
C6H5C2H5	2	485	5.425	0.4	0.0
1.0					
C6H4O2	2	485	5.425	0.4	0.0
1.0					
HOC6H4CH3	2	567	5.60	1.6	0.0
1.0					
C6H5CH2OH	2	572	5.82	1.7	0.0
1.0					
bi-C6H5CH2	2	620	7.24	0.0	0.0
1.0					
C5H5OH	2	464.800	5.290	0.000	10.320
0.000 ! as C5H4OH, ZD99					
C5H4OH	2	464.800	5.290	0.000	10.320
0.000 ! benze					
o-C6H4	2	464.8	5.29	0.00	10.32

0.000 !	benze					
C6H5C6H5		2	676.5	6.31	0.00	20.00
1.000 !	biphe					
OC6H4CH3		2	567	5.6	1.6	0.0
1.000						
C10H8		2	630.4	6.18	0.00	16.50
1.000 !	naphthalene					
C6H4CH3		2	495.3	5.68	0.43	12.30
1.000 !						
NC12H26		2	789.980	7.047	0.000	0.000
1.000 !	n-dodecane					
PXC12H25		2	789.980	7.047	0.000	0.000
1.000 !						
SXC12H25		2	789.980	7.047	0.000	0.000
1.000 !						
S2XC12H25		2	789.980	7.047	0.000	0.000
1.000 !						
S3XC12H25		2	789.980	7.047	0.000	0.000
1.000 !						
S4XC12H25		2	789.980	7.047	0.000	0.000
1.000 !						
S5XC12H25		2	789.980	7.047	0.000	0.000
1.000 !						
C12H24		2	775.294	7.090	0.000	0.000
1.000 !	1-dodecene					
PXC12H23		2	775.294	7.090	0.000	0.000
1.000 !						
NC11H24		2	750.460	6.834	0.000	0.000
1.000 !	n-undecane					
PXC11H23		2	750.460	6.834	0.000	0.000
1.000 !						
SXC11H23		2	750.460	6.834	0.000	0.000
1.000 !						
S2XC11H23		2	750.460	6.834	0.000	0.000
1.000 !						
S3XC11H23		2	750.460	6.834	0.000	0.000
1.000 !						
S4XC11H23		2	750.460	6.834	0.000	0.000
1.000 !						
S5XC11H23		2	750.460	6.834	0.000	0.000
1.000 !						
C11H22		2	763.817	6.688	0.000	0.000
1.000 !	1-undecene					
PXC11H21		2	763.817	6.688	0.000	0.000
1.000 !						
NC10H22		2	704.917	6.675	0.000	0.000
1.000 !	n-decane					
PXC10H21		2	704.917	6.675	0.000	0.000
1.000 !						
SXC10H21		2	704.917	6.675	0.000	0.000
1.000 !						

S2XC10H21	2	704.917	6.675	0.000	0.000
1.000 !					
S3XC10H21	2	704.917	6.675	0.000	0.000
1.000 !					
S4XC10H21	2	704.917	6.675	0.000	0.000
1.000 !					
C10H20	2	698.122	6.578	0.000	0.000
1.000 ! 1-decene					
PXC10H19	2	698.122	6.578	0.000	0.000
1.000 !					
NC9H20	2	660.032	6.467	0.000	0.000
1.000 ! n-nonane					
PXC9H19	2	660.032	6.467	0.000	0.000
1.000 !					
SXC9H19	2	660.032	6.467	0.000	0.000
1.000 !					
S2XC9H19	2	660.032	6.467	0.000	0.000
1.000 !					
S3XC9H19	2	660.032	6.467	0.000	0.000
1.000 !					
S4XC9H19	2	660.032	6.467	0.000	0.000
1.000 !					
C9H18	2	655.390	6.331	0.000	0.000
1.000 ! 1-nonene					
PXC9H17	2	655.390	6.331	0.000	0.000
1.000 !					
NC8H18	2	613.127	6.250	0.000	0.000
1.000 ! n-octane					
PXC8H17	2	613.127	6.250	0.000	0.000
1.000 !					
SXC8H17	2	613.127	6.250	0.000	0.000
1.000 !					
S2XC8H17	2	613.127	6.250	0.000	0.000
1.000 !					
S3XC8H17	2	613.127	6.250	0.000	0.000
1.000 !					
C8H16	2	608.488	6.100	0.000	0.000
1.000 ! 1-octene					
PXC8H15	2	608.488	6.100	0.000	0.000
1.000 !					
NC7H16	2	564.030	6.004	0.000	0.000
1.000 ! n-heptane					
PXC7H15	2	564.030	6.004	0.000	0.000
1.000 !					
SXC7H15	2	564.030	6.004	0.000	0.000
1.000 !					
S2XC7H15	2	564.030	6.004	0.000	0.000
1.000 !					
S3XC7H15	2	564.030	6.004	0.000	0.000
1.000 !					
C7H14	2	557.947	5.876	0.000	0.000
1.000 ! 1-heptene					

PXC7H13		2	557.947	5.876	0.000	0.000
1.000 !						
NC6H14		2	512.225	5.742	0.000	0.000
1.000 !	n-hexane					
PXC6H13		2	512.225	5.742	0.000	0.000
1.000 !						
SXC6H13		2	512.225	5.742	0.000	0.000
1.000 !						
S2XC6H13		2	512.225	5.742	0.000	0.000
1.000 !						
C6H12		2	504.629	5.628	0.000	0.000
1.000 !	1-hexene					
PXC6H11		2	504.629	5.628	0.000	0.000
1.000 !						
NC5H12		2	458.182	5.445	0.000	0.000
1.000 !	n-pentane					
PXC5H11		2	458.182	5.445	0.000	0.000
1.000 !						
SXC5H11		2	458.182	5.445	0.000	0.000
1.000 !						
S2XC5H11		2	458.182	5.445	0.000	0.000
1.000 !						
C5H10		2	448.508	5.342	0.000	0.000
1.000 !	1-pentene					
PXC5H9		2	448.508	5.342	0.000	0.000
1.000 !						
PC12H25O2		2	805.031	7.102	0.000	0.000
1.000						
P12OOHX2		2	805.031	7.102	0.000	0.000
1.000						
SOO12OOH		2	877.052	7.457	0.000	0.000
1.000						
OC12OOH		2	839.348	7.273	0.000	0.000
1.000						
C6H11		2	504.629	5.628	0.000	0.000
1.000 !	1-hexene					
SXC6H11		2	504.629	5.628	0.000	0.000
1.000 !						
S2XC6H11		2	504.629	5.628	0.000	0.000
1.000 !						
SAXC6H11		2	504.629	5.628	0.000	0.000
1.000 !						
cC6H11		2	464.8	5.29	0.00	0.000
1.000 !	benze					
cC6H10		2	464.8	5.29	0.00	0.000
1.000 !	benze					
cC6H11O2		2	464.8	5.29	0.00	0.000
1.000 !						
cC6H10O2H-2		2	464.8	5.29	0.00	0.000
1.000 !						
SOOcC6O2H		2	464.8	5.29	0.00	0.000

1.000	!				
SOOcC6O	2	464.8	5.29	0.00	0.000
1.000	!				
PXCH2cC5H9	2	464.8	5.29	0.00	0.000
1.000	! benze				
CH2cC5H8	2	464.8	5.29	0.00	0.000
1.000	! benze				
C6H10-13	2	504.629	5.628	0.000	0.000
1.000	!				
SAX4-2C6H11	2	504.629	5.628	0.000	0.000
1.000	!				
PXCH2-4-1C5H9	2	504.629	5.628	0.000	0.000
1.000	!				
CH3cC5H83	2	464.8	5.29	0.00	0.000
1.000	! benze				
cC5H9	2	357.000	5.180	0.000	0.000
1.000	! C5H6				
cC5H8	2	357.000	5.180	0.000	0.000
1.000	! C5H6				
SXC5H9	2	357.000	5.180	0.000	0.000
1.000					
C5H8-13	2	357.000	5.180	0.000	0.000
1.000					
C5H8-12	2	357.000	5.180	0.000	0.000
1.000					
C5H8-14	2	357.000	5.180	0.000	0.000
1.000					
PXCH2-3-1C4H7	2	357.000	5.180	0.000	0.000
1.000					
SAXC5H9	2	357.000	5.180	0.000	0.000
1.000					
!					
! Cycloalkanes model species					
!					
C4H9cC6H11	2	717.126	6.229	0.13	15.00
1.000	! C6H5C2H3				
C4H9cC6H10O	2	717.126	6.229	0.13	15.00
1.000	! C6H5C2H3				
C4H9cC6H9OOH	2	717.126	6.229	0.13	15.00
1.000	! C6H5C2H3				
C5H84C4H9CHO	2	717.126	6.229	0.13	15.00
1.000	! C6H5C2H3				
C4H9cC6H9O3	2	717.126	6.229	0.13	15.00
1.000	! C6H5C2H3				
C10H20-5	2	698.122	6.578	0.000	0.000
1.000	! 1-decene				
C4H9-2-1C6H11	2	698.122	6.578	0.000	0.000
1.000	!				
CH3-5-1C9H17	2	698.122	6.578	0.000	0.000
1.000	!				
C3H7-3-1C7H13	2	698.122	6.578	0.000	0.000

1.000 !					
C2H5-4-1C8H15	2	698.122	6.578	0.000	0.000
1.000 !					
PXC4H8cC6H11	2	546.2	6.00	0.13	15.00
1.000 ! C6H5C2H3					
SXC4H8cC6H11	2	546.2	6.00	0.13	15.00
1.000 !					
S2XC4H8cC6H11	2	546.2	6.00	0.13	15.00
1.000 !					
S3XC4H8cC6H11	2	546.2	6.00	0.13	15.00
1.000 !					
C4H9TXcC6H10	2	546.2	6.00	0.13	15.00
1.000 !					
C4H9S2XcC6H10	2	546.2	6.00	0.13	15.00
1.000 !					
C4H9S3XcC6H10	2	546.2	6.00	0.13	15.00
1.000 !					
C4H9S4XcC6H10	2	546.2	6.00	0.13	15.00
1.000 !					
PX10-4C10H19	2	698.122	6.578	0.000	0.000
1.000 ! 1-decene					
PXC4H8-2-1C6H11	2	698.122	6.578	0.000	0.000
1.000 !					
PX10-5C10H19	2	698.122	6.578	0.000	0.000
1.000 !					
PXC3H6-3-1C7H13	2	698.122	6.578	0.000	0.000
1.000 !					
S4XC10H19	2	698.122	6.578	0.000	0.000
1.000 !					
PXC2H4-4-1C8H15	2	698.122	6.578	0.000	0.000
1.000 !					
PXCH2-5-1C9H17	2	698.122	6.578	0.000	0.000
1.000 !					
SAX6-4C10H19	2	698.122	6.578	0.000	0.000
1.000 !					
SAX4-5C10H19	2	698.122	6.578	0.000	0.000
1.000 !					
SAXC10H19	2	698.122	6.578	0.000	0.000
1.000 !					
SAXC4H8-2-1C6H11	2	698.122	6.578	0.000	0.000
1.000 !					
C3H7-3-TAX1C7H13	2	698.122	6.578	0.000	0.000
1.000 !					
C2H5-4-SAX1C8H14	2	698.122	6.578	0.000	0.000
1.000 !					
CH3-5-SAX1C9H16	2	698.122	6.578	0.000	0.000
1.000 !					
C3H7cC6H11	2	670.219	6.032	0.13	15.00
1.000 ! C6H5C2H3					
C3H7cC6H1000	2	670.219	6.032	0.13	15.00
1.000 ! C6H5C2H3					

C3H7cC6H9OOH	2	670.219	6.032	0.13	15.00
1.000 ! C6H5C2H3					
C5H84C3H7CHO	2	670.219	6.032	0.13	15.00
1.000 ! C6H5C2H3					
C3H7cC6H9O3	2	670.219	6.032	0.13	15.00
1.000 ! C6H5C2H3					
C9H18-4	2	655.390	6.331	0.000	0.000
1.000 ! 1-nonene					
C3H7-2-1C6H11	2	655.390	6.331	0.000	0.000
1.000 !					
C3H7-3-1C6H11	2	655.390	6.331	0.000	0.000
1.000 !					
CH3-4-1C8H15	2	655.390	6.331	0.000	0.000
1.000 !					
C2H5-4-1C7H13	2	655.390	6.331	0.000	0.000
1.000 !					
PXC3H6cC6H11	2	546.2	6.00	0.13	15.00
1.000 ! C6H5C2H3					
SXC3H6cC6H11	2	546.2	6.00	0.13	15.00
1.000 !					
S2XC3H6cC6H11	2	546.2	6.00	0.13	15.00
1.000 !					
C3H7S2XcC6H10	2	546.2	6.00	0.13	15.00
1.000 !					
C3H7S3XcC6H10	2	546.2	6.00	0.13	15.00
1.000 !					
C3H7TXcC6H10	2	546.2	6.00	0.13	15.00
1.000 !					
C3H7S4XcC6H10	2	546.2	6.00	0.13	15.00
1.000 !					
PX9-3C9H17	2	655.390	6.331	0.000	0.000
1.000 !					
PX9-4C9H17	2	655.390	6.331	0.000	0.000
1.000 !					
C3H7-2-PXC6H10	2	655.390	6.331	0.000	0.000
1.000 !					
S3XC9H17	2	655.390	6.331	0.000	0.000
1.000 !					
PXC3H6-3-1C6H11	2	655.390	6.331	0.000	0.000
1.000 !					
PXC2H4-4-1C7H13	2	655.390	6.331	0.000	0.000
1.000 !					
PXCH2-5-1C8H15	2	655.390	6.331	0.000	0.000
1.000 !					
SAX5-3C9H17	2	655.390	6.331	0.000	0.000
1.000 !					
C3H7-3-TAX1C6H10	2	655.390	6.331	0.000	0.000
1.000 !					
C3H7-2-SAXC6H10	2	655.390	6.331	0.000	0.000
1.000 !					
SAX6-4C9H17	2	655.390	6.331	0.000	0.000

1.000 !					
SAXC9H17	2	655.390	6.331	0.000	0.000
1.000 !					
C2H5-4-SAX1C7H12	2	655.390	6.331	0.000	0.000
1.000 !					
CH3-5-SAX1C8H14	2	655.390	6.331	0.000	0.000
1.000 !					
C3H5cC6H11	2	630.303	5.769	0.13	15.00
1.000 ! C6H5C2H3					
C2H5cC6H11	2	546.2	6.00	0.13	15.00
1.000 !					
C2H5cC6H1000	2	546.2	6.00	0.13	15.00
1.000 !					
C2H5cC6H9OOH	2	546.2	6.00	0.13	15.00
1.000 !					
C5H84C2H5CHO	2	546.2	6.00	0.13	15.00
1.000 !					
C2H5cC6H9O3	2	546.2	6.00	0.13	15.00
1.000 !					
C8H16-3	2	608.488	6.100	0.000	0.000
1.000 ! 1-octene					
C2H5-2-1C6H11	2	608.488	6.100	0.000	0.000
1.000 !					
CH3-5-1C7H13	2	608.488	6.100	0.000	0.000
1.000 !					
C2H5-4-1C6H11	2	608.488	6.100	0.000	0.000
1.000 !					
C2H5-3-1C6H11	2	608.488	6.100	0.000	0.000
1.000 !					
PXC2H4cC6H11	2	546.2	6.00	0.13	15.00
1.000 ! C6H5C2H3					
SXC2H4cC6H11	2	546.2	6.00	0.13	15.00
1.000 !					
C2H5TXcC6H10	2	546.2	6.00	0.13	15.00
1.000 !					
C2H5S2XcC6H10	2	546.2	6.00	0.13	15.00
1.000 !					
C2H5S3XcC6H10	2	546.2	6.00	0.13	15.00
1.000 !					
C2H5S4XcC6H10	2	546.2	6.00	0.13	15.00
1.000 !					
PX8-2C8H15	2	608.488	6.100	0.000	0.000
1.000 ! 1-octene					
C2H5-2-PXC6H10	2	608.488	6.100	0.000	0.000
1.000 !					
PX8-3C8H15	2	608.488	6.100	0.000	0.000
1.000 !					
C2H5-3-PXC6H10	2	608.488	6.100	0.000	0.000
1.000 !					
S2XC8H15	2	608.488	6.100	0.000	0.000

1.000 !					
PXC2H4-4-1C6H11	2	608.488	6.100	0.000	0.000
1.000 !					
PXCH2-5-1C7H13	2	608.488	6.100	0.000	0.000
1.000 !					
SAX4-2C8H15	2	608.488	6.100	0.000	0.000
1.000 !					
C2H5-2-SAX1C6H10	2	608.488	6.100	0.000	0.000
1.000 !					
SAX5-3C8H15	2	608.488	6.100	0.000	0.000
1.000 !					
C2H5-3-TAX1C6H10	2	608.488	6.100	0.000	0.000
1.000 !					
SAXC8H15	2	608.488	6.100	0.000	0.000
1.000 !					
C2H5-4-SAX1C6H10	2	608.488	6.100	0.000	0.000
1.000 !					
CH3-5-SAX1C7H12	2	608.488	6.100	0.000	0.000
1.000 !					
PX1-4C8H15	2	608.488	6.100	0.000	0.000
1.000 !					
PX1-3C8H15	2	608.488	6.100	0.000	0.000
1.000 !					
S4XC8H15	2	608.488	6.100	0.000	0.000
1.000 !					
PXC2H4-2-1C6H11	2	608.488	6.100	0.000	0.000
1.000 !					
PXCH2-3-1C7H13	2	608.488	6.100	0.000	0.000
1.000 !					
C2H3cC6H11	2	568.428	5.642	0.13	15.00
1.000 ! C6H5C2H3					
C8H14-13	2	608.488	6.100	0.000	0.000
1.000 !					
CH3cC6H11	2	495.3	5.68	0.43	12.30
1.000 ! C6H5CH3					
CH3cC6H10OO	2	495.3	5.68	0.43	12.30
1.000 ! C6H5CH3					
CH3cC6H9OOH	2	495.3	5.68	0.43	12.30
1.000 ! C6H5CH3					
C5H84CH3CHO	2	495.3	5.68	0.43	12.30
1.000 ! C6H5CH3					
CH3cC6H9O3	2	495.3	5.68	0.43	12.30
1.000 ! C6H5CH3					
CH2-3-1C7H12	2	557.947	5.876	0.000	0.000
1.000 ! 1-heptene					
PXCH2-2-C6H13	2	557.947	5.876	0.000	0.000
1.000 !					
CH3-2-SXC6H12	2	557.947	5.876	0.000	0.000
1.000 !					
C7H14-2	2	557.947	5.876	0.000	0.000

1.000 !					
CH3-2-1C6H11	2	557.947	5.876	0.000	0.000
1.000 !					
CH3-5-1C6H11	2	557.947	5.876	0.000	0.000
1.000 !					
CH3-4-1C6H11	2	557.947	5.876	0.000	0.000
1.000 !					
CH3-3-1C6H11	2	557.947	5.876	0.000	0.000
1.000 !					
PXCH2cC6H11	2	495.3	5.68	0.43	12.30
1.000 ! C6H5CH3					
CH3TXcC6H10	2	495.3	5.68	0.43	12.30
1.000 !					
CH3S2XcC6H10	2	495.3	5.68	0.43	12.30
1.000 !					
CH3S4XcC6H10	2	495.3	5.68	0.43	12.30
1.000 !					
CH3S3XcC6H10	2	495.3	5.68	0.43	12.30
1.000 ! 1-heptene					
CH3-2-PXC6H10	2	557.947	5.876	0.000	0.000
1.000 !					
PX7-2C7H13	2	557.947	5.876	0.000	0.000
1.000 !					
CH3-3-PXC6H10	2	557.947	5.876	0.000	0.000
1.000 !					
SXC7H13	2	557.947	5.876	0.000	0.000
1.000 !					
SAXC7H13	2	557.947	5.876	0.000	0.000
1.000 !					
CH3-4-PXC6H10	2	557.947	5.876	0.000	0.000
1.000 !					
PXCH2-5-1C6H11	2	557.947	5.876	0.000	0.000
1.000 !					
CH3-5-SAXC6H10	2	557.947	5.876	0.000	0.000
1.000 !					
SAX4-2C7H13	2	557.947	5.876	0.000	0.000
1.000 !					
CH3-4-SAXC6H10	2	557.947	5.876	0.000	0.000
1.000 !					
CH3-2-SAXC6H10	2	557.947	5.876	0.000	0.000
1.000 !					
CH3-3-TAXC6H10	2	557.947	5.876	0.000	0.000
1.000 !					
PAXCH2-2-1C6H11	2	557.947	5.876	0.000	0.000
1.000 !					
PX1-3C7H13	2	557.947	5.876	0.000	0.000
1.000 !					
PXCH2-3-1C6H11	2	557.947	5.876	0.000	0.000
1.000 !					
S3XC7H13	2	557.947	5.876	0.000	0.000
1.000 !					
PXC2H4-2-1C5H9	2	557.947	5.876	0.000	0.000

1.000 !					
C2H5-2-SAX1C5H9	2	557.947	5.876	0.000	0.000
1.000 !					
C7H12-13	2	557.947	5.876	0.000	0.000
1.000 !					
C7H12-16	2	557.947	5.876	0.000	0.000
1.000 !					
CH2-3-1C6H10	2	557.947	5.876	0.000	0.000
1.000 !					
CH2cC6H10	2	537.375	5.348	0.43	12.30
1.000 ! C6H5CH3					
cC6H12	2	464.8	5.29	0.00	0.000
1.000 ! benze					
cC6H1100	2	464.8	5.29	0.00	0.000
1.000 ! benze					
cC6H1000H	2	464.8	5.29	0.00	0.000
1.000 ! benze					
C5H9CHO	2	464.8	5.29	0.00	0.000
1.000 ! benze					
C6H1003	2	464.8	5.29	0.00	0.000
1.000 ! benze					
CH3-2-1C5H9	2	504.629	5.628	0.000	0.000
1.000 ! 1-hexene					
PXCH2-3-1C5H9	2	504.629	5.628	0.000	0.000
1.000 !					
PX1-3C6H11	2	504.629	5.628	0.000	0.000
1.000 !					
PAXCH2-2-1C5H9	2	504.629	5.628	0.000	0.000
1.000 !					
PX6-2C6H11	2	504.629	5.628	0.000	0.000
1.000 !					
PXC2H4-2-1C4H7	2	504.629	5.628	0.000	0.000
1.000 !					
CH3S3XcC5H8	2	495.3	5.68	0.43	12.30
1.000 ! C6H5CH3					
C6H10-15	2	504.629	5.628	0.000	0.000
1.000 !					
C6H10-12	2	504.629	5.628	0.000	0.000
1.000 !					
C2H5-2-C4H513	2	504.629	5.628	0.000	0.000
1.000 !					
CH2-3-1C5H8	2	504.629	5.628	0.000	0.000
1.000 !					
C2H3-2-1C4H7	2	504.629	5.628	0.000	0.000
1.000 !					
SAXC6H9-13	2	504.629	5.628	0.000	0.000
1.000 !					
SAXC6H9-15	2	504.629	5.628	0.000	0.000
1.000 !					
SAXcC6H9	2	464.8	5.29	0.00	0.000

```

1.000 ! benze
CH2-3-SAXC5H7      2   504.629    5.628    0.000    0.000
1.000 !
cC6H8-13           2   464.8      5.29     0.00     0.000
1.000 !
C6H8-135           2   504.629    5.628    0.000    0.000
1.000 !
SAXcC6H7           2   464.8      5.29     0.00     0.000
1.000 !
PXCH2-2-C4H9       2   448.508    5.342    0.000    0.000
1.000 ! 1-pentene
CH3-2-1C4H7        2   448.508    5.342    0.000    0.000
1.000 !
C2H3cC3H5          2   357.000    5.180    0.000    0.000
1.000 ! C5H6
PAXCH2-2-1C4H7     2   448.508    5.342    0.000    0.000
1.000 !
CH3-2-PXC4H6       2   448.508    5.342    0.000    0.000
1.000 !
PX5-2C5H9          2   448.508    5.342    0.000    0.000
1.000 !
CH3-2-C4H5-13      2   448.508    5.342    0.000    0.000
1.000 !
PAXCH2-2-C4H5      2   448.508    5.342    0.000    0.000
1.000 !
SAXC4H7            2   357.000    5.176    0.000    0.000
1.000 ! C4H7

```

1-15: Species name

16-80: Molecular parameters

molecule index: 0 = atom, 1= linear molec.

2 = nonlinear molec.

L-J potential well depth, e/kb (K)

L-J collision diameter, s,

Dipole moment, f, Debye

Polarizability, ` ,

Rotational relaxation number, Zrot at 298K

Comments

!

! Delete the block below if you do not use the revised tranfit
program (see <http://ae->

[www.usc.edu/research/combustion/CombustionKinetics/Mechanisms/USC-](http://www.usc.edu/research/combustion/CombustionKinetics/Mechanisms/USC-Mech%20II/USC_Mech%20II.htm)
[-Mech%20II/USC_Mech%20II.htm](http://www.usc.edu/research/combustion/CombustionKinetics/Mechanisms/USC-Mech%20II/USC_Mech%20II.htm))

!

END

```

H HE      -9.66994265100   2.10026266000   -0.07705964500
0.00546112600 ! Middha et al, Proc. Comb. Inst., Vol. 29
0.93003284006   0.08015000695   -0.00947327267
0.00063458775
0.87637862374   0.10238278295   -0.01480299828
0.00098803605
1.06001553391  -0.05992751365    0.01026504945  -

```



```

0.00073450868
H H2 -11.74984983000 3.15068443400 -0.25747189600
0.01589155500 ! Middha et al, Proc. Comb. Inst., Vol. 29
0.68564849197 0.15339038119 -0.01367350360
0.00032210353
0.67794933764 0.13747070299 -0.01105868963
0.00016576525
0.65119387990 0.08215979427 -0.00438944167 -
0.00027358319
H2 HE -12.75127347000 3.42444798700 -0.28472577300
0.01593170100 ! Middha et al, Proc. Comb. Inst., Vol. 29
0.59534394712 0.20780905298 -0.02484767627
0.00100127755
0.67714740207 0.13579177260 -0.01142533631
0.00018885880
0.65191818266 0.08365135783 -0.00445010155 -
0.00025986744
H AR -9.05107284400 1.61614185700 -0.00287779500
0.00130541500 ! AIChE 2002
0.68819287418 0.15342306998 -0.01769949486
0.00088795976
0.69683113086 0.17157988788 -0.02435683182
0.00136547873
0.67026727852 0.11433417790 -0.01504070012
0.00051875848
N H2 -11.06296595000 2.35003553100 -0.10371499000
0.00580309100 ! Stallcop et al, Phys. Rev. A, 64, Art. 042722
1.31576376016 -0.13458345098 0.02492533153 -
0.00119098283
6.99070003974 -2.59649971924 0.37720200602 -
0.01788555212
1.28549476326 -0.20526851249 0.03796449261 -
0.00230740895
N N2 -14.50976666000 3.27038987700 -0.22411274000
0.01070436600 ! Stallcop et al, Phys. Rev. A, 64, Art. 042722
1.28549476326 -0.20526851249 0.03796449261 -
0.00230740895
1.31470940230 -0.12581573177 0.02093874922 -
0.00091239288
1.18530004024 -0.00109904512 -0.00679031552
0.00082436382
H O2 -11.04103178000 2.40427694900 -0.10279690200
0.00532644300 ! Stallcop et al, Phys. Rev. A, 64, Art. 042722
1.29254489763 -0.18498887975 0.04271031056 -
0.00260823132
1.99269990199 -0.27220069165 0.02059506743
0.00016444098
1.27566027457 -0.22786150854 0.04449949355 -
0.00274619496
O O2 -14.60250025000 3.29049804400 -0.22351565500
0.01068641100 ! Stallcop et al, Phys. Rev. A, 64, Art. 042722
1.29827044958 -0.17304622424 0.03635310801 -

```

```
0.00206726443
  9.96160341198 -3.95288550918 0.58275322682 -
0.02828930035
  1.26594984746 -0.24767207966 0.04946972829 -
0.00300929402
H N2 -13.27028844000 3.51865269300 -0.29664901800
0.01643138100 ! Stallcop et al, J. Chem. Phys., 97, 3431 (1992)
  1.33864596568 -0.08545398502 0.00922905086
0.00004406488
  -2.20299987672 1.59160087079 -0.25339378410
0.01364477086
  1.27615648812 -0.22593374251 0.04641828877 -
0.00310151225
H2 N2 -10.99943193000 2.20257995900 -0.08115516500
0.00440608700 ! Stallcop et al, Phys. Rev. A, 62, Art. 062709
  1.31648435027 -0.13202102692 0.02416204045 -
0.00120258929
  1.94229781522 -0.41910587564 0.06711915359 -
0.00336850295
  1.29072759648 -0.19301215992 0.03398993578 -
0.00196835629
N2 N2 -16.51750614000 4.05271572500 -0.34593622800
0.01671006600 ! Stallcop et al, Phys. Rev. A, 62, Art. 062709
  1.35301607939 -0.05405097875 -0.00113356164
0.00059799157
  3.61489786826 -1.08630677454 0.15481851859 -
0.00723438967
  1.25620046061 -0.26881554497 0.05577645068 -
0.00340833729
H2 H2 -9.96095484000 2.05602189500 -0.06497689600
0.00413678100 ! Stallcop et al, J. Thermophys. Heat Tra., 12, 514
(1998)
  1.32208755845 -0.12074925804 0.02204710917 -
0.00105955055
  3.63140155962 -1.13979323643 0.16942078618 -
0.00812678015
  1.29811062932 -0.17814060954 0.02956707397 -
0.00170200851
ENDDIFF
```

D.2 The Lumped JetSurf Mechanism

```

!
! Trial version of a lumped model of n-dodecane pyrolysis
! JetSurF 2.5 version a
! June 2013
! Hai Wang
!
! *****
*****
!
! USC Mech ver 2.0
! Release date: May 2007
!
! The reaction model includes the high-temperature chemistry of
! H2/CO/C1-C4 compounds.
!
! How to cite:
! Hai Wang, Xiaqing You, Ameya V. Joshi, Scott G. Davis, Alexander Laskin,
! Fokion Egolfopoulos, and Chung K. Law, USC Mech Version II.
! High-Temperature Combustion Reaction Model of H2/CO/C1-C4 Compounds.
! http://ignis.usc.edu/USC_Mech_II.htm, May 2007.
!
! *****
*****
!
! Please contact Hai Wang at haiw@usc.edu for questions and comments
!
! *****
*****
! CO+OH, OH+HO2 and CO+HO2 Updated May 2007 by Xiaqing You.
! *****
*****
! Last updated April 2005 for H2/CO Chemistry by Ameya Joshi
! *****
*****
!           Revised H2/CO high temperature Combustion Mechanism
!
!           Scott Davis, Ameya Joshi, and Hai Wang
! Department of Mechanical Engineering, University of Delaware, Newark, DE
19716
!
!           January 2003
!
! *****
*****
!
! Added the mechanism of n-butane combustion
! Added the mechanism of benzene and toluene combustion
!
! Ameya Joshi and Hai Wang, October 2001
!
! *****
*****

```

```

!           A Detailed Kinetic Model of 1,3-Butadiene Combustion
!
!           Alexander Laskin and Hai Wang
!Department of Mechanical Engineering, University of Delaware, Newark, DE
19716
!
!           Chung K. Law
!Department of Mechanical and Aerospace Engineering, Princeton University
!
!           June 1999
!
!*****
!*****
! Reference sources can be found at the end of the file.
!
!=====
=====
ELEMENTS
O  H  C  N  AR  HE
END
SPECIES
!
NC12H26
!
AR  N2
HE
!
H      O      OH      HO2      H2      H2O      H2O2
O2
!
C      CH      CH2      CH2*      CH3      CH4
HCO     CH2O     CH3O     CH2OH     CH3OH     CO      CO2
C2O
!
C2H      C2H2      H2CC      C2H3      C2H4      C2H5      C2H6
HCCO     HCCOH     CH2CO     CH3CO     CH2CHO     CH2OCH     CH3CHO
CH2OCH2
!
C3H3      pC3H4      aC3H4      cC3H4      aC3H5      CH3CCH2      CH3CHCH
C3H6      nC3H7      iC3H7      C3H8
CH2CHCO   C2H3CHO     CH3CHOCH2  CH3CH2CHO  CH3COCH3
!
C4H2      nC4H3      iC4H3      C4H4      nC4H5      iC4H5      C4H5-2
c-C4H5
C4H6      C4H612     C4H6-2     C4H7      iC4H7      C4H81      C4H82
iC4H8
pC4H9     sC4H9      iC4H9      tC4H9     C4H10     iC4H10
!
H2C4O     C4H4O      CH2CHCHCHO      CH3CHCHCO
C2H3CHOCH2
C4H6O23   CH3CHCHCHO      C4H6O25

```

```

!
C5H4O      C5H5O (1,3)  C5H5O (2,4) C5H4OH    C5H5OH    C5H5      C5H6
1C5H7
!
C6H2      C6H3      1-C6H4      o-C6H4      C6H5      C6H6
!
C6H5CH2    C6H5CH3    C6H5C2H    C6H5O      C6H5OH    C6H4O2
C6H5CO     C6H5CHO     C6H5CH2OH OC6H4CH3    HOC6H4CH3
C6H4CH3
!
!bi-C6H5CH2
!C6H5C6H5
!C10H8
!
!CH2      - triplet methylene
!CH2*     - singlet methylene
!H2CC     - vinylidene
!aC3H5    - allyl
!CH3CCH2  - CH3-*C=CH2
!CH3CHCH  - CH3-CH=CH*
!nC3H7    - CH3-CH2-CH2*
!iC3H7    - CH3-*CH-CH3
!CH2OCH   - CH2OCH* radical of ethylene oxide
!nC4H3    - *CH=CH-CCH
!iC4H3    - CH2C*-CCH
!nC4H5    - *CH=CH-CH=CH2
!iC4H5    - CH2=C*-CH=CH2
!iC4H7    2-methylpropen-3-yl      H2C=C (CH3) (CH2)
! C4H10    n-butane                  CH3CH2CH2CH3
! iC4H10   i-butane                  CH (CH3) 3
! pC4H9    1-butyl                   CH3CH2CH2CH2
! sC4H9    2-butyl                   CH3CH2CHCH3
! tC4H9    t-butyl                   C (CH3) 3
! iC4H9    i-butyl                   CH2CH (CH3) 2
! C4H81    1-butene                  CH3CH2CHCH2
! C4H82    2-butene                  CH3CHCHCH3
! iC4H8     i-butene                  H2C=C (CH3) 2
!C4H5-2    - CH3-CC-*CH2
!C4H7      - *CH2-CH2-CH=CH2
!CH2CHCO   - CH2=CH-*CO
!C5H5      - cyclopentadienyl
!CH2CHCHCHO - *CH2-CH=CH-CHO
!CH3CHCHCO - CH3-CH=CH-*CO
!C6H3      - *CH=CH-CC-CCH
!C6H5      - phenyl
!C5H5O     - cyclopentadienyloxy radical
!C5H4OH    - cyclopentadienolyl radical
!C6H5CH2   - benzyl
!C6H5O     - phenoxy radical
!CH2OCH2   - ethylene oxide
!C4H6      - 1,3-butadiene
!C4H612    - 1,2-butadiene

```

```

!C4H6-2      - 2-butyne
!C4H81       - 1-butene
!C2H3CHO     - acrolein
!CH3CHOCH2   - propylene oxide
!CH3COCH3    - acetone
!C5H6        - cyclopentadiene
!H2C4O       - CH2=C=C=O
!C4H4O       - furan
!C2H3CHOCH2  - ethenyloxirane
!C4H6O23     - 2,3-dihydrofuran
!CH3CHCHCHO  - crotonaldehyde
!C4H6O25     - 2,5-dihydrofuran
!l-C6H4      - CH2=CH-CC-CCH
!o-C6H4      - benzyne
!C6H6        - benzene
!C5H4O       - 2,4-cyclopentadiene, 1-one
!C6H5CH3     - toluene
!C6H5OH      - phenol
!C6H5C2H     - phenylacetylene
!C6H5C2H3    - styrene
!C10H8       - naphthalene
!C5H5CH3     - methylcyclopentadiene
!C5H4CH2     - fulvene
REACTIONS
!
! Lumped - most condensed form
!
! (1) All alkyl radicals are assumed to be in chemical equilibrium among
the isomers
! (2) beta-scission of the isomers leads to fragmentation
! (3) All 1-alkene species are assumed to dissociate to allyl + an primary
alkyl radical
!
NC12H26      =>
0.3117CH3+0.1884C2H4+0.9924C2H5+0.7895C3H6+0.7327nC3H7+0.2246C4H81+0.5
359pC4H9+0.5727aC3H5 6.82E+32 -4.85 89800.
NC12H26+H    =>H2
+0.2548CH3+0.1859C2H4+0.7773C2H5+0.7773C3H6+0.5731nC3H7+0.2548C4H81+0.
4190pC4H9+1.0242aC3H5 4.005E+06 2.51 4415.22
NC12H26+CH3=>CH4+0.2548CH3+0.1859C2H4+0.7773C2H5+0.7773C3H6+0.5731nC3H
7+0.2548C4H81+0.4190pC4H9+1.0242aC3H5 9.45E-07 5.96 4747.0
NC12H26+OH
=>H2O+0.2548CH3+0.1859C2H4+0.7773C2H5+0.7773C3H6+0.5731nC3H7+0.2548C4H
81+0.4190pC4H9+1.0242aC3H5 1.64+10 1.03 196.7
NC12H26+O2
=>HO2+0.2548CH3+0.1859C2H4+0.7773C2H5+0.7773C3H6+0.5731nC3H7+0.2548C4H
81+0.4190pC4H9+1.0242aC3H5 4.18E+14 0.00 47626.8
NC12H26+HO2=>H2O2+0.2548CH3+0.1859C2H4+0.7773C2H5+0.7773C3H6+0.5731nC3
H7+0.2548C4H81+0.4190pC4H9+1.0242aC3H5 3.09E+04 2.90 14857.66
!
! ---- Optimized C1-C4 mechanism ----
!

```

H+O2<=>O+OH	2.6023E+16	-0.671	17041.00
O+H2<=>H+OH	3.8390E+04	2.700	6260.00
OH+H2<=>H+H2O	2.1384E+08	1.510	3430.00
2OH<=>O+H2O	3.5700E+04	2.400	-2110.00
2H+M<=>H2+M	1.0000E+18	-1.000	0.00
AR/0.63/ HE/0.63/ H2/0.00/ H2O/0.00/ CO2/0.00/			
2H+H2<=>2H2	9.0000E+16	-0.600	0.00
2H+H2O<=>H2+H2O	6.0000E+19	-1.250	0.00
2H+CO2<=>H2+CO2	5.5000E+20	-2.000	0.00
H+OH+M<=>H2O+M	2.5102E+22	-2.000	0.00
AR/0.38/ HE/0.38/ H2/2.00/ H2O/6.30/ CO/1.75/ CO2/3.60/			
O+H+M<=>OH+M	4.7140E+18	-1.000	0.00
AR/ 0.70/ HE/ 0.70/ H2/ 2.00/ H2O/12.00/ CO/ 1.75/ CO2/ 3.60/			
2O+M<=>O2+M	1.2000E+17	-1.000	0.00
AR/ 0.83/ HE/ 0.83/ H2/ 2.40/ H2O/15.40/ CO/ 1.75/ CO2/ 3.60/			
H+O2+M<=>HO2+M	5.2413E+19	-1.397	94.56
AR/0.00/ HE/0.00/ H2/0.00/ H2O/0.00/ O2/0.00/ CO/0.00/			
CO2/0.00/			
H+O2+H2<=>HO2+H2	5.2204E+19	-1.397	94.56
H+2O2<=>HO2+O2	3.8564E+19	-1.395	82.11
H+O2+CO<=>HO2+CO	6.3427E+19	-1.398	103.74
H+O2+CO2<=>HO2+CO2	1.3670E+20	-1.408	150.94
H+O2+H2O<=>HO2+H2O	7.9988E+20	-1.438	217.44
H+O2+AR<=>HO2+AR	6.4519E+18	-1.190	57.52
H+O2+HE<=>HO2+HE	6.4519E+18	-1.190	57.52
H2+O2<=>HO2+H	7.3580E+05	2.433	53502.00
2OH(+M)<=>H2O2(+M)	7.4000E+13	-0.370	0.00
LOW / 1.3400E+17 -0.584 -2293.00/			
TROE/ 0.7346 94.00 1756.00 5182.00 /			
AR/0.70/ HE/0.70/ H2/2.00/ H2O/6.00/ CO/1.75/ CO2/3.60/			
HO2+H<=>O+H2O	3.9700E+12	0.000	671.00
HO2+H<=>2OH	6.4286E+13	0.000	295.00
HO2+O<=>OH+O2	2.0000E+13	0.000	0.00
2HO2<=>O2+H2O2	1.3000E+11	0.000	-1630.00
DUPLICATE			
2HO2<=>O2+H2O2	3.5070E+14	0.000	12000.00
DUPLICATE			
OH+HO2<=>H2O+O2	2.6415E+13	0.000	-500.00
H2O2+H<=>HO2+H2	1.2100E+07	2.000	5200.00
H2O2+H<=>OH+H2O	2.4100E+13	0.000	3970.00
H2O2+O<=>OH+HO2	9.6300E+06	2.000	3970.00
H2O2+OH<=>HO2+H2O	2.0000E+12	0.000	427.00
DUPLICATE			
H2O2+OH<=>HO2+H2O	2.6700E+41	-7.000	37600.00
DUPLICATE			
CO+O(+M)<=>CO2(+M)	1.8000E+10	0.000	2384.00
LOW / 1.5500E+24 -2.790 4191.00/			
AR/ 0.70/ HE/ 0.70/ H2/ 2.00/ H2O/12.00/ CO/ 1.75/ CO2/ 3.60/			
CO+OH<=>CO2+H	6.8417E+04	2.053	-355.67
DUPLICATE			
CO+OH<=>CO2+H	5.7340E+12	-0.664	331.83
DUPLICATE			


```

CO+O2<=>CO2+O          2.5300E+12    0.000    47700.00
CO+HO2<=>CO2+OH         3.0100E+13    0.000    23000.00
HCO+H<=>CO+H2          1.3692E+14    0.000     0.00
HCO+O<=>CO+OH           3.0000E+13    0.000     0.00
HCO+O<=>CO2+H           3.0000E+13    0.000     0.00
HCO+OH<=>CO+H2O         3.4066E+13    0.000     0.00
HCO+M<=>CO+H+M          1.0023E+17   -1.000    17000.00
H2/2.00/ H2O/0.00/ CO/1.75/ CO2/3.60/
HCO+H2O<=>CO+H+H2O      9.5033E+17   -1.000    17000.00
HCO+O2<=>CO+HO2         1.2209E+10    0.807    -727.00
CO+H2 (+M) <=>CH2O (+M)  4.3000E+07    1.500    79600.00
    LOW / 5.0700E+27   -3.420    84350.00/
    TROE/ 0.9320      197.00     1540.00     10300.00 /
AR/0.70/ H2/2.00/ H2O/6.00/ CH4/2.00/ CO/1.50/ CO2/2.00/
C2H6/3.00/
C+OH<=>CO+H             5.0000E+13    0.000     0.00
C+O2<=>CO+O             5.8000E+13    0.000    576.00
CH+H<=>C+H2             1.1077E+14    0.000     0.00
CH+O<=>CO+H             5.7000E+13    0.000     0.00
CH+OH<=>HCO+H           3.0000E+13    0.000     0.00
CH+H2<=>CH2+H           1.1070E+08    1.790    1670.00
CH+H2O<=>CH2O+H         5.7100E+12    0.000   -755.00
CH+O2<=>HCO+O           2.4453E+13    0.000     0.00
CH+CO (+M) <=>HCCO (+M)  5.0000E+13    0.000     0.00
    LOW / 2.6900E+28   -3.740    1936.00/
    TROE/ 0.5757      237.00     1652.00     5069.00 /
AR/0.70/ H2/2.00/ H2O/6.00/ CH4/2.00/ CO/1.50/ CO2/2.00/
C2H6/3.00/
CH+CO2<=>HCO+CO         3.4000E+12    0.000     690.00
HCO+H (+M) <=>CH2O (+M)  1.0900E+12    0.480   -260.00
    LOW / 1.3500E+24   -2.570    1425.00/
    TROE/ 0.7824      271.00     2755.00     6570.00 /
AR/0.70/ H2/2.00/ H2O/6.00/ CH4/2.00/ CO/1.50/ CO2/2.00/
C2H6/3.00/
CH2+H (+M) <=>CH3 (+M)   2.5000E+16   -0.800     0.00
    LOW / 3.2000E+27   -3.140    1230.00/
    TROE/ 0.6800      78.00     1995.00     5590.00 /
AR/0.70/ H2/2.00/ H2O/6.00/ CH4/2.00/ CO/1.50/ CO2/2.00/
C2H6/3.00/
CH2+O<=>HCO+H           8.0000E+13    0.000     0.00
CH2+OH<=>CH2O+H         2.0000E+13    0.000     0.00
CH2+OH<=>CH+H2O         1.1300E+07    2.000    3000.00
CH2+H2<=>H+CH3          5.0000E+05    2.000    7230.00
CH2+O2<=>HCO+OH         1.0452E+13    0.000    1500.00
CH2+O2<=>CO2+2H         2.6030E+12    0.000    1500.00
CH2+HO2<=>CH2O+OH       2.0000E+13    0.000     0.00
CH2+C<=>C2H+H           5.0000E+13    0.000     0.00
CH2+CO (+M) <=>CH2CO (+M) 8.1000E+11    0.500    4510.00
    LOW / 2.6900E+33   -5.110    7095.00/
    TROE/ 0.5907      275.00     1226.00     5185.00 /
AR/0.70/ H2/2.00/ H2O/6.00/ CH4/2.00/ CO/1.50/ CO2/2.00/
C2H6/3.00/

```

CH2+CH<=>C2H2+H	4.0000E+13	0.000	0.00
2CH2<=>C2H2+H2	3.2000E+13	0.000	0.00
CH2*+N2<=>CH2+N2	1.5000E+13	0.000	600.00
CH2*+AR<=>CH2+AR	9.0000E+12	0.000	600.00
CH2*+H<=>CH+H2	3.0000E+13	0.000	0.00
CH2*+O<=>CO+H2	1.5000E+13	0.000	0.00
CH2*+O<=>HCO+H	1.5000E+13	0.000	0.00
CH2*+OH<=>CH2O+H	3.0000E+13	0.000	0.00
CH2*+H2<=>CH3+H	7.0000E+13	0.000	0.00
CH2*+O2<=>H+OH+CO	2.6684E+13	0.000	0.00
CH2*+O2<=>CO+H2O	1.2000E+13	0.000	0.00
CH2*+H2O (+M) <=>CH3OH (+M)	2.0000E+13	0.000	0.00
LOW / 2.7000E+38 -6.300 3100.00/			
TROE/ 0.1507 134.00 2383.00 7265.00 /			
H2/2.00/ H2O/6.00/ CH4/2.00/ CO/1.50/ CO2/2.00/ C2H6/3.00/			
CH2*+H2O<=>CH2+H2O	3.0000E+13	0.000	0.00
CH2*+CO<=>CH2+CO	9.0000E+12	0.000	0.00
CH2*+CO2<=>CH2+CO2	7.0000E+12	0.000	0.00
CH2*+CO2<=>CH2O+CO	1.4000E+13	0.000	0.00
CH2O+H (+M) <=>CH2OH (+M)	5.4000E+11	0.454	3600.00
LOW / 1.2700E+32 -4.820 6530.00/			
TROE/ 0.7187 103.00 1291.00 4160.00 /			
H2/2.00/ H2O/6.00/ CH4/2.00/ CO/1.50/ CO2/2.00/ C2H6/3.00/			
CH2O+H (+M) <=>CH3O (+M)	5.4000E+11	0.454	2600.00
LOW / 2.2000E+30 -4.800 5560.00/			
TROE/ 0.7580 94.00 1555.00 4200.00 /			
H2/2.00/ H2O/6.00/ CH4/2.00/ CO/1.50/ CO2/2.00/ C2H6/3.00/			
CH2O+H<=>HCO+H2	2.3000E+10	1.050	3275.00
CH2O+O<=>HCO+OH	3.9000E+13	0.000	3540.00
CH2O+OH<=>HCO+H2O	3.4300E+09	1.180	-447.00
CH2O+O2<=>HCO+HO2	1.0000E+14	0.000	40000.00
CH2O+HO2<=>HCO+H2O2	1.0000E+12	0.000	8000.00
CH2O+CH<=>CH2CO+H	9.4600E+13	0.000	-515.00
CH3+H (+M) <=>CH4 (+M)	1.0109E+16	-0.630	383.00
LOW / 1.9717E+33 -4.760 2440.00/			
TROE/ 0.7830 74.00 2941.00 6964.00 /			
AR/0.70/ H2/2.00/ H2O/6.00/ CH4/2.00/ CO/1.50/ CO2/2.00/			
C2H6/3.00/			
CH3+O<=>CH2O+H	8.2024E+13	0.000	0.00
CH3+OH (+M) <=>CH3OH (+M)	9.4185E+13	0.000	0.00
LOW / 4.0365E+38 -6.300 3100.00/			
TROE/ 0.2105 83.50 5398.00 8370.00 /			
H2/2.00/ H2O/6.00/ CH4/2.00/ CO/1.50/ CO2/2.00/ C2H6/3.00/			
CH3+OH<=>CH2+H2O	5.6000E+07	1.600	5420.00
CH3+OH<=>CH2*+H2O	7.7281E+12	0.000	0.00
CH3+O2<=>O+CH3O	3.4776E+13	0.000	28800.00
CH3+O2<=>OH+CH2O	3.6000E+10	0.000	8940.00
CH3+HO2<=>CH4+O2	1.0000E+12	0.000	0.00
CH3+HO2<=>CH3O+OH	3.0217E+13	0.000	0.00
CH3+H2O2<=>CH4+HO2	2.4500E+04	2.470	5180.00
CH3+C<=>C2H2+H	5.0000E+13	0.000	0.00
CH3+CH<=>C2H3+H	3.0000E+13	0.000	0.00

```

CH3+HCO<=>CH4+CO          8.4800E+12    0.000    0.00
CH3+CH2O<=>CH4+HCO        3.3200E+03    2.810    5860.00
CH3+CH2<=>C2H4+H          4.0000E+13    0.000    0.00
CH3+CH2* <=> C2H4+H        1.2000E+13    0.000   -570.00
2CH3 (+M) <=> C2H6 (+M)    2.4359E+16   -0.970    620.00
    LOW / 2.0337E+50   -9.670    6220.00/
    TROE/ 0.5325      151.00    1038.00    4970.00 /
AR/0.70/ H2/2.00/ H2O/6.00/ CH4/2.00/ CO/1.50/ CO2/2.00/
C2H6/3.00/
2CH3<=>H+C2H5              5.5838E+12    0.100   10600.00
CH3+HCCO<=>C2H4+CO        5.0000E+13    0.000    0.00
CH3+C2H<=>C3H3+H          2.4100E+13    0.000    0.00
CH3O+H (+M) <=> CH3OH (+M) 5.0000E+13    0.000    0.00
    LOW / 8.6000E+28   -4.000    3025.00/
    TROE/ 0.8902      144.00    2838.00    45569.00 /
H2/2.00/ H2O/6.00/ CH4/2.00/ CO/1.50/ CO2/2.00/ C2H6/3.00/
CH3O+H<=>CH2OH+H          3.4000E+06    1.600    0.00
CH3O+H<=>CH2O+H2          2.0000E+13    0.000    0.00
CH3O+H<=>CH3+OH           3.2000E+13    0.000    0.00
CH3O+H<=>CH2*+H2O         1.6000E+13    0.000    0.00
CH3O+O<=>CH2O+OH          1.0000E+13    0.000    0.00
CH3O+OH<=>CH2O+H2O        5.0000E+12    0.000    0.00
CH3O+O2<=>CH2O+HO2        4.2800E-13    7.600   -3530.00
CH2OH+H (+M) <=> CH3OH (+M) 1.8000E+13    0.000    0.00
    LOW / 3.0000E+31   -4.800    3300.00/
    TROE/ 0.7679      338.00    1812.00    5081.00 /
H2/2.00/ H2O/6.00/ CH4/2.00/ CO/1.50/ CO2/2.00/ C2H6/3.00/
CH2OH+H<=>CH2O+H2         2.0000E+13    0.000    0.00
CH2OH+H<=>CH3+OH           1.2000E+13    0.000    0.00
CH2OH+H<=>CH2*+H2O         6.0000E+12    0.000    0.00
CH2OH+O<=>CH2O+OH          1.0000E+13    0.000    0.00
CH2OH+OH<=>CH2O+H2O        5.0000E+12    0.000    0.00
CH2OH+O2<=>CH2O+HO2        1.8000E+13    0.000    900.00
CH4+H<=>CH3+H2            6.6000E+08    1.620   10840.00
CH4+O<=>CH3+OH             1.0200E+09    1.500    8600.00
CH4+OH<=>CH3+H2O           9.6400E+07    1.600    3120.00
CH4+CH<=>C2H4+H            6.0000E+13    0.000    0.00
CH4+CH2<=>2CH3             2.4600E+06    2.000    8270.00
CH4+CH2* <=> 2CH3           1.6000E+13    0.000   -570.00
CH4+C2H<=>C2H2+CH3         1.8100E+12    0.000    500.00
CH3OH+H<=>CH2OH+H2         1.7000E+07    2.100    4870.00
CH3OH+H<=>CH3O+H2          4.2000E+06    2.100    4870.00
CH3OH+O<=>CH2OH+OH         3.8800E+05    2.500    3100.00
CH3OH+O<=>CH3O+OH          1.3000E+05    2.500    5000.00
CH3OH+OH<=>CH2OH+H2O       1.4400E+06    2.000   -840.00
CH3OH+OH<=>CH3O+H2O        6.3000E+06    2.000    1500.00
CH3OH+CH3<=>CH2OH+CH4      3.0000E+07    1.500    9940.00
CH3OH+CH3<=>CH3O+CH4       1.0000E+07    1.500    9940.00
C2H+H (+M) <=> C2H2 (+M)   1.0000E+17   -1.000    0.00
    LOW / 3.7500E+33   -4.800    1900.00/
    TROE/ 0.6464      132.00    1315.00    5566.00 /
AR/0.70/ H2/2.00/ H2O/6.00/ CH4/2.00/ CO/1.50/ CO2/2.00/

```

```

C2H6/3.00/
C2H+O<=>CH+CO          5.0000E+13    0.000    0.00
C2H+OH<=>H+HCCO         2.0000E+13    0.000    0.00
C2H+O2<=>HCO+CO         5.0000E+13    0.000   1500.00
C2H+H2<=>H+C2H2         4.9000E+05    2.500   560.00
C2O+H<=>CH+CO           5.0000E+13    0.000    0.00
C2O+O<=>2CO             5.0000E+13    0.000    0.00
C2O+OH<=>2CO+H          2.0000E+13    0.000    0.00
C2O+O2<=>2CO+O          2.0000E+13    0.000    0.00
HCCO+H<=>CH2*+CO        1.0350E+14    0.000    0.00
HCCO+O<=>H+2CO          1.0000E+14    0.000    0.00
HCCO+O2<=>OH+2CO        1.9104E+12    0.000   854.00
HCCO+CH<=>C2H2+CO       5.0000E+13    0.000    0.00
HCCO+CH2<=>C2H3+CO      3.0000E+13    0.000    0.00
2HCCO<=>C2H2+2CO        1.0000E+13    0.000    0.00
HCCO+OH<=>C2O+H2O       3.0000E+13    0.000    0.00
C2H2 (+M) <=>H2CC (+M)   8.0000E+14   -0.520  50750.00
    LOW / 2.4500E+15   -0.640  49700.00/
H2/2.00/ H2O/6.00/ CH4/2.00/ CO/1.50/ CO2/2.00/ C2H4/2.50/
C2H6/3.00/
C2H3 (+M) <=>C2H2+H (+M) 3.6323E+08    1.620  37048.20
    LOW / 2.4137E+27   -3.400  35798.72/
    TROE/ 1.9816    5383.70    4.29    -0.08 /
AR/0.70/ H2/2.00/ H2O/6.00/ CH4/2.00/ CO/1.50/ CO2/2.00/
C2H2/3.00/ C2H4/3.00/ C2H6/3.00/
C2H2+O<=>C2H+OH         4.6000E+19   -1.410  28950.00
C2H2+O<=>CH2+CO         4.0800E+06    2.000   1900.00
C2H2+O<=>HCCO+H         1.6124E+07    2.000   1900.00
C2H2+OH<=>CH2CO+H       2.1800E-04    4.500  -1000.00
C2H2+OH<=>HCCOH+H       5.0400E+05    2.300  13500.00
C2H2+OH<=>C2H+H2O       3.3700E+07    2.000  14000.00
C2H2+OH<=>CH3+CO        4.8300E-04    4.000  -2000.00
C2H2+HCO<=>C2H3+CO      1.0000E+07    2.000   6000.00
C2H2+CH2<=>C3H3+H       1.2000E+13    0.000   6620.00
C2H2+CH2* <=>C3H3+H     2.0000E+13    0.000    0.00
C2H2+C2H<=>C4H2+H       9.6000E+13    0.000    0.00
C2H2+C2H (+M) <=>nC4H3 (+M) 8.3000E+10    0.899  -363.00
    LOW / 1.2400E+31   -4.718  1871.00/
    TROE/ 1.0000    100.00    5613.00    13387.00 /
H2/2.00/ H2O/6.00/ CH4/2.00/ CO/1.50/ CO2/2.00/ C2H2/2.50/
C2H4/2.50/ C2H6/3.00/
C2H2+C2H (+M) <=>iC4H3 (+M) 8.3000E+10    0.899  -363.00
    LOW / 1.2400E+31   -4.718  1871.00/
    TROE/ 1.0000    100.00    5613.00    13387.00 /
H2/2.00/ H2O/6.00/ CH4/2.00/ CO/1.50/ CO2/2.00/ C2H2/2.50/
C2H4/2.50/ C2H6/3.00/
C2H2+HCCO<=>C3H3+CO     1.0000E+11    0.000   3000.00
C2H2+CH3<=>pC3H4+H      2.4218E+09    1.100  13644.00
C2H2+CH3<=>aC3H4+H      5.1400E+09    0.860  22153.00
C2H2+CH3<=>CH3CCH2      4.9900E+22   -4.390  18850.00
C2H2+CH3<=>CH3CHCH      3.2000E+35   -7.760  13300.00
C2H2+CH3<=>aC3H5        2.6800E+53  -12.820  35730.00

```

H2CC+H<=>C2H2+H	1.0000E+14	0.000	0.00
H2CC+OH<=>CH2CO+H	2.0000E+13	0.000	0.00
H2CC+O2<=>2HCO	1.0000E+13	0.000	0.00
H2CC+C2H2 (+M) <=>C4H4 (+M)	3.5000E+05	2.055	-2400.00
LOW / 1.4000E+60 -12.599 7417.00/			
TROE/ 0.9800 56.00 580.00 4164.00 /			
H2/2.00/ H2O/6.00/ CH4/2.00/ CO/1.50/ CO2/2.00/ C2H2/3.00/			
C2H4/3.00/ C2H6/3.00/			
H2CC+C2H4<=>C4H6	1.0000E+12	0.000	0.00
CH2CO+H (+M) <=>CH2CHO (+M)	3.3000E+14	-0.060	8500.00
LOW / 3.8000E+41 -7.640 11900.00/			
TROE/ 0.3370 1707.00 3200.00 4131.00 /			
AR/0.70/ H2/2.00/ H2O/6.00/ CH4/2.00/ CO/1.50/ CO2/2.00/			
C2H2/3.00/ C2H4/3.00/ C2H6/3.00/			
CH2CO+H<=>HCCO+H2	5.0000E+13	0.000	8000.00
CH2CO+H<=>CH3+CO	1.5000E+09	1.430	2690.00
CH2CO+O<=>HCCO+OH	1.0000E+13	0.000	8000.00
CH2CO+O<=>CH2+CO2	1.7500E+12	0.000	1350.00
CH2CO+OH<=>HCCO+H2O	7.5000E+12	0.000	2000.00
HCCOH+H<=>CH2CO+H	1.0000E+13	0.000	0.00
C2H3+H (+M) <=>C2H4 (+M)	6.0800E+12	0.270	280.00
LOW / 1.4000E+30 -3.860 3320.00/			
TROE/ 0.7820 207.50 2663.00 6095.00 /			
AR/0.70/ H2/2.00/ H2O/6.00/ CH4/2.00/ CO/1.50/ CO2/2.00/			
C2H2/3.00/ C2H4/3.00/ C2H6/3.00/			
C2H3+H<=>C2H2+H2	8.8020E+13	0.000	0.00
C2H3+H<=>H2CC+H2	6.3960E+13	0.000	0.00
C2H3+O<=>CH2CO+H	4.8000E+13	0.000	0.00
C2H3+O<=>CH3+CO	4.8000E+13	0.000	0.00
C2H3+OH<=>C2H2+H2O	3.0110E+13	0.000	0.00
C2H3+O2<=>C2H2+HO2	1.3400E+06	1.610	-383.40
C2H3+O2<=>CH2CHO+O	9.6120E+11	0.290	11.00
C2H3+O2<=>HCO+CH2O	3.8410E+16	-1.390	1010.00
C2H3+HO2<=>CH2CHO+OH	1.0000E+13	0.000	0.00
C2H3+H2O2<=>C2H4+HO2	1.2100E+10	0.000	-596.00
C2H3+HCO<=>C2H4+CO	9.0330E+13	0.000	0.00
C2H3+HCO<=>C2H3CHO	1.8000E+13	0.000	0.00
C2H3+CH3<=>C2H2+CH4	3.9200E+11	0.000	0.00
C2H3+CH3 (+M) <=>C3H6 (+M)	2.5000E+13	0.000	0.00
LOW / 4.2700E+58 -11.940 9769.80/			
TROE/ 0.1750 1340.60 60000.00 10139.80 /			
AR/0.70/ H2/2.00/ H2O/6.00/ CH4/2.00/ CO/1.50/ CO2/2.00/			
C2H4/3.00/ C2H6/3.00/			
C2H3+CH3<=>aC3H5+H	1.5000E+24	-2.830	18618.00
C2H3+C2H2<=>C4H4+H	2.0000E+18	-1.680	10600.00
C2H3+C2H2<=>nC4H5	9.3000E+38	-8.760	12000.00
C2H3+C2H2<=>iC4H5	1.6000E+46	-10.980	18600.00
2C2H3<=>C4H6	1.5000E+42	-8.840	12483.00
2C2H3<=>iC4H5+H	1.2000E+22	-2.440	13654.00
2C2H3<=>nC4H5+H	2.4000E+20	-2.040	15361.00
2C2H3<=>C2H2+C2H4	9.6000E+11	0.000	0.00
CH2CHO<=>CH3+CO	7.8000E+41	-9.147	46900.00

```

CH2CHO+H (+M) <=> CH3CHO (+M)                1.0000E+14    0.000    0.00
    LOW / 5.2000E+39    -7.297    4700.00/
    TROE/ 0.5500    8900.00    4350.00    7244.00 /
H2/2.00/ H2O/6.00/ CH4/2.00/ CO/1.50/ CO2/2.00/ C2H2/3.00/
C2H4/3.00/ C2H6/3.00/
CH2CHO+H<=>CH3CO+H                5.0000E+12    0.000    0.00
CH2CHO+H<=>CH3+HCO                9.0000E+13    0.000    0.00
CH2CHO+H<=>CH2CO+H2                2.0000E+13    0.000    4000.00
CH2CHO+O<=>CH2CO+OH                2.0000E+13    0.000    4000.00
CH2CHO+OH<=>CH2CO+H2O              1.0000E+13    0.000    2000.00
CH2CHO+O2<=>CH2CO+HO2              1.4000E+11    0.000    0.00
CH2CHO+O2<=>CH2O+CO+OH              1.8000E+10    0.000    0.00
CH3+CO (+M) <=> CH3CO (+M)          4.8500E+07    1.650    6150.00
    LOW / 7.8000E+30    -5.395    8600.00/
    TROE/ 0.2580    598.00    21002.00    1773.00 /
AR/0.70/ H2/2.00/ H2O/6.00/ CH4/2.00/ CO/1.50/ CO2/2.00/
C2H2/3.00/ C2H4/3.00/ C2H6/3.00/
CH3CO+H (+M) <=> CH3CHO (+M)          9.6000E+13    0.000    0.00
    LOW / 3.8500E+44    -8.569    5500.00/
    TROE/ 1.0000    2900.00    2900.00    5132.00 /
H2/2.00/ H2O/6.00/ CH4/2.00/ CO/1.50/ CO2/2.00/ C2H2/3.00/
C2H4/3.00/ C2H6/3.00/
CH3CO+H<=>CH3+HCO                9.6000E+13    0.000    0.00
CH3CO+O<=>CH2CO+OH                3.9000E+13    0.000    0.00
CH3CO+O<=>CH3+CO2                1.5000E+14    0.000    0.00
CH3CO+OH<=>CH2CO+H2O              1.2000E+13    0.000    0.00
CH3CO+OH<=>CH3+CO+OH              3.0000E+13    0.000    0.00
CH3CO+HO2<=>CH3+CO2+OH            3.0000E+13    0.000    0.00
CH3CO+H2O2<=>CH3CHO+HO2            1.8000E+11    0.000    8226.00
CH3+HCO (+M) <=> CH3CHO (+M)          1.8000E+13    0.000    0.00
    LOW / 2.2000E+48    -9.588    5100.00/
    TROE/ 0.6173    13.08    2078.00    5093.00 /
H2/2.00/ H2O/6.00/ CH4/2.00/ CO/1.50/ CO2/2.00/ C2H2/3.00/
C2H4/3.00/ C2H6/3.00/
CH3CHO+H<=>CH3CO+H2                4.1000E+09    1.160    2400.00
CH3CHO+H<=>CH4+HCO                5.0000E+10    0.000    0.00
CH3CHO+O<=>CH3CO+OH                5.8000E+12    0.000    1800.00
CH3CHO+OH<=>CH3CO+H2O              2.3500E+10    0.730    -1110.00
CH3CHO+CH3<=>CH3CO+CH4              2.0000E-06    5.600    2460.00
CH3CHO+HCO<=>CO+HCO+CH4            8.0000E+12    0.000    10400.00
CH3CHO+O2<=>CH3CO+HO2              3.0000E+13    0.000    39100.00
CH2OCH2<=>CH3+HCO                 3.6300E+13    0.000    57200.00
CH2OCH2<=>CH3CHO                  7.2600E+13    0.000    57200.00
CH2OCH2<=>CH4+CO                  1.2100E+13    0.000    57200.00
CH2OCH2+H<=>CH2OCH+H2              2.0000E+13    0.000    8300.00
CH2OCH2+H<=>C2H3+H2O              5.0000E+09    0.000    5000.00
CH2OCH2+H<=>C2H4+OH              9.5100E+10    0.000    5000.00
CH2OCH2+O<=>CH2OCH+OH             1.9100E+12    0.000    5250.00
CH2OCH2+OH<=>CH2OCH+H2O            1.7800E+13    0.000    3610.00
CH2OCH2+CH3<=>CH2OCH+CH4           1.0700E+12    0.000    11830.00
CH2OCH+M<=>CH3+CO+M                3.1600E+14    0.000    12000.00
CH2OCH+M<=>CH2CHO+M                5.0000E+09    0.000    0.00

```

```

CH2OCH+M<=>CH2CO+H+M          3.0000E+13    0.000    8000.00
C2H4+M<=>H2+H2CC+M          9.6835E+14    0.000    54250.00
AR/0.70/ H2/2.00/ H2O/6.00/ CH4/2.00/ CO/1.50/ CO2/2.00/
C2H6/3.00/
C2H4+H (+M) <=> C2H5 (+M)      1.2385E+09    1.463    1355.00
    LOW / 1.8365E+39    -6.642    5769.00/
    TROE/ -0.5690      299.00    9147.00    -152.40 /
AR/0.70/ H2/2.00/ H2O/6.00/ CH4/2.00/ CO/1.50/ CO2/2.00/
C2H6/3.00/
C2H4+H<=>C2H3+H2          4.9990E+07    1.900    12950.00
C2H4+O<=>C2H3+OH          1.7425E+07    1.900    3740.00
C2H4+O<=>CH3+HCO          1.6032E+07    1.830    220.00
C2H4+O<=>CH2+CH2O          3.8400E+05    1.830    220.00
C2H4+OH<=>C2H3+H2O          4.2804E+06    2.000    2500.00
C2H4+HCO<=>C2H5+CO          1.0000E+07    2.000    8000.00
C2H4+CH<=>aC3H4+H          3.0000E+13    0.000    0.00
C2H4+CH<=>pC3H4+H          3.0000E+13    0.000    0.00
C2H4+CH2<=>aC3H5+H          2.0000E+13    0.000    6000.00
C2H4+CH2*<=>H2CC+CH4        5.0000E+13    0.000    0.00
C2H4+CH2*<=>aC3H5+H          5.0000E+13    0.000    0.00
C2H4+CH3<=>C2H3+CH4        4.4628E+05    2.000    9200.00
C2H4+CH3<=>nC3H7            3.3000E+11    0.000    7700.00
C2H4+C2H<=>C4H4+H          1.2000E+13    0.000    0.00
C2H4+O2<=>C2H3+HO2          4.2200E+13    0.000    60800.00
C2H4+C2H3<=>C4H7            7.9300E+38    -8.470    14220.00
C2H4+HO2<=>CH2OCH2+OH        2.8200E+12    0.000    17100.00
C2H5+H (+M) <=> C2H6 (+M)      5.2100E+17    -0.990    1580.00
    LOW / 1.9900E+41    -7.080    6685.00/
    TROE/ 0.8422      125.00    2219.00    6882.00 /
AR/0.70/ H2/2.00/ H2O/6.00/ CH4/2.00/ CO/1.50/ CO2/2.00/
C2H6/3.00/
C2H5+H<=>C2H4+H2          2.0000E+12    0.000    0.00
C2H5+O<=>CH3+CH2O          1.6040E+13    0.000    0.00
C2H5+O<=>CH3CHO+H          8.0200E+13    0.000    0.00
C2H5+O2<=>C2H4+HO2          2.0000E+10    0.000    0.00
C2H5+HO2<=>C2H6+O2          3.0000E+11    0.000    0.00
C2H5+HO2<=>C2H4+H2O2          3.0000E+11    0.000    0.00
C2H5+HO2<=>CH3+CH2O+OH        2.4000E+13    0.000    0.00
C2H5+H2O2<=>C2H6+HO2          8.7000E+09    0.000    974.00
C2H5+CH3 (+M) <=> C3H8 (+M)    4.9000E+14    -0.500    0.00
    LOW / 6.8000E+61    -13.420    6000.00/
    TROE/ 1.0000      1000.00    1433.90    5328.80 /
AR/0.70/ H2/2.00/ H2O/6.00/ CH4/2.00/ CO/1.50/ CO2/2.00/
C2H6/3.00/
C2H5+C2H3 (+M) <=> C4H8 (+M)    1.5000E+13    0.000    0.00
    LOW / 1.5500E+56    -11.790    8984.50/
    TROE/ 0.1980      2277.90    60000.00    5723.20 /
AR/0.70/ H2/2.00/ H2O/6.00/ CH4/2.00/ CO/1.50/ CO2/2.00/
C2H6/3.00/
C2H5+C2H3<=>aC3H5+CH3        3.9000E+32    -5.220    19747.00
C2H6+H<=>C2H5+H2          1.1500E+08    1.900    7530.00
C2H6+O<=>C2H5+OH          8.9800E+07    1.920    5690.00

```

C2H6+OH<=>C2H5+H2O	3.4550E+06	2.120	870.00
C2H6+CH2*=>C2H5+CH3	4.0000E+13	0.000	-550.00
C2H6+CH3<=>C2H5+CH4	6.1400E+06	1.740	10450.00
C3H3+H<=>pC3H4	1.5000E+13	0.000	0.00
C3H3+H<=>aC3H4	2.5000E+12	0.000	0.00
C3H3+O<=>CH2O+C2H	2.0000E+13	0.000	0.00
C3H3+O2<=>CH2CO+HCO	3.0000E+10	0.000	2868.00
C3H3+HO2<=>OH+CO+C2H3	8.0000E+11	0.000	0.00
C3H3+HO2<=>aC3H4+O2	3.0000E+11	0.000	0.00
C3H3+HO2<=>pC3H4+O2	2.5000E+12	0.000	0.00
C3H3+HCO<=>aC3H4+CO	2.5000E+13	0.000	0.00
C3H3+HCO<=>pC3H4+CO	2.5000E+13	0.000	0.00
C3H3+HCCO<=>C4H4+CO	2.5000E+13	0.000	0.00
C3H3+CH<=>iC4H3+H	5.0000E+13	0.000	0.00
C3H3+CH2<=>C4H4+H	5.0000E+13	0.000	0.00
C3H3+CH3 (+M) <=>C4H612 (+M)	1.5000E+12	0.000	0.00
LOW / 2.6000E+57 -11.940 9770.00/			
TROE/ 0.1750 1340.60 60000.00 9769.80 /			
AR/0.70/ H2/2.00/ H2O/6.00/ CH4/2.00/ CO/1.50/ CO2/2.00/			
C2H6/3.00/			
C3H3+C2H2<=>C5H5	6.8700E+55	-12.500	42025.00
2C3H3=>C6H5+H	5.0000E+12	0.000	0.00
2C3H3=>C6H6	2.0000E+12	0.000	0.00
C3H3+C4H4<=>C6H5CH2	6.5300E+05	1.280	-4611.00
C3H3+C4H6<=>C6H5CH3+H	6.5300E+05	1.280	-4611.00
aC3H4+H<=>C3H3+H2	1.3000E+06	2.000	5500.00
aC3H4+H<=>CH3CHCH	5.4000E+29	-6.090	16300.00
aC3H4+H<=>CH3CCH2	9.4600E+42	-9.430	11190.00
aC3H4+H<=>aC3H5	1.6173E+59	-13.540	26949.00
aC3H4+O<=>C2H4+CO	2.0000E+07	1.800	1000.00
aC3H4+OH<=>C3H3+H2O	5.3000E+06	2.000	2000.00
aC3H4+CH3<=>C3H3+CH4	1.3000E+12	0.000	7700.00
aC3H4+CH3<=>iC4H7	2.0000E+11	0.000	7500.00
aC3H4+C2H<=>C2H2+C3H3	1.0000E+13	0.000	0.00
pC3H4<=>cC3H4	1.2000E+44	-9.920	69250.00
pC3H4<=>aC3H4	5.1500E+60	-13.930	91117.00
pC3H4+H<=>aC3H4+H	6.2700E+17	-0.910	10079.00
pC3H4+H<=>CH3CCH2	1.6600E+47	-10.580	13690.00
pC3H4+H<=>CH3CHCH	5.5000E+28	-5.740	4300.00
pC3H4+H<=>aC3H5	4.9100E+60	-14.370	31644.00
pC3H4+H<=>C3H3+H2	1.3000E+06	2.000	5500.00
pC3H4+C3H3<=>aC3H4+C3H3	6.1400E+06	1.740	10450.00
pC3H4+O<=>HCCO+CH3	7.3000E+12	0.000	2250.00
pC3H4+O<=>C2H4+CO	1.0000E+13	0.000	2250.00
pC3H4+OH<=>C3H3+H2O	1.0000E+06	2.000	100.00
pC3H4+C2H<=>C2H2+C3H3	1.0000E+13	0.000	0.00
pC3H4+CH3<=>C3H3+CH4	1.8000E+12	0.000	7700.00
cC3H4<=>aC3H4	4.8900E+41	-9.170	49594.00
aC3H5+H (+M) <=>C3H6 (+M)	1.9560E+14	0.000	0.00
LOW / 1.3007E+60 -12.000 5967.80/			
TROE/ 0.0200 1096.60 1096.60 6859.50 /			
AR/0.70/ H2/2.00/ H2O/6.00/ CH4/2.00/ CO/1.50/ CO2/2.00/			


```

C2H6/3.00/
aC3H5+H<=>aC3H4+H2          1.8000E+13    0.000    0.00
aC3H5+O<=>C2H3CHO+H          5.6820E+13    0.000    0.00
aC3H5+OH<=>C2H3CHO+2H        4.2000E+32   -5.160   30126.00
aC3H5+OH<=>aC3H4+H2O          6.0000E+12    0.000    0.00
aC3H5+O2<=>aC3H4+HO2          4.9900E+15   -1.400   22428.00
aC3H5+O2<=>CH3CO+CH2O         1.1900E+15   -1.010   20128.00
aC3H5+O2<=>C2H3CHO+OH         1.8200E+13   -0.410   22859.00
aC3H5+HO2<=>C3H6+O2           2.6600E+12    0.000    0.00
aC3H5+HO2<=>OH+C2H3+CH2O      9.1740E+12    0.000    0.00
aC3H5+HCO<=>C3H6+CO           6.0000E+13    0.000    0.00
aC3H5+CH3 (+M) <=>C4H81 (+M)  9.9200E+13   -0.320   -262.30
      LOW / 3.8787E+60  -12.810  6250.00/
      TROE/ 0.1040    1606.00    60000.00    6118.40 /
AR/0.70/ H2/2.00/ H2O/6.00/ CH4/2.00/ CO/1.50/ CO2/2.00/
C2H6/3.00/
aC3H5+CH3<=>aC3H4+CH4          3.0000E+12   -0.320   -131.00
aC3H5<=>CH3CCH2                7.0600E+56  -14.080   75868.00
aC3H5<=>CH3CHCH                5.0000E+51  -13.020   73300.00
aC3H5+C2H2<=>1C5H7             8.3800E+30   -6.242   12824.00
CH3CCH2<=>CH3CHCH              1.5000E+48  -12.710   53900.00
CH3CCH2+H<=>pC3H4+H2           3.3400E+12    0.000    0.00
CH3CCH2+O<=>CH3+CH2CO           6.0000E+13    0.000    0.00
CH3CCH2+OH<=>CH3+CH2CO+H        5.0000E+12    0.000    0.00
CH3CCH2+O2<=>CH3CO+CH2O         1.0000E+11    0.000    0.00
CH3CCH2+HO2<=>CH3+CH2CO+OH      2.0000E+13    0.000    0.00
CH3CCH2+HCO<=>C3H6+CO           9.0000E+13    0.000    0.00
CH3CCH2+CH3<=>pC3H4+CH4         1.0000E+11    0.000    0.00
CH3CCH2+CH3<=>iC4H8             2.0000E+13    0.000    0.00
CH3CHCH+H<=>pC3H4+H2           3.3400E+12    0.000    0.00
CH3CHCH+O<=>C2H4+HCO            6.0000E+13    0.000    0.00
CH3CHCH+OH<=>C2H4+HCO+H         5.0000E+12    0.000    0.00
CH3CHCH+O2<=>CH3CHO+HCO          1.0000E+11    0.000    0.00
CH3CHCH+HO2<=>C2H4+HCO+OH       2.0000E+13    0.000    0.00
CH3CHCH+HCO<=>C3H6+CO           9.0000E+13    0.000    0.00
CH3CHCH+CH3<=>pC3H4+CH4         1.0000E+11    0.000    0.00
C3H6+H (+M) <=>nC3H7 (+M)       1.3300E+13    0.000   3260.70
      LOW / 6.2600E+38   -6.660  7000.00/
      TROE/ 1.0000    1000.00    1310.00    48097.00 /
AR/0.70/ H2/2.00/ H2O/6.00/ CH4/2.00/ CO/1.50/ CO2/2.00/
C2H6/3.00/
C3H6+H (+M) <=>iC3H7 (+M)       1.3300E+13    0.000   1559.80
      LOW / 8.7000E+42   -7.500  4721.80/
      TROE/ 1.0000    1000.00    645.40    6844.30 /
AR/0.70/ H2/2.00/ H2O/6.00/ CH4/2.00/ CO/1.50/ CO2/2.00/
C2H6/3.00/
C3H6+H<=>C2H4+CH3              7.7840E+21   -2.390   11180.00
C3H6+H<=>aC3H5+H2              1.2923E+05    2.500   2490.00
C3H6+H<=>CH3CCH2+H2            4.0000E+05    2.500   9790.00
C3H6+H<=>CH3CHCH+H2            8.0400E+05    2.500  12283.00
C3H6+O<=>CH2CO+CH3+H           8.0000E+07    1.650    327.00
C3H6+O<=>C2H3CHO+2H            4.0640E+07    1.650    327.00

```

C3H6+O<=>C2H5+HCO	3.5735E+07	1.650	-972.00
C3H6+O<=>aC3H5+OH	1.8000E+11	0.700	5880.00
C3H6+O<=>CH3CCH2+OH	6.0000E+10	0.700	7630.00
C3H6+O<=>CH3CHCH+OH	1.2100E+11	0.700	8960.00
C3H6+OH<=>aC3H5+H2O	2.5017E+06	2.000	-298.00
C3H6+OH<=>CH3CCH2+H2O	1.1000E+06	2.000	1450.00
C3H6+OH<=>CH3CHCH+H2O	2.1400E+06	2.000	2778.00
C3H6+HO2<=>aC3H5+H2O2	9.6000E+03	2.600	13910.00
C3H6+CH3<=>aC3H5+CH4	2.2000E+00	3.500	5675.00
C3H6+CH3<=>CH3CCH2+CH4	8.4000E-01	3.500	11660.00
C3H6+CH3<=>CH3CHCH+CH4	1.3500E+00	3.500	12848.00
C3H6+C2H3<=>C4H6+CH3	7.2300E+11	0.000	5000.00
C3H6+HO2<=>CH3CHOCH2+OH	1.0900E+12	0.000	14200.00
C2H3CHO+H<=>C2H4+HCO	1.0800E+11	0.454	5820.00
C2H3CHO+O<=>C2H3+OH+CO	3.0000E+13	0.000	3540.00
C2H3CHO+O<=>CH2O+CH2CO	1.9000E+07	1.800	220.00
C2H3CHO+OH<=>C2H3+H2O+CO	3.4300E+09	1.180	-447.00
C2H3CHO+CH3<=>CH2CHCO+CH4	2.0000E+13	0.000	11000.00
C2H3CHO+C2H3<=>C4H6+HCO	2.8000E+21	-2.440	14720.00
CH2CHCO<=>C2H3+CO	1.0000E+14	0.000	27000.00
CH2CHCO+H<=>C2H3CHO	1.0000E+14	0.000	0.00
CH3CHOCH2<=>CH3CH2CHO	1.8400E+14	0.000	58500.00
CH3CHOCH2<=>C2H5+HCO	2.4500E+13	0.000	58500.00
CH3CHOCH2<=>CH3+CH2CHO	2.4500E+13	0.000	58800.00
CH3CHOCH2<=>CH3COCH3	1.0100E+14	0.000	59900.00
CH3CHOCH2<=>CH3+CH3CO	4.5400E+13	0.000	59900.00
iC3H7+H (+M) <=>C3H8 (+M)	2.4000E+13	0.000	0.00
LOW / 1.7000E+58 -12.080 11263.70/			
TROE/ 0.6490 1213.10 1213.10 13369.70 /			
AR/0.70/ H2/2.00/ H2O/6.00/ CH4/2.00/ CO/1.50/ CO2/2.00/			
C2H6/3.00/			
iC3H7+H<=>CH3+C2H5	1.4000E+28	-3.940	15916.00
iC3H7+H<=>C3H6+H2	3.2000E+12	0.000	0.00
iC3H7+O<=>CH3CHO+CH3	9.6000E+13	0.000	0.00
iC3H7+OH<=>C3H6+H2O	2.4000E+13	0.000	0.00
iC3H7+O2<=>C3H6+HO2	1.3000E+11	0.000	0.00
iC3H7+HO2<=>CH3CHO+CH3+OH	2.4000E+13	0.000	0.00
iC3H7+HCO<=>C3H8+CO	1.2000E+14	0.000	0.00
iC3H7+CH3<=>CH4+C3H6	2.2000E+14	-0.680	0.00
nC3H7+H (+M) <=>C3H8 (+M)	3.6000E+13	0.000	0.00
LOW / 3.0100E+48 -9.320 5833.60/			
TROE/ 0.4980 1314.00 1314.00 50000.00 /			
AR/0.70/ H2/2.00/ H2O/6.00/ CH4/2.00/ CO/1.50/ CO2/2.00/			
C2H6/3.00/			
nC3H7+H<=>C2H5+CH3	3.7000E+24	-2.920	12505.00
nC3H7+H<=>C3H6+H2	1.8000E+12	0.000	0.00
nC3H7+O<=>C2H5+CH2O	9.6000E+13	0.000	0.00
nC3H7+OH<=>C3H6+H2O	2.4000E+13	0.000	0.00
nC3H7+O2<=>C3H6+HO2	9.0000E+10	0.000	0.00
nC3H7+HO2<=>C2H5+OH+CH2O	2.4000E+13	0.000	0.00
nC3H7+HCO<=>C3H8+CO	6.0000E+13	0.000	0.00
nC3H7+CH3<=>CH4+C3H6	1.1000E+13	0.000	0.00

C3H8+H<=>H2+nC3H7	1.3000E+06	2.540	6756.00
C3H8+H<=>H2+iC3H7	1.3000E+06	2.400	4471.00
C3H8+O<=>nC3H7+OH	1.9000E+05	2.680	3716.00
C3H8+O<=>iC3H7+OH	4.7600E+04	2.710	2106.00
C3H8+OH<=>nC3H7+H2O	1.4000E+03	2.660	527.00
C3H8+OH<=>iC3H7+H2O	2.7000E+04	2.390	393.00
C3H8+O2<=>nC3H7+HO2	4.0000E+13	0.000	50930.00
C3H8+O2<=>iC3H7+HO2	4.0000E+13	0.000	47590.00
C3H8+HO2<=>nC3H7+H2O2	4.7600E+04	2.550	16490.00
C3H8+HO2<=>iC3H7+H2O2	9.6400E+03	2.600	13910.00
C3H8+CH3<=>CH4+nC3H7	9.0300E-01	3.650	7153.00
C3H8+CH3<=>CH4+iC3H7	1.5100E+00	3.460	5480.00
C4H2+H<=>nC4H3	1.1000E+42	-8.720	15300.00
C4H2+H<=>iC4H3	1.1000E+30	-4.920	10800.00
C4H2+OH<=>H2C4O+H	6.6000E+12	0.000	-410.00
C4H2+C2H<=>C6H2+H	9.6000E+13	0.000	0.00
C4H2+C2H<=>C6H3	4.5000E+37	-7.680	7100.00
H2C4O+H<=>C2H2+HCCO	5.0000E+13	0.000	3000.00
H2C4O+OH<=>CH2CO+HCCO	1.0000E+07	2.000	2000.00
nC4H3<=>iC4H3	4.1000E+43	-9.490	53000.00
nC4H3+H<=>iC4H3+H	2.5000E+20	-1.670	10800.00
nC4H3+H<=>C2H2+H2CC	6.3000E+25	-3.340	10014.00
nC4H3+H<=>C4H4	2.0000E+47	-10.260	13070.00
nC4H3+H<=>C4H2+H2	3.0000E+13	0.000	0.00
nC4H3+OH<=>C4H2+H2O	2.0000E+12	0.000	0.00
nC4H3+C2H2<=>1-C6H4+H	2.5000E+14	-0.560	10600.00
nC4H3+C2H2<=>C6H5	9.6000E+70	-17.770	31300.00
nC4H3+C2H2<=>o-C6H4+H	6.9000E+46	-10.010	30100.00
iC4H3+H<=>C2H2+H2CC	2.8000E+23	-2.550	10780.00
iC4H3+H<=>C4H4	3.4000E+43	-9.010	12120.00
iC4H3+H<=>C4H2+H2	6.0000E+13	0.000	0.00
iC4H3+OH<=>C4H2+H2O	4.0000E+12	0.000	0.00
iC4H3+O2<=>HCCO+CH2CO	7.8600E+16	-1.800	0.00
C4H4+H<=>nC4H5	1.3000E+51	-11.920	16500.00
C4H4+H<=>iC4H5	4.9000E+51	-11.920	17700.00
C4H4+H<=>nC4H3+H2	6.6500E+05	2.530	12240.00
C4H4+H<=>iC4H3+H2	3.3300E+05	2.530	9240.00
C4H4+OH<=>nC4H3+H2O	3.1000E+07	2.000	3430.00
C4H4+OH<=>iC4H3+H2O	1.5500E+07	2.000	430.00
C4H4+O<=>C3H3+HCO	6.0000E+08	1.450	-860.00
C4H4+C2H<=>1-C6H4+H	1.2000E+13	0.000	0.00
nC4H5<=>iC4H5	1.5000E+67	-16.890	59100.00
nC4H5+H<=>iC4H5+H	3.1000E+26	-3.350	17423.00
nC4H5+H<=>C4H4+H2	1.5000E+13	0.000	0.00
nC4H5+OH<=>C4H4+H2O	2.0000E+12	0.000	0.00
nC4H5+HCO<=>C4H6+CO	5.0000E+12	0.000	0.00
nC4H5+HO2<=>C2H3+CH2CO+OH	6.6000E+12	0.000	0.00
nC4H5+H2O2<=>C4H6+HO2	1.2100E+10	0.000	-596.00
nC4H5+HO2<=>C4H6+O2	6.0000E+11	0.000	0.00
nC4H5+O2<=>CH2CHCHCHO+O	3.0000E+11	0.290	11.00
nC4H5+O2<=>HCO+C2H3CHO	9.2000E+16	-1.390	1010.00
nC4H5+C2H2<=>C6H6+H	1.6000E+16	-1.330	5400.00

nC4H5+C2H3<=>C6H6+H2	1.8400E-13	7.070	-3611.00
iC4H5+H<=>C4H4+H2	3.0000E+13	0.000	0.00
iC4H5+H<=>C3H3+CH3	2.0000E+13	0.000	2000.00
iC4H5+OH<=>C4H4+H2O	4.0000E+12	0.000	0.00
iC4H5+HCO<=>C4H6+CO	5.0000E+12	0.000	0.00
iC4H5+HO2<=>C4H6+O2	6.0000E+11	0.000	0.00
iC4H5+HO2<=>C2H3+CH2CO+OH	6.6000E+12	0.000	0.00
iC4H5+H2O2<=>C4H6+HO2	1.2100E+10	0.000	-596.00
iC4H5+O2<=>CH2CO+CH2CHO	2.1600E+10	0.000	2500.00
C4H5-2<=>iC4H5	1.5000E+67	-16.890	59100.00
iC4H5+H<=>C4H5-2+H	3.1000E+26	-3.350	17423.00
C4H5-2+HO2<=>OH+C2H2+CH3CO	8.0000E+11	0.000	0.00
C4H5-2+O2<=>CH3CO+CH2CO	2.1600E+10	0.000	2500.00
C4H5-2+C2H2<=>C6H6+H	5.0000E+14	0.000	25000.00
C4H5-2+C2H4<=>C5H6+CH3	5.0000E+14	0.000	25000.00
C4H6<=>iC4H5+H	5.7000E+36	-6.270	112353.00
C4H6<=>nC4H5+H	5.3000E+44	-8.620	123608.00
C4H6<=>C4H4+H2	2.5000E+15	0.000	94700.00
C4H6+H<=>nC4H5+H2	1.3300E+06	2.530	12240.00
C4H6+H<=>iC4H5+H2	6.6500E+05	2.530	9240.00
C4H6+H<=>C2H4+C2H3	1.4600E+30	-4.340	21647.00
C4H6+H<=>pC3H4+CH3	2.0000E+12	0.000	7000.00
C4H6+H<=>aC3H4+CH3	2.0000E+12	0.000	7000.00
C4H6+O<=>nC4H5+OH	7.5000E+06	1.900	3740.00
C4H6+O<=>iC4H5+OH	7.5000E+06	1.900	3740.00
C4H6+O<=>CH3CHCHCO+H	1.5000E+08	1.450	-860.00
C4H6+O<=>CH2CHCHCHO+H	4.5000E+08	1.450	-860.00
C4H6+OH<=>nC4H5+H2O	6.2000E+06	2.000	3430.00
C4H6+OH<=>iC4H5+H2O	3.1000E+06	2.000	430.00
C4H6+HO2<=>C4H6O25+OH	1.2000E+12	0.000	14000.00
C4H6+HO2<=>C2H3CHOCH2+OH	4.8000E+12	0.000	14000.00
C4H6+CH3<=>nC4H5+CH4	2.0000E+14	0.000	22800.00
C4H6+CH3<=>iC4H5+CH4	1.0000E+14	0.000	19800.00
C4H6+C2H3<=>nC4H5+C2H4	5.0000E+13	0.000	22800.00
C4H6+C2H3<=>iC4H5+C2H4	2.5000E+13	0.000	19800.00
C4H6+C3H3<=>nC4H5+aC3H4	1.0000E+13	0.000	22500.00
C4H6+C3H3<=>iC4H5+aC3H4	5.0000E+12	0.000	19500.00
C4H6+aC3H5<=>nC4H5+C3H6	1.0000E+13	0.000	22500.00
C4H6+aC3H5<=>iC4H5+C3H6	5.0000E+12	0.000	19500.00
C4H6+C2H3<=>C6H6+H2+H	5.6200E+11	0.000	3240.00
C4H612<=>iC4H5+H	4.2000E+15	0.000	92600.00
C4H612+H<=>C4H6+H	2.0000E+13	0.000	4000.00
C4H612+H<=>iC4H5+H2	1.7000E+05	2.500	2490.00
C4H612+H<=>aC3H4+CH3	2.0000E+13	0.000	2000.00
C4H612+H<=>pC3H4+CH3	2.0000E+13	0.000	2000.00
C4H612+CH3<=>iC4H5+CH4	7.0000E+13	0.000	18500.00
C4H612+O<=>CH2CO+C2H4	1.2000E+08	1.650	327.00
C4H612+O<=>iC4H5+OH	1.8000E+11	0.700	5880.00
C4H612+OH<=>iC4H5+H2O	3.1000E+06	2.000	-298.00
C4H612<=>C4H6	3.0000E+13	0.000	65000.00
C4H6-2<=>C4H6	3.0000E+13	0.000	65000.00
C4H6-2<=>C4H612	3.0000E+13	0.000	67000.00

C4H6-2+H<=>C4H612+H	2.0000E+13	0.000	4000.00
C4H6-2+H<=>C4H5-2+H2	3.4000E+05	2.500	2490.00
C4H6-2+H<=>CH3+pC3H4	2.6000E+05	2.500	1000.00
C4H6-2<=>H+C4H5-2	5.0000E+15	0.000	87300.00
C4H6-2+CH3<=>C4H5-2+CH4	1.4000E+14	0.000	18500.00
C2H3CHOCH2<=>C4H6O23	2.0000E+14	0.000	50600.00
C4H6O23<=>CH3CHCHCHO	1.9500E+13	0.000	49400.00
C4H6O23<=>C2H4+CH2CO	5.7500E+15	0.000	69300.00
C4H6O23<=>C2H2+CH2OCH2	1.0000E+16	0.000	75800.00
C4H6O25<=>C4H4O+H2	5.3000E+12	0.000	48500.00
C4H4O<=>CO+pC3H4	1.7800E+15	0.000	77500.00
C4H4O<=>C2H2+CH2CO	5.0100E+14	0.000	77500.00
CH3CHCHCHO<=>C3H6+CO	3.9000E+14	0.000	69000.00
CH3CHCHCHO+H<=>CH2CHCHCHO+H2	1.7000E+05	2.500	2490.00
CH3CHCHCHO+H<=>CH3CHCHCO+H2	1.0000E+05	2.500	2490.00
CH3CHCHCHO+H<=>CH3+C2H3CHO	4.0000E+21	-2.390	11180.00
CH3CHCHCHO+H<=>C3H6+HCO	4.0000E+21	-2.390	11180.00
CH3CHCHCHO+CH3<=>CH2CHCHCHO+CH4	2.1000E+00	3.500	5675.00
CH3CHCHCHO+CH3<=>CH3CHCHCO+CH4	1.1000E+00	3.500	5675.00
CH3CHCHCHO+C2H3<=>CH2CHCHCHO+C2H4	2.2100E+00	3.500	4682.00
CH3CHCHCHO+C2H3<=>CH3CHCHCO+C2H4	1.1100E+00	3.500	4682.00
CH3CHCHCO<=>CH3CHCH+CO	1.0000E+14	0.000	30000.00
CH3CHCHCO+H<=>CH3CHCHCHO	1.0000E+14	0.000	0.00
CH2CHCHCHO<=>aC3H5+CO	1.0000E+14	0.000	25000.00
CH2CHCHCHO+H<=>CH3CHCHCHO	1.0000E+14	0.000	0.00
C4H7<=>C4H6+H	2.4800E+53	-12.300	52000.00
C4H7+H (+M) <=>C4H81 (+M)	3.6000E+13	0.000	0.00
LOW / 3.0100E+48 -9.320 5833.60/			
TROE/ 0.4980 1314.00 1314.00 50000.00 /			
AR/0.70/ H2/2.00/ H2O/6.00/ CH4/2.00/ CO/1.50/ CO2/2.00/			
C2H6/3.00/			
C4H7+H<=>CH3+aC3H5	2.0000E+21	-2.000	11000.00
C4H7+H<=>C4H6+H2	1.8000E+12	0.000	0.00
C4H7+O2<=>C4H6+HO2	1.0000E+11	0.000	0.00
C4H7+HO2<=>CH2O+OH+aC3H5	2.4000E+13	0.000	0.00
C4H7+HCO<=>C4H81+CO	6.0000E+13	0.000	0.00
C4H7+CH3<=>C4H6+CH4	1.1000E+13	0.000	0.00
iC4H7+H (+M) <=>iC4H8 (+M)	2.0000E+14	0.000	0.00
LOW / 1.3300E+60 -12.000 5967.80/			
TROE/ 0.0200 1096.60 1096.60 6859.50 /			
AR/0.70/ H2/2.00/ H2O/6.00/ CH4/2.00/ CO/1.50/ CO2/2.00/			
C2H6/3.00/			
iC4H7+H<=>CH3CCH2+CH3	2.6000E+45	-8.190	37890.00
iC4H7+O<=>CH2O+CH3CCH2	9.0000E+13	0.000	0.00
iC4H7+HO2<=>CH3CCH2+CH2O+OH	4.0000E+12	0.000	0.00
C4H81+H (+M) <=>pC4H9 (+M)	1.3300E+13	0.000	3260.70
LOW / 6.2600E+38 -6.660 7000.00/			
TROE/ 1.0000 1000.00 1310.00 48097.00 /			
AR/0.70/ H2/2.00/ H2O/6.00/ CH4/2.00/ CO/1.50/ CO2/2.00/			
C2H6/3.00/			
C4H81+H (+M) <=>sC4H9 (+M)	1.3300E+13	0.000	1559.80
LOW / 8.7000E+42 -7.500 4721.80/			

```

TROE/ 1.0000 1000.00 645.40 6844.30 /
AR/0.70/ H2/2.00/ H2O/6.00/ CH4/2.00/ CO/1.50/ CO2/2.00/
C2H6/3.00/
C4H81+H<=>C2H4+C2H5 1.3872E+22 -2.390 11180.00
C4H81+H<=>C3H6+CH3 3.5232E+22 -2.390 11180.00
C4H81+H<=>C4H7+H2 6.5000E+05 2.540 6756.00
C4H81+O<=>nC3H7+HCO 3.3000E+08 1.450 -402.00
C4H81+O<=>C4H7+OH 1.5000E+13 0.000 5760.00
DUPLICATE
C4H81+O<=>C4H7+OH 2.6000E+13 0.000 4470.00
DUPLICATE
C4H81+OH<=>C4H7+H2O 7.0000E+02 2.660 527.00
C4H81+O2<=>C4H7+HO2 2.0000E+13 0.000 50930.00
C4H81+HO2<=>C4H7+H2O2 1.0000E+12 0.000 14340.00
C4H81+CH3<=>C4H7+CH4 4.5000E-01 3.650 7153.00
C4H82+H (+M) <=>sC4H9 (+M) 1.3300E+13 0.000 1559.80
LOW / 8.7000E+42 -7.500 4721.80/
TROE/ 1.0000 1000.00 645.40 6844.30 /
AR/0.70/ H2/2.00/ H2O/6.00/ CH4/2.00/ CO/1.50/ CO2/2.00/
C2H6/3.00/
C4H82+H<=>C4H7+H2 3.4000E+05 2.500 2490.00
C4H82+O<=>C2H4+CH3CHO 2.4000E+08 1.650 327.00
C4H82+OH<=>C4H7+H2O 6.2000E+06 2.000 -298.00
C4H82+O2<=>C4H7+HO2 5.0000E+13 0.000 53300.00
C4H82+HO2<=>C4H7+H2O2 1.9000E+04 2.600 13910.00
C4H82+CH3<=>C4H7+CH4 4.4000E+00 3.500 5675.00
iC4H8+H (+M) <=>iC4H9 (+M) 1.3300E+13 0.000 3260.70
LOW / 6.2600E+38 -6.660 7000.00/
TROE/ 1.0000 1000.00 1310.00 48097.00 /
AR/0.70/ H2/2.00/ H2O/6.00/ CH4/2.00/ CO/1.50/ CO2/2.00/
C2H6/3.00/
iC4H8+H<=>iC4H7+H2 1.2000E+06 2.540 6760.00
iC4H8+H<=>C3H6+CH3 8.0000E+21 -2.390 11180.00
iC4H8+O<=>2CH3+CH2CO 1.2000E+08 1.650 327.00
iC4H8+O<=>iC3H7+HCO 3.5000E+07 1.650 -972.00
iC4H8+O<=>iC4H7+OH 2.9000E+05 2.500 3640.00
iC4H8+OH<=>iC4H7+H2O 1.5000E+08 1.530 775.00
iC4H8+HO2<=>iC4H7+H2O2 2.0000E+04 2.550 15500.00
iC4H8+O2<=>iC4H7+HO2 2.7000E+13 0.000 50900.00
iC4H8+CH3<=>iC4H7+CH4 9.1000E-01 3.650 7150.00
C2H4+C2H5<=>pC4H9 1.5000E+11 0.000 7300.00
pC4H9+H (+M) <=>C4H10 (+M) 3.6000E+13 0.000 0.00
LOW / 3.0100E+48 -9.320 5833.60/
TROE/ 0.4980 1314.00 1314.00 50000.00 /
AR/0.70/ H2/2.00/ H2O/6.00/ CH4/2.00/ CO/1.50/ CO2/2.00/
C2H6/3.00/
pC4H9+H<=>2C2H5 3.7000E+24 -2.920 12505.00
pC4H9+H<=>C4H81+H2 1.8000E+12 0.000 0.00
pC4H9+O<=>nC3H7+CH2O 9.6000E+13 0.000 0.00
pC4H9+OH<=>C4H81+H2O 2.4000E+13 0.000 0.00
pC4H9+O2<=>C4H81+HO2 2.7000E+11 0.000 0.00
pC4H9+HO2<=>nC3H7+OH+CH2O 2.4000E+13 0.000 0.00

```

```

pC4H9+HCO<=>C4H10+CO          9.0000E+13    0.000    0.00
pC4H9+CH3<=>C4H81+CH4          1.1000E+13    0.000    0.00
C3H6+CH3 (+M) <=>sC4H9 (+M)      1.7000E+11    0.000    7403.60
    LOW / 2.3100E+28   -4.270   1831.00/
    TROE/ 0.5650    60000.00    534.20    3007.20 /
AR/0.70/ H2/2.00/ H2O/6.00/ CH4/2.00/ CO/1.50/ CO2/2.00/
C2H6/3.00/
sC4H9+H (+M) <=>C4H10 (+M)      2.4000E+13    0.000    0.00
    LOW / 1.7000E+58  -12.080   11263.70/
    TROE/ 0.6490    1213.10    1213.10    13369.70 /
AR/0.70/ H2/2.00/ H2O/6.00/ CH4/2.00/ CO/1.50/ CO2/2.00/
C2H6/3.00/
sC4H9+H<=>2C2H5                1.4000E+28   -3.940   15916.00
sC4H9+H<=>C4H81+H2             3.2000E+12    0.000    0.00
sC4H9+H<=>C4H82+H2             2.1000E+12    0.000    0.00
sC4H9+O<=>CH3CHO+C2H5          9.6000E+13    0.000    0.00
sC4H9+OH<=>C4H81+H2O           2.4000E+13    0.000    0.00
sC4H9+OH<=>C4H82+H2O           1.6000E+13    0.000    0.00
sC4H9+O2<=>C4H81+HO2           5.1000E+10    0.000    0.00
sC4H9+O2<=>C4H82+HO2           1.2000E+11    0.000    0.00
sC4H9+HO2<=>CH3CHO+C2H5+OH      2.4000E+13    0.000    0.00
sC4H9+HCO<=>C4H10+CO           1.2000E+14    0.000    0.00
sC4H9+CH3<=>CH4+C4H81           2.2000E+14   -0.680    0.00
sC4H9+CH3<=>CH4+C4H82           1.5000E+14   -0.680    0.00
C3H6+CH3 (+M) <=>iC4H9 (+M)      9.6000E+10    0.000    8003.60
    LOW / 1.3000E+28   -4.270   2431.10/
    TROE/ 0.5650    60000.00    534.20    3007.20 /
AR/0.70/ H2/2.00/ H2O/6.00/ CH4/2.00/ CO/1.50/ CO2/2.00/
C2H6/3.00/
iC4H9+H (+M) <=>iC4H10 (+M)      3.6000E+13    0.000    0.00
    LOW / 3.2700E+56  -11.740   6430.80/
    TROE/ 0.5060    1266.60    1266.60    50000.00 /
AR/0.70/ H2/2.00/ H2O/6.00/ CH4/2.00/ CO/1.50/ CO2/2.00/
C2H6/3.00/
iC4H9+H<=>iC3H7+CH3             1.9000E+35   -5.830   22470.00
iC4H9+H<=>iC4H8+H2             9.0000E+11    0.000    0.00
iC4H9+O<=>iC3H7+CH2O           9.6000E+13    0.000    0.00
iC4H9+OH<=>iC4H8+H2O           1.2000E+13    0.000    0.00
iC4H9+O2<=>iC4H8+HO2           2.4000E+10    0.000    0.00
iC4H9+HO2<=>iC3H7+CH2O+OH       2.4100E+13    0.000    0.00
iC4H9+HCO<=>iC4H10+CO           3.6000E+13    0.000    0.00
iC4H9+CH3<=>iC4H8+CH4           6.0000E+12   -0.320    0.00
tC4H9 (+M) <=>iC4H8+H (+M)      8.3000E+13    0.000    38150.40
    LOW / 1.9000E+41   -7.360   36631.70/
    TROE/ 0.2930    649.00    60000.00    3425.90 /
AR/0.70/ H2/2.00/ H2O/6.00/ CH4/2.00/ CO/1.50/ CO2/2.00/
C2H6/3.00/
tC4H9+H (+M) <=>iC4H10 (+M)      2.4000E+13    0.000    0.00
    LOW / 1.4700E+61  -12.940   8000.00/
    TROE/ 0.0000    1456.40    1000.00    10000.50 /
AR/0.70/ H2/2.00/ H2O/6.00/ CH4/2.00/ CO/1.50/ CO2/2.00/
C2H6/3.00/

```

tC4H9+H<=>iC3H7+CH3	2.6000E+36	-6.120	25640.00
tC4H9+H<=>iC4H8+H2	5.4200E+12	0.000	0.00
tC4H9+O<=>iC4H8+OH	1.8000E+14	0.000	0.00
tC4H9+O<=>CH3COCH3+CH3	1.8000E+14	0.000	0.00
tC4H9+OH<=>iC4H8+H2O	1.8000E+13	0.000	0.00
tC4H9+O2<=>iC4H8+HO2	4.8000E+11	0.000	0.00
tC4H9+HO2<=>CH3+CH3COCH3+OH	1.8000E+13	0.000	0.00
tC4H9+HCO<=>iC4H10+CO	6.0000E+13	0.000	0.00
tC4H9+CH3<=>iC4H8+CH4	3.8000E+15	-1.000	0.00
CH3COCH3+H<=>H2+CH2CO+CH3	1.3000E+06	2.540	6756.00
CH3COCH3+O<=>OH+CH2CO+CH3	1.9000E+05	2.680	3716.00
CH3COCH3+OH<=>H2O+CH2CO+CH3	3.2000E+07	1.800	934.00
CH3+CH3CO<=>CH3COCH3	4.0000E+15	-0.800	0.00
nC3H7+CH3 (+M) <=>C4H10 (+M)	1.9300E+14	-0.320	0.00
LOW / 2.6800E+61 -13.240 6000.00/			
TROE/ 1.0000 1000.00 1433.90 5328.80 /			
AR/0.70/ H2/2.00/ H2O/6.00/ CH4/2.00/ CO/1.50/ CO2/2.00/			
C2H6/3.00/			
2C2H5 (+M) <=>C4H10 (+M)	1.8800E+14	-0.500	0.00
LOW / 2.6100E+61 -13.420 6000.00/			
TROE/ 1.0000 1000.00 1433.90 5328.80 /			
AR/0.70/ H2/2.00/ H2O/6.00/ CH4/2.00/ CO/1.50/ CO2/2.00/			
C2H6/3.00/			
C4H10+H<=>pC4H9+H2	9.2000E+05	2.540	6756.00
C4H10+H<=>sC4H9+H2	2.4000E+06	2.400	4471.00
C4H10+O<=>pC4H9+OH	4.9000E+06	2.400	5500.00
C4H10+O<=>sC4H9+OH	4.3000E+05	2.600	2580.00
C4H10+OH<=>pC4H9+H2O	3.3000E+07	1.800	954.00
C4H10+OH<=>sC4H9+H2O	5.4000E+06	2.000	-596.00
C4H10+O2<=>pC4H9+HO2	4.0000E+13	0.000	50930.00
C4H10+O2<=>sC4H9+HO2	8.0000E+13	0.000	47590.00
C4H10+HO2<=>pC4H9+H2O2	4.7600E+04	2.550	16490.00
C4H10+HO2<=>sC4H9+H2O2	1.9000E+04	2.600	13910.00
C4H10+CH3<=>pC4H9+CH4	9.0300E-01	3.650	7153.00
C4H10+CH3<=>sC4H9+CH4	3.0000E+00	3.460	5480.00
iC3H7+CH3 (+M) <=>iC4H10 (+M)	1.4000E+15	-0.680	0.00
LOW / 4.1600E+61 -13.330 3903.40/			
TROE/ 0.9310 60000.00 1265.30 5469.80 /			
AR/0.70/ H2/2.00/ H2O/6.00/ CH4/2.00/ CO/1.50/ CO2/2.00/			
C2H6/3.00/			
iC4H10+H<=>iC4H9+H2	1.8000E+06	2.540	6760.00
iC4H10+H<=>tC4H9+H2	6.0000E+05	2.400	2580.00
iC4H10+O<=>iC4H9+OH	4.3000E+05	2.500	3640.00
iC4H10+O<=>tC4H9+OH	1.5700E+05	2.500	1110.00
iC4H10+OH<=>iC4H9+H2O	2.3000E+08	1.530	775.00
iC4H10+OH<=>tC4H9+H2O	5.7300E+10	0.510	64.00
iC4H10+HO2<=>iC4H9+H2O2	3.0000E+04	2.550	15500.00
iC4H10+HO2<=>tC4H9+H2O2	3.6000E+03	2.550	10500.00
iC4H10+O2<=>iC4H9+HO2	4.0000E+13	0.000	50900.00
iC4H10+O2<=>tC4H9+HO2	4.0000E+13	0.000	44000.00
iC4H10+CH3<=>iC4H9+CH4	1.3600E+00	3.650	7150.00
iC4H10+CH3<=>tC4H9+CH4	9.0000E-01	3.460	4600.00


```

!-----
!
! Reactions of C6H2
!
!C6H2 + H = C6H3                                4.30E+45 -10.15    13250.0
! 20 Torr 97WAN/FRE
!C6H2 + H = C6H3                                2.60E+46 -10.15    15500.0
! 90 Torr 97WAN/FRE
! C6H2 + H = C6H3                                1.10E+30  -4.92     10800.0
! 760 Torr 97WAN/FRE
!
! Reactions of C6H3
!
!C6H3 + H = C4H2 + C2H2                          2.40E+19  -1.60     2800.0
! 20 Torr RRKM 97WAN/FRE
!C6H3 + H = C4H2 + C2H2                          3.70E+22  -2.50     5140.0
! 90 Torr RRKM 97WAN/FRE
! C6H3 + H = C4H2 + C2H2                          2.80E+23  -2.55    10780.0
! 760 Torr RRKM 97WAN/FRE
!
!C6H3 + H = 1-C6H4                              4.20E+44 -10.27     7890.0
! 20 Torr RRKM 97WAN/FRE
!C6H3 + H = 1-C6H4                              5.30E+46 -10.68     9270.0
! 90 Torr RRKM 97WAN/FRE
! C6H3 + H = 1-C6H4                              3.40E+43  -9.01    12120.0
! 760 Torr RRKM 97WAN/FRE
!
! C6H3+H = C6H2+H2                                3.00E+13   0.00
0.0 !97WAN/FRE
! C6H3+OH = C6H2+H2O                             4.00E+12   0.00
0.0 !97WAN/FRE
!
!1-C6H4 + H = C6H5                               4.40E+74 -19.09    25800.
! 10 Torr RRKM 97WAN/FRE
!1-C6H4 + H = C6H5                               3.60E+77 -20.09    28100.
! 20 Torr RRKM 97WAN/FRE
!1-C6H4 + H = C6H5                               4.70E+78 -20.10    29500.
! 90 Torr RRKM 97WAN/FRE
! 1-C6H4 + H = C6H5                               1.70E+78 -19.72    31400.
! 760 Torr RRKM 97WAN/FRE
!1-C6H4 + H = C6H5                               3.90E+69 -16.63    34100.
! 7600 Torr RRKM 97WAN/FRE
!
!1-C6H4 + H = o-C6H4+ H                         8.70E+45  -9.61    22300.
! 10 Torr RRKM 97WAN/FRE
!1-C6H4 + H = o-C6H4+ H                         2.20E+47  -9.98    24000.
! 20 Torr RRKM 97WAN/FRE
!1-C6H4 + H = o-C6H4+ H                         9.70E+48 -10.37    27000.
! 90 Torr RRKM 97WAN/FRE
! 1-C6H4 + H = o-C6H4+ H                         1.40E+54 -11.70    34500.
! 760 Torr RRKM 97WAN/FRE

```

```

!!l-C6H4 + H = o-C6H4+ H                    5.70E+55 -11.98    41900.
! 7600 Torr RRKM 97WAN/FRE
!
  l-C6H4 + H = C6H3 + H2                    1.330E+06    2.530
9240.00 ! = C4H4+H
  l-C6H4 + OH = C6H3 + H2O                  3.100E+06    2.000
430.00 ! see notes
!
!C4H2 + C2H2 = o-C6H4                      1.40E+07    1.453    25407
! kinf 300-2500 K, 83 kcal/mol, rot
  C4H2 + C2H2 = o-C6H4                      5.00E+78   -19.31    67920.
! 5 atm
!
  o-C6H4 + OH = CO + C5H5                    1.00E+13    0.00    0.
! Estimated
!
!*****
*****
!
! The following is the ring destruction sybmodel
!
!*****
*****
!
! Reactions of toluene (C6H5CH3)
!
  C6H5 + CH3 = C6H5CH3                      1.380E+13    0.000    46.0
! 99-TOK-LIN (added 5/2)
  C6H5CH3 + O2 = C6H5CH2 + HO2              3.000E+14    0.000
42992.00 ! 98-ENG-FIT
  C6H5CH3 + OH = C6H5CH2 + H2O              1.620E+13    0.000
2770.00 ! 05-VAS-DAV
  C6H5CH3 + OH = C6H4CH3 + H2O              1.333E+08    1.420
1450.00 ! 5/6 * c6h6+oh
  C6H5CH3 + H = C6H5CH2 + H2                1.259E+14    0.000
8359.00 ! 90-HIP-REI
  C6H5CH3 + H = C6H6 + CH3                  1.930E+06    2.170
4163.00 ! 01-TOK-LIN (added 5/2)
  C6H5CH3 + O = OC6H4CH3 + H                2.600E+13    0.000
3795.00 ! 82-NIC-GUM
  C6H5CH3 + CH3 = C6H5CH2 + CH4             3.160E+11    0.000
9500.00 ! 76-KER-PAR
  C6H5CH3 + C6H5 = C6H5CH2 + C6H6          2.103E+12    0.000
4400.00 ! 88-FAH-STE
  C6H5CH3 + HO2 = C6H5CH2 + H2O2           3.975E+11    0.000
14069.00 ! 94-BAULCH
  C6H5CH3 + HO2 = C6H4CH3 + H2O2           5.420E+12    0.000
28810.00 ! 94-BAULCH
!
! Reactions of benzyl radical (C6H5CH2)
!
  C6H5CH2 + H (+M) = C6H5CH3 (+M)          1.000E+14    0.000

```

```

0.00 ! kinf (assumed, reduced from 2.6E14)
                                LOW /1.100E+103 -24.63
14590.00 / ! k0 (RRKM)
                                TROE /0.431 383. 152.
4730. /
                                H2/2/ H2O/6/ CH4/2/ CO/1.5/ CO2/2/
C2H6/3/
C6H5CH2 + H = C6H5 + CH3 1.500E+66 -13.940 64580.00
! RRKM at 1 atm,
C6H5CH2 + O = C6H5CHO + H 4.000E+14 0.000
0.00 ! (90a-HIP-REI)
C6H5CH2 + OH = C6H5CH2OH 2.000E+13 0.000
0.00 ! 90a-HIP-REI
C6H5CH2 + HO2 = C6H5CHO + H + OH 5.000E+12 0.000 0.00
! 90a-HIP-REI
C6H5CH2 + C6H5OH = C6H5CH3 + C6H5O 1.050E+11 0.000
9500.00 ! 92-EMD-BRE, est.
C6H5CH2 + HOC6H4CH3 = C6H5CH3 + OC6H4CH3 1.050E+11 0.000
9500.00 ! 92-EMD-BRE, est.
!
! Reactions of benzyl alcohol (C6H5CH2OH)
!
C6H5CH2OH + OH = C6H5CHO + H2O + H 5.000E+12 0.000 0.00
! 90a-HIP-REI
C6H5CH2OH + H = C6H5CHO + H2 + H 8.000E+13 0.000 8235.00
! 92-EMD-BRE, est.
C6H5CH2OH + H = C6H6 + CH2OH 1.200E+13 0.000
5148.00 ! 92-EMD-BRE, est.
C6H5CH2OH + C6H5 = C6H5CHO + C6H6 + H 1.400E+12 0.000 4400.00
! 92-EMD-BRE, est.
!
! Reactions of benzaldehyde (C6H5CHO)
!
C6H5 + HCO = C6H5CHO 1.000E+13 0.000
0.00 ! Est.
C6H5CHO = C6H5CO + H 3.980E+15 0.000
86900.00 ! 86-GRE, Eamodified
C6H5CHO + O2 = C6H5CO + HO2 1.020E+13 0.000
38950.00 ! est. Tsang
C6H5CHO + OH = C6H5CO + H2O 2.350E+10 0.730
-1110.00 ! est., (CH3CHO+OH)
C6H5CHO + H = C6H5CO + H2 4.100E+09 1.160
2400.00 ! est., (CH3CHO+H).
C6H5CHO + H = C6H6 + HCO 1.930E+06 2.170
4163.00 ! est., (C6H5CH3 + H = C6H6 + CH3)
C6H5CHO + O = C6H5CO + OH 5.800E+12 0.000
1800.00 ! est., (CH3CHO+O)
C6H5CHO + C6H5CH2 = C6H5CO + C6H5CH3 2.000E-06 5.600
2460.00 ! est. (C6H5CHO + CH3)
C6H5CHO + CH3 = C6H5CO + CH4 2.000E-06 5.600
2460.00 ! est. (CH3CHO+CH3).
C6H5CHO + C6H5 = C6H5CO + C6H6 2.103E+12 0.000

```

```

4400.00 ! est.(C6H5CH3+C6H5)
  C6H5CO + H2O2 = C6H5CHO + HO2          1.800E+11    0.000
8226.00 ! est.(CH3CO+H2O2 = CH3CHO+HO2)
!
! Reactions of cresoxy radical (OC6H4CH3)
!
  OC6H4CH3 + H (+M) = HOC6H4CH3 (+M)      1.000E+14    0.000
0.00 ! Estimated (C6H5O + H -> C6H5OH) / 2.5
                                  LOW / 4.000E+93 -21.840
13880.0 / ! 96-DAV-WAN, 97-WAN-FRE
                                  TROE / 0.043 304.2 60000. 5896.4
/
                                  H2/2.0/ H2O/6.0/ CH4/2.0/ CO/1.5/
CO2/2.0/
  OC6H4CH3 + H = C6H5O + CH3              1.930E+06    2.170
4163.00 ! est, =(C6H5CH3+H=C6H6+CH3)
  OC6H4CH3 + O = C6H4O2 + CH3             8.000E+13    0.000
0.00 ! est.
!
! Reactions of cresol (HOC6H5CH3)
!
  HOC6H4CH3 + OH = OC6H4CH3 + H2O         6.000E+12    0.000
0.00 ! 88-HE-MAL
  HOC6H4CH3 + H = OC6H4CH3 + H2           1.150E+14    0.000
12400.00 ! 88-HE-MAL
  HOC6H4CH3 + H = C6H5CH3 + OH            2.210E+13    0.000
7910.00 ! 88-HE-MAL
  HOC6H4CH3 + H = C6H5OH + CH3            1.200E+13    0.000
5148.00 ! 92-EMD-BRE, est.
!
! Reaction of benzoyl radical (C6H5CO)
!
  C6H5CO = C6H5 + CO                      5.270E+14    0.000
29013.00 ! 00-NAM-LIN (rep 5/1)
!
! Reactions of benzene (C6H6)
!
  C6H5 + H (+M) = C6H6 (+M)               1.000E+14    0.000
0.00 !
                                  LOW / 6.600E+75 -16.300
7000.00 /! (HW, RRKM)
                                  TROE / 1.0 0.1 584.9 6113.
/
                                  H2/2.0/ H2O/6.0/ CH4/2.0/ CO/1.5/
CO2/2.0/
!
  C6H6 + OH = C6H5 + H2O                  3.985E+05    2.286
1058.00 ! Fit,AJ
  C6H6 + OH = C6H5OH + H                  1.300E+13    0.000
10600.00 ! 92BAU/COB
  C6H6 + O = C6H5O + H                    1.390E+13    0.000
4910.00 ! 50% split 82-NIC-GUM

```

```

C6H6 + O = C5H5 + HCO                                1.390E+13   0.000
4530.00 ! 50% split based on McKinnon
C6H5 + H2 = C6H6 + H                                5.707E+04   2.430
6273.00 ! 97-MEB-LIN
!
! Reactions of phenyl radical (C6H5)
!
C6H5 (+M) = o-C6H4 + H (+M)                          4.300E+12   0.616   77313.
! RRKM 00-HAI-FRE
                                LOW/ 1.000E+84 -18.866
90064    /
                                TROE/ 0.902, 696., 358., 3856.
/
                                H2/2.0/ H2O/6.0/ CH4/2.0/ CO/1.5/
CO2/2.0/
!
C6H5 + H = o-C6H4 + H2                                2.000E+11   1.100
24500.00 ! 01-MEB-LIN 1 atm
C6H5 + O2 = C6H5O + O                                2.600E+13   0.000
6120.00 ! 94-FRA-HER
C6H5 + O2 = C6H4O2 + H                                3.000E+13   0.000
8980.00 ! 94-FRA-HER
C6H5 + O = C5H5 + CO                                1.000E+14   0.000
0.00 ! 94-FRA-HER
C6H5 + OH = C6H5O + H                                3.000E+13   0.000
0.00 ! Est.
C6H5 + HO2 = C6H5O + OH                              3.000E+13   0.000
0.00 ! Est.

C6H5 + HO2 = C6H6 + O2                                1.000E+12   0.000
0.00 ! Estimated, 10/01
C6H5 + CH4 = C6H6 + CH3                                3.890E-03   4.570
5256.00 ! 99-TOK-LIN (added 5/1)
C6H5 + C2H6 = C6H6 + C2H5                              2.100E+11   0.000
4443.00 ! 01-PAR-LIN (added 5/2)
C6H5 + CH2O = C6H6 + HCO                              8.550E+04   2.190
38.00 ! 00-CHO-LIN (added 5/1)
!
!C6H5 + C6H5 = BIPHENYL                                3.800E+31  -5.750
7950.00 ! 97-WAN-FRE, 20 torr
!C6H5 + C6H5 = BIPHENYL                                6.100E+25  -4.000
5590.00 ! 97-WAN-FRE, 90 torr
!C6H5 + C6H5 = BIPHENYL                                2.000E+19  -2.050
2900.00 ! 97-WAN-FRE, 760 torr

!C6H6 + C6H5 = BIPHENYL+H                              5.600E+12  -0.074
7550.00 ! 97-WAN-FRE, 20 torr
!C6H6 + C6H5 = BIPHENYL+H                              1.500E+14  -0.450
8915.00 ! 97-WAN-FRE, 90 torr
!C6H6 + C6H5 = BIPHENYL+H                              1.100E+23  -2.920
15890.00 ! 97-WAN-FRE, 760 torr
!

```

```

! Reactions of benzoquinone (p-C6H4O2)
!
C6H4O2 = C5H4O + CO                                7.400E+11    0.000
59000.00 ! 94-FRA-HER
C6H4O2 + H = CO + C5H5O(1,3)                        4.300E+09    1.450
3900.00 ! est. HW k = kinf[C6H6 + H]
C6H4O2 + O = 2CO + C2H2 + CH2CO                    3.000E+13    0.000    5000.00
! est. HW, ??
!
! Reactions of phenoxy radical (C6H5O)
!
C6H5O + H = C5H5 + HCO                            1.000E+13    0.000    12000.00 !
added 9/25
C6H5O + H = C5H6 + CO                              5.000E+13    0.000
0.00 ! added 9/25
C6H5O = CO + C5H5                                  3.760E+54 -12.060
72800.00 ! DAVIS, RRKM 1 atm (Ea reduced by 1.5 kcal/mol = change in
hf, ch650)
C6H5O + O = C6H4O2 + H                             2.600E+10    0.470
795.00 ! MEB-LIN-95 (added 9/23)
!
! Reactions of phenol (C6H5OH)
!
C6H5OH = C5H6 + CO                                  1.000E12     0.000
60808.00 ! 98-HOR-FRA (added 9/25)
C6H5OH + OH = C6H5O + H2O                          2.950E+06    2.000
-1312.00 ! 90-KNI-KOC
C6H5OH + H = C6H5O + H2                            1.150E+14    0.000
12398.00 ! 88-HE-MAL
C6H5OH + O = C6H5O + OH                             2.810E+13    0.000
7352.00 ! 92-EMD-BRE, est. as 1/6 of CH3C6H4CH3 + O from 82-NIC-GUM
C6H5OH + C2H3 = C6H5O + C2H4                       6.000E+12    0.000
0.00 ! 92-EMD-BRE, est. from phenol + OH
C6H5OH + nC4H5 = C6H5O + C4H6                      6.000E+12    0.000
0.00 ! 92-EMD-BRE, est. from phenol + OH
C6H5OH + C6H5 = C6H5O + C6H6                      4.910E+12    0.000
4400.00 ! 88-FAH-STE
!
! Reactions of cyclopentadiene (C5H6)
!
C5H6 + H = C2H2 + aC3H5                             7.740E+36   -6.180
32890.00 ! 98-ZHO-BOZ
C5H6 + H = 1C5H7                                    8.270E+126  -32.30
82348.00 ! 02-MOS-LIN
C5H6 + H = C5H5 + H2                                3.030E+08    1.710
5590.00 ! 02-MOS-LIN
C5H6 + O = C5H5 + OH                                4.770E+04    2.710
1106.00 ! 98-ZHO-BOZ est.
C5H6 + O = C5H5O(1,3) + H                          8.910E+12   -0.150
590.00 ! 98-ZHO-BOZ, C5H5O1_1
DUPLICATE
C5H6 + O = C5H5O(1,3) + H                          5.600E+12   -0.060

```

```

200.00 ! 98-ZHO-BOZ, C5H5O1_2
      DUPLICATE
      C5H6 + O = nC4H5 + CO + H      8.700E+51 -11.090   33240.00
! 98-ZHO-BOZ
      C5H6 + OH = C5H5 + H2O          3.080E+06   2.000
0.00 ! 98-ZHO-BOZ est.
      C5H6 + HO2 = C5H5 + H2O2        1.100E+04   2.600
12900.00 ! 98-ZHO-BOZ est.
      C5H6 + O2 = C5H5 + HO2          4.000E+13   0.000
37150.00 ! 98-ZHO-BOZ est.
      C5H6 + HCO = C5H5 + CH2O        1.080E+08   1.900
16000.00 ! 98-ZHO-BOZ est.
      C5H6 + CH3 = C5H5 + CH4         0.180E+00   4.000
0.00 ! 98-ZHO-BOZ est.
      C5H5 + H (+M) = C5H6 (+M)       1.000E+14   0.000
0.00 ! 92-EMD-BRE, est., 94-FRA-HER
      LOW / 4.400E+80 -18.280
12994.0 / !96-DAV-WAN, 97-WAN-FRE
      TROE / 0.068 400.7 4135.8 5501.9
/
      H2/2.0/ H2O/6.0/ CH4/2.0/ CO/1.5/
CO2/2.0/
!
! Reactions of cyclopentadienyl radical (C5H5)
!
      C5H5 + O2 = C5H5O(2,4) + O      7.780E+15  -0.730   48740.00
! 10/18
      C5H5 + O = C5H5O(2,4)          1.120E-12   5.870
-17310.00 !10/18
      C5H5 + O = C5H4O + H            5.810E+13  -0.020
20.00 ! 98-ZHO-BOZ
      C5H5 + O = nC4H5 + CO           3.200E+13  -0.17
440.00 !ZHO-BOZ-98 added 10/08
      C5H5 + OH = C5H4OH + H          3.510E+57 -12.180   48350.00
! 98-ZHO-BOZ
      C5H5 + OH = C5H5O(2,4) + H      1.360E+51 -10.460
57100.00 !10/18
      C5H5 + HO2 = C5H5O(2,4) + OH    6.270E+29  -4.690
11650.00 !10/18
      C5H5 + OH = C5H5OH              6.490E+14  -0.850
-2730.00 ! 98-ZHO-BOZ, C5H5OH
      DUPLICATE
      C5H5 + OH = C5H5OH              1.150E+43  -8.760
18730.00 ! 98-ZHO-BOZ, 1-C5H5OH
      DUPLICATE
      C5H5 + OH = C5H5OH              1.060E+59 -13.080
33450.00 ! 98-ZHO-BOZ, 2-C5H5OH
      DUPLICATE
      C5H5 + O2 = C5H4O + OH          1.800E+12   0.080
18000.00 ! RRKM 1 atm
!C5H5 + C5H5 = C10H8 + 2H            6.430E+12   0.000
4000.00 ! 98-KER-KIE (added 5/12)

```

```

!
! Reactions of cyclopentadienols (1,3-, 2,4- and 1,4-C5H5OH)
!
C5H5OH + H = C5H5O(2,4) + H2 1.150E+14 0.000
15400.00 ! as C6H5OH + H = C6H5O + H2 + 3 kcal/mol E barrier
C5H5OH + H = C5H4OH + H2 1.200E+05 2.500
1492.00 ! est. C5H6 + H = C5H5 + H2
C5H5OH + OH = C5H5O(2,4) + H2O 6.000E+12 0.000
0.00 ! as C6H5OH + OH = C6H5O + H2O
C5H5OH + OH = C5H4OH + H2O 3.080E+06 2.000
0.00 ! est. C5H6 + OH = C5H5 + H2O
C5H5O(2,4) + H = C5H5OH 1.000E+14 0.000
0.00 ! est. HW
!
! Reactions of C5H5O(2,4)
!
C5H5O(2,4) = C5H4O + H 2.000E+13 0.000
30000.00 ! (est. HW)
C5H5O(2,4) + O2 = C5H4O + HO2 1.000E+11 0.000
0.00 ! (est. HW)
!
! Reactions of C5H5O(1,3)
!
C5H4O + H = C5H5O(1,3) 2.000E+13 0.000
2000.00 ! Est. HW, see notes
C5H5O(1,3) = c-C4H5 + CO 1.000E+12 0.000
36000.00 ! Est. (very rough) from C6H5O
C5H5O(1,3) + O2 = C5H4O + HO2 1.000E+11 0.000
0.00 ! Est. HW
!
! Reactions of cyclopentadienone (C5H4O)
!
C5H4OH = C5H4O + H 2.100E+13 0.000
48000.00 ! Est. EBG
C5H4O = 2C2H2 + CO 6.200E+41 -7.870
98700.00 !RRKM (10/18)
!
C5H4O + H = CO + c-C4H5 4.300E+09 1.450
3900.00 ! Est. HW = C6H6 + H kinf, possibly too large
C5H4O + O = CO + HCO + C3H3 6.200E+08 1.450 -858.00
! Est. HW = C4H6 + O
!
! Ractions of c-C4H5
!
c-C4H5 + H = C4H6 1.000E+13 0.000
0.00 ! Est. HW, fast c-C4H6 -> C4H6 - Lifshitz
c-C4H5 + H = C2H4 + C2H2 1.000E+13 0.000
0.00 ! Est. HW
c-C4H5 + O = CH2CHO + C2H2 1.000E+14 0.000
0.00 ! Est. HW
c-C4H5 + O2 = CH2CHO + CH2CO 4.800E+11 0.000
19000.00 ! Est. HW, C3H5+O2

```



```

c-C4H5 = C4H4 + H                                3.000E+12    0.000
52000.00 ! Est. HW
c-C4H5 = C2H3 + C2H2                                2.000E+12    0.000
58000.00 ! Est. HW
!
! Reactions of 1,4-pentadien-3-yl (1-C5H7)
!
aC3H5 + C2H3 = 1C5H7 + H                            1.000E+13    0.000
0.00 ! Est.
1C5H7 + O = C2H3CHO + C2H3                            5.000E+13    0.000
0.00 ! Est.
1C5H7 + OH = C2H3CHO + C2H4                            2.000E+13    0.000
0.00 ! Est.
END
=====
References and Notes:
!-----
-----

GRI      - Frenklach, M.; Wang, H.; Goldenberg, M.; Smith, G.P.; Golden,
D.M.;
          Bowman, C.T.; Hanson, R.K.; Gardiner, W.C.; Lissiansky, V.
          GRI-Mech: An Optimized Chemical Reaction Mechanism for Methane
          Combustion (version GRI-Mech 1.2), GRI Report No. GRI-95/0058,
          Gas Research Institute, Chicago, 1995.

GRI#      - the rate constants for these reactions were taken with the
branching
          ratio of 1:5 ( GRI-mech1.2 uses 1:1 ratio), as was reported
in the
          followed work: Michael, J.V.; Wagner, A.F.
Ber.Bunsenges.Phys.Chem.
          1990, 94, 2453.

GRI##     - reaction products were modified from the GRI-mech1.2 mechanism,
          see reference 97WAN/FRE for detales

GRI###     - reaction products were modified from the GRI-mech1.2

NIST DB    - Westly, F.; Herron, J.T.; Cvetanovich, R.J.; Hampson R.F.;
Mallard,
          W.G. NIST - chemical Kinetics Standard Referncew Data Base 17,
ver.
          5.0

67LAM/CHR  - Lambert, R.M.; Christie, M.I.; Linnet, J.W.
J.Chem.Soc.Chem.Comm.
          1967, 388.

76CRA/LUT  - Crawford, R.J.; Lutener, S.B.; Cockcroft, R.D. Can.J.Chem.
1976, 54,

```

- 3364.
- 77FLO - Flowers, M.C. J.Chem.Soc., Faraday Trans. 1977, 73, 1927.
- 78BOG/HAN - Bogan, D.J.; Hand, C.W. J.Phys.Chem. 1978, 82, 2067.
- 83HOM/WEL - Homman, K.H.; Wellman, C., Ber.Bunsenges.Phys.Chem. 1983, 87, 609.
- 83LIF/BEN - Lifshitz, A.; Ben-Hamou, H. J.Phys.Chem. 1983, 87, 1782.
- 83WAR/BOC - Warnatz, J.; Bockhorn, H.; Moser, A.; Wenz, H. Th. 19th Symposium
(international) on Combustion, The Combustion Institute,
Pittsburgh,
1983, p.197.
- 84COL/BIT - Cole, J.A.; Bittner, J.D.; Longwell, J.P.; Howard, J.B.
Combust.
Flame 1984, 56, 51.
- 84BOL/KEE - Baldwin, R.R.; Keen, A.; Walker, R.W. J.Chem.Soc., Faraday
Trans.
1984, 80, 435.
- 84PER - Perry, R.A. Combust.Flame 1984, 58, 221.
- 84WAR - Warnatz, J. "Rate coefficients in C/H/O system", in "Combustion
Chemistry" (Ed W.C. Gardiner, Jr.) Springer-Verlag, NY 1984,
p.197.
- 85BAL/HIS - Baldwin, R.R.; Hisham, M.W.M; Walker, R.W. Th. 20th symposium
(international) on Combustion, The Combustion Institute,
Pittsburgh,
1985, p.743.
- 86FRA/BHA - Frank, F.; Bhaskarn, K.A.; Just, Th. 21th symposium
(international)
on Combustion, The Combustion Institute, Pittsburgh, 1988,
p.885.
- 86LIF/BID1 - Lifshitz, A.; Bidani, M. J.Phys.Chem. 1986, 90, 6011.
- 86LIF/BID2 - Lifshitz, A.; Bidani, M. J.Phys.Chem. 1986, 90, 5373.
- 86ROB/TSA - Robaugh, D.; Tsang, W. J.Phys.Chem. 1986, 90, 4159.
- 86TSA/HAM - Tsang, W.; Hampson, R.F. J.Phys.Chem.Ref.Data 1986, 15, 1087.
- 87MAH/MAR - Machmud, K.; Marshall, P.; Fontijn, A. J.Phys.Chem. 1987, 91,
1568.

- 87WU/KER - Wu, C.H.; Kern, R.D. J.Phys.Chem. 1987, 91, 6291.
- 88BOH/TEM - Bohland, T.; Temp, F.; Wagner, H.G. 21th Symposium
(international)
on Combustion, The Combustion Institute, Pittsburgh, 1988,
p.841.
- 88HE/MAL - He, Y.Z.; Mallard, W.J.; Tsang, W. J.Phys.Chem. 1988, 92, 2196.
- 88KER/SIN - Kern, R.D.; Singh, H.J.; Wu, C.H. Int.J.Chem.Kin., 1988, 20,
731.
- 88LIU/MUL - Liu, A.; Mulac, W.A.; Jonah, C.D. J.Phys.Chem. 1988, 92, 131.
- 88LIU/MUL1 - Liu, A.; Mulac, W.A.; Jonah, C.D. J.Phys.Chem. 1988, 92, 3821.
- 88SLA/GUT - Slagle, I.R.; Gutman, D. 21th symposium (international) on
Combustion, The Combustion Institute, Pittsburgh, 1988,
p.875.
- 88TSA - Tsang, W. J.Phys.Chem.Ref.Data 1988, 17, 887.
- 89FAH/STE - Fahr, A.; Stein, S.E. 22th symposium (international) on
Combustion, The Combustion Institute, Pittsburgh, 1989,
p.1023.
- 89LIF/BID - Lifshitz, A.; Bidani, M. J.Phys.Chem. 1989, 93, 1139.
- 89MIL/BOW - Miller, J.A.; Bowman, C.T. Prog.Energy Combust.Sci. 1989, 15,
287.
- 89SLA/BER - Slagle, I.R.; Bernhardt, J.R.; Gutman, D. 22th symposium
(international) on Combustion, The Combustion Institute,
Pittsburgh,
1989, p.953.
- 89WAL - Walker, R.W. 22th symposium (international) on Combustion, The
Combustion Institute, Pittsburgh, 1989, p.883.
- 89WES/DEA - Westmoreland, P.R.; Dean, A.M.; Howard, J.B.; Longwell J.P.
J.Phys.Chem. 1989, 93, 8171.
- 90BOZ/DEA - Bozzelli, J.W.; Dean, A.M. J.Phys.Chem. 1990, 94, 3313.
- 90DEAN - Dean A.M. J. Phys. Chem., 1990, 94, 1432
- 91KO/ADU - Ko, T.; Adusei, G.Y.; Fontijn, A. J.Phys.Chem. 1991, 95, 9366.
- 91SHI/MIC - Shin, K.S.; Michael, J.V. J.Phys.Chem. 1991, 95, 5864.
- 91TSA - Tsang, W. J.Phys.Chem.Ref.Data 1991, 20, 221.

- 92BAU/COB - Baulch, D.L.; Cobos, C.J.; Cox, R.A.; Frank, P.; Hayman, G.; Just, Th.; Kerr, J.A.; Murrells, T.; Pilling, M.J.; Troe, J.; Walker, R.W.; Warnatz, J. J.Phys.Chem.Ref.Data 1992, 21, 411.
- 92EMD/BRE - Emdee, J.L.; Brezinsky, K.; Glassman, I. J.Phys.Chem. 1992, 96, 2151.
- 92KOS/FUK - Koshi, M.; Fukluda, K.; Kamiya, K.; Matsui, H. J.Phys.Chem. 1992, 96, 9839.
- 92MIL/MEL - Miller, J.A.; Melius, C.F. Combust.Flame 1992, 91, 21.
- 92SLA/BEN - Slagle, I.R.; Benscira, A.; Xing, S-B.; Gutman, D. 24th symposium (international) on Combustion, The Combustion Institute, Pittsburgh, 1992, p.653.
- 92WAN - Wang, H., Ph.D. Thesis, The Pennsylvania State University, University Park, PA, 1992
- 93ADU/FON - Adusei, G.Y.; Fontijn, A. J.Phys.Chem. 1993, 97, 1406.
- 93ADU/FON# - total rate constant for C4H6+O reaction was taken from the reference 92ADU/FON, the products and the branching ratio were proposed in the present work.
- 93FAR/MOR - Fahrat, S.K.; Morter, C.L.; Glass, G.P. J.Phys.Chem. 1993, 97, 12789.
- 94BUTH - Buth, R.; Hoyermann, K.; Seeba, J. 25th Symposium, 1998. p321
- 94FRA/HER - Frank, P.; Herzler, J.; Just, Th.; Wahl, C. 25th symposium (international) on Combustion, The Combustion Institute, Pittsburgh, 1994, p.833.
- 94LIF/TAM - Lifshitz, A.; Tamburu, C. J.Phys.Chem. 1994, 98, 1167.
- 95LEU/LIN - Leung, K.M.; Linstedt, R.P. Combust.Flame 1995, 102, 129.
- 95PAU/VOL - Pauwels, J-F.; Volponi, J. V.; Miller, J.A. Combust.Sci.Tech. 1995, 110/111, 249.
- 95MEB/LIN - Lin, M.C. and Mebel, A.M.; J. Phys. Organic Chem. 1995, 8, 407-420
- 96ADU/BLU - Adusei, G.Y.; Blue, A.S.; Fontijn, A. J.Phys.Chem. 1996, 100, 16921.

- 96ADU/BLU#- total rate constant for $\text{pC}_3\text{H}_4 + \text{O}$ reaction was taken from the reference 96ADU/BLU, the products and the branching ratio were taken from the reference 98DAV/LAW
- 96HEC/HIP - Heckmann, E.; Hippler, H.; Troe, J. C. 26th symposium (international) on Combustion, The Combustion Institute, Pittsburgh, 1996, p.543.
- 96HID/HIG - Hidaka, Y.; Higashihara, T.; Ninomiya, N.; Masaoka, H.; Nakamura, T.; Kawano, H. *Int.J.Chem.Kin.* 1996, 28, 137z.
- 96KNY/BEN - Knyazev, V.D.; Benscira, A.; Stoliarov, S.I.; Slagle, I.R. *J.Phys.Chem.* 1996, 100, 11343.
- 96KNY/SLA - Knyazev, V.D.; Slagle, I.R. *J.Phys.Chem.* 1996, 100, 16899.
- 96MEB/DIA - Mebel, A.M.; Diau, E.W.G.; Lin, M.C.; Morokuma, K. *J.Phys.Chem.* 1996, 118, 9759.
- 96WUR/McG - Wurmel, J.; McGuinness, M.; Simmie, J.M. *J.Chem.Soc., Faraday Trans.* 1996, 92(5), 715.
- 97JON/BAC - Jones, J.; Bacskay, G.B.; Mackie, J.C. *J.Phys.Chem.A* 1997, 101, 7105.
- 97MEB/LIN - Mebel, A.M.; Lin, M.C.; Yu, T.; Morokuma, K. *J.Phys.Chem.A* 1997, 101, 3189.
- 97WAN/FRA - Wang, H.; Frenklach, M. *Combust.Flame* 1997, 110, 173.
- 98DAV/LAW - Davis, S.G.; Law, C.K.; Wang, H. 27th Symposium (international) on Combustion, The Combustion Institute, Pittsburgh, 1998, p.305.
- 98KER/KIE - Kern, R.D.; Zhang, Q.; Yao, J.; Jursic B.S.; Tranter, R.S.; Greybill, M.A.; Kiefer, J.H. 27th Symposium (international) on Combustion, The Combustion Institute, 1998
- 98HOR/FRA - Horn C, Roy K, Frank P and Just T; 27th Symposium (international) on Combustion, The Combustion Institute, Pittsburgh, 1998, p.321
- 99DAV/LAW - Davis, S.G.; Law, C.K.; Wang, H. *J.Phys.Chem.* 1999, in press.
- 99LAS/WAN - Laskin, A.; Wang, H. *Chem.Phys.Lett.*, 1999, 303, 43.
- 99TOK/LIN - Tokmakov, I.V.; Park, J.; Gheyas, S.; Lin, M.C. *J. Phys. Chem.A* 1999,

103, 3636
00CHO/LIN - Choi, Y.M.; Xia, W.S.; Park, J.; Lin, M.C. J. Phys. Chem.A 2000,
104, 7030
00NAM/LIN - Nam, Gi-Jung; Xia, Wensheng; Park, J.; Lin, M.C. J. Phys. Chem.A
2000, 104, 1233
00HAI/FRE - Wang, H.; Laskin, A.; Moriarty, N.; Frenklach, M. 28th Symposium
(international) on Combustion, The combustion Institute, 2000.
96DAV/WAN - Davis, S.G.; Wang, H.; Brezinsky, K.; Law, C.K. 26th Symposium
(international) on Combustion, The Combustion Institute,
Pittsburgh,
1996, p.1025.
01PAR/LIN - Park, J.; Gheysa, S.; Lin, M.C. Int. J. Chem. Kinet. 2001, 33,
64
01TOK/LIN - Tokmakov, I.V.; Lin, M.C. Int. J. Chem. Kinet. 2001, 33,
633-653.
01MEB/LIN - Mebel A.M., Lin M.C., Chakraborty D., Park J., Lin S.H. and
Lee Y.T.
; J.Chem. Phys. 114, 19, 2001, 8421.
02MOS/LIN - Moskaleva L.V. and Lin M.C. 29th Combustion Symposium, 2002,
1319.
05/VAS/DAV - Vasudevan, V.; Davidson, D. F.; Hanson, R. K. J. Phys. Chem.
A 2005, 109, 3352

Bibliography

- Aamir D Abid, Joaquin Camacho, David A Sheen, and Hai Wang. Evolution of soot particle size distribution function in burner-stabilized stagnation n-dodecane- oxygen-argon flames. *Energy & Fuels*, 23(9):4286–4294, 2009.
- A Agosta, NP Cernansky, DL Miller, T Faravelli, and E Ranzi. Reference components of jet fuels: kinetic modeling and experimental results. *Experimental Thermal and Fluid Science*, 28(7):701–708, 2004.
- National Laboratory Argonne. Commercial trucks aviation marine modes railroads pipelines off-road equipment. Technical report, Argonne National Laboratory, 2013. URL <http://www.osti.gov/bridge>.
- A. Bardosova. *Flow Reactor Study of Oxidation of Dimethyl Ether and Methane Binary Mixtures at Intermediate Temperatures*. PhD thesis, Stanford University, 2011.
- Philip R. Bevington and D. Keith Robinson. *Data Reduction and Error Analysis*. Mc Graw Hill, third edition, 2002.
- G Bikas and N Peters. Kinetic modelling of *n*-decane combustion and autoignition: Modeling combustion of *n*-decanem. *Combustion and Flame*, 126(1):1456–1475, 2001.
- D Bradley and AG Entwistle. Determination of the emissivity, for total radiation, of small diameter platinum-10% rhodium wires in the temperature range 600-1450 c. *British Journal of Applied Physics*, 12(12):708, 1961.

- Alexander Burcat and Branko Ruscic. *Third millenium ideal gas and condensed phase thermochemical database for combustion with updates from active thermochemical tables*. Argonne National Laboratory Argonne, IL, 2005. URL <http://garfield.chem.elte.hu/Burcat/BURCAT.THR>.
- CLEEN. Cleen program. URL https://www.faa.gov/about/office_org/headquarters_offices/apl/research/aircraft_technology/cleen/reports/.
- Meredith Colket, Tim Edwards, Skip Williams, Nicholas P Cernansky, David L Miller, Fokion Egolfopoulos, Peter Lindstedt, Kalyanasundaram Seshadri, Frederick L Dryer, Chung K Law, et al. Development of an experimental database and kinetic models for surrogate jet fuels. In *45th AIAA Aerospace Sciences Meeting and Exhibit*, pages 2007–770, 2007.
- James A Cooke, Matteo Bellucci, Mitchell D Smooke, Alessandro Gomez, Angela Violi, Tiziano Faravelli, and Eliseo Ranzi. Computational and experimental study of jp-8, a surrogate, and its components in counterflow diffusion flames. *Proceedings of the Combustion Institute*, 30(1):439–446, 2005.
- HJ Curran, P Gaffuri, William J Pitz, and Charles K Westbrook. A comprehensive modeling study of n-heptane oxidation. *Combustion and flame*, 114(1-2):149–177, 1998.
- Philippe Dagaut. On the kinetics of hydrocarbons oxidation from natural gas to kerosene and diesel fuel. *Physical Chemistry Chemical Physics*, 4(11):2079–2094, 2002.
- KD Dahm, PS Virk, R Bounaceur, F Battin-Leclerc, PM Marquaire, R Fournet, E Daniau, and M Bouchez. Experimental and modelling investigation of the thermal decomposition of n-dodecane. *Journal of Analytical and Applied Pyrolysis*, 71(2):865–881, 2004.
- A D’Anna, M Alfe, B Apicella, A Tregrossi, and A Ciajolo. Effect of fuel/air ratio and aromaticity on sooting behavior of premixed heptane flames. *Energy & Fuels*, 21(5):2655–2662, 2007.
- DF Davidson, Z Hong, GL Pilla, A Farooq, RD Cook, and RK Hanson. Multi-species time-history measurements during n-dodecane oxidation behind reflected shock waves. *Proceedings of the Combustion Institute*, 33(1):151–157, 2011.

- Alexander C Davis and Joseph S Francisco. Ab initio study of hydrogen migration across n-alkyl radicals. *The Journal of Physical Chemistry A*, 115(14):2966–2977, 2011.
- Stephen Dooley, Sang Hee Won, Joshua Heyne, Tanvir I Farouk, Yiguang Ju, Frederick L Dryer, Kamal Kumar, Xin Hui, Chih-Jen Sung, Haowei Wang, et al. The experimental evaluation of a methodology for surrogate fuel formulation to emulate gas phase combustion kinetic phenomena. *Combustion and Flame*, 159(4):1444–1466, 2012.
- C Doute, J-L Delfau, R Akrich, and C Vovelle. Chemical structure of atmospheric pressure premixed n-decane and kerosene flames. *Combustion Science and Technology*, 106(4-6): 327–344, 1995.
- Francis Dryer, Jeffrey Haas, Tanvir Santner, Marcus Farouk, and Chaos. Interpreting chemical kinetics from complex reaction-advection-diffusion systems: Modeling of flow reactor and related experiments. *Progress Energy Combustion Science*, 2014. Accepted for Publication.
- Fokion N Egolfopoulos. Development of detailed and reduced kinetics mechanisms for surrogates of petroleum-derived and synthetic jet fuels. Technical report, DTIC Document, 2011.
- Y Feng, JT Niiranen, A Bencsura, VD Knyazev, D Gutman, and W Tsang. Weak collision effects in the reaction ethyl radical. dblrw. ethene+ hydrogen. *The Journal of Physical Chemistry*, 97(4):871–880, 1993.
- Laurent YM Gicquel, Gabriel Staffelbach, and Thierry Poinso. Large eddy simulations of gaseous flames in gas turbine combustion chambers. *Progress in Energy and Combustion Science*, 38(6):782–817, 2012.
- David Goodwin. Cantera: An object-oriented software toolkit for chemical kinetics, thermodynamics, and transport processes. URL <https://code.google.com/p/cantera/>.
- Joel M Hall and Eric L Petersen. An optimized kinetics model for oh chemiluminescence at high temperatures and atmospheric pressures. *International journal of chemical kinetics*, 38(12):714–724, 2006.

- Peter E Hamlington, Alexei Y Poludnenko, and Elaine S Oran. Interactions between turbulence and flames in premixed reacting flows. *Physics of Fluids (1994-present)*, 23(12): 125111, 2011.
- MA Hanning-Lee, NJB Green, MJ Pilling, and SH Robertson. Direct observation of equilibration in the system $\text{h} + \text{c}_2\text{h}_4 = \text{c}_2\text{h}_5$: standard enthalpy of formation of the ethyl radical. *Journal of physical chemistry*, 97(4):860–870, 1993.
- Olivier Herbinet, Paul-Marie Marquaire, Frédérique Battin-Leclerc, and René Fournet. Thermal decomposition of n-dodecane: Experiments and kinetic modeling. *Journal of analytical and applied pyrolysis*, 78(2):419–429, 2007.
- J.O. Hinze. *Turbulence*. Mc, first edition, 1959.
- AT Holley, Y Dong, MG Andac, FN Egolfopoulos, and T Edwards. Ignition and extinction of non-premixed flames of single-component liquid hydrocarbons, jet fuels, and their surrogates. *Proceedings of the Combustion Institute*, 31(1):1205–1213, 2007.
- AT Holley, XQ You, E Dames, H Wang, and FN Egolfopoulos. Sensitivity of propagation and extinction of large hydrocarbon flames to fuel diffusion. *Proceedings of the Combustion Institute*, 32(1):1157–1163, 2009.
- S Humer, A Frassoldati, S Granata, T Faravelli, E Ranzi, R Seiser, and K Seshadri. Experimental and kinetic modeling study of combustion of jp-8, its surrogates and reference components in laminar nonpremixed flows. *Proceedings of the Combustion Institute*, 31(1):393–400, 2007a.
- S Humer, A Frassoldati, S Granata, T Faravelli, E Ranzi, R Seiser, and K Seshadri. Experimental and kinetic modeling study of combustion of jp-8, its surrogates and reference components in laminar nonpremixed flows. *Proceedings of the Combustion Institute*, 31(1):393–400, 2007b.
- IEA. Iea statistics: Co2 emissions from fuel combustion highlights. Technical report, IEA, 2013.

- Saeed Jahangirian, Stephen Dooley, Francis M Haas, and Frederick L Dryer. A detailed experimental and kinetic modeling study of n-decane oxidation at elevated pressures. *Combustion and Flame*, 159(1):30–43, 2012.
- James K. Klein James T. Edwards, Linda M. Shafer. Us airforce hydroprocessed renewable jet (hrj) fuel research. Technical report, University of Dayton Research Institute, 2012.
- Chunsheng Ji, Enoch Dames, Yang L Wang, Hai Wang, and Fokion N Egolfopoulos. Propagation and extinction of premixed c5–c12, n-alkane flames. *Combustion and Flame*, 157(2):277–287, 2010.
- Andreas M Kempf. Les validation from experiments. *Flow, Turbulence and Combustion*, 80(3):351–373, 2008.
- Kamal Kumar and Chih-Jen Sung. Laminar flame speeds and extinction limits of preheated n-decane/o₂/n₂ and n-dodecane/o₂/n₂ mixtures. *Combustion and Flame*, 151(1):209–224, 2007a.
- Kamal Kumar and Chih-Jen Sung. Laminar flame speeds and extinction limits of preheated n-decane/o₂/n₂ and n-dodecane/o₂/n₂ mixtures. *Combustion and Flame*, 151(1):209–224, 2007b.
- Kenneth Kuo. *Principles of Combustion; Section 1.5: Methods of Measurement of Gas-Phase Reaction Rates*. John Wiley and Sons, 2nd edition edition, 2005.
- Matthew S Kurman, Robert H Natelson, Nicholas P Cernansky, and David L Miller. Speciation of the reaction intermediates from n-dodecane oxidation in the low temperature regime. *Proceedings of the Combustion Institute*, 33(1):159–166, 2011.
- Ning Liu, Chunsheng Ji, and Fokion N Egolfopoulos. Ignition of non-premixed c3–c12 n-alkane flames. *Combustion and Flame*, 159(2):465–475, 2012.
- Megan E MacDonald, Wei Ren, Yangye Zhu, David F Davidson, and Ronald K Hanson. Fuel and ethylene measurements during n-dodecane, methylcyclohexane, and iso-cetane pyrolysis in shock tubes. *Fuel*, 103:1060–1068, 2013.

- Megan Edwards MacDonald. *DECOMPOSITION KINETICS OF THE ROCKET PROPELLANT RP-1 AND ITS CHEMICAL KINETIC SURROGATES*. PhD thesis, Stanford University, 2012.
- Tomasz Malewicki and Kenneth Brezinsky. Experimental and modeling study on the pyrolysis and oxidation of n-decane and n-dodecane. *Proceedings of the Combustion Institute*, 34(1):361–368, 2013.
- Nick M Marinov, William J Pitz, Charles K Westbrook, Antonio M Vincitore, Marco J Castaldi, Selim M Senkan, and Carl F Melius. Aromatic and polycyclic aromatic hydrocarbon formation in a laminar premixed n-butane flame. *Combustion and Flame*, 114(1):192–213, 1998.
- AM Mebel, EWG Diau, MC Lin, and K Morokuma. Ab initio and rrkm calculations for multichannel rate constants of the $\text{c}_2\text{h}_3 + \text{o}_2$ reaction. *Journal of the American Chemical Society*, 118(40):9759–9771, 1996.
- Wayne K Metcalfe, Sinéad M Burke, Syed S Ahmed, and Henry J Curran. A hierarchical and comparative kinetic modeling study of c_1 - c_2 hydrocarbon and oxygenated fuels. *International Journal of Chemical Kinetics*, 45(10):638–675, 2013.
- James A Miller and Stephen J Klippenstein. The $\text{h} + \text{c}_2\text{h}_2 (+ \text{m}) = \text{c}_2\text{h}_3 (+ \text{m})$ and $\text{h} + \text{c}_2\text{h}_4 (+ \text{m}) = \text{c}_2\text{h}_5 (+ \text{m})$ reactions: Electronic structure, variational transition-state theory, and solutions to a two-dimensional master equation. *PCCP. Physical chemistry chemical physics*, 6(6):1192–1202, 2004.
- Christopher J Montgomery, SM Cannon, MA Mawid, and B Sekar. Reduced chemical kinetic mechanisms for jp-8 combustion. Technical report, DTIC Document, 2002.
- Amir Mze-Ahmed, Kamal Hadj-Ali, Philippe Dagaut, and Guillaume Dayma. Experimental and modeling study of the oxidation kinetics of n-undecane and n-dodecane in a jet-stirred reactor. *Energy & Fuels*, 26(7):4253–4268, 2012.
- Krithika Narayanaswamy. *Chemical Kinetic Modeling of Jet Fuel Surrogates*. PhD thesis, Stanford, 2013.

- Krithika Narayanaswamy, Perrine Pepiot, and Heinz Pitsch. A chemical mechanism for low to high temperature oxidation of n-dodecane as a component of transportation fuel surrogates. *Combustion and Flame*, 161(4):866 – 884, 2014. ISSN 0010-2180. doi: <http://dx.doi.org/10.1016/j.combustflame.2013.10.012>. URL <http://www.sciencedirect.com/science/article/pii/S0010218013003866>.
- N Peters. Multiscale combustion and turbulence. *Proceedings of the Combustion Institute*, 32(1):1–25, 2009.
- S Prucker, W Meier, and W Stricker. A flat flame burner as calibration source for combustion research: Temperatures and species concentrations of premixed h₂/air flames. *Review of scientific instruments*, 65(9):2908–2911, 1994.
- E Ranzi, T Faravelli, P Gaffuri, E Garavaglia, and A Goldaniga. Primary pyrolysis and oxidation reactions of linear and branched alkanes. *Industrial & engineering chemistry research*, 36(8):3336–3344, 1997.
- E Ranzi, M Dente, A Goldaniga, G Bozzano, and T Faravelli. Lumping procedures in detailed kinetic modeling of gasification, pyrolysis, partial oxidation and combustion of hydrocarbon mixtures. *Progress in Energy and Combustion Science*, 27(1):99–139, 2001.
- E Ranzi, A Frassoldati, R Grana, A Cuoci, T Faravelli, AP Kelley, and CK Law. Hierarchical and comparative kinetic modeling of laminar flame speeds of hydrocarbon and oxygenated fuels. *Progress in Energy and Combustion Science*, 38(4):468–501, 2012.
- Eliseo Ranzi, Alessio Frassoldati, Silvia Granata, and Tiziano Faravelli. Wide-range kinetic modeling study of the pyrolysis, partial oxidation, and combustion of heavy n-alkanes. *Industrial & engineering chemistry research*, 44(14):5170–5183, 2005.
- Artur Ratkiewicz and Thanh N Truong. Kinetics of the c–c bond beta scission reactions in alkyl radical reaction class. *The Journal of Physical Chemistry A*, 116(25):6643–6654, 2012.

- Edward R Ritter. Therm: A computer code for estimating thermodynamic properties for species important to combustion and reaction modeling. *Journal of chemical information and computer sciences*, 31(3):400–408, 1991.
- C. C. Schmidt. *Flow Reactor Study of the Effect of Pressure on the Thermal de-NO_x Reaction*. PhD thesis, Stanford University, 2001.
- Linda M Shafer, Richard C Striebich, Jeff Gomach, and Tim Edwards. Chemical class composition of commercial jet fuels and other specialty kerosene fuels. *American Institute of Aeronautics and Astronautics*, paper, 7972:6–9, 2006.
- David A Sheen and Hai Wang. The method of uncertainty quantification and minimization using polynomial chaos expansions. *Combustion and Flame*, 158(12):2358–2374, 2011a.
- David A Sheen and Hai Wang. Combustion kinetic modeling using multispecies time histories in shock-tube oxidation of heptane. *Combustion and Flame*, 158(4):645–656, 2011b.
- David A Sheen, Xiaoqing You, Hai Wang, and Terese Løvås. Spectral uncertainty quantification, propagation and optimization of a detailed kinetic model for ethylene combustion. *Proceedings of the Combustion Institute*, 32(1):535–542, 2009.
- Hsi-Ping S Shen, Justin Steinberg, Jeremy Vanderover, and Matthew A Oehlschlaeger. A shock tube study of the ignition of n-heptane, n-decane, n-dodecane, and n-tetradecane at elevated pressures. *Energy & Fuels*, 23(5):2482–2489, 2009a.
- Hsi-Ping S Shen, Justin Steinberg, Jeremy Vanderover, and Matthew A Oehlschlaeger. A shock tube study of the ignition of n-heptane, n-decane, n-dodecane, and n-tetradecane at elevated pressures. *Energy & Fuels*, 23(5):2482–2489, 2009b.
- Hongbo Si, Sayak Banerjee, and C.T. Bowman. Evaluation of a mixing-reacting model for interpretation of flow reactor data. 2011.

- B. Sirjean, E. Dames, D. A. Sheen, X. You, C. Sung, A.T. Holley, F.N. Egolfopoulos, H. Wang, S.S. Vasu, D.F. Davidson, R.K. Hanson, H. Pitsch, C.T. Bowman, A. Kelley, C.K. Law, W. Tsang, N.P. Cernansky, D.L. Miller, Violi, and A. R. P. Lindstedt. A high-temperature chemical kinetic model of n-alkane oxidation, jetsurf version 1.0, September 15 2009. URL <http://www.stanford.edu/group/haiwanglab/JetSurF/JetSurF1.0/>.
- Baptiste Sirjean, Enoch Dames, Hai Wang, and Wing Tsang. Tunneling in hydrogen-transfer isomerization of n-alkyl radicals. *The Journal of Physical Chemistry A*, 116(1): 319–332, 2011.
- GP Smith, DM Golden, M Frenklach, NW Moriarty, B Eiteneer, M Goldenberg, CT Bowman, RK Hanson, S Song, WC Gardiner Jr, et al. Gri-mech 3.0 (1999). URL: http://www.me.berkeley.edu/gri_mech, 1999.
- AH Sully, EA Brandes, and RB Waterhouse. Some measurements of the total emissivity of metals and pure refractory oxides and the variation of emissivity with temperature. *British Journal of Applied Physics*, 3(3):97, 1952.
- W Tsang, I Awan, S McGovern, JA Manion, H Bockhorn, A DAnna, AF Sarofim, and H Wang. *Soot Precursors from Real Fuels: The Unimolecular Reactions of Fuel Radicals*. KIT Scientific Publishing: Karlsruhe, 2009a.
- Wing Tsang. Thermal decomposition of some alkyl halides by a shock-tube method. *The Journal of Chemical Physics*, 41(8):2487–2494, 1964.
- Wing Tsang, James A Walker, and Jeffrey A Manion. Single-pulse shock-tube study on the decomposition of 1-pentyl radicals. In *Symposium (International) on Combustion*, volume 27, pages 135–142. Elsevier, 1998.
- Wing Tsang, James A Walker, and Jeffrey A Manion. The decomposition of normal hexyl radicals. *Proceedings of the Combustion Institute*, 31(1):141–148, 2007.
- Wing Tsang, W Sean McGivern, and Jeffrey A Manion. Multichannel decomposition and isomerization of octyl radicals. *Proceedings of the Combustion Institute*, 32(1):131–138, 2009b.

- SS Vasu, DF Davidson, Z Hong, V Vasudevan, and RK Hanson. n-dodecane oxidation at high-pressures: Measurements of ignition delay times and oh concentration time-histories. *Proceedings of the Combustion Institute*, 32(1):173–180, 2009.
- PS Veloo, S Jahangirian, and FL Dryer. An experimental and kinetic modeling study of the two stage autoignition kinetic behavior of c 7, c 10, c 12, and c 14 n-alkanes. In *Spring Technical Meeting, Central States Section of the Combustion Institute*, 2012.
- A Violi, S Yan, EG Eddings, AF Sarofim, S Granata, T Faravelli, and E Ranzi. Experimental formulation and kinetic model for jp-8 surrogate mixtures. *Combustion Science and Technology*, 174(11-12):399–417, 2002.
- K. M. Walters. *A Flow-Reactor Study of Vitiated Ethane Oxidation at Intermediate Temperatures*. PhD thesis, Stanford University, 2008.
- Feng Wang, Dong Bo Cao, Gang Liu, Jie Ren, and Yong Wang Li. Theoretical study of the competitive decomposition and isomerization of 1-hexyl radical. *Theoretical Chemistry Accounts*, 126(1-2):87–98, 2010.
- Hai Wang, Xiaoqing You, Ameya V Joshi, Scott G Davis, Alexander Laskin, Fokion Egolopoulos, and Chung K Law. Usc mech version ii. *High-temperature combustion reaction model of H₂*, 2, 2007.
- P Wang, NA Platova, J Fröhlich, and U Maas. Large eddy simulation of the preccinsta burner. *International Journal of Heat and Mass Transfer*, 70:486–495, 2014.
- Jürgen Warnatz. The structure of laminar alkane-, alkene-, and acetylene flames. In *Symposium (International) on Combustion*, volume 18, pages 369–384. Elsevier, 1981.
- Jürgen Warnatz. Chemistry of high temperature combustion of alkanes up to octane. In *Symposium (International) on Combustion*, volume 20, pages 845–856. Elsevier, 1985.
- Valérie Warth, Frédérique Battin-Leclerc, René Fournet, Pierre-Alexandre Glaude, Guy-Marie Côme, and Gérard Scacchi. Computer based generation of reaction mechanisms for gas-phase oxidation. *Computers & chemistry*, 24(5):541–560, 2000.

- Charles K Westbrook, William J Pitz, Olivier Herbinet, Henry J Curran, and Emma J Silke. A comprehensive detailed chemical kinetic reaction mechanism for combustion of n-alkane hydrocarbons from n-octane to n-hexadecane. *Combustion and Flame*, 156(1): 181–199, 2009.
- X You. *A Theoretical Study of Normal Alkane Combustion*. PhD thesis, University of Southern California, 2008.
- Xiaoqing You, Fokion N Egolfopoulos, and Hai Wang. Detailed and simplified kinetic models of n-dodecane oxidation: The role of fuel cracking in aliphatic hydrocarbon combustion. *Proceedings of the combustion institute*, 32(1):403–410, 2009.
- Zhenwei Zhao, Marcos Chaos, Andrei Kazakov, and Frederick L Dryer. Thermal decomposition reaction and a comprehensive kinetic model of dimethyl ether. *International Journal of Chemical Kinetics*, 40(1):1–18, 2008.
- Th N Zwietering. The degree of mixing in continuous flow systems. *Chemical Engineering Science*, 11(1):1–15, 1959.
- Th N Zwietering. A backmixing model describing micromixing in single-phase continuous-flow systems. *Chemical engineering science*, 39(12):1765–1778, 1984.